AGARDograph 105

Space Navigation Guidance and Control

Editor
J. E. MILLER M.I.T.

AGARD

The Advisory group for Aerospace Research and Development (AGARD) initiated in 1951 is part of the North Atlantic Treaty Organization and consists of a number of permanent specialist scientific panels and committees from NATO countries. These panels are responsible for sponsoring technical meetings and symposia and the publication of technical papers.

Part of the AGARD publishing programme takes the form of good quality letterpress bound volumes of symposia proceedings or monographs on significant areas of aeronautical research and development.

Technivision Limited of Maidenhead, England have set up a publishing organization based on their wide technological background and utilizing their existing staff of Authors and Editors together with expanded art and production departments.

AGARDograph 105

This volume presents an overall picture of the basic requirements, design philosophy and equipment for the guidance and control of the Apollo moon landing vehicle. The information is arranged in separate papers by specialist authors. Earlier papers state the problems and discuss the solutions; the text is assisted in these tasks by numerous diagrams. Later papers present detailed information on the design and construction of the vital items required to satisfy the solutions derived in the earlier papers. The information provides a valuable guide to the methods used for interplanetary journeys, rendezvous and soft landings.

The authors are part of the senior design staff of the Instrument Laboratory of the Massachusetts Institute of Technology which was responsible for the inertial navigational system for the Polaris Submarines.

The book is printed in uninterrupted pages of text to facilitate rapid reading with the illustrations grouped so that there is no necessity to turn the book round to consult them. The index provided is designed for rapid reference and indicates the relevant information area thus facilitating the use of the book by students.

$15.50

AGARDOGRAPH 105

Space Navigation Guidance and Control

THE ADVISORY GROUP
FOR AEROSPACE RESEARCH AND DEVELOPMENT OF
THE NORTH ATLANTIC TREATY ORGANIZATION

Authors

Dr. C. S. DRAPER

Dr. W. WRIGLEY

D. G. HOAG

Dr. R. H. BATTIN

J. E. MILLER

D. A. KOSO

Dr. A. L. HOPKINS

Dr. W. E. VANDER VELDE

Editor

J. E. MILLER

all of

MASSACHUSETTS INSTITUTE OF TECHNOLOGY

Published by

TECHNIVISION LIMITED
MAIDENHEAD, ENGLAND

Set in Baskerville 10 on 11 pt
Printed and Bound
by

W. and J. MACKAY and CO LTD
LONDON and CHATHAM, ENGLAND

LIBRARY OF CONGRESS
CARD NO 66–28575
THE ADVISORY GROUP FOR AEROSPACE
RESEARCH AND DEVELOPMENT

CONTENTS

PREFACE

The material in this book was assembled to support a series of lectures to be given by the authors in Europe in June 1965, under the sponsorship of the Advisory Group for Aerospace Research and Development, an agency of NATO.

The general subject of Space Vehicle Control Systems is the subject of discussion with particular application to the present Manned Lunar Landing Program. The man-machine interaction along with requirements of the mission are first described. These mission requirements in terms of specific hardware along with the performance requirements and underlying reasons for choice are next explained. Lastly, the theoretical background, the system analysis and the derivation of the control functions to integrate the hardware into a precision guidance, navigation and control system are discussed. The book is organized into seven sections following the pattern of the lectures.

Section 1 provides an historical background to the fundamental problems of guidance and navigation. The basic physical phenomenon and associated instrument techniques are discussed.

Section 2 continues with background information going more specifically into the problems and approach of the guidance, navigation and control oı the Apollo manned lunar landing mission. This section illustrates some of the basic philosophy and approaches to the Apollo tasks, such as the success enhancing decision to provide equipment that will perform all necessary operations on-board and using all ground base help when available.

Section 3 concerns in detail the analytic foundation for performing on-board calculations for navigation and guidance. The achievement of a unified and universal set of equations provides an economy in on-board computer program to perform all the various mission tasks.

Section 4 covers in detail the mechanization of the inertial sensor equipment of the Apollo guidance and control system.

Section 5 provides the same visibility into the optical navigation sensors and measurement techniques.

Section 6 provides background and specific techniques in the mechanization of on-board digital computers. Application to the Apollo mission illustrates several problems of interest such as the methods for providing reasonable and straightforward astronaut data input and readout.

Section 7 concerns the specific problems and solutions of vehicle attitude control under conditions both of rocket powered flight and the free-fall coast conditions. The Apollo mission provides a diversity of examples of this area of technology in the control schemes of the command and service module, the lunar landing vehicle, and the earth entry configuration.

The general problems of Space Navigation, Guidance, and Control requires a great variety of disciplines from the engineering and scientific fields. The successful completion of any one space mission or phase of a space mission requires a team effort with a unified approach. Of equal importance are the

software deliveries and performance with the hardware. This lecture series is an attempt to integrate many of the disciplines involved in creating successful and accurate space vehicle control systems.

These lectures represent, on everyone's part, an interplay between equipment and theory. While in each case emphasis may be on one or the other, in the whole equal emphasis is applied.

All sections may be treated as separate entities; however, in the case of Section 3 through 7 it is helpful to have the background of Section 2. There is a cross reference between sections to avoid unnecessary duplication.

It is observed that the authors have emphasized the Apollo mission and hardware as examples in their treatment of the subjects. This is partially because of their intimate familiarity with Apollo in the development work at the Instrumentation Laboratory of M.I.T. and partially because Apollo provides, in an existing program, an excellent example in its multiple requirements and diversity of problems. Because Apollo is currently under development, no particular attempt has been made to make reference only to the latest configuration details. Indeed, the authors have utilized various stages of the Apollo development cycle without specific identification in every case, as they provide the guidance, navigation or control technique example desired.

The authors wish to express their appreciation to NASA for the opportunity to participate in the lecture series and for permission to use material from the research and development contracts NAS 9–153 and NAS 9–4065. They also recognize that this does not constitute approval by NASA of this material. In addition, they wish to thank the many members of M.I.T.'s Instrumentation Laboratory who are working on the Apollo system, for their inspiration and generation of material.

PART I

GUIDANCE – BASIC PRINCIPLES

Dr. C. Stark Draper
Dr. Walter Wrigley

DR. CHARLES STARK DRAPER

Charles Stark Draper is Professor and Head of the Department of Aeronautics and Astronautics and Director of the Instrumentation Laboratory. Dr. Draper is responsible for an extended curriculum of courses in the fields of instrument engineering and fire control. These courses include regular instruction by the Instrument Section of the Department of Aeronautics and also work leading to degrees for Navy and Air Force officers in armament and fire control. In addition, Dr. Draper has written extensively in the fields of instrumentation and control and has served as consulting engineer to many aeronautical companies and instrument manufacturers. He holds a number of patents for measurement and control equipment.

Dr. Draper was born in Windsor, Missouri, on October 2, 1901. In 1922 he received a Bachelor of Arts degree in Psychology from Stanford University. He then entered M.I.T., where he earned a B.S. in Electrochemical Engineering in 1926; a S.M. without specification of department and a Sc.D. in Physics in 1938.

Dr. Draper is President of the International Academy of Astronautics and his many memberships include the American Academy of Arts and Sciences, the National Academy of Sciences and the American Institute of Aeronautics and Astronautics. In 1965 President Johnson personally awarded the National Medal of Science to Dr. Draper for his "many engineering achievements for the defense of the country".

DR. WALTER WRIGLEY

Walter Wrigley is Professor of Instrumentation and Astronautics, Educational Director of the Instrumentation Laboratory, and Acting Director of the Experimental Astronomy Laboratory at the Massachusetts Institute of Technology. He has been active in the development of basic concepts for fire control and navigation systems and has written extensively in these and related fields.

Dr. Wrigley was born in Brockton, Mass., on March 26, 1913. He received his Bachelor of Science degree in 1934 and a Sc.D. in Physics in 1941, both from M.I.T.

Prior to joining the Instrumentation Laboratory in 1946, Dr. Wrigley served as project engineer with the Sperry Gyroscope Company. He has served on numerous military and civilian advisory boards. Dr. Wrigley is a registered Professional Engineer in Massachusetts, a member of the Scientific Advisory Board for the Chief of Staff of the Air Force, an Associate Fellow of the American Institute of Aeronautics and Astronautics and a member of several professional and honorary societies.

PART I

GUIDANCE – BASIC PRINCIPLES

INTRODUCTION

Guidance is the process of collecting and applying information for the purpose of generating maneuver commands to control vehicle movements. In effect, this process represents closure of the essential control feedback branch that has to be associated with structure and propulsion in order for any vehicle system to operate successfully. Strong airframes and powerful engines can provide the capability for flight, but without control to give stability, guidance to determine proper paths and to generate maneuver commands for realizing these paths, the most sophisticated and expensive craft are of no practical value. The finest airplane will not begin to serve as a means of transportation until the pilot takes his seat and assumes the functions of control and guidance. It is true that in recent times the demands of these functions have often gone beyond the abilities of human senses, human muscles and the speed of human thought processes. Man must now retain his hold on the command of many situations through his invention, production and application of inanimate devices that aid or replace his own limited powers for direct action. The collective brains of mankind are again demonstrating the ages-old truth that thought is very powerful among the factors that determine progress. Advances in the technology of control and guidance have been substantial during the past two decades, but these advances have generated much misunderstanding, controversy and often strong opposition as the demands for attention and funding support have increased. However, the spectacular results that have been achieved, particularly in the fields of ballistic missiles, submarines, satellites and space vehicles, have tended to reduce this resistance and to encourage the development of a technology essential to the advancement and perhaps the survival of our country.

A wide spectrum of possibilities for the future has already been revealed by results now in the records, but essential decisions associated with a continuation of work toward pioneering improvements in performance remain to be made in the near future. Matters of national policy, strategy, tactics, economics, politics, company profits and human emotions are so intermixed with basic physical laws and technological developments that any significant clarifications of basic problems associated with guidance and control are certainly helpful in forming plans for constructive action. The authors of this paper hope to provide some assistance by a discussion of basic principles, requirements, mechanization features and natural performance limitations of components and of systems to meet the needs of military operations. Representative numerical values for typical cases are cited, but specific results from particular equipments are not presented.

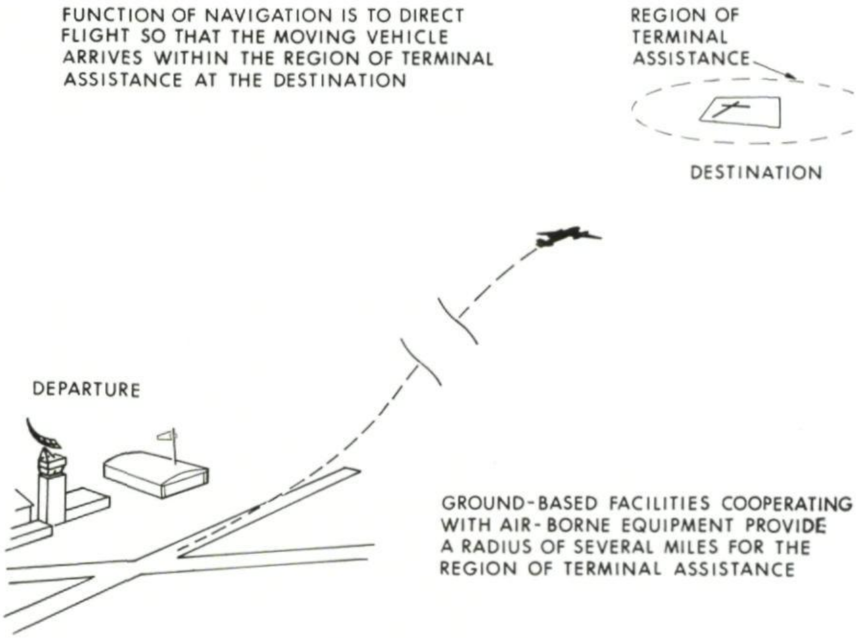

FIG. 1–1 Navigation

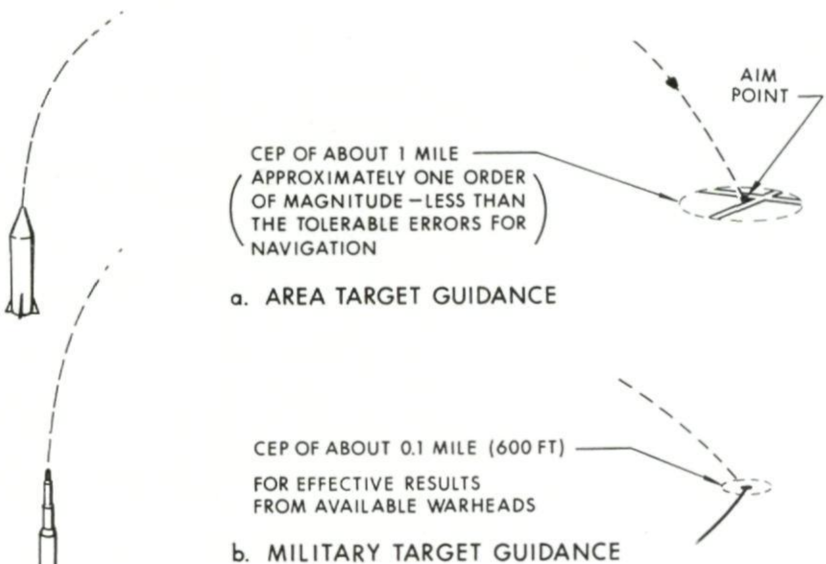

FIG. 1–2 Guidance

CHAPTER 1–1

PROBLEMS OF GUIDANCE

The traditional method of directing the motion of a vehicle from a port of departure to a port of destination is based on the position and direction information generated by navigation. This situation is suggested by Fig. 1–1. Because the terminal phases of many missions are made to depend upon direct contacts with facilities at the destination, the accuracy required of navigation is in general not very great. If navigation can bring a vehicle into an area extending a few miles around the destination, its function has been accomplished. For flights covering not more than a few hours it follows that performance inaccuracies not greater than one to three miles for each hour of flight are often considered satisfactory for navigation systems. Attacks on area targets with weapons able to cause destruction over areas several miles in radius is suggested in Fig. 1–2a. The purposes of such attacks can be served by control and guidance systems giving CEP's – Circular Error Probability (the radius in which half of a significant number of flights would terminate) with the order of one nautical mile. This inaccuracy should be substantially independent of range and time of flight.

Any scheme of navigation or guidance that does not use direct contacts based on either natural or artificial electromagnetic (or acoustic) radiation, must depend upon the identification of points on the earth's surface in terms of measured distances from established bench marks or by means of angles between local gravity directions with respect to coordinate axes fixed in the earth. The association of these directions with points on a theoretical mapping surface makes it possible to identify well-surveyed positions on the earth with inaccuracies somewhat less than one-tenth of a nautical mile. This means that a CEP of one-tenth nautical mile as the performance goal for the instrumentation of navigation and guidance systems is consistent with the map grids now available. Effective attacks on many military targets, such as bridges and hardened missile sites, which can be given map locations within one-tenth nautical mile require inaccuracies around the aim point of approximately the same one-tenth mile order of magnitude. Figure 1–2b suggests the situation associated with a ballistic attack on a hardened missile site.

Control, navigation and guidance always involve a reference coordinate system with axes having known working relationships with directions in the space used for defining the essential path of motion. This definition involves directions with respect to the reference coordinates, and also distances and motion between the guided entity and the destination or target. In practice, the reference coordinates may be established in several ways and the essential distances may also be indicated by various methods. Figure 1–3 illustrates one of the simplest situations for guidance with one airplane making an attack on another craft with guns. The problem is for the attacker to fly a path which causes projectiles from his armament to strike the target. His problem

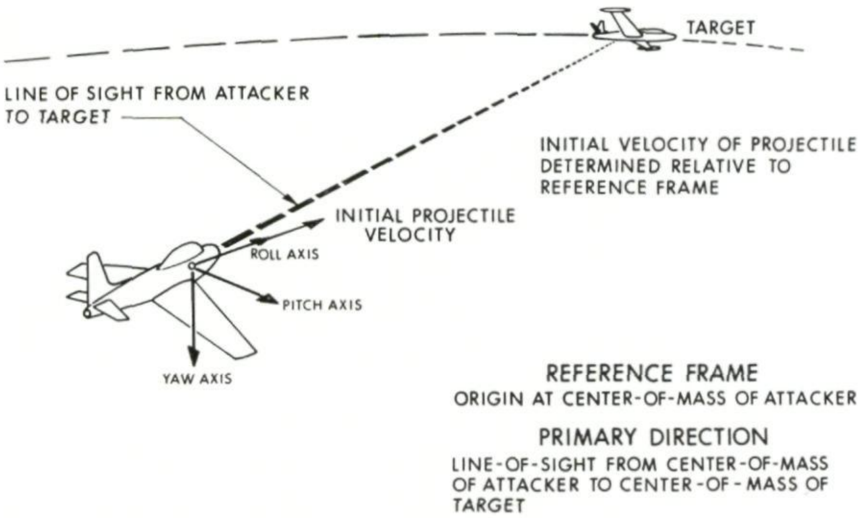

FIG. 1–3 Line of sight guidance – reference frame in vehicle

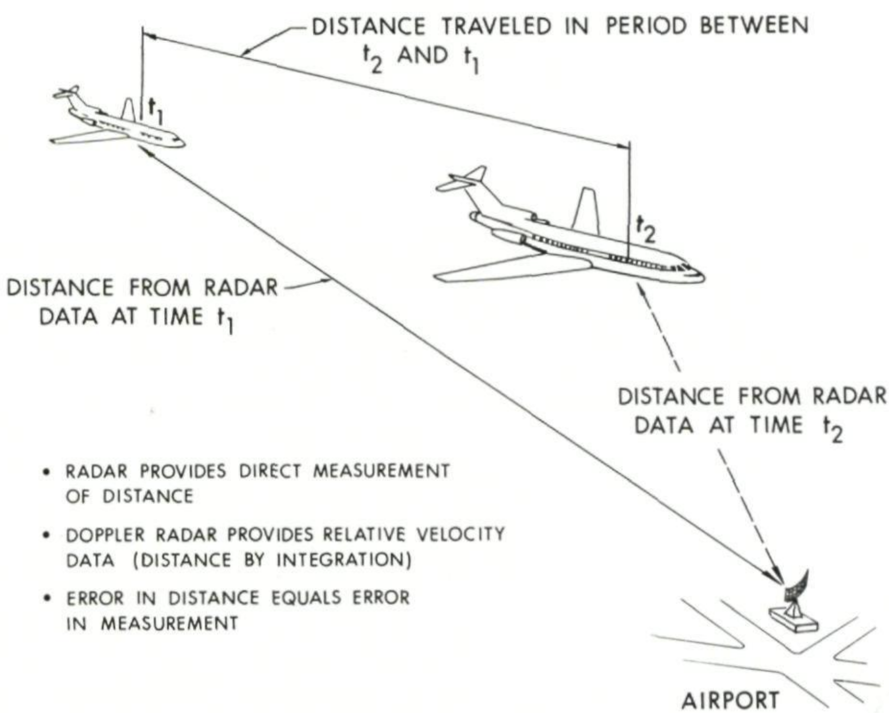

FIG. 1–4 Position change information or radiation contact measurements

centers around the line of sight to the target with reference coordinates for maneuvers fixed in the attacking plane. Usually roll, pitch and yaw axes fixed to the aircraft would be instinctively chosen for judging direction and magnitude of maneuvers. Success is achieved when the attacker flies so that his gunfire destroys the target.

Navigation and guidance present situations that are more complex than the circumstances of an air-to-air duel because direct visual line-of-sight contact with the destination is not generally possible, so that a reference space outside the moving vehicle is necessary in order to describe positions and motions. When flight paths are between points associated with the earth's surface it is natural to use earth's coordinates established by north and the vertical for reference purposes. It is also reasonable to use radiation such as radio and radar for determining distance and direction. Situations of many kinds appear, depending upon circumstances, but it is possible to illustrate the principles involved in terms of the diagrams of Figs. 1–4, 1–5 and 1–6.

Figure 1–4 suggests the situation in which ground-based equipment having a known orientation with respect to earth coordinates has artificial radiation contacts with the moving vehicle. When these contacts are by pulse tracking radar distance measurements are direct and give position when combined with indications of direction from tracking signals. Figure 1–5 illustrates the relationship of distances between points on the earth's surface to angles between gravitational vectors at the points in question. Measurements of directions of gravity are generally associated with positions by the means of celestial navigation procedures. In these methods the gravity vector angles from lines of sight to selected stars are corrected for earth's rotation and then related to map information. It is noted on the figure that an inaccuracy of 60 seconds of arc (one minute of arc) gives a position inaccuracy of 6 000 feet (one nautical mile), while inaccuracies of 6 seconds of arc and 1 second of arc correspond to 600 feet and 100 feet respectively.

Figure 1–6 illustrates the indication of distance moved by a vehicle over the surface of the earth by integration of signals from an accelerometer with its input axis stabilized along the direction of vehicle motion. One integration of these signals from a given initial instant gives changes in velocity. A second integration gives changes in position. Assuming perfect orientation of the input axis during a one-hour time of flight, an average accelerometer inaccuracy of 30×10^{-6} earth gravity leads to approximately 6 000 feet inaccuracy in the indication of distance traveled. Under similar circumstances accelerometer inaccuracies of 3×10^{-6} and 0.5×10^{-6} earth gravity produce approximately 600 feet and 100 feet respectively. The use of a vehicle-borne accelerometer implies that the means to stabilize the member on which it is mounted be aligned with the direction of the earth gravity vectors which identify positions on the earth's surface. On the basis of numbers given in Fig. 1–6, initial alignment inaccuracies of 6 arc-seconds, 0.6 arc-seconds and 0.1 arc-second will mean position inaccuracies of 6 000 feet, 600 feet and 100 feet respectively. Additional inaccuracies of similar magnitude will accumulate if the orientational reference keeping the accelerometer input axis at right angles to the local gravity directions drifts at average rates that accumulate the given angular inaccuracies.

It is convenient to express these drift rates in terms of earth's rate for the

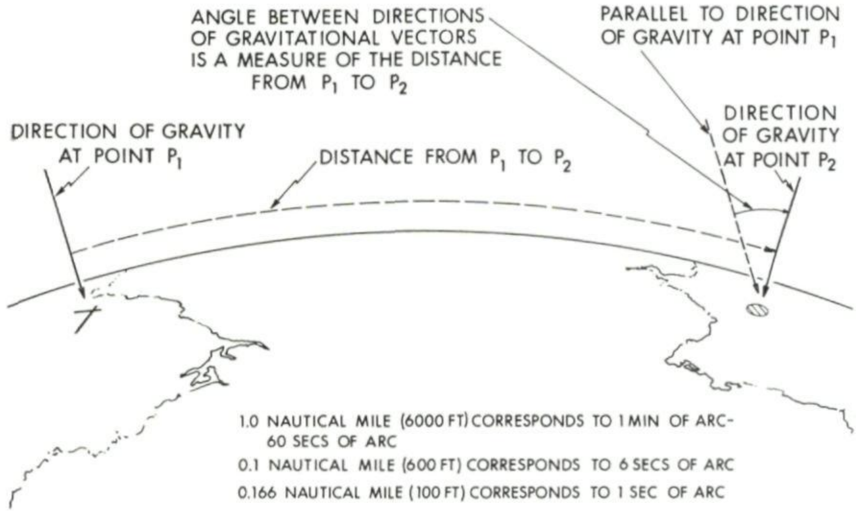

FIG. 1–5 Position information from measurement of angle between gravity vector direction

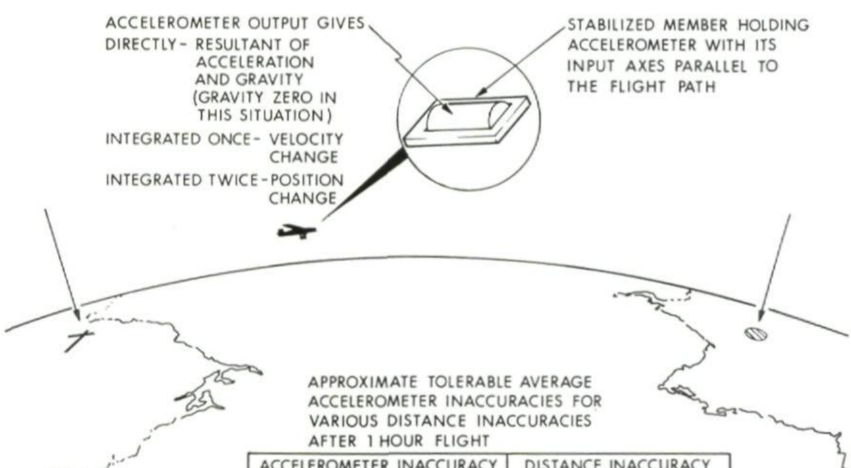

ACCELEROMETER INACCURACY	DISTANCE INACCURACY
30×10^{-6} EARTH GRAVITY	1 N. MILE 6000 FEET
3×10^{-6} EARTH GRAVITY	0.1 N. MILE 600 FEET
0.5×10^{-6} EARTH GRAVITY	0.0166 N. MILE 100 FEET

FIG. 1–6 Position and velocity changes from integration of accelerometer measurement taken along flight paths

purposes of describing system performance. Earth's rate called an "eru" unit is 15 degrees per hour or 900 minutes per hour. One-thousandth of earth's rate (called one milli-earth-rate-unit, one meru) is thus one minute per hour (0.015 degree per hour) which corresponds to a position inaccuracy of about one nautical mile per hour. This means that one-tenth nautical mile (600 feet) corresponds to one-tenth meru (0.0015 degree per hour, or 6 seconds per hour) while 100 feet corresponds to 0.0167 meru (0.00025 degree per hour, 1 arc-second per hour). It is to be noted that the numbers mentioned are only rough approximations. Any mechanization would require higher performance from its individual components in order to account for the interactions that inevitably exist in complete systems.

In summary, it appears that radiation link inaccuracy is directly that of the instrumentation used. When gravitational directions are used to indicate positions, a 60 arc-second error gives one nautical mile error, with the corresponding error for 100 feet being one arc-second. If one-hour flight time is allowed to accumulate these errors the stabilization drift error must be less than 1 meru (0.015 degree per hour) for one mile error in an hour while a drift of 0.0167 meru (0.00025 degree per hour, 1 arc-second per hour) is required if not more than 100 feet position error is to be developed in one hour. When signals from an accelerometer with its input along the vehicle flight path are used to generate position change data, one mile error in one hour needs an accelerometer inaccuracy of about 30×10^{-6} earth gravity, while 100 feet error in one hour needs accelerometer performance in the range of 0.5×10^{-6} earth gravity.

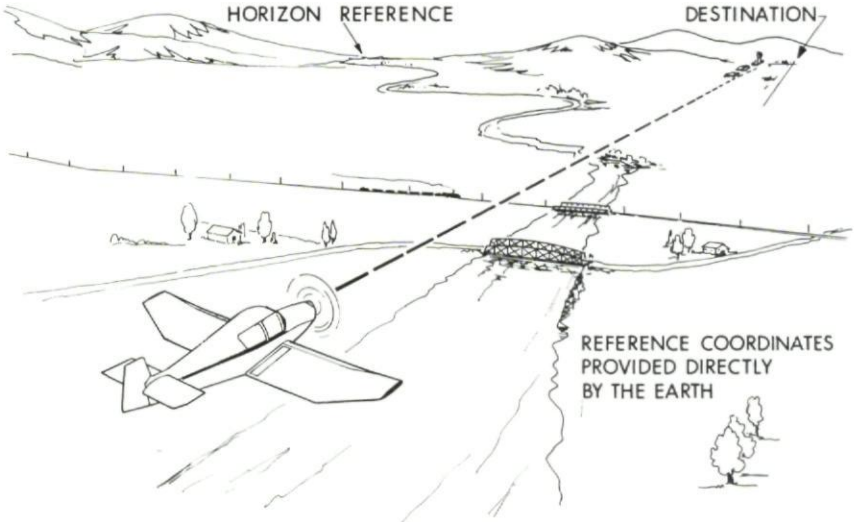

FIG. 1–7 Navigation by visual contact with earth

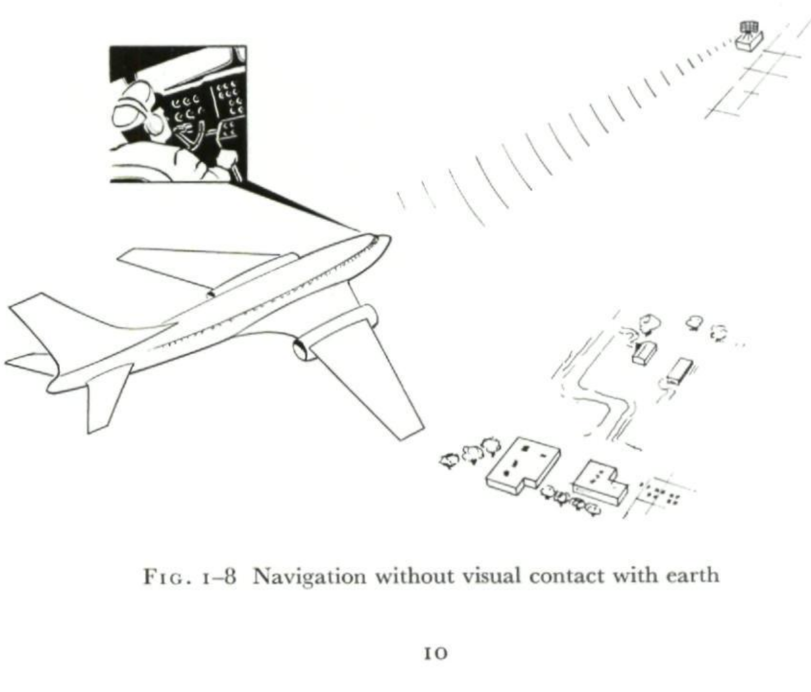

FIG. 1–8 Navigation without visual contact with earth

CHAPTER 1–2

GEOMETRICAL ASPECTS OF GUIDANCE AND CONTROL

From the standpoint of basic geometry the problem of navigation and guidance is that of commanding vehicles to move so that they reach the vicinity of destinations or effectively hit pre-selected targets. In order for this process to be at all possible a reference space in which knowledge of relative location and motion between the guided vehicle and its goal must be available. With this knowledge in hand it may be processed and compared with desired location and motion to determine indicated deviations from which correction maneuver commands can be generated. Geometrical reference space for navigation and guidance is not unique, but may be chosen in many ways to be convenient for the problem under consideration.

Figure 1–7 illustrates a simple situation in which a guided vehicle and its target are linked by a direct line of sight. This line is the geometrical entity that determines the maneuvers carried out by the pilot as he flies to the vicinity of his target. His own airplane acts for him as the reference space for these maneuvers; no outside body is involved. Here his reference space is naturally provided by the earth in good weather with the horizon and landmarks to give him the vertical and north as a setting for the location of his destination. In effect, the earth supplies three coordinate directions for judging angles and a ground-fixed point at the destination for estimating distance and velocity along these axes.

Figure 1–8 shows how the situation changes when clear visual contacts with the ground are lost because of night, weather or terrain. Under these circumstances it is universal practice to use gyroscopic instruments responsive to gravity for vertical indications and controlled by north-seeking devices for azimuth to establish a set of coordinates for directional reference purposes. It is significant to note that these instruments by-pass the structure of the vehicle by which they are carried and act as self-contained equipment in providing orientational reference coodinates. With visual contacts eliminated, artificial radiation links at radio and radar frequencies are used to establish distances and directions from known ground-based stations to the vehicle. Thus, directional information in earth coordinates is provided by both onboard and remote equipment, while indications of distance come from the radiation links with known points on the earth.

Figure 1–9 illustrates the situation that exists when both visual contacts for judging orientation and artificial radiation links for indications of position are not available. The devices providing orientational reference information must be improved to have several orders of magnitude smaller error rates than the orientational reference needed for the situation of Fig. 1–8. By giving the geometrical reference member an initial alignment accurately related to earth coordinates at a known point, changes in location may be indicated

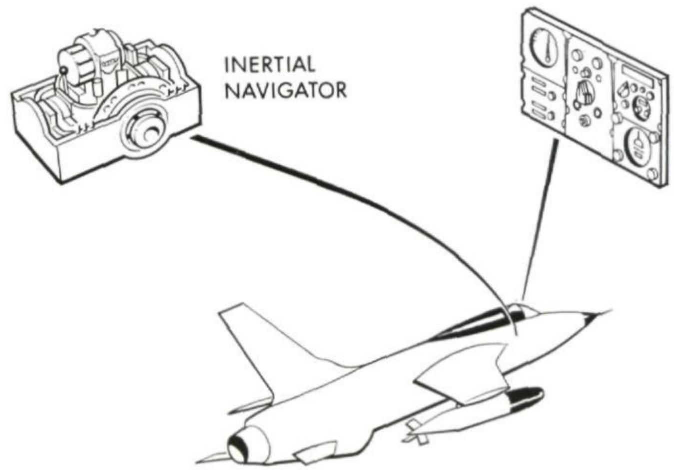

FIG. 1–9 Navigation with both visual and artificial radiation contacts with ground lost

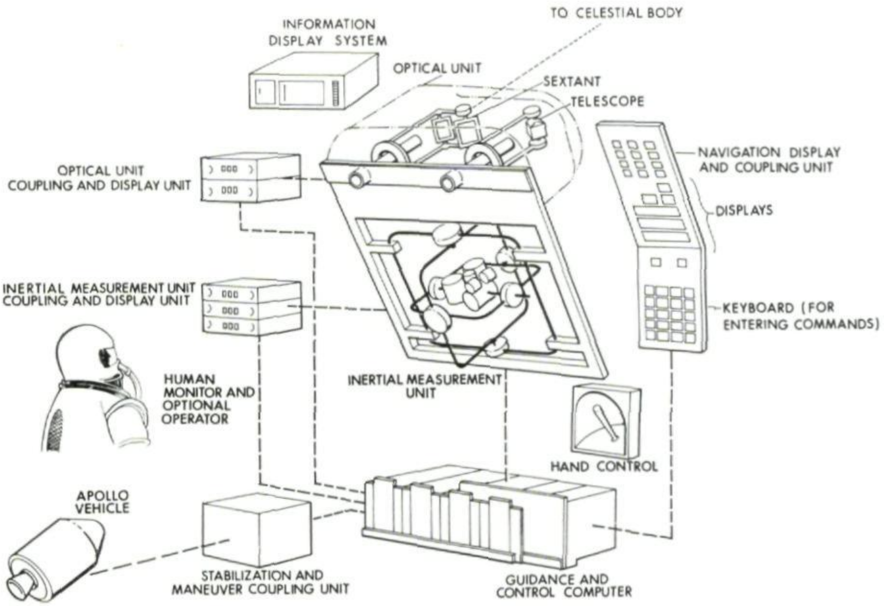

FIG. 1–10 Mechanism elements of Apollo guidance system

by effectively carrying out the double integration of accelerometer output, or by following changes in direction of the earth's gravity vector. This means, in effect, that earth coordinates for a selected time and place must have been transferred to a self-contained system aboard the guided vehicle. With the good equipment performance necessary to provide information continuously and accurately on earth space directions and properly mounted accelerometers with output signals processed by computers, a self-contained system will indicate location and velocity with respect to its point of departure. A system which operates in this way is called an INERTIAL GUIDANCE SYSTEM. Systems of this kind are universally used in ballistic missiles and in submarines when guidance without outside contacts is important. Inertial guidance systems for service over the earth are implemented in many ways, but the necessity remains for an accurate, continuously available, self-contained geometrical reference related in a known way to the external space in which guidance is to be performed. A number of typical mechanizations are described briefly in a later section of this report.

When guidance is considered for vehicles to operate not in the near vicinity of the earth but in regions for which the earth, moon, planets and stars effectively approach mass points, coordinates aligned in earth space lose their usefulness. Rather, it is necessary to employ geometrical reference coordinates associated with stars and planets. For example, celestial sphere coordinates, or some other directions such as a line directed toward the sun, may be set into an inertially stabilized reference member. Figure 1–10 shows the essential features of the Apollo Guidance System which is to be used on manned flights to the moon and return. This system must deal reliably and accurately with some fifteen or twenty different problems of guidance ranging from earth launching through earth orbit, mid-course to the moon, moon orbit, moon landing and return to orbit, and finally through space to landing at a pre-selected point on the earth.

An inertial member with provisions for either manual or automatic alignment with earth coordinates or celestial coordinates is used as the geometrical reference during acceleration phases of the trip. Visually or automatically established lines of sight to known stars and to landmarks on the earth and the moon are used as the basis for determining location and velocity during mid-course flight. Data from these observations are processed by a digital computer which supplies both navigational information and guidance commands for system operation, which may be completely automatic as self-contained equipment, completely manual or partially automatic with monitoring by on-board human pilots, or with remote monitoring by ground-based supervisors through radio and radar links. It is probable that the Apollo Guidance Systems which have already been conceived, designed, built, tested and delivered will be useful models for Space Guidance Systems of the future.

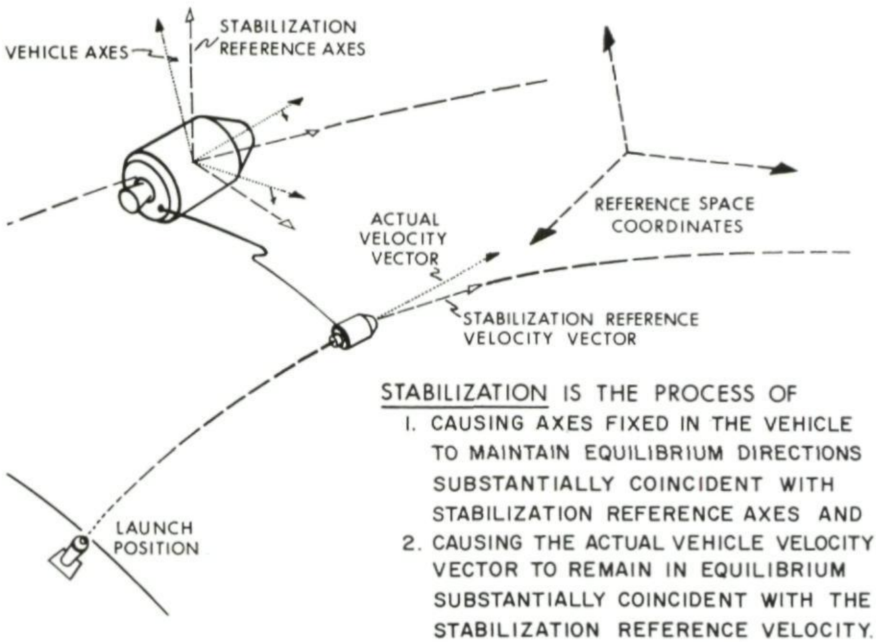

FIG. 1–11 Stabilization

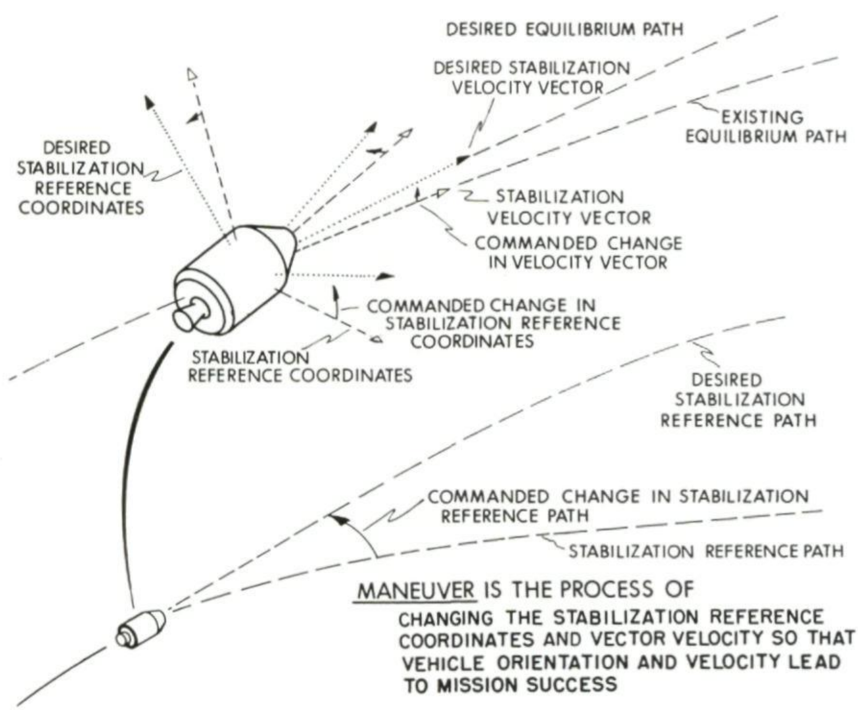

FIG. 1–12 Maneuver

CHAPTER 1–3

FUNCTIONAL REQUIREMENTS OF SYSTEMS AND THEIR COMPONENTS FOR CONTROL AND GUIDANCE

Figure 1–11 represents the essential geometrical function of stabilization in terms of right-angled three-coordinate axis systems associated with the spaces concerned. A set of stabilization reference coordinates is established by some instrumental means or by direct visual contact to a space either identical with or related to the space in which vehicle motion is to be guided. An essential duty of the control system is to cause axes fixed to the vehicle structure to remain continually close to the stabilization reference axes, and also to keep the vehicle velocity vector substantially identical with a stabilization reference velocity vector which has a direction and a magnitude established in some way with respect to the reference space in which the vehicle path is defined.

Figure 1–12 represents maneuver, a second control system function in which the stabilization reference coordinates and the stabilization reference motion are changed with respect to the vehicle path reference space in the ways necessary to accomplish missions. The control system inputs that serve this purpose are maneuver commands generated from plans, programs, feedback data, environmental data, and other information by a guidance system. The nature and functions of this system are illustrated by the diagram of Fig. 1–13.

Figures 1–14 and 1–15 suggest the control and guidance situation that existed during the early days of manned flight. Without a pilot to complete the information handling feedback loop of control and guidance, an airplane was completely useless. Plans and programs were stored in the man's brain, stabilization references and airplane conditions were noted by human senses and processed in the pilot's mind to generate maneuver commands that were applied to the airplane control levers by his hands and feet.

Figures 1–16 and 1–17 illustrate the control and guidance situation that commonly exists today in jet aircraft. Human pilots continue to be used in the control and guidance systems, but their senses are greatly extended by radio, radar and many instruments, their muscle forces are boosted by servo power and their ability to solve complex problems is extended by computers. All these appurtenances certainly improve the effectiveness of control and guidance, but the pilot's position as an "on-line" component in both the control and guidance loops means that his limitations in ability to solve complex problems rapidly and properly handle situations requiring too rapid responses set boundaries to the possible performance of the overall system.

Figures 1–18 and 1–19 suggest the circumstances that exist in rocket powered vehicles that, because of limited payload capacities, one-way missions, hostile environments and severe programs must operate with self-

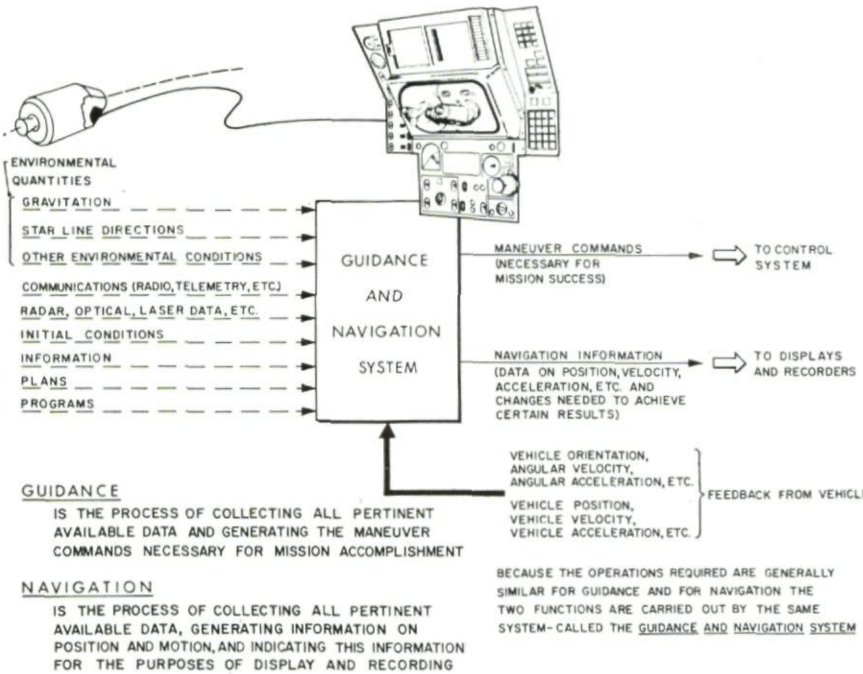

Fig. 1–13 Guidance

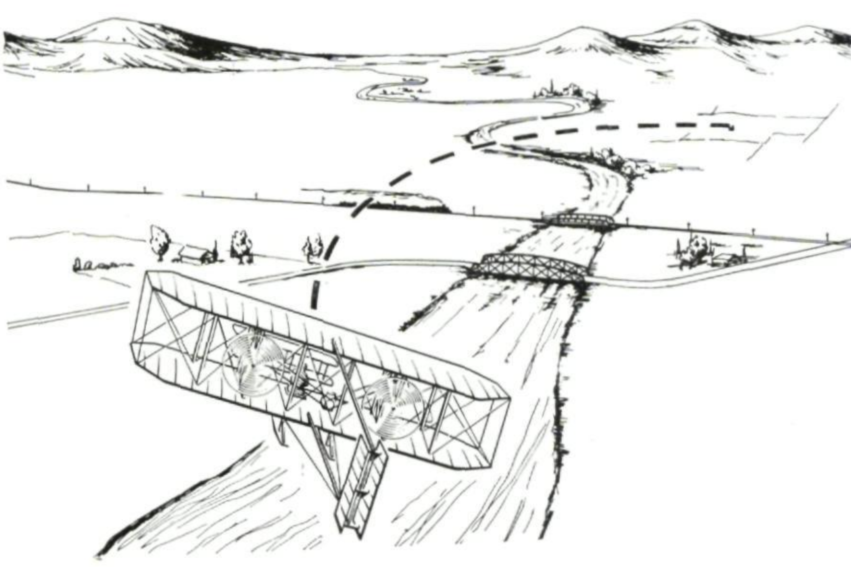

Fig. 1–14 Guidance – human operator

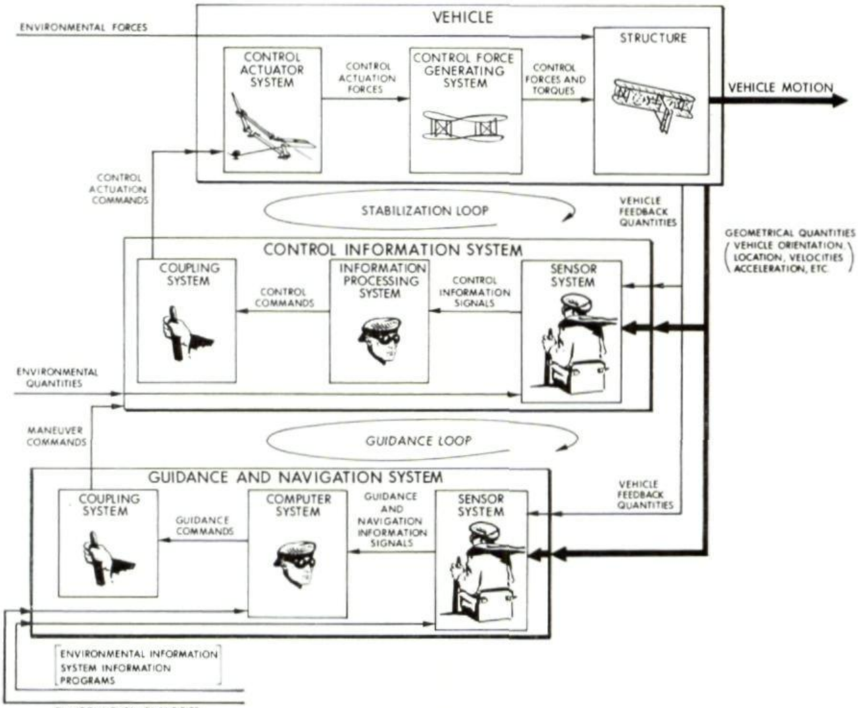

FIG. 1–15 Guidance and control system – human operator

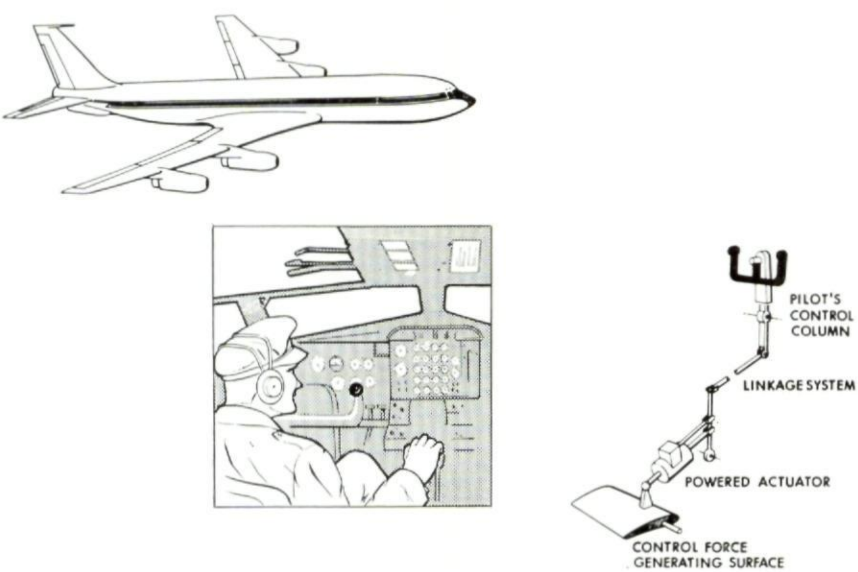

FIG. 1–16 Extension of human operator's senses and power

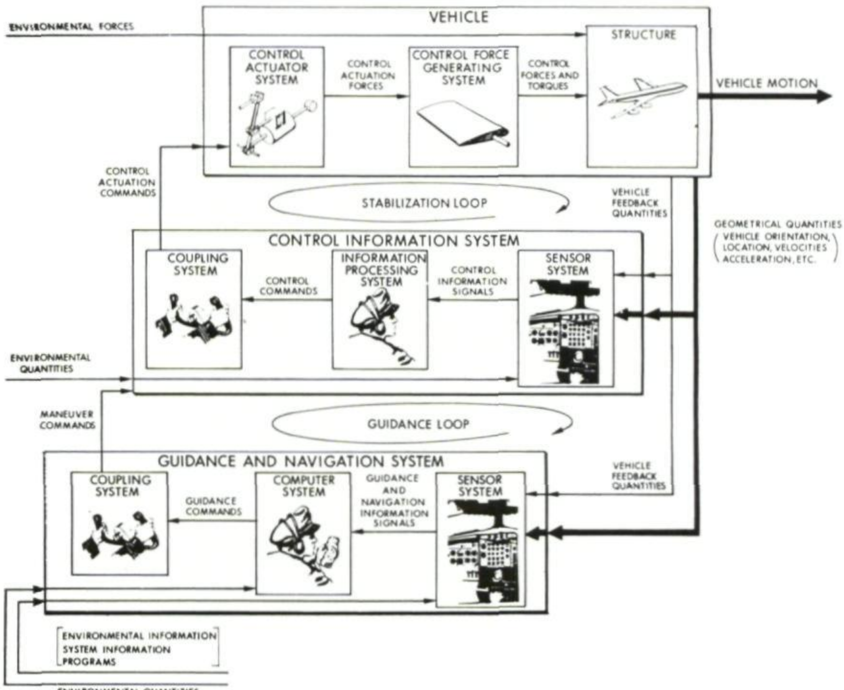

FIG. 1–17 Guidance and control system – human operator's senses and power extended

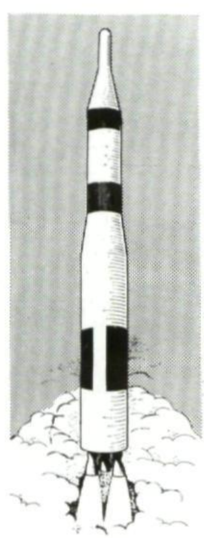

FIG. 1–18 Automatically guided flight vehicle

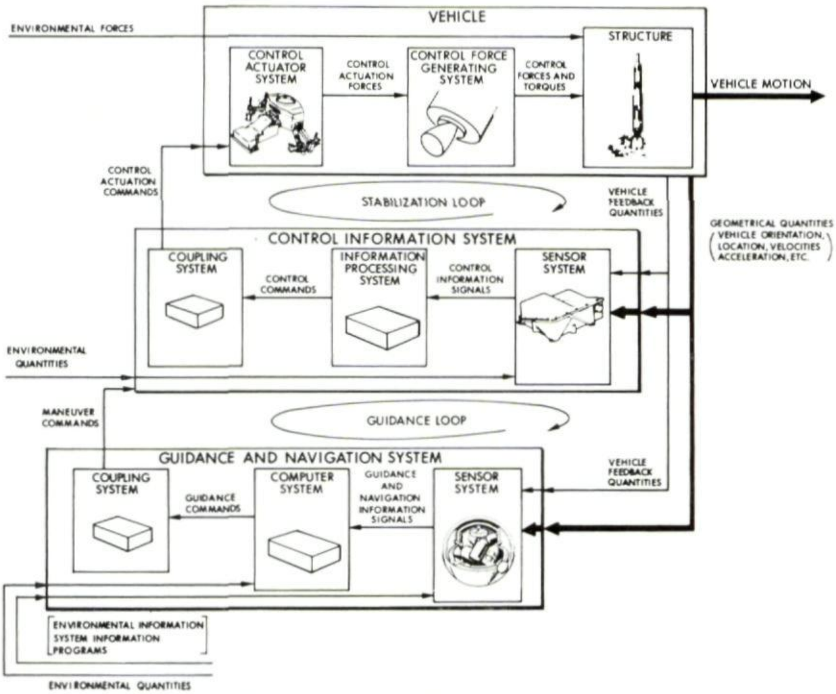

FIG. 1–19 Guidance and control system – automatic operator

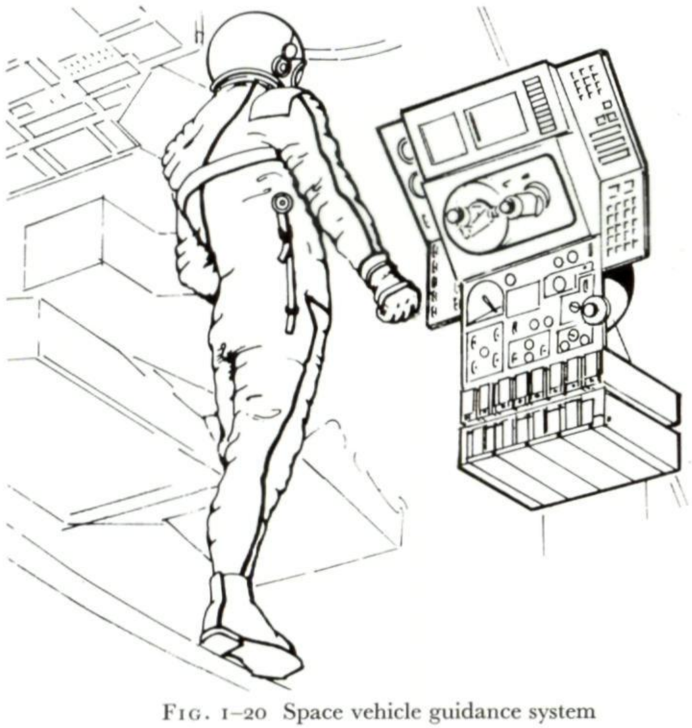

FIG. 1–20 Space vehicle guidance system

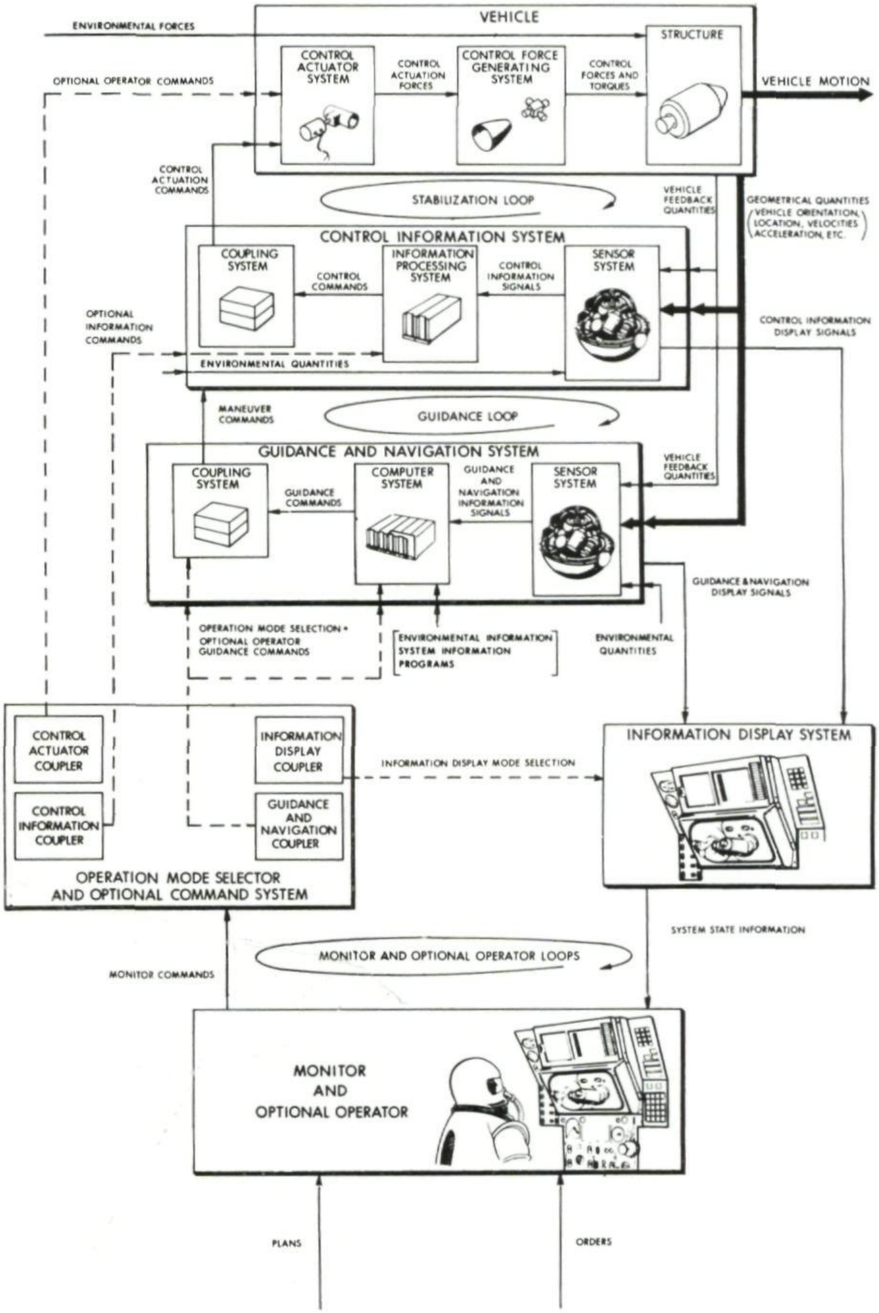

FIG. 1–21 Functional diagram of complete vehicle guidance system with optional monitor command operation

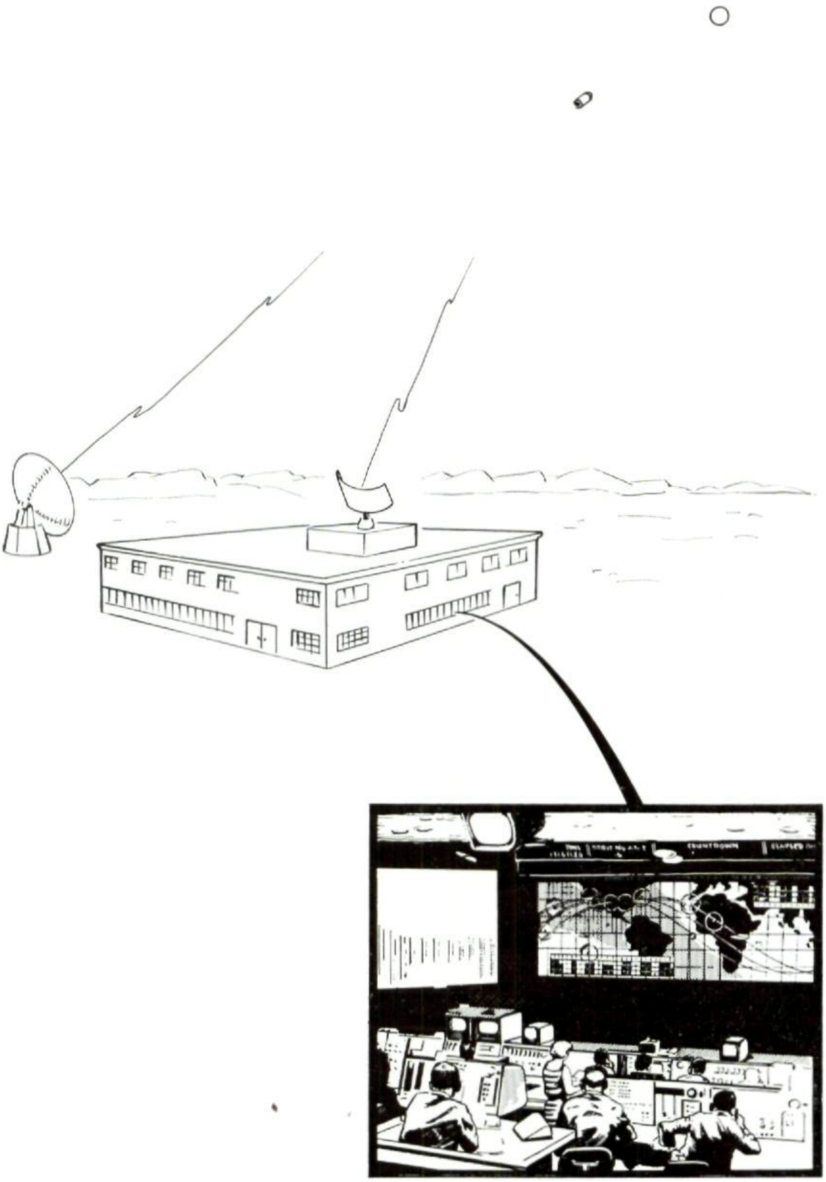

FIG. 1–22 Ground based monitor system

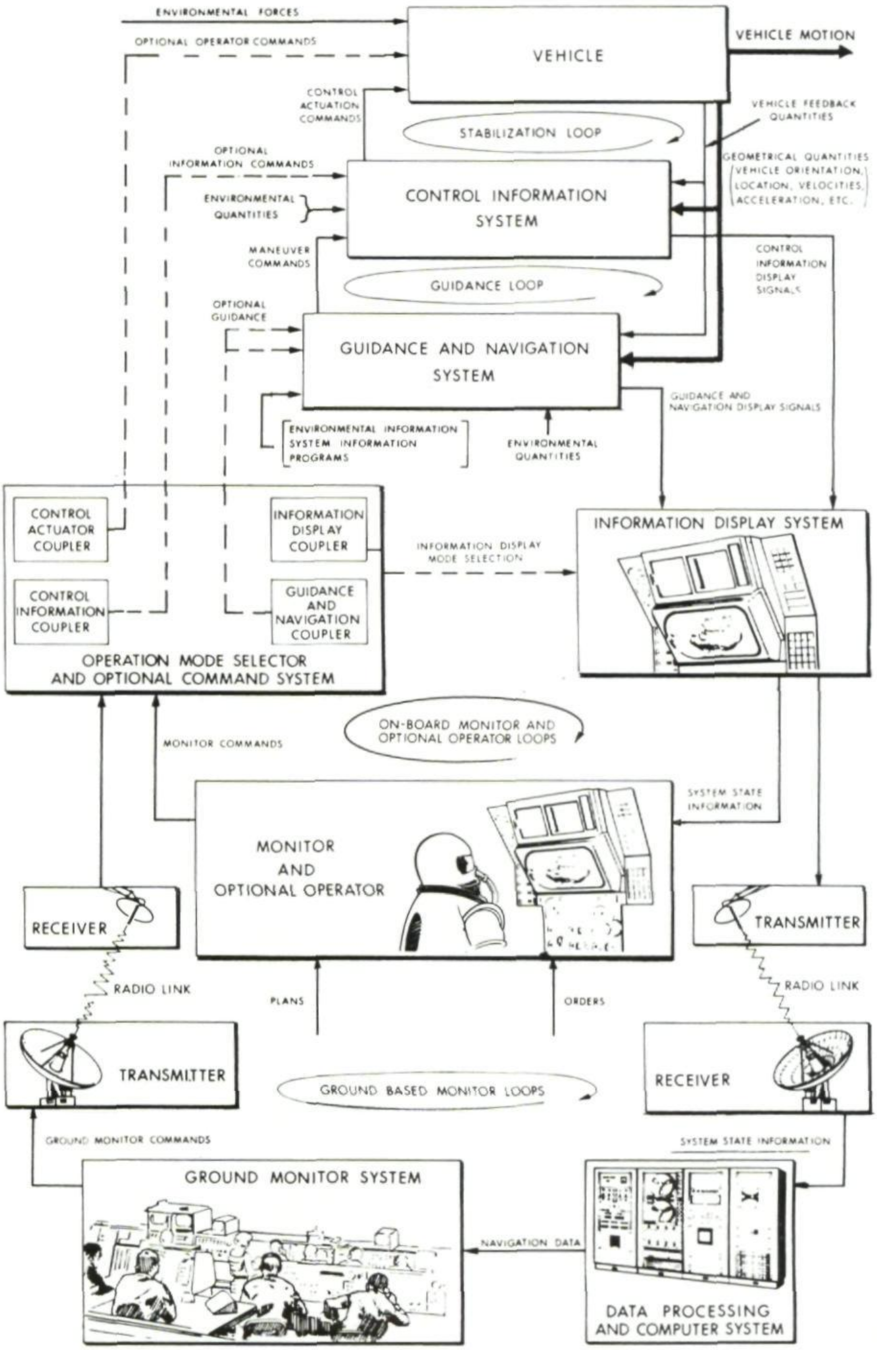

FIG. 1–23 Control and guidance system with ground based monitor

contained automatic control and guidance systems. The absence of restrictions imposed by human limitations makes it possible to realize ballistic missiles and other vehicles with capabilities well beyond those in which men provide control and guidance functions as "on-line" components.

Figures 1–20 and 1–21 illustrate the situation that exists in the control and guidance system of a manned vehicle to operate in the astronautical regions above the earth's atmosphere and beyond the earth's gravitational field. The control and guidance systems are automatic with orientational and translational references provided by an inertially stabilized member, and a set of three accelerometers rigidly mounted on this member with input axes set in an orthogonal configuration. A telescope and a space sextant with their line-of-sight directions adjustable and transferable through a computer to the inertial reference member give information for correcting reference member alignment. Observations by the human pilot or by automatic optional tracking also supply data for a computing system to calculate positions in space and to generate correction maneuver commands.

Flight condition data displayed by the automatic control and guidance system to the human pilot provide the information for monitoring system operation. A set of controls forming the operation mode selector and optional command system make it possible for the pilot to determine the mode in which the overall system works. He may select any sort of configuration from full automatic, in which he only observes operation, to completely manual, in which he acts to close servo-loops by continued on-line operation.

Figures 1–22 and 1–23 suggest the complete configuration used by Apollo in which a ground-monitoring system connected by radio, radar and possibly visual up and down links to the flight vehicle. The earth-based system acts as an information collecting and monitoring branch in parallel with the on-board pilot monitor. Information and suggestions may be sent to the space vehicle, whether or not they are accepted in any given case depends on operating doctrine and the circumstances of particular cases.

CHAPTER I–4

STATE OF TECHNOLOGY OF COMPONENTS FOR CONTROL, NAVIGATION AND GUIDANCE SYSTEMS

Radiation links which are generally employed to implement friendly environments have the function of establishing contacts from transmitters to receivers, transponders and reflecting bodies. These links provide communications by voice, by telemetry and by signals of other kinds. Pulsed and continuous wave radar indicate line-of-sight directions and distances. Lasers and ordinary searchlights also offer powerful radiation links, particularly for satellites and space vehicles. In the current state of radiation link technology which allows determination of distances within a few feet, the links themselves do not impose limiting restrictions on the performance of navigation and guidance systems as far as distance measurements are concerned. The ability of radiation links to determine line-of-sight directions with inaccuracies less than one milliradian is adequate for the needs associated with navigation and guidance.

Carefully surveyed ground station sites with commonly available indicators of the vertical provide earth reference coordinates of such high accuracy that radiation beam orientations may be taken as substantially perfect. On the other hand, radiation links established by airborne transmitters generally have adequate ability to measure distances, but have restricted ranges due to limitations on size, weight and power consumption of the geometrical stabilization member. For these reasons the accuracy of directional tracking is not so good as that obtained from ground stations. A generally more severe limitation of air-borne radiation link equipment is introduced by inaccuracies of reference coordinate equipment which will always be greater than the corresponding inaccuracies of transmitters rigidly fixed to the earth. This source of reduced performance may be serious, and, in any case, must be given careful consideration in evaluating the errors of any particular system.

Computing systems receive essential information and carry out the mathematical processes necessary to generate required outputs. The problems solved range from trigonometric transformations to the determination of position and velocity from accelerometer output signals. In terms of a rough analogy, computers perform the same functions that the brain of a pilot provides when a human being acts as the on-line date processing component in navigation and guidance equipment. The current technology of computers, particularly those based on digital operations, is so well developed that units of ample capacity, speed and reliability with reasonable sizes, weights and power consumptions are available for use in guidance systems. Improvements in all essential computer features including resistance to environmental interference effects are now in progress. It is certain that mechanization of computing functions is not now and will not in the future be a limiting factor on navigation and guidance systems.

Engineering problems associated with angle sensing servomechanisms,

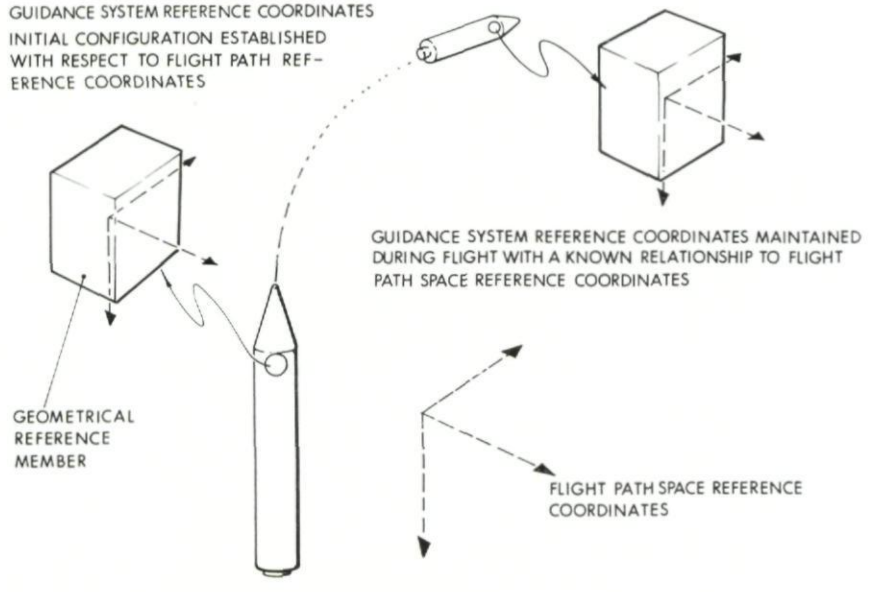

FIG. 1–24 Relationship of guidance system reference co-ordinates to flight path reference co-ordinates

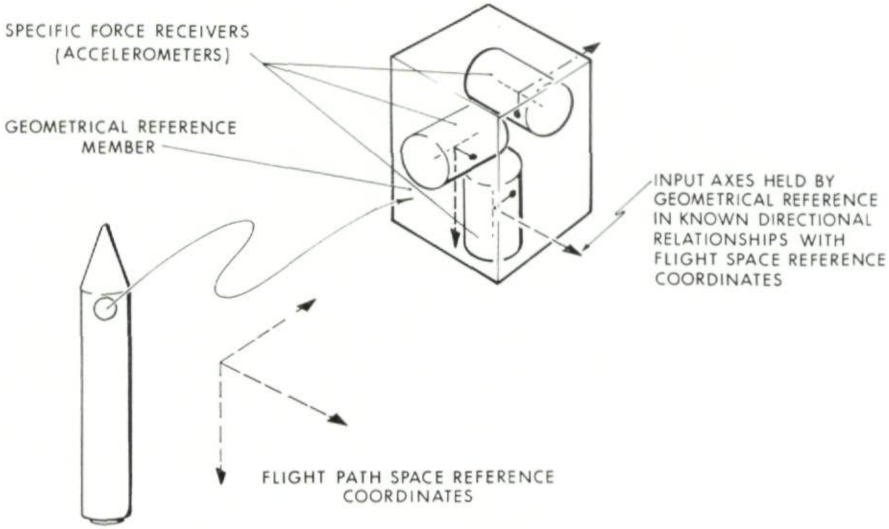

FIG. 1–25 Specific force receiver (accelerometer) system

data transmission, mechanical design, etc., have current solutions that are generally satisfactory with advances certain to appear in the near future. Except in certain special situations these factors do not limit the performance of equipment for navigation and guidance.

Guidance system coordinates related in a known way to reference directions of the space in which the desired path of the guided vehicle is defined are easily established when rigid or optical connections to the ground are available. When the guidance system is vehicle-borne its necessary reference coordinates must be established with a known relationship to external space and maintained with this relationship defined during the progress of guided flight. This situation is suggested by the diagram of Fig. 1–24 with the guidance system coordinates initially established before flight with known geometrical relationships to the flight path space reference coordinates.

For the purposes of guidance, the system coordinates must continue to provide a geometrical reference that accurately represents the flight path space as the vehicle moves to complete its mission. Because mechanical connections are impossible and radiation links between the vehicle and the flight path reference space generally absent, the only possibility for realizing satisfactory guidance system reference coordinates lies in the use of inertial principles. Properly applied, these principles make it possible to mechanize a member which either remains non-rotating with respect to inertial space, or moves in a quantitative way with respect to this space. Details of arrangements to accomplish such results are discussed in the next section of this paper.

Current technology is easily able to provide guidance system reference coordinates representing flight space coordinates within one minute of arc for each hour of operation. The arc-second accuracy required by military guidance for hard targets is more difficult to achieve, but is feasible with proper attention to design and production of components. The principles available, typical arrangements and performance realized are discussed in the next section.

Specific force receivers, the devices commonly called accelerometers, are the only available means for on-board sensing translational vehicle motion when radiation links with the environment are not available. A commonly used configuration of specific force receivers is to mount three units rigidly to the geometrical reference member with their input axes aligned with the guidance reference axes. This arrangement is suggested in the diagram of Fig. 1–25.

Signals from the three specific force receivers represent the resultant components of gravity force and inertia reaction force along each of the three axes. With the geometrical relationships of these axes to the flight space reference axes known, calculations based on these signals make it possible for the computer to generate output signals giving the changes in vehicle location and velocity occurring after the start of system operation. Assuming perfect alignment of the guidance system reference coordinates with the flight-space reference coordinates and perfect computer operation, errors in indicated location and motion are due to imperfections in specific force receiver performance. Performance matching the requirements of navigation is easy to realize, while military guidance for hard point targets is within the capabilities of today's advanced technology. The mechanizations that afford these results are described in a later section.

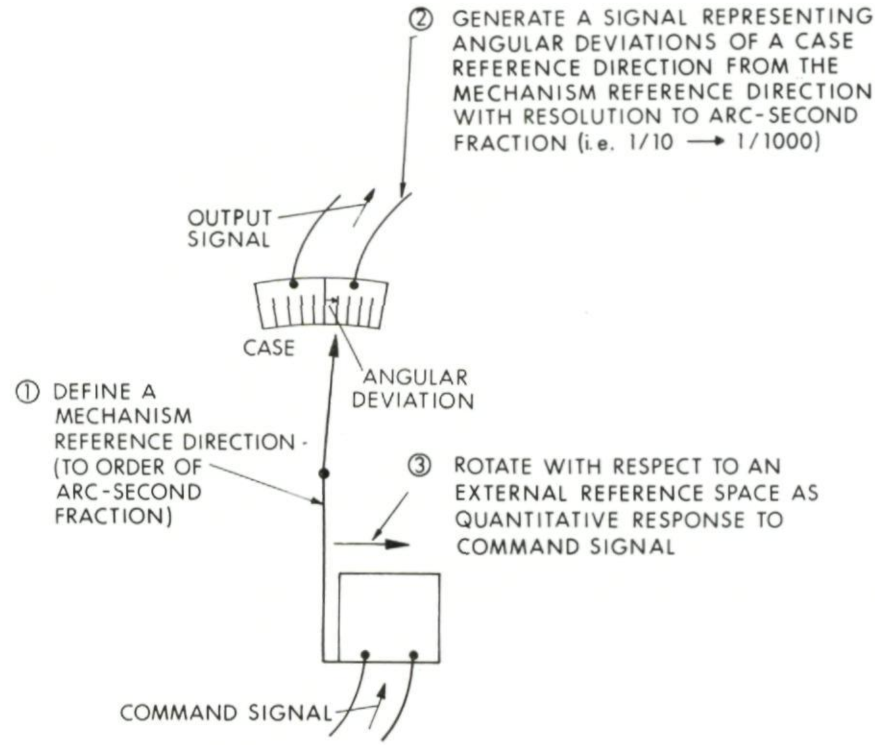

④ RELIABLE CONTINUOUS OPERATION FOR INDEFINITE PERIOD (SEVERAL YEARS AT LEAST)

⑤ REASONABLE POWER CONSUMPTION

⑥ REASONABLE SIZE AND WEIGHT

⑦ REASONABLE COST

FIG. 1–26 General requirements for instrumental components to mechanize guidance system reference directions

CHAPTER 1–5

GYROSCOPIC UNITS FOR REALIZATION OF GUIDANCE SYSTEM REFERENCE COORDINATES

Reference coordinates for vehicle-borne guidance systems with satisfactory performance must fulfill the general requirements summarized in Fig. 1–26. The basic functions are: (1) to provide continuously available mechanism reference directions; (2) to provide accurate control of the reference directions with respect to a selected external reference space in response to command signals; (3) to provide angular output signals that accurately represent deviations of case fixed reference directions from the mechanism reference directions. In addition to these essential performance characteristics, practical instruments must be reliable, of reasonable size and weight, and be available at acceptable cost.

Gyroscopic principles may be applied to mechanize practical instruments for providing guidance system reference directions. The theory involved is associated with applications of the Newtonian Laws of Mechanics to rapidly spinning symmetrical rotors. It is relatively simple to discuss this theory in terms of vectors representing rotational quantities in accordance with the commonly used "right hand" conventions that are summarized in Fig. 1–27. The central idea is that a rotational quantity such as angular velocity or angular momentum may be described by a vector along the axis of rotation with its length proportional to the magnitude of the quantity, and the head of its arrow related to the direction of rotation by the "right-hand screw rule".

Figure 1–28 suggests the basic operating principle of a gyroscopic element. When the gyroscopic element definition condition of constant spin velocity exists Newton's Law of dynamics leads to the conclusion that a torque applied to the rotor at right angles to the spin axis causes the angular momentum vector to change its orientation with respect to inertial space with an angular velocity of precession proportional to the magnitude of the torque and having a sense that always turns the angular momentum vector toward the torque vector.

One way of using the gyroscopic element to realize mechanism reference directions for guidance system purposes is to set up an angular momentum vector and then carefully to reduce all torque components on the rotor to zero about any axis at right angles to the spin axis. In this torque-less condition the angular momentum vector maintains an orientation with respect to inertial space that is completely determined by the direction about which the spinning torque originally built up the angular momentum of the rotor. Once the spin angular momentum vector direction is established it becomes useful for reference purposes only through the medium of signals that represent angles between the spin axis and reference directions fixed to the case within which the rotor spins. Figure 1–29 suggests the situation that exists

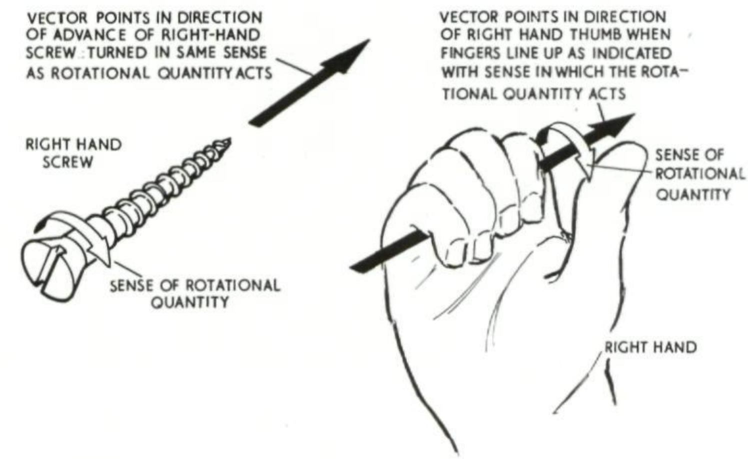

(a) Right hand rules for the relationships between a rotational quantity and the vector representing the quantity

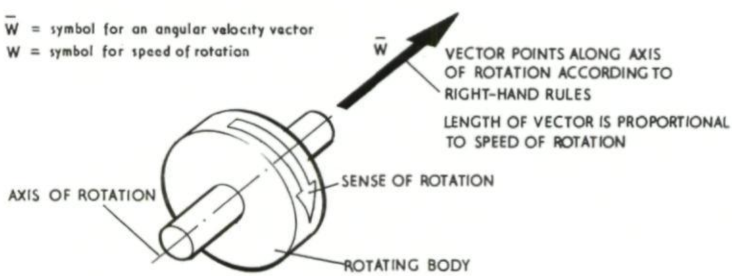

(b) Vector representation of angular velocity

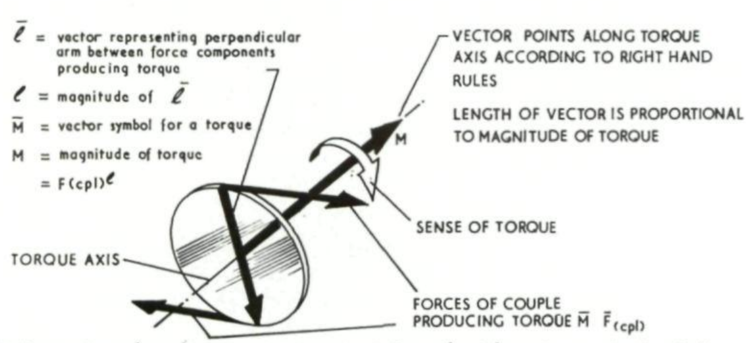

For this diagram, the term 'torque' has a meaning identical with the word 'couple' as used in conventional mechanics.

(c) Vector representation of a torque

FIG. 1–27a Vector conventions for rotational quantities

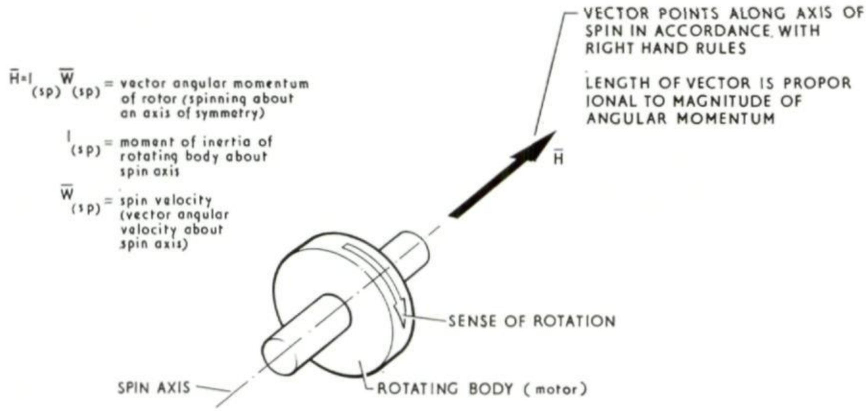

(d) Vector representation for the angular momentum of a spinning rotor

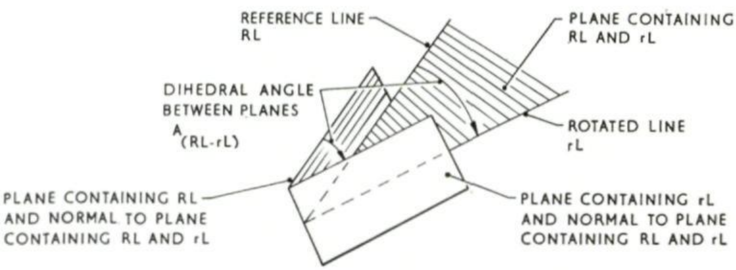

(e) Angle represented on a dihedral angle between planes

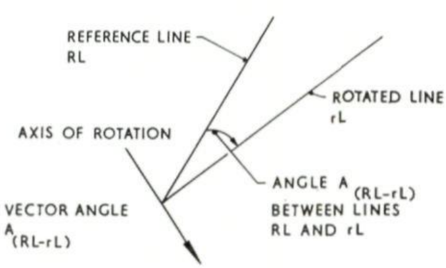

(f) Angle represented on a rotational vector

FIG. 1–27b Vector conventions for rotational quantities

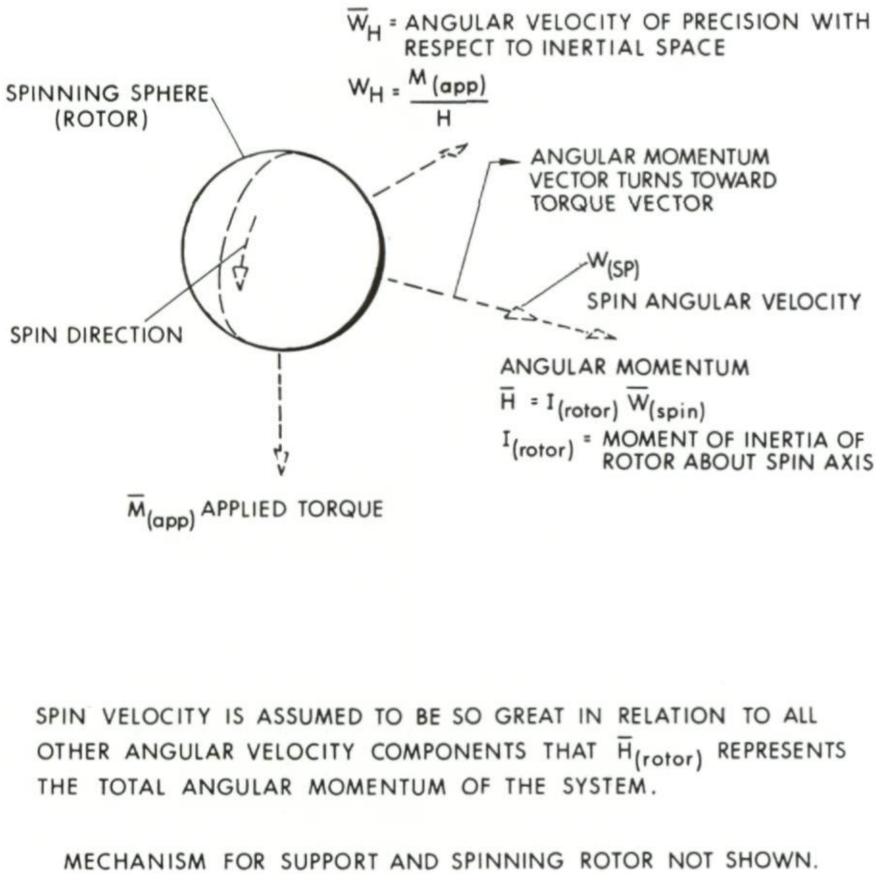

FIG. 1–28 Basic operating principles of the gyroscopic element

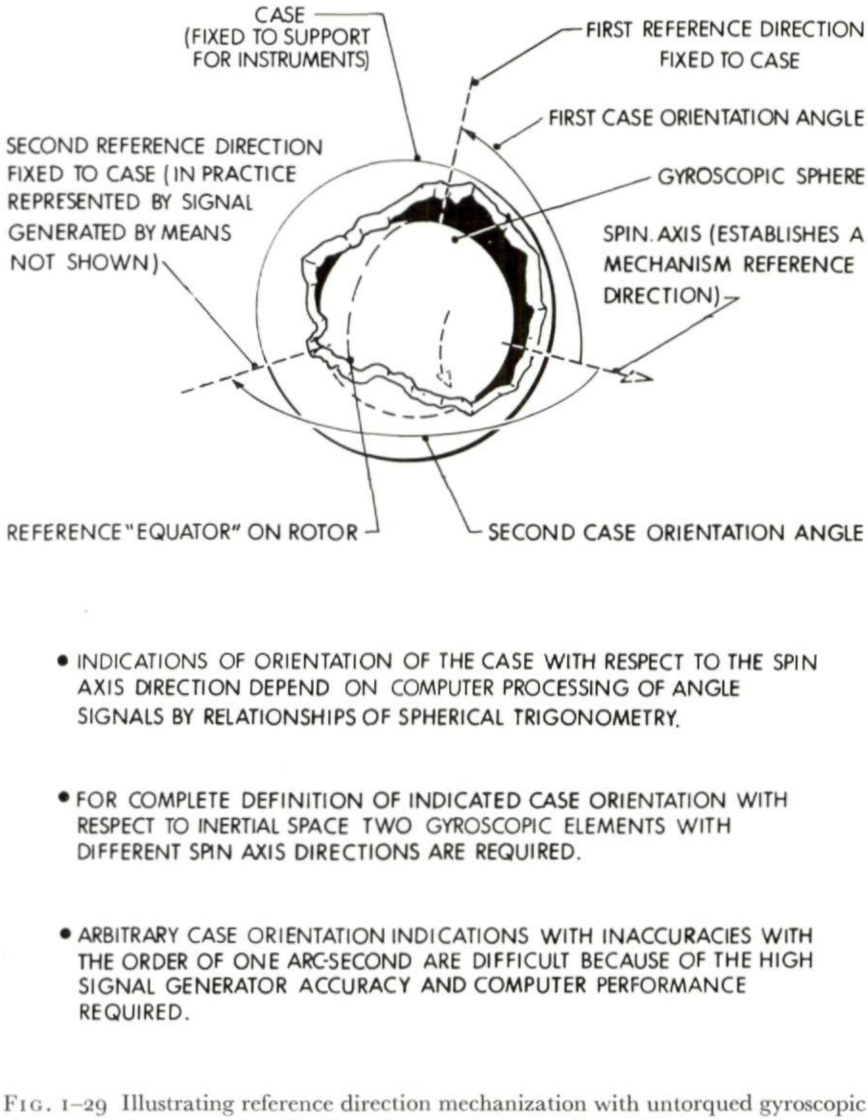

FIG. 1–29 Illustrating reference direction mechanization with untorqued gyroscopic elements and computed indication of case orientation from direct rotor-case angle signals

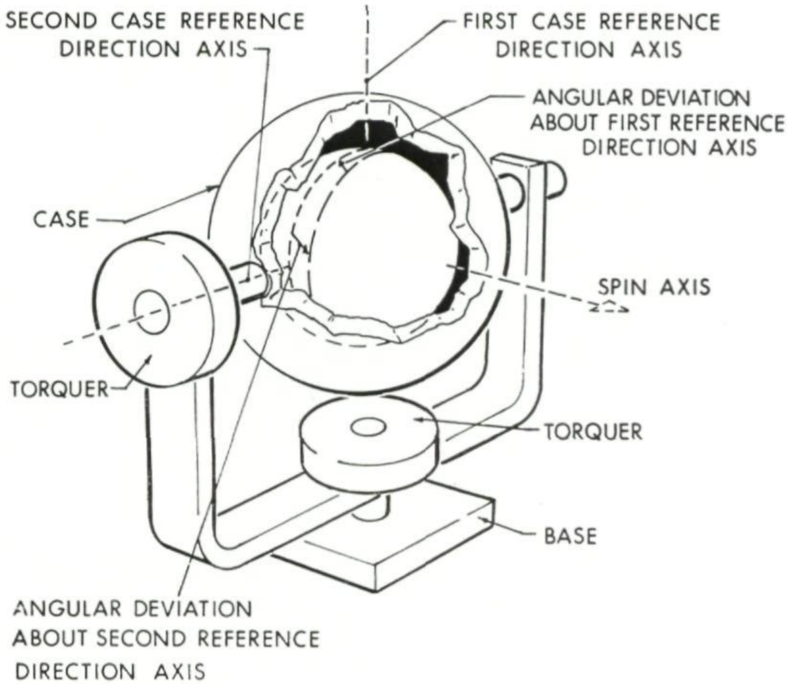

READOUT OF ANGLES

ANGULAR DEVIATIONS ABOUT THE CASE REFERENCE DIRECTION AXES (IN THE PLANE OF THE ROTOR SPIN EQUATOR WHEN THE ANGULAR DEVIATIONS ARE ZERO) ARE RECEIVED BY SIGNAL GENERATORS GIVING OUTPUTS PROPORTIONAL TO DEVIATIONS OF THE REFERENCE DIRECTIONS FROM PERPENDICULARITY TO THE SPIN AXIS.

THESE SIGNALS APPLIED AS SERVO-DRIVE INPUTS TO GIMBAL TORQUERS ACT TO KEEP THE CASE AS A CONTROLLED MEMBER IN ALIGNMENT WITH THE SPIN AXIS.

ANY SATISFACTORY SERVO-SYSTEM MAINTAINS THE ANGULAR DEVIATIONS SMALL - ONE SEC. OF ARC REPRESENTS REASONABLE PERFORMANCE.

FIG. 1–30 Illustration of two-axis mechanism reference system based on servo-driven gimbals and the untorqued gyroscopic element

when a case is rigidly fixed to some base that may have any arbitrary changes in orientation with respect to inertial space. The position of the case with respect to the reference direction can be indicated in terms of the two angles between perpendicular lines fixed to the case and the spin axis. Signals representing these two angles may be processed by a computer to give information about the position of the case with respect to the spin axis in terms suitable for any particular problem of control and guidance.

The situation that is generally of practical interest requires information on the orientation of the case with respect to some specified external reference space. It is obvious that any single direction such as a spin axis cannot specify angular positions of the case about the spin direction, so that a second gyroscope element with its spin axis having some projection at right angles to the first spin axis is required for any complete indication of case orientation in three dimensional space. When two spin axis directions are available for mechanism reference purposes, the common position of two gyro unit cases rigidly connected together gives all the needed information. It is to be noted that the interpretation of this information depends on the continuous operation of a computer to carry out complex trigonometrical calculations. The relationships of spherical trigonometry are such that computations generally give results of varying accuracy as case orientations change by large angles with respect to spin axis directions. This fact, coupled with difficulties of achieving satisfactory signals from large components of case-to-gyro rotor angles in the fractional arc-second region means that the "large deviation angle" configuration illustrated in Fig. 1–29 is not suitable for the mechanism reference coordinate indications of high performance guidance systems.

Problems of mechanism reference coordinates associated with sensing and transformation of large angles are usually eliminated, so far as gyro units themselves are concerned, by mounting the unit cases on a member having three degrees of angular freedom with respect to the base by which it is carried, and providing power drives of some kind to overcome inaccuracy-producing torques due to inertia and friction. Figure 1–30 suggests the essential features of such an arrangement for two degrees of freedom with angular deviation signals between the case and the spin axis direction used to energize gimbal torquer drives through the operation of electrical servo-systems not shown in the diagram. With proper servo designs, the case-to-spin axis angular deviations may be maintained small; in practice to the order of one arc-second by using good angle sensors and tight servo-loops. Because only small angles are involved and accurately matched sensitivities are unimportant, difficulties associated with accurate signals are greatly reduced from those involved in collecting data on large angles. Combinations of the signals from two perpendicular case directions in a plane at right angles to the spin axis are required to command proper responses from the two torquers. Relatively low performance resolvers on the gimbal axes are sufficient to serve the needs of servo loop control. It is unnecessary to include a separate trigonometric computer in the system.

The diagram of Fig. 1–30 illustrates a single rotor arrangement providing two-degree-of-freedom isolation of a controlled member (the case) from base motion. Any complete system requires three-degree-of-freedom angular isolation. In practice this situation is very often met by an arrangement like

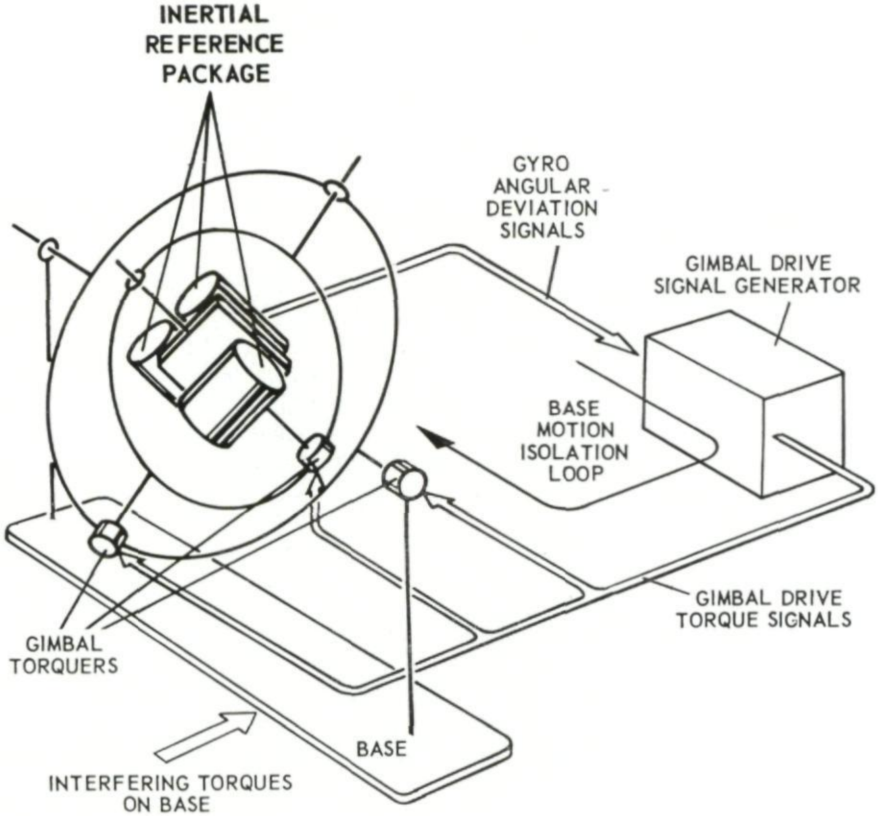

FIG. 1–31 Illustration of arrangement of three-degree-of-freedom servo-driven gimbals to isolate mechanism reference members from base motion

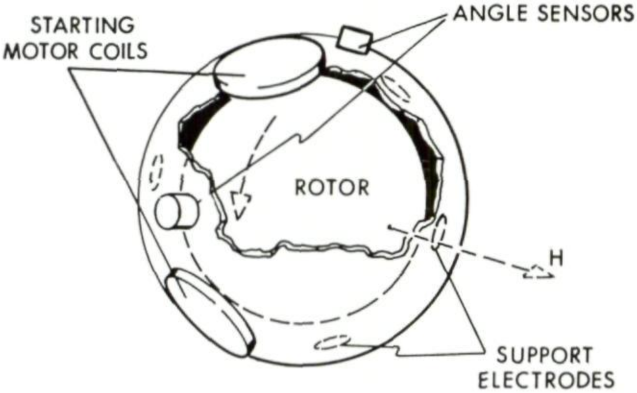

FEATURES

- INITIAL SPIN TORQUE ONLY (ROTOR COASTS DURING OPERATION)
- ONE MOVING PART
- FIELD PROVIDES BEARING FOR SPINNING MEMBER
- FIELD SUPPORT ALSO PROVIDES TWO DEGREES OF FREEDOM FOR ANGULAR MOMENTUM VECTOR
- ANGLE SIGNAL GENERATOR RECEIVES COMPONENTS OF SINGLE ANGLE
- SENSITIVE TO ANGULAR MOTION ABOUT ALL AXES AT RIGHT ANGLE TO SPIN AXIS
- ADAPTED TO TORQUE-FREE OPERATION ONLY

FIG. 1–32 Basic features of the non-viscous field (electromagnetic, electrostatic) supported two-degree-of-freedom gyro unit

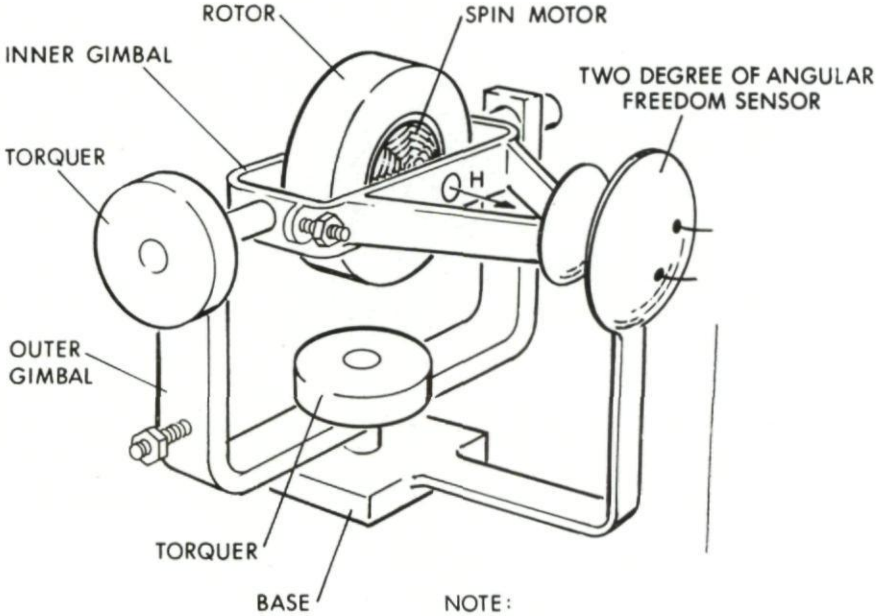

NOTE:
ROTOR AND ITS BEARINGS MAY BE ENCLOSED IN A HERMETICALLY SEALED CAN AND SUBSTANTIALLY SUPPORTED BY FLOTATION IN A FLUID CONTAINED WITHIN AN OUTER CASE

FEATURES

- SPIN MOTOR SUSTAINS ROTOR SPEED CONSTANT INDEFINITELY
- SPIN BEARINGS LIMIT ROTOR TO ROTATION ABOUT SPIN AXIS FIXED TO INNER GIMBAL
- TWO DEGREES OF ANGULAR FREEDOM FOR ANGULAR MOMENTUM VECTOR PROVIDED BY GIMBALS
- ANGLE DEVIATION SIGNALS REPRESENT COMPONENTS OF SINGLE ANGLE
- SENSITIVE TO ANGULAR MOTION ABOUT ALL AXES AT RIGHT ANGLES TO SPIN AXIS
- TORQUERS ON GIMBALS MAKE IT POSSIBLE TO CHANGE ORIENTATION OF SPIN AXIS AS A QUANTITATIVELY ACCURATE RESPONSE TO COMMAND SIGNALS

FIG. 1–33 Basic features of the gimbal supported two-degree-of-freedom gyro units

that suggested in the diagram of Fig. 1–31. In this figure, three gyro units, each with one degree of freedom, are shown on the inertial reference package instead of the two that would be needed if gyro elements like that of Fig. 1–30 were used. For the situation illustrated, the nature of the gyro units is immaterial so long as they provide the function of sensing and representing angular deviations in terms of usable signals. Gyro units of many types have been conceived and a few have been reduced to successful practice. Strong discussions of relative merit for various mechanizations continue and are not likely to be settled until working equipment is tested under operational conditions. However, an understanding of the patterns in which fundamental principles may be applied is surely helpful for effective evaluations of performance data from test results. The discussion that follows is intended to help with this understanding by describing the features and problems associated with typical classes of gyro units.

All gyro units are designed around a relatively strong component of angular momentum with its direction rigidly fixed to some member which has freedom to move within the instrument case. For the instruments that have proved to be successful in the present state of technology, this angular momentum is generated by a spinning rotor of some kind. Figure 1–32 illustrates the simplest arrangement in which a single moving part, a rotor having a generally spherical form, is supported on forces generated by electromagnetic or electrostatic fields so configured that the resultant damping forces acting on the rotor are very low. This characteristic makes it possible for a rotor forced into rotation by eddy-current motor action to continue coasting with a high velocity spin for considerable periods of time such as days, weeks or months after the driving torque has been removed. When the spherical rotor runs within a spherical case in the arrangement suggested by Fig. 1–32, the frictionless support not only provides a spin bearing but also allows for complete angular freedom of the case with respect to the spin axis. Sensors for angles between references fixed to the case and the spin axis supply signals that yield orientational reference information after processing by a computer.

The inviscid field supported rotor gyro unit is attractive because of its simplicity, but start-up of spin is an awkward process requiring considerable time with the spin direction determined by the orientation of the case during the time the spin torque is acting. Nutation, i.e. an oscillatory change in direction of the angular momentum vector, is generated during the starting operation and must be damped out. The inviscid field supported rotor arrangement does not lend itself to the controlled application of torque components for adjusting the direction of the angular momentum vector, a circumstance which makes it practically impossible to align the spin axis direction directly and accurately with external reference case coordinates. This means that auxiliary means to provide special positioning of the case with respect to external coordinates must be used. The required equipment tends to be cumbersome and difficult to use. This circumstance makes it unlikely that inviscid field supported sphere gyro units will be as satisfactory for the purposes of high performance guidance systems as other units that allow self-alignment of the system in which they operate.

Gyro units with inviscid field supported spherical rotors also present

certain other difficulties. These problems stem from the inaccessibility of spinning rotors for balancing and other adjustments while the complete gyro unit is in operation with all the environmental conditions adjusted to those of operational use. Another matter of basic importance that remains to be resolved is that of the effects of vibration and acceleration on a gyroscopic system with zero damping. It is certainly very desirable to measure environmental effects and to determine overall system performance as soon as possible. Because gyro rotor behavior cannot be refined by mass changes made directly on spinning spheres, it is not possible to refine gyro performance by adjustments. In practice the operation of each individual sphere must be calibrated in combination with a computing system to determine performance coefficients that can be applied during operation to reduce imperfections in behaviour by calculation rather than through adjustment or compensation of the mechanism.

Practical problems of design, engineering, production and operation for gyro units may be simplified by separating the various functions that must be provided within a gyro unit in ways that allow each aspect of performance to be given individual adjustments and compensation with a minimum of coupling effects that lead to inaccuracies in operation. Figure 1–33 suggests the basic features of the typical two-degree-of-freedom gyro unit with:

(a) Angular momentum provided by the rotation of a spinning wheel-like rotor, carried by an inner gimbal through shaft and journal bearings that may be ball, roller or hydro-dynamic with gaseous or fluid lubricant.

(b) Spin angular velocity sustained (no coasting in operation) with constant speed by a continuously acting motor.

(c) Two degrees of angular freedom with respect to the case provided by gimbals (fluid, ball or roller supported).

(d) Generation of angular deviation signals restricted to small magnitudes, by reception of spherical displacements of the case with respect to the spin axis.

(e) Accurate changes in angular momentum orientation with respect to inertial space by direct response to command input for gimbal torquers.

(f) Balance adjustments available during unit operation by means of threaded nuts on the two gimbals. These adjustments make it possible to approach the ideal condition of gyro unit insensitivity to gravity and acceleration by adjusting the center of mass so that it approaches coincidence with the point of support provided by the gimbals.

In some designs this mechanical support may be supplemented by flotation forces provided by liquid within the clearance between hermetically sealed thin shell gimbals.

When its base is mounted on a structure which rotates with respect to inertial space the two-degree-of-freedom gyro unit gives output signals which represent spin axis angular deviations about axes perpendicular to the spin axis, from a reference position of the case. This reference position is determined by the orientation of the case in which the angle output signal has its null level. Command signals to the torquers make it possible to change the reference orientation as desired without any need for taking base orientation

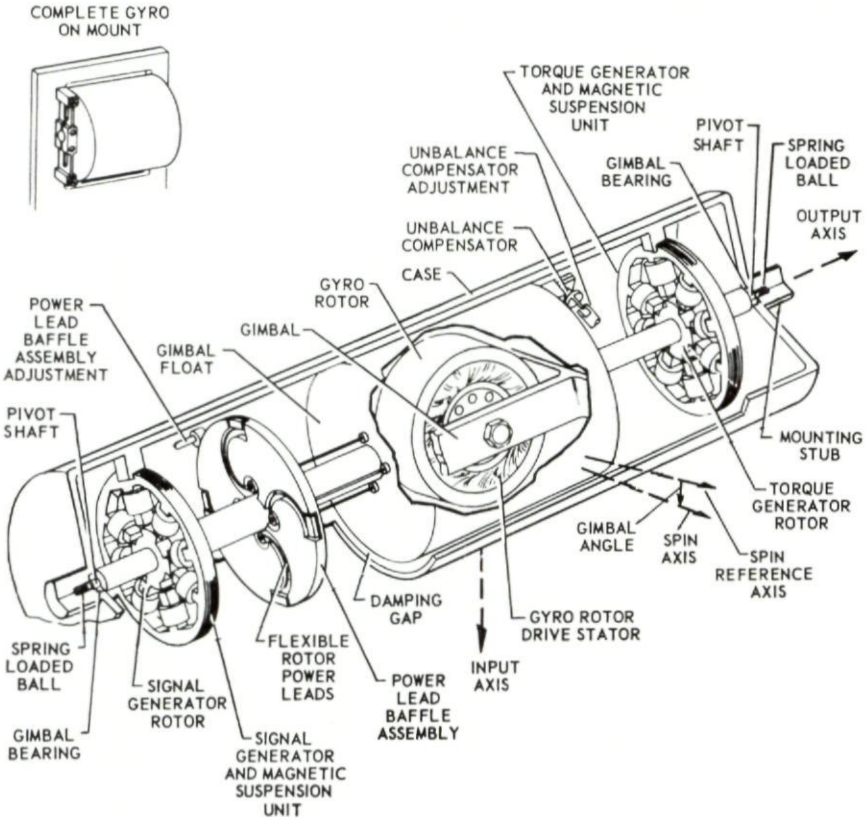

FIG. 1–34 Basic features of single-degree-of-freedom floated integrating gyro unit

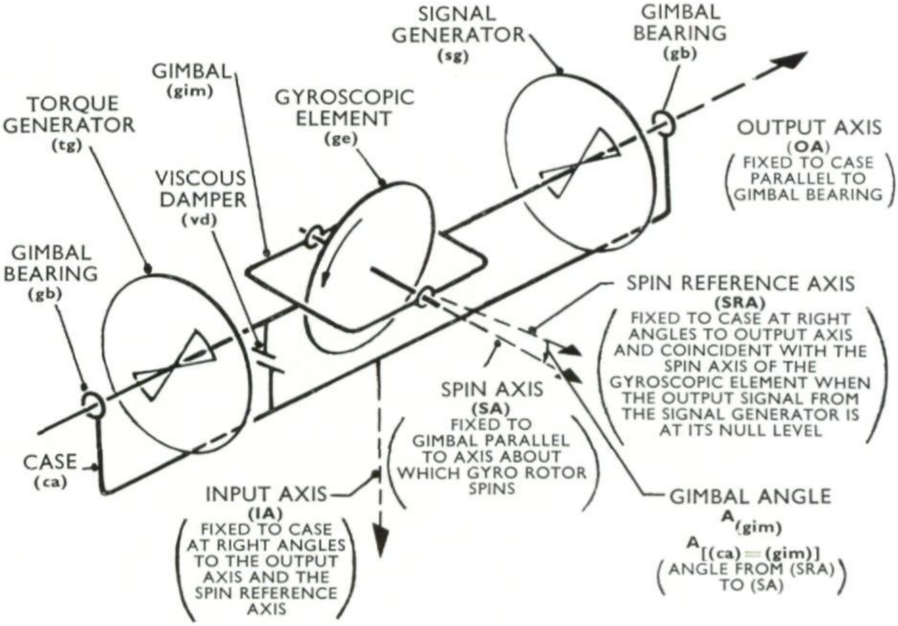

NOTES:

1. POSITIVE SENSES SHOWN BY THE ARROWS ARE CHOSEN SO THAT **(IA)**, **(SRA)**, AND **(OA)** FORM A RIGHT-HANDED SYSTEM.
2. THE GYRO UNIT TEMPERATURE CONTROL POWER IS SUPPLIED TO A MOUNTING BLOCK ADAPTED TO RECEIVE THE GYRO UNIT CASE. THE FLOW OF POWER IS CONTROLLED BY THE DAMPER TEMPERATURE SETTING.
3. THE SYMBOL $\mathbf{A}_{[(ref)-(cmprd)]}$ REPRESENTS THE ANGLE A MEASURED FROM THE REFERENCE DIRECTION ((**ref**) IN THE SUBSCRIPT) TO THE COMPARED DIRECTION ((cmpd) IN THE SUBSCRIPT).

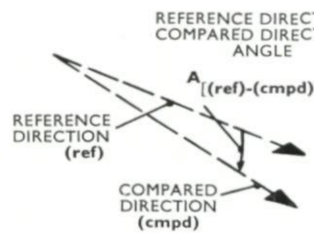

(ca)—THE STRUCTURE THAT GIVES SUPPORT FOR THE INTERNALWORKING PARTS OF THE GYRO UNIT, ENCLOSES THE PARTS, AND CARRIES PROVISIONS FOR EXTERNAL CONNECTIONS OF ALL KINDS.

(tg)—COMPONENT FOR RECEIVING INPUT SIGNALS AND PRODUCING CORRESPONDING OUTPUT TORQUE APPLIED TO THE GIMBAL ABOUT THE OUTPUT AXIS.

(dmp)—SUBSYSTEM RECEIVING ANGULAR VELOCITY OF THE GIMBAL WITH RESPECT TO THE CASE AS ITS INPUT AND PRODUCING AS OUTPUT A RETARDING TORQUE ACTING ON THE GIMBAL ABOUT THE OUTPUT AXIS WITH A MAGNITUDE PROPORTIONAL TO THE MAGNITUDE OF THE ANGULAR VELOCITY OF THE GIMBAL WITH RESPECT TO THE CASE.

—**(gu)**—THIS ENTITY MADE UP OF THE COMPONENTS REPRESENTED IN THIS DIAGRAM AND ALL THE ADDITIONAL PARTS NECESSARY FOR A SINGLE PACKAGE TO CARRY OUT THE FUNCTIONS OF A GYRO UNIT.

—**(sg)**—COMPONENT FOR RECEIVING THE ANGLE OF THE SPIN AXIS WITH RESPECT TO THE CASE AS INPUT AND PRODUCING A CORRESPONDING SIGNAL THAT SERVES AS THE OUTPUT SIGNAL FROM THE GYRO UNIT.

(gim)—STRUCTURE CARRYING THE BEARINGS FOR THE SPINNING ROTOR OF THE GYROSCOPIC ELEMENT, ROTORS FOR THE TORQUE GENERATOR AND SIGNAL GENERATOR, PART OF THE DAMPER, FLOAT SEALS AND STRUCTURE, BALANCE ADJUSTMENTS, STOPS, PIVOTS, ETC.

FIG. 1–35 Line schematic diagram for the single-degree-of-freedom floated Integrating Gyro Unit

into account. This possibility of directly relating gyro unit angular momentum to an external space reference direction gives the torqued two-degree-of-freedom gimbal supported gyro unit a considerable advantage over inviscid field supported spherical rotor units.

The gimbal supported two-degree-of-freedom gyro unit overcomes some of the difficulties stemming from the multiple function characteristics of inviscid field spherical rotor supports. Adjustments can be made during operation by gimbal balancing adjustments, indefinite operating periods are achieved, accurate control of angular momentum directions is made possible and various other results of practical importance are attained. However, the difficulties associated with accurately maintaining coincidence between the point of support provided by two coincident gimbals and the center of mass of an articulated structure limit the quality of performance available from the two-degree-of-freedom gyro unit and considerably increase the difficulty of manufacture for units of even medium performance levels. The output of deviations in terms of a conical angle subject to the coupling effects that tend to accompany the precession and nutation of a two-degree-of-freedom gyro rotor is also troublesome when accuracies in the region of fractional arc-seconds are desired.

Some difficulties of two-degree-of-freedom units are reduced when the mechanical gimbal system is replaced by a spherical gas bearing arrangement which allows both rotor spin action and angular freedom between the spin reference direction and the case. Balancing problems still exist and the gas bearing is always subject to sharply defined upper limits of resistance to shock and vibration, but many practical gyro units using this mechanization are in operational use. All two-degree-of-freedom gyro units are essentially untorqued for the purposes of sensing angular deviations. This means that the obtainable resolution in terms of angular velocity components about axes of sensitivity for the unit depends on the angle defined by the minimum usable output from the signal generator. This generally corresponds to angles so large that detection of small components of earth's rate (in the region of one arc-second per hour) is generally not practical.

Single-degree-of-freedom gyro units with the basic features illustrated in Figs. 1–34 and 1–35 make it possible to realize practical gyro units with the characteristics required of angular deviation sensing instruments for guidance systems able to reliably provide the low CEP range needed for hard point military targets. The design philosophy involved is the direct antithesis of the single moving part philosophy of the inviscid field supported sphere gyro unit in which refining adjustments to the rotor are impossible during operation and accurate direct alignment of angular momentum axis to external reference space is not available. In the floated integrating single-degree-of-freedom gyro unit each function is carefully separated from others and with the exception of dynamic balancing for the rotor, may be refined toward ultimate performance with the complete gyro unit in normal operation.

As suggested by Figs. 1–34 and 1–35 angular momentum is provided by a rotor with its spin sustained indefinitely by a driving motor. The spin axis bearings which support the rotor from the single gimbal may be either ball bearing or hydrodynamic journal bearings lubricated by air. With good design and manufacture both types have demonstrated high performance

and lifetimes of many thousands of hours. Gas bearings consume somewhat more power at starting and in operation than ball bearings. Gas bearings are much more liable to damage than balls when subjected to torques before their full supporting power has been developed during start-up, and they are also more vulnerable to catastrophic failure under either steady or vibratory high accelerations. It appears that gas bearings are suitable for environments of limited severity, while ball bearings are adaptable to wider ranges of environmental conditions. Both types are now in use and can be applied in single-degree-of-freedom gyro units at the preference of the designer.

Single-degree-of-freedom motion is provided by a chamber enclosing the gyro rotor, which is largely supported on the flotation pressure gradients built up by gravitational and inertia reaction forces in a dense, highly viscous fluid contained in the clearance volume between the float and the hermetically sealed case. In operation, the temperatures of the solid parts and the fluid are closely controlled, so that the buoyancy support remains substantially constant. The small remaining imperfection in flotation is effectively reduced to zero by single axis magnetic support units at either end of the float, which is thus suspended within the case without even the slightest rubbing contact between solid parts.

Complementing the buoyancy and magnetic supporting forces are forces generated by hydrodynamic forces and torques generated when the heavy fluid is forced to flow between parts of the clearance space. The resultant support minimizes distorting stress on the gimbal because of the distributed nature of the loads. The overall result is a system effectively immune to the mechanical effects of acceleration, vibration and shock within selected design ranges.

The use of high viscosity fluids for gimbal support means that high level drag forces are developed by motion of the float within the case. The forces not only provide support during dynamic conditions but also develop a drag torque about the gimbal freedom axis of the float. This torque is proportional to the angular velocity of the float with respect to the case about this axis, which is carefully made at right angles to the spin axis of the gyro rotor. Under gyroscopic principles a rotation of the angular momentum vector about the input axis which is at right angles to the gimbal axis and also the spin axis, causes the gyro rotor to exert a torque on the gimbal about its axis of freedom which, for this reason, is called the output axis. This torque is absorbed by the accelerational inertia reaction of the float and by viscous drag in the fluid. The inertia reaction torque causes the gyro unit to exhibit a time constant with the order of one thousandth second, while the viscous drag torque causes the float angular velocity within the case to be proportional to the case angular velocity with respect to inertial space about the input axis. The result is that the float output angle with respect to the case is proportional to the angle turned through by the case with respect to inertial space about the input axis. This action leads the name "integrating gyro unit" for instruments with the features of Fig. 1–34.

Because of the absence of rubbing friction between solid parts and the utilization of viscous drag as a primary factor in operation, the proportionality between input angle and float output angle is effectively perfect over the

operating range of a few minutes of arc down to a lower limit that is surely less than one thousandth of an arc-second.

In operation, the single-degree-of-freedom integrating gyro unit is suitable for use only under circumstances in which gimbal deflection angles are limited to a few seconds of arc. This condition is favorable for signal generator designs which can be constructed to give very low null signals and high sensitivity outputs when connected to feasible electronic circuits. Signals defining less than 0.01 arc-seconds are achievable with carefully designed generators and good electronics.

As shown in Fig. 1–34 balance adjustments for the float have the form of nuts on screws attached to the float. By providing means for turning these nuts from outside the case with the unit in full operation, it becomes possible to place the center of mass on the output axis so accurately that the total effects of unbalance torques under one earth gravity may be reduced to the level of one meru or less.

Flexible leads carefully selected for low hysteresis and substantially floated in the suspension fluid are used to carry power to the gyro rotor within the gimbal float. By careful design and the use of a refining adjustment accessible from outside the case, the effects of power lead torque may be reduced to a level of one meru or less.

With single axis operation and accurately controlled centralization of the moving element, torque generators are feasible in which the output is very closely proportional to the electrical input. This characteristic makes the single-degree-of-freedom integrating gyro unit a very useful and flexible component for applications of many kinds.

The features described in general terms coupled with an absolutely necessary careful control of temperature, rotor power, electrical excitation, mechanical mounting, connectors, etc., make it possible to reduce gyro performance uncertainties to levels between 0.01 and 0.001 meru. By proper compensation and/or correction of various basic effects which are measurable by inspection techniques, gyro performance substantially identical with the uncertainty levels may be achieved in practical operation.

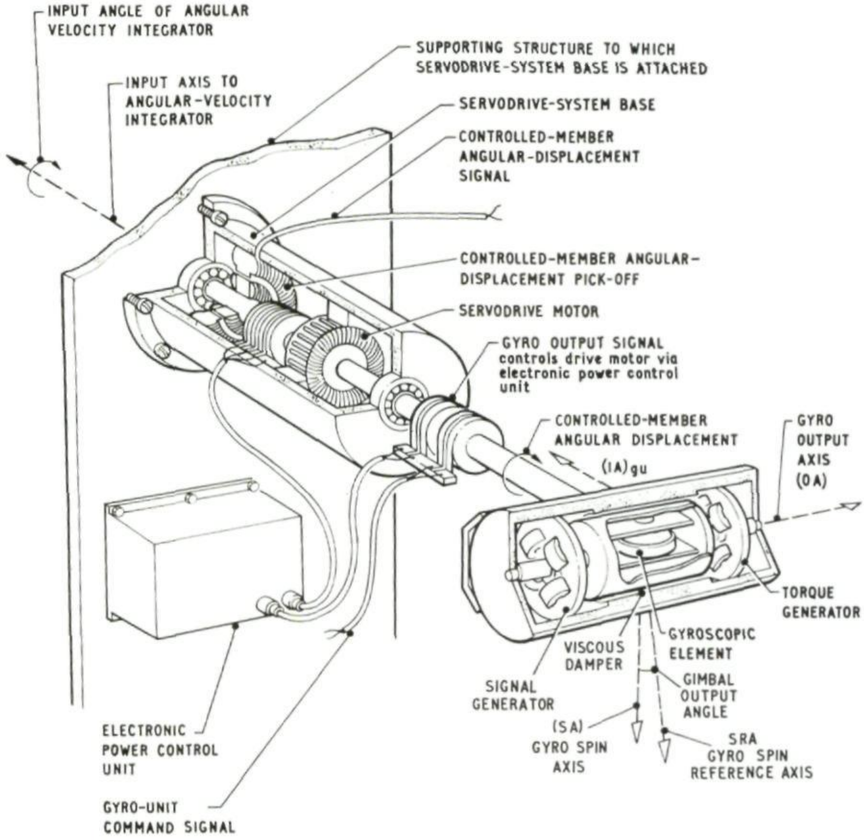

FIG. 1–36 Pictorial schematic diagram illustrating basic features of the single axis servo-driven stabilization with inertial-space angular deviation sensed by the single-degree-of-freedom floated integrating gyro unit

CHAPTER 1–6

BASIC PRINCIPLES OF GYRO UNIT APPLICATIONS

Single-degree-of-freedom gyro unit systems as components are combined with many more devices to produce a coordinated overall result in guidance systems. The particular function of any single gyro unit is to translate the resultant of rotations about its input axis with respect to inertial space and command inputs to its torque generator into a resultant signal that represents the angle deviation of the float from the position for which the output signal has its null level. In effect, the output signal represents the angular deviation of the case about the input axis from a reference position established by the null level of the signal. Command inputs to the torque generator have the effect of rotating the reference position with an angular velocity proportional to the signal.

Figure 1–36 is an illustrative pictorial schematic diagram in terms of a single axis system suggesting the basic features and operating principles of a typical gyro unit – servo-driven controlled member combination. For the arrangement of this figure which provides functions similar to those of the geometrical reference member of an inertial guidance system, it is assumed that the command input is zero except perhaps for small compensations for calibrated imperfections of the particular gyro unit involved. When, for any reason, the base of the servo-drive moves so that the gyro unit is rotated away from its reference orientation about the input axis, or a torque is imposed from any other source, a gyro output signal is generated. Through slip rings this signal is applied as input to the servo-drive system which applies torque to the controlled member to force it back to the orientation for which the gyro unit case has its reference position. As a result of this continued action of the servo in overcoming disturbing torques, the case effectively holds its reference position about the input axis no matter how the base may move. Operation of this is typical of geometrical stabilization.

The servo-drive-gyro unit combination of Fig. 1–36 provides several functions for inertial guidance systems. The broad natures of these functions are suggested by the diagrams of Fig. 1–37. When no command signal is applied to the gyro unit, the servo-drive stabilizes the input axis orientation of a controlled member on the basis of angular deviation signals from the gyro unit. Command signal integration appears when an input is supplied to the gyro unit torque motor. The resulting torque on the float causes rotation which produces an output signal. This signal acts as an input to the servo so that the controlled member turns in the proper direction to reduce the output signal. Except for dynamic response effects, which may be reduced to negligible levels by proper servo design, the operation described may be made to rotate the controlled member about the input axis with an angular velocity effectively proportional in magnitude to the magnitude of the command

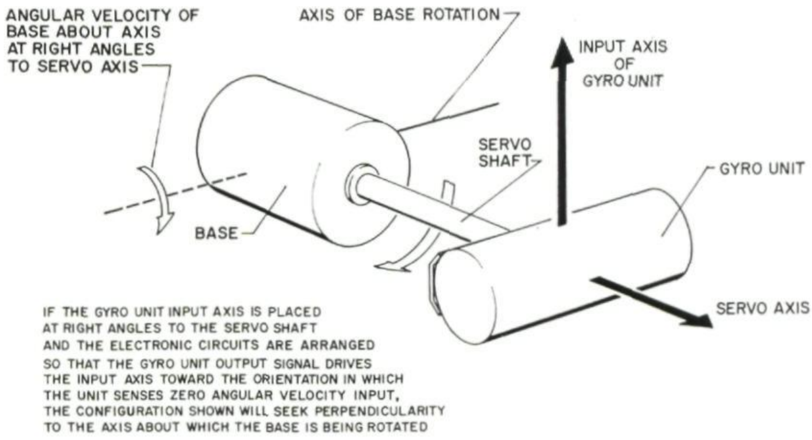

FIG. 1–37 (a) Angular velocity direction sensor

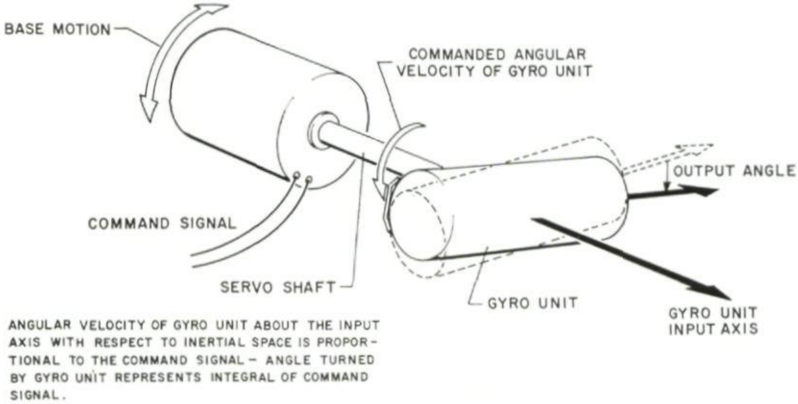

FIG. 1–37 (b) Space integration

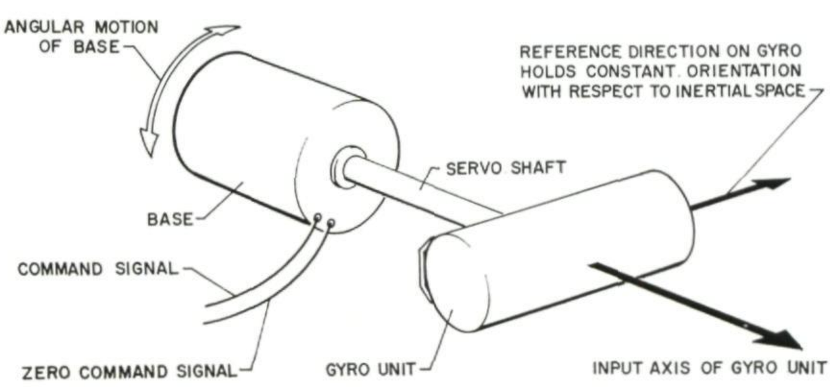

FIG. 1–37 (c) Stabilization – base motion isolation

signal. Directional senses are determined by phasing or polarity changes of the command signal. The resulting effect of the signal is that the angle turned through with respect to inertial space by the controlled member about the input axis is proportional to the time integral of the command signal.

Another mode of gyro-unit operation that is generally similar to the space integrator result described is that in which the command signals are applied to the gyro unit to keep the output signal at null as the controlled member is forced to rotate in any arbitrary way with respect to inertial space about the input axis. With this mode of operation, integration of the command signal over any given time interval represents the total angle turned through by the controlled member during the same interval. It is to be noted that with this type of operation, the servo-drive of Fig. 1–37 has no significant function beyond providing a shaft for controlled member rotation. In practice, command signals may be direct current, alternating current, or electrical pulses. Pulses are especially suitable for command signals, because they may be easily adapted as inputs-outputs for digital computers. Integration with pulses is particularly easy, as the process involved is a matter of simple counting.

When the axis of base rotation is about an axis perpendicular to the servo-drive axis and the gyro unit is adjusted on the controlled member so that its input axis is at right angles to the servo axis, the arrangement may be used to indicate the direction of the axis about which the base is being rotated. In effect, if the input axis is inclined so that it receives a component of the base angular velocity, the gyro unit case is forced to rotate about its input axis so that it generates an output signal which causes the servo to turn the case so that its input axis is at right angles to the base rotation axis. By giving the gyro unit performance that enables it to respond consistently to, say, one millionth of the magnitude of the base angular velocity, the direction of the gyro unit input axis may be made to indicate perpendicularity to the base rotation with an inaccuracy with the order of one arc-second. This mode of operation using components now available, makes it possible to align controlled members to north with sufficient accuracy for the operation of high performance guidance systems.

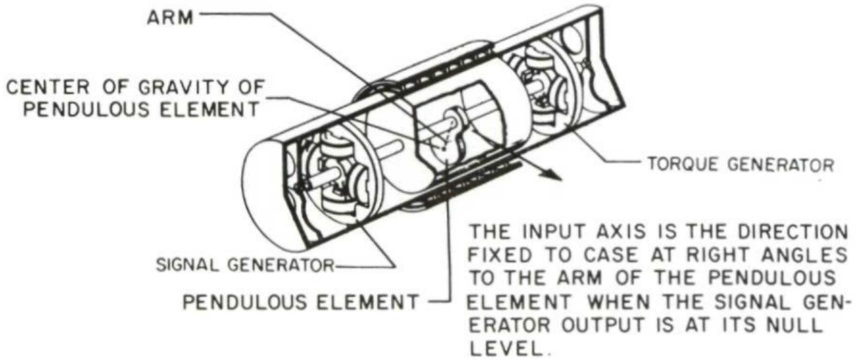

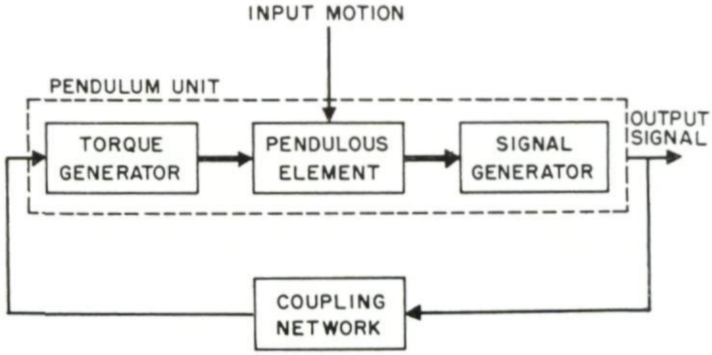

FIG. 1–38 Basic features of the single-degree-of-freedom pulsed integrating pendulum for receiving specific force

CHAPTER 1–7

SPECIFIC FORCE RECEIVERS

All instruments designed to receive specific force depend upon a sensitive element that is essentially an unbalanced mass. This mass is arranged so that it imposes a force, or a torque, on some member that is restrained in a calibratable way. Figure 1–38 illustrates the use of a floated-magnetic suspension carried pendulum restrained by a torque generator fed by pulses under the control of float angle signals. The integral of specific force (the resultant of gravity and inertia reaction force) is obtained by counting the pulses required to keep the float angle on its null position.

Figure 1–39 suggests the features of a pendulous gyro-servo-drive specific force receiver in which the calibrated balancing torque for the output of the unbalanced mass is provided by the gyroscopic output torque from a constant speed spinning rotor driven by a servo to keep the output signal at its null level. Since the required angular velocity about the gyro input axis is proportional the balancing torque, the angle turned by the gyro unit case in a given time interval is a measure of the specific force integral for the same time. This calibration relationship depends upon interactions between two absolutely linear, non-saturable effects (both depending only on Newton's Laws of Dynamics) so that the range of accurate operation is basically limited only by servo design considerations. By using digitalizing signal generators for the servo-axis, the integrated output appears in terms of pulses suitable for direct use as digital computer inputs.

The requirements of position location for center-of-mass positions to be maintained in order to realize various drift rates with typical gyro units are summarized in the table of Fig. 1–41. These numbers also suggest that specific force receivers must have their unbalanced mass centers positioned within very small tolerances if inaccuracies of 10^{-6} earth's gravity are to be maintained over a range including some tens of gravity.

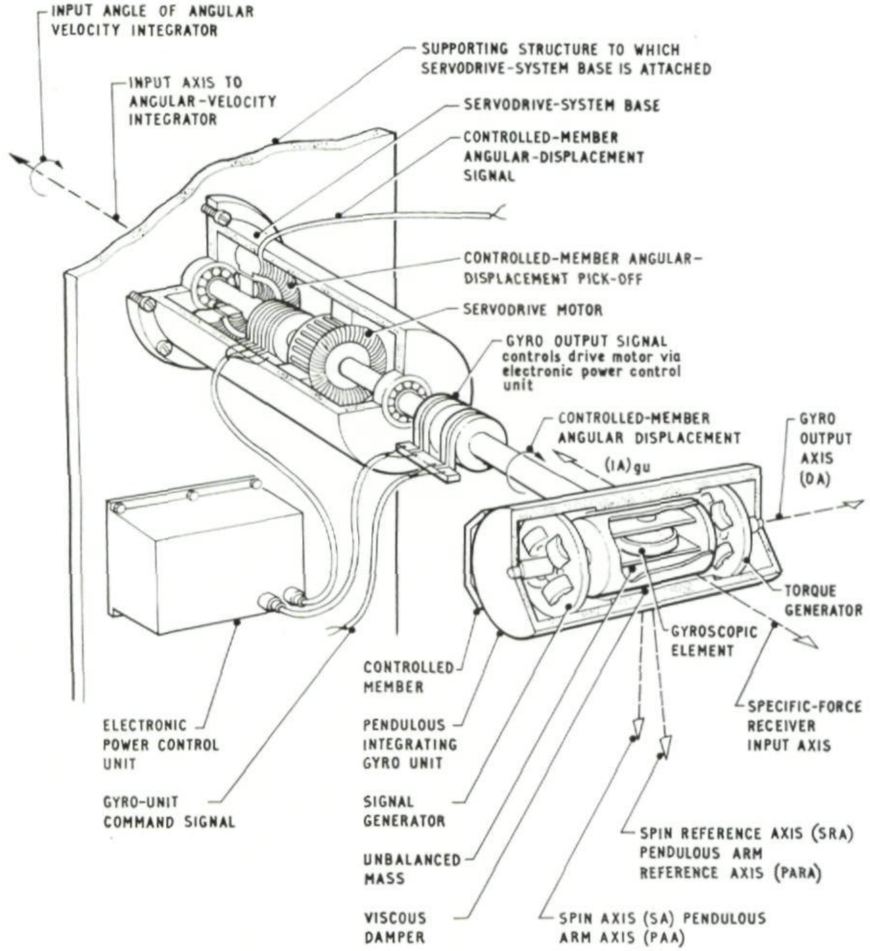

FIG. 1–39 Pictorial schematic diagram showing basic features of the single axis single-degree-of-freedom pendulum single-degree-of-freedom gyro unit integrating special force receiver

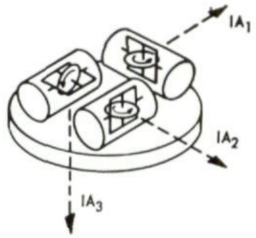

Schematic drawing of single-degree-of-freedom gyro package

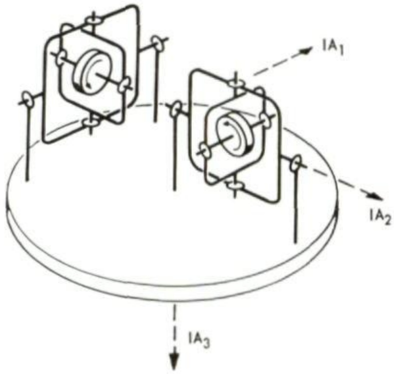

Schematic drawing of two-degree-of-freedom gyro package

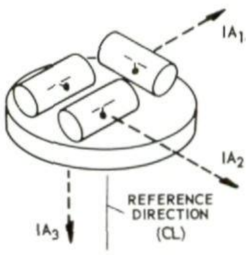

Schematic drawing of accelerometer package

FIG. 1–40a Basic elements of typical geometrical reference packages

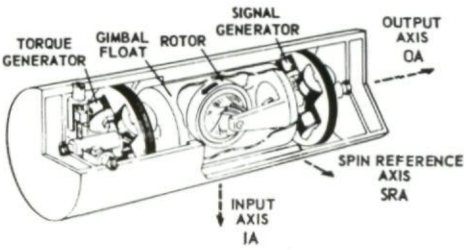

Pictorial drawing of single-degree-of-freedom gyro unit

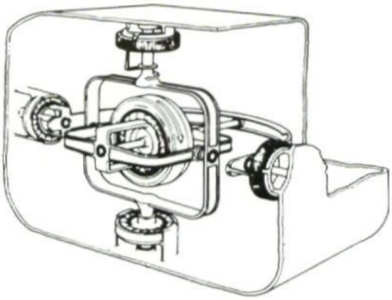

Pictorial drawing of two-degree-of-freedom gyro unit

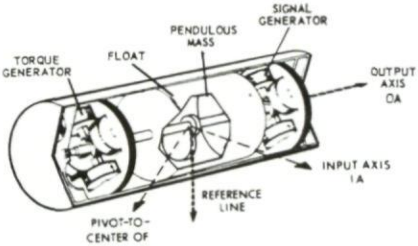

Pictorial drawing of a single-degree-of-freedom specific force receiving unit

FIG. 1–40b Basic elements of typical geometrical reference packages

Drift Rate		Center-of-Mass Position with Respect to Output Axis $(arm)_{(cg)}$				
In Earth Angular Velocity Units	In $\frac{\text{Radians}}{\text{Second}}$	In Centimeters	In Microinches	In Angstroms	In Lattice Constants (approx) of Aluminum, Steel, or Beryllium*	
1 eru	$0{\cdot}73 \times 10^{-4}$	$1{\cdot}46 \times 10^{-4}$	57·5	$1{\cdot}46 \times 10^{4}$	$\cong 0{\cdot}5 \times 10^{4}$ or	5000
1 deru	$0{\cdot}73 \times 10^{-5}$	$1{\cdot}46 \times 10^{-5}$	5·75	$1{\cdot}46 \times 10^{3}$	$0{\cdot}5 \times 10^{3}$	500
1 ceru	$0{\cdot}73 \times 10^{-6}$	$1{\cdot}46 \times 10^{-6}$	0·575	$1{\cdot}46 \times 10^{2}$	$0{\cdot}5 \times 10^{2}$	50
1 meru	$0{\cdot}73 \times 10^{-7}$	$1{\cdot}46 \times 10^{-7}$	0·0575	$1{\cdot}46 \times 10$	$0{\cdot}5 \times 10$	5
1 d meru	$0{\cdot}73 \times 10^{-8}$	$1{\cdot}46 \times 10^{-8}$	0·00575	1·46	0·5	1/2
1 e meru	$0{\cdot}73 \times 10^{-9}$	$1{\cdot}46 \times 10^{-9}$	0·000575	0·146	0·05	1/20
1 m meru	$0{\cdot}73 \times 10^{-10}$	$1{\cdot}46 \times 10^{-10}$	0·0000575	0·0146	0·005	1·200

* The lattice constants of aluminum, steel and beryllium are approximately 3 angstrom units, that is, 3×10^{-8} centimeter.

FIG. 1–41 Approximate centre-of-mass position in terms of distance along the spin axis for typical gyro units

CHAPTER 1–8

INERTIAL SYSTEMS

Inertial guidance systems all require the instrumentation of reference coordinates accurately aligned with the external space used for flight path reference purposes. In addition, specific force receivers rigidly mounted on the reference member are needed to produce signals that represent specific force components. A typical arrangement is suggested by the diagram of Fig. 1–42. Controlled member stabilization maintains the reference coordinates and specific force receiver outputs give computer inputs representing components along known axes. These outputs, processed by the computer, give control, navigation and guidance outputs without the necessity of geometrical transformations based on gimbal orientations.

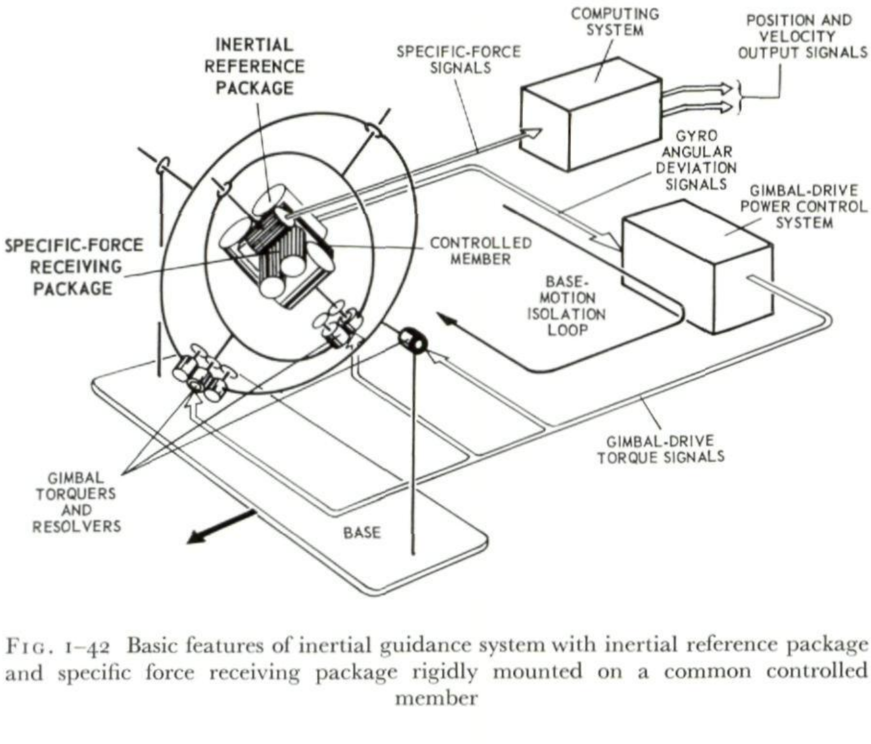

FIG. 1–42 Basic features of inertial guidance system with inertial reference package and specific force receiving package rigidly mounted on a common controlled member

REFERENCES

1. Schuler, M., "Die Storung von Pendel-und Kreiselapparaten durch die Beschleunigung des Fahrzeuges". Phys. Z., Vol. 24, p. 344, 1923.
2. Ishlinsky, A. Yu., "Equations for the Problem of Determining the Position of a Moving Object by Means of Gyroscopes and Accelerometers". Prikladnaya Matematika i Mekhanika, Vol. XXI, No. 6, pp. 725–9, Moscow, 1957.
3. Pitman, G. R. (editor), "Inertial Guidance". John Wiley, New York, 1962.
4. Draper, C. S., Wrigley, W., and Hovorka, J., "Inertial Guidance". Pergamon Press, New York, 1962.
5. Markey, W., and Hovorka, J., "The Mechanics of Inertial Position and Heading Indication". Methuen, London, 1961.
6. Broxmeyer, C., "Inertial Navigation Systems". McGraw-Hill, New York, 1964.
7. Wrigley, W., Woodbury, R. B., and Hovorka, J., "Inertial Guidance". S.M.F. Paper FF–16, Inst. of the Aerospace Sciences, New York, 1957.
8. Draper, C. S., Wrigley, W., Hovorka, J., and Marshall, R. E., "Non-Linear Effects in Radio-Monitored Inertial Guidance Systems". IUTAM Symposium, Kiev, 1961.
9. Draper, C. S., "Mechanization of Inertial Guidance Systems". Gyrodynamics, H. Ziegler (editor), pp. 92–118, Springer-Berlin, 1963.
10. O'Donnell, C. F. (editor), "Inertial Navigation Analysis and Design". McGraw-Hill, New York, 1964.
11. Leondes, C. T. (editor), "Guidance and Control of Aerospace Vehicles". McGraw-Hill, New York, 1963.
12. Fernandez, M., and Macomber, G. R., "Inertial Guidance Engineering". Prentice-Hall, Englewood Cliffs, 1962.
13. Savant, C. J., Jr., Howard, R. C., Solloway, C. B., and Savant, C. A., "Principles of Inertial Navigation". McGraw-Hill, New York, 1961.
14. Locke, A. S., "Guidance". D. Van Nostrand, Princeton, 1955.
15. Cannon, R. H., Jr., "Alignment of Inertial Guidance Systems by Gyrocompassing-Linear Theory". J. Aerospace Sci., Vol. 28, No. 11, 1961.
16. Duncan, D. B., "Combined Doppler Radar and Inertial Navigation Systems". Proc. Nat. Electronic Conf., Chicago, 1958.
17. "Theoretical Background of Inertial Navigation for Submarines". M.I.T., Instrumentation Laboratory, Report R-9, 1952.
18. Hellman, H., "The Development of Inertial Navigation". Navigation, Vol. 9, No. 2, 1962.
19. McClure, C. L., "Theory of Inertial Guidance". Prentice-Hall, Englewood Cliffs, 1960.
20. Slater, J. M., "Newtonian Navigation". Electromechanical Design, Vol. 6, 1962.

21. Wrigley, W., "Schuler Tuning Characteristics in Navigational Instruments". Navigation, 1950.
22. Wrigley, W., "Single-Degree-of-Freedom Gyroscopes". M.I.T. Instrumentation Laboratory, Report R-375, References: 1, 7–18, 24, 25, 38 and 40, 1952.
23. Ziegler, H. (editor), "Gyrodynamics". Springer-Berlin, 1963.
24. Draper, C. S., Whitaker, H. P., and Young, L. R., "The Roles of Men and Instruments in Control and Guidance Systems for Spacecraft". XVth International Astronautical Congress, Warsaw, 1964.
25. Brown, K., and Weiser, P. (editors), "Ground Support Systems for Missiles and Space Vehicles". McGraw-Hill, New York, 1961.

PART 2

THE NAVIGATION, GUIDANCE AND CONTROL OF A MANNED LUNAR LANDING

David G. Hoag

DAVID G. HOAG

David G. Hoag is an Associate Director of Instrumentation Laboratory, Massachusetts Institute of Technology. He is assigned to the technical direction of design and development of the guidance-navigation system the Laboratory is developing for the National Aeronautics and Space Administration's Apollo spacecraft. Prior to his present assignment, Mr. Hoag was in charge of technical design of the inertial guidance system for the Navy's Polaris missile which the Laboratory developed.

Mr. Hoag was born October 11, 1925, in Boston. He was graduated from Chauncy Hall School, Boston, in 1943, and entered M.I.T. that year as a member of the Navy V-12. He received his Bachelor of Science degree in Electrical Engineering from M.I.T. in 1946, and his Master of Science degree in Instrumentation from M.I.T. in 1950.

Mr. Hoag joined the Instrumentation Laboratory in 1946, and worked for several years on gun fire control systems and ship-launched missile fire control systems for the Navy. He became an Assistant Director of the Laboratory in 1955, and was placed in charge of all technical design aspects of the Polaris guidance system when the Laboratory later assumed responsibility for that work. He was appointed an Associate Director in 1963.

PART 2

THE NAVIGATION, GUIDANCE AND CONTROL OF A MANNED LUNAR LANDING

INTRODUCTION

Among the many extensions of old disciplines and development of new technologies needed in man's present rush into space flight is that of the subject of this book; the measurement and control of spacecraft position, velocity and orientation in support of space mission objectives. In this chapter, we will introduce more specifically the nature of the problem in order to provide a background of definition and approach for the following chapters which deal with actual details of specific problems and their solutions.

One might choose the words "spacecraft rotational and translational management" as being descriptive of the subject. The parameters of concern are the time history of the three degrees of freedom describing spacecraft orientation and the time history of the three degrees of freedom describing spacecraft position.

Spacecraft missions such as those being flown today operate in phases which alternate with a short period of powered or accelerated (that motion with respect to the free-fall arising from non-gravitational forces) flight followed by a long period of free-fall coasting. This is a consequence of the character of available propulsion typical in the chemical rocket. The nature of the rotational and translational management problems differ markedly between the free-fall and thrusting accelerated conditions. Thus it becomes convenient to separate discussions and base definitions on paired combinations of the "rotational" or "translational" and the "free-fall" or "accelerated" aspects of the subject. This results in the following definitions of four often-used terms:

(a) NAVIGATION
Translational measurement and control in free-fall

(b) ATTITUDE CONTROL
Rotational measurement and control in free-fall

(c) THRUST VECTOR CONTROL
Rotational measurement and control during acceleration

(d) GUIDANCE
Translational measurement and control during acceleration

Unfortunately two minor flaws mar this symmetrical array of definitions. First, the process of "navigation" probably ought not to be constrained only to free-fall flight. Indeed, the determination of position and velocity during any phase of flight might be a better definition of navigation. We can take the view, then, that navigation is one of the functions of the guidance process – as will be seen. Second, using "thrust vector control" for the title associated with rotational measurement and control during accelerated flight

appears to exclude similar operations during phases where aerodynamic forces – not rocket thrust – are causing the acceleration. This occurs during the important phases of planetary atmospheric entry using drag and lift forces for deceleration and steering.

Recognizing these qualifications, the following chapter covers the problems of each of the four situations.

CHAPTER 2–1

THE BACKGROUND AND THE PROBLEM OF SPACECRAFT GUIDANCE, NAVIGATION AND CONTROL

NAVIGATION

Translational measurement and control in free-fall

Navigation as defined herein is the process of measurement and computation to determine the existing present position and probable future position of a vehicle. It is concerned only with the translational aspects of motion – i.e. position and velocity – and is considered here temporarily to be applicable only to the free-fall coasting conditions of spacecraft. It includes those processes necessary to determine needed trajectory corrections as well as to compute the initial conditions of major powered maneuvers. In this sense it has "control" aspects as well as "measurement" in that it includes activity to modify the spacecraft's path.

In non-thrusting flight out in space the forces on the craft which determine its motion are dominated by the Newtonian gravitation attraction of the near bodies – the earth, moon, sun and planets. Generally the vehicle is influenced primarily by one body and follows nearly the classical Keplerian conic path. The effects of forces other than that of the point mass central body can usually be treated as deviations or perturbations to the simpler motion. A non-exhaustive listing of typical perturbing effects are: (1) Mass distribution within central body, e.g. oblateness of earth, triaxiality of moon, (2) Attraction of more remote bodies, (3) Atmospheric drag, (4) Solar radiation pressure, (5) Meteroid impact and (6) Magnetic and electric field interactions with spacecraft.

In a given situation it is usually possible to ignore all but a few of the perturbing effects and predict the future trajectory of the vehicle with satisfactory accuracy many hours to many days into the future, using knowledge of present position and velocity. However, for a given accuracy, the prediction finally deteriorates due to ignored perturbing effects and due to the accuracy limitations of the initial conditions and the extrapolation model.

Because of the relatively predictable nature of spacecraft trajectories in free coasting flight continuous measurement of position and velocity is unnecessary. Measurements are needed periodically to correct for the slow deviation of the actual spacecraft from the predicted path.

Practical navigation measurements in free coasting flight all utilize electromagnetic radiation at appropriate wavelengths to sense spacial relationships among the spacecraft and the near bodies of the solar system. These measurements can be categorized into two types: first, those made earth-based by remote tracking of the spacecraft from suitable stations on the earth and, second, those made from on board using sensing devices on the craft itself. Only the first of these has yet been applied; all U.S. spacecraft and as far as

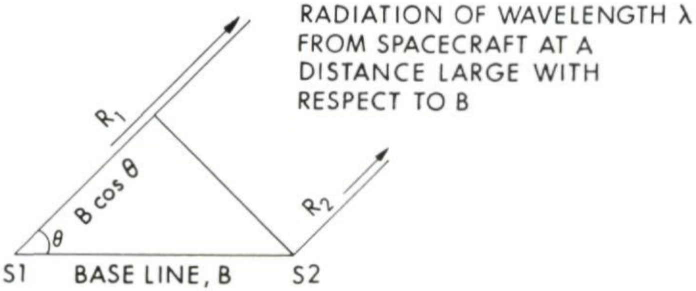

$$B\cos\theta = R_1 - R_2 \qquad \Delta\phi = \text{PHASE DIFFERENCE } (S1, S2)$$

$$\cos\theta = \frac{R_1 - R_2}{B} \qquad R_1 - R_2 = \frac{\lambda}{2\pi}\Delta\phi$$

$$\cos\theta = \frac{\lambda}{B}\,\frac{\Delta\phi}{2\pi}$$

FIG. 2–1 Short base line interferometric direction measurement

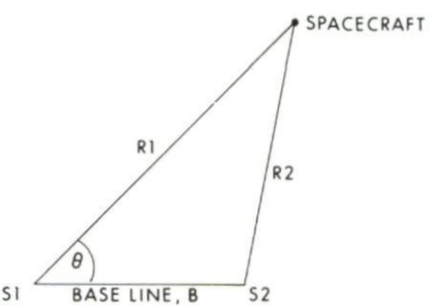

$$R_2^2 = R_1^2 + B^2 - 2R_1B\cos\theta$$

$$\cos\theta = \frac{R_1^2 - R_2^2 + B^2}{2R_1B} = \frac{R_1^2 - R_2^2}{2R_1B} + \frac{B}{2R_1}$$

$$\cos\theta = \frac{(R_1 - R_2)}{B}\left(1 - \frac{R_1 - R_2}{2R_1}\right) + \frac{B}{2R_1}$$

$$\cong \frac{R_1 - R_2}{B} \text{ when } B << R_1, R_2$$

FIG. 2–2 Long base line inverse triangulation direction measurement

we know all Soviet vehicles have been navigated using earth-based tracking measurements only.

Earth-Based Navigation – Earth-based tracking for navigation usually uses radar frequencies with the cooperative use of transmitting beacons or transponders on the spacecraft being tracked. Optical wavelengths have seen use but suffer from the problem of obscuring cloud cover.

Radio tracking for navigation is founded upon: (1) the fixed and well-known speed of light in space, (2) the use of highly accurate time bases and stable frequency sources and (3) the ingenuity and accuracy with which precise phase measurement can be made between two signals in the presence of interfering noise.

Earth-Based Range Measurement – For measurement of spacecraft range the earth station transmits a periodic waveform on a high frequency carrier to the spacecraft, which in turn is equipped to re-radiate this waveform back to the earth. The distance to and from the spacecraft is proportional to the phase lag of the waveform as received from the spacecraft with respect to the transmitted waveform to the spacecraft. Range resolution, then, is that fraction of a wavelength with which the phase can be measured. A 100 mc carrier, for instance, has a wavelength of 3 meters and range resolution well inside this dimension is straightforward. Lower frequency modulation tones with longer wavelengths must be used to resolve the ambiguities and thereby determine the more significant figures of the number representing measured range. For spacecraft this technique depends upon a transponder in the spacecraft which will receive the transmission and re-radiate with controlled phase-shift an appropriate correlated signal to the ground station.

Although range tracking, as defined, has almost micrometer resolution capability, several limitations on the total overall accuracy exist. The most apparent, of course, is our knowledge of the exact speed of light. This is currently known to about 1 part in 10^6. Without calibration correction as discussed below, this means a range error of 150 kilometers in a spacecraft distance of one astronomical unit. At lunar distances this reduces to the order of 400 meters.

Range rate information is measured by the rate of change of phase shift of the received signal, or more familiarly, by the equivalent doppler frequency shift.

Earth-Based Direction Measurement – The most common direction measurement technique from earth stations is a sort of inverted triangulation using multiple receivers on accurately known baselines. If this baseline array is suitably short the received signals can be simultaneously processed, in the same earth-based equipment, to perform an interferometric measure of the differences in range of the spacecraft from the various receivers, as shown on Fig. 2–1. It is a technique which still offers many advantages, particularly the fact that the spacecraft need carry only a radio beacon transmitter which does not need to be interrogated from the ground.

For these short baselength systems the differences in phases of the various received waveforms can be measured with extreme precision. A 3-meter signal wavelength (100 mc) can be resolved by phase measurement to 3 millimeters, for example, utilizing techniques such as heterodyning to a

lower frequency and precision timing. On a 150 meter baselength this corresponds to 20 microradians (4 seconds of arc) of angular resolution of spacecraft directions which lie near normal to the baseline. If a spacecraft is at one astronomical unit distance, for instance, this is position resolution of across the line of sight of 3 000 kilometers. At the shorter lunar distances this reduces to about 8 kilometers.

For the usual horizontal array of receivers, it is seen that best directional accuracy is obtained for conditions with the spacecraft direction near perpendicular to the baseline. As the vehicle gets near in line with the baseline the angular resolution degenerates inversely as the sine of the angle from the baseline. Moreover, near the horizon, earth atmospheric refraction uncertainty degenerates the total indicated direction accuracy.

For greater accuracy in direction measurement the baseline can be increased. However, several problems interfere with proportional accuracy improvement of longer baselines in comparison with the short baseline interferometric systems. First, wide separation of the receiving stations prevents accurate, simultaneous, direct phase comparison of the received signals. Also the direction is no longer a direct function of the range difference, as illustrated in Fig. 2–2. So rather than using range differences obtained directly by phase comparison, the total range values from the several stations must be individually collected and then processed for determination of direction.

Realization of directional measurement accuracy improvement by increasing baselength requires that the range measurement and baseline errors accumulate less rapidly than does the baseline increase. The practicability of this can be seen by examining the accuracy needed in the baseline to maintain and improve the previous 20 microradian error derived above for the short 150 meter baselength. If the baselength is increased to 1 500 kilometers a 20 microradian error results from baseline errors of 30 meters. To obtain an improvement to 2 microradians direction error the 1 500 kilometer baseline must be known to 3 meters. However, at this precision and better, a serious question arises about achieving this necessary accuracy of earth station location. This is clearly a problem of survey and geodesy. The precise knowledge of the size and the shape of the earth is a question actively being pursued and about which agreement does not now exist.

Earth-based tracking ranging and directional measurements described above provide the basis for determining directly all components of the position and velocity of a spacecraft. The error values of our hypothetical models above by no means provide the accuracy limit from ground tracking. Considerable improvement for a given station array can be demonstrated by calibration techniques in tracking targets and applying corrections to fit the known target motions.

Spacecraft-Based Navigation – Spacecraft-borne navigation measurement tends more to optical frequency direction measurement rather than the radio frequency direct ranging that is so accurate for ground tracking. For relatively close work, however, direct ranging using radio frequencies with rendezvous or landing radars becomes possible, albeit necessary. But further from the planets and other targets direct measurement of range or range rate or the use of radio frequencies has not appeared attractive to the designers due to the weight and power penalties.

Spacecraft on-board directional measurements are those made to the near bodies – the sun, moon, earth and other planets. The stars provide no position data because of their extreme distances. But because of this distance they are most excellent references against which to measure directions to the nearer bodies. In a sense, then, on-board navigation is performed by observing the near bodies relative to the background stars. This can be done indirectly by measuring the angles sequentially from a gyro stabilized base to the stars and the near body. Alternately a direct and simultaneous measurement of the angle between a reference star and the near body with a suitable sextant-like instrument avoids an accumulation of errors with which the former sequential technique must cope.

The ancient sextant, updated and refined with a suitable telescope for image resolution and with a precision angle readout of the deflecting mirror, can provide in a reasonable size an accurate measure of the angle between a feature of a near body and a star superimposed upon that feature in the field of view. The "feature" alluded to is some distinct point of known coordinates on the planet to which the direction is being measured. The center of the planetary disk naturally comes to mind, but identifiable surface landmark features and horizons which can be related to planet coordinates are easier and more accurate for visual use, particularly under crescent illumination.

From sextant and sextant-like measurements directions can be determined with accuracies, for instance, of the order of 50 microradians to targets with an additional target feature positional accuracy of the order of 1 000 meters. For distances greater than 20 000 kilometers the 50 microradians dominates. Closer to the planet, however, navigation is limited by the location knowledge of the target features being used.

Each such angle measurement from the spacecraft provides a locus surface of spacecraft position at the time of measurement. Several together, if made simultaneously, define position uniquely at the common loci intersection, as shown in Fig. 2–3. In this hypothetical situation we see that range information is determined indirectly from the combination of direction data in a fashion not unlike triangulation, where the baseline is the known distance and direction between the target features of the planets. This also, in effect, is of the same nature as stadiometric ranging, made by measuring the apparent diameter of a planet disk.

Measurements separated in time can provide the basis for velocity determination. To obtain three components of position in the presence of spacecraft motion, one would desire the simultaneous measurement of at least three directional components. Practical considerations make time sequential directional measurements easier and no direct computation of position or velocity is possible by purely geometric calculations. Schemes such as used in Apollo and described in Part 3 of this book depend upon the use of an on-board computer, programmed to accept the sequence of single coordinate navigation data and the precise time each measurement occurred. Each datum point is received and used to update and improve in an optimum fashion the six dimensional state vector of the spacecraft, recognizing the expected error in each measurement, the current estimate of state vector error and the motion constraints of the spacecraft in free-fall.

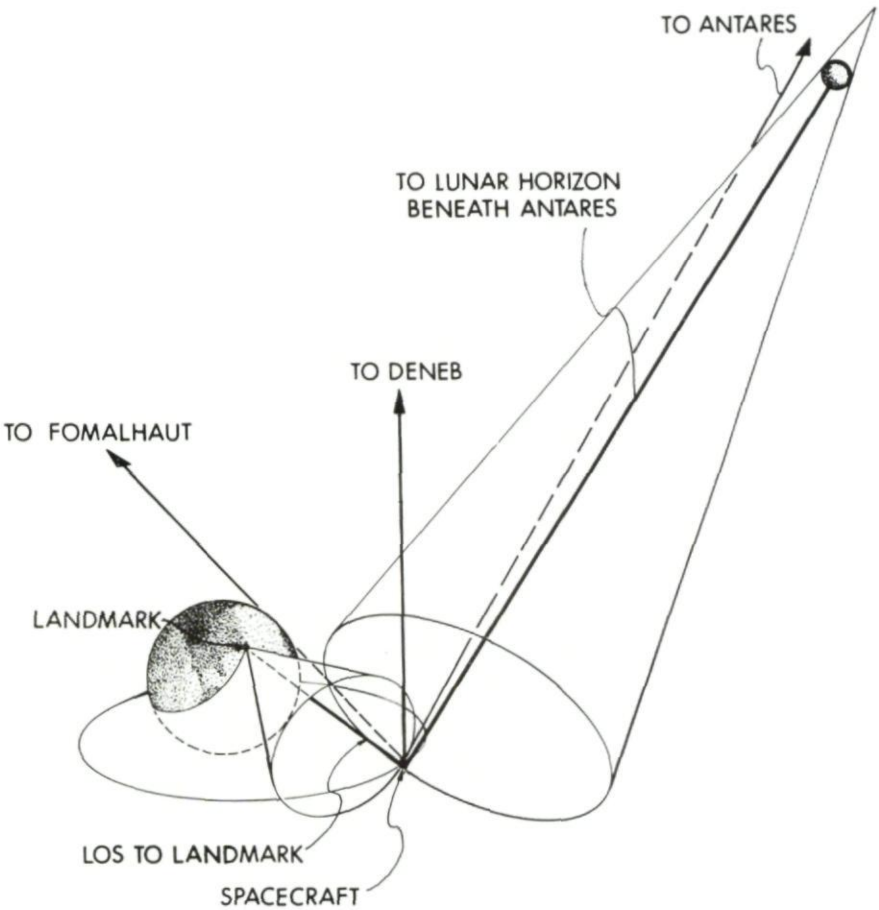

FIG. 2–3 Geometry of navigational fix in space

Ground-Based and Spacecraft-Based Navigation Measurement Comparison – We can compare the similarities and differences between navigation of a spacecraft in free fall using earth-based tracking measurements and using vehicle-borne direction measurements as follows:

(a) The two categories of navigation measurement complement each other in that earth-based tracking gives strong results along the line of sight from earth, while on-board measurement can add strength across the line of sight. The latter is particularly accurate at distances from earth and with respect to a target planet.

(d) Both categories depend upon optimum processing of data points taken over a period of time, recognizing known measurement uncertainties and spacecraft motion as constrained by orbital mechanics. Both categories use the past history of data to determine present position and velocity as limited by data uncertainty and can predict future motion further limited by the imperfect knowledge of the forces on the spacecraft due to the space environment.

(c) Availability of earth-based navigation data from a given station is dependent upon the spacecraft being sufficiently above the horizon for that station. Spacecraft-based navigation measurements must compete for control availability with other operations of the spacecraft.

(d) Earth-based navigation stations can support simultaneously only a limited number of missions. Spacecraft-based equipment, of course, is solely available for the use of that mission.

(e) Earth-based navigation tracking facilities are most limited by economic factors in the attempt to gain more capability by the use of many large radio tracking installations with complex communication networks and data processing centers. Spacecraft-based navigation is limited more by the weight that can be carried in the sensors and data-processing computers on board.

(f) Earth-based navigation tracking facilities have the strong advantage of multiple use and re-use in sequential support of many types of missions. Spacecraft based navigation equipment is, in a sense, consumed and only in missions where the equipment is recovered would re-use be possible.

(g) Earth-based navigation measurements fail while the spacecraft is passing behind its target planet. This is unfortunate since efficient orbital insertion and transearth orbital escape maneuvers always occur behind the moon and have a strong probability of being out of sight for other planets.

(h) Earth-based navigation is vulnerable to enemy action against military spacecraft. Spacecraft-based navigation measurement can be strictly passive for military use and is invulnerable to jamming or sabotage.

ATTITUDE CONTROL

Rotational measurement and control in free-fall

Attitude control is the process of aligning the spacecraft to a desired orientation with respect to a suitable reference framework and in response to input commands. As defined here the operation of attitude control applies to free fall coasting flight only. The diverse nature of the problem is seen in

terms of: (a) the orientation requirements, (b) the attitude sensing techniques, (c) the nature of the disturbing torques and (d) the techniques of applying the control torques. These will be discussed briefly to show the wide spectrum of problems and solutions that appear in designing attitude control systems for spacecraft.

The orientation requirements are naturally a function of the vehicle's mission and the associated operating constraints:

(a) Scientific payloads of a radiation or field sensing nature generally have pointing requirements for the sensitive axis of the instrument. Often these aiming requirements are not particularly stringent, but again others such as astronomical telescopes can require the utmost in accuracy and stability of aiming.

(b) Spacecraft management orientation constraints generally are of a low order of accuracy. These include (1) aiming of solar cells for gathering energy to support power consuming equipment, (2) aiming of communication, telemetry, transponder and beacon antennas toward earth and (3) the maintenance of thermal balance by controlling attitude with respect to the sun.

(c) Navigation and guidance functions require attitude control arising from (1) the need to point the operating field of the navigation sensors towards the desired portion of the sky and (2) the need for initial pointing of the rocket thrust axis just prior to ignition for a trajectory correction or major maneuver.

This multitude of possible requirements can lead to impossible conflicting situations which are sometimes relieved only by mounting the light-weight instruments on articulating gimbals to make them at least partially independent on spacecraft attitude.

The attitude sensing function is also performed in a number of ways:

(a) In some cases radiation sensing instruments requiring pointing can be made to track the sensed flux themselves by providing error signals to the control system.

(b) For earth orbital spacecraft the most common attitude sensing uses infrared horizon detectors to indicate spacecraft orientation deviations from local vertical. These, used in conjunction with a gyroscope reference, can also provide the attitude about the local vertical with respect to the orbital plane. This process is similar to the earthbound gyrocompass in that the pendulum is replaced by the horizon detectors and the earth's rotation is replaced by the rotation in orbit.

(c) Basic attitude sensing for small cislunar and interplanetary vehicles most often depends upon a sun seeker/tracker to set up a vehicle axis with respect to the sun, combined with a star tracker offset by an adjustable angle to acquire and track a star so as to provide attitude sensing about that sun line.

(d) Once an orientation reference is established this can be maintained by the use of gyroscopes to detect deviations from the reference. Gyroscopes also provide capability to meter orientation changes accurately from the attitude established by other means.

The disturbance torques upset spacecraft orientation and cause the need for correction from the control system:

(a) Lightweight vehicles can be affected by the relatively weak forces associated with the space environment. For spacecraft with large unsymmetric surfaces with respect to the center of mass, radiation pressure from the sun is a significant torque disturbance. Lightweight vehicles also may be affected by interaction of electrical current loops or other spacecraft magnetic sources with the earth's field. Electrostatic forces, unsymmetric atmospheric drag and the integrated effect of micrometeoroids have also been suggested as a source of disturbance torques.

(b) Vehicles having one long dimension resulting in a wide difference in the principal moments of inertia can be strongly affected by differential gravity forces when near a massive planet.

(c) Spacecraft will experience disturbance torques any time mass is thrown off. This can occur, for instance, by the boiloff venting of cryogenic fuel or oxidizer or the offloading of other wastes.

(d) Relative acceleration of masses within the vehicle cause a redistribution of angular momentum arising from associated torques. Speed changes of on-board rotating machinery, the pumping or sloshing of fluids or the process of erection of solar panels or antennas are examples. On manned craft the movements of the crew cause significant disturbance.

Control torques to counteract these disturbances or to reorient the vehicle can utilize any of three phenomena:

(a) The weak forces associated with the space environment can be utilized in a passive or semipassive attitude control. Self-aligning mechanisms based upon solar radiation pressure, magnetic field torques or gravity gradient unbalances can provide weak but often adequate restoring torques to a stable orientation satisfactory for some missions. Some form of energy dissipation for damping oscillations must be provided.

(b) Small reaction rocket engines arrayed to provide suitable torque couples depend upon angular momentum transfer to the exhausted gas. These are usually chemical or cold gas low thrust engines designed for as many on-off cycles as demanded by the control loop. Control is characterized by pulsed operation of the jet and limit cycle oscillation about the desired attitude.

(c) Flywheel or gyroscope momentum exchange systems achieve control torque by either accelerating a heavy flywheel or precessing a spinning gyro. Unlike the jet or rocket systems above, only power is consumed and operation is not limited by the amount of working fluid carried. However, there is a capacity limit in the sense that there is a maximum momentum that can be stored by practical speeds of heavy flywheels or gyrowheels. Thus, in application, these momentum exchange systems are used in conjunction with periodic use of a jet or other type of external torques to "desaturate" the system back within its control range. Finally, a simple spin of the whole spacecraft itself can often provide adequate simple means of stabilization.

The design of attitude control systems is complicated by a number of factors. The classical equations of motion under assumptions of spacecraft

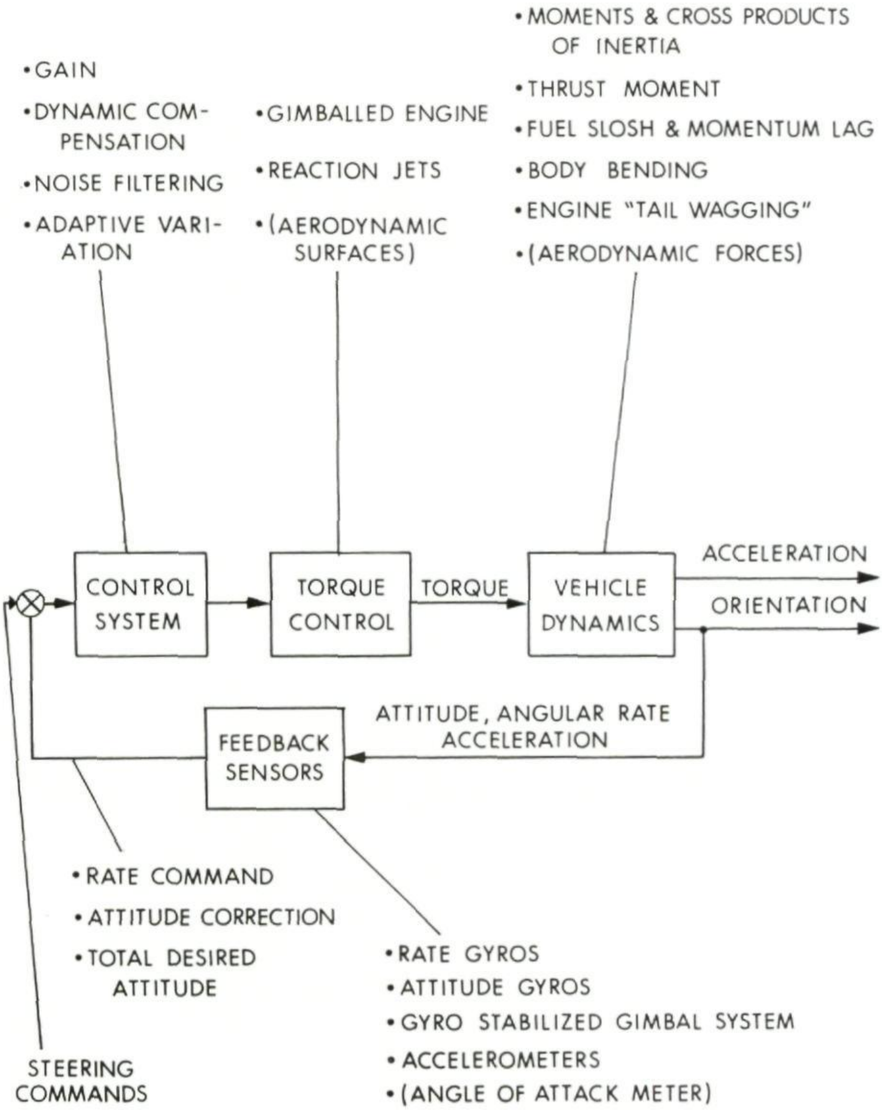

FIG. 2-4 Thrust vector stabilization and control

rigidity are straightforward. But even though it is theoretically possible to predict the rotational motions of the vehicle, a simple control system cannot make large rotational changes directly when the desired axis of rotation does not coincide with one of the principal axes of inertia. Usually the torquing axes are close to these principal axes and large rotational maneuvers are made sequentially axis by axis. This is admittedly less efficient than a hypothetical control system that would control to the shortest path achieved by applying a single initial torque impulse on the necessary axis. This impulse would create that angular momentum vector which will carry the vehicle into the desired orientation by free tumbling rotation where a second impulse could stop it.

The energy used in a rotational maneuver is directly a function of the speed with which the maneuver must be accomplished. Rather than build up kinetic energy in a fast turn only to cancel it again at the destination orientation with an opposite impulse, the designers tend towards very slow rotation rates for the large turns when mission requirements permit. Another complicating factor occurs when the spacecraft carries a significant mass of fluid fuel. A practical attitude control cannot measure the angular momentum contribution of this fluid, since its loose coupling to spacecraft allows it independent motion. Again the theoretically most efficient application of control torque cannot be achieved by simple attitude control systems.

Reaction jet control engines are characterized by fixed torque levels during firing and a wearout or lifetime limit on the number or duration of individual firings. Since disturbance torques are generally less than the available control torque, the attitude control system provides on-off cycles of firing resulting in a limit cycle oscillation about the desired orientation. The total jet fuel used and the number of on-off cycles should be minimized by optimization of the control system.

THRUST VECTOR CONTROL

Rotational measurement and control during acceleration

Thrust vector stabilization and control is the closed-loop process which (a) keeps the vehicle attitude from tumbling under the high forces of engine firing and (b) accepts turning or guidance steering commands to change the direction of engine-caused acceleration.

Figure 2–4 illustrates a generalization of acceleration vector stabilization and control. In order to illustrate the variations possible, the boxes in the figure may contain one or more of the aspects listed with "dot" prefix adjacent to the boxes. These systems are characterized by appropriate feedback to provide a stable control of angle or angular velocity of the thrusting vehicle. The loop also accepts input steering commands from guidance to achieve a particular desired thrust direction.

The design constraints on thrust vector stabilization and control systems represented by Fig. 2–4 vary considerably. The figure lists typical variations possible in the spacecraft body dynamics and the torque producing control devices. Most of these characteristics are not only gross nonlinearities but are time variant and interacting as well. The design is further complicated by necessary constraints on dynamic response to inputs and disturbances. It is usually restricted by allowable limits on angular acceleration, angle of

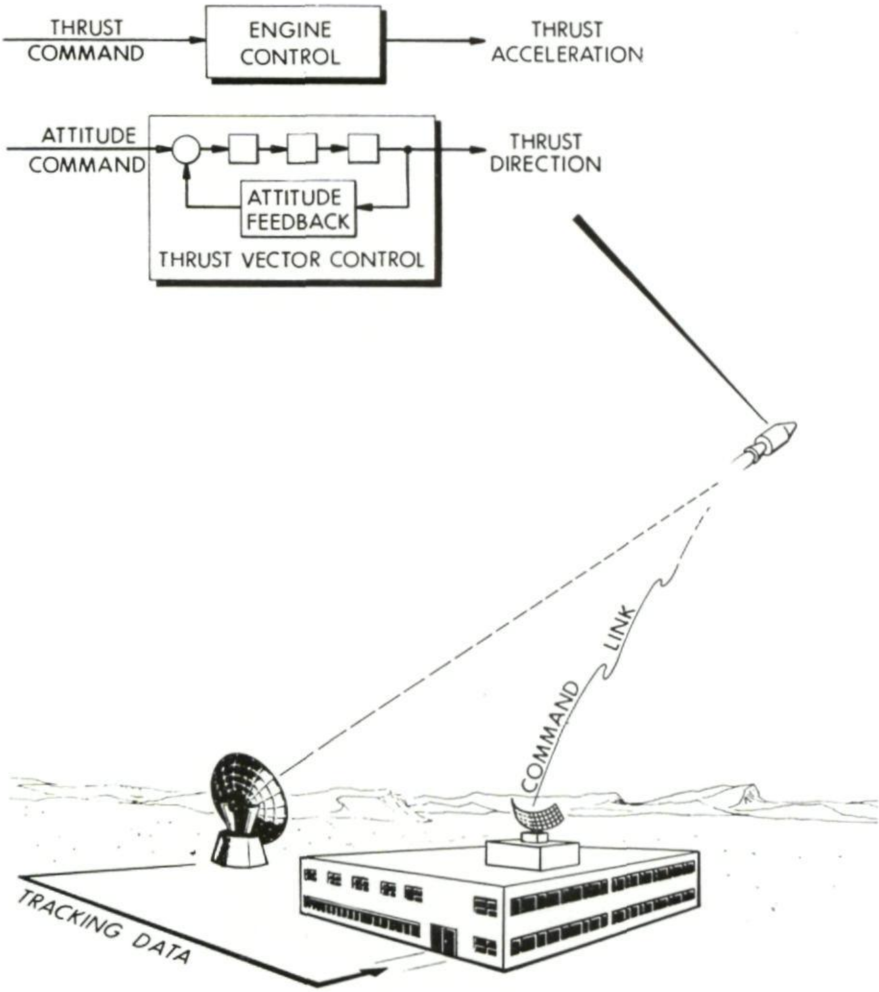

FIG. 2-5 Radio command guidance

attack and other variables depending on structural and controllability considerations. All this and the usual concern about reliability, weight, cost etc. makes design particularly difficult.

GUIDANCE

Translational measurement and control during acceleration

Guidance is the process of measurement and computation necessary to provide steering signals to the thrust vector control system and signals to modulate engine thrust level in order to achieve vehicle acceleration to a desired trajectory. Modulation of engine thrust level in the more common case of a non-throttleable engine consists only of turn-on and cutoff commands.

Earth-Based Tracking Guidance – Powered steering of some of the early U.S.A. ballistic missiles and of workhorse spacecraft launch vehicles used ground tracking data in a radio command guidance illustrated in Fig. 2–5. This type of guidance is characterized by a continuous ground tracking monitor of position and velocity changes during the powered phases and a radio command to the vehicle to change the direction of thrust appropriately – and finally to signal thrust termination. A basic requirement is an attitude reference system carried aboard the vehicle. This is illustrated in Fig. 2–5 as the attitude feedback, implemented with gyros for instance, as part of the thrust vector control system.

Far from the earth, delays occur associated with necessary longer smoothing of the noisier tracking signals and delays associated with the finite speed of electromagnetic propagation. For deep space spacecraft requiring short burn trajectory corrections of moderate accuracy these delays are not significant, since the ground command need only specify the direction and length of burn required. However, for precise long duration maneuvers the thrust vector control alone cannot assure accuracy in metering the direction or magnitude of the specified velocity change. And far from the earth the mentioned delays in the receipt of the steering commands make loop closure corrections of questionable effectiveness. Here inertial guidance is the only practical method of powered steering control.

On-Board Inertial Guidance – Inertial guidance, Fig. 2–6, is based upon measurements of vehicle motion using self-contained instruments which do not depend upon radiation sensing. In every inertial guidance system three types of measurements are made involving distinctive instruments: (a) angular rate or direction using gyroscopic devices, (b) linear acceleration using restrained test masses in accelerometers and (c) time using precision reference frequency sources. The integration with time of the sensed acceleration in the indicated direction with proper recognition of known gravity field forces is the essence of the navigation portion of inertial guidance. The implied processes are accomplished in a computer with the result of generating corrective steering commands to the thrust vector control system. Since inertial guidance of the type described can only integrate vehicle motion into changes in position, velocity and orientation, accurate initial conditions are required in these parameters before the accelerated guidance phase is started. Initial conditions in position and velocity are provided by navigation prior to the accelerated phase. Initial conditions in orientation come from the attitude control systems or directly from stellar references.

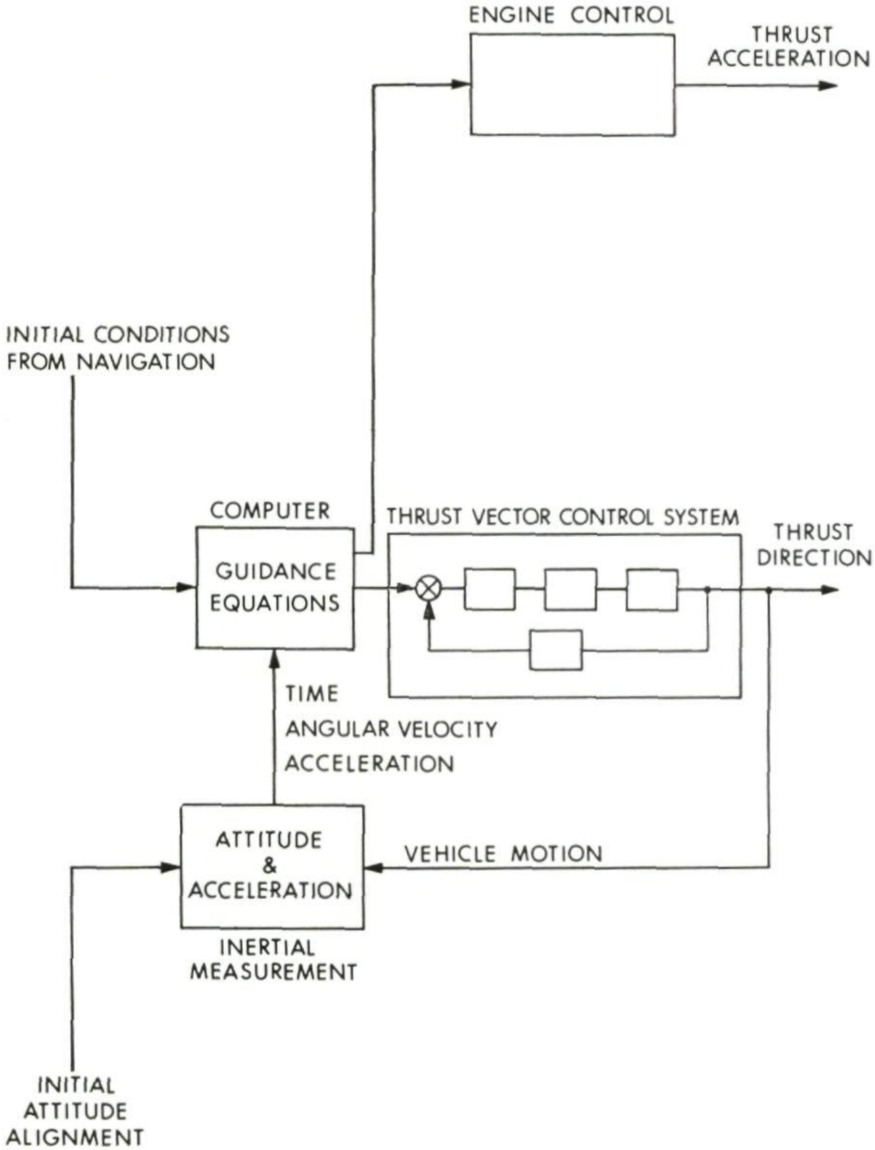

FIG. 2–6 Inertial guidance

One well-debated problem with inertial guidance is the presence of an increasing error of the inertially derived orientation and navigation with time. When an error in the gyro data, commonly called gyro drift, is processed in the computer the direction of the controlled acceleration is in error. When an error in the acceleration sensing exists, again the direction of acceleration as well as magnitude of acceleration and the controlled length of motor burning are affected undesirably. However, due to the motivation to perfect inertial instruments for their well adapted use in military guidance and navigation, the technology is advanced to the point that inertial guidance performance can be kept well ahead of needs for spacecraft missions in controlling accelerated flight. Furthermore, spacecraft inertial guidance can be tolerant of error, in the sense that errors in the resulting trajectory usually can be measured later by navigation and corrected with a short burn of the propulsion.

It is perhaps pertinent to examine these last statements with respect to two propulsion situations which undoubtedly will exist in the future. The first is that of the high specific impulse low thrust electric engines. Here the very low thrust to mass ratio requires long periods of controlled engine operation – measured in weeks. In such long periods inertial guidance measurement alone, without recourse to periodic external navigation measurements, would be unacceptable even if the inertial sensing were perfect. The inertial system cannot sense the perturbations in trajectory caused by the imperfectly known gravitational forces. Such systems then require periodic navigation by on-board or ground-tracking measurements. It is doubtful whether these navigation checks would be needed any more often than during the coasting free-fall phases with the more conventional chemical engine mission.

The second future propulsion situation is that which will exist with high thrust nuclear rockets providing more abundant total impulse. In this realm, mission times will be shortened by longer burning to higher interplanetary velocities than permitted with current chemical engines. In spite of the larger velocity changes to be measured during thrust by the inertial sensing, the dramatic shortening of the subsequent time of flight is enough to decrease required measurement precision for the same accuracy in arrival at the destination planet or orbit.

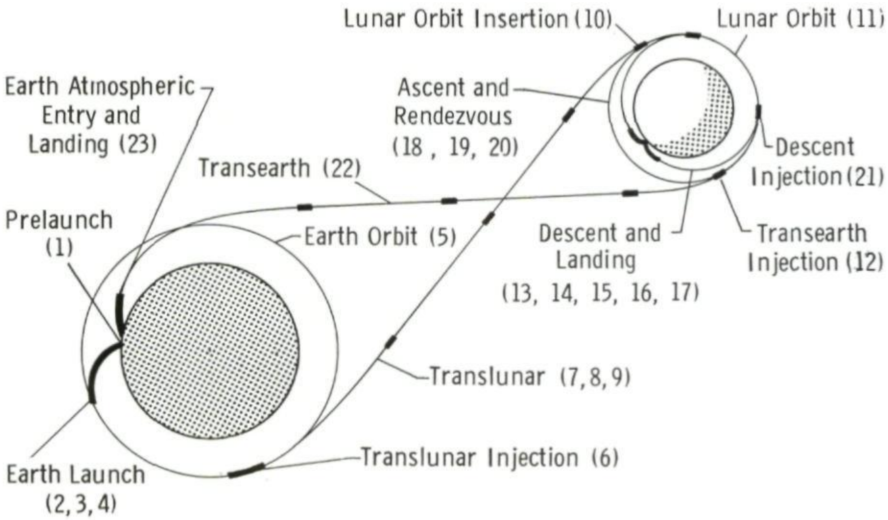

FIG. 2–7 The overall Apollo mission

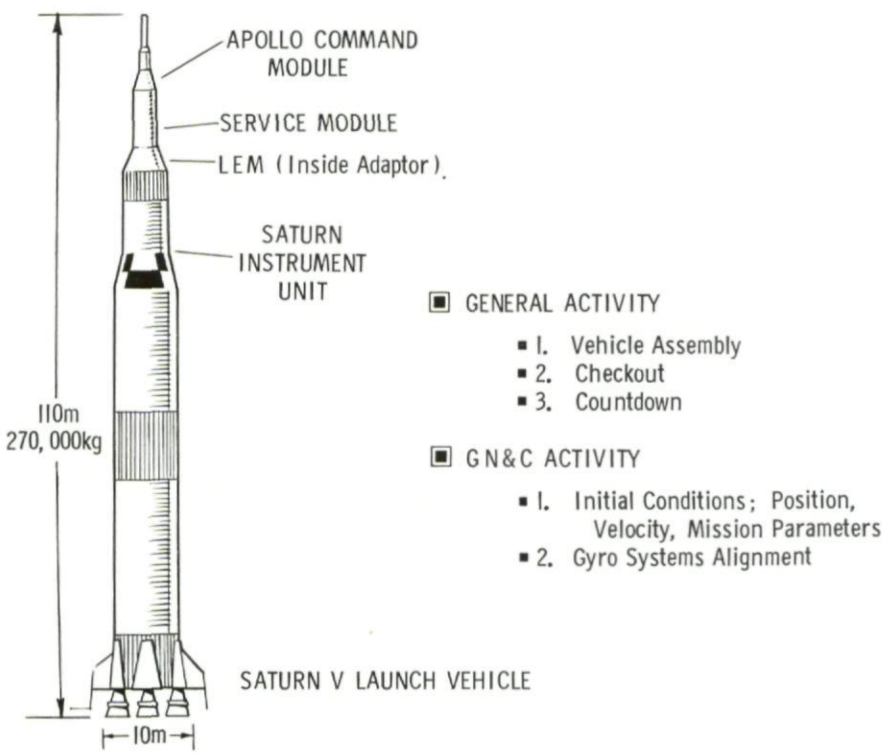

FIG. 2–8 Phase 1 – prelaunch

CHAPTER 2–2

GUIDANCE, NAVIGATION AND CONTROL TASKS IN THE APOLLO MISSION

Much insight into problems of space flight has been gained from the extensive study and hardware development during the last four years in the Apollo program for a manned lunar landing. Using Apollo as an example, specific spacecraft guidance, navigation and control tasks are illustrated in this chapter.

The overall Apollo mission trajectory is summarized in Fig. 2–7. The heavy lines correspond to the short accelerated maneuvers which are separated by the much longer free coasting phases. The trajectory on this figure is purposefully distorted as are also some of the following figures in order to show features of the phases more clearly. The numbers on Fig. 2–7 relate to the following mission phase subdivisions.

The prelaunch phase includes an intensive and intricate schedule of activity to prepare and verify the equipment for flight. Automatic programmed checkout equipment perform the exhaustive tests of the major subassemblies. Testing continues during the final countdown. Activity of interest here concerns the preparation of the two operating sets of guidance equipment for the launch. The Saturn guidance equipment located in the Saturn Instrument Unit will control the launch vehicle. The Apollo guidance equipment, located in the Command Module (CM) where the crew of three lie in their protective couches, will provide a monitor of Saturn guidance during launch. A third set of guidance equipment, located in the Lunar Excursion Module (LEM) which is inside the protective LEM adapter, is used later near the moon.

Ground support equipment communicates directly with the Saturn and Apollo CM guidance computers to read in initial conditions and mission and trajectory constants as they vary as a function of countdown status. Both sets of inertial guidance sensors are aligned to a common vertical and launch azimuth framework. The vertical is achieved in both cases by erection loops sensing gravity. Azimuth in Saturn is measured optically from the ground and controlled by means of an adjustable prism mounted on the stable member. Azimuth in Apollo is aligned optically on board by the astronauts and held by gyro compassing action. During countdown both systems are tied to an earth frame reference. Just before liftoff both systems respond to signals to release the coordinate frames simultaneously from the earth reference to the non-rotating inertial reference to be used during boost flight.

During first stage flight the Saturn guidance system controls the vehicle by swiveling the outer four rocket engines. During the initial vertical flight the vehicle is rolled from its launch azimuth to the flight path azimuth. Following this the Saturn guidance controls the vehicle in an open loop preprogrammed pitch designed to pass safely through the period of high

aerodynamic loading. Inertial sensed acceleration signals are not used during this phase to guide to desired path but rather the lateral accelerometers help control the vehicle to stay within the maximum allowed angle of attack. Stable control is achieved in overcoming the effects of flexure bending, fuel slosh and aerodynamic loading by the use of properly located sensors and control networks.

Both the Saturn and Apollo Command Module guidance systems continuously measure vehicle motion and compute position and velocity. In addition the Apollo system compares the actual motion history with that to be expected from the Saturn control equations so as to generate an error display to the crew. This and many other sensing and display arrangements monitor the flight. If abort criteria indicate the crew can fire the launch escape system. This is a rocket attached on a tower to the top of the command module to lift it rapidly away from the rest of the vehicle. Parachutes are later deployed for the landing. In a normal flight the first stage is allowed to burn to near complete fuel depletion as sensed by fuel level meters before first stage engine shutdown is commanded.

Shortly after the initial fuel settling ullage and the firing of second stage thrust, the aerodynamic pressure reduces to zero as the vehicle passes out of the atmosphere. At this time the launch escape system is jettisoned. Aborts now, if necessary, would normally be accomplished using the Apollo Service Module propulsion to accelerate the Command Module away from the rest of the vehicle. Since the problems of aerodynamic structure loading are unimportant in second stage flight, the Saturn guidance system now steers the vehicle towards the desired orbital insertion conditions using propellant optimizing guidance equations. Thrust control is achieved by swiveling the outer four engines of the second stage.

During second stage flight the Apollo Command Module guidance system continues to compute vehicle position and velocity. Also this system computes any of several other possible parameters of the flight to be displayed to the crew for monitoring purposes. In addition, the free-fall time to atmospheric entry and the corresponding entry peak acceleration are displayed to allow the crew to judge the abort conditions existing.

The third Saturn stage or SIVB has a single engine for main propulsion which is gimballed for thrust vector control. Roll control is achieved by use of the SIVB roll attitude control thrusters. The Saturn guidance system continues to steer the vehicle to orbital altitude and speed. When orbit is achieved the main SIVB propulsion is shut down.

During second and third stage boost flight the Apollo Command Module has the capability, on astronaut option, to take over the SIVB stage guidance function if the Saturn guidance system indicates failure. If this switchover occurs the mission presumably could be continued. More drastic failures would require an abort using the Service Module propulsion. In this case the Apollo computer is programmed to provide several abort trajectories: (a) immediate safe return to earth, (b) return to a designated landing site or (c) abort into orbit for later return to earth. SIVB engine shutdown occurs about 12 minutes after liftoff at 185 km altitude near circular orbit. The Apollo spacecraft configuration remains attached to the Saturn SIVB stage in earth orbit. The Saturn system controls attitude by on-off commands to

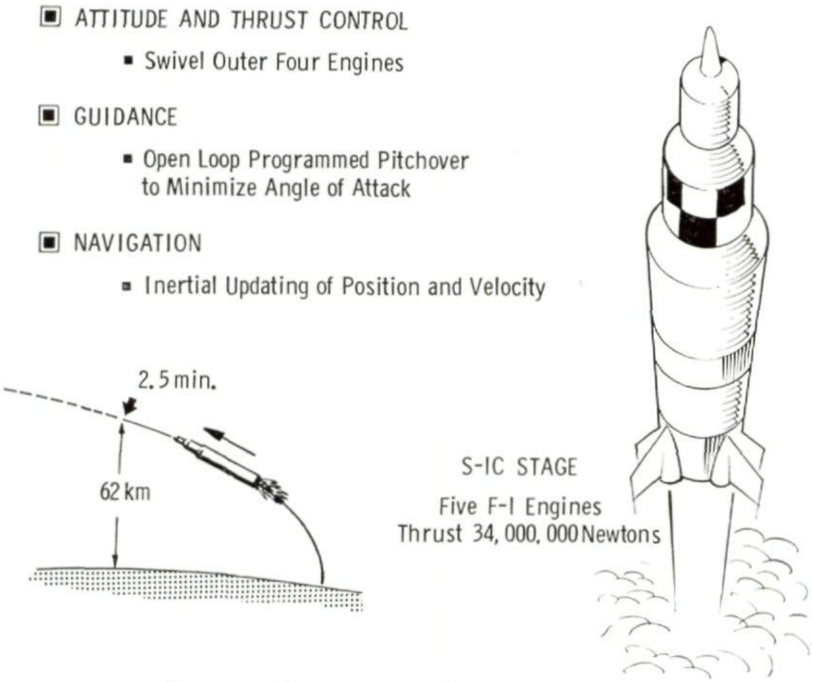

FIG. 2–9 Phase 2 – earth launch – first stage

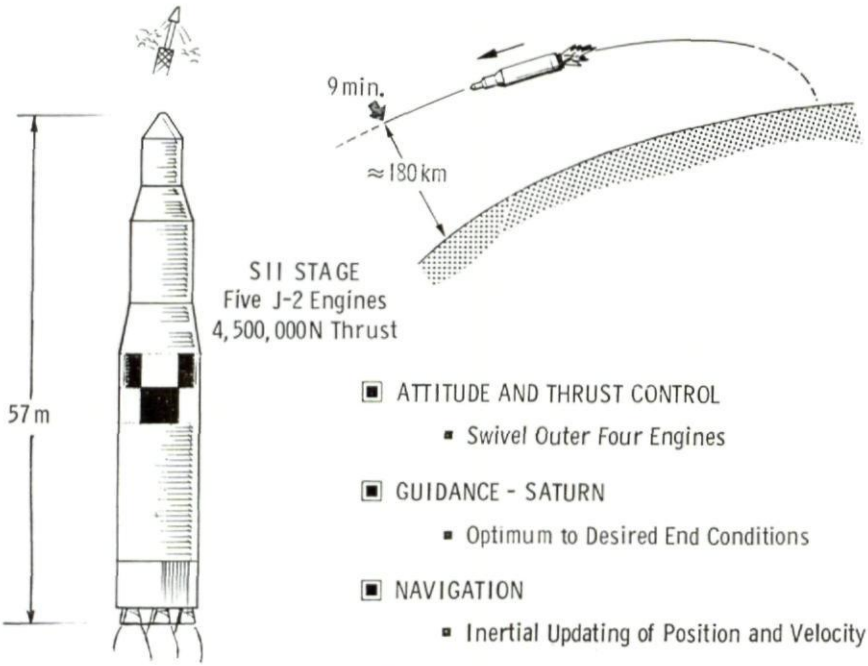

FIG. 2–10 Phase 3 – second stage

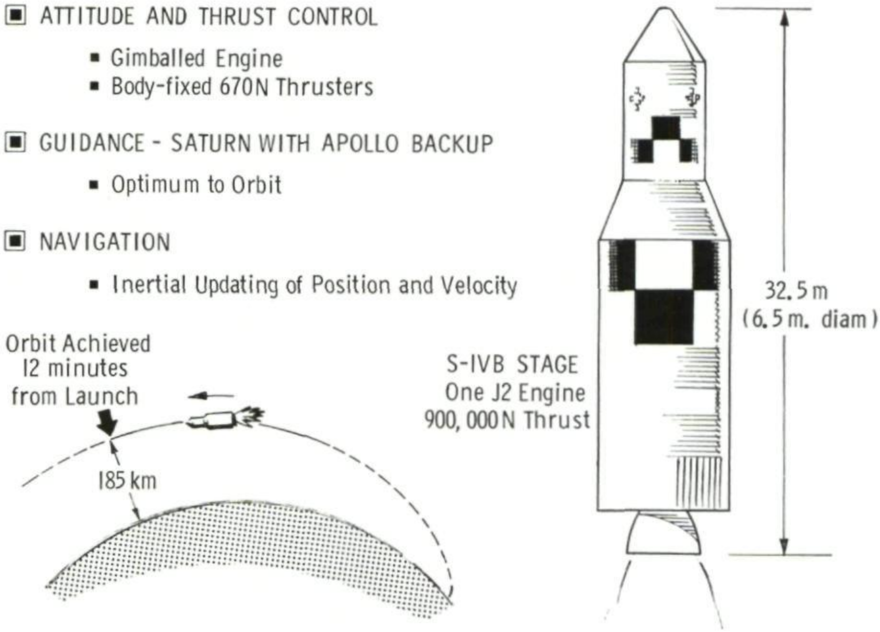

FIG. 2-11 Phase 4 – earth launch – third stage

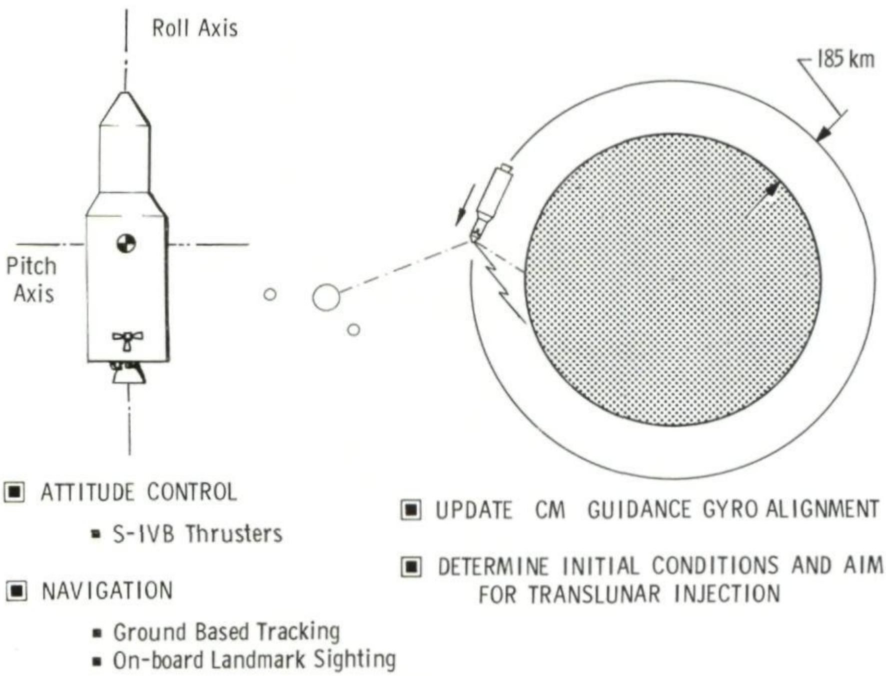

FIG. 2-12 Phase 5 – earth orbit

two of the small fixed attitude thrusters for pitch and to four more shared for yaw and roll.

Ground tracking navigation data telemetered from the Manned Space Flight Network (MSFN) stations is available to correct the position and velocity of the Saturn navigation system and provide navigation data for the Apollo navigation system. In Apollo the crew also can make on-board navigation measurements for on-board determination of the ephemeris by making landmark or horizon direction sightings using a special optical system. The Apollo inertial equipment alignment will also be updated by star sightings with the same optical system. For these measurements the crew has manual command control of attitude through the Saturn system. Normally, limited roll maneuvers are required to provide optical system visibility to both stars and earth. The Apollo on-board navigation measurements include accelerometer measurement of the small thrust occurring during the pressure venting of the cryogenic propellant tanks of the SIVB. Typically, the earth orbital phase lasts for several hours before the crew signals the Saturn system to initiate the translunar injection at the next opportunity.

Translunar injection is performed using a second burn of the Saturn SIVB propulsion, preceeded, of course, by an ullage maneuver using the small thrusters. Saturn guidance and control systems again provide the necessary steering and thrust vector control to the near parabolic velocity which for crew safety considerations puts the vehicle on a so-called "free return" trajectory to the moon. The system aims to this trajectory which ideally is constrained to pass behind the moon and return to earth entry conditions without additional propulsion.

As before, the Apollo guidance system independently generates appropriate parameters for display to the crew for monitoring purposes. It is recognized that a display of a large error by Apollo does not necessarily indicate Saturn system malfunction, because an error in Apollo system operation could instead be the fault. The identification of the failed system may be indicated by another of the available displays or by ground tracking information relayed to the crew. If the Saturn guidance system indicates failure, steering takeover by the Apollo is possible without need for aborting the mission. The translunar injection thrusting maneuver continues for slightly over 5 minutes duration before the SIVB stage is commanded its final shutdown.

The spacecraft configuration injected onto the translunar free-fall path must be reassembled for the remaining operations. The astronaut pilot separates the Command and Service Modules (CSM) from the LEM which is housed inside the adapter in front of the SIVB stage. He then turns around the CSM for docking to the LEM. To do this the pilot has a three-axis left-hand translation controller and a three-axis right-hand rotational controller. Output signals from these controllers are processed to modulate appropriately the firing of the 16 low thrust reaction control jets for the maneuver. The normal response from the translation controller is proportional vehicle acceleration in the indicated direction. The normal response from the rotational controller is proportional to vehicle angular velocity about the indicated axis.

During the separation and turnaround maneuver of the CSM the SIVB

control system holds the LEM attitude stationary. This allows for a simple docking maneuver of the command module to the LEM docking hatch. The SIVB, Saturn instrument unit and LEM adapter are staged to leave the Apollo spacecraft in the translunar configuration. Final docking is complete less than 6.5 hours from liftoff at the launching pad.

Very soon after injection into the translunar free-fall coast phase navigation measurements are made and processed to examine the acceptability of the trajectory. These data will probably indicate the need for an early midcourse maneuver to correct error in the flight path before it propagates with time into larger values which would needlessly waste correction maneuver fuel.

Once this first correction is made – perhaps a couple of hours from injection – the navigation activity on board can proceed at a more leisurely pace. Ground tracking data can be telemetered to the craft any time it is available. Using this ground data and/or on-board sextant type of landmark to star angle measurements the on-board computer can correct the knowledge of the spacecraft state vector – position and velocity. The astronaut navigator can examine with the help of the computer each datum input available – whether from ground tracking telemetered to the craft or taken on board – to see how it could change the indicated position and velocity before he accepts it into the computer state vector correction program. In this way the effects of mistakes in data gathering or transmission can be minimized.

The navigator will examine periodically the computer's estimate of indicated uncertainty in position and velocity and the estimate of indicated velocity correction required to improve the present trajectory. If the indicated position and velocity uncertainty is suitably small and the indicated correction is large enough to be worth the effort in making, then the crew will prepare for the indicated midcourse correction. Each midcourse velocity correction will first require initial spacecraft orientation to put the estimated direction of the thrust axis along the desired acceleration direction. Once thrust direction is aimed, the rocket is fired under measurement and control of the guidance system. Use of the guidance system requires that the inertial measurement system be aligned. This latter is done by optical star direction sightings.

Typical midcourse corrections are expected to be of the order of 10 meters/sec. If the required correction happens to be very small, it would be made by using the small reaction control thrusters. Larger corrections would be made with a short burn of the main service propulsion rocket. It is expected that about three of these midcourse velocity corrections will be made on the way to the moon. The direction and magnitude of each will adjust the trajectory so that the moon is finally approached near a desired plane and pericynthian altitude which provides for satisfactory conditions for the lunar orbit insertion.

For lunar orbit insertion, as with all normal thrusting maneuvers using the service propulsion of the spacecraft, the inertial guidance system is first aligned using star sightings. Then the system generates initial conditions and steering parameters based upon the navigation measure of position and velocity and the requirements of the maneuver. The guidance initiates engine turn-on, controls the direction of the acceleration appropriately and signals engine shutdown when the maneuver is complete. The lunar orbit insertion maneuver is intended to put the spacecraft in a near circular orbit of

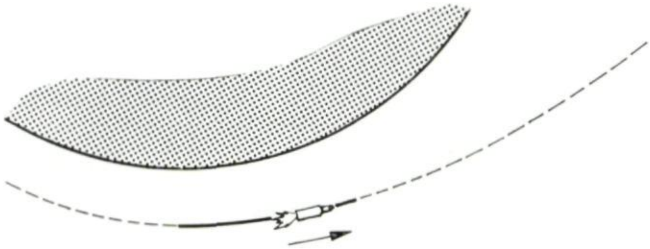

- THRUST
  - Second Burn of S-IVB
- GUIDANCE - SATURN WITH APOLLO BACKUP
  - Steer Into "Free-Return" Trajectory to the Moon
- NAVIGATION
  - Inertial Update of Position and Velocity

FIG. 2–13 Phase 6 – translunar injection

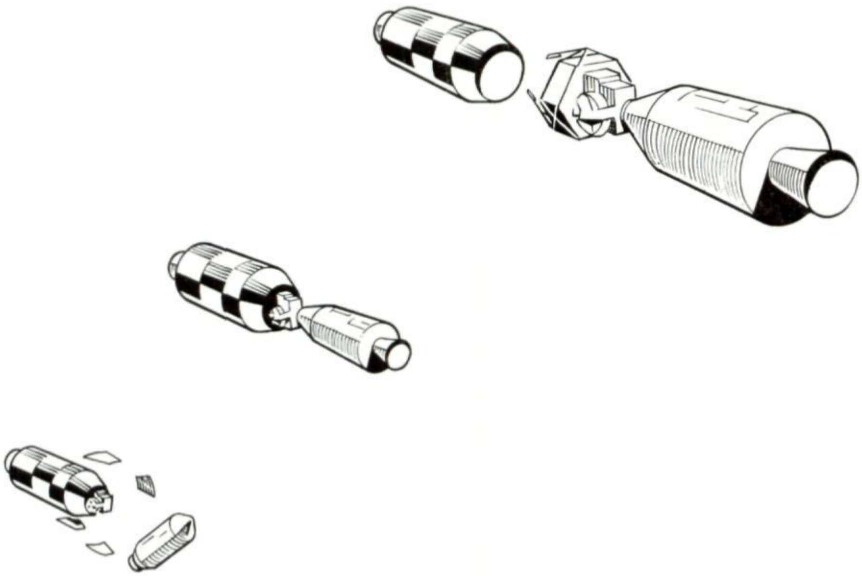

FIG. 2–14 Phase 7 – transposition and docking

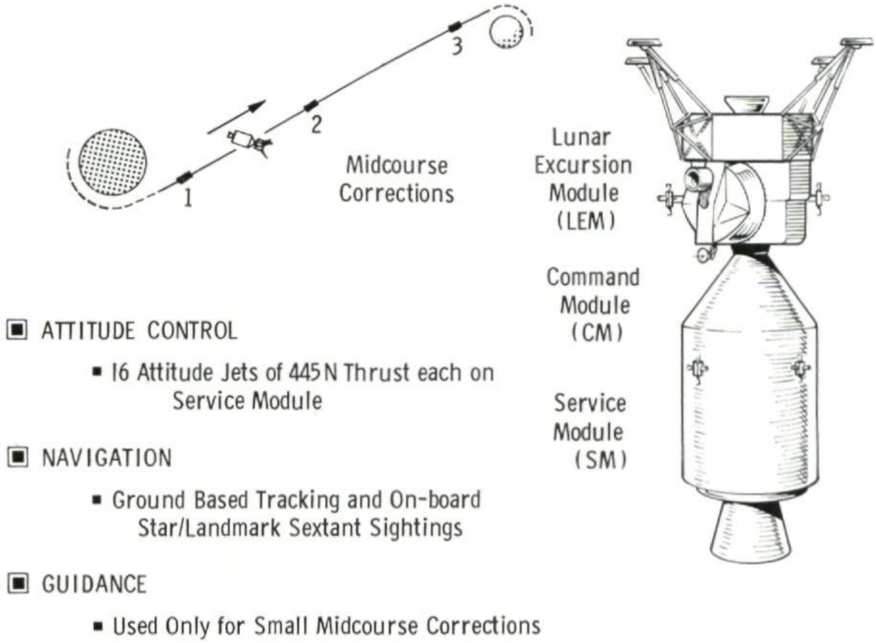

FIG. 2–15 Phase 8 – translunar coast

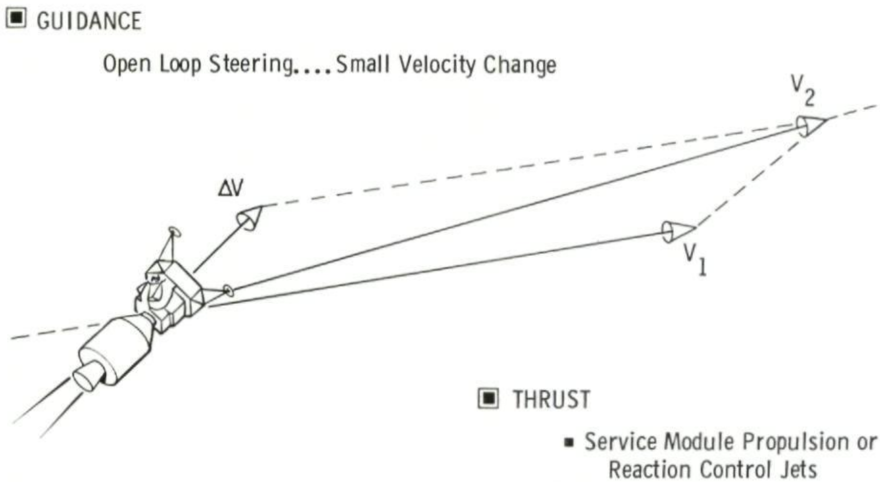

FIG. 2–16 Phase 9 – midcourse correction

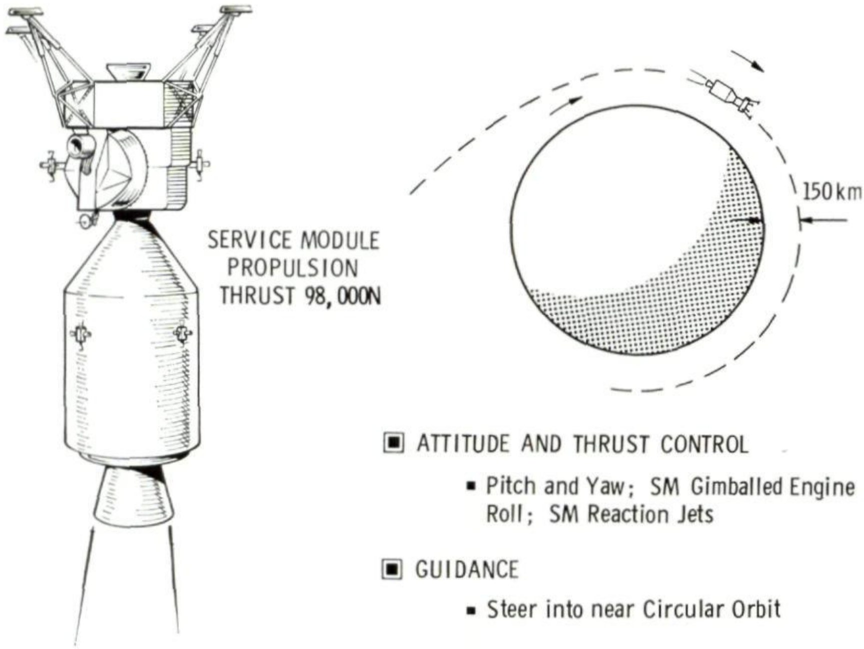

FIG. 2–17 Phase 10 – lunar orbit insertion

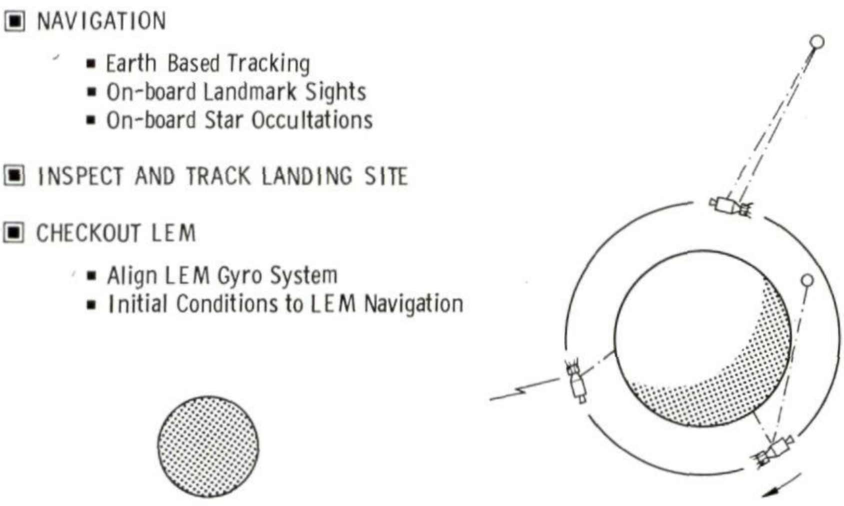

FIG. 2–18 Phase 11 – lunar orbit

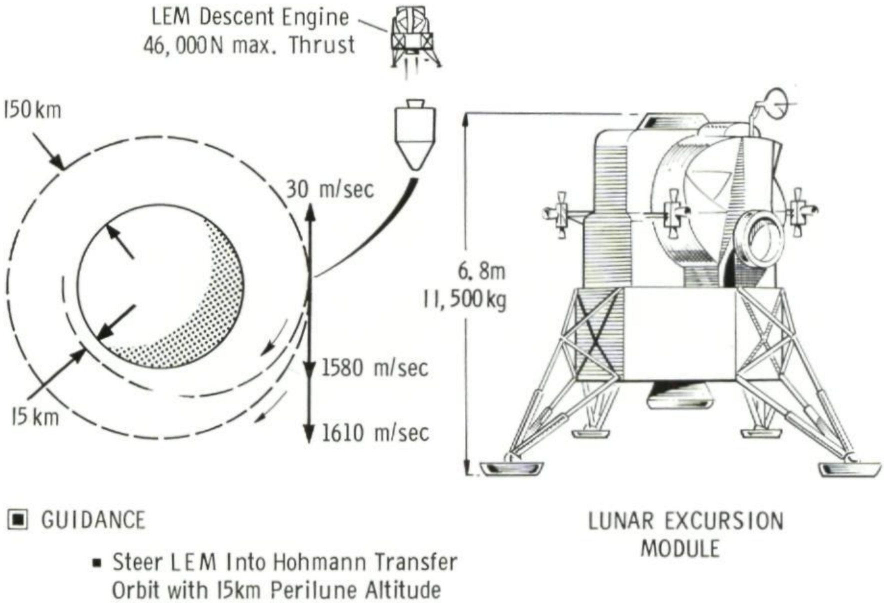

FIG. 2–19 Phase 12 – LEM descent orbit injection

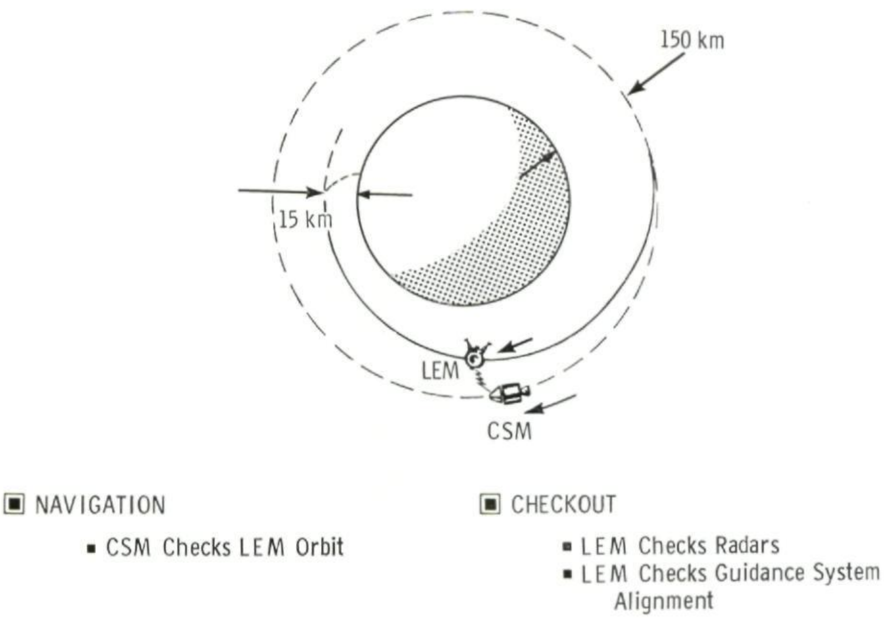

FIG. 2–20 Phase 13 – LEM descent orbit coast

approximately 150 km altitude. The plane of the orbit is selected to pass over the landing region on the front of the moon.

In lunar orbit, navigation measurements are made to update the knowledge of the actual orbital motions. The navigation measurement data are processed in the computer, using much of the same program as in the translunar phase. Several sources of data are possible. Direction measurement to lunar landmarks or horizons and earth based radio tracking telemetered data are similar to the measurements used earlier in the flight in earth orbit. Because of the lack of lunar atmosphere occultation time events of identified stars by the lunar limb are easily made measurements. Orbital period measurements are available by timing successive passages over the same terrain feature or successive occultations of the same star. Sufficient measurements must be made to provide accurate initial conditions for the guidance system in the LEM for its controlled descent to the lunar surface. Before separation of the LEM this landing area is examined by the crew, using the magnifying optics in the command module. At this time, direction measurements to a particular surface feature can relate a desired landing site or area to the existing indicated orbital ephemeris in the computer. These particular landing coordinates become part of the LEM guidance system initial conditions received from the command module.

After two of the crew transfer to the LEM and separate from the Command and Service Module (CSM), the remaining man in the CSM will continue orbital navigation as necessary to keep sufficient accuracy in the indicated CSM position and velocity. The LEM guidance system will have been turned on and received a checkout earlier in lunar orbit before separation and received initial conditions from the CSM. Starting about twenty minutes before initiation of the LEM descent injection maneuver the vehicles are separated, the LEM guidance system receives final alignment from star sightings and the attitude for the maneuver is assumed. The maneuver is made using the LEM descent stage propulsion under control of the LEM guidance system. During the short burn, the throttling capability of the descent engine is exercised as a check of its operation. The maneuver is a 30 meter per second velocity change to reduce the velocity from the 1 600 meter/sec orbital velocity for a near Hohmann transfer to a 15 km altitude pericynthian which is is timed to occur at a range of about 370 kilometers short of the final landing area.

During the free-fall phases of the LEM descent, the CSM can make tracking measurements of the LEM direction for confirmation of LEM orbit with respect to the CM. For that part of the trajectory in the front of the moon the earth tracking can also provide an independent check. The LEM, during appropriate parts of this coasting orbit, will check the operation of its radar equipment. The directional tracking and ranging operation of the Rendezvous Radar is checked against the radar transponder on the CSM. This also provides data to the LEM computer for an added descent orbit check. At lower altitudes the LEM landing radar on the descent stage is operated for checks using the moon surface return. Alignment updating of the LEM guidance system can be performed if desired. The CM from orbit can monitor this phase of the LEM descent using the tracking systems and on-board computer.

As pericynthian is approached, the proper LEM attitude for the powered descent phase is achieved by signals from the guidance system. This phase starts at the 15 kilometer altitude pericynthian of the descent coast phase. The descent engine is re-ignited and this velocity and altitude reducing maneuver is controlled by the LEM inertial guidance system. The descent stage engine is capable of thrust level throttling over the range necessary to provide initial braking and to provide controlled hover above the lunar surface. Engine throttle setting is commanded by the guidance system to achieve proper path control, although the pilot can override this signal if desired.

Thrust vector direction control of the descent stage is achieved by a combination of body-fixed reaction jets and limited gimballing of the engine. The engine gimbal angles follow guidance commands in a slow loop so as to cause the thrust direction to pass through the vehicle center of gravity. This minimizes the need for continuous fuel wasting torques from the reaction jets. During all phases of the descent the operations of the various systems are monitored. The mission could be aborted for a number of reasons. If the primary guidance system performing the descent control is still operating satisfactorily, it would control the abort back to rendezvous with the CSM. If the primary guidance system has failed, a simple independent abort guidance system can steer the vehicle back to conditions for rendezvous.

For normal mission, the braking phase continues until the altitude drops to about 4 kilometers or so. Then guidance control and trajectory enter the final approach operation. One significant feature of this phase is that the controlled trajectory is selected to provide visibility of the landing area to the LEM crew. The vehicle attitude, descent rate and direction of flight are all essentially constant, so that the landing point being controlled by the guidance appears fixed with relation to the window. A simple reticle pattern in the window, as shown, indicates this landing point in line with the number indicated by computer display. The pilot may observe that the landing point being indicated is in an area of unsatisfactory surface features with relation to other areas nearby. He can then elect to select a new landing point for the computer control by turning the vehicle about the thrust axis until the reticle intersects the better area. He then hits a "mark" button to signal the computer, reads the reticle number which is in line with this area into the computer and then allows the guidance to redirect the path appropriately. This capability allows early change of landing area and fuel efficient control to the new area which otherwise might have to be performed wastefully later during hover.

Automatic guidance control during the terminal phase uses weighted combinations of inertial sensing and landing radar data, the weighting depending upon expected uncertainties in the measurements. The landing radar include altitude measurement and a three-beam doppler measurement of three components of LEM velocity with respect to the lunar surface. At any point in the landing the pilot can elect to take over partial or complete control of the vehicle. For instance, one logical mixed mode would have altitude descent rate controlled automatically by modulation of the thrust magnitude and pilot manual control of attitude for maneuvering horizontally.

The final approach phase will end near the lunar surface, and the spacecraft will enter a hover phase. This phase can have various possibilities of

■ THRUST VECTOR CONTROL

- 3 - Axis Control Using Reaction Jets
- Engine Gimballed for Trim Correction

■ ENGINE

- Near Full Throttle Under Guidance System Control

■ GUIDANCE

- Inertial Sensing with Some Radar data at Lower Altitudes

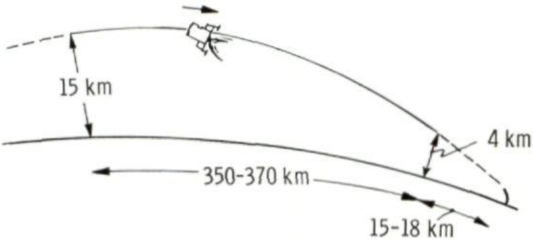

Fig. 2–21 Phase 14 – LEM powered descent braking phase

■ ENGINE

- Throttled to near 2 meters / sec / sec Under Guidance Control

■ GUIDANCE - MIXED INERTIAL AND RADAR SENSING

- Under Automatic Control With Constant Attitude
- Astronaut May Redesignate Landing Site

or

- Various Levels of Manual Control

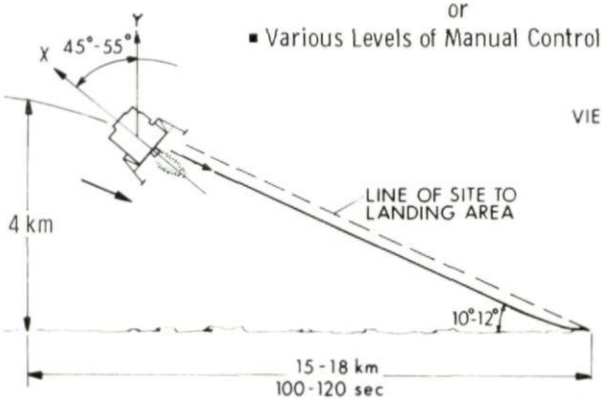

FIG. A

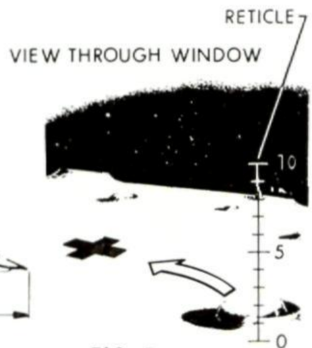

FIG. B

Fig. 2–22 Phase 15 – LEM powered descent final approach

■ GUIDANCE

- Various Mixtures of Manual and Automatic
- Radar and Visual Correction Until Surface Obscured by Dust, Then...
- All Inertial For Touchdown at Low Velocity

■ TRAJECTORY

- Mission Groundrules and Pilot Option

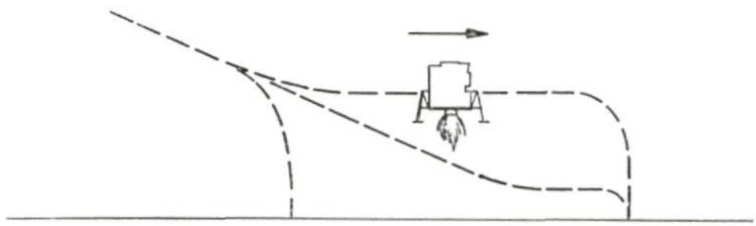

FIG. 2–23 Phase 16 – landing and touchdown

■ ACTIVITY

- Checkout Systems
- Exploration, Experimentation, etc

■ GUIDANCE AND NAVIGATION

- Track CSM Overhead
- Align Guidance for Ascent

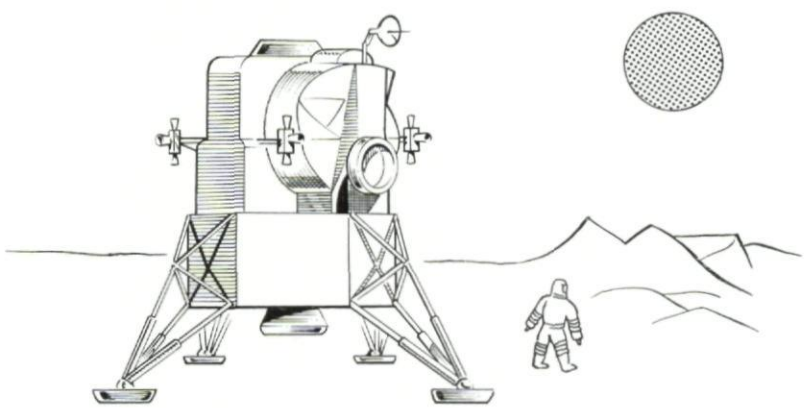

FIG. 2–24 Phase 17 – lunar surface operation

initial altitude and forward velocity depending upon mission groundrules, pilot option and computer program yet to be decided. Descent stage fuel allowance provides for approximately two minutes of hover before touchdown must be accomplished or abort on the ascent stage initiated. The crew will make final selection of the landing point and maneuver to it either by tilting the vehicle or by operating the reaction jets for translation acceleration. The inertial system altitude and velocity computation is updated by the landing radar so that as touchdown is approached good data are available from the inertial sensors as the flying dust and debris caused by the rocket exhaust degrade radar and visual information. Touchdown must be made with the craft near vertical and at sufficiently low velocity.

The period on the moon will naturally include considerable activity in exploration, experimentation and sample gatherings. Also during this stay time LEM spacecraft systems will be checked and prepared for the return. The ephemeris of the CSM in orbit is continually updated and the information relayed to the LEM crew and computer. The LEM rendezvous radar also can track the CSM as it passes overhead to provide further data upon which to base the ascent guidance parameters. The inertial guidance gets final alignment from optical star direction sightings prior to the start of ascent. The vertical components of this alignment could also be achieved by accelerometer sensing of lunar gravity in a vertical erection loop. Liftoff must be timed to achieve the desired trajectory for rendezvous with the CSM.

Normal direct ascent launches are timed and controlled to cutoff conditions resulting in a coasting intercept with the CSM. Emergency launches from the lunar surface can be initiated at any time by entering a holding orbit at low altitude until the phasing is proper for transfer to the CSM. A desirable constraint on all ascent powered maneuvers as well as abort maneuvers during the landing is that the following coasting trajectory be near enough circular so as to be clear of intersection with the lunar surface. This is a safety consideration to allow for the possibility of failure of the engine to restart. If the LEM engine thus fails, the LEM can then safely coast until a pickup maneuver by the CSM is accomplished.

The initial part of the ascent trajectory is a vertical rise followed by pitch-over as commanded by the guidance equations. The ascent engine maneuvers are under the control of the LEM inertial guidance system. The engine has a fixed mounted nozzle. Thrust vector control is achieved by operation of the sixteen reaction jets which are mounted on the ascent stage. The engine thrust cannot be throttled, but the necessary signals from guidance will terminate burning when a suitable rendezvous coast trajectory is achieved.

If the launch point lies in the plane of the CSM orbit, efficient ascending coasting trajectories would cover 180 degrees central angle to the rendezvous point. Several effects will cause the launch point to be removed from the CSM plane resulting in trajectories either somewhat more or somewhat less than 180 degrees. Immediately after injection into the ascending coasting rendezvous trajectory, the rendezvous radar on the LEM will start making direction and range measurements to the CSM upon which the LEM computer will base its navigation using a process almost identical to that used in navigation of the midcourse phase between earth and moon. From this navigation the LEM computer will determine small velocity corrections

to be made by LEM reaction control jets to establish the collision or intercept trajectory with the CSM more accurately. These corrections will be made as often as the radar based navigation measurements justify. The coasting continues until the range to the CSM is reduced to approximately 10 kilometers when the terminal rendezvous phase begins.

The terminal rendezvous phase consists of a series of braking thrust maneuvers under control of the LEM guidance system which uses data from its inertial sensors and the rendezvous radar. The objective of these operations is to reduce the velocity of the LEM relative to the CSM to zero at a point near the CSM. This leaves the pilot in the LEM in a position to initiate a manual docking with the CSM using the translation and rotation control of the LEM reaction jets. Although these maneuvers would normally be done with the LEM, propulsion or control problems in the LEM could require the CSM to take the active role. After final docking the LEM crew transfer to the CSM and the LEM is then jettisoned and abandoned in lunar orbit.

Navigation measurements made while in lunar orbit determine the proper initial conditions for transearth injection. These are performed as before using on-board and ground-based tracking data as available. The guided transearth injection maneuver is made normally under the control of the primary inertial guidance system. Several backup means are available to cover possible failures in the primary system. The injection maneuver is controlled to put the spacecraft on a free-fall coast to satisfactory entry conditions near earth. The time of midcourse transearth coast must be adjusted by the injection to account for earth's rotation motion of the recovery area and as limited by the entry maneuver capability.

The transearth coast is very similar to the translunar coast phase. During the long coasting phases going to and from the moon the systems and crew must control the spacecraft orientation as required. Typical midcourse orientation constraints are those to assure the high gain communication antenna is within its gimbal limits to point to earth or that the spacecraft attitude is not held fixed to the local heating effect of the sun for too long a period. During the long periods of free-fall flight going to and from the moon when the inertial measurement system is not being used for controlling velocity corrections, the inertial system is turned off to conserve power supply energy.

On-board and ground-based measurements provide for navigation upon which is based a series – normally three – of midcourse correction maneuvers during transearth flight. The aim point of these corrections is the center of the safe earth entry corridor suitable for the desired landing area. This safe corridor is expressed as a variation of approximately ± 32 kilometers in the vacuum perigee. A too-high entry could lead to an uncontrolled skipout of the atmosphere; a too-low entry might lead to atmospheric drag accelerations exceeding the crew tolerance. After the final safe entry conditions are confirmed by the navigation before entry phase starts, the inertial guidance is aligned, the Service Module is jettisoned and the initial entry attitude of the Command Module is achieved.

Initial control of entry attitude is achieved by guidance system commands to the twelve reaction jets on the command module surface. As the atmo-

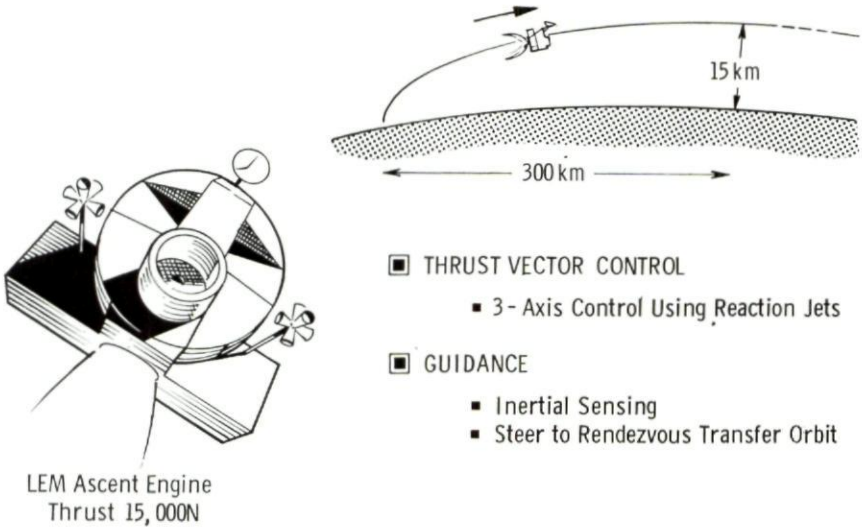

FIG. 2-25 Phase 18 – LEM ascent

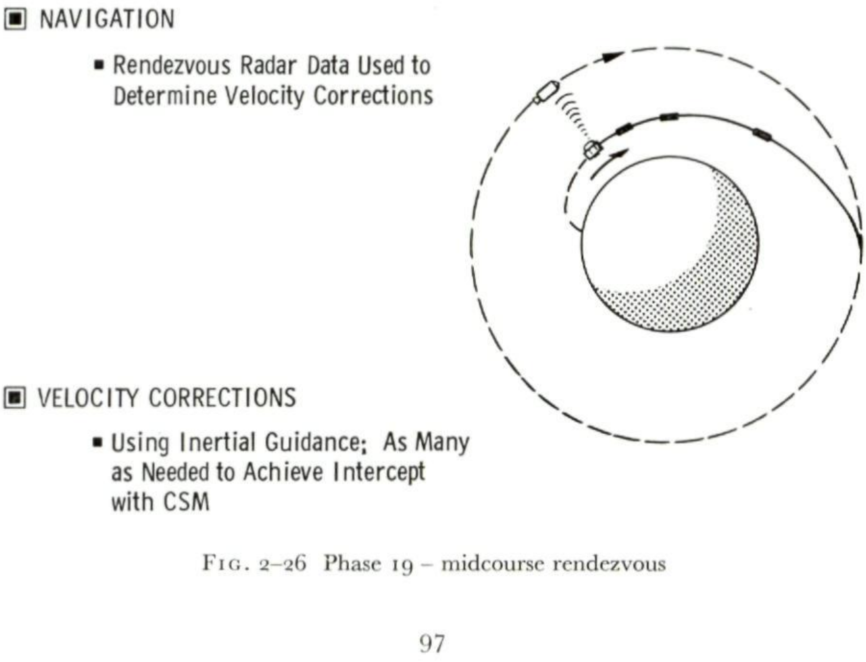

FIG. 2-26 Phase 19 – midcourse rendezvous

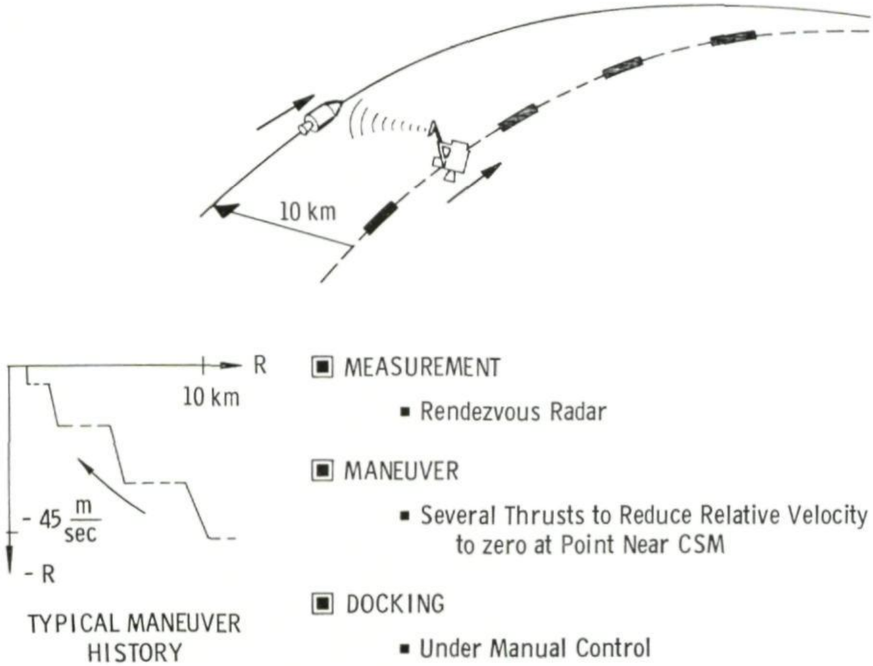

FIG. 2–27 Phase 20 – terminal rendezvous and docking

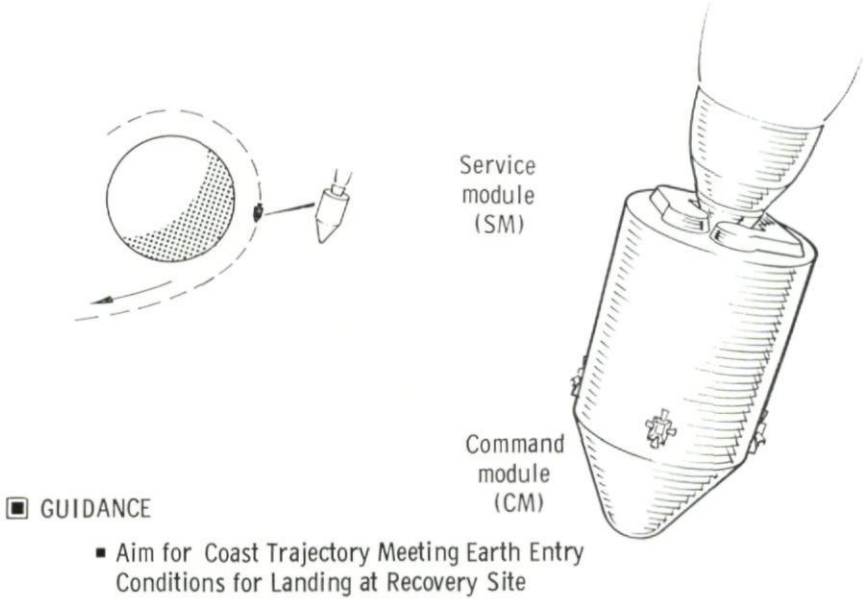

FIG. 2–28 Phase 21 – transearth injection

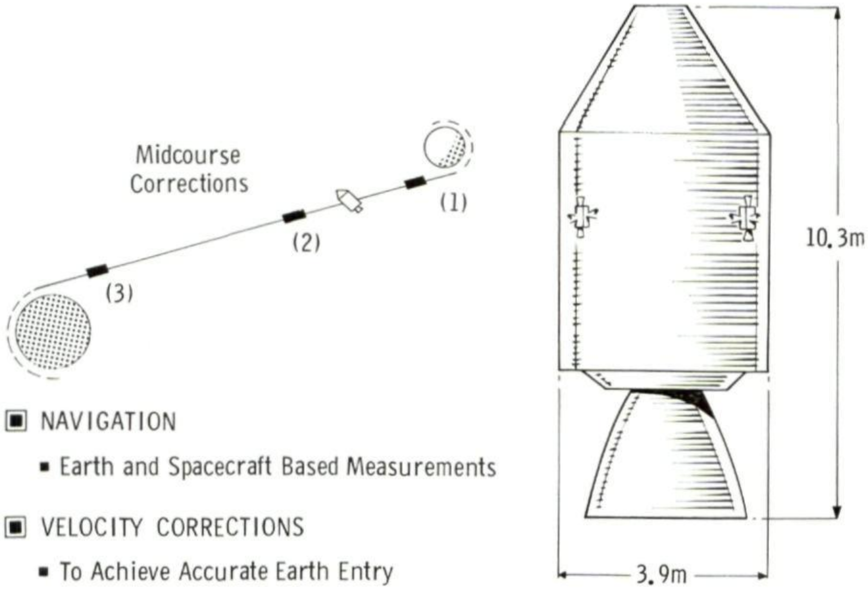

FIG. 2–29 Phase 22 – transearth coast

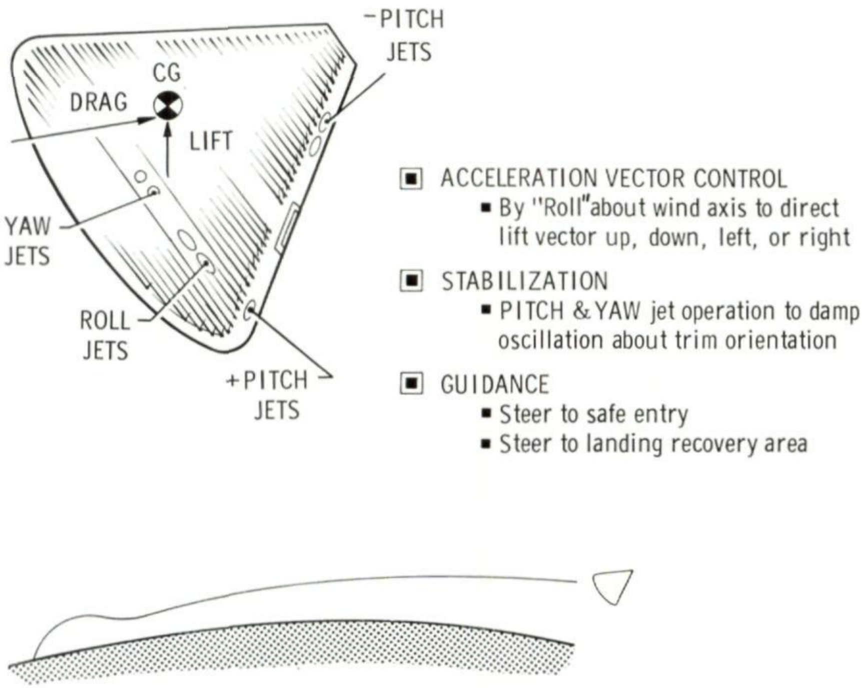

FIG. 2–30 Phase 23 – earth atmospheric entry

sphere is entered, aerodynamic forces create torques determined by the shape and center of mass location. If initial orientation was correct, these torques are in a direction towards a stable trim orientation with heat shield forward and flight path nearly parallel to one edge of the conical surface. The control system now operates the reaction jets to damp out oscillation about this trim orientation. The resulting angle of attack of the entry shape causes an aerodynamic lift force which can be used for entry path control by rolling the vehicle about the wind axis under control of the guidance system. Range control is achieved by rolling so that an appropriate component of that lift is either up or down as required. Track or across range control is achieved by alternatively choosing as required the side the horizontal lift component appears.

The early part of the entry guidance is concerned with the safe reduction of the high velocity through the energy dissipation effect of the drag forces. Later at lower velocity the objective of controlling to the earth recovery landing area is included in the guidance. This continues until velocity is reduced and position achieved for deployment of a drag parachute. Final letdown is normally by three parachutes to a water landing.

CHAPTER 2–3

GUIDANCE, NAVIGATION AND CONTROL INSTRUMENTATION IN APOLLO

The choice of sensors and data processors for guidance, navigation and control used in Apollo is governed by the nature of the spacecraft and its mission as described in the previous chapter. Two Apollo design guidelines will be mentioned at the outset.

First, although full use will be made of all earth-based help, the spacecraft systems are designed to have the capability of completing the mission and returning without the use of earth-based tracking data or computation support. This provides protection against critical lack of earth coverage or failure in communication. However, earth-based data will be available most of the time which will be supported by measurements from the on-board equipment.

The second guideline recognizes the diverse nature of the mission and the variations in spacecraft configuration. The guidance, navigation and control equipment is designed to provide a great deal of flexibility in its utilization. This is manifest in the fact that identical subsystems are used in the two independent systems controlling the command module and the lunar excursion module. This flexibility extends also to the development of the necessary operation equations expressed in the flight computer programs. The unified approach of these to handle the various thrusting and coasting computation chores with a universal compact set of programs is described in Part 3. In this chapter we will describe the selection and design of hardware.

INERTIAL MEASUREMENT SYSTEM

The choice of inertial guidance over radio command guidance can be easily justified . . . perhaps most dramatically by recognition of the velocity change maneuvers which necessarily must occur behind the moon. Here the guidance measurements must be made by on-board sensors during the lunar orbit insertion and escape maneuvers out of sight of the earth where ground data are not available. Even were it not for the fact that the earth is blind with respect to these maneuvers, it is extremely doubtful that radio command could function for large velocity change maneuvers at lunar distances.

The choice of inertial guidance mechanization might not be so obvious. The two major configurations for inertial measurements are: (a) gyro stabilized gimbal-mounted platform and (b) vehicle frame mounted sensors. Each has advantages.

The gyro stabilized gimballed platform has had many years of success and experience gained primarily by its use in guidance of military ballistic missiles. Its superior performance is largely due to the isolation of the gyros and accelerometers provided by the gimbals and their servos. Further, the outputs are in a convenient form; vehicle attitude Euler angles appear

STABILISED PLATFORM

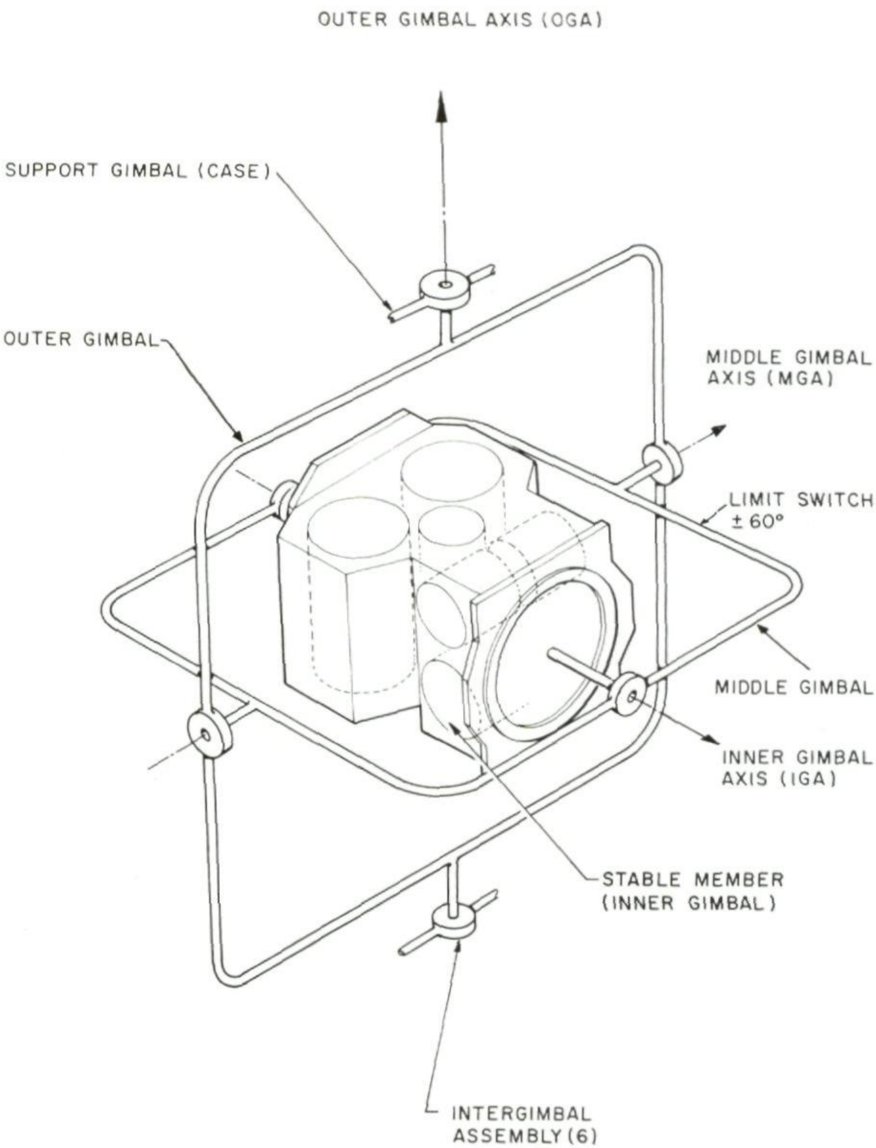

FIG. 2–31 Schematic of the inertial measurement unit

directly as the angles of the gimbals and acceleration measurement appears directly as components in the non-rotating coordinate frame of the stable member "platform".

Alternately, the vehicle frame or body-mounted inertial sensors offer promise of dramatic savings in size, weight and convenience in mounting. Unlike the gyros on the gimballed system which merely must indicate the small deviations from initial attitude for closed loop gimbal control, the body-mounted gyros must measure precisely the whole angular velocity experienced by the vehicle. Moreover, problems are introduced in achieving good gyro and accelerometer performance because of this large angular velocity the units must tolerate about all axes. Finally the outputs are not always in a direct useful form. Angular orientation of the vehicle is indicated only by properly transforming and integrating the body-fixed coordinates of angular motion indicated by the gyros into either an Euler angle set or a matrix of direction cosines. With either of these, the body-mounted accelerometer signals can be resolved from the rotating spacecraft coordinates into an inertial frame. All these calculations require a computer of considerable speed and accuracy to prevent accumulation of excessive error.

The choice made in Apollo for both the Command Module and LEM spacecrafts was the use of the gimbal stabilized member mounting of the sensors for the primary systems. The superior demonstrated performance provides a conservative margin of safety in economical use of rocket fuel for the major mission completion maneuvers. The secondary backup or abort guidance systems in each spacecraft, however, capitalize upon the size and convenient installation advantages of body-mounted sensors. Here the more modest performance is quite ample for the crew safety abort maneuvers in case of primary guidance system failure.

The Apollo primary guidance gimbal system – or IMU for Inertial Measurement Unit – is shown schematically in Fig. 2–31. This IMU is seen to carry three single-degree-of-freedom gyros which provide necessary error signals to stabilize in space the orientation of the inner member by servo drives on each axis. There are three of these rotational axes of the gimbal system as shown in the figure. A three degree of gimbal system such as this can present problems due to a phenomena called "gimbal lock". Gimbal lock would occur when the outer axis is carried by spacecraft motion to be parallel to the inner axis. In this position, all three axes of gimbal freedom lie in a plane and no axis is in a direction to absorb instantaneously rotation about an axis perpendicular to this plane. Thus, at gimbal lock the inner stable member can be pulled off its space alignment. Even though a three-degree-of-freedom gimbal system allows geometrically any relative orientation, the required outer gimbal angular acceleration needed at gimbal lock to maintain stabilization will exceed servo capability.

One direct solution to gimbal lock problems is to add a fourth gimbal and axis of freedom which can be driven so as to keep the other three axes from getting near a common plane. However, the cost in complexity and weight for a fourth gimbal is considerable. Fortunately, in Apollo the operations with the IMU are such that gimbal lock can be easily avoided, and a simple three-degree-of-freedom gimbal system is entirely satisfactory. This will be made clear in the following paragraph.

FIG. 2–32 Inertial measurement unit for system 600F (LEM functional)

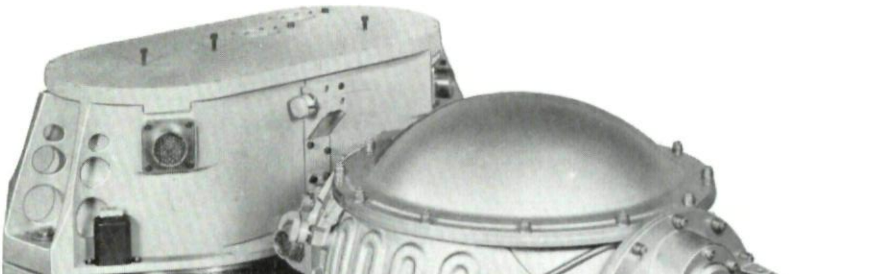

FIG. 2–33 Optics (left) and IMU (right) on navigation base

The Apollo IMU will normally be turned off during all long coasting periods not requiring its use. This is done primarily to save power and corresponding fuel cell battery reactant. (Reactant savings of the order of 20 kilograms have been estimated.) For this reason, the guidance system provides for in-flight inertial system alignment against star references before the start of each accelerated phase of the mission. This allows the inner stable member alignment to be chosen for each use in the most logical orientation. Simplifications can result in the computer generation of steering commands if the "X" accelerometer axis on the stable member is aligned in some direction near parallel to the expected thrust (or entry atmospheric drag). This happens also to be optimum with respect to inertial sensor measurement error effects in velocity measurement. Since the "X" accelerometer is perpendicular to the inner gimbal axis, the direction of this inner axis can be chosen as required. For each mission phase involving rocket burning or atmospheric drag, the trajectory and the thrust or drag lie fairly close to some fixed plane. The inner gimbal axis is them aligned somewhere nearly perpendicular to this plane. All required large maneuvers result mostly in inner gimbal motion, thus avoiding the difficulty of approaching gimbal lock associated with large middle gimbal angles. Finally, because large roll maneuvers are desirable (for instance during entry for the Command Module) the outer gimbal axis is mounted to the spacecraft along or near the roll axis so that no restriction on roll maneuver ever exists.

Because the details of the design and operation of the critical inertial sensors – gyros and accelerometers – to be mounted on the stable member of the gimbal system are of particular importance and interest, this subject is covered separately in Part 4. However, an overall view of the inertial measurement unit is shown in Fig. 2–32. In this photograph the spherical gimbal halves and case cover are removed to show the appearance of the components mounted on the stable member and on the axes of the gimbals.

INERTIAL SYSTEM ALIGNMENT

As mentioned above, the inertial measurement system is turned off during the longer free-fall coasting periods to conserve power supply energy. Even were it not for this, unavoidable drift of the inertially derived attitude reference would require periodic in-flight alignment to the precise orientation required for measuring the large guided maneuvers. The use of identified star directions for the inertial system alignment introduces the question of physically relating the sensed star direction to inertial system stable member orientation. The problem from one point of view could be minimized by mounting the star sensor or sensors directly on the stable member itself. This would impose a most severe limitation of field of view of sky available and puts unpermissible constraints on spacecraft attitudes during the alignment. Even a measured two degree of rotational freedom of the star sensor axis on the stable member limits flexibility and compromises design more than can be tolerated.

The alternative of mounting the star sensor telescope separately near the spacecraft skin where its line of sight can be articulated to cover a large portion of the sky means far more freedom in spacecraft attitude during inertial system alignment. In Apollo a rigid structure called the navigation

base which is strain-free mounted to the spacecraft provides a common mounting structure for the star alignment telescope and the base of the inertial measurement gimbal system. Figure 2–33 shows this arrangement for the Command Module system. (In this photograph the eyepieces of the optics are not attached.) By means of precision angle transducers on each of the axes of the telescope and on each of the axes of the inertial system gimbals, the indicated angles can be processed in the on-board computer to generate the star direction components in inertial system stable member coordinates. This provides the computer with part of the needed stable member orientation data, except no information is provided for rotation about the star line. The use of a second star, at an angle far enough removed from this line, completes the full three-axis stable member orientation measurement. With this information the stable member orientation can then be changed under computer command, if desired, to the orientation optimum for use of the guidance maneuvers.

It is recognized that the above procedure has many sources of error in achieving inertial system alignment. For example, each axis of rotation of the star telescope and the inertial system gimbals must be accurately orthogonal (or at a known angle) with respect to the adjacent axis on the same structure. This is a problem of precision machining, accurate bearings and stable structures. Each angle transducer on each axis of the star telescope and the inertial system gimbals must have minimum error in indicated angle. This includes initial zeroing, transducer angle function errors and digital quantization errors for the computer inputs. By careful attention to minimizing each of these and other error sources, probable Apollo inertial system alignment error of the order of 0.1 milliradian is achieved, an accuracy which exceeds requirements by a comfortable margin.

OPTICAL MEASUREMENT SYSTEM

Besides providing for inertial system alignment as described above, the optical system also provides the on-board measurement capability for orbital and midcourse navigation of the command module. The single-line-of-sight direction measurement referenced to the stable member used for inertial system alignment can be well utilized also in low earth or lunar orbit for navigation. However, for on-board navigation during the translunar and transearth phases, accuracy requirements are met only by a two-line-of-sight sextant type of instrument. Two separate Command Module optical instruments are mounted on the navigation base which also supports the inertial measurement unit. These are the two-line-of-sight sextant and the single-line-of-sight scanning telescope.

The sextant and its features are illustrated diagramatically in Fig. 2–34. It is essentially a two-line-of-sight instrument providing magnification for manual visual use as well as special sensors for automatic use. It is seen in the figure that one of the lines of sight of the sextant, identified with the landmark side of the navigation angle, is undeflected by the instrument and is thereby fixed to the spacecraft. To aim this line then, the spacecraft must be turned in space appropriately by means of orientation commands to the attitude control system. The second line identified with the star side of the navigation angle can be pointed in space through the use of two servo motor drives

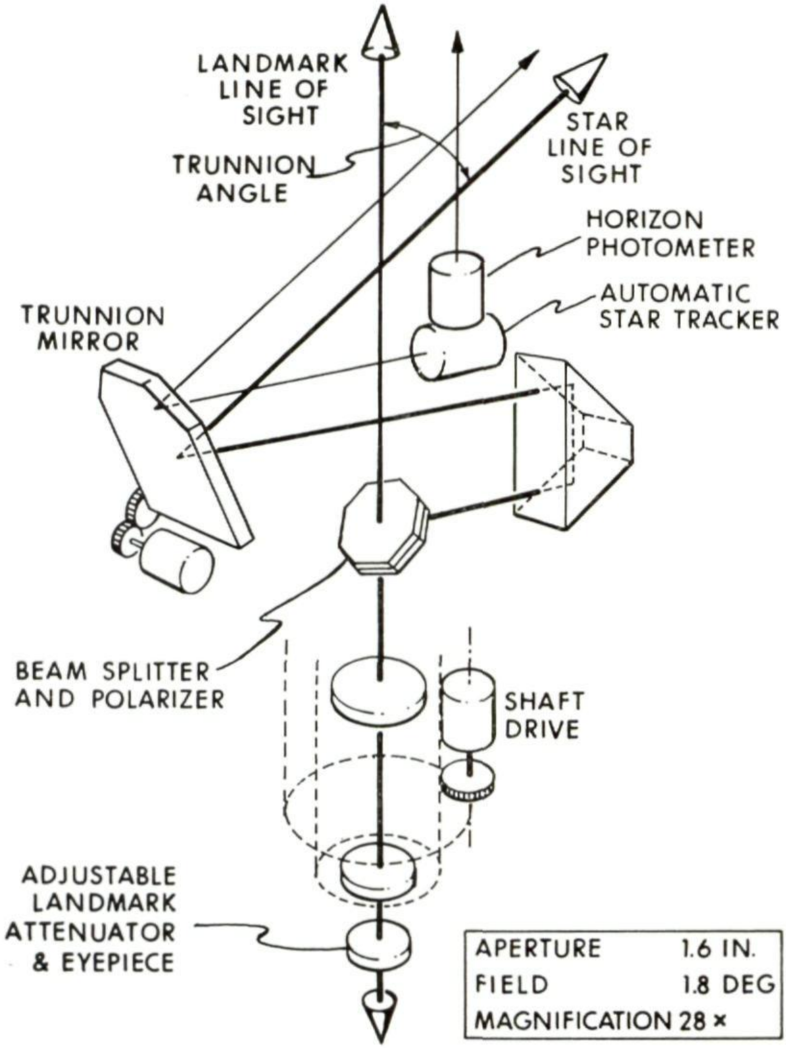

FIG. 2–34 Sextant schematic

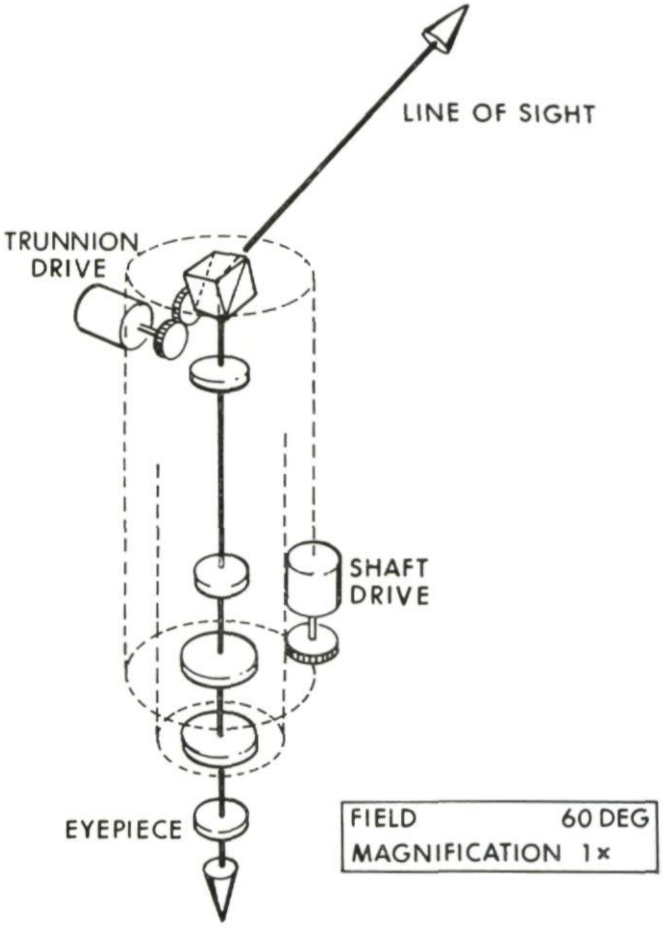

FIG. 2–35 Scanning telescope – schematic

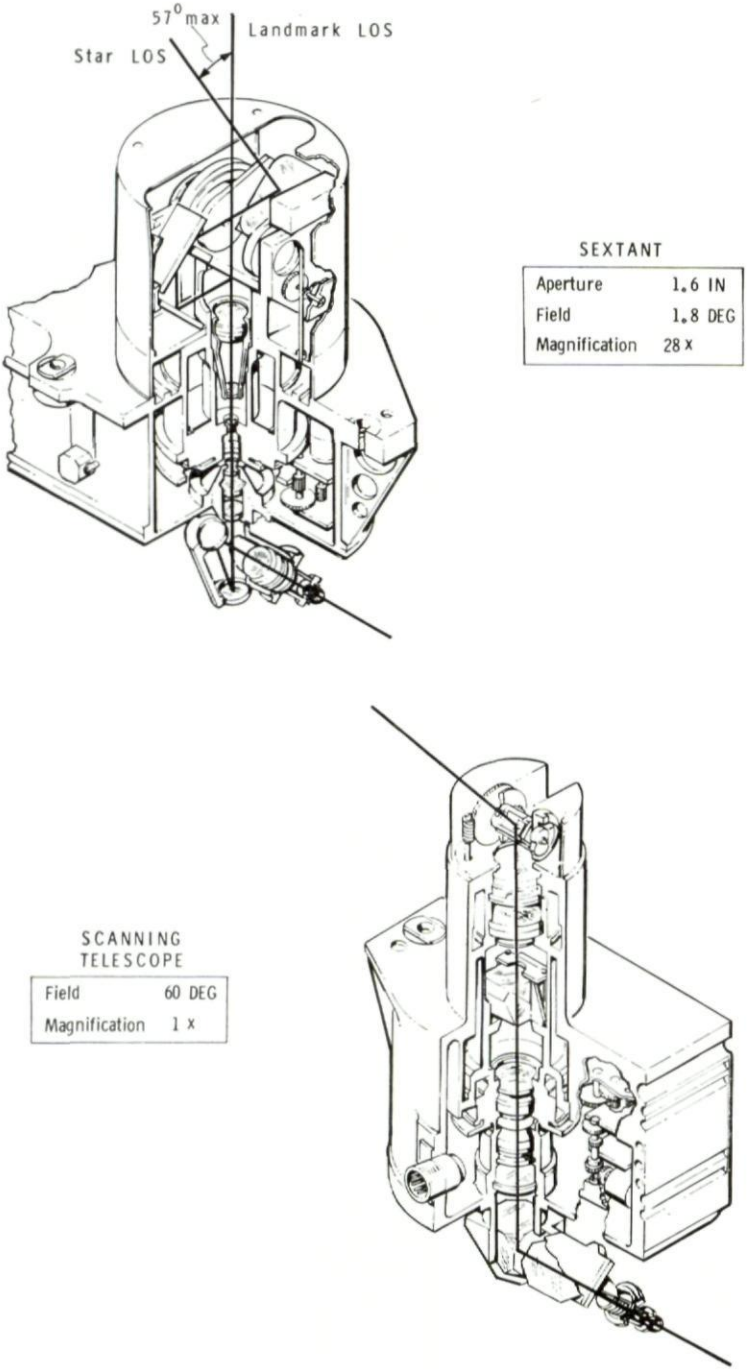

FIG. 2-36 Optical unit – sextant and scanning telescope

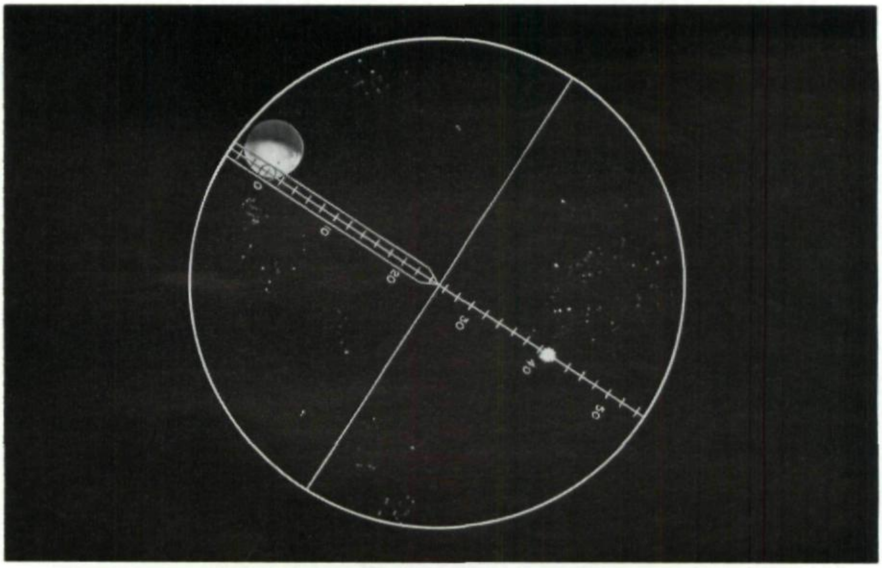

FIG. 2–37 Telescope view – midcourse navigation

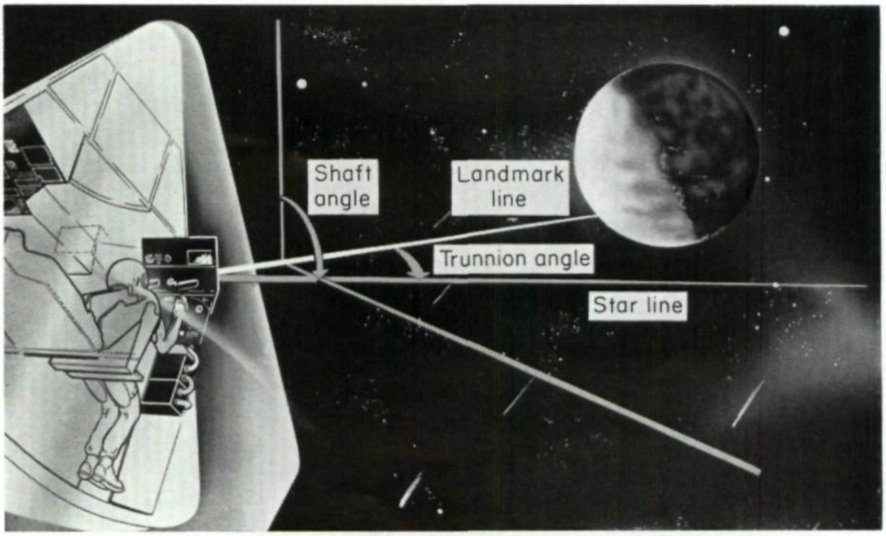

FIG. 2–38 Spacecraft orientation – midcourse navigation sighting

illustrated schematically. One axis of this motion – called the shaft axis – is parallel to the landmark line and changes the plane in which the navigation angle is measured by rotating the head of the instrument as a whole. The second axis – trunnion axis – sets the navigation angle by tilting of the trunnion axis mirror. A precision angle data transducer on this mirror provides a direct measure of the navigation angle for the navigation routine of the computer. An angle transducer on the shaft axis completes the data needed by the computer of the indicated star direction when the instrument is used for inertial system alignment.

The light arriving along the landmark line is polarized before being combined in the beam splitter mirror with the light along the star line, so that the navigator can adjust the landmark background brightness relative to the star intensity by means of an eyepiece polarizer. The sextant also uses the trunnion mirror in conjunction with a star tracker sensor to provide automatic star tracking error signals to the shaft and trunnion drives. Mounted with its sensitive axis along the landmark line is a second automatic detector called a horizon photometer. This device senses the brightness of a small portion of the sun illuminated horizon for use as one side of the navigation angle. This is described in more detail in Part 5.

Because the 28 power magnification of the visual section of the sextant results in less than a 2 degree diameter field of view, the second instrument, the scanning telescope, provides a wide field acquisition capability for the sextant to find and acquire objects in the sky. The use of an entirely separate optical instrument rather than a combined variable power instrument using one set of line-of-sight articulation drives is justified by the simpler mechanical and optical configuration and the sighting redundancy two units provide.

The scanning telescope illustrated in Fig. 2–35 has shaft and trunnion pointing of its single line of sight. The shaft angle always is made to follow the sextant shaft angle by servo action when the optics system power is on. The trunnion can be selected by the astronaut to (a) follow the sextant trunnion and hence look along the star line, (b) be driven to zero and hence look along the landmark line, or (c) be driven to a fixed angle of 25 degrees. This latter provides for ease in simultaneous acquisition of landmark and star, since the scanning telescope will indicate the image along the landmark line by a reticle point 25 degrees from the center of the field and will indicate possible stars available by trunnion motion in the sextant field of view on a diametrical reticle line. Figure 2–37 shows the view through the scanning telescope during acquisition. Generally, the navigator will preset the trunnion to the expected navigation angle indicated by the computer as the preliminary step in the acquisition process.

Under manual visual control, the shaft and trunnion drives of the telescope are commanded by a left-hand two-axis controller. By this controller, the navigator can point the scanning telescope and the sextant star line. At his right hand, the navigator has spacecraft attitude controllers with which he can rotate the spacecraft to position the landmark line. His midcourse cislunar sighting strategy is to set up the measurement situation illustrated in Fig. 2–38. With his right hand controls, he gets the identified landmark within the field of view of the sextant at a slow spacecraft rotation drift. He need then only provide occasional minimum impulses from the appropriate

attitude jets to keep the landmark within the field while with his left hand he positions the star image to superimposition on the landmark. When this is achieved, Fig. 2–39, he pushes a "mark" button which signals the computer to record the navigation trunnion angle and time. From these data the computer updates the navigation state vector.

The unity power wide field of view of the scanning telescope is also suitable for navigation direction measurements to landmarks in low earth or moon orbit. The wide field of view makes landmark recognition easy. Landmark direction measurement accuracy of the order of 1 milliradian as referenced to the pre-aligned attitude of inertial system and as limited by the unity magnification is sufficient for landmark ranges under a few hundred kilometers. In low orbit, the inertial measurement gimbal system must be on and pre-aligned with two star sightings. Then the navigator acquires and tracks landmarks as they pass beneath him, pushing the mark button when he judges he is best on target, Fig. 2–40. The computer then records optics angles, inertial measurement unit gimbal angles and time to provide the navigation data. In all uses of stars and landmarks for navigation the computer must be told by the navigator the identifying code or coordinates of the star and/or landmark. These appear on the navigator's maps and charts to help his memory.

ON-BOARD COMPUTER

The relatively large amount of on-board data processing required for Apollo guidance, navigation and control can be met only by the capabilities of a specially designed digital computer. The special requirements define a computer which would provide for:

(a) Logic, memory, word length and speed capability to fit the needs of the problems handled.

(b) Real time data processing of several problems simultaneously on a priority basis.

(c) Efficient and yet easily understood communication with the astronauts for display of operations and data as well as manual input provisions for instructions and data.

(d) Capability of ground control through radio links as well as telemetering of on-board operations and data to the ground.

(e) Multiple signal interfaces of both a discrete and continuously variable nature.

The design features of this computer are covered in detail in Part 6. But perhaps the many input and output signals should be discussed briefly here because of the large part these interfaces take in determining the system configuration and in understanding system tasks and operation. Rather than a listing of interfaces the important ones will be discussed by groups in the following paragraphs.

Inputs to the computer of a discrete or two-state nature are handled as contact closures or voltage signals. These offer no difficulty except for the computer activity needed to keep appraised of them. Important urgent signals of this nature – such as an abort command or the time critical "mark" signals – go to special circuits which interrupt computer activity to be processed before other activity is resumed or modified. Less critical signals indicating

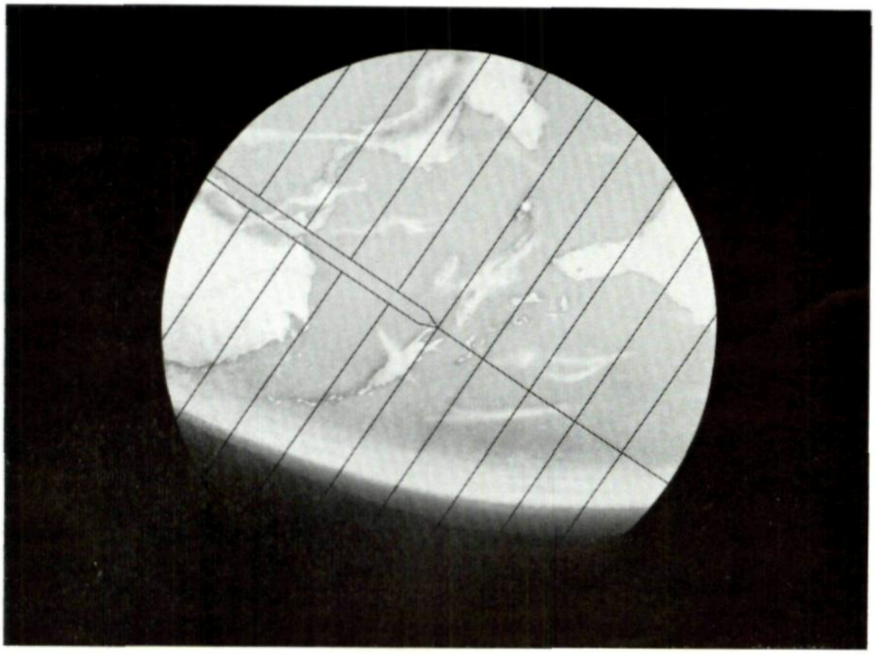

FIG. 2–39 Sextant view – midcourse navigation

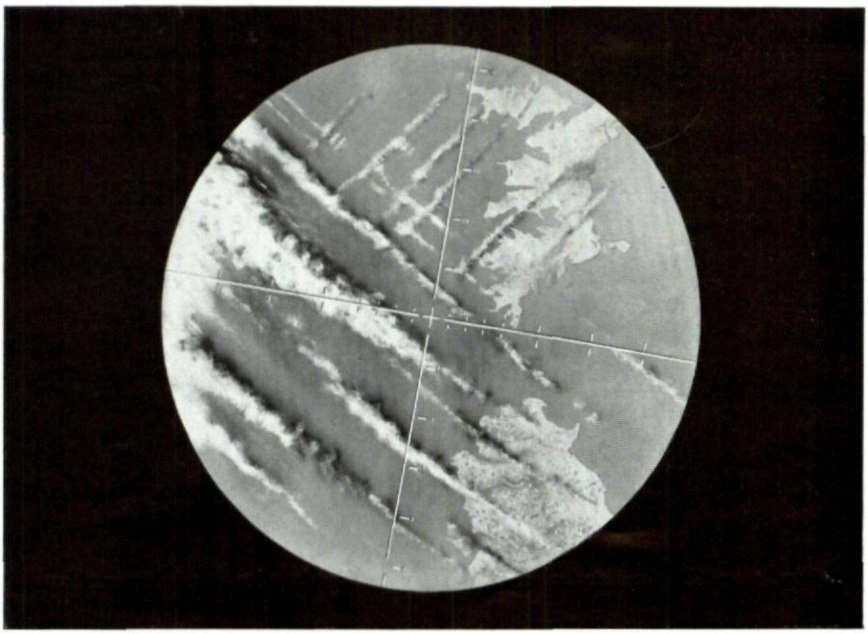

FIG. 2–40 Telescope view – orbital navigation

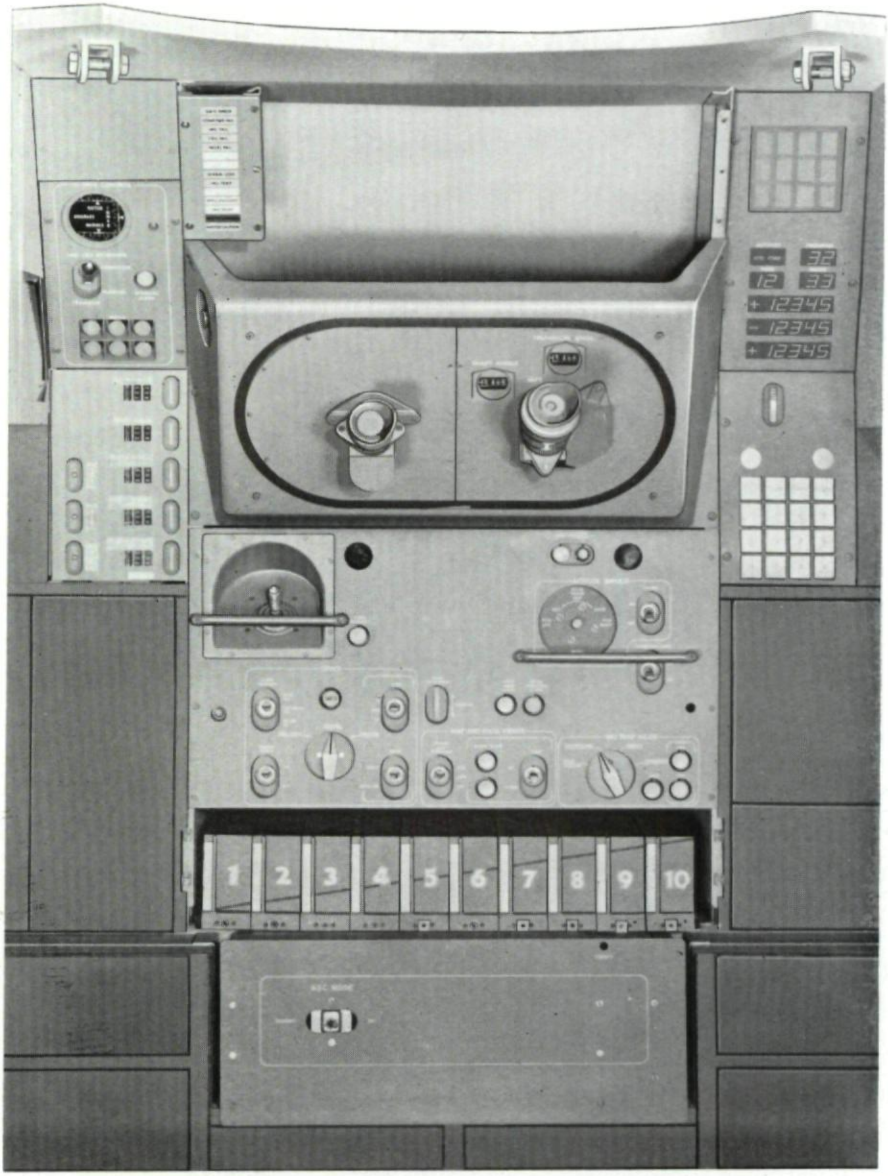

FIG. 2-41 Displays and controls – command module lower equipment bay

states of the various equipment or requiring less urgent action are examined by the program periodically as necessary.

Discrete signal outputs are of two types. Time critical ones such as that which signals engine thrust cutoff consist of high frequency pulse trains which are gated on at the time of the programmed event and detected remotely where the action is requested. Slower discrete outputs are either gated d.c. voltages or relay contact closures set by a state matrix which drives the appropriate relay coils. The majority of these relays are used to set the states of the electroluminescent number displays readout of the computer display and keyboard. Others change operating modes of the associated spacecraft systems or are used to light status or warning lights. Direct earth communication to and from the computer requires circuits associated with the interface with the radio receiver and transmitter to convert between the serial code of the telemetry and the parallel format of the computer.

Other variables into the computer are handled by input counters which sum pulses transmitted as the indicated variable changes through fixed increments. Velocity increments, for instance, measured by the inertial system accelerometers are handled in this way. Some variable outputs, such as the command torquing of the inertial system gyros to change alignment, appear as output increment pulses on appropriate lines.

Perhaps the most difficult class of computer interfaces is handled by the use of auxiliary pieces of equipment called Coupling Data Units – or CDU's for short. The CDU's provide the means for coupling with the digital computer the sine and cosine analog signals from the resolver type of angle transducers used on the optics and inertial gimbal system axes. There are five of these CDU's, one each associated with optics shaft, optics trunnion and the three axes of the inertial unit gimbal system. The details of the operation and construction of the CDU's are described in Part 4.

DISPLAYS AND CONTROLS

The preceeding sections have introduced the needs and characteristics of three Apollo guidance, navigation and control subsystems: (a) the inertial measuring equipment, (b) the optical measurement equipment and (c) the digital computer data processing equipment. Because Apollo is by its very purpose a manned mission, the provision for system operation by the crew is essential. This identifies the need for the fourth subsystem, the displays and controls.

The provisions to involve the astronaut might appear as an unnecessary complication. Indeed, many tasks are best left to the machine; those that are too tedious or require too much energy, speed of response or accuracy outside man's capabilities. But the utilization of man in many of the tasks of guidance, navigation and control more than pays for the display and control hardware needed. His involvement without any doubt enhances mission success significantly. Consider man's judgement and adaptability, his decision-making capability in the face of the unanticipated and his unique ability to recognize and evaluate patterns. Of this latter, consider his unsurpassed faculty to pick out a particular navigation star from the heavens or to evaluate a suitable touchdown spot on the moon. Displays and controls were designed in Apollo to provide the crew with visibility into and command

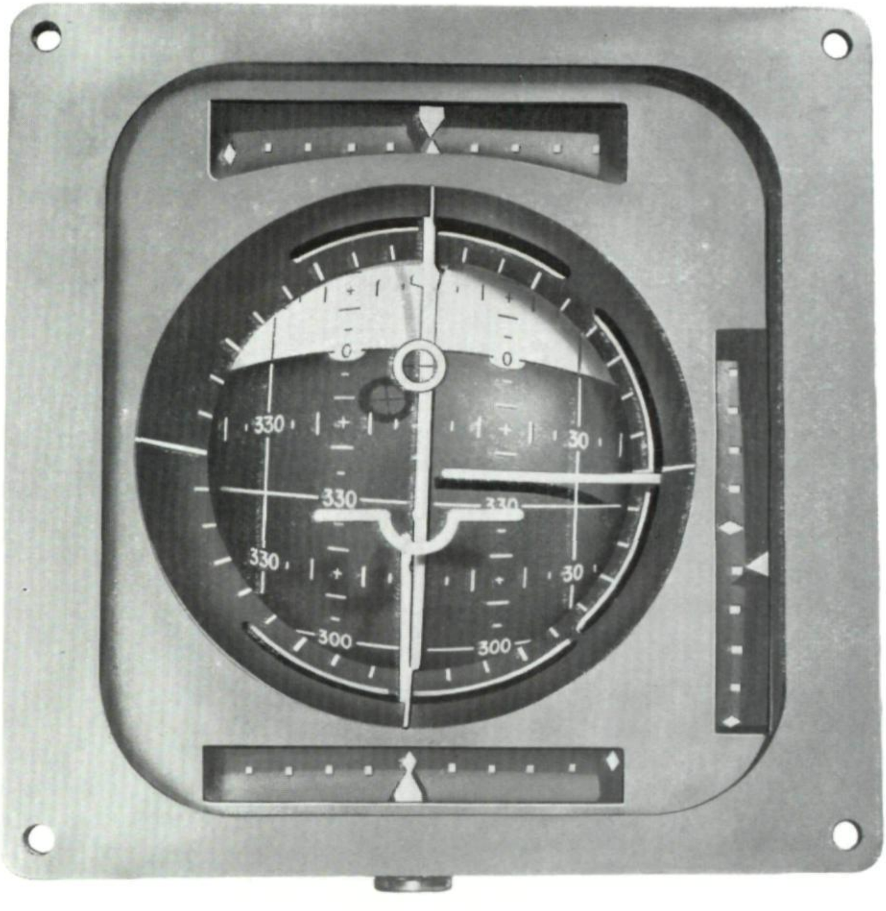

FIG. 2–42 Ball attitude indicator

over the guidance, navigation and control tasks. In most of these tasks then, the astronaut can select either to be intimately involved in the procedures or allow full automatic operation which he will be able to monitor at his discretion.

In the command module, the navigator has displays and controls illustrated in Fig. 2–41. The eyepieces of the sextant and scanning telescope appear prominently beside each other. Just below these eyepieces is a control panel used primarily for operating the optics. The left-hand optics hand controller and the right-hand spacecraft attitude minimum impulse controller appear at the top of this panel. At the bottom of this panel are operating mode selector switches. The inertial system mode controls and displays appear to the left and above the eyepieces. Directly to the left are the five coupling data units with a display of the associated variable of each. To the right is the numerical readout and keyboard associated with the computer. Features of this are described with the computer in Part 6.

Tabulations of data, lists of procedures and maps and charts of landmarks and stars will be provided in a bound book or could alternately be projected on a microfilm projector. Space for this projector appears near the top of Fig. 2–41. Controls to operate the film drives and projection lamp are seen on the center panel. The numbered modules below the optics control panel contain the miscellaneous analog electronics that operate the equipment. Below this is the digital computer.

Separated from the displays and controls described and on the main panel in front of the pilot's couch certain important guidance data are displayed. A second display and keyboard of the digital computer is mounted here. This unit is functionally in parallel with the one used by the navigator so that the majority of guidance and navigation functions can be operated and observed from either station.

Also visible to the pilot is a ball attitude indicator and associated needles, Fig. 2–42. The spacecraft orientation is indicated to the pilot by the attitude of the ball which is driven in three axes by the three axes of the inertial measurement unit gimbals. Also, the three components of attitude error generated by the guidance system are displayed by the position of three pointers which cross the face of the instrument. Vehicle attitude rates measured by three vehicle mounted rate gyros are displayed by three more pointers around the sides of the instrument. Other displays showing guidance, navigation and control system status also are available for the pilot on the main panel along with a complex array of equipment associated with other systems for control mode selection and display.

EQUIPMENT INSTALLATION IN SPACECRAFT

The installation of the guidance and navigation equipment in the command module is illustrated in the cutaway view, Fig. 2–43. This shows the navigator operating the displays and controls at the lower equipment bay where the majority of the guidance and navigation equipment is located. Other control equipment is distributed around the spacecraft. During launch boost into earth orbit and during return entry when the acceleration forces are high, the navigator must leave his station as shown and lie in the protective couch in the center between his companions. Sufficient controls

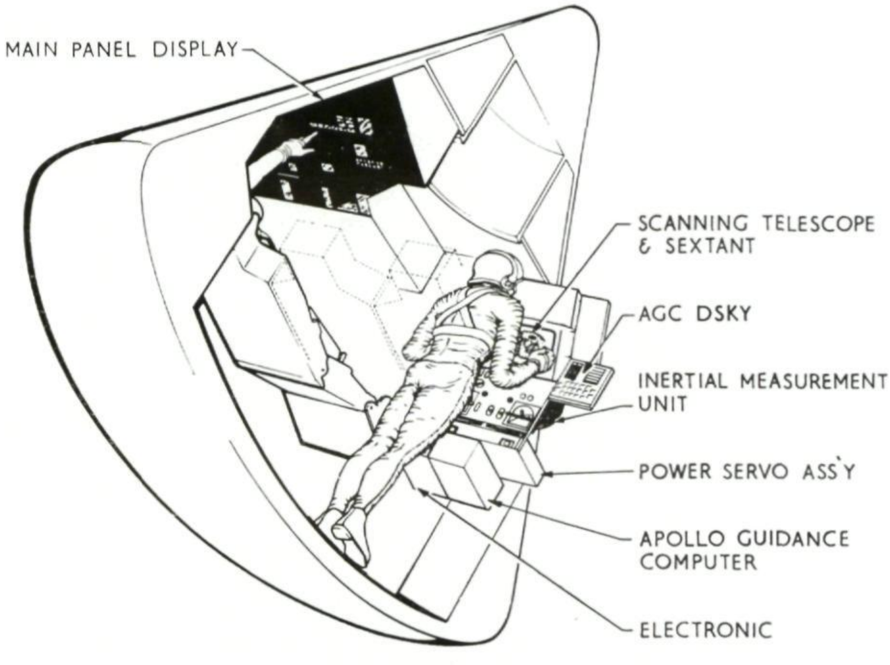

FIG. 2–43 Location of the guidance and navigation system in the command module

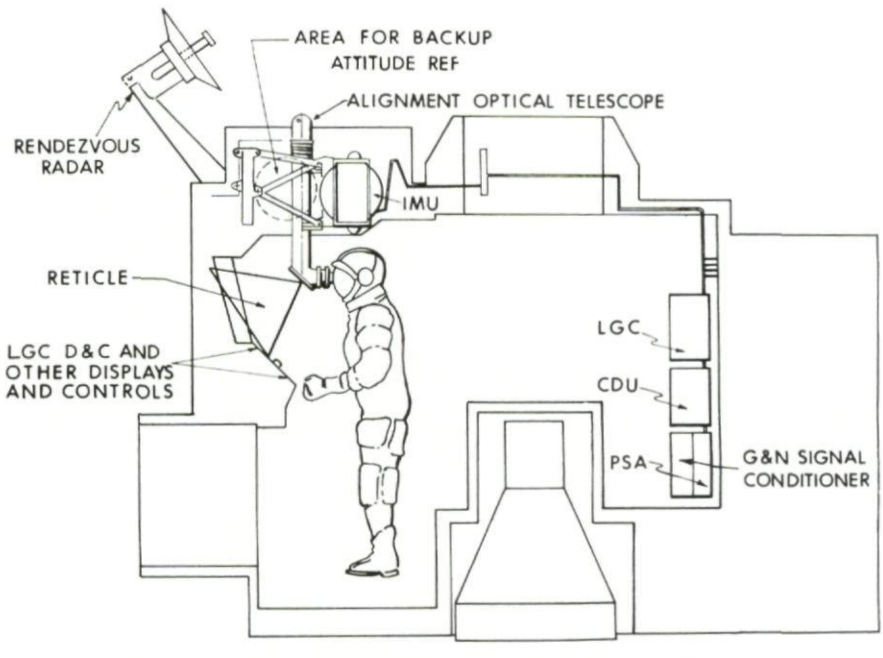

FIG. 2–44 Location of the guidance and navigation system in the lunar excursion module

and displays as described above are on the main panel in front of the couches to perform all the guidance and navigation functions except for those requiring visual use of the optics. Thus, for the limited period near the earth when the navigator cannot be stationed in front of the eyepieces at the lower equipment bay, use of optics is through the automatic features only.

The installation in the LEM is shown in Fig. 2–44. The inertial measurement unit (IMU), the LEM guidance computer (LGC), the coupling data units (CDU's) and support electronics of the power servo assembly (PSA) are all identical to those used in the command module. Since the LEM activity, when separated from the command module, does not require optical navigation sightings, a simpler optical alignment telescope is installed on a navigation base with the inertial measurement unit and is used only for aligning the stable member of the latter. Also unique to the LEM are the two radars. The rendezvous radar is mounted near the inertial unit so that direction data can be related between the two. The landing radar is on the descent stage, not shown, and is therefore discarded on the lunar surface after it has served its function during landing.

OVERALL BLOCK DIAGRAMS

The signal interconnections among the various equipments which constitute or have some part in the guidance, navigation and control are illustrated in Fig. 2–45 and Fig. 2–46 for the command module and LEM systems, respectively. The equipment and signals shown on these figures can, for the most part, be related to material already discussed. A detailed explanation is not given here, since the intent is only to show the general nature of the equipment interfaces, the similarity and difference between the command module and LEM systems and the central role of the guidance computer in each case.

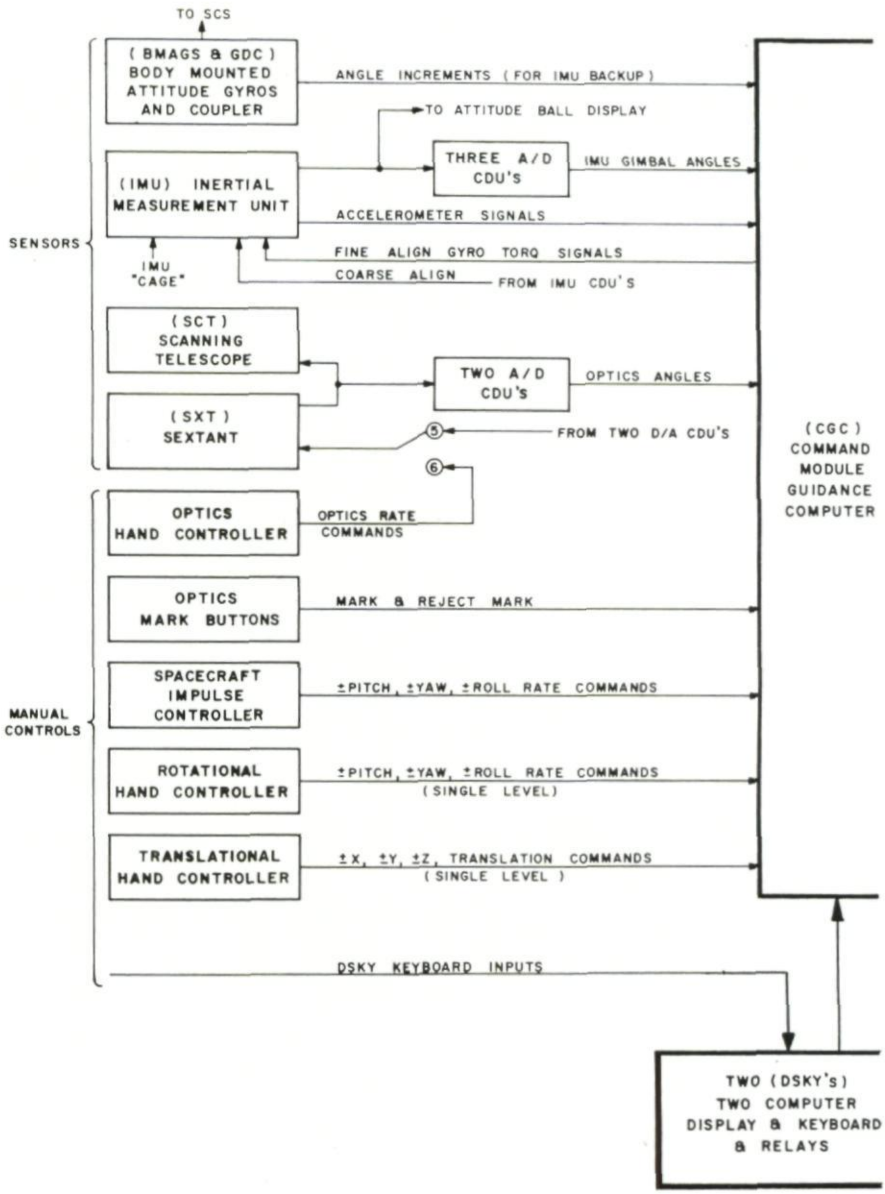

FIG. 2–45a Guidance navigation and control interconnections in command module

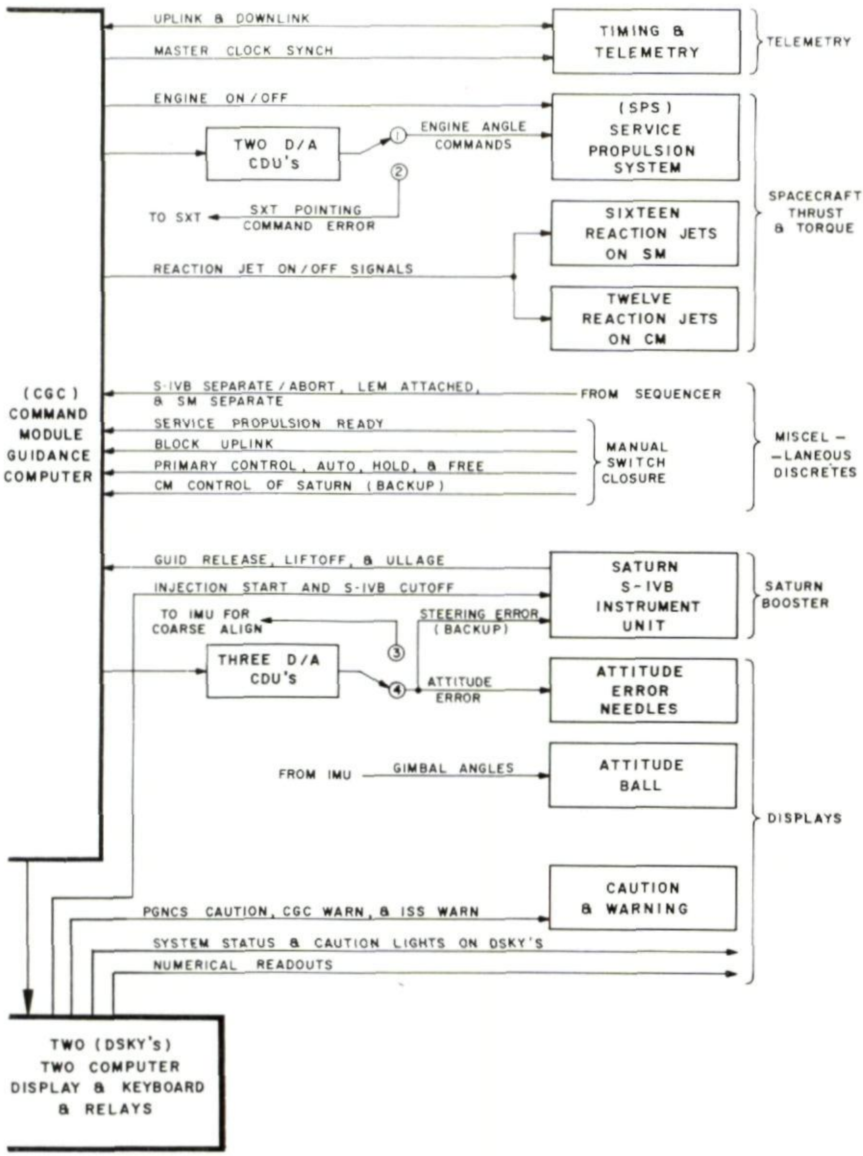

FIG. 2-45b Guidance navigation and control interconnections in command module

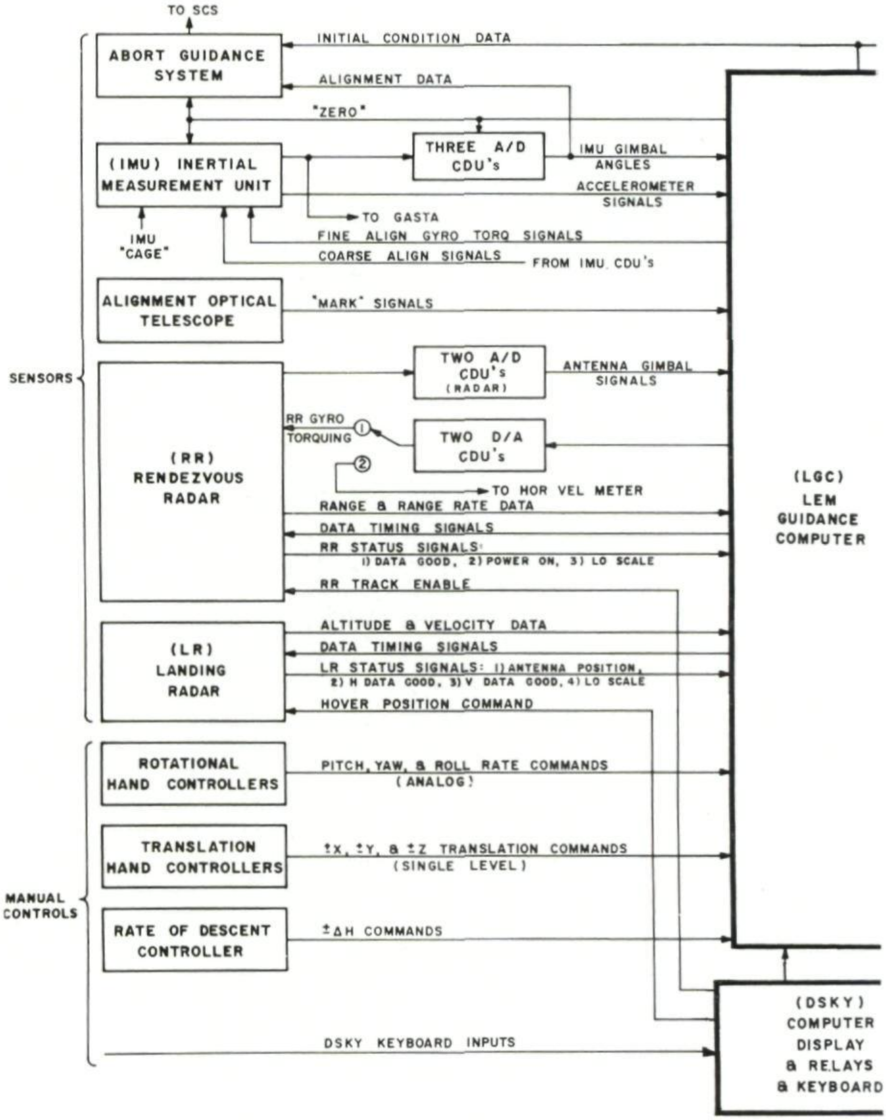

Fig. 2–46a Guidance, navigation and control interconnections in LEM

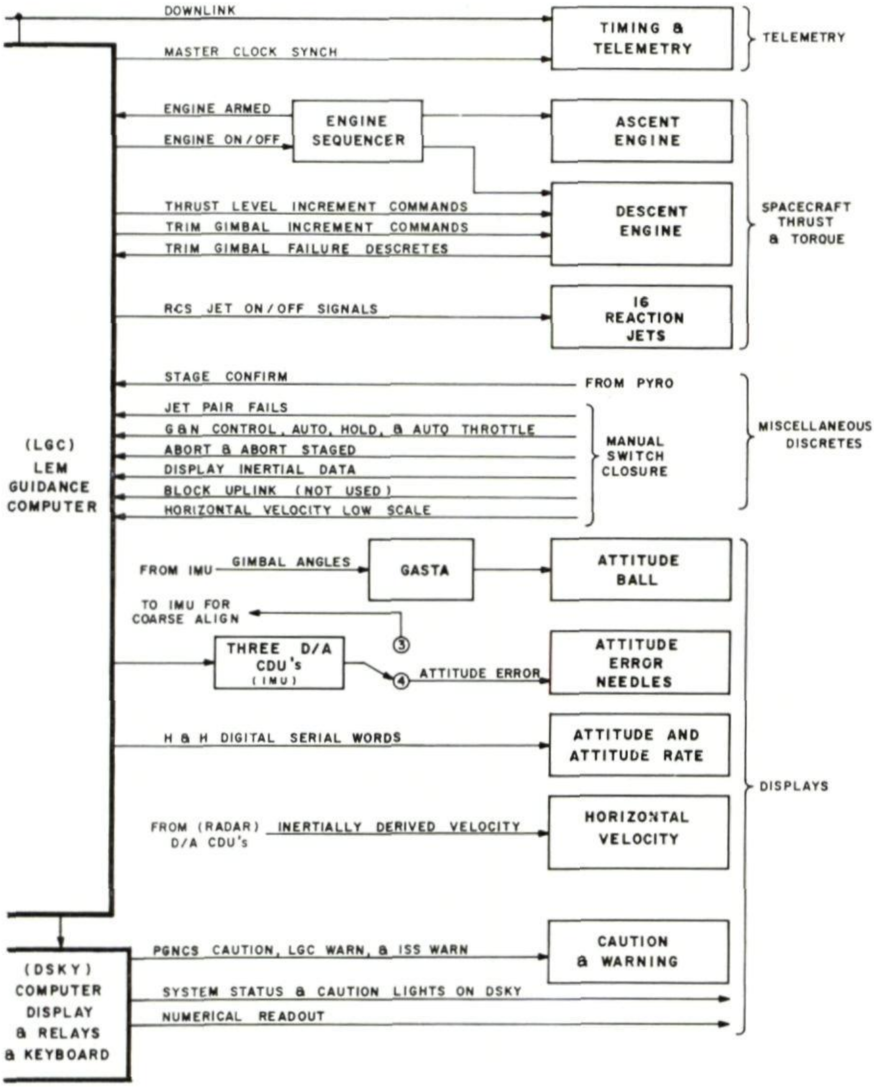

FIG. 2-46b Guidance, navigation and control interconnections in LEM

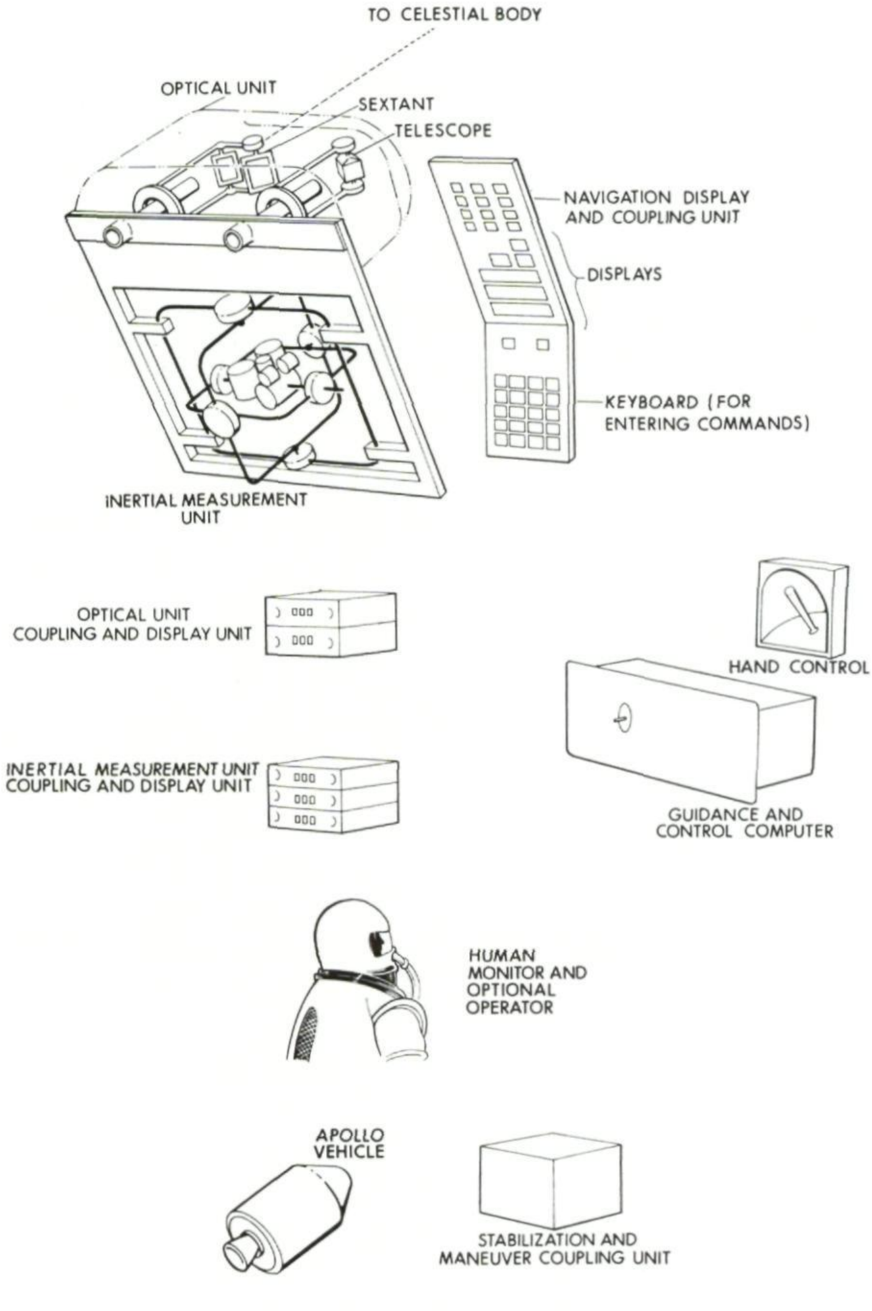

FIG. 2–47 Equipment arrangement in the command module lower equipment bay

CHAPTER 2-4

OPERATION MODES OF GUIDANCE, NAVIGATION AND CONTROL APOLLO COMMAND MODULE BLOCK I

The system that has been described so far can be seen to have a high degree of flexibility in performing the many tasks of concern. In this chapter a series of diagrams are used to show briefly the equipment involved and the information flow in operations with these tasks.

Figure 2–47 shows the installed arrangement of the equipment in the Block I command module. In the following figures this equipment is shown separated in order to trace signal paths more easily. The Block I equipment configuration lends itself better to the tasks of this chapter than the later more integrated Block II equipment which will finally perform the lunar landing.

Figure 2–48 is the key figure of the series. Here the principal subsystems of the Block I command module guidance and navigation are arrayed and identified for use in the subsequent figures. The sensors of the system are shown in the top center; the two optical instruments, sextant and scanning telescope and the inertial measurement unit (IMU) are all mounted on the common rigid navigation base. At top left are the two sets of coupling data units (CDU's) to provide the communication of the optics and IMU angles with the computer shown at the center. The computer display and keyboard (DSKY) is at upper right. The whole vehicle – command and service modules – is represented by the figure center right. The separate stabilization and control system of the Block I system is bottom right. The astronaut navigator is shown bottom left surrounded by several of the important controls.

The first mode is that of powered flight guidance, Fig. 2–49. The signals from the accelerometers on the IMU are processed within the computer where the steering equations develop a desired thrusting attitude of the vehicle to achieve the desired direction of acceleration. This is treated as a commanded attitude which is compared in the CDU's with actual attitude measured by the IMU. The difference is a steering error which is sent to the SCS to control the vehicle. Resulting vehicle motion is sensed by the IMU to complete the feedback. When the required velocity change is achieved, the computer sends a rocket engine shutdown signal. The crew can monitor the whole operation by the display of appropriate variables on the DSKY such as the components of velocity yet to be gained. Before the IMU can be used for an operation such as this, it must be aligned to the desired spacial orientation. This process is described next.

IMU alignment is normally performed in two stages: "coarse" and "fine". The first step of coarse alignment is to give the computer a reasonably accurate knowledge of spacecraft attitude with respect to the celestial framework being used. Illustrated in Fig. 2–50, the navigator sights sequentially two stars

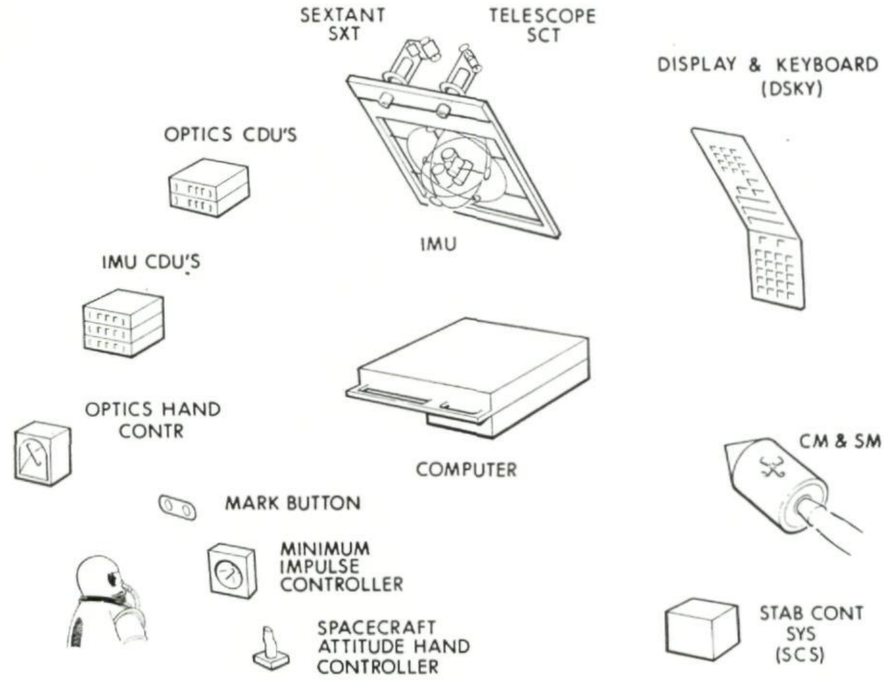

Fig. 2–48 Sub-system identification

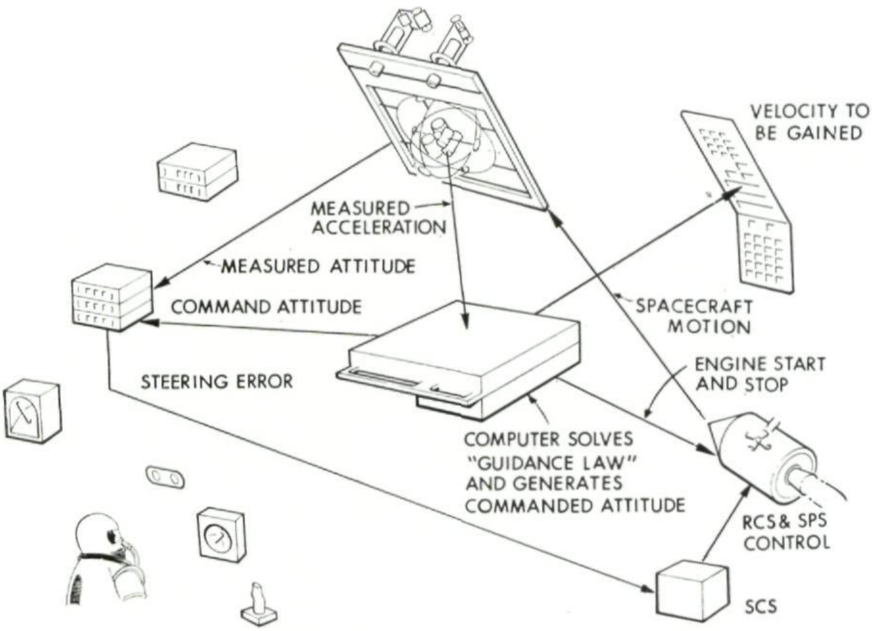

Fig. 2–49 Guidance steering control

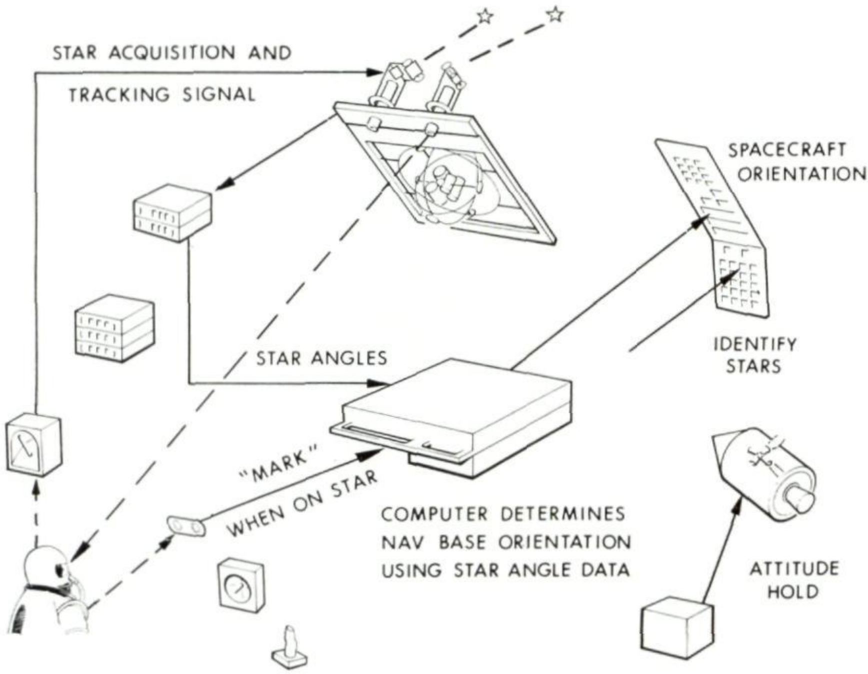

Fig. 2–50 IMU coarse alignment, step 1

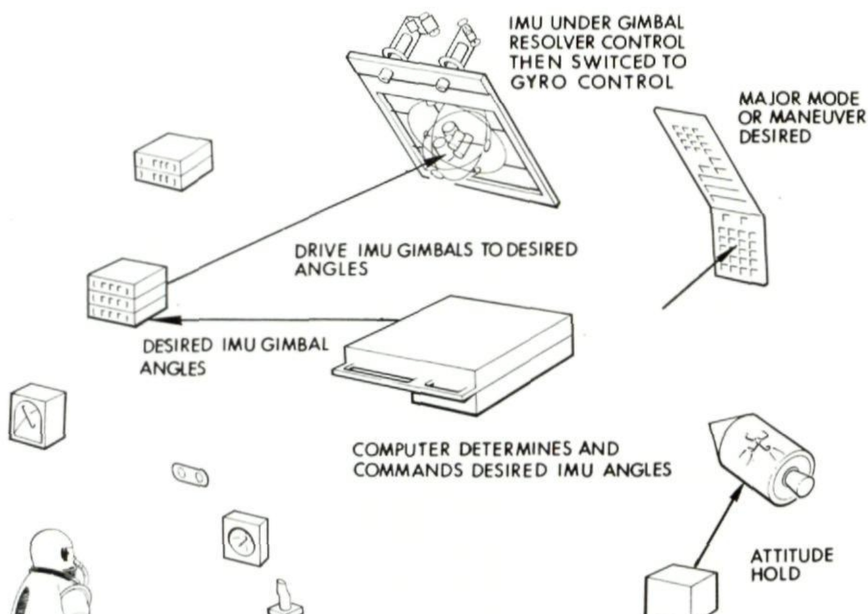

Fig. 2–51 IMU coarse alignment, step 2

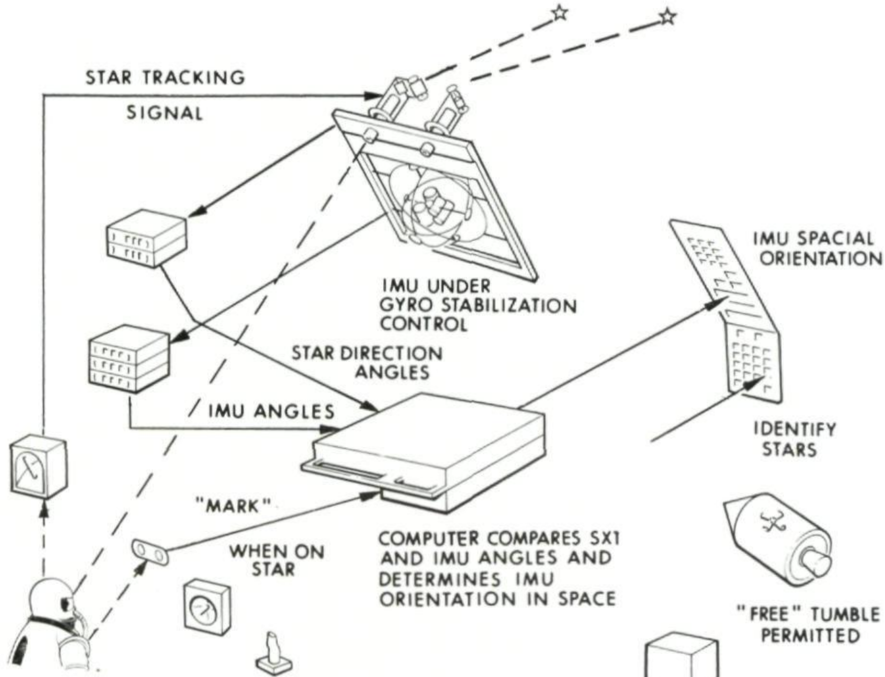

FIG. 2–52 Manual IMU fine alignment, step 1

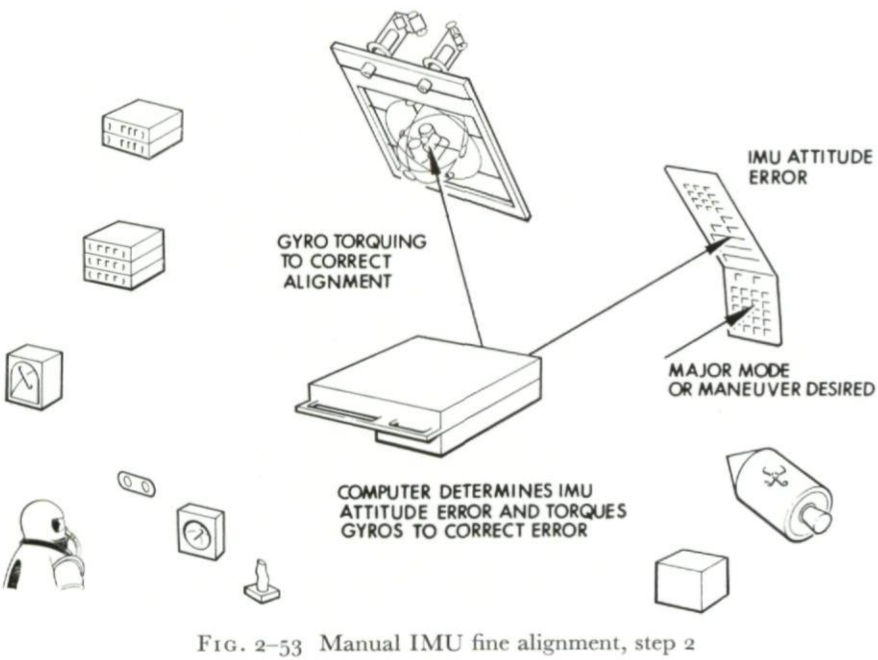

FIG. 2–53 Manual IMU fine alignment, step 2

using the scanning telescope (SCT). The star image is sensed by the navigator who uses his left hand optics controller to command the SCT prism such as to center the star on the reticle. He pushes the mark button when he achieves satisfactory tracking which signals the computer to read the SCT angles being transmitted it by the optics CDU's. A second star direction at a reasonably large angle from the first is similarly measured. The navigator identifies which stars are being used to the computer through the keyboard of the DSKY. With these data the computer determines in three dimensions the spacecraft attitude which is held reasonably fixed by a gyro control attitude hold of the SCS during all of these coarse alignment operations.

In step two of coarse alignment shown in Fig. 2–51, the computer determines desired IMU gimbal angles based upon its knowledge of spacecraft attitude and the guidance maneuver which will be next performed. These desired angle signals sent to the IMU through the CDU are quickly matched by the IMU gimbal servos in response to error signals developed on the angle transducers on each gimbal axis. At this point the IMU gimbal servos are then switched over to the gyro stabilization error signals to hold the achieved orientation.

In the first step of fine alignment shown in Fig. 2–52, two star directions are again measured by the navigator. This time he uses the high magnification of the sextant (SXT) with the precision readout on the star line in order to achieve necessary accuracy. The IMU is presumed to be under gyro stabilization control and to be reasonably close to the desired orientation. On each of two stars which the navigator identifies to the computer, the navigator signals "mark" when he achieves precise alignment on the SXT crosshair. On these signals the computer simultaneously reads the SXT and IMU angles being transmitted through the CDU's. With these data the computer determines star directions in IMU stable member coordinates from which the spatial orientation of the IMU being held by gyro control can be computed. The spacecraft attitude need not be held fixed during these fine alignment operations as long as the angular velocity is small enough to permit accurate star tracking by the navigator.

In step two shown in Fig. 2–53 the computer determines the existing IMU attitude error based upon the desired attitude as determined from the next use of the IMU such as for a particular guided maneuver. The computer then meters out the necessary number of gyro torquing pulses necessary to precess the gyros and the IMU to correct the IMU alignment error. The two steps of fine alignment can be repeated if desired to obtain more precision when the torquing precession angle is large.

On-board navigation measurements in low orbit can be performed either using landmark references as shown on the above figure or using other references as described later. In Fig. 2–54, the navigator first aligns the IMU as previously described and then tracks identified landmarks as they pass beneath him using the SCT. When he is on target he signals "mark" and the computer records IMU and SCT angles and time so as to compute landmark direction in the coordinate frame of the aligned IMU. These direction measurements are then used to update the computer's estimate of position and velocity and the computer's estimate of error in these parameters. These data can be displayed to the astronauts if desired.

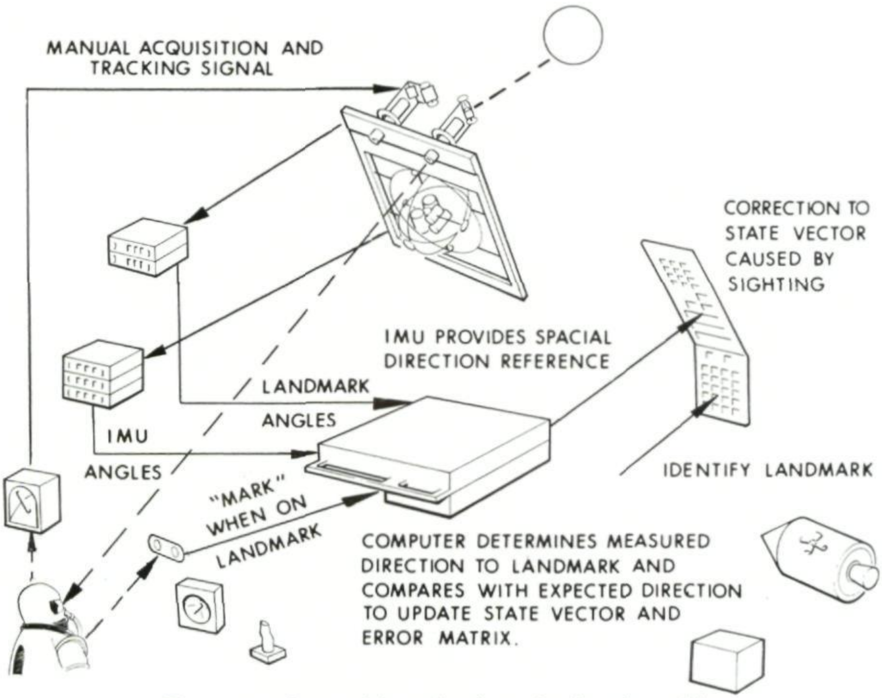

FIG. 2–54 Low orbit navigation – landmark tracking

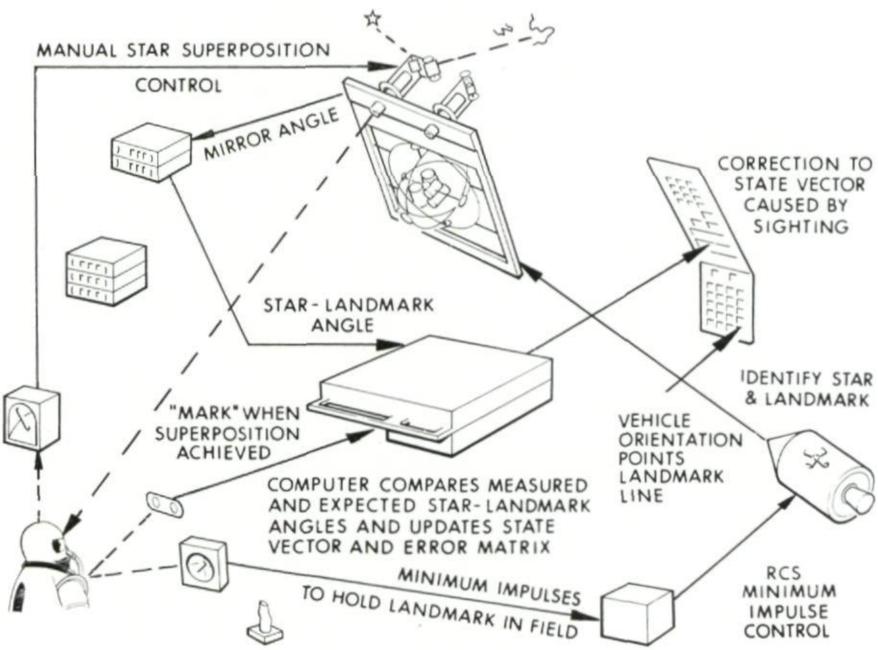

FIG. 2–55 Midcourse navigation – manual star landmark measurement

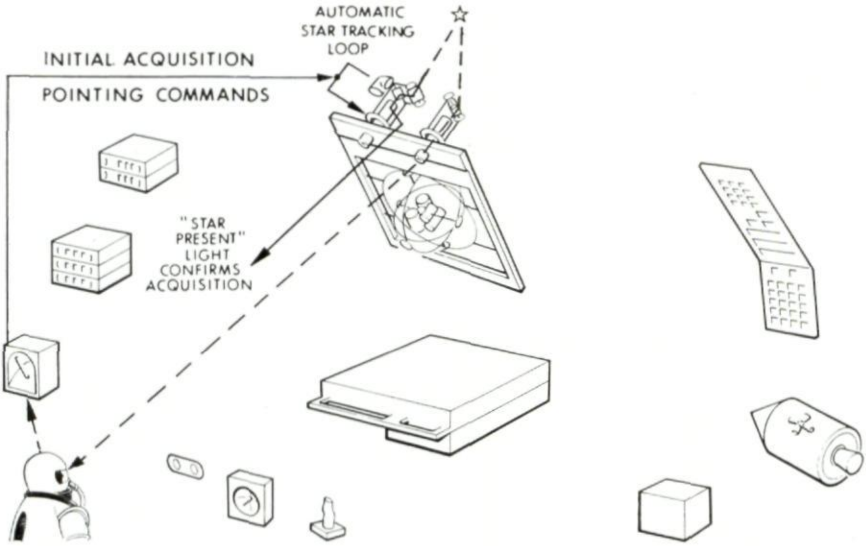

FIG. 2–56 Illuminated horizon – manual navigation measurement, step 1

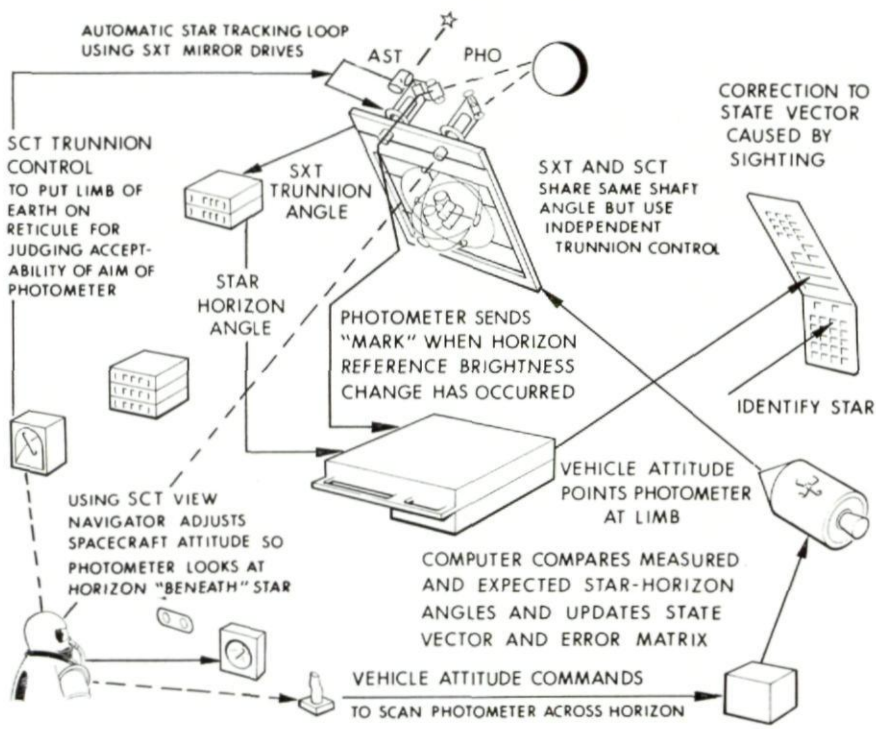

FIG. 2–57 Illuminated horizon – manual navigation measurement, step 2

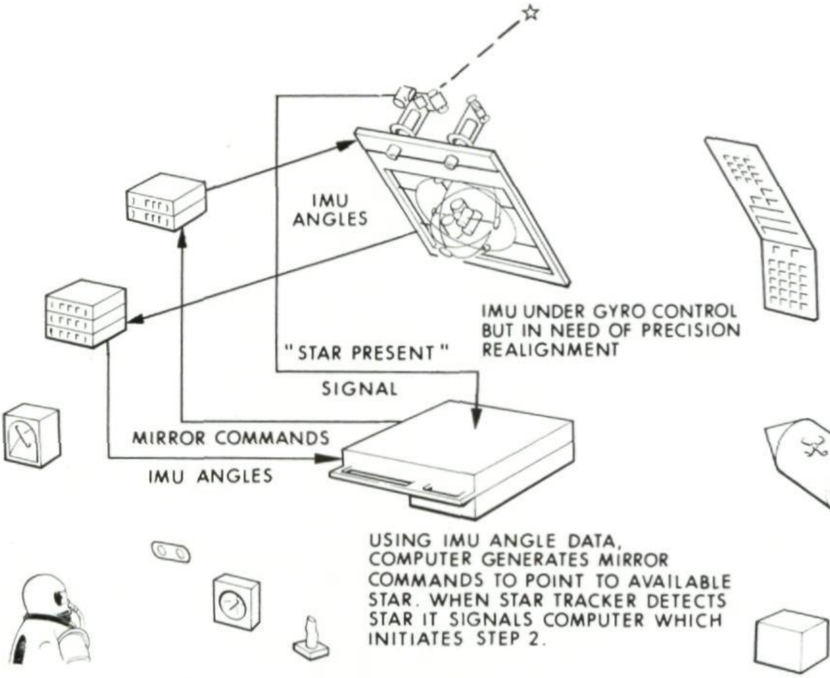

FIG. 2–58 Automatic IMU fine alignment, step 1

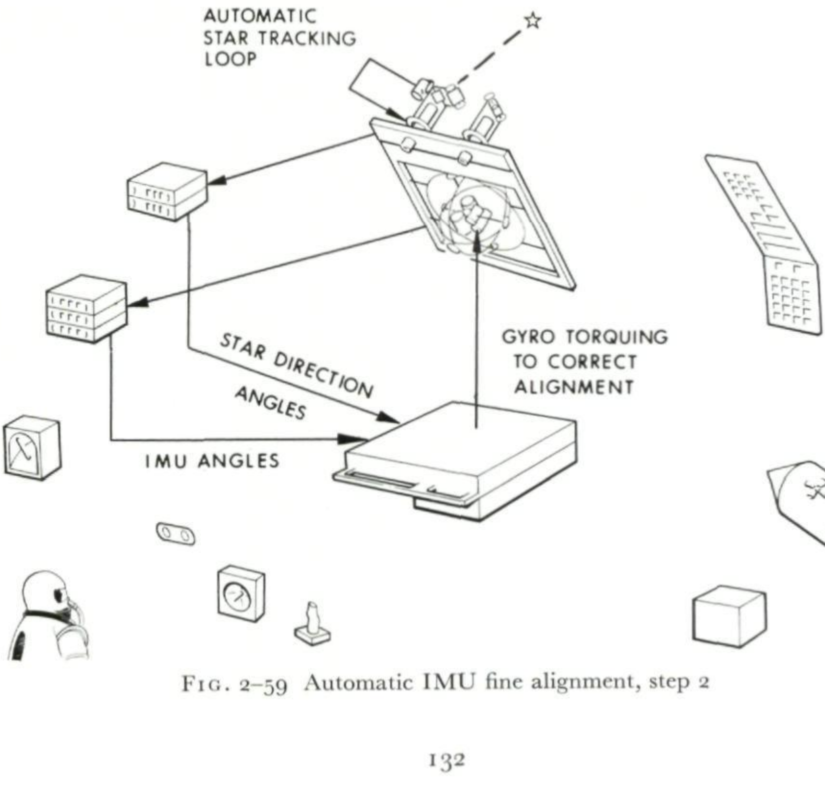

FIG. 2–59 Automatic IMU fine alignment, step 2

Although this assumes identified landmarks of known coordinates, unidentified landmark features can be used as described in Part 5.

The use of the sextant to measure the angle between identified stars and landmarks for midcourse navigation is described with Fig. 2–55. The acquisition process using the scanning telescope is assumed already to have been performed so that the desired star and landmark images appear in the SXT field of view. With his right hand the navigator periodically commands jet impulses to hold the landmark in the field of view by controlling spacecraft attitude and the body-fixed landmark line. With his left hand he controls the sextant mirror to superimpose the star image onto the landmark. When this superposition is satisfactory he signals "mark" and the computer records the measured navigation angle and time. These numbers are then further processed in the computer navigation routines. The computer displays the correction to the state vector which would be caused by this sighting, so that the navigator is given a basis to reject a faulty measurement before it is incorporated into the navigation.

The use for navigation of the automatic star tracker (AST) and photometer (PHO) is shown in two steps. In the first step, shown in Fig. 2–56, the navigator uses the scanning telescope (SCT) to acquire the navigation star with the automatic star tracker on the sextant. Acquisition is confirmed by a "star present" light signalled from the star tracker.

In step two, shown in Fig. 2–57, the navigator maneuvers spacecraft attitude manually to point the body-fixed horizon photometer line to the illuminated horizon by observing the geometry through the SCT. The SCT has a reticle pattern which permits the navigator to judge when the photometer is looking in the plane containing the star and the centre of the planet. This puts the photometer sensitive area directly beneath the star. His task is then to sweep the photometer line in this plane through the horizon. When the sensed brightness drops to half the peak value, the photometer automatically sends a "mark" to the computer so that the resulting navigation angle and time can be recorded. This operation can be performed using the sun illuminated limb of either the moon or earth. Operation with the earth depends upon the systematic brightness of the atmospheric scattered light with altitude described in Part 5. The navigation measurement process described uses astronaut control in positioning the Photometer line. If the IMU is on and aligned, this process could be completely automatic through computer control program.

The automatic star tracker on the sextant provides the capability of automatic IMU alignment as illustrated in Fig. 2–58 and Fig. 2–59. Without astronaut help, however, the star tracker cannot acquire a known alignment star unless the IMU is already roughly aligned to provide a coarse direction reference. The automatic IMU alignment capability described here, then, is most useful to re-correct the IMU drift after a long period of IMU operation.

In the first step, shown in Fig. 2–58, the computer points the sextant to the expected star direction through the optics CDU's based upon the vehicle attitude measured by the IMU. Presumably the star tracker now senses the desired star within its acquisition field of view and signals the computer that the star is detected.

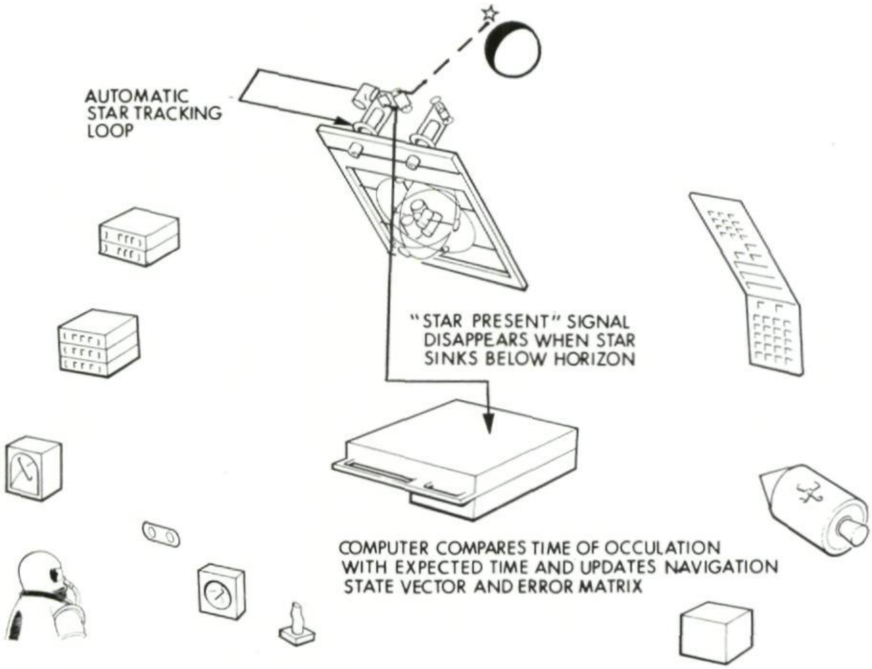

FIG. 2–60 Star occulation by moon – automatic navigation measurement

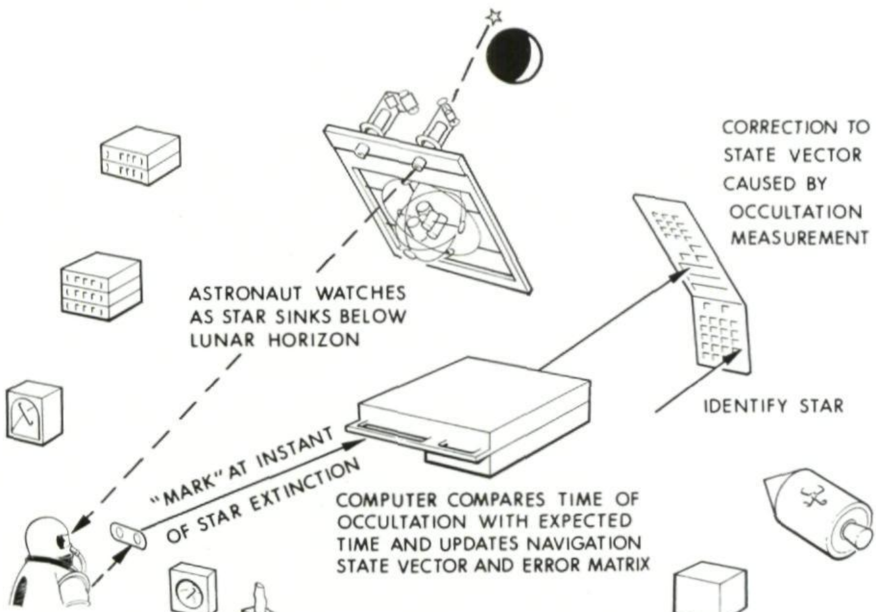

FIG. 2–61 Star occulation by moon – manual navigation measurement

In step two, shown in Fig. 2–59, the computer now changes equipment mode to send the star tracker error signals to the sextant drives so as to track the star automatically. The computer then reads simultaneously the sextant and IMU angles in order to determine two components of the actual IMU misalignment. This latter is corrected by computer torquing signals to the IMU gyros as described previously. Acquisition and tracking of a second star completes the automatic fine alignment in three degrees of freedom.

The automatic star tracker provides the means for making automatic star occultation navigation measurements with the moon, as shown in Fig. 2–60. An acquisition by the star tracker as shown in Fig. 2–56 or Fig. 2–58 is required, of course, as an initial step. While the star is being tracked the instrument generates a "star present" signal for the computer which is based upon the detected star light energy. As the star sinks below the lunar horizon due to the orbital motion of the spacecraft, the star present signal disappears at the moment of occultation. The time of this event is measured by the computer as a point of the navigation data. A similar process is possible using the earth's limb, but this requires a more elaborate star present detection. The star intensity diminishes gradually due to dispersion and scattering as the beam sinks into the earth's atmosphere. Besides the automatic occultation measurement just described, a manual detection is possible, of course, as shown in Fig. 2–61. This is of advantage, since it does not require that the optics system electronics be turned on. In fact, the event can be observed by the astronaut through the window and timed with a separate stopwatch for transmission to the earth for use in aiding ground-based navigation measurement.

CHAPTER 2–5

SPACECRAFT SAFETY CONSIDERATIONS OF GUIDANCE, NAVIGATION AND CONTROL

Although the risk is actually small, the Apollo crew, when they embark in their spacecraft admittedly put their life in jeopardy. However, unlike the more traditional pioneers and adventurers, the men flying the Apollo missions will leave in a spacecraft only after their safety is assured. Crew survival will be a most strong concern in the preparation for the voyage. The National Aeronautics and Space Administration has set high safety standards. The crew, in a checked-out vehicle leaving the earth launching pad for the lunar surface, should have a 90% probability of accomplishing the lunar landing mission and have a 99.9% probability of returning to earth safely whether having been able to complete the mission or not. These goals are sought by consideration of all parts of the Apollo program; mission planning, spacecraft design, crew training, testing methods etc. In this chapter we are concerned only with the Apollo safety aspects under consideration in the guidance, navigation and control systems.

Much can be said about the means of producing complex equipment which has an extremely low failure probability. Questions of discipline in basic design, parts selection, manufacturing techniques, qualification methods, testing procedures and other reliability enhancing techniques are much debated. We will bypass this well-treated subject and look at aspects of design and planning which accept the occurrence of failure without the occurrence of disaster. The tolerance to failure in Apollo systems is based primarily on the deliberate design guideline that any single failure should, if at all possible, leave enough working equipment remaining to bring the crew safely home. Although for practical reasons this guideline cannot be met everywhere, the number of safety critical flight items that have no back-up is quite small.

ABORT TRAJECTORIES

The guidance and navigation equipment is designed with enough flexibility in hardware and in computer program to support the measurements and maneuvers necessary for all reasonable mission abort trajectories required due to failures in other parts of the spacecraft. Depending upon the nature of this failure and the phase of the mission in which the failure occurs, the crew can initiate an abort by so informing the flight computer and setting the proper condition of the appropriate propulsion systems. In some situations the pilot can inform the computer which of three types of abort he wishes: (1) time critical aborts which require fastest return using all available propulsion, (2) propulsion critical aborts which require optimum use of available fuel in energy efficient orbital transfers and (3) normal aborts which use trajectories which are constrained to achieve a landing on one of the prepared

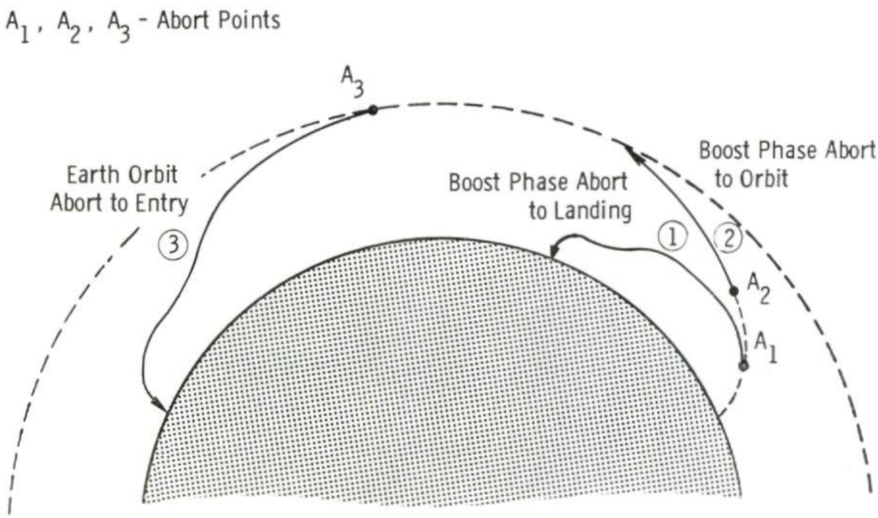

FIG. 2–62 Near earth abort trajectories

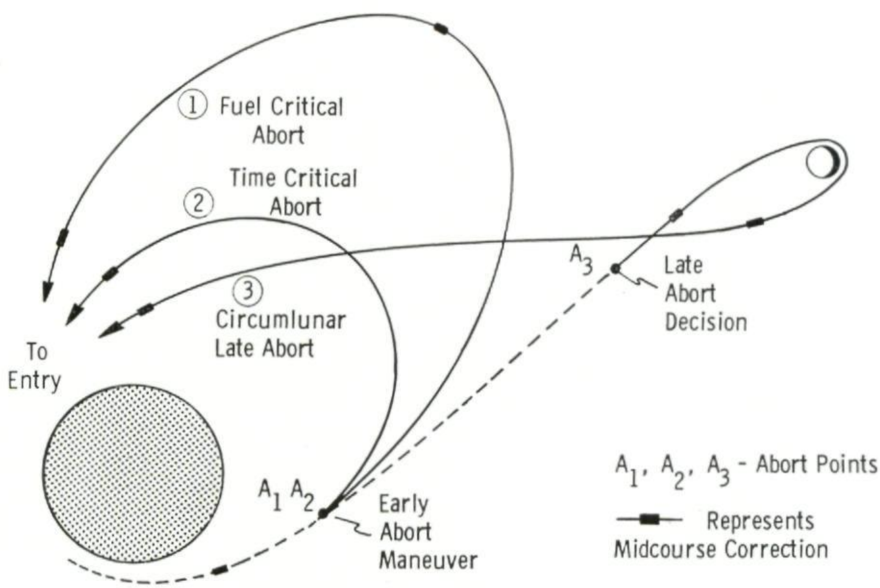

FIG. 2–63 Translunar coast abort trajectories

earth recovery areas. The computer can inform the crew about the times of flight and propulsion usage for each of the above aborts so that the abort mode decision can be made.

The abort trajectory to be determined and controlled by the guidance and navigation equipment depends upon the mission phase in which the abort decision is made. Figure 2–62 illustrates the three abort trajectory types pertinent to operations near the earth. Trajectory 1 on the diagram is direct abort to earth during launch boost ascent. It is flown when the failure is of a nature requiring immediate return to earth or where sufficient propulsion is not available to fly trajectory 2. Abort trajectory 2 continues the flight into earth orbit using an upper stage of the vehicle. It has the advantage of better choice of landing recovery area by selecting the phasing of the return maneuver. It further permits a possible continuation of the flight, but obviously of more limited mission scope. The descent from orbit, trajectory 3, is similar to the earth orbit returns already flown by the Soviet and American manned orbital flights.

Aborts that can be initiated after Apollo has been committed through translunar injection are illustrated in Fig. 2–63. Trajectories 1 and 2 on this figure are typical of the paths flows for aborts initiated during the first part of the translunar coast. Trajectory 1 illustrates a fuel optimum direct return to earth. Trajectory 2 illustrates the full fuel usage quick return to earth. At some point in the translunar coast, the time to earth return is quicker if the spacecraft coasts around behind the moon and then continues home, trajectory 3. All of these cislunar aborts will require careful navigation. Navigation is required before the abort is initiated upon which to base the abort injection guided maneuver. After this maneuver, navigation is needed upon which to base small midcourse corrections to assure accurate arrival at the safe earth entry conditions.

After arrival into lunar orbit, aborts either may be an immediate trans-earth injection or may necessarily be preceeded by recovery of the two men in the LEM. Figure 2–64 illustrates the trajectories and operations involved with the LEM aborts. Trajectory 1 illustrates a typical abort initiated during the LEM descent. The abort trajectory injection, begun at point A_1, is guided and controlled to put the LEM in a fairly high elliptical trajectory so that the phasing is proper for rendezvous to meet the orbiting command module at point R_1. Midcourse corrections, not shown, are necessary based upon navigation from the rendezvous radar on earth tracking data. Unfortunately much of the trajectory occurs behind the moon out of sight of the earth tracking facility. This might suggest use of a low altitude holding orbit such as described below to provide better phasing of the rendezvous for earth coverage.

Trajectory 2 of Fig. 2–64 illustrates a typical LEM emergency abort from the lunar surface. Here it is supposed that a failure has occurred – such as fuel tank leakage or life support system failure – that requires immediate ascent without waiting until the CSM is in the proper position for a normal ascent and rendezvous. The powered phase is guided to put the LEM in a low altitude clear perilune orbit where it will hold until it catches up appropriately with the orbiting command module. At the proper point the ascent engine is fired again for transfer and rendezvous using midcourse corrections

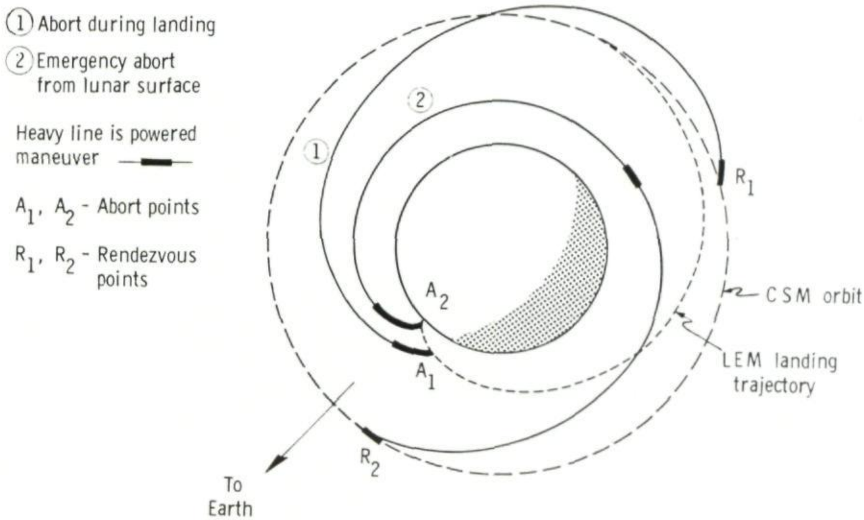

FIG. 2–64 LEM operation abort trajectories

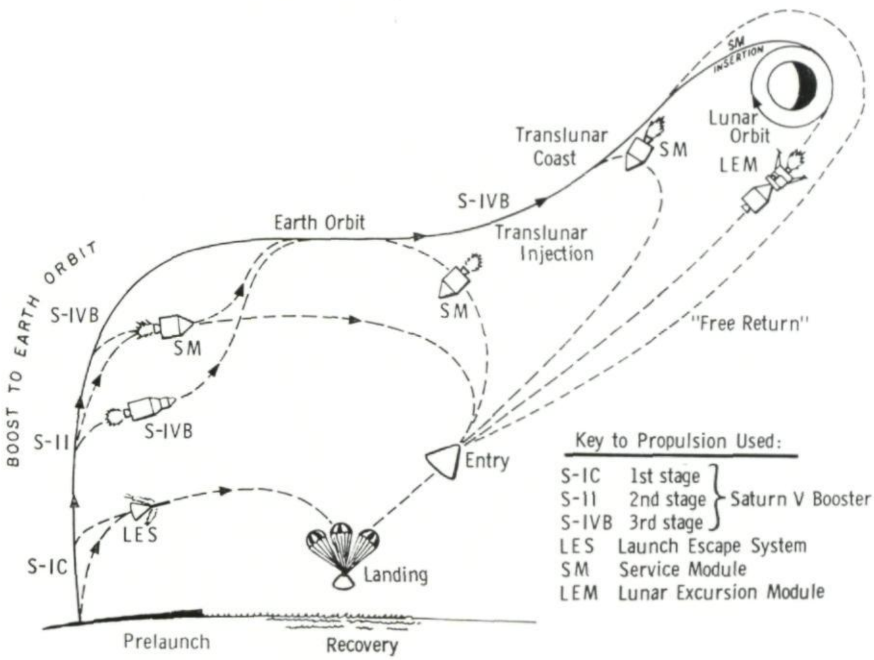

FIG. 2–65 Propulsion failure abort paths

as required. Alternately, once the LEM succeeds in getting into a holding orbit, it can assume if necessary, a passive role and allow the CSM to maneuver for rendezvous and crew pickup.

CONTROL OF PROPULSION FAILURE BACKUPS

The Apollo guidance and control equipment will be designed to operate with abnormal propulsion and loading configurations for given mission phases to provide abort capabilities covering failure in any of the primary rocket engines. Figure 2–65 is a rather fanciful diagram showing examples of aborts of this nature. The heavy ascending line traces out the normal mission phases from prelaunch to lunar orbit. The dashed lines trace out abort paths through alternate propulsion sources to cover failures of the normal rocket used in each phase. These paths are numbered on the diagram and are explained briefly below:

(a) This is the use of the launch escape system providing aborts during the period from on the pad before liftoff until atmospheric exit during the early part of the second stage burn. No measurement is necessary by the guidance system for launch escape aborts; the system is designed to pull the command module safely past and far enough away from an exploding booster for a low velocity entry and normal CM parachute landing.

(b) A failure of the second stage during ascent might be of a nature to allow thrusting in the third SIVB Saturn stage into earth orbit. This would naturally deplete SIVB fuel sufficiently to prevent continuation of a lunar mission.

(c) Again during second stage boost and during third stage as well, the abort may be made to an immediate entry trajectory and landing using the command module propulsion and the spacecraft guidance and control systems.

(d) Aborts using service module propulsion during third stage boost may also be made into earth orbit. A second burn of the service module would then initiate descent to a selected landing site.

(e) If the abort is initiated while in earth orbit the service module propulsion would be used for descent assuming it still functions. If not, the small reaction jets could be used in a limited retrograde translational burn or series of burns so as to capture the atmosphere.

(f) On the way to the moon the service module propulsion could be used to inject into the return orbits described previously.

(g) If the service module rocket has failed the flight can continue around the moon on the "free return" path using the reaction jets in translation maneuvers to perform the necessary midcourse maneuvers determined by navigation.

(h) If the service module propulsion fails while in lunar orbit before the LEM separation and descent, the LEM propulsion and LEM guidance and control systems can be used to inject the command module onto the necessary transearth trajectory.

These examples of propulsion failure abort paths illustrate dramatically the necessary flexibility and universality needed of the Apollo guidance, navigation and control systems.

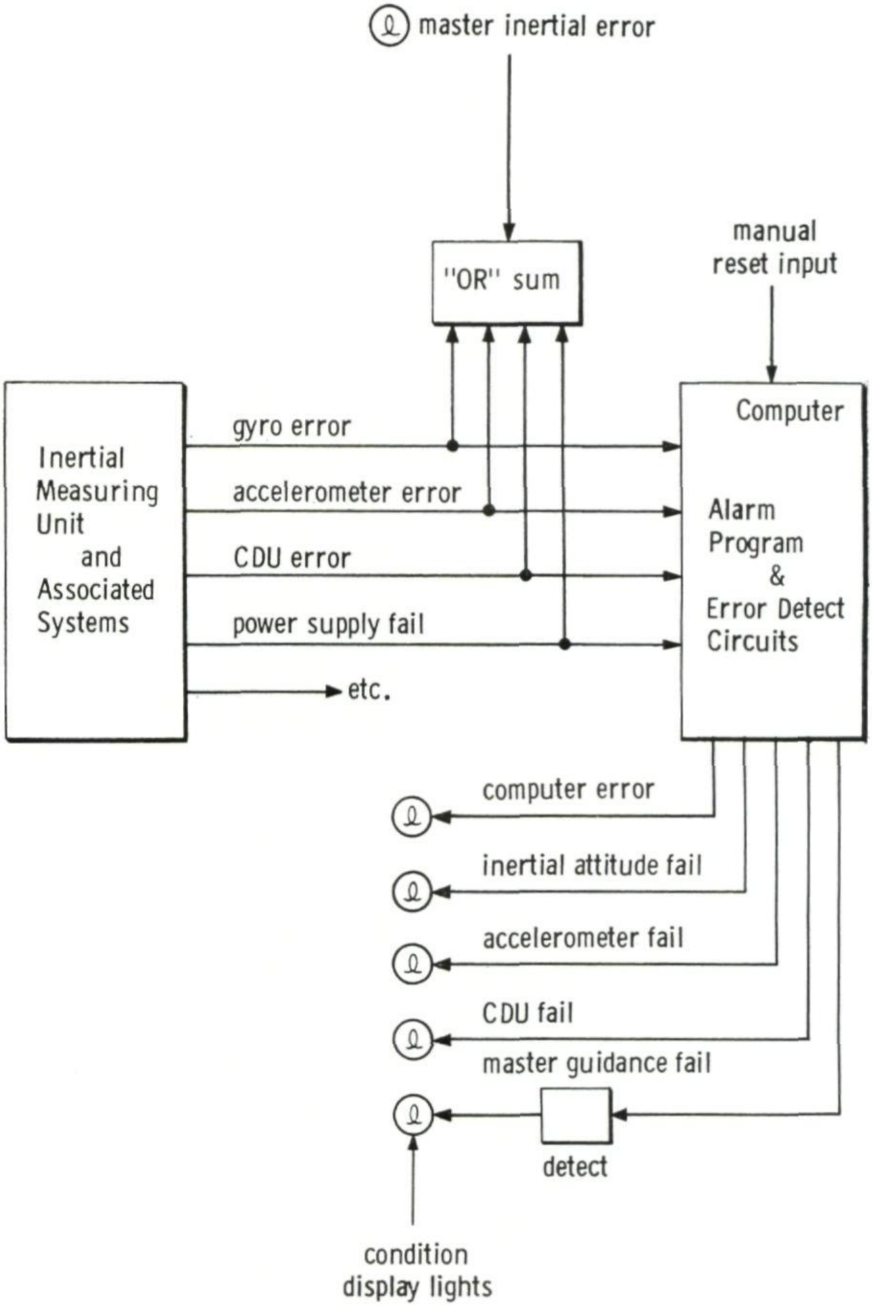

FIG. 2–66 Failure detection – command module primary guidance system

FAILURE DETECTION AND ALARM

A central aspect of mission safety is the early detection of system failure. Part of this detection is in the systematic on-board testing during the stress-free coasting phases to assure the needed systems are functioning. Of more interest, perhaps, is the automatic failure detection features which immediately signal appropriate alarms during the stressed accelerated phases of rocket thrust or entry. It is with the help of these alarms that the crew can initiate appropriate abort action immediately as necessary. As an example, we will limit this discussion to the automatic failure detection of the guidance system in the command module as used during guided flight.

Figure 2–66 is a simplified diagram of this failure detection system. The box at the bottom represents the inertial system. The signals coming out are error detections. Shown is "gyro error" which is a signal which exists when any of the gyro gimbal stabilization loop servo errors exceed a preselected detection level. The "accelerometer error" and "CDU error" have similar properties with detection of any of the accelerometer servo loop errors and coupling display unit servo loop errors. The "power supply fail" signals deviations of the inertial system power supply voltages from preselected levels. Each of these detections is sent to the computer as well as being separately summed to light a master inertial system error display light. During system turn-on or mode switching this light is expected to operate briefly during the transient but will extinguish itself in a normal system.

The computer contains its own error detection programs and circuitry which may light a master computer error light. If this occurs for transient reasons, the astronaut will succeed in extinguishing it by pushing a reset button. The computer program will examine its error and the inertial system detections and will light appropriate fail lights. The "inertial attitude fail" signals that the inertial system alignment is lost and the crew should use a backup system if re-alignment cannot be accomplished. The "accelerometer fail" indicates that the acceleration data in the guidance is faulty and the primary guidance steering cannot be used. In this latter case, however, the inertial attitude data may still be correct for use in a backup mode. A similar situation occurs with the "CDU fail" light.

The last light is a "master guidance fail" which has special features which makes it fail-safe. The computer program examines periodically, at a fixed frequency, all of the previous failure detections and if it finds none the program sends out a pulse of a particular duration. If this pulse keeps occurring at the expected frequency, then the detector inhibits lighting the "master guidance fail". Otherwise this signal lights up. If any of these lights operate the crew is trained to take appropriate emergency backup action.

NAVIGATION REDUNDANCY

The originally stated premise that a single failure should leave the system with enough capability to return safely should now be examined. With respect to navigation this is quite straightforward with the use of both on-board and ground-based provisions. If ground tracking navigation data are unavailable because of a loss of communications, then the on-board system can perform all the necessary navigation.

If the on-board navigation capability fails the ground can provide the

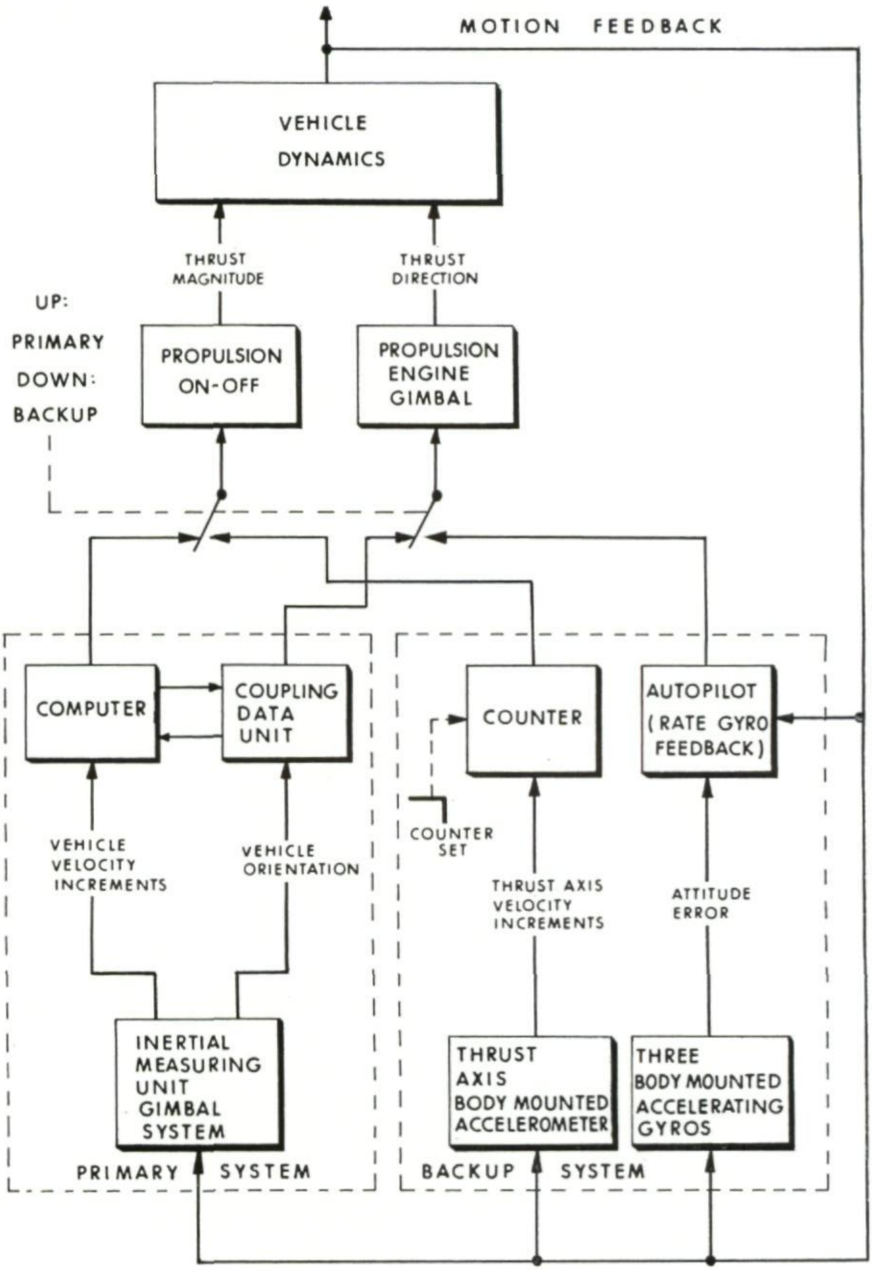

FIG. 2–67 Primary and backup guidance concept

necessary data. This applies to the failure of either the optics system or the on-board computer. For a failed computer, on-board navigation data can be telemetered for ground processing to aid in the ground determination of the necessary abort maneuver. If the optics system drives have failed, star occultation events can be observed, either by spacecraft attitude aiming of the optics or directly through the window. These events are useful navigation data for the computer.

GUIDANCE AND CONTROL BACKUP

Failure in the primary guidance equipment requires the use of an alternate backup system to provide safe return of the crew. The redundancy concept used is illustrated in Fig. 2–67. The figure has been simplified to illustrate more clearly the principles involved.

The primary system involving the inertial measurement unit gimbal system, the flight digital computer and the associated coupling data unit, constitutes a complete, flexible, accurate and fuel efficient guidance and control having the capability to perform all the maneuvers required to complete the mission. The backup system is simpler, smaller and of more modest endowment, being able to make the more simple maneuvers to return the crew after the failure of the primary system has aborted the mission. Figure 2–67 shows a backup using three body-mounted single-degree-of-freedom integrating gyros which provide attitude error signals over a limited angular range. These errors are treated as steering commands to a simple autopilot to hold vehicle direction fixed during an abort thrusting maneuver. Engine cutoff is signalled by the integrated output of a single body axis accelerometer mounted with its sensitive axis along the nominal thrust axis. The integrator consists of a simple preset counter giving as an output an engine shutdown signal when the sum of the accelerometer output velocity increments reaches a level equal to the total velocity desired of the maneuver.

The crew, using data telemetered from the ground, will pre-align the thrust axis in the required abort maneuver direction by aiming the vehicle with respect to the stars. The ground instructions to do this will recognize the expected offset of the thrust axis from the vehicle roll axis. The maneuvers are restricted to accelerations in a fixed direction but of any magnitude set into the acceleration counter. If large magnitude velocity changes are required, then the more limited accuracy of this backup system will result in significant errors. These can be corrected by a much smaller maneuver after a short coast based upon the ground tracking of the abort trajectory.

This backup guidance system just explained is a somewhat simplified description of that used in the command module. The LEM has been given a more complex abort guidance system to perform more accurately the critical and complex abort maneuvers near the moon's surface. This LEM abort system consists of three body-mounted rate-measuring gyros, three body-mounted accelerometers and a small computer to perform necessary transformations of gyro and accelerometer data. This computer also generates steering commands appropriate for abort at any phase of LEM operation to rendezvous conditions with the orbiting command module.

Satisfactory vehicle control also requires three-axis spacecraft torquing during the free-fall and accelerating phases. Optimum redundancy in the

hardware to drive the engine gimbals is provided. The sixteen reaction jets on the service module and the sixteen reaction jets on the LEM allow a limited number of jet failures without unacceptable loss of rotational control or translational control. Likewise the necessary rotational control of the command module is provided by a redundant assembly of twelve reaction jets for use during earth atmospheric entry. Various levels of automatic, semi-automatic and manual control can be selected by the crew to utilize the subsystems available and working. In the limit, the pilot or a surviving companion can use direct hand control commands to the reaction jets and the engine gimbals and a view of the stars as reference directions to provide him with the last level of emergency backup.

PART 3

EXPLICIT AND UNIFIED METHODS OF SPACECRAFT GUIDANCE

Dr. Richard H. Battin

DR. RICHARD H. BATTIN

Dr. Richard H. Battin, Deputy Associate Director of Instrumentation Laboratory, Massachusetts Institute of Technology, is a specialist in space trajectories, guidance concepts and in the programming of space guidance computers. He is in charge of the Space Guidance Analysis Group which is charged with both theoretical analysis and programming of the on-board guidance computer for the Laboratory's development of the guidance system that will be used aboard the Project Apollo spacecraft.

Dr. Battin was born in Atlantic City, N.J., March 3, 1925, and was graduated from Forest Park High School, Baltimore, Md., in 1942. He received the S.B. degree in electrical engineering from M.I.T. in 1945 and served in the Navy as a Supply Corps officer for one year. He returned to M.I.T. in 1946 as an instructor in mathematics and a research assistant in meterology, studying atmospheric circulations. He was awarded the Ph.D. degree in Applied Mathematics from M.I.T. in 1951. Dr. Battin joined the Instrumentation Laboratory in 1951 as a research mathematician working on fire control and inertial navigation systems and later became head of the Laboratory's Computing Devices Group.

From 1956 to 1958, Dr. Battin was a senior staff member in the Operations Research Group of Arthur D. Little, Inc., working on digital data processing for business and industrial research. Since returning to the Instrumentation Laboratory in 1958, Dr. Battin has been engaged primarily in interplanetary navigation theory and development.

Dr. Battin is the author of the book "Astronautical Guidance" (New York; McGraw-Hill, Inc., 1964) and co-author of the book, "Random Processes in Automatic Control" (New York; McGraw-Hill, 1956). He has published numerous articles in professional journals dealing with meteorology, analog and digital computing techniques, stochastic processes, interplanetary trajectories and navigation. He is a member of Sigma Xi and an Associate Fellow of the American Institute of Aeronautics and Astronautics.

PART 3

EXPLICIT AND UNIFIED METHODS OF SPACECRAFT GUIDANCE

INTRODUCTION

Of fundamental importance in the design of space guidance systems is the creation of both flexible techniques and versatile instrumentation which have a wide range of applicability but neither compromise mission accuracy nor place an undue burden on propulsion requirements. Minimal constraints on the system and methods of its operation should be imposed by detailed mission objectives which are subject to frequent and last minute revision. In partial fulfillment of these goals, the development of explicit guidance techniques is warranted to reduce any dependence on precomputed reference orbits or specific rocket engine characteristics.

During the evolution of a space flight program such as Apollo, the ultimate mission objective is attained progressively by a series of intermediate flights. Each successive flight is planned as a direct extension of the previous one so that the need for special equipment and untried techniques can be minimized. The success of this approach is enhanced through the development of unified guidance methods. Then the guidance requirements for each new mission phase can be met as a specific application of a general guidance principle.

The two fundamental tasks of a guidance system are to maintain accurate knowledge of spacecraft position and velocity and to provide steering commands for required changes in course. It is the purpose here to review some of the current techniques for solving the guidance problem emphasizing those methods which are consistent with the explicit and unified philosophy of design.

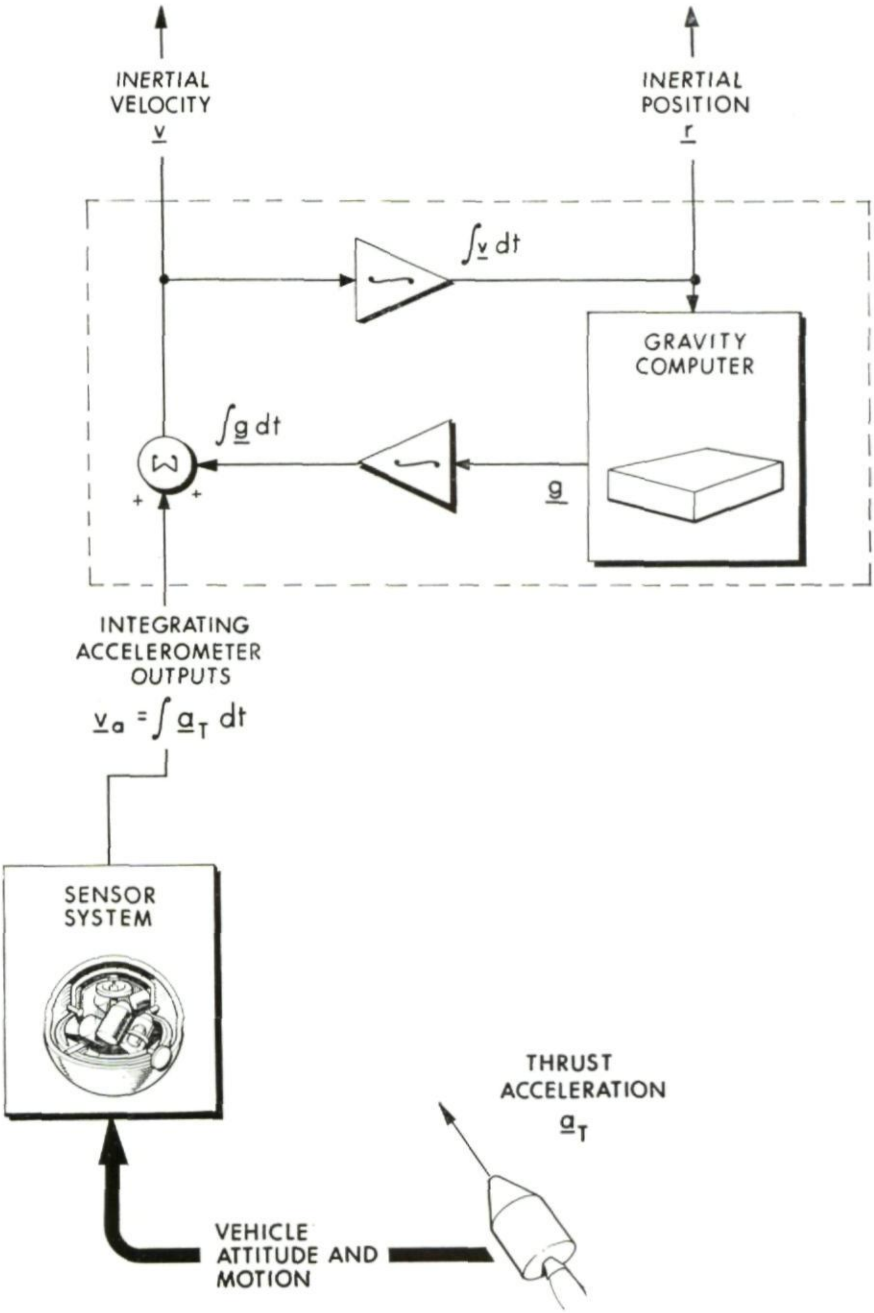

Fig. 3-1 Accelerated flight navigation system

CHAPTER 3–1

ACCELERATED FLIGHT NAVIGATION

The task of periodic determination of position and velocity, customarily referred to as navigation, divides naturally into two parts – accelerated flight and coasting flight. For navigation during an accelerated maneuver, the system frequently includes inertial instruments capable of measuring thrust acceleration along three mutually orthogonal axes which are nonrotating. A guidance computer is then required to perform accurate integrations and gravity calculations on a real-time basis.

A functional diagram of the basic computations required of the navigation system is shown in Fig. 3–1. Incremental outputs from inertially stabilized integrating accelerometers, together with components of gravitational acceleration computed as functions of inertial position in a feedback loop, are summed to give the components of inertial velocity. The ultimate precision attainable is, of course, limited by the accuracy of the inertial instruments, the speed of the guidance computer and the knowledge of the initial conditions.

GRAVITY COMPUTER

The gravity calculations may be performed in a straightforward manner. The equations of motion for a vehicle moving in a gravitational field are

$$\frac{d\underline{r}}{dt} = \underline{v} \qquad \frac{d\underline{v}}{dt} = \underline{g} + \underline{a}_T \qquad \text{(Eq. 3–1)}$$

where $\underline{r}$ and $\underline{v}$ are the position and velocity vectors with respect to an inertial frame of reference. The measured acceleration vector $\underline{a}_T$ of the vehicle is defined to be the vehicle acceleration resulting from the sum of rocket thrust and aerodynamic forces, if any, and would be zero if the vehicle moved under the action of gravity alone. The vector sum of $\underline{a}_T$ and $\underline{g}$, the gravitational vector, represents the total vehicle acceleration.

A simple computational algorithm, by means of which position and velocity are obtained as a first order difference equation calculation, follows:

$$\begin{aligned} \Delta\underline{v}_a(t_n) &= \underline{v}_a(t_n) - \underline{v}_a(t_{n-1}) \\ \underline{r}(t_n) &= \underline{r}(t_{n-1}) + \underline{v}(t_{n-1})\,\Delta t + \frac{1}{2}\underline{g}_{n-1}\,(\Delta t)^2 + \frac{1}{2}\Delta\underline{v}_a(t_n)\,\Delta t \qquad \text{(Eq. 3–2)} \\ \underline{v}(t_n) &= \underline{v}(t_{n-1}) + \Delta\underline{v}_a(t_n) + \frac{1}{2}(\underline{g}_n + \underline{g}_{n-1})\,\Delta t \end{aligned}$$

The vector $\underline{v}_a$ is the time integral of the non-gravitational acceleration forces, the components of which are the outputs of the three mutually orthogonal integrating accelerometers as shown in Fig. 3–2. The gravitational vector $\underline{g}_n$ is a function of position at time t_n. In the figure, only a simple spherical gravitation field is considered.

Since velocity is updated by means of the average effective gravity over

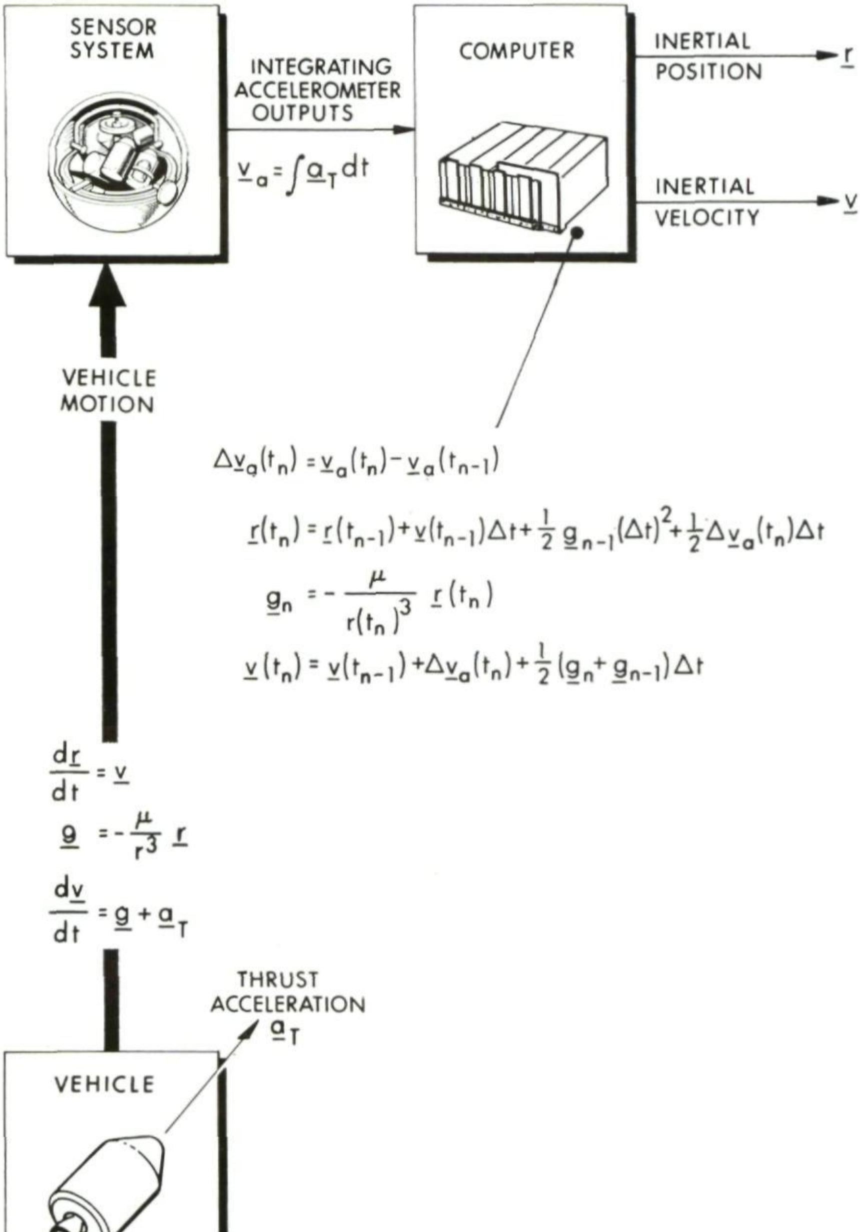

FIG. 3-2 Accelerated flight navigation

the interval of one time step, this method has been termed the "average g" method. A careful error analysis of a vehicle in earth orbit has shown this algorithm to yield errors of the order of 100 feet and 0.2 feet per second after a period of 35 minutes using a 2 second time step and rounding all additions to 8 decimal digits. The errors will increase for a smaller time step due to the effects of accumulated round off errors and will also increase for larger time steps as truncation errors become significant. When compared to typical accelerometer scale factor errors, the error in the computational algorithm seems to be several orders of magnitude smaller.

BODY-MOUNTED SENSORS

During recent years increasing attention has been devoted to the so-called "gimballess inertial measurement unit" in which the inertial sensors are mounted directly to the spacecraft (see Bumstead and Vander Velde (1) and Wiener (2)). Although many advantages might accrue in terms of system weight, volume, power, cost, packaging flexibility, reliability and maintainability, the realization of a satisfactory design is not without significant problems. Unlike the environment provided by a gimballed system, the body mounted inertial instruments are subjected to substantial angular velocity which tends to exaggerate performance errors. Also, the role of the guidance computer is expanded since the angular orientation of the vehicle must also be determined by integration of measured angular velocities. It is most convenient if the outputs of the body mounted accelerometers are immediately transformed into an inertially stabilized coordinate frame so that the navigation or guidance problem can be solved just as if a physically stabilized platform had been employed.

As indicated in Fig. 3-3, the body fixed coordinates and the inertial coordinates of the thrust acceleration vector are related by a transformation matrix of direction cosines. The additional computations required of the guidance computer involve the updating of the matrix and using it to transform vectors from one frame of reference to the other. The transformation matrix R is readily shown to satisfy a first order differential equation with a coefficient matrix Ω whose elements are the components of the angular velocity of the body fixed coordinate frame measured in body coordinates.

Currently, pulse-torqued integrating gyros are the most promising candidates for angular velocity sensors. However, since their basic output consists of angular increments rather than angular velocity, the accuracy with which the transformation matrix differential equation may be integrated is adversely affected. The use of a higher order integration rule provides no advantage over simple rectangular integration since the basic data from the gyro has already an uncertainty of the order of the square of the gyro quantization error.

The accuracy attainable by a gimballess inertial system is limited primarily by the maximum angular velocities to which the vehicle is subjected. The required sampling time of the integrating gyros is inversely proportional to this maximum angular velocity and the time step used for integrating the direction cosine differential equations must be of the same order of magnitude as the gyro sampling time. If the sample time is very short, a digital differential analyzer may prove to be the best solution to the problem of selecting a

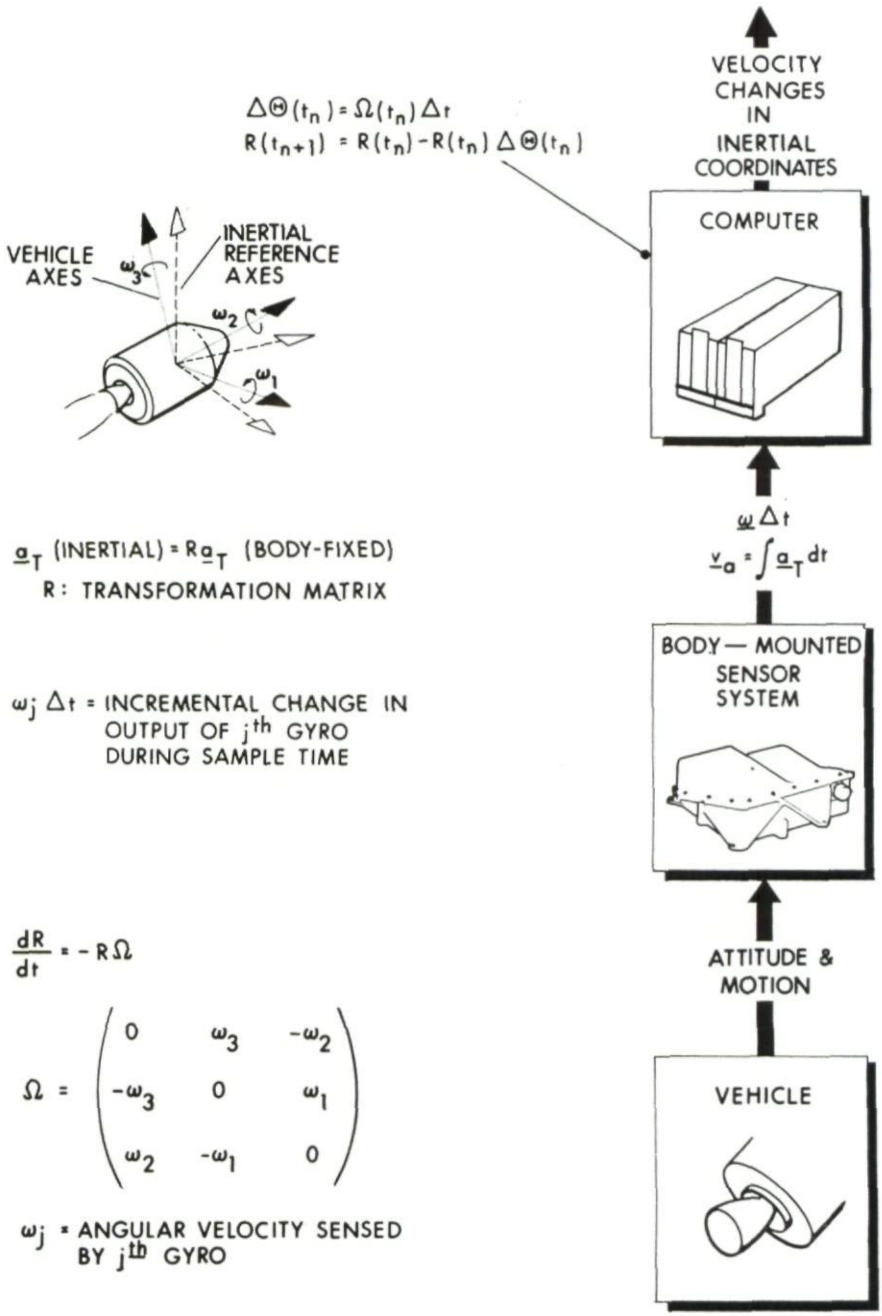

FIG. 3–3 Navigation using body mounted sensors

guidance computer. On the other hand, if the sampling time is long enough to permit the use of a general purpose computer, there may be sufficient time remaining in which to process the navigation and/or steering equations. This is, of course more satisfactory, for then one has the possibility of satisfying all or most of the complete system computation requirements with a single computer.

CHAPTER 3–2

COASTING FLIGHT NAVIGATION

Spacecraft navigation during prolonged coasting flight is performed by appropriate utilization of periodic measurements of convenient physical quantities such as (a) distance, velocity, elevation and azimuth from well-established reference points, (b) angles between lines of sight to known celestial objects. (c) star occultations and (d) apparent planet diameters. Since navigation measurements are more accurately made when the sensors are in proximity to the data source, vehicle-borne and ground-based instrumentation can serve in complementary roles.

COMPARISON OF METHODS

The data processing aspects of the navigation problem have been the subject of much research during recent years. The classical method of the astronomer, called the "method of differential corrections", is cumbersome for large amounts of observational data and is not well suited to implementation in a vehicle-borne computer. Blackman, in a recent paper (3), gives an excellent review of several of the new methods contrasting them with the classical approach and with each other.

Currently, the statistical methods of optimum linear estimation theory seem to hold the most promise. The statistical method of maximum likelihood, which is based on the concept of maximizing a particular conditional probability, has received much attention. Optimum filter theory, whose goal is to find a linear estimator that minimizes some function of the variances and covariances of the uncertainties in the estimated state vector, provides an alternate method of attack. Although the subject may be approached from a variety of points of view, Potter and Stern (4) have shown that all such methods lead to equivalent results if the measurement uncertainties have Gaussian distributions.

RECURSIVE NAVIGATION

The scope of this chapter does not permit a thorough development of the mathematics underlying the so-called "recursive method" of spacecraft position and velocity estimation; however this is adequately treated in reference (5). The method, which is particularly well-suited to both vehicle-borne and ground-based computation, is under active consideration for use in the Apollo guidance computer as well as in the Mission Control Center at the Manned Spacecraft Center, Houston, Texas.

The estimate of position and velocity is maintained in the computer in non-rotating rectangular coordinates and is referenced to either the earth or the moon. An earth centered equatorial coordinate system is used when the vehicle is outside of the lunar sphere of influence. Inside of this sphere the center of coordinates coincides with the center of the moon. The extrapola-

tion of position and velocity is made by a direct numerical integration of the equations of motion.

The basic equation may be written in vector form as:

$$\frac{d^2}{dt^2}\underline{r}_{PV} + \frac{\mu_P}{r^3_{PV}}\underline{r}_{PV} = \underline{a}_d \qquad \text{(Eq. 3-3)}$$

where $\underline{r}_{PV}$ is the vector position of the vehicle with respect to the primary body P which is either the earth or moon and μ_P is the gravitational constant of P. The vector $\underline{a}_d$ is the vector acceleration which prevents the motion of the vehicle from being precisely a conic with P at the focus. If a_d is small compared with the central force field, direct use of Eq. 3–3 is inefficient. As an alternative, the integration may be accomplished employing the technique of differential accelerations suggested by Encke.

Encke's Method – At time t_0 the position and velocity vectors $\underline{r}_{PV}(t_0)$ and $\underline{v}_{PV}(t_0)$ define an osculating orbit. The vector difference $\underline{\delta}\ (t)$ satisfies the following differential equation

$$\frac{d^2}{dt^2}\underline{\delta} = \frac{\mu_P}{r^3_{PV(C)}}\left[\left(1 - \frac{r^3_{PV(C)}}{r^3_{PV}}\right)\underline{r}_{PV} - \underline{\delta}\right] + \underline{a}_d \qquad \text{(Eq. 3-4)}$$

subject to the initial conditions:

$$\underline{\delta}(t_0) = 0 \qquad \frac{d}{dt}\underline{\delta}(t_0) = \underline{v}(t_0) = 0$$

where $\underline{r}_{PV(C)}$ is the osculating conic position vector. The numerical difficulties which would arise from the evaluation of the coefficient of $\underline{r}_{PV}$ in Eq. 3–4 may be avoided. Since:

$$\underline{r}_{PV}\ (t) = \underline{r}_{PV(C)}\ (t) + \underline{\delta}\ (t) \qquad \text{(Eq. 3-5)}$$

it follows that:

$$1 - \frac{r^3_{PV(C)}}{r^3_{PV}} = -f(q_C) = 1 - (1 + q_C)^{3/2}$$

where:

$$q_C = \frac{(\underline{\delta} - {}^2\underline{r}_{PV}) \cdot \underline{\delta}}{r^2_{PV}} \qquad \text{(Eq. 3-6)}$$

The function $f(q)$ may be conveniently evaluated from:

$$f(q) = q\,\frac{3 + 3q + q^2}{1 + (1 + q)^{3/2}} \qquad \text{(Eq. 3-7)}$$

Encke's method may now be summarized as follows:

(a) Position in the osculating orbit is calculated from:

$$\underline{r}_{PV(C)}\ (t) = \left[1 - \frac{x^2}{r_{PV}(t_0)}\,C(\alpha_0 x^2)\right]\underline{r}_{PV}(t_0) + \left[(t-t_0) - \frac{x^3}{\sqrt{\mu_P}}\,S(\alpha_0\, x^2)\right]\underline{v}_{PV}(t_0) \qquad \text{(Eq. 3-8)}$$

where:

$$\alpha_0 = \frac{2}{r_{PV}(t_0)} - \frac{v_{PV}(t_0)^2}{\mu_P} \qquad \text{(Eq. 3-9)}$$

and x is determined as the root of Kepler's equation in the form:

$$\sqrt{\mu_P}(t-t_0) = \frac{\underline{r}_{PV}(t_0) \cdot \underline{v}_{PV}(t_0)}{\sqrt{\mu_P}} x^2 C(\alpha_0 x^2) + [1 - r_{PV}(t_0)\alpha_0] x^3 S(\alpha_0 x^2) + r_{PV}(t_0) x \qquad \text{(Eq. 3–10)}$$

The special transcendental functions S and C are defined by:

$$S(x) = \frac{1}{3!} - \frac{x}{5!} + \frac{x^2}{7!} - \ldots \qquad \text{(Eq. 3–11)}$$

$$C(x) = \frac{1}{2!} - \frac{x}{4!} + \frac{x^2}{6!} - \ldots$$

(b) Deviations from the osculating orbit are obtained by a numerical integration of

$$\frac{d^2}{dt^2} \underline{\delta}(t) = -\frac{\mu_P}{r^3_{PV(C)}(t)} [f(q)\, \underline{r}_{PV}(t) + \underline{\delta}(t)] + \underline{a}_d(t) \qquad \text{(Eq. 3–12)}$$

The first term on the right hand side of the last equation must remain small, i.e. of the same order as $\underline{a}_d(t)$, if the method is to be efficient. As the deviation vector $\underline{\delta}$ grows in magnitude this term will eventually increase in size. Therefore, in order to maintain the efficiency, a new osculating orbit should be defined by the true position and velocity. The process of selecting a new conic orbit from which to calculate deviations is called rectification. When rectification occurs, the initial conditions of the differential equation for $\underline{\delta}$ are again zero and the right hand side is simply the perturbation acceleration $\underline{a}_d$ at the time of rectification.

(c) The position vector $\underline{r}_{PV}(t)$ is computed from Eq. 3–5 using Eq. 3–8. The velocity vector $\underline{v}_{PV}(t)$ is then computed as:

$$\underline{v}_{PV}(t) = \underline{v}_{PV(C)}(t) + \underline{v}(t) \qquad \text{(Eq. 3–13)}$$

where:

$$\underline{v}_{PV(C)}(t) = \frac{\sqrt{\mu_P}}{r_{PV}(t_0)\, r_{PV(C)}(t)} [\alpha_0 x^3 S(\alpha_0 x^2) - x]\, \underline{r}_{PV}(t_0) + \left[1 - \frac{x^2}{r_{PV(C)}(t)} C(\alpha_0 x^2)\right] \underline{v}_{PV}(t_0) \qquad \text{(Eq. 3–14)}$$

Disturbing Acceleration – The form of the disturbing acceleration $\underline{a}_d$ to be used depends on the phase of the mission. In earth orbit only the gravitational anomalies arising from the non-spherical shape of the earth need be considered. During translunar and transearth flight the gravitational attraction of the sun and the secondary body Q (either earth or moon) are relevant forces. In lunar orbit it may be necessary to consider forces arising from the non-spherical shape of the moon. A summary of the various cases appears below.

(a) Earth Orbit

$$\underline{a}_d = \frac{\mu_E}{r^2_{EV}} \sum_{k=2}^{4} J_k \left(\frac{r_{eq}}{r_{EV}}\right)^k [P'_{k+1}(\cos\phi)\, \underline{i}_{EV} - P'_k(\cos\phi)\, \underline{i}_z] \qquad \text{(Eq. 3–15)}$$

where:

$$P'_2 (\cos \phi) = 3 \cos \phi$$
$$P'_3 (\cos \phi) = \tfrac{1}{2} (15 \cos^2 \phi - 3)$$
$$P'_4 (\cos \phi) = \tfrac{1}{3} (7 \cos \phi \, P'_3 - 4 P'_2)$$
$$P'_5 (\cos \phi) = \tfrac{1}{4} (9 \cos \phi \, P'_4 - 5 P'_3)$$

are the derivatives of the Legendre polynomials:
Cos $\phi = \underline{i}_{EV} \cdot \underline{i}_z$ is the cosine of the angle ϕ between the unit vector $\underline{i}_{EV}$ in the direction of of $\underline{r}_{EV}$ and the unit vector $\underline{i}_z$ in the direction of the north pole; r_{eq} is the equatorial radius of the earth; and J_2, I_3, J_4 are the coefficients of the second, third and fourth harmonics of the earth's potential function. The subscript E denotes the center of the earth as the origin of coordinates.
(b) Translunar and Transearth Flight

$$\underline{a}_d = -\frac{\mu_Q}{r^3_{QV}} [f(q_Q) \underline{r}_{PQ} + \underline{r}_{PV}] - \frac{\mu S}{r^3_{SV}} [f(q_S) \underline{r}_{PS} + \underline{r}_{PV}] \quad \text{(Eq. 3–16)}$$

where the subscripts Q and S denote the secondary body and the sun, respectively. Thus, for example, $\underline{r}_{PS}$ is the position vector of the sun with respect to the primary body. The arguments $q_{(\,)}$ are calculated from

$$q_{(\,)} = \frac{(\underline{r}_{PV} - 2\underline{r}_{P(\,)}) \cdot \underline{r}_{PV}}{r^2_{P(\,)}} \quad \text{(Eq. 3–17)}$$

and the function f from Eq. 3–7.

Ephemeris data for the positions of the moon relative to the earth $\underline{r}_{EM}$ and the sun relative to the earth-moon barycenter $\underline{r}_{BS}$ are required as functions of time. The position of the sun relative to the primary planet $\underline{r}_{PS}$ is then computed from

$$\underline{r}_{PS}(t) = \underline{r}_{BS}(t) + \frac{\mu_Q}{\mu_P + \mu_Q} \underline{r}_{PQ} \quad \text{(Eq. 3–18)}$$

In the vicinity of the lunar sphere of influence a change in origin of coordinates is made. Thus:

$$\begin{aligned} \underline{r}_{PV}(t) - \underline{r}_{PQ}(t) &= \underline{r}_{QV}(t) \rightarrow \underline{r}_{PV}(t) \\ \underline{v}_{PV}(t) - \underline{v}_{PQ}(t) &= \underline{v}_{QV}(t) \rightarrow \underline{v}_{PV}(t) \end{aligned} \quad \text{(Eq. 3–19)}$$

(c) Lunar Orbit

$$\begin{aligned} \underline{a}_d = -\frac{3\mu_M r_m^2 C'}{2 r_{MV}^4} \Bigg(& \left\{ \frac{B-A}{C} [1 - 5 (\underline{i}_{MV} \cdot \underline{i}_\eta)^2] + \right. \\ & \left. + \frac{C-A}{C} [1 - 5 (\underline{i}_{MV} \cdot \underline{i}_\xi)^2] \right\} (\underline{i}_{MV} \cdot \underline{i}_\xi) \underline{i}_\xi \\ & + \left\{ \frac{B-A}{C} [3 - 5 (\underline{i}_{MV} \cdot \underline{i}_\eta)^2] + \right. \\ & \left. + \frac{C-A}{C} [1 - 5 (\underline{i}_{MV} \cdot \underline{i}_\xi)^2] \right\} (\underline{i}_{MV} \cdot \underline{i}_\eta) \underline{i}_\eta \\ & + \left\{ \frac{B-A}{C} [1 - 5 (\underline{i}_{MV} \cdot \underline{i}_\eta)^2] + \right. \\ & \left. + \frac{C-A}{C} [3 - 5 (\underline{i}_{MV} \cdot \underline{i}_\xi)^2] \right\} (\underline{i}_{MV} \cdot \underline{i}_\xi) \underline{i}_\xi \Bigg) \end{aligned} \quad \text{(Eq. 3–20)}$$

where A, B, C are the principal moments of inertia of the moon, r_m is the radius of the moon, C' is C divided by the product of the mass of the moon and the square of its radius, $\underline{i}_\xi$, $\underline{i}_\eta$, $\underline{i}_\zeta$ are the selenographic coordinate unit vectors, and $\underline{i}_{MV}$ is the unit vector in the direction of $\underline{r}_{MV}$.

Navigation Measurements – Periodically, the position and velocity of the spacecraft must be brought into accord with optical or radar observations made with either on-board or ground-based sensors. At the time a measurement is made the best estimate of spacecraft position and velocity is the extrapolated estimate maintained in the computer and denoted by $\underline{r}_{PV}$ and $\underline{v}_{PV}$ as shown in Fig. 3–4. From this estimate, it is possible to determine an estimate of the quantity to be measured such as an angle, range from a tracking station or range rate. When the predicted value of this measurement is compared with the actual measured quantity, the difference is used to improve the estimated position and velocity vector.

(a) The Measurement Geometry Vector

An important feature of the recursive navigation method is that measurement data from a wide variety of sources may be incorporated within the same framework of computation. Associated with each measurement is a six-dimensional vector $\underline{b}$ representing, to a first order of approximation, the variation in the measured quantity q which would result from variations in the components of position and velocity. Thus, each measurement establishes a component of the spacecraft state vector along the direction of the $\underline{b}$ vector in state space.

Specifically, if $\underline{b}_1$ and $\underline{b}_2$ are the upper and lower three-dimensional partitions of the six-dimensional b vector and if $\delta\tilde{q}$ is the difference between the value of the quantity as actually measured and the expected value as computed from the current values of $\underline{r}_{PV}$ and $\underline{v}_{PV}$, then:

$$\delta\tilde{q} = \underline{b}_1 \,.\, \delta\underline{r}_{PV} + \underline{b}_2 \cdot \delta\underline{v}_{PV} \qquad \text{(Eq. 3–21)}$$

where $\delta\underline{r}_{PV}$ and $\delta\underline{v}_{PV}$ are the changes in the computed values of position and velocity necessary to make the estimated state of the vehicle compatible with the observation.

As examples of both ground-based and on-board measurements we may list the following:

1. Radar Range Measurement

$$\underline{b}_1 = \underline{i}_{RV}$$
$$\underline{b}_2 = 0$$
$$q = r_{RV}$$

where r_{RV} is the range of the vehicle from the radar site and $\underline{i}_{RV}$ is a unit vector in the direction of the vehicle from the site.

2. Radar Range Rate Measurement

$$\underline{b}_1 = \frac{1}{r_{RV}}\,\underline{i}_{RV} \times (\underline{v}_{RV} \times \underline{i}_{RV})$$
$$\underline{b}_2 = \underline{i}_{RV}$$
$$q = \underline{v}_{RV} \cdot \underline{i}_{RV}$$

where $\underline{v}_{RV}$ is the velocity of the vehicle with respect to the radar site.

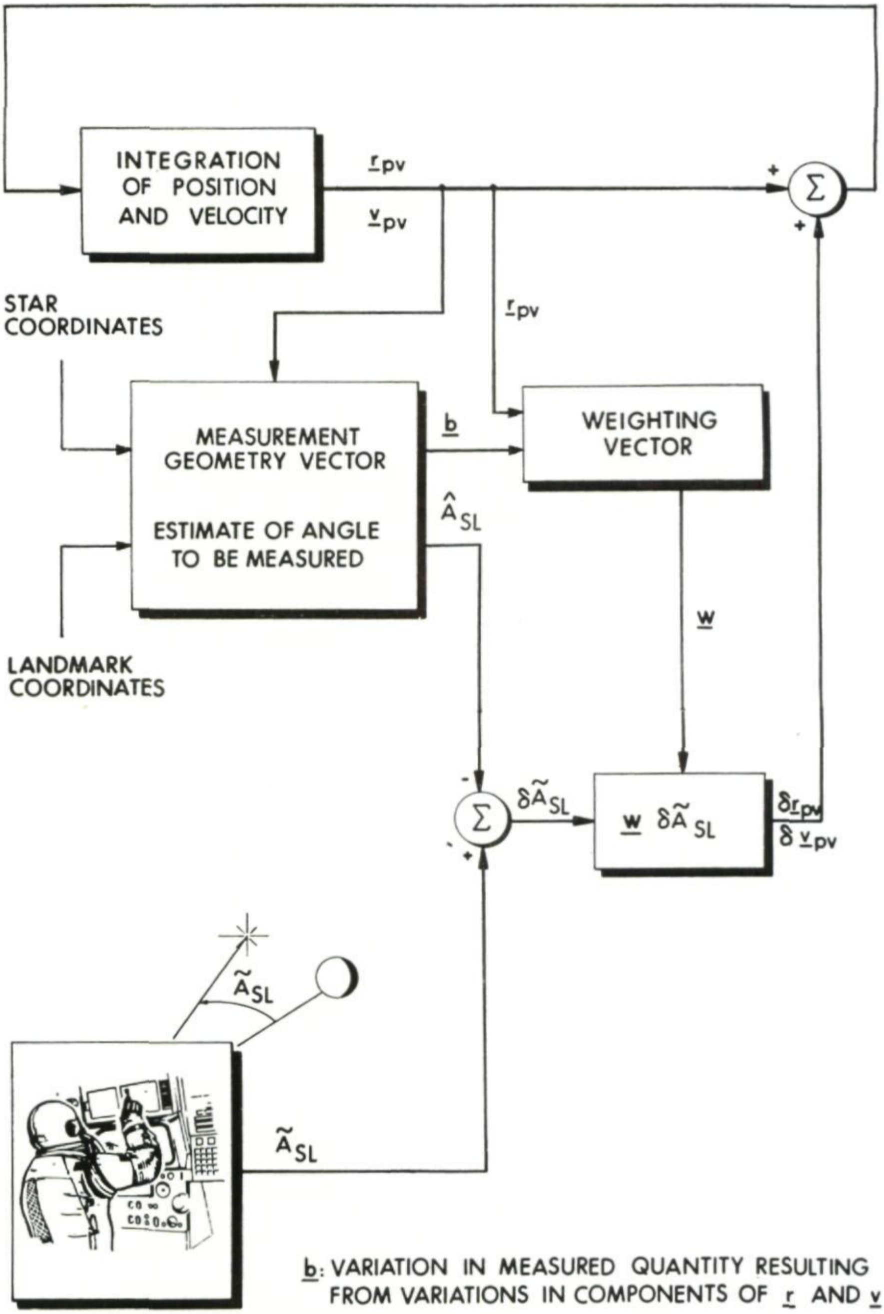

FIG. 3-4 Coasting flight navigation computation

3. Star-Landmark Measurement

$$\underline{b}_1 = \frac{1}{r_{LV}} \text{ UNIT } [\underline{i}_s - (\underline{i}_s \cdot \underline{i}_{LV})\, \underline{i}_{LV}]$$

$$\underline{b}_2 = 0$$

$$q = \cos^{-1} (-\underline{i}_{LV} \cdot \underline{i}_s)$$

where r_{LV} is the distance of the vehicle from the landmark and i_{LV} is a unit vector in the direction of the vehicle from the landmark. The unit vector i_s gives the direction of the star. The notation UNIT ( ) indicates a unit vector in the direction of the quantity ( ).

4. Star-Horizon Measurement

$$\underline{b}_1 = \frac{1}{\sqrt{r_{PV}^2 - r_{PH}^2}} \text{ UNIT } \Big\{ \sqrt{r_{PV}^2 - r_{PH}^2} \times$$

$$\text{UNIT } [\underline{i}_s - (\underline{i}_s \cdot \underline{i}_{PV})\underline{i}_{PV}] - r_{PH}\, \underline{i}_{PV} \Big\}$$

$$\underline{b}_2 = 0$$

$$q = \cos^{-1} (-\underline{i}_{PV} \cdot \underline{i}_s) - \sin^{-1} \frac{r_{PH}}{r_{PV}}$$

where $\underline{r}_{PV}$ is a vector from the selected planet to the vehicle and r_{PH} is the altitude of the horizon from the center of the planet. If the far horizon is chosen for the measurement, then r_{PH} must be negative.

(b) The Error Transition Matrix

Six measurements made simultaneously would provide a set of six equations of the form of Eq. 3–21. If the directions of the associated $\underline{b}$ vectors span the state space, then the vector changes $\delta\underline{r}_{PV}$ and $\delta\underline{v}_{PV}$ could be obtained by inversion of the six-dimensional coefficient matrix each of whose rows were elements of the $\underline{b}$ vectors.

Both the problems of simultaneous measurements and matrix inversion can be avoided in such a manner that measurement data may be incorporated sequentially as it is obtained. For this purpose, it is necessary to maintain statistical data in the guidance computer in the form of a six-dimensional correlation matrix $E(t)$ of estimation errors. If $\epsilon(t)$ and $\underline{v}(t)$ are the errors in the estimates of the position and velocity vector, respectively, then the six-dimensional correlation matrix $E(t)$ is defined by Eq. 3–22.

The transpose of a vector or a matrix is denoted by a superscript T.

$$E(t) = \begin{pmatrix} \overline{\underline{\epsilon}(t)\ \underline{\epsilon}(t)^T} & \overline{\underline{\epsilon}(t)\ \underline{v}(t)^T} \\ \overline{\underline{v}(t)\ \underline{\epsilon}(t)^T} & \overline{\underline{v}(t)\ \underline{v}(t)^T} \end{pmatrix} \qquad \text{(Eq. 3–22)}$$

Because of accumulated numerical inaccuracies, it is possible that this correlation matrix may fail to remain positive definite after a large number of computations as it theoretically must. A recent innovation to avoid this problem, which has also the advantage of significantly reducing the total computational requirements, is to replace the correlation matrix by a matrix $W(t)$, called the error transition matrix. The $W(t)$ matrix has the property:

$$E(t) = W(t)\ W(t)^T \qquad \text{(Eq. 3–23)}$$

and thus, in a sense, is the square root of the correlation matrix. If needed,

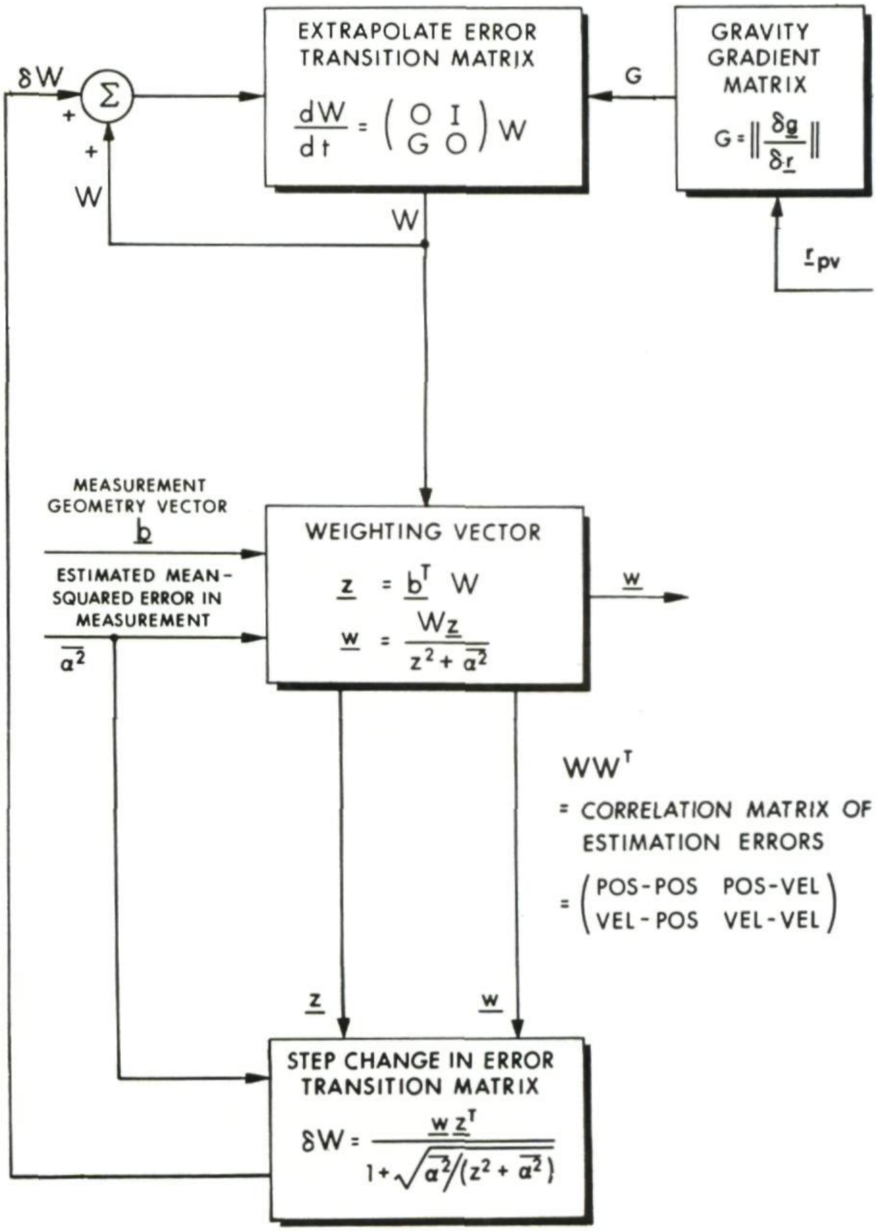

FIG. 3-5 Weighting vector calculations

the correlation matrix may be determined as the product of the matrix $W(t)$ and its transpose, thereby guaranteeing it to be at least positive semi-definite.

Extrapolation of the matrix $W(t)$ is made by direct numerical integration of the differential equation:

$$\frac{dW}{dt} = \begin{pmatrix} O & I \\ G(t) & O \end{pmatrix} W \qquad \text{(Eq. 3-24)}$$

where $G(t)$ is the three-dimensional gravity gradient matrix. The matrices I and O are the three-dimensional identity and zero matrices, respectively. If the W matrix is partitioned as:

$$W = \begin{pmatrix} \omega_1 & \omega_2 & \ldots\ldots & \omega_6 \\ \dfrac{d\omega_1}{dt} & \dfrac{d\omega_2}{dt} & \ldots\ldots & \dfrac{d\omega_6}{dt} \end{pmatrix} \qquad \text{(Eq. 3-25)}$$

then the extrapolation may be accomplished by successively integrating the vector differential equations:

$$\frac{d^2}{dt^2}\omega_i = G(t)\omega_i \quad i = 1, 2, \ldots, 6 \qquad \text{(Eq. 3-26)}$$

The $G(t)$ matrix for translunar and transearth flight is readily shown to be:

$$G(t) = \frac{\mu_E}{r_{EV}^5(t)}\left[3\underline{r}_{EV}(t)\,\underline{r}_{EV}(t)^T - r_{EV}^2(t)\,\mathrm{I}\right] + \frac{\mu_M}{r_{MV}^5(t)}\left[3\underline{r}_{MV}(t)\,\underline{r}_{MV}(t)^T - r_{MV}^2(t)\,\mathrm{I}\right]$$

so that the differential equations for the $\omega_i(t)$ vectors are simply:

$$\begin{aligned} \frac{d^2}{dt^2}\omega_i = {} & \frac{\mu_E}{r_{EV}^3(t)}\left\{3\,[\underline{i}_{EV}(t)\cdot\omega_i(t)]\,\underline{i}_{EV}(t) - \omega_i(t)\right\} \\ & + \frac{\mu_M}{r_{MV}^3(t)}\left\{3\,[\underline{i}_{MV}(t)\cdot\omega_i(t)]\,\underline{i}_{MV}(t) - \omega_i(t)\right\} \\ & i = 1, 2, \ldots, 6 \end{aligned} \qquad \text{(Eq. 3-27)}$$

(c) The Weighting Vector

By algebraically combining the W matrix, the $\underline{b}$ vector and a mean-squared a *priori* estimation error $\overline{a^2}$ in the measurement, there are produced a weighting vector $\underline{w}$ and the step change to be made in the error transition matrix to reflect the changes in the uncertainties in the estimated quantities as a result of the measurement. The weighting vector $\underline{w}$ has six components and is determined so that the observational data is utilized in a statistically optimum manner. The required calculation is given as a flow diagram in Fig. 3-5.

The computation may be conveniently organized in terms of the vector partitions of the W matrix as given in Eq. 3-25. If $\underline{w}_1$ and $\underline{w}_2$ are the three-dimensional upper and lower partitions of the weighting vector, then we have:

$$z_i = \omega_i \cdot b_1 + \frac{d\omega_i}{dt} . \underline{b}_2 \qquad i = 1, 2, \ldots, 6$$

$$\beta = \frac{1}{\overline{a^2} + \sum_{i=1}^{6} z_i^2} \qquad \text{(Eq. 3–28)}$$

$$\underline{w}_1 = \sum_{i=1}^{6} z_i \omega_i$$

$$\underline{w}_2 = \sum_{i=1}^{6} z_i \frac{d\omega_i}{dt}$$

Finally, the navigation parameters are updated according to:

$$\begin{aligned} &\underline{r}_{PV} + \underline{w}_1 \, \delta\tilde{q} \rightarrow \underline{r}_{PV} \\ &\underline{v}_{PV} + \underline{w}_2 \, \delta\tilde{q} \rightarrow \underline{v}_{PV} \\ &\omega_i - \gamma z_i \underline{w}_1 \rightarrow \omega_i \\ &\frac{d\omega_i}{dt} - \gamma z_i \underline{w}_2 \rightarrow \frac{d\omega_i}{dt} \end{aligned} \qquad i = 1, 2, \ldots 6 \qquad \text{(Eq. 3–29)}$$

where:

$$\gamma = \frac{1}{1 + \sqrt{\beta \, \overline{a^2}}}$$

(d) Numerical Integration

The extrapolation of navigation parameters requires the solution of seven second order vector differential equations, specifically Eq. 3–12 and Eq. 3–27. These are all special cases of the form:

$$\frac{d^2}{dt^2} \underline{y} = \underline{f} \, (\underline{y}) \qquad \text{(Eq. 3–30)}$$

in which the right hand side is a function of the independent variable and time only. Nyström's method (6) is particularly well-suited to this form and gives an integration method of fourth order accuracy. The second order system is written as:

$$\frac{d}{dt} \underline{y} = \underline{z} \qquad \frac{d}{dt} \underline{z} = \underline{f}(\underline{y}) \qquad \text{(Eq. 3–31)}$$

and the formulae are summarized below:

$$\begin{aligned} \underline{y}_{n+1} &= \underline{y}_n + \underline{\phi}(\underline{y}_n) \, \Delta t \\ \underline{z}_{n+1} &= \underline{z}_n + \underline{\psi}(\underline{y}_n) \, \Delta t \\ \underline{\phi}(\underline{y}_n) &= \underline{z}_n + \frac{1}{6} (\underline{k}_1 + 2\underline{k}_2) \, \Delta t \\ \underline{\psi}(\underline{y}_n) &= \frac{1}{6} (\underline{k}_1 + 4\underline{k}_2 + \underline{k}_3) \\ \underline{k}_1 &= \underline{f}(\underline{y}_n) \\ \underline{k}_2 &= \underline{f}(\underline{y}_n + \frac{1}{2} \underline{z}_n \, \Delta t + \frac{1}{8} \underline{k}_1 \, (\Delta t)^2) \\ \underline{k}_3 &= \underline{f}(\underline{y}_n + \underline{z}_n \, \Delta t + \frac{1}{2} \underline{k}_2 \, (\Delta t)^2) \end{aligned} \qquad \text{(Eq. 3–32)}$$

For efficient use of computer storage as well as computing time the computations should be performed in the following order:
(a) Eq. 3–12 is solved using the Nyström formulae Eq. 3–32. The position of the sun and moon are required at times t_n, $t_n + 1/2\ \Delta t$, $t_n + \Delta t$ to be used in the evaluation of the vectors $\underline{k}_1, \underline{k}_2, \underline{k}_3$ respectively. It is necessary to preserve the values of the vectors $\underline{r}_{EV}$ and $\underline{r}_{EM}$ at these times for use in the solution of Eq. 3–27.
(b) Eq. 3–27 is solved one set at a time using formulae Eq. 3–32 together with the values of $\underline{r}_{EV}$ and $\underline{r}_{EM}$ which resulted from the first step.

Many of the advantages of the recursive navigation method are now readily apparent. Although linear techniques are still employed, it has been possible to remove any dependence on a reference or pre-computed orbit. Within the framework of a single computational algorithm, measurement data from any source may be incorporated sequentially as obtained. Sensitive numerical computations, such as the inversion of matrices, are avoided.

PARAMETER ESTIMATION

The coasting flight navigation procedure just outlined is capable of generalization to include the estimation of quantities in addition to position and velocity by the simple expedient of increasing the dimensions of the state vector beyond six. For example, one might wish to estimate biases or cross-correlations in the optical or radar instruments, the frequency of a satellite-borne doppler source or even astronomical quantities such as distances and gravitational constants.

MEASUREMENT SCHEDULE

For effective application of this navigation method, an efficient observation schedule should be prepared. An elementary procedure, which has been found to be quite effective for this purpose, is described in reference (5). At each of a number of discrete times, appropriately spaced along the flight path, that measurement is selected from a variety of possible observations, which would result in the greatest reduction in mean-squared position uncertainty at the destination. In order to control the number of measurements and prevent an unnecessarily lengthy schedule, a measurement is required to produce a significant reduction in the potential miss distance or it will not be made.

The simple strategy described above, in which only currently available information is exploited, does not, of course, insure an optimum schedule, since the uncertainties in position and velocity at the target clearly depend on the entire measurement schedule. A method of improving a measurement schedule iteratively, employing an adjoint of the correlation matrix, has been developed. The technique has been shown to converge always to essentially the same schedule starting from a variety of nominal measurement schedules. A numerical example, reported by Denham and Speyer (7), gives a minimum rms uncertainty in position at the terminal point which is 10% less than the value obtained using the more elementary method.

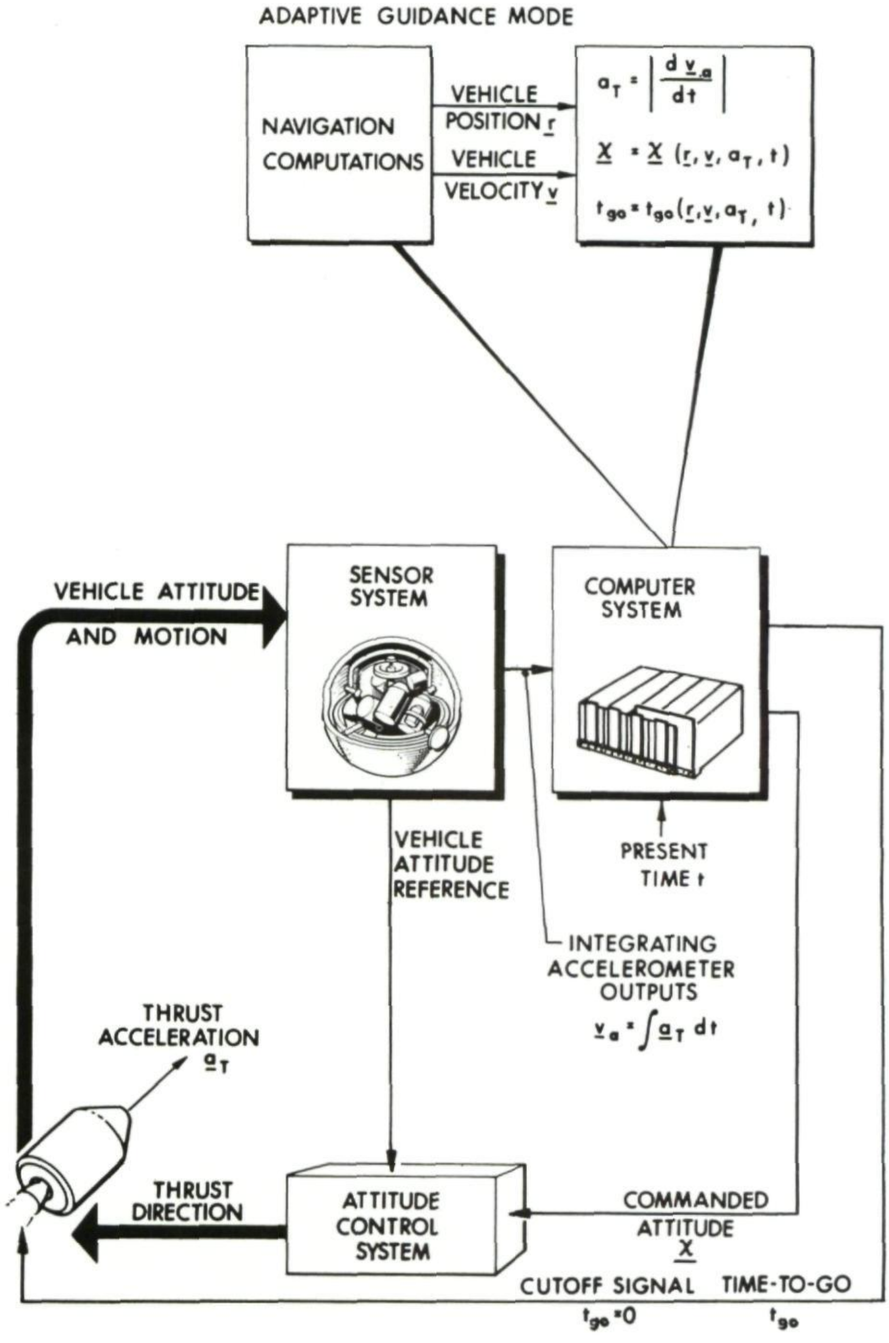

Fig. 3–6 Powered flight guidance system

CHAPTER 3–3

POWERED-FLIGHT GUIDANCE

The task of providing steering commands, frequently called guidance, separates naturally into two categories – major and minor maneuvers. Launch into parking orbit, transfer to lunar or interplanetary orbit, insertion into orbit and landing are all examples of major thrusting maneuvers and differ markedly from the minor orbit changes typified by mid-course velocity corrections. In either case, the guidance problem is always a boundary value problem subject to a variety of constraints of which fuel conservation, vehicle maneuverability and time are examples.

Explicit solutions to the problem of guidance during periods of major thrusting require relatively complex calculations to be performed in flight on a time-critical basis. Considering the modest size and capabilities of vehicle-borne computers contrasted with the more familiar commercial machines, the design of feasible explicit methods presents a considerable challenge. Several of the more promising guidance techniques currently under development are compared in this chapter.

ADAPTIVE GUIDANCE MODE

The guidance method developed at Marshall Space Flight Center for the Saturn rocket and termed the Adaptive Guidance Mode (8) is conceptually simple and easily described. The form of the guidance and cutoff equations is invariant with changing missions and vehicles and therefore is in accord with the requirements of a unified method. However, significantly large quantities of ground computations are required to determine certain coefficients needed in the mechanization.

The vector values of position and velocity, the scalar magnitude of thrust acceleration and time are updated continuously during powered flight. At each instant the present values of these quantities may be considered as initial conditions for the remainder of the flight. Ideally, one would determine the optimum trajectory from present conditions to desired terminal conditions and command a thrust direction from this optimum solution. This is, of course, impractical, so that the techniques of the calculus of variations are employed to generate a volume of expected trajectories for specific vehicles and missions. Numerical curve fitting methods are employed to obtain satisfactory series solutions for the guidance and cutoff commands.

A functional diagram for the Saturn guidance system is shown in Fig. 3–6. During flight the thrust acceleration magnitude is computed approximately once per second by differentiating the outputs of the integrating accelerometers and taking the square root of the sum of the squares of the resulting derivatives. Guidance and cutoff commands are computed as polynomial functions of position, velocity, thrust acceleration and time at intervals of approximately one second. During the burning of the first stage

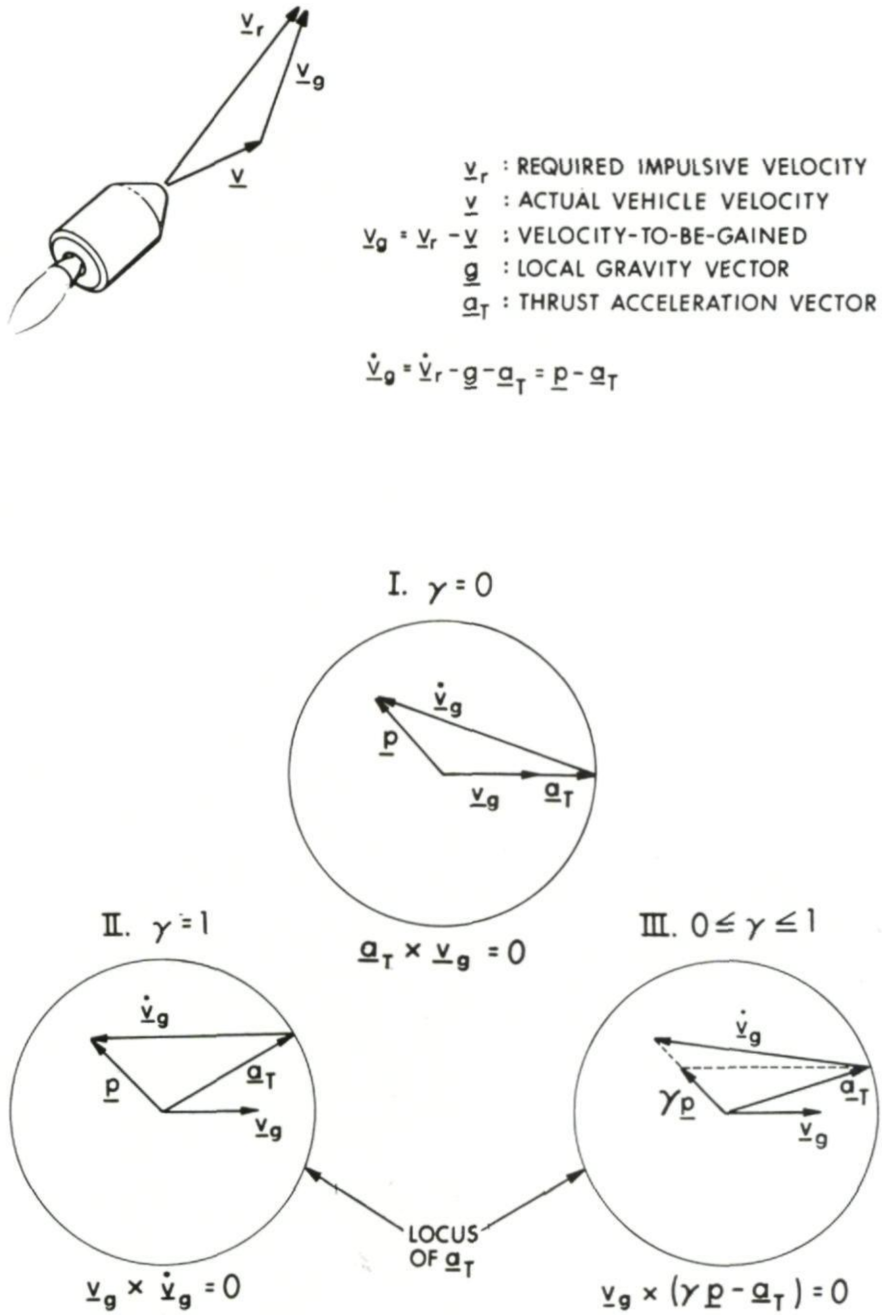

FIG. 3–7 Velocity-to-be-gained methods

of Saturn, the guidance program is obtained as a polynomial expansion in time only because of structural and control problems.

The chief difficulty with the Adaptive Guidance Mode is determining the best method of representing the volume of expected trajectories which provide minimum fuel consumption. The required number of terms in the polynomials to obtain acceptable accuracy has been found to vary from 40 to 60 depending on the mission.

VELOCITY-TO-BE-GAINED METHODS

Conic orbits can be exploited to advantage in solving many guidance problems. For those major orbital transfer maneuvers which can be accomplished conceptually by a single impulsive velocity change, an instantaneous velocity-to-be-gained vector based on conic orbits can often be defined and the vehicle steered to null this vector. Refer to Fig. 3–7 and let a vector v_r be defined, corresponding to the present vehicle location r, as the instantaneous velocity required to satisfy a set of stated mission objectives. The velocity difference v_g between v_r and the present vehicle velocity v is then the instantaneous velocity-to-be-gained.

Two convenient guidance laws are immediately apparent which will assure that all three components of the vector v_g are simultaneously driven to zero. First, we may orient the vehicle to align the thrust acceleration vector a_T with the direction of the velocity-to-be-gained vector. Alternatively, since a convenient expression can be developed for the time rate of change of the v_g vector, we may direct the vector a_T to cause the vector v_g to be parallel to v_g and oppositely directed. If the thrust acceleration magnitude is not sufficiently large it may not be possible to align the vector v_g with its derivative. However, with typical chemical rockets for which the burning time is relatively short, no difficulty has been encountered with this guidance logic.

A combination of these two techniques leads to a highly efficient steering law which compares favorably with calculus of variations optimum solutions (9). The scalar mixing parameter γ is chosen empirically to maximize fuel economy during the maneuver. A constant value of γ is usually sufficient for a particular mission phase; however, if required, it may be allowed to vary as a function of some convenient system variable.

A functional diagram illustrating the computation of the error signal required for control purposes is shown in Fig. 3–8. The position, velocity and gravitation vectors are computed from the outputs of integrating accelerometers as described earlier in the section on navigation. The required impulsive velocity needed to achieve mission objectives is determined as a function of the position vector and used to calculate the velocity-to-be-gained. Numerical differentiation of the required velocity vector and the accelerometer outputs, using values stored from the previous sample time, provides two important ingredients of the error signals. When properly scaled, the system output is a vector rate of command whose magnitude is proportional to the small angular differences between the actual and commanded thrust acceleration vectors and whose direction defines the direction of vehicle rotation required to null the error. Near the end of the maneuver, when the velocity-to-be-gained is small, cross-product steering is terminated,

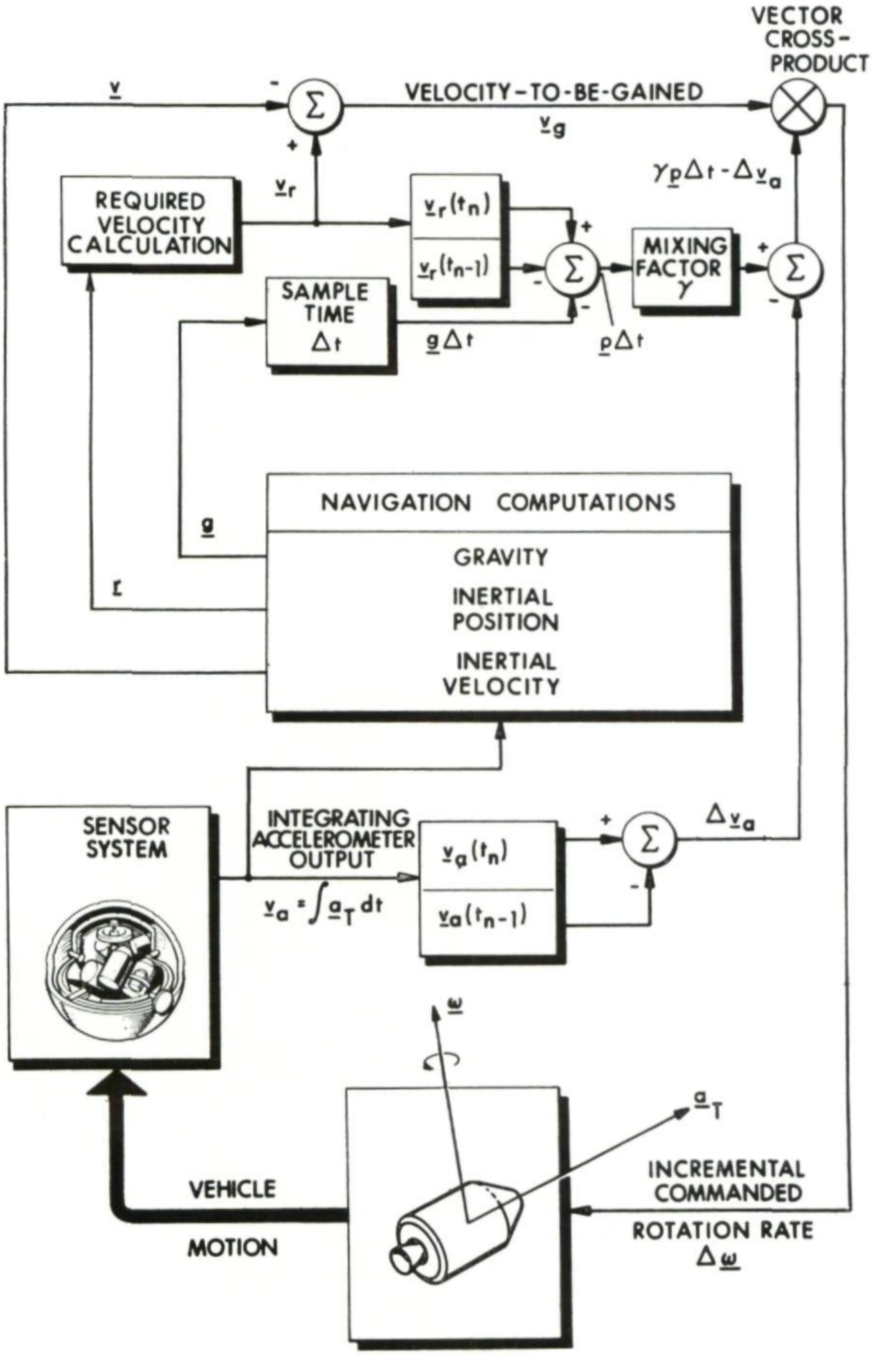

FIG. 3–8 Velocity-to-be-gained steering

the vehicle holds a constant attitude and engine cutoff is made on the basis of the magnitude of the $\underline{v}_g$ vector.

This guidance technique is being considered for steering the Apollo Command Module during the following mission phases, (a) translunar injection which refers to the process of transfer from earth parking orbit to a trajectory linking earth and moon, (b) transfer from a hyperbolic approach trajectory to a circular orbit of the moon, and (c) transearth injection or transfer from a lunar orbit to an earth-bound trajectory.

For each of these maneuvers, the required impulsive velocity is as follows:

(a) Translunar Injection

The required velocity for translunar injection is defined as that velocity, at the present position, that will place the vehicle on a conic passing through a specified time. Specifically, this velocity vector $\underline{v}_r$ is calculated from:

$$\underline{v}_r = \sqrt{\frac{\mu_E}{2}}\,[A(\underline{i}_c + \underline{i}_r) + B(\underline{i}_c - \underline{i}_r)] \qquad \text{(Eq. 3-33)}$$

where:

$$A = \pm\sqrt{\frac{1}{s-c} - \frac{1}{2a}}$$

$$B = \operatorname{sgn}(t_m - t)\sqrt{\frac{1}{s} - \frac{1}{2a}}$$

In these formulae, c is the linear distance from the present position $\underline{r}$ to the target position $\underline{r}_T$; s is the semi-perimeter of the triangle formed by the vectors $\underline{r}$ and $\underline{r}_T$; a is the semimajor axis of the conic; t is the time of flight; and t_m is the time to fly the minimum energy path from $\underline{r}$ to $\underline{r}_T$. The choice of upper or lower sign in the expression for A is made according as the transfer angle is less than or greater than 180°, respectively. The target point is actually offset by a calibrated amount from the desired position to account for gravitational perturbations. To simplify the computational load the fixed time requirement is readily approximated by holding constant the semimajor axis of the conic at a pre-determined value.

(b) Circular Orbit Insertion

To guide a vehicle into a circular orbit of the moon by a rocket braking maneuver initiated on an approach trajectory, the vector $\underline{v}_r$ may be defined as that velocity impulse required at the present position to circularize the orbit in a specified plane. If $\underline{r}$ is the position vector of the vehicle relative to the moon and $\underline{i}_n$ is the unit normal to the desired orbit plane, then:

$$\underline{v}_r = \sqrt{\frac{\mu_M}{r}}\,(\underline{i}_r \times \underline{i}_n) \qquad \text{(Eq. 3-34)}$$

The shape and orientation of the final orbit is controlled by this means, but direct control of the orbital radius is not possible. However, there is an empirical relationship between the final radius and the pericenter of the approach trajectory, so that a desired radius can be established by an appropriate selection of the approach orbit.

(c) Transearth Injection

In the vicinity of the moon the spacecraft trajectory is very nearly hyperbolic. Therefore, the required velocity for transearth injection from

lunar orbit may be conveniently defined by the magnitude v_∞ and direction $\underline{i}_\infty$ of the asymptotic velocity $\underline{v}_\infty$. Thus:

$$\underline{v}_r = \frac{v_\infty}{2} \left[(D+1)\, \underline{i}_\infty + (D-1)\, \underline{i}_r \right] \qquad \text{(Eq. 3–35)}$$

where:

$$D = \sqrt{1 + \frac{4\mu_M}{r v_\infty^2 \, (1 + \underline{i}_r \cdot \underline{i}_\infty)}}$$

The direction in space that the thrust vector should be oriented at the beginning of a power flight maneuver is determined from the equation:

$$\underline{a}_T = \gamma \underline{p} + (q - \underline{i}_g \cdot \gamma \underline{p})\, \underline{i}_g \qquad \text{(Eq. 3–36)}$$

where $\underline{i}_g$ is a unit vector in the direction of the $\underline{v}_g$ vector and

$$q = \sqrt{a_T^2 - (\gamma p)^2 + (\underline{i}_g \cdot \gamma \underline{p})^2}$$

The quantities $\underline{v}_g$ and $\underline{p}$ are both continuous functions through the ignition point and, thus, their computation can be started to align the vehicle initially prior to the firing of the engine.

TERMINAL STATE VECTOR CONTROL

The explicit technique just discussed is workable if it is possible, at thrust termination, to define the required velocity as a function of position and thereby eliminate the need for position control. On the other hand, when burn-out position and velocity are independently specified, an alternate guidance method, based on an explicit solution of the powered flight dynamics, is frequently applicable (10). As examples, consider the problems of insertion of a vehicle into a circular orbit at a pre-specified altitude which lies in a prescribed plane, soft-landing a vehicle on the surface of the moon and orbital rendezvous.

The guidance computations, needed for solving explicitly the more general boundary value problem, involve a determination of the time remaining before thrust termination. For fixed thrust rocket problems, the termination time is calculated cyclically by an iteration process in such a manner as to control the final velocity along one coordinate axis. As a part of the calculation, the effective exhaust velocity of the rocket engine, based on a mathematical model of the engine performance, is needed.

When the vehicle is propelled by a controllable thrust engine, the magnitude of the thrust acceleration can be commanded to cause burn-out to occur at a pre-specified terminal time. In this case, the time-to-go is a trivial calculation. Prior to thrust initiation, the thrust termination time is chosen according to criteria which depend on the particular guidance problem. For orbital rendezvous, the time and desired terminal position and velocity are chosen from a knowledge of the target vehicle ephemeris. For a lunar landing, the terminal time is selected to maximize the initial thrust acceleration.

The development of an explicit steering equation for a controllable thrust engine, which will guide a vehicle to a desired set of terminal conditions, is based on the solution to the following simple variational problem.

Let it be required to find the acceleration program $\underline{a}(t)$, which will minimize the functional:

$$\mathcal{J} = \int_{t}^{t_D} a(\tau)^2 \, d\tau \qquad \text{(Eq. 3-37)}$$

where t is present time and t_D is the desired terminal time. If $\underline{a}(t)$ is the total acceleration influencing the vehicle motion, then:

$$\frac{d\underline{r}}{dt} = \underline{v} \qquad \frac{d\underline{v}}{dt} = \underline{a}(t) \qquad \text{(Eq. 3-38)}$$

subject to the boundary conditions:

$$\begin{aligned} \underline{r}(t) &= \underline{r} \qquad \underline{r}(t_D) = \underline{r}_D \\ \underline{v}(t) &= \underline{v} \qquad \underline{v}(t_D) = \underline{v}_D \end{aligned} \qquad \text{(Eq. 3-39)}$$

This minimization problem is readily solved using the calculus of variations. By introducing the two vector Lagrange multipliers $\underline{\lambda}$ and $\underline{\eta}$ we may combine Eq. 3–37 and Eq. 3–38 in the form:

$$\mathcal{J} = \int_{t}^{t_D} \left\{ \underline{a}(\tau)^T \underline{a}(\tau) + \underline{\lambda}^T \left(\frac{d\underline{r}}{dt} - \underline{v} \right) + \underline{\eta}^T \left[\frac{d\underline{v}}{dt} - \underline{a}(\tau) \right] \right\} d\tau$$

for which the Euler-Lagrange equations are found to be:

$$\begin{aligned} &\frac{d}{dt} \underline{\lambda}^T = 0 \\ &\frac{d}{dt} \underline{\eta}^T + \underline{\lambda}^T = 0 \\ &-2\underline{a}(t)^T + \underline{\eta}^T = 0 \end{aligned} \qquad \text{(Eq. 3-40)}$$

The solution of Eq. 3–40 yields:

$$\underline{a}(t) = \underline{c}_1 + \underline{c}_2 t$$

and the constants of integration c_1 and c_2 are chosen to satisfy the boundary conditions of Eq. 3–39. The final result is simply:

$$\underline{a}(t) = \frac{4}{t_{go}} (\underline{v}_D - \underline{v}) + \frac{6}{t_{go}^2} [\underline{r}_D - (\underline{r} + \underline{v}_D \, t_{go})]$$

where:

$$t_{go} = t_D - t$$

is the time-to-go before termination.

In a guidance maneuver the total acceleration $a(t)$ is the sum of thrust acceleration $a_T(t)$ and gravity $g(r)$. If the gravity vector were a constant, then the exact solution to the guidance problem would be:

$$a_T = \frac{4}{t_{go}} (v_D - v) + \frac{6}{t_{go}^2} [r_D - (r + v_D \, t_{go})] - g \qquad \text{(Eq. 3-41)}$$

In the problems of practical interest, the vector $\underline{g}$ is not constant and the

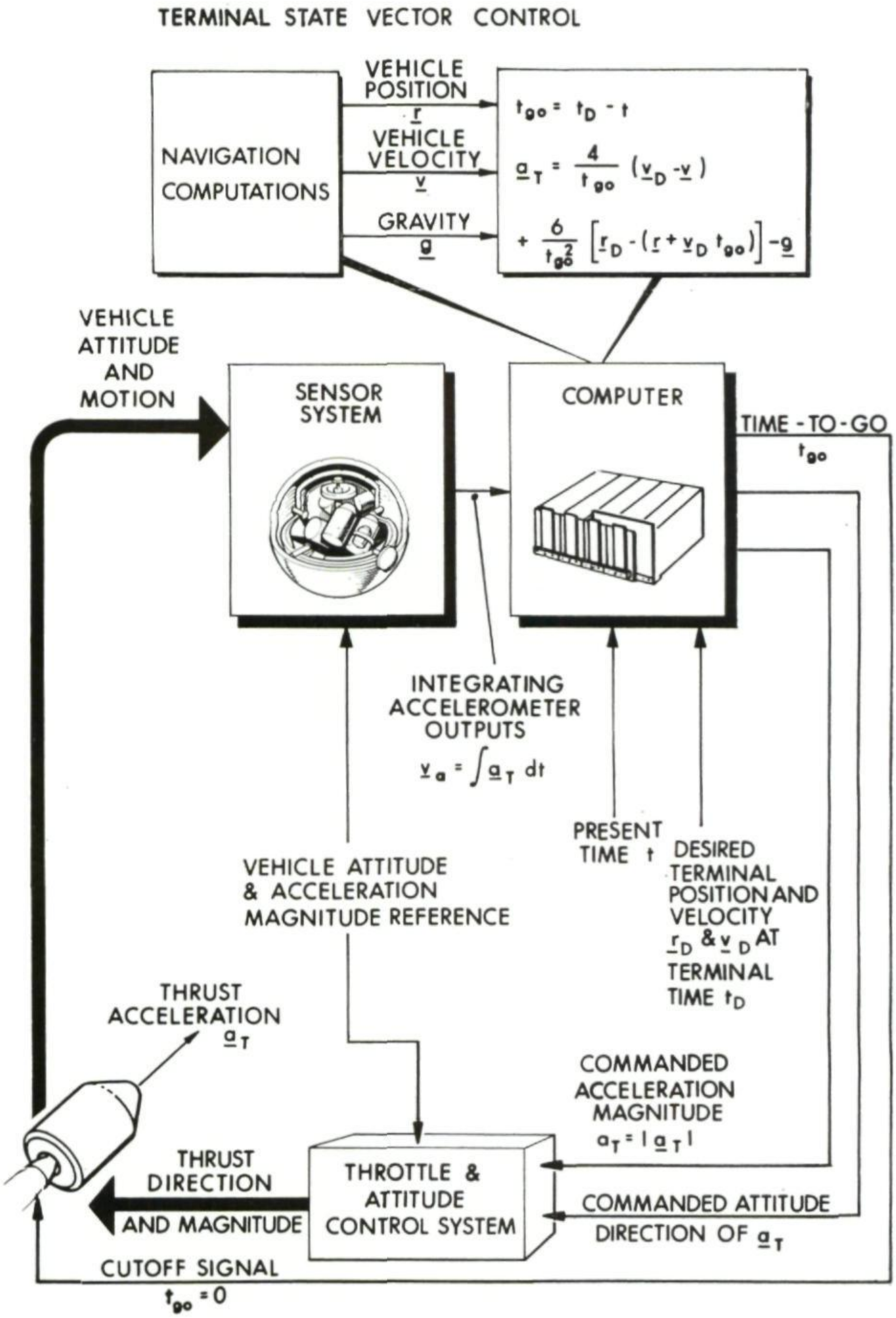

FIG. 3–9 Variable thrust guidance system

integral-square criterion of Eq. 3–37 is not appropriate for fuel minimization. However, it happens that Eq. 3–41 does provide a nearly optimum steer law for a wide variety of problems.

Figure 3–9 illustrates the guidance computations required to achieve a given terminal position and velocity at a specified time with a throttleable rocket engine. From the navigation system the present position, velocity, gravitational acceleration and time are determined and the direction and magnitude of the thrust acceleration to be commanded are calculated. As the terminal conditions are approached, time-to-go approaches zero and the computation clearly becomes unstable. The singularity is readily avoided, with only slight loss in potential performance, by holding time-to-go constant in the guidance expression when it is less than a pre-assigned amount. Engine cutoff can then be commanded when the actual time-to-go reaches zero.

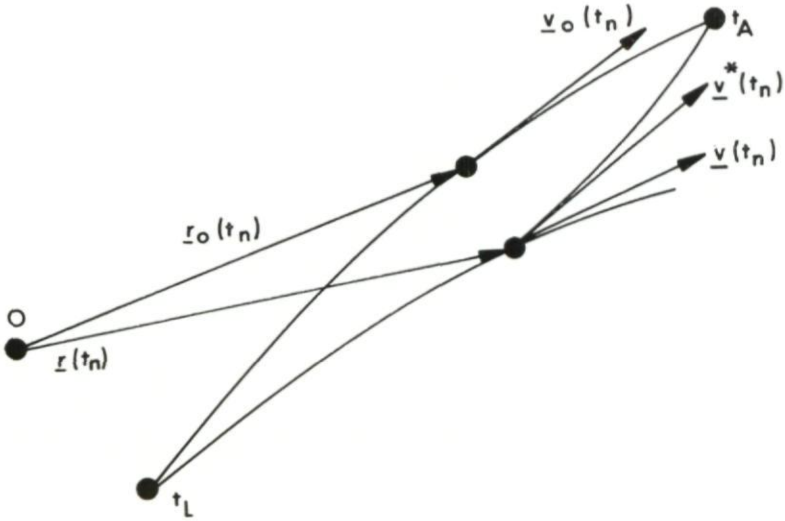

$$C^* = \left\| \frac{\delta \underline{v}^*}{\delta \underline{r}} \right\|$$

$$\delta \underline{r}_n = \underline{r}(t_n) - \underline{r}_o(t_n)$$
$$\delta \underline{v}_n = \underline{v}(t_n) - \underline{v}_o(t_n)$$

VELOCITY CORRECTION

$$\Delta \underline{v}_n^* = C_n^* \, \delta \underline{r}_n - \delta \underline{v}_n$$

FIG. 3–10 Linearized guidance theory

CHAPTER 3–4

MID-COURSE GUIDANCE

LINEARIZED GUIDANCE THEORY

Techniques of guidance and navigation of a spacecraft in interplanetary or cislunar space are often based on the method of linearized perturbations. The approach is to linearize the equations of motion by a series expansion about a nominal or reference orbit in which only first-order terms are retained. The resulting equations are far simpler and superposition techniques, as well as all of the powerful tools of linear analysis, may be exploited to obtain solutions to a wide variety of navigation and guidance problems.

Consider, for example, the guidance problem illustrated in Fig. 3–10. A vehicle is launched into orbit at time t_L and moves under the influence of one or more gravity fields to reach a target point at time t_A. Let $\underline{r}_0(t_n)$ and $\underline{v}_0(t_n)$ be the position and velocity vectors at time t_n for a vehicle traveling along a reference path connecting the initial and final points. Because of errors, the true position and velocity vectors $\underline{r}(t_n)$ and $\underline{v}(t_n)$ will deviate from the associated reference quantities. If the deviations from the reference path are always small, so that linearization techniques are applicable, the velocity correction $\Delta\underline{v}_n{}^*$ may be computed as a linear combination of the position and velocity deviations. The three-dimensional matrix $C_n{}^*$ is the matrix of partial derivatives, with respect to the components of $\underline{r}$, of the components of the velocity vector $\underline{v}^*$ required to reach the target from position r.

For these calculations to remain valid it is, of course, necessary to restrict the magnitude of the deviations from the corresponding nominal values. Another disadvantage of the method is that all possible times of velocity corrections must be anticipated and associated values of the C^* matrix stored in the guidance computer. Also to provide an adequate launch window, a family of reference trajectories is mandatory and the guidance computer storage requirements rapidly become excessive using this approach.

EXPLICIT TECHNIQUES

The quantity of stored data required for mid-course guidance maneuvers can be markedly reduced if explicit techniques are employed using conic arcs suitably modified to account for small non-central force field effects. Both fixed and variable-time-of-arrival velocity corrections can be calculated and the procedures will be illustrated by two specific examples.

Fixed-Time-of-Arrival Guidance – Because of initial errors arising from a failure to inject the spacecraft in an appropriate trajectory to the moon, a velocity correction is frequently required after a few hours of coasting flight. During the post-injection phase, an accurate determination of the vehicle's orbit is made using navigation techniques as previously discussed. An intermediate target point $\underline{r}_T$ is selected as the position on the lunar sphere of influence through which the reference vehicle would pass at the reference time.

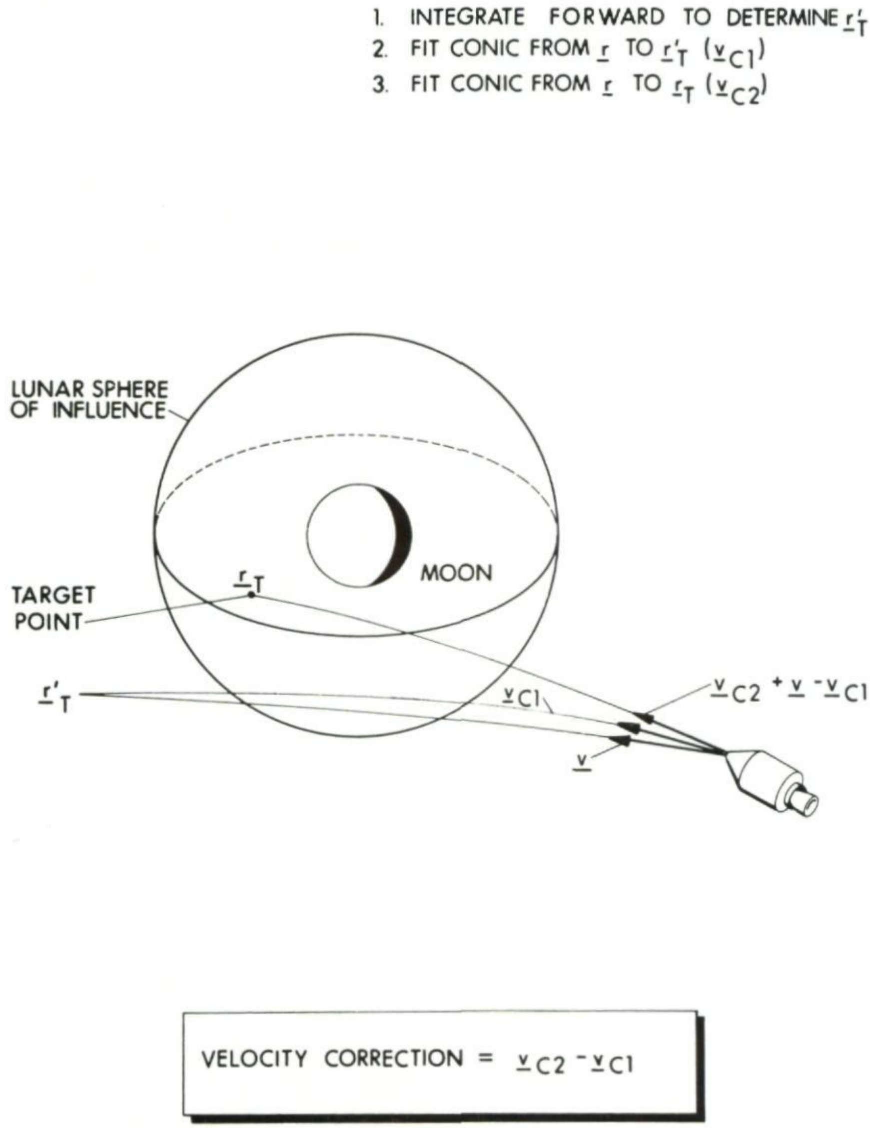

FIG. 3–11 Fixed-time-of-arrival midcourse correction

Refer to Fig. 3–11 and let r and v be the position and velocity estimates of the vehicle at the time a correction is to be made. Using the trajectory integration routine, which is a part of the coast phase navigation program, the position of the vehicle is extrapolated to determine the point r_T' at which the spacecraft would be found at the target reference time if no corrective action were taken. By calculating the conic arc connecting the position vectors r and r_T' in the same time interval, the conic velocity vector v_{c1} at r is determined. The difference between the conic velocity and the vehicle's actual velocity is a good measure of the effect of lunar and solar perturbations. A second conic arc connecting the vehicle position vector r and the desired target point r_T produces the conic velocity vector v_{c2}. If this velocity is corrected for the effect of perturbations, the velocity necessary to reach the desired target from position r is obtained. Thus, an excellent approximation to the required velocity correction is just the difference between the two conic velocities. The computation may, of course, be repeated iteratively to achieve any desired degree of convergence. However, in practice, one computation cycle is usually sufficient.

Fixed-time-of-arrival guidance may be summarized as follows:

(a) The conic velocity required at r to arrive at r_T' is calculated from

$$v_{c1} = \operatorname{sgn}(\pi^2 - x)\sqrt{\frac{\mu_E[2 - xC(x)]}{4s}}\,(\underline{i}_c - \underline{i}_r) \pm$$

$$\pm\sqrt{\frac{\mu_E[2 - yC(y)]}{4(s - c)}}\,(\underline{i}_c + \underline{i}_r) \qquad \text{(Eq. 3–42)}$$

where μ_E is the gravitational constant of the earth, $\underline{i}_r$ is a unit vector in the direction of $\underline{r}$, $\underline{i}_c$ is a unit vector in the direction of $\underline{r}_T' - \underline{r}$, and s is the semi-perimeter of the triangle formed by $\underline{r}$ and $\underline{r}_T'$. The quantities x and y are determined as the roots of the equations:

$$\sqrt{\mu_E}\,\Delta t = \left[\frac{s}{C(x)}\right]^{3/2} S(x) \pm \left[\frac{s - c}{C(y)}\right]^{3/2} S(y) \qquad \text{(Eq. 3–43)}$$

$$sC(y) = (s - c)x\,C(x)$$

where Δt is the time difference between the reference time of arrival and present time. The special transcendental functions S and C are defined in Eq. 3–11. The choice of the upper and lower signs in Eq. 3–42 and Eq. 3–43 is made according to whether the angle between $\underline{r}$ and $\underline{r}_T'$ is less than or greater than 180 degrees, respectively.

(b) The conic velocity v_{c2} for attaining $\underline{r}_T$ is computed by repeating step A with $\underline{r}_T$ substituted for $\underline{r}_T'$.

(c) The estimated velocity correction is then given by

$$\Delta v = v_{c2} - v_{c1} \qquad \text{(Eq. 3–44)}$$

Variable-Time-of-Arrival Guidance – When a velocity correction is made in the vicinity of the moon the arrival time at perilune may be allowed to vary thereby reducing substantially the required velocity correction as well as the terminal velocity deviation from its nominal value. Specifically, let the desired terminal conditions at the moon be a specified altitude at perilune

r_p = DESIRED PERILUNE ALTITUDE

$\underline{1}_n$ = UNIT NORMAL TO DESIRED PLANE

p = PARAMETER OF CONIC ORBIT

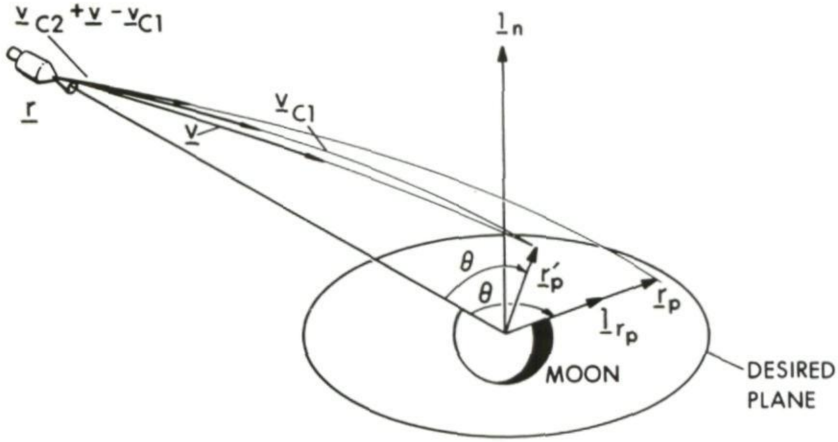

INSENSITIVITY DIRECTION

$$\underline{1}_D = \text{UNIT}\left[-(1-\cos\theta)^2\ \underline{1}_{r_p} + \left(1-\cos\theta+\frac{\mu}{r_p}\right)\sin\theta\ \underline{1}_{r_p}\times\underline{1}_n\right]$$

$$\boxed{\text{VELOCITY CORRECTION} = (\underline{v}_{C2}-\underline{v}_{C1}) - \underline{1}_D \cdot (\underline{v}_{C2}-\underline{v}_{C1})\,\underline{1}_D}$$

FIG. 3-12 Variable-time-of-arrival midcourse correction

and a fixed plane in which the perilune vector is to lie. Again, as shown in Fig. 3–12, the trajectory is extrapolated forward in time to locate the perilune vector $\underline{r}_p'$ which would result in the absence of a velocity correction. A conic arc with $\underline{r}_p'$ as perilune and connecting the position vector r is then determined to obtain a measure of the gravitational perturbation. The desired perilune vector $\underline{r}_p$ is calculated from $\underline{r}_p'$ by scaling its length to correspond to the required perilune distance and then rotating it into the required plane while keeping the central angle θ fixed. A second conic arc with $\underline{r}_p$ as perilune is calculated and the difference between the two conic velocities again provides an excellent approximation to the necessary velocity correction.

Theoretically, the desired plane should not be fixed in space, but should rotate with the moon. However, the change in perilune arrival time combined with the moon's own rotation leads to terminal deviations which are smaller than the navigation uncertainties. Hence, it is sufficiently accurate to aim for a fixed plane when approaching perilune.

Perilune guidance may be summarized as follows:

(a) The conic velocity $\underline{v}_{c1}$ required at $\underline{r}$ to attain pericenter at $\underline{r}_p'$ is computed from:

$$\underline{v}_{c1} = \frac{\sqrt{\mu_M p}}{r\, r_p' \sin\theta}\left\{\underline{r}_p' - \left[1 - \frac{r_p}{p}(1-\cos\theta)\right]\underline{r}\right\} \qquad \text{(Eq. 3–45)}$$

where θ is the angle between $\underline{r}$ and $\underline{r}_p'$, and p, the parameter of the conic, is given by:

$$p = \frac{r\, r_p'\,(1 - \cos\theta)}{r_p' - r\cos\theta} \qquad \text{(Eq. 3–46)}$$

(b) The pericenter vector $\underline{r}_p'$ is rotated into the desired plane and scaled to the desired length r_p by means of:

$$\underline{r}_p = r_p\left[\sqrt{1 + \beta\cos\theta}\ \text{UNIT}\ (\underline{i}_n \times \underline{i}_r) + \beta\underline{i}_n \times (\underline{i}_n \times \underline{i}_r)\right] \qquad \text{(Eq. 3–47)}$$

where:

$$\beta = -\frac{\cos\theta}{1 - (\underline{i}_n \cdot \underline{i}_r)^2}$$

The unit vector $\underline{i}_n$ is normal to the desired plane in the direction of the angular momentum vector.

The conic velocity $\underline{v}_{c2}$, required to attain pericenter at $\underline{r}_p$, is then calculated by repeating step A with $\underline{r}_p$ in place of $\underline{r}_p'$.

(d) The magnitude of the required velocity correction may be further reduced by noting that there is a direction along which a velocity change may be made without altering the altitude at pericenter. If the component of velocity correction along this insensitive direction is deducted from the total correction, the effect will be simply a small rotation of the perilune vector r_p. This insensitive direction is computed from

$$\underline{i}_D = \text{UNIT}\left[-(1 - \cos\theta)^2\,\underline{i}_{r_p} + \sin\theta\left(1 - \cos\theta + \frac{p}{r_p}\right)\underline{i}_r \times \underline{i}_n\right] \qquad \text{(Eq. 3–48)}$$

where $\underline{i}_{r_p}$ is a unit vector in the direction of $\underline{r}_p$.

(e) The estimated velocity correction is then given by the component of the

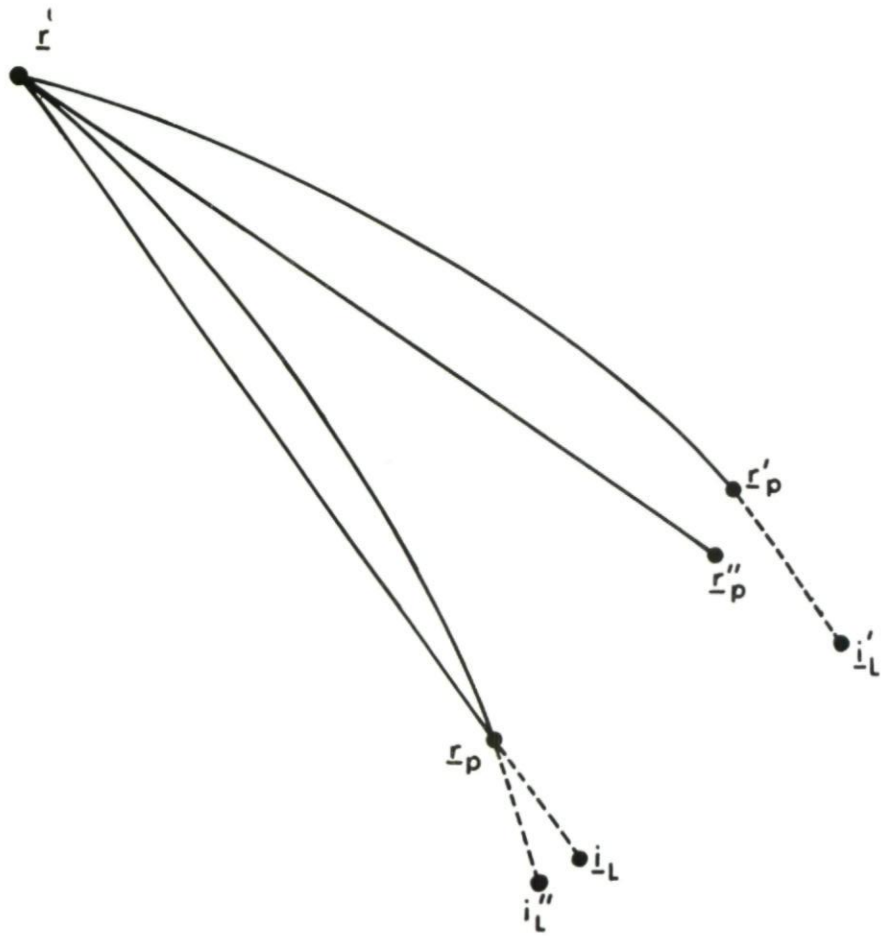

Fig. 3-13 Geometry of perigee guidance

vector $\underline{v}_{c2} - \underline{v}_{c1}$ in the plane perpendicular to $\underline{i}_D$ and is calculated from

$$\Delta \underline{v} = (\underline{v}_{c2} - \underline{v}_{c1}) - \underline{i}_D \cdot (\underline{v}_{c2} - \underline{v}_{c1})\, \underline{i}_D \qquad \text{(Eq. 3-49)}$$

During transearth flight it is not sufficient to aim for a fixed plane when making a velocity correction to the vicinity of the earth. The desired terminal conditions are a vacuum perigee distance (which is equivalent to an entry angle) and a landing site fixed to the earth. This type of velocity correction, called perigee guidance, is an extension of perilune guidance with the plane determined so that the spacecraft will be directed to the desired landing site.

Inherent in perigee guidance is a timing problem which necessitates taking into account the correction to be made in estimating the time of arrival at perigee. The change in perigee time due to a correction that alters the perigee distance from $\underline{r}_p'$ to $\underline{r}_p$ is given by the empirically determined formula $kr(r_p' - r_p)$, where k has been found experimentally to be 16×10^{-10} hr/mi^2. A simple calculation shows that a velocity correction, which is made at the lunar sphere of influence (about 200000 miles from the earth) and which changes the perigee distance by 500 miles, alters the perigee arrival time by nearly ten minutes.

Let δt_p be the estimated deviation in perigee arrival time in hours, $\underline{i}_{L_0}$ a unit vector in the direction of the landing site at the nominal time of arrival, and a_0 the nominal angle from perigee to $\underline{i}_{L0}$. Assuming that the spacecraft travels on the average at circular orbital speed during entry, the deviation in the angle through which the earth rotates is given by:

$$\delta A = \frac{\pi}{12}\,\delta t_p + \frac{a - a_0}{16} \qquad \text{(Eq. 3-50)}$$

where a is the actual angle from perigee to the landing site. When the earth rotates through an angle δA, the landing site changes from $\underline{i}_{L_0}$ to $\underline{i}_L$ according to:

$$\underline{i}_L = \begin{pmatrix} \cos \delta A & -\sin \delta A & 0 \\ \sin \delta A & \cos \delta A & 0 \\ 0 & 0 & 1 \end{pmatrix} \underline{i}_{L_0} \qquad \text{(Eq. 3-51)}$$

The angle a satisfies:

$$a = \begin{cases} \cos^{-1}(\underline{i}_r \cdot \underline{i}_L) - \theta \\ \\ 2\pi - \cos^{-1}(\underline{i}_r \cdot \underline{i}_L) - \theta \end{cases} \qquad \text{(Eq. 3-52)}$$

where the choice of the first or second equation is made according to whether the angle between $\underline{i}_r$ and $\underline{i}_L$ is greater or less than 180 degrees, respectively. The desired plane is then determined by the initial position $\underline{r}$ and the landing site vector $\underline{i}_L$ calculated from Eq. 3-50, Eq. 3-51 and Eq. 3-52.

If the spacecraft trajectory was indeed planar, the steps outlined in the discussion of perilune guidance would be adequate for calculating the velocity correction. Unfortunately, the non-planar characteristics are sufficiently pronounced that an additional step is required before the perilune guidance technique can be applied.

In Fig. 3-13 is represented, schematically, an edge-wise view of the trajectory problem in which a planar path appears as a straight line. The

unmodified perilune guidance method would cause the vehicle to head for a landing site at $\underline{i}_L''$ instead of $\underline{i}_L$. To counteract this effect, the vector $\underline{r}_p'$ is projected ahead to $\underline{i}_L'$, the position the spacecraft would achieve on an uncorrected trajectory at the time the target landing site is at $\underline{i}_L$. Then a false perigee position $\underline{r}_p''$, in the plane determined by $\underline{r}$ and $\underline{i}_L'$, is used in place of $\underline{r}_p'$.

Perigee guidance may be summarized as follows:

(a) The estimated change in time of arrival at perigee is calculated from

$$\delta t_p = \delta t_p' + kr(r_p - r_p') \qquad \text{(Eq. 3–53)}$$

where $\delta t_p'$ is the deviation in perigee time obtained in the extrapolation of $\underline{r}$ and $\underline{v}$ to perigee $\underline{r}_p'$.

(b) The position of the desired landing site is found by solving the transcendental Eq. 3–50, Eq. 3–51 and Eq. 3–52 for $\underline{i}_L$ and α.

(c) The unit vector i_L' is calculated from

$$\underline{i}_L' = \underline{i}_{r_p} \cos \alpha + \underline{i}_{v_p} \sin \alpha \qquad \text{(Eq. 3–54)}$$

where $\underline{i}_{r_p}$ and $\underline{i}_{v_p}$ are unit vectors in the directions of the position and velocity vectors at $\underline{r}_p'$.

(d) The false perigee vector is located using Eq. 3–47 with the substitutions:

$$\pm \text{UNIT}\ (\underline{i}_r \times \underline{i}_L') \rightarrow \underline{i}_n$$
$$r_p' \rightarrow r_p$$
$$\underline{r}_p' \rightarrow \underline{r}_p$$

(e) The unit vector normal to the desired plane is computed from:

$$i_n = \pm \text{UNIT}\ (i_r \times i_L)$$

(f) The remaining calculations are exactly as outlined in steps (a) through (e) for perilune guidance. In the determination of the vector $\underline{i}_n$ in steps (d) and (e) above, the upper or lower sign is selected according to whether the angle between $\underline{i}_r$ and either $\underline{i}_L'$ or $\underline{i}_L$, whichever is relevant, is greater or less than 180 degrees, respectively.

OPTIMUM GUIDANCE POLICIES

In an effort to compensate for initial errors by means of a mid-course velocity correction, new errors will inevitably be made which must again be corrected. The problem of determining when and how to perform impulsive corrections to a spacecraft orbit can be classified as a multistage decision process. Various guidance policies have been proposed and the new mathematical techniques of dynamic programming and steepest ascent optimization theory have been used with some success in an attempt to formulate an optimum policy. Several useful guidance policies are described and compared by Curkendall and Pfeiffer (11) in a recent paper.

As with all applications of dynamic programming techniques, the computational requirements are extensive and rapidly become impractical as the dimension of the problem increases. The results obtained by Arcon (12) and Orford (13) using this approach have been rather limited and numerical examples are restricted to problems of only one or two dimensions rather than six.

Denham and Speyer (7) have formulated a method of improving a velocity correction schedule iteratively using steepest ascent techniques in a manner similar to that mentioned earlier for optimizing measurement schedules. No numerical results are yet available.

Unfortunately the Monte Carlo approach to the determination of velocity-correction times remains the most practical method. The lack of mathematical elegance and an overabundance of computer usage time, which characterize this technique, are nevertheless balanced by the capability of utilizing a realistic, rather than an oversimplified, mathematical model.

REFERENCES

1. BUMSTEAD, R. M., and VANDER VELDE, W. E., "Navigation and Guidance Systems Employing a Gimballess IMU". Progress in Astronautics and Aeronautics, Vol. 13, pp. 391–419, Academic Press, New York, 1964.
2. WIENER, T. F., "Theoretical Analysis of Gimballess Inertial Reference Equipment Using Delta-Modulated Instruments". M.I.T. Instrumentation Laboratory Sc.D. Thesis T-300, Cambridge, Mass., March 1962.
3. BLACKMAN, R. B., "Methods of Orbit Refinement". Bell Telephone Technical Journal, Vol. 43, pp. 885–909, May 1964.
4. POTTER, J. E., and STERN, R. G., "Statistical Filtering of Space Navigation Measurements". Progress in Astronautics and Aeronautics, Vol. 13, pp. 775–801, Academic Press, New York, 1964.
5. BATTIN, R. H., "Astronautical Guidance". McGraw-Hill Book Company, Inc., New York, 1964.
6. HENRICI, P., "Discrete Variable Methods in Ordinary Differential Equations". John Wiley and Sons, Inc., New York, 1962.
7. DENHAM, W. F., and SPEYER, J. L., "Optimal Measurement and Velocity Correction Programs for Midcourse Guidance". AIAA Journal, Vol. 2, pp. 896–907, May 1964.
8. MOORE, F., BROOKS, and BROOKS, M., "Saturn Ascending Phase Guidance and Control Techniques". Progress in Astronautics and Aeronautics, Vol. 10, pp. 183–209, Academic Press, New York, 1963.
9. MARTIN, F. H., "Closed-Loop Near-Optimum Steering for a Class of Space Missions". M.I.T. Instrumentation Laboratory Sc.D. Thesis T-413, Cambridge, Massachusetts, May 1965.
10. CHERRY, G. W., "E Guidance: A Universal, Explicit, Optimizing Guidance Law for Rocket-Propelled Flight". AIAA/ION Astrodynamics, Guidance and Control Conference Paper 64–638, Massachusetts Institute of Technology, Cambridge, Massachusetts, August 1964.
11. CURKENDALL, D. W., and PFEIFFER, C. G., "Discussion of Guidance Policies for Multiple-Impulse Corrections of the Trajectory of a Spacecraft". Progress in Astronautics and Aeronautics, Vol. 13, pp. 667–87, Academic Press, New York, 1964.
12. ADVANCED RESEARCH CONSULTANTS, "Some Aspects of Midcourse Guidance". Report R62–5, Lexington, Massachusetts, July 1962.
13. ORFORD, R. J., "Optimization of Stochastic Final Value Control Systems Subject to Constraints". Grumman Aircraft Engineering Corporation, Report RE-157, Bethpage, New York, May 1962.

PART 4

INERTIAL MEASUREMENT UNITS AND PULSE TORQUING

John E. Miller

JOHN E. MILLER

John E. Miller, Deputy Associate Director of Instrumentation Laboratory, Massachusetts Institute of Technology, heads the Laboratory group that is developing the inertial measurement unit for the Project Apollo spacecraft guidance system. Mr. Miller was born April 30, 1925, at Aberdeen, S.D., and was graduated from high school there in 1943. He served in the U.S. Army from 1943 to 1945 prior to appointment to the United States Military Academy, West Point, N.Y., where he was graduated in 1949.

Mr. Miller served in the U.S. Air Force from 1949 to 1958 and during this period was sent to M.I.T. for graduate study. He was awarded the M.S. degree in instrumentation in 1953. Also while serving as an Air Force officer, Mr. Miller taught inertial navigation and automatic control at the Air Force Institute of Technology, Dayton, O. He joined the Instrumental Laboratory in 1959 and initially worked on the development of accelerometers used in the Mark II guidance system the Laboratory designed for the Navy's Polaris missile.

PART 4

INERTIAL MEASUREMENT UNITS AND PULSE TORQUING

INTRODUCTION

The Inertial Measurement Unit, IMU, provides three fundamental functions in a space guidance system. It establishes a non-rotating computing coordinate frame oriented to a desired inertial reference such that acceleration is measured in that frame. It provides information to a guidance computer of the orientation of that coordinate frame with respect to the control member, the spacecraft. It provides a measure of the specific force of the spacecraft (usually the integral of the specific force) in suitable form to the guidance computer.

The Apollo IMU is a three degree of freedom gimbal system utilizing integrating gyroscopes to detect angular deviations of the stable member with respect to inertial space, and to provide along with their servo electronics the establishment of a non-rotating member. On this stable member are three accelerometers in an orthogonal triad. The accelerometers are single degree of freedom pendulums with a digital pulse restraining system. Angle information as to the orientation of the computing coordinate frame, stable member, with respect to the navigation base is derived from a two speed resolver system mounted on each axis of the IMU. This resolver system provides knowledge of the stable member to both the astronaut and to the computer; to the astronaut by the means of a ball indicating system with resolvers servo controlled to follow the resolvers on the IMU. The ball has the same gimbal order as the IMU. The same resolver system by means of a Coupling Data Unit, CDU, provides to the computer quantized angle increments for changes in gimbal angles. The CDU couples angle information to and from the guidance computer, performing both analog to digital and digital to analog conversion.

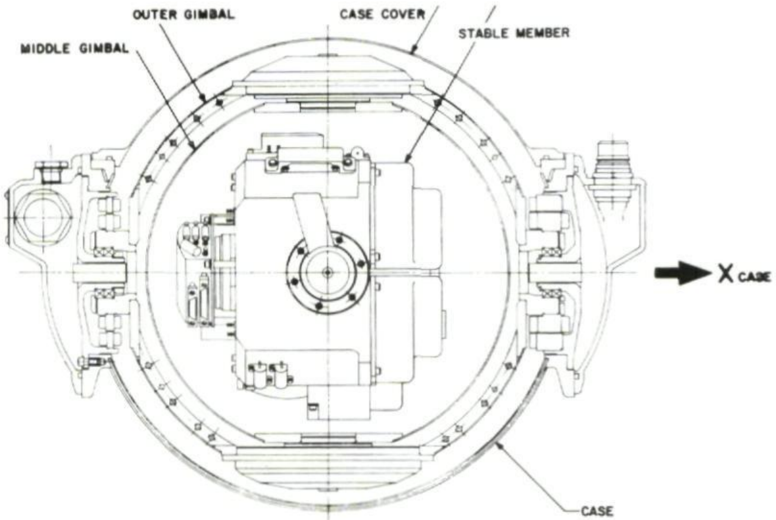

NOTES:

1. INERTIAL COMPONENT INPUT AXIS DIRECTIONS SHOWN WITH GIMBALS IN ZERO POSITION
2. X_{SC}, Y_{SC}, & Z_{SC} AXES ARE IN THE SAME DIRECTION AS X_{CASE}, Y_{CASE}, & Z_{CASE} AXES
3. X_{SC}, Y_{SC}, & Z_{SC} ARE SPACECRAFT AXES WITH X_{SC} ALONG THRUST DIRECTION

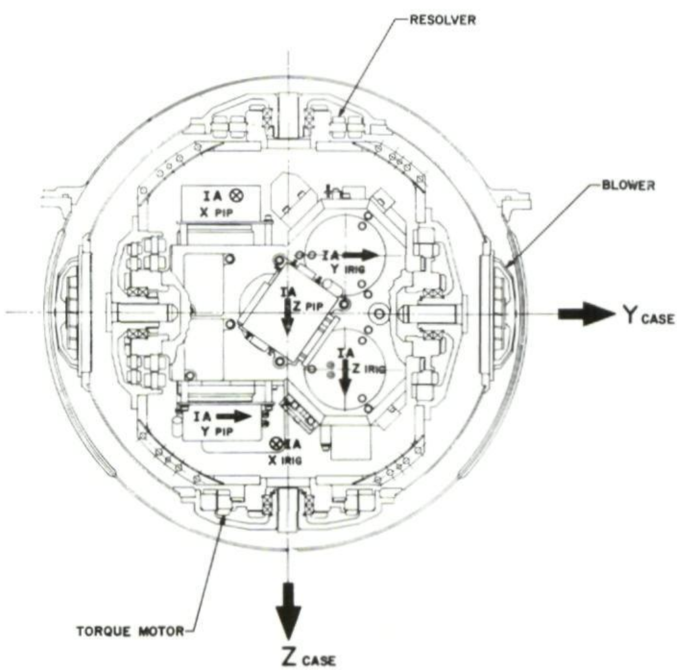

FIG. 4–1 Inertial measurement unit

CHAPTER 4–1

THE APOLLO INERTIAL MEASUREMENT UNIT

Thermal and Mechanical – The Apollo Inertial Measurement Unit (IMU) is a three degree of freedom gimbaled system. The reasons for using this inertial measurement configuration have been previously stated. The IMU is described from the stable member to the case using Fig. 4–1. The inertial components are three single-degree-of-freedom Inertial Reference Integrating Gyroscopes (IRIG) and three single-degree-of-freedom Pulsed Integrating Pendulums (PIP). These components are mounted on the inner member which is referred to as the stable member. It is the member which will be non-rotating with respect to the fixed stars except by the drift of the gyroscopes. The stable member also contains necessary electronics. Three degrees of freedom are obtained by coupling the stable member to a middle gimbal by means of an intergimbal assembly to provide one axis of rotation. Likewise a degree of freedom is provided between the middle and the outer gimbal and the outer gimbal and the case. Mounting pads are used as a means of precision alignment of the case onto the navigation base.

The gyroscopes and accelerometers are temperature controlled. The case of the IMU provides a hermetically sealed environment containing air at atmospheric pressure with leak rates less than 10^{-5} cc of He/sec equivalent. There is in the case an integral coolant passage for a heat sink. This integral coolant passage is formed by placing a pattern on a sheet of aluminum. This sheet of aluminum is roll bonded to another sheet except in the area of the pattern where no bonding takes place. The piece or case is formed and machined to the proper dimensions. The coolant passage is then inflated using air to form a coolant passage where the pattern has been placed. This provides a means of making a leak-free integral coolant passage over a spherical surface. Water and glycol at 7°C from the spacecraft coolant system is circulated at a rate of 15 Kg/hour and the pressure drop in the IMU is less than 703 Kg/M^2.

The required operation of the IMU is for ambient pressure of zero for 14 days and environmental extremes from -18°C to $+65$°C. It may see these ambient structure temperatures depending upon orientation of the spacecraft with respect to the sun. The temperature of the gyroscopes and accelerometers is controlled by means of a thermostatic control system. Heat flow is from the stable member to the case and coolant. Around the stable member is a dead air space. The gyroscopes are controlled to 57°C and the accelerometers to 54°C. The major source of power is in the gyroscope wheels with smaller amounts in electromagnetic components such as torquers. A pair of blowers on the outer gimbal provide heat transfer by moving air over the middle gimbal and the case. There is insulation over the case that is shown in Figure 4–2 primarily because the case will be below the dew point. This is particularly true at the launch at Cape Kennedy.

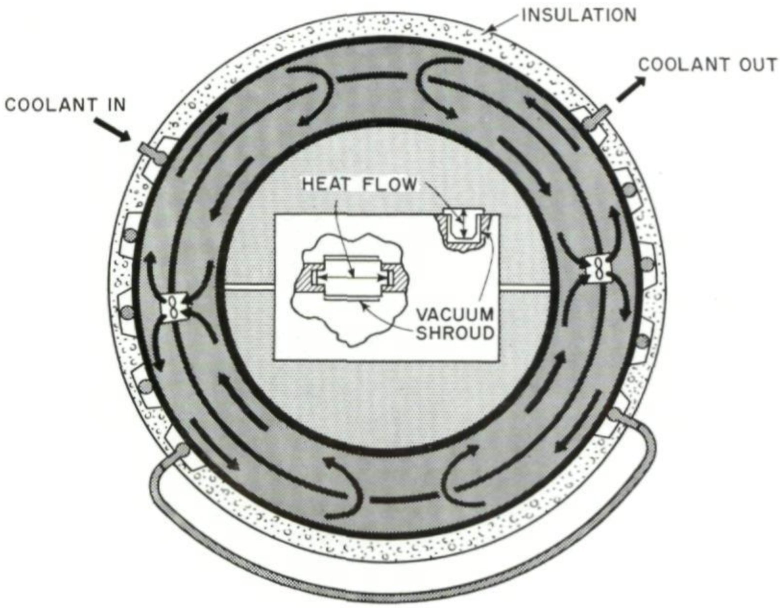

FIG. 4–2 IMU heat transfer diagram

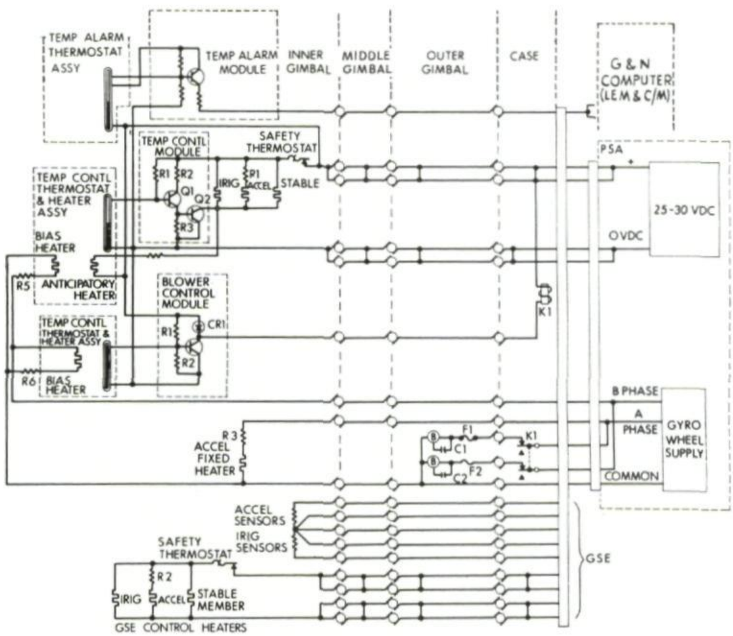

FIG. 4–3 Block II IMU temperature control system schematic diagram

A mercury thermostat senses the stable member temperature by being mounted on the appropriate position of the stable member. A single thermostat is used to control the temperature of six inertial components. The thermostat energizes an end-mount heater on the pendulum, end-mount heaters on each end of each gyro and two stable member heaters. The inertial components have a vacuum shroud around the cylindrical wall to prevent circumferential gradients. All heat flow is thus axial which is done to reduce uncertainty torques. The thermostat dead zone is 0.17°C. A thermostat heater is used to prevent long delays and to control the limit cycle amplitudes of the inertial components. This heater is the anticipatory heater. Fixed heat is applied to the thermostat to set the absolute temperature of the inertial components.

Mounted on the outer gimbal are a pair of blowers, one on each end of a diameter. These also are thermostatically controlled, their purpose is to increase the dynamic range of the temperature control loop in the presence of environmental disturbances. Each inertial component is held to a constant temperature $\pm\frac{1}{3}$°C under all environmental temperature and pressure design conditions. The blower control loop is required only under conditions of high environmental conditions or high heat dissipation on the stable member. About 18 watts are dissipated under normal operating conditions on the stable member. The principal portion of this power, about 14 watts, is in the gyro wheels. A complete temperature control diagram is shown in Figure 4–3. The principal problems of design have been the reliable control of six inertial instruments with a single thermostat and the design of a precision temperature control system both under accelerating and free fall conditions with wide variations in the environmental disturbances.

The temperature difference between IRIGs and PIPs is adjusted by properly proportioning the amount of power in each heater. This balance is obtained by adjustment of R_1. (Refer to Fig. 4–3 and 4–4). As the power required to maintain the thermostat in its limit cycle operation is varied, because of environmental or power changes, the temperature error of the IRIGs and PIPs can change proportional to the power required. This proportionality can be adjusted to be either plus or minus, and is adjusted to zero. This results in a zero temperature error, or very nearly so, over the full power range possible. There is a fixed bias heat applied to the PIPs to bring them to their operating temperature under normal conditions. As the PIP temperature deviations are subject to gyro power dissipation, this fixed heat is from the same power supply as the gyro wheels.

The performance of the temperature control system may be seen in Fig. 4–5. The thermostat cycle of operation at 50% duty cycle is 0.17°C, while at the same time the gyroscope limit cycle has been attenuated to 0.36 millidegree C° and that of the accelerometers to 5 millidegree C°. The stable member temperature continues to drop as the control power is increased, as one would expect. But the inertial component temperature remains constant throughout the power range. The blower extends the dynamic range of operation, is used infrequently and is limit cycled by a thermostat. There is a separate sensor to detect temperature out of limits to caution the astronaut should this occur. In addition, high limit mechanical thermostats are used in every heater power line to prevent an overheated condition. These are

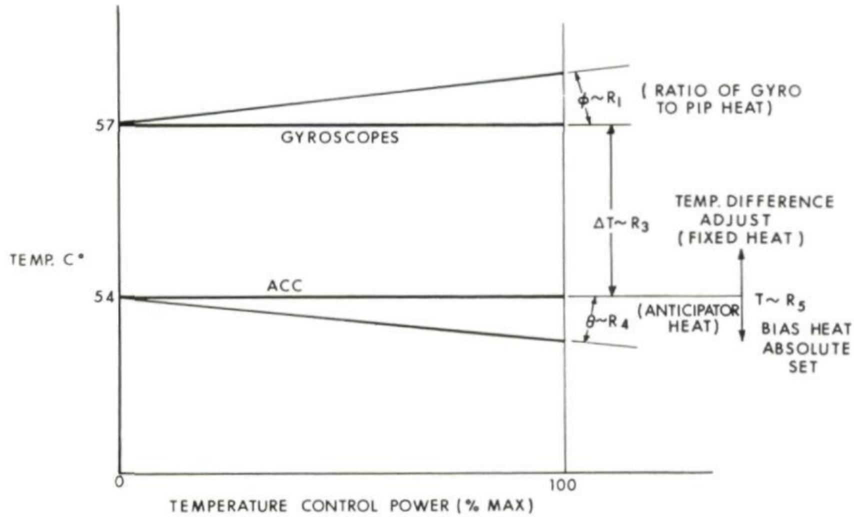

FIG. 4–4 IMU temperature control trimming resistor functions

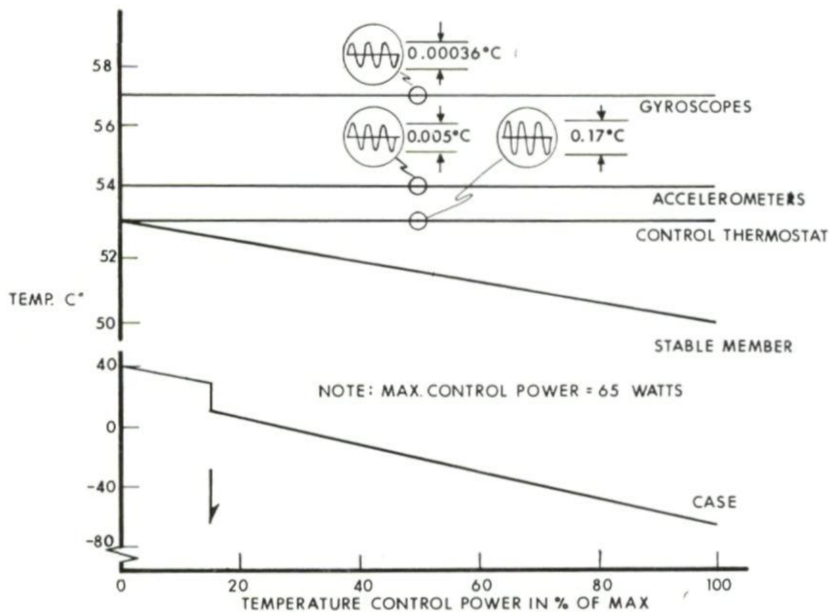

FIG. 4–5 IMU temperature profile vs temperature control power

set to open the heater power at a temperature of about 5°C over the normal control temperature. These have been rarely used, but when necessary have prevented damage to valuable equipment.

The GSE (Ground Support Equipment) heaters and sensors have been provided for ground handling. The IMU once assembled is maintained at temperature. This necessitates times and places of operation where normal power may not be available. Separate heaters and sensors are provided isolated from airborne control. Thus it is possible with the system in the spacecraft to be maintained at temperature with a portable temperature controller with normal power off or on.

Vibration – Before proceeding into the vibration environment it is well to discuss some of the mechanical construction features. The stable member itself is a sintered block of beryllium with drilled holes for each inertial component. These inertial components are pre-aligned in a test stand and assembled into the stable member in an aligned condition. This saves considerable adjustment of alignment at later stages of testing. A pre-wired harness with connectors is laid on to the stable member and interconnection is made. At each end of the stable member are intergimbal assemblies. These house the slip rings to electrically interconnect rotating members. The slip rings are 40 or 50 circuit elements depending upon axis location, the larger number required at the middle and outer axis. Much effort has gone into the design of reliable rotary slip rings which will give unlimited angular freedom of motion. There is a double pair of brushes for each circuit spaced 0.64 mm apart. Each circuit with two feet of No. 30 AWG has less than $\frac{1}{3}$ of an ohm resistance. Electrical coupling does take place between adjacent circuits. Coupling is approximately inversely proportional to the spacing between circuits. With proper selection of circuit placement on the slip ring cross coupling effects can be reduced to negligible amounts. Each contact is rated for 2 amps of current. Only heater power utilizes this much current while everything else is less than 1 amp. High current carrying load slip rings are paralleled for reliability reasons. Early design considerations allow for about 10% spares. As the design progresses toward maturity these spares are usually reduced and finally all utilized.

The gimbal construction is spherical. Gimbals are interconnected by means of an intergimbal assembly which contains the resolvers, d.c. gimbal torque motors, slip rings, stub shaft and a duplex pair of preloaded bearings. Surrounding the stable member is the middle gimbal, and surrounding the middle gimbal is the outer gimbal which is next to the case. The intergimbal assemblies contain either a resolver or a d.c. torque motor. Each axis utilizes one d.c. torque motor and a single resolver which is both a single speed resolver and a sixteen speed resolver utilizing the same excitation winding. In addition, on the inner axis is a gyro error resolver to resolve X and Z gyro error voltages by the angle of the inner gimbal. Each axis has a duplex pair of preloaded bearings. These intergimbal assemblies are again made of beryllium for the housing and stub shaft in order to decrease weight.

The IMU, as a mechanical element, forms a system of masses, springs and dampers, with non-linear behavior. As a complex mechanical system it will resonate at certain frequencies. The lowest frequency resonant vibration ratio of the amplitude of the stable member to that of the input to the case

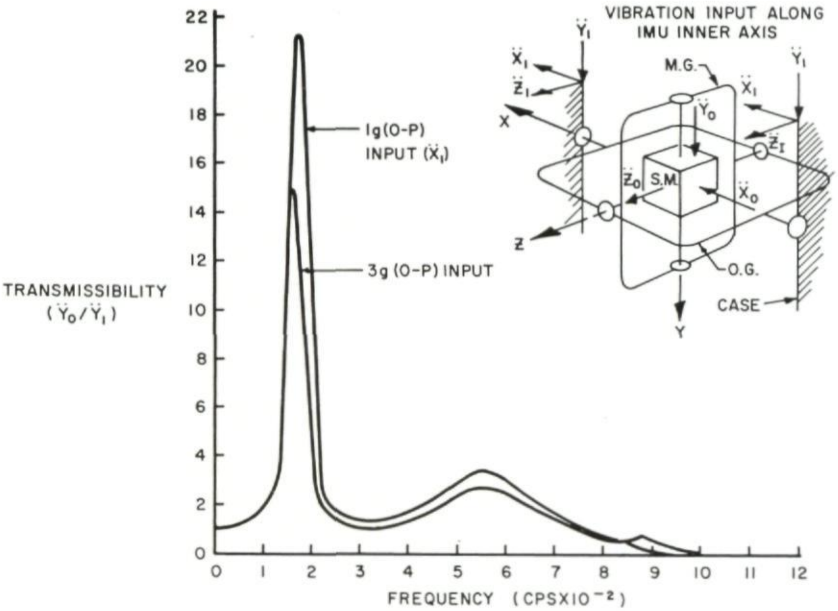

FIG. 4–6 Apollo IMU–VM (12.5) vibration test results – stable member response curves

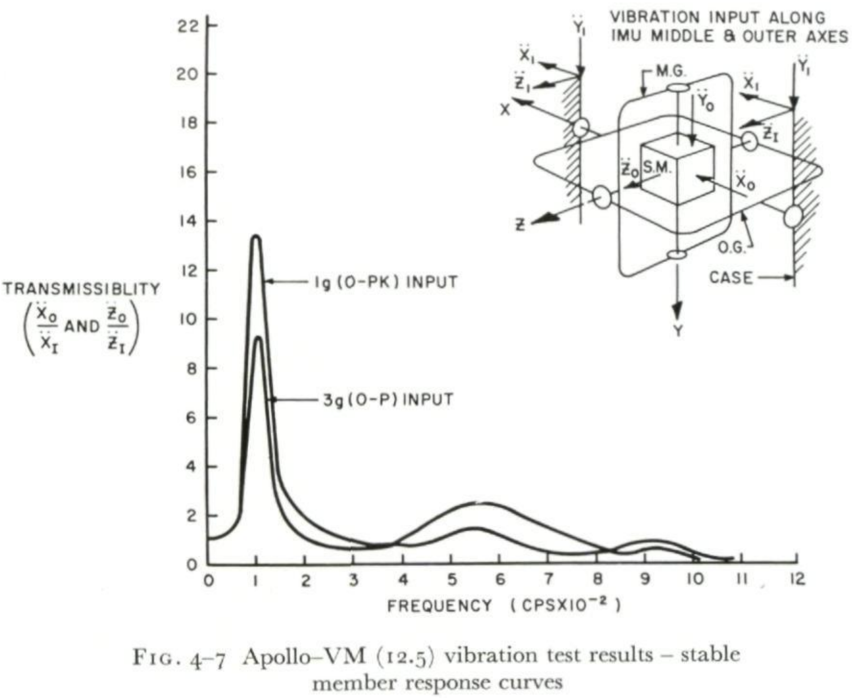

FIG. 4–7 Apollo–VM (12.5) vibration test results – stable member response curves

is the greatest. This ratio, called transmissibility, is non-linear in that the ratio decreases with increasing input amplitudes. The elements must be structurally sound enough to withstand the flight environment. Shown in Fig. 4–6 and 4–7 is the transmissiblity of the IMU. The expected flight environment is less 0.044 g^2/cps. Each IMU is given a workmanship vibration test from 20 to 20000 cps of at least 1g rms input along each axis. The resonant peaks may be reduced by adding vibration dampers along each axis which provide a Coulomb friction force for motion along the axis but which do not change the friction torque about the axis.

Gyroscopes and Stabilization – The gyroscopes used are single-degree-of-freedom integrating gyroscopes of a type previously described (1). The angular momentum is $\frac{10^6}{2}$ gm cm²/sec developed by a wheel supported by a pair of preloaded ball bearings with a 13 n preload. This wheel has a hysteresis ring on it with a motor stator surrounding it on the inside of a spherical float. The float is a beryllium member again designed to yield the highest ratio of wheel to float weight. Flexible power leads carry power from the cast to the float. These power leads create less than 1/2 dyne cm of torque on the float. The fluid used for buoyant support is a brominated fluorocarbon with a density of 2.385 gms/cc at 58°C. The fluid is fractionally distilled to yield polymers of approximately the same length and nearly the same viscosity. This prevents fluid stratification under operating and storage conditions. The damping about the output axis is $4.6 \cdot 10^5$ dyne cm/radian/sec. In addition to the fluid support there is an electromagnetic suspension system to provide both axial and radial suspension of the float with respect to the case. Such suspension systems have been previously described (2).

The axis definition for the instrument has previously been described. Shown in Fig. 4–9 is the signal generator which develops a voltage modulated by the angle of the float with respect to the case A_{c-f}. This is the rotation of the stable member about the gyro non-rotating input axis. There is with each gyroscope a set of prealignment hardware. This provides integrally with each pre-aligned instrument the following items:

(a) Suspension Capacitors for Microsyn Suspension
(b) Temperature Sensor Normalization
(c) End Mount Heater Pre-aligned to Gyro IA
(d) Torque Generator Normalization
(e) Signal Generator Preamplifier with normalized gain

The gyro is prealigned on a test stand with the input axis aligned about the output axis relative to a slot in the mounting ring. The alignment is carried over to the stable member where a pin is precisely located to pick up the slot. The use of prealigned components has made assembly techniques simpler and has brought about excellent correlation between component and system performance of the gyroscope. Deviations in performance between component and system are less than 10 meru (milliearth rate unit). 1 meru = 0.015 degrees per hour.

Each gimbal axis contains a d.c. torque motor used to null the deviations of the gyro input axis with respect to the case. These direct drive motors have been designed with sensitivities of 1.65 nm/amp. The gyro error signals are fed to the gimbal servo amplifier which with its proper dynamic compensa-

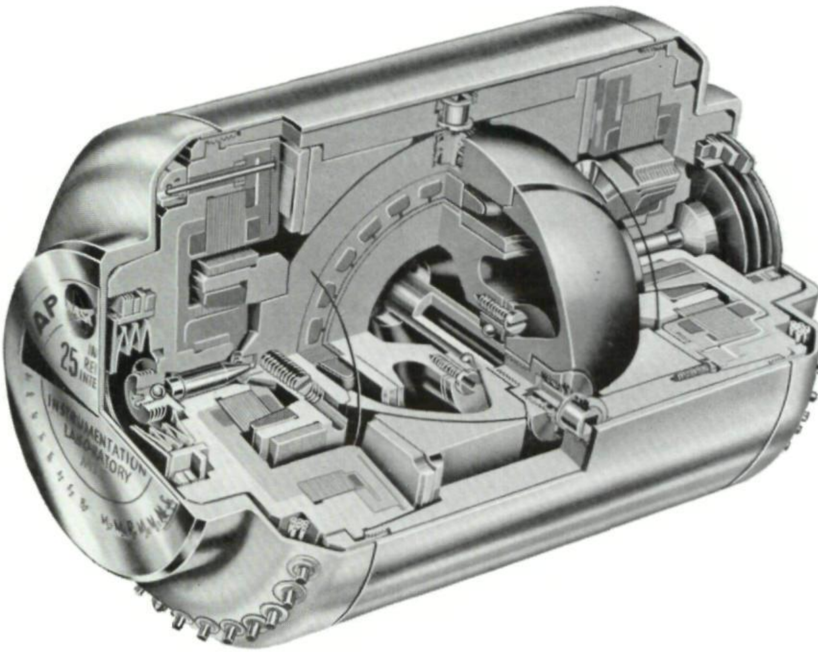

FIG. 4–8 Apollo II IRIG

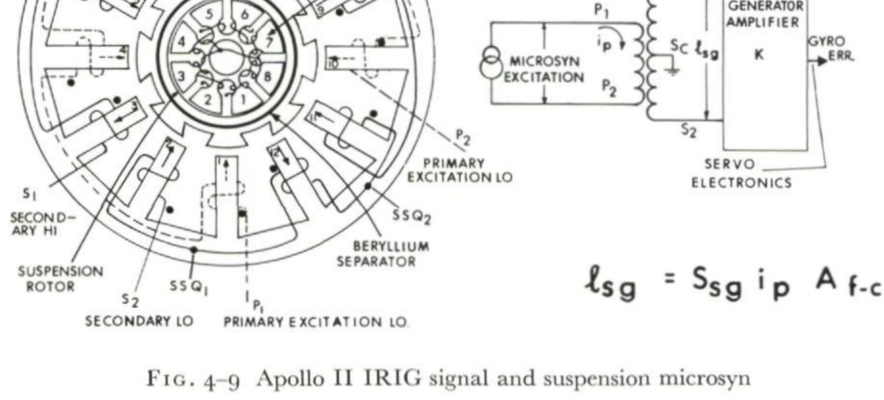

FIG. 4–9 Apollo II IRIG signal and suspension microsyn

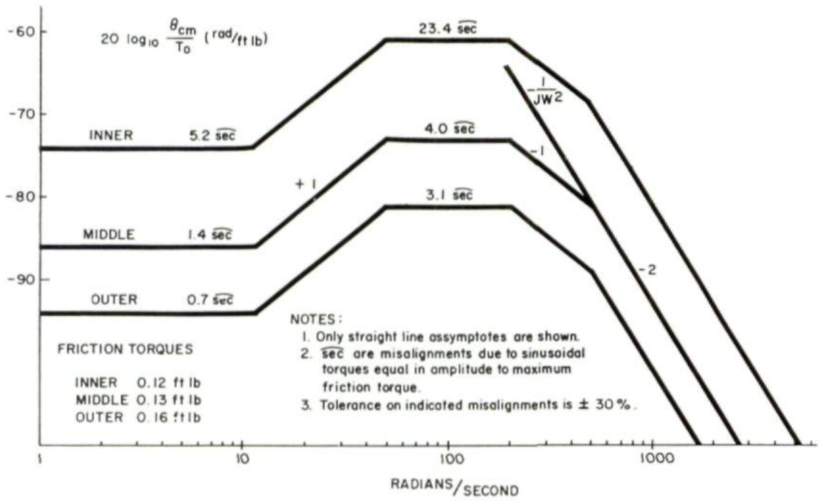

FIG. 4–10 Inertial platform misalignment due to friction torques vs frequency

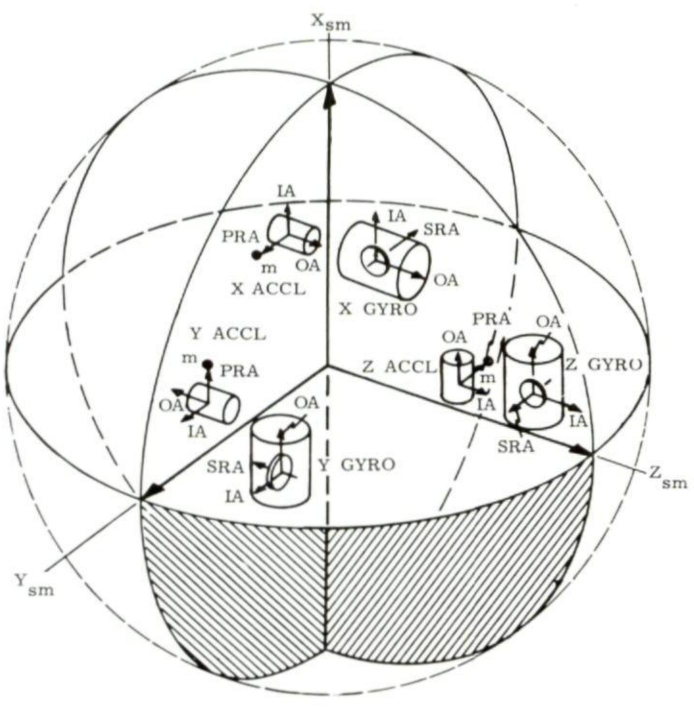

FIG. 4–11 Stable member geometry

$\Delta V = 3106.880$ m/sec. Max. Acceleration $= 12.160$ m/sec^2

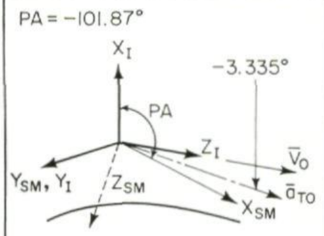			Error Coefficient	Final Position Error in Target Axes in feet			Final Velocity Error in Target Axes in ft/sec		
				Alt.	Track	Range	Alt.	Track	Range
STABLE Member	Initial S.M. Alignment Errors	$A_{(SM)XI}$	0.2 mr		99			0.82	
		$A_{(SM)YI}$	0.2 mr	277		−77	2.09		−0.46
		$A_{(SM)ZI}$	0.2 mr		−261			−1.86	
ACCELEROMETER	Accel. IA Non-orthogonality	X to Y	0.10 mr						
		X to Z	0.10 mr	−1		−6	−0.0002		0.0008
		Y to Z	0.10 mr						
	Bias Error	ACBX	0.2 cm/sec^2	−70		−305	−0.46		−1.94
		ACBY	0.2 cm/sec^2		−313			−1.99	
		ACBZ	0.2 cm/sec^2	316		−72	2.08		−0.46
	Scale Factor Error	SFEX	100 PPM	−31		−136	−0.23		−0.99
		SFEY	100 PPM		0			0	
		SFEZ	100 PPM	−7		2	−0.004		0.0004
	Accel. Sq. Sensitive Indication Error	NCXX	10 $\mu g/g^2$	−3		−13	−0.03		−0.11
		NCYY	10 $\mu g/g^2$		0			0	
		NCZZ	10 $\mu g/g^2$	0.08		−0.02	0.0006		−0.0001
GYRO	Bias Drift Drift Time before Traj. start: 15 min. (Init. Mlm. = 0.33 mr for 5 meru drift)	BDX							
		Direct effect	5 meru		0.4			−0.03	
		Eff. on Init. Mlm.			163.1			1.35	
		Combined eff.			163.5			1.32	
		BDY							
		Direct effect	5 meru	59		−14	0.66		−0.12
		Eff. on Init. Mlm.		454		−126	3.44		−0.76
		Combined eff.		513		−140	4.10		−0.88
		BDZ							
		Direct effect	5 meru		59			0.65	
		Eff. on Init. Mlm.			−428			−3.05	
		Combined eff.			−369			−2.40	
	Acceleration Sensitive Drift	ADIAX	15 meru/g^2		0.3			−0.08	
		ADSRAY	10 meru/g^2	7		−2	0.05		−0.012
		ADIAZ	15 meru/g^2		−11			−0.08	
	Acceleration Squared Sensitive Drift	$A^2D_{(IA)(IA)X}$	1 meru/g^2		−0.03			−0.006	
		$A^2D_{(SRA)(SRA)Y}$	1 meru/g^2	0.07		−0.02	0.0007		−0.0001
		$A^2D_{(IA)(IA)Z}$	1 meru/g^2		0.07			0.0006	

FIG. 4–12 Translunar injection trajectory cut-off coefficients

tion are used to stabilize the inner member. The performance of the gimbal servos is best described by their ability to attenuate angular deviations of the stable member in the presence of torque disturbances. Shown in Fig. 4–10 is the performance of each axis of the IMU gimbal servo. Among the design problems are the mode switching from coarse align (resolver control) to fine align (gyro control), synchronization from turn-on or switch over conditions, performance under power supply changes, gain changes from geometrical variations and torque disturbances.

Gyro torquing is required for precision alignment of the stable member at prelaunch and for in-flight alignment. The fine alignment procedure and mechanization has previously been described. The gyroscope has a torque generator used in a digital torque command loop. This loop accepts commands from the computer by a pulse train with equal pulse width spacing. The torque commanded is a constant magnitude and modulated only by the time interval. The computer could thus command one equivalent pulse incremental angle ($2\pi/2^{21}$ radians/pulse). One precision current switch is used for all three gyroscopes and the commands are multiplexed in one selector network. The torque level control will be described later. (See Chapter 4–2.) The torque generator is normalized in gain to command a fixed angular velocity for a fixed current. This digital angle command from the computer to the IMU permits the stable member to be oriented within the uncertainty of the angle read system ($\Delta\theta = 40$ arc sec). It, furthermore, has the advantage of no current applied to the gyro during periods other than alignment. The gyroscopes are oriented on the stable member with Y and Z gyro output axis along X_{sm}. This axis is usually aligned along the thrust axis. This inertial component orientation reduces the acceleration sensitive torques in the gyros. The Y_{sm} axis is usually aligned such that it is normal to the plane of maneuver. For this reason the X gyro SRA is along Y_{sm} as can be seen in Fig. 4–11. For the same reason the Z SRA axis is along Y_{sm}.

The largest error contributors per unit of error following any maneuver are the premaneuver errors. That is to say that the effects of gyro drift during thrusting create less error uncertainty in position and velocity at the end of thrust period than those misalignments due to drift between alignment and start of thrust. The error in free fall from the time of alignment to the start of any acceleration maneuver is time dependent upon the gyro non-acceleration sensitive drift (bias drift). As an example the ratio of error created by 1 meru of drift for 15 minutes prior to the start of translunar injection to that error created by the same drift during thrusting is approximately 400 : 1. Tables of error coefficients for two thrusting maneuvers are shown in Fig. 4–12 and Fig. 4–13. This same fact is readily apparent. Every effort has been made to reduce gyro bias drift uncertainty and magnitude.

The torque generator has been designed to be d.c. torqued with low residual magnetism uncertainty torques. It is a twelve pole stator with an eight pole rotor creating 4 500 dyne cm of torque with a current excitation of 0.1 amps. The beryllium separator prevents the use of the microsyn excitation as a reset coil or degausser for the rotor. Dipole storage in the rotor and stator would create residual torque in the gyro and this torque magnitude and sign would be a function of its past history. It would be possible to return

(V_0 = 36,200 ft/sec, $_0$ = −6.0 deg., Max. G = 5.45, Platf. Angle = −35.7°)

PA = −35.7°

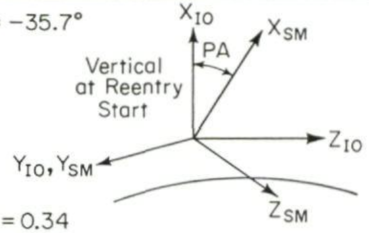

L/D = 0.34

			Error Coefficient	Final Position Error in Target Axes in feet: Alt.	Track	Range
STABLE Member	Initial S.M. Alignment Errors ° (Uncorrelated)	$A_{(SM)XI}$	0.2 mr	130	946	28
		$A_{(SM)YI}$	0.2 mr	−2,360	−6	376
		$A_{(SM)ZI}$	0.2 mr	−44	1,796	101
ACCELEROMETER	Accel. IA Non-orthogonality	X to Y	0.1 mr			
		X to Z	0.1 mr	−1,172	−3	23
		Y to Z	0.1 mr			
	Bias Error	ACBX	0.2 cm/sec^2	−1,593	−4	32
		ACBY	0.2 cm/sec^2	−4	−1,361	0
		ACBZ	0.2 cm/sec^2	35	0	−1,369
	Scale Factor Error	SFEX	100 PPM	215	1	−8
		SFEY	100 PPM	0	−52	0
		SFEZ	100 PPM	−26	0	1,007
	Accel. Sq. Sensitive Indication Error	NCXX	10 $\mu g/g^2$	−49	0	1
		NCYY	10 $\mu g/g^2$	0	−20	0
		NCZZ	10 $\mu g/g^2$	7	0	−281
GYRO	Bias Drift Drift Time before Traj. start: 45 min. (Init. Mlm. = 0.98 mr for 5 meru drift)	BDX Direct effect	5 meru	1	852	7
		BDX Eff. on Init. Mlm.		641	4,655	139
		BDX Combined eff.		642	5,507	146
		BDY Direct effect	5 meru	−937	−1	−9
		BDY Eff. on Init. Mlm.		−11,618	−28	1,850
		BDY Combined eff.		−12,555	−29	1,841
		BDZ Direct effect	5 meru	−11	19	1
		BDZ Eff. on Init. Mlm.		−217	8,840	499
		BDZ Combined eff.		−228	8,859	500
	Acceleration Sensitive Drift	ADIAX	15 meru/g	−1	−879	10
		ADSRAY	10 meru/g	−2,832	−4	9
		ADIAZ	15 meru/g	17	−33	−3
	Acceleration Squared Sensitive Drift	$A^2 D(IA)(IA)X$	1 meru/g^2	0	113	0
		$A^2 D(SRA)(SRA)Y$	1 meru/g^2	−808	−1	13
		$A^2 D(IA)(IA)Z$	1 meru/g^2	−8	−3	1

FIG. 4–13 3 700 kilometers earth re-entry trajectory errors

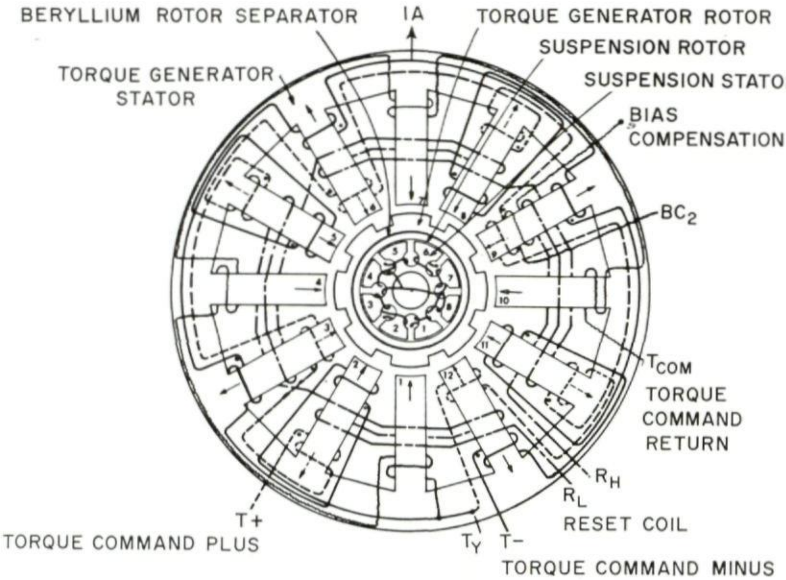

FIG. 4–14 Apollo II torque generator and suspension

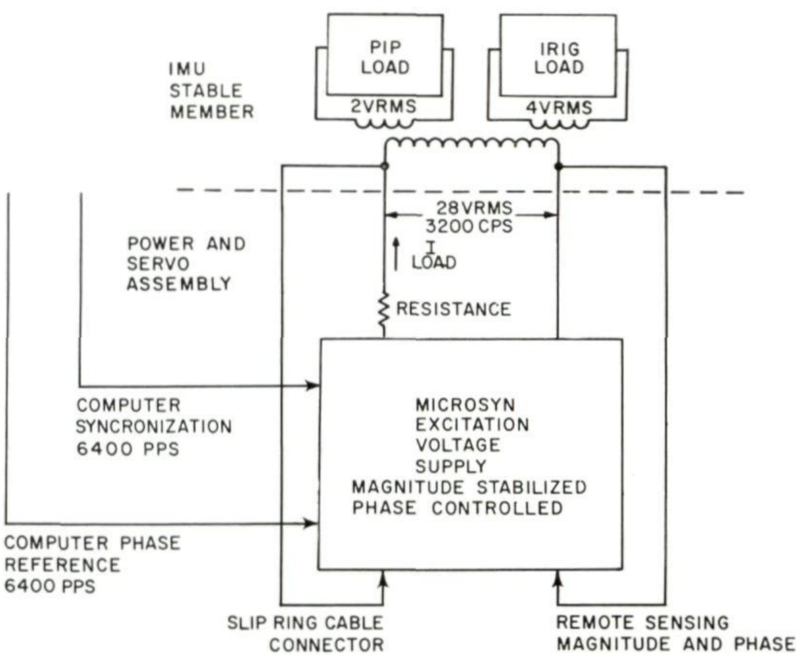

FIG. 4–15 Microsyn excitation voltage supply

the state of the magnetic material to its original condition in most cases by appropriate commands from the computer. However, the use of a reset coil with a.c. excitation from the microsyn excitation voltage supply serves to keep the state of the magnetic material constant following any pulse torque commands from the computer.

There is a winding around each set of three poles which acts as a reset winding for both rotor and stator. Further use of this reset winding may be made if one recognizes that if the flux through one stator pole were unbalanced there would be a torque created on the float. The bias compensation winding on pole nine is used to create a torque equal and opposite to all the non-gravity sensitive torques and thus reduce the bias drift to zero. The torques creating bias drift come from two sources, flex leads and microsyns. The microsyn torques are proportional to the microsyn excitation voltage squared. The bias compensation winding torque changes due to excitation voltage changes are exactly equal and of negative polarity relative to the microsyn torque changes from the same source. Only the flex lead torque magnitude may be compensated by the bias winding.

The microsyn excitation for both gyros and accelerometers is from a single source located in the power and servo assembly, PSA. The voltage level on the IMU stable member is stable to within 1% of the value required (2 volts for the PIPs and 4 volts for the IRIGs) under the design disturbance conditions. The magnitude and phase of the voltage on the stable member is controlled. All a.c. power supplies are synchronized to the guidance computer clock. D.C. to d.c. converter or d.c. supplies using multivibrators as a.c. sources for rectification are also synchronized to the computer.

The method of synchronization is to use a multivibrator which will free run at a lower frequency without the computer pulses. This will assure operation of the IMU power supplier in the event of a computer failure. With the computer pulses these supplies will be synchronized. In addition, the microsyn excitation supply voltage is phase locked to the computer. The voltage stability and phase stability is required at the inertial component. For power transmission there is a step down transformer on the stable member. This reduces the slip ring current and the voltage drop effects due to slip ring, cable and connector resistance. The stable member voltage is sensed at the primary transformer side and compared to a voltage and phase reference. Phase is controlled to within $\pm \frac{1}{2}^\circ$ of the computer reference. On the stable member each PIP has the same length of wire from the transformer to the PIP input terminals on the instrument.

CHAPTER 4–2

THE PULSED INTEGRATING PENDULOUS ACCELEROMETER (PIPA)

Basic Operation – The PIPA block diagram is shown in Fig. 4–16. The inertial sensor is a single-degree-of-freedom pendulum with a pendulosity of $\frac{1}{4}$ gm cm. The pendulum is mounted on the stable member and is non-rotating with respect to inertial space. The signal generator is a variable reluctance device termed a signal generator microsyn. It is excited from a sinusoidal source which is synchronized and phase locked to the guidance computer. The signal generator output is voltage modulated by the angle of the pendulum float with respect to case (A_{c-f}) and the float angular velocity $(\dot{A}_{c-f})$. The voltage may be considered to contain only float angle information. This signal, amplified, is used in an interrogator. The interrogator is a peak detecting device used to determine sign and magnitude of the float angle at discrete times. These discrete times are the computer clock times (ΔT) synchronized with sinusoidal excitation. Only float angle sign is determined and the operation is binary. The interrogator output is a command to torque the float angle to null. The current switch directs a constant current source into either the odd poles or even poles of an eight pole torque microsyn. The torque generator creates a torque either positive or negative proportional to the square of the current in the windings. Current is controlled constant by comparison of a precision voltage reference with the voltage drop across a precision resistor in the current loop.

Dynamic Operation – The basic loop equation is neglecting uncertainty torques about the output axis and making the small angle assumption: $\cos A_{c-f} = 1$, $\sin A_{c-1} = A_{c-f}$.

$$J \ddot{A}_{I-f} + C \dot{A}_{c-f} = M_{tg} + ml\, a_{IA} \qquad \text{(Eq. 4–1)}$$

Where:

J = Float inertia

C = Damping about the output axis

A_{c-f} = Float angle with respect to the case $(c-f)$

A_{I-f} = Float angle with respect to inertial space

M_{tg} = Torque generator torque

a_{IA} = Acceleration along the input axis

$$V_{IA} = \int_o^t a_{IA}\, dt$$

Integrating yields:

$$J \dot{A}_{I-f} + C A_{c-f} + \text{Initial conditions} = \int_o^t M_{tg}\, dt + ml \int_o^t a_{IA}\, dt$$

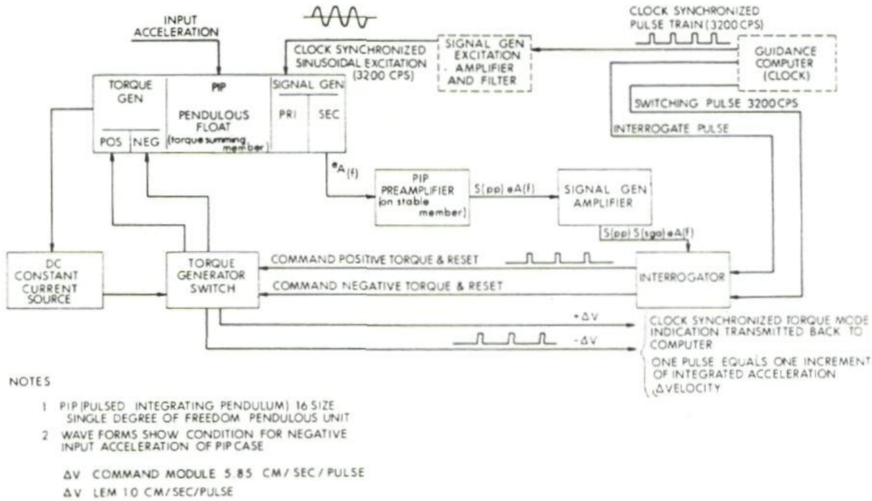

FIG. 4–16 PIP accelerometer block diagram

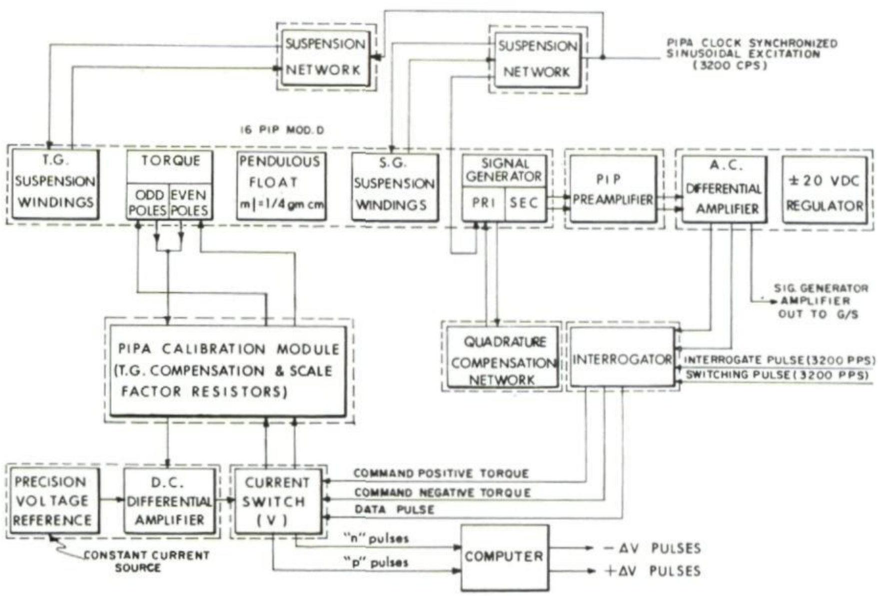

FIG. 4–17 PIP accelerometer module block diagram

Considering the float storage and initial conditions for the accelerometer as an error (velocity stored, V_s):

$$V_s = \int_o^t M_{tg}\, dt + ml\, V_{IA}$$

$$ml\, V_{IA} - V_s = -\int_o^t M_{tg}\, dt \qquad \text{(Eq. 4–2)}$$

Since M_{tg} is controlled to be constant and permitted to change sign only at discrete times (ΔT) the integral may be replaced by summation:

$$ml\, V_{IA} - V_s = -\sum_o^{n+p} M_{tg}\, \Delta T = \Delta T\, M_{tg}\, (n-p) \qquad \text{(Eq. 4–3)}$$

where n = number of negative torque commands
p = number of positive torque commands

Neglecting for the moment V_s:

$$V_{IA} = \frac{M_{tg}}{ml}\, \Delta T\, (n-p) \qquad \text{(Eq. 4–4)}$$

The accelerometer scale factor (SF) is then $\dfrac{M_{tg}\, \Delta T}{ml}$ per pulse and the integrated acceleration or velocity increment per pulse is the scale factor. The net velocity is the net number of minus and plus torque commands, $(n-p)$ sign considered, times the scale factor.

The torque is constantly applied and only switched in direction. The system then behaves as a relay system with a delay due to sampling but no hysteresis. The system limit cycles and the limit cycle behavior is of importance near zero input acceleration as the stored velocity is a function of the magnitude of the limit cycle. The dynamic behaviour may be described by collecting together all linear elements (the pendulum, amplifiers, signal generators, etc) as $G\,(s)$ and the switching of torque as a relay either at $+1$ or -1 together with the sampler as $N\,(s)$. (See Fig. 4–19.)

$$\frac{O}{I} = \frac{G\,(s)\, N\,(s)}{1 + G\,(s)\, N\,(s)}$$

This loop will oscillate when:

$$1 + G\,(s)\, N\,(s) = O$$

or:

$$G\,(s) = -\frac{1}{N\,(s)}$$

Consider for an example only the dynamics of the inertial component as the linear plant:

$$G\,(s) = \frac{K}{s\,(1 + \frac{Js}{G})} \qquad \text{(Eq. 4–5)}$$

The non-linear element, the switch, may be treated using the describing

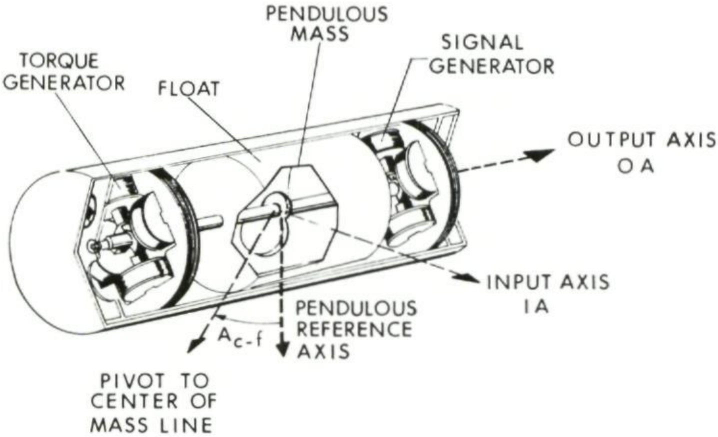

FIG. 4–18 Pulsed integrating pendulum schematic

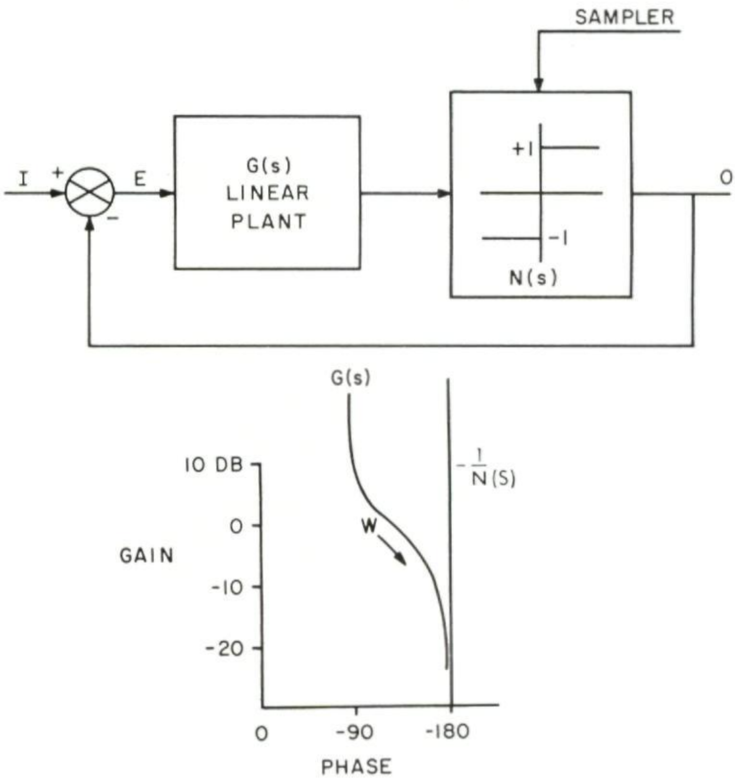

FIG. 4–19 Relay control system

function technique (3). The gain-phase plot of these two functions $G(s)$ and $\frac{-1}{N(s)}$ is shown in Fig. 4–20. The intersection of $G(s)$ and $\frac{-1}{N(s)}$ would indicate that oscillations would exist at infinite frequency of zero amplitude. This however neglects the phase delay due to sampling. While the phase delay due to sampling may be introduced on the gain phase plot it is equally valid to introduce it on the phase plot alone. The limit cycle oscillation is constrained by the interrogator to have a period of integral multiples of the clock time, ΔT. The stored velocity, V_s, is proportional to the magnitude of the limit cycle and it is therefore, desirable to have it small. The phase delay due to the sampler is $\frac{2\pi}{n}$ where n is the number of ΔT's per cycle in the limit cycle. The addition of the phase delay to $G(s)$ shows intersections with $\frac{-1}{N(s)}$ and thus satisfies the conditions for $G(s) = \frac{-1}{N(s)}$. The moding or limit cycle may be described as 1:1 where there is one sampling pulse per half cycle. A $n{:}n$ mode is where there are n sampling pulses per half cycle. The phase delays are shown as lines of phase shift at frequency $w = \frac{\pi}{n \Delta T}$. The illustrated graph shows as possible limit cycles either the 1:1 or 2:2 mode, and it is impossible to have a 3:3 or higher mode limit cycle operation.

It is possible here to decrease the moding by decreasing the ratio of J/C. For a physical instrument the value of J is fairly firmly established and not much alteration is possible. However, a fairly wide viscosity range of damping fluid is possible. This would seem to indicate that increasing the damping would reduce the limit cycle to its lowest mode. Such is usually the case; however, one must now consider the signal-to-noise ratio of the instrument. As the damping increases the float motion decreases. It becomes then a question of the smallest detectable float angle. That is to say what is the minimum angle from null at which you can positively identify the float as positive or negative.

From previously, $V_s = J\dot{A}_{c-f} + CA_{c-f} +$ initial conditions. Assuming initial conditions are zero and near null the minimum angle of detection is $A_{c-f} = A_m$. At this point the damping torque is much greater than the inertia reaction torque therefore:

$$\dot{A}_{c-f} = \frac{M_{tg}}{C} \qquad \text{(Eq. 4–6)}$$

$$V_s = \frac{J}{C} M_{tg} + C\,A_m \qquad \text{(Eq. 4–7)}$$

The damping for minimum stored velocity is:

$$C = \sqrt{\frac{J\,M_{tg}}{A_m}} \qquad \text{(Eq. 4–8)}$$

This relationship is heuristically correct in that a smaller detectable angle (higher signal-to-noise ratio) will permit increased damping, while decreasing J will reduce the float time constant. Increasing torque, M_{tg} will, in the same time interval, increase float angle equivalent to reducing A_m.

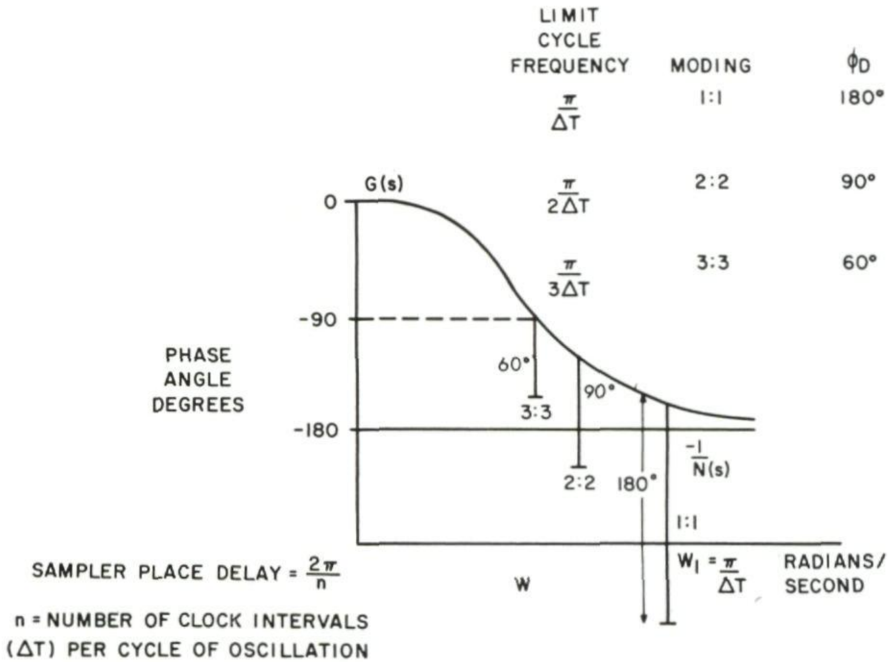

FIG. 4–20 PIPA limit cycle

FIG. 4–21 16 pulsed integrating pendulum, Mod. D

PIP – The physical inertial component, the pendulum (PIP), is a single-degree-of-freedom pendulum. The pendulum is floated both to reduce friction uncertainty and to provide damping about all three axes. The output axis damping is to provide good dynamic behavior while the damping about the other axes is to provide geometrical stabilization of the float with respect to the case. This is necessary to assure stability of performance. There is an electromagnetic suspension system called ducosyn to provide both axial and radial centering forces to additionally stabilize the float with respect to the case. The float is a hollow cylindrical beryllium piece with ferrite rotors cemented on each end. There is a pivot shaft used for axial and radial stops of the suspension system. The pendulosity, $\frac{1}{4}$ gm cm, is adjusted by a pin and screw which also serve as the output axis stop limiting rotation of A_{c-f} to less than $\pm 1°$. On a diameter perpendicular to the pendulous axis are two screws used to achieve flotation.

Surrounding the float is the damping block. The damping fluid and the clearances between the float and the case set the damping to about 120 000 dyne cm/radian/second. Located in the damping block are four bellows for volume compensation. On each end is the end housing which has the electromagnetic syspension system on the inner rotor and the signal generator or torque generator on the outer rotor. The rotor itself is a one piece device. The torque generator is an eight pole device with windings on the even poles for negative torque and on the odd poles for positive torque. The torque is proportional by the sensitivity of the torque generator, S_{tg}, and to the square of the current. The damping fluid is the only mechanical connection between the float and the case. This has made a pendulum with a friction uncertainty level of less than 0.02 dyne centimeters when only the suspensions and signal generator are excited. The float inertia about the pivot as output axis is approximately 14 gm/cm². The float time constant, J/C, is about 100 microseconds. The pendulum time constant for the float with the input reference axis and output axis perpendicular to gravity is eight minutes.

The signal generator is an eight pole device with limitations identical to those of the torque generator. It uses a primary excitation and a differential center tapped secondary. The signal generator is resistive and capacitive tuned for a second order system damping ratio of nearly unity and natural frequency slightly greater than the carrier frequency. This prevents excessive phase delays of the signal generator from affecting the moding and yet reduces high frequency noise generated and picked up in the signal generator.

The effects of an elastic restraint, K, may be seen by considering the basic equation:

$$J\,\ddot{A}_{I-f} + C\,\dot{A}_{c-f} + K\,A_{c-f} = M_{tg} + ml\,a_{IA} \qquad \text{(Eq. 4–9)}$$

K = elastic restraint coefficient

for the average values of the angle $\bar{A}_{c-f}$. This eliminates the limit cycle when considering small inputs:

$$J\,\ddot{\bar{A}}_{c-f} + C\,\dot{\bar{A}}_{c-f} + K\,\bar{A}_{c-f} = ml\,a_{IA} \qquad \text{(Eq. 4–10)}$$

Considering the inertia reaction torque small with respect to the damping torque and elastic restraint torque:

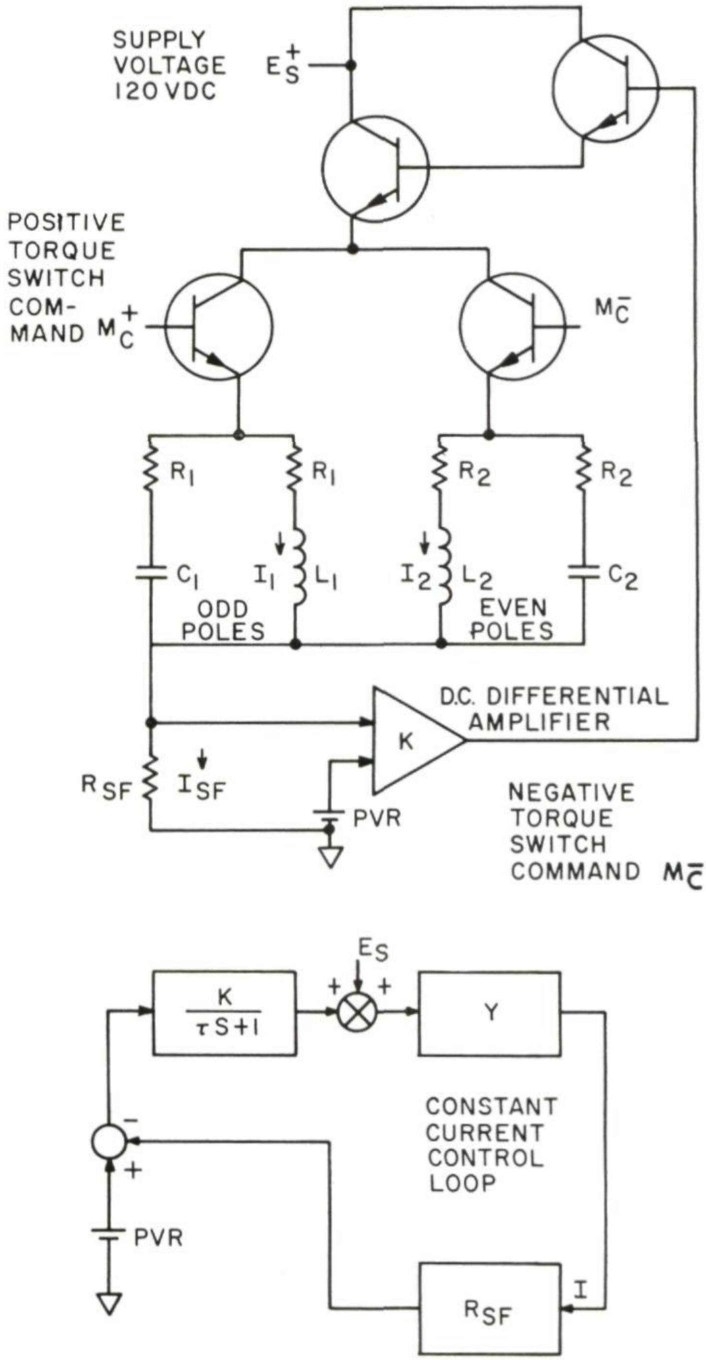

FIG. 4-22 Current control and current switch

$$C\,\dot{\bar{A}}_{c-f} + K\,\bar{A}_{c-f} = ml\,a_{IA}$$

$$\bar{A}_{c-f} = \frac{ml\,a_{IA}}{K}\left[1 - e^{-\frac{Kt}{C}}\right] \qquad \text{(Eq. 4–11)}$$

This is to say a finite positive K reduces the average angle through which the float will rotate. Any elastic restraint will alter the time at which an output, ΔV, will be indicated. A positive K will increase the apparent integration time and a negative K will decrease the apparent integration time. The limiting positive K case shows an interesting concept. Consider that there is corresponding to a ΔV an equivalent average float angle ΔA.

$$\Delta\dot{A} = A\,\Delta T = \frac{M_{tg}}{C}\,\Delta t \qquad \text{(Eq. 4–12)}$$

For a steady state case as $t \longrightarrow \infty$:

$A_{c-f} = \Delta A$ as a necessary condition for integrating an input acceleration

$$\frac{ml\,a_{IA}}{K} = \frac{M_{tg}}{C}\,\Delta T$$

or:

$$K = \frac{ml\,a_{IA}}{M\,\Delta T}\,C = \frac{C\,a_{IA}}{\Delta V} \qquad \text{(Eq. 4–13)}$$

This shows the minimum detectable input acceleration under conditions of a finite elastic restraint. Furthermore, this shows that increasing C reduces the effect of elastic restraint. We again return to the criteria of the minimum detectable angle A_m. For the optimum damping:

$$K \leqq \frac{a_{IA}\,ml}{\Delta T}\sqrt{\frac{J}{A_m\,M_{tg}}} = \frac{a_{IA}}{\Delta V}\sqrt{\frac{J\,M_{tg}}{A_m}} \qquad \text{(Eq. 4–14)}$$

Refer to Fig. 4–22. The torque generator flats to create a pseudo-salient pole are not just a single planar surface. There are multiple planar surfaces near the cylindrical rotor portion designed to reduce the elastic restraint to a negligibly small value. The accelerometer itself is the best means of measuring the elastic restraint coefficient. The minimum detectable acceleration is below 0.05 cm/sec^2.

Scale Factor and Bias – The constant current loop with the reference and switching is shown in Fig. 4–23. A d.c. differential amplifier compares the voltage drop across a scale factor resistor with that of a precision voltage reference. The torque generator of the PIP is a V connected microsyn torque generator. Torque is developed proportional to the difference of the squares of the current in odd poles and even poles. Switching of current is controlled by appropriate drive voltages to the basis of the switch transistors for $M_{\underline{c}}^{+}$ or $M_{\underline{c}}^{-}$. The network of resistances and capacitance associated with each torque are chosen to make the impedance of the switched network resistive. That is to say $\frac{L_1}{R_1} = R_1C_1$. This, for the amplifier, has the output impedance always resistive. As will be shown later, it is desirable to have the voltage across the compensated windings as high as possible to reduce the current

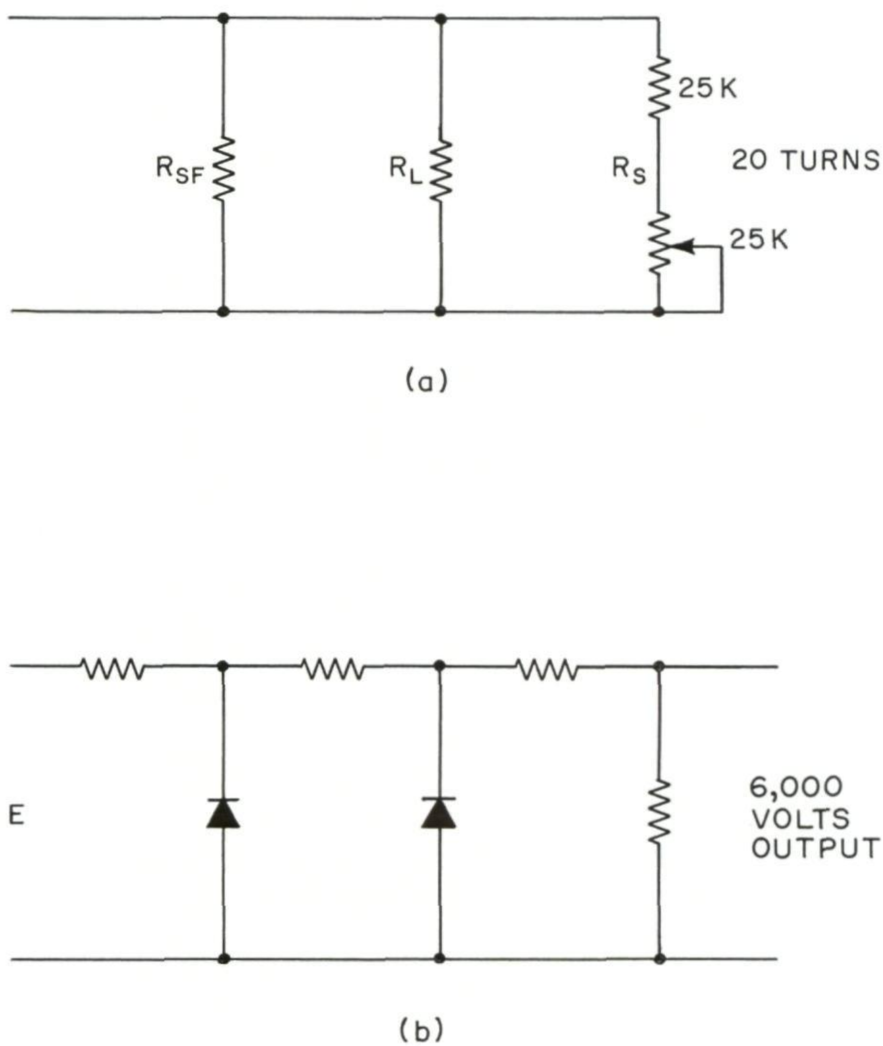

FIG. 4–23 Precision voltage reference, circuit diagram

rise time. However, the upper limit is controlled by the breakdown voltage of transistors used in this switching application. The amplifier gain is chosen to reduce the effects of supply voltage disturbances to acceptable limits. The dynamic response of the amplifier is chosen to reduce the current squared effects due to supply voltage changes to an acceptable value:

$$\frac{I}{E} = \frac{\dfrac{\Upsilon}{\Upsilon R_{SF} K}}{\tau s + 1} + 1 \qquad \text{(Eq. 4–15)}$$

For a change of E_s of 10% or 12 volts the gain, $K = 200\,000$, is determined such that the current changes are less than 10 ppm. Dynamic response of the control loop, principally controlled by the amplifier, is set to minimize current transients. Loop compensation is required for stability and also to control current transients due to switching. The current rise time for the current in the torque generator (I_1, I_2) is desired to be as small as possible. The amplifier drive impedance is tuned to be resistive to minimize current transients. Thus the torque generator impedance is tuned to be resistive with the addition of a resistor and capacitor. The current rise time, L_1/R_1 is then controlled by R_1, since L_1 is controlled by the torque generator. The current requirement, I_{SF}, is determined from the scale factor requirement and the torque generator sensitivity. This leaves only the supply voltage, E_S, as the variable for R_1 determination. The desire to increase R_1 is then determined as a compromise between the desire to increase R_1 and the limitation of E_S for voltage breakdown reasons, V_{CE}, of the current control transistors. Based upon the current state of the art for reliable producible transistors 120 volts was chosen as a suitable compromise. In the steady state case this leaves about 80 volts across C_1 or C_2.

The stability of the current loop is determined by two other important items, the scale factor resistor and the voltage reference, called Precision Voltage Reference, PVR. Precision resistors with low temperature coefficients are commercially available. The method used for setting the desired conductance is to normalize all PVR's to a particular value, 6 000 volts, and then adjust two fixed values R_L and R_{SF} with the ratio $\frac{R_L}{R_{SF}}$ between 100 and 1 300. (See Fig. 4–23a.)

With this method precision adjustment is possible by the use of the potentiometer. Resistance stability is generally better than 3 ppm/year with temperature coefficients of less than 3 ppm/C° deviation.

The Precision Voltage Reference is a cascaded zener diode voltage source. (See Fig. 4–23b.)

The second stage is chosen for a voltage where the temperature coefficient of the diode is nearly zero. This is slightly greater than 6 volts, which is the point at which the temperature coefficient changes sign. The resistor divider network on the output is the normalization of the PVR to 6 000 volts. Voltage deviations of the PVR are less than 10 ppm/year with changes due to temperature less than 3 ppm/C°. This then forms the major portion of the constant current loop.

As in any accelerometer the stability of parameters in one of the most important considerations. From previously:

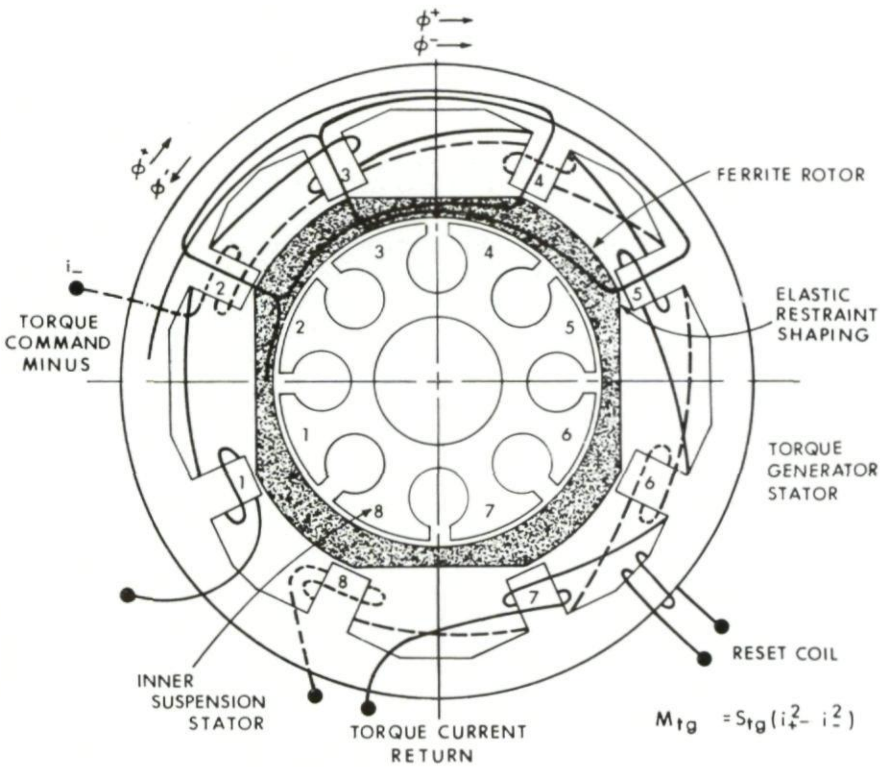

FIG. 4–24 Apollo 16 PIP Mod. D torque generator schematic diagram

$$SF = \frac{S_{tg}\, i^2\, \Delta T}{ml}$$

$$dSF = \frac{\delta SF}{\delta S_{tg}} dS_{tg} + \frac{\delta SF}{\delta i} di + \frac{\delta SF}{\delta \Delta T} + \frac{\delta SF\, d\, ml}{\delta\, ml} \qquad \text{(Eq. 4-16)}$$

$$\frac{dSF}{SF} = \frac{dS_{tg}}{S_{tg}} + \frac{2\, di}{i} + \frac{d\Delta T}{\Delta T} - \frac{d\, ml}{ml}$$

This is the fundamental relation describing stability of the scale factor. Mechanization is required to minimize these changes. The pendulosity is very stable. The current control has been previously described to minimize $\frac{di}{i}$. A single computer pulse train is used for switching the torque. As a precaution against any modulation of the switching pulse amplitude and the resulting timing changes a second pulse train, the interrogration pulse, preceding the switching pulse, is used to set the state of the gates to allow switching with the switch pulse. This eliminates any apparent elastic restraint effects which might result from summing the float angle information with the switching pulse.

The primary scale factor stability parameter is the torque generator sensitivity. The torque generator sensitivity is proportional to the permeability and inversely proportional to the gap. The gap is controlled by the magnetic suspension system with radial force restraints of 11.6 n/mm and about 1/20 this stiffness for the axial restraint.

The stabilization of the permeability requires a number of things. First a review of the torque generator will show that at the stator locations between poles there are alternate locations of d.c. and a.c. flux. These d.c. flux regions are locations where memory can be maintained. This memory may be erased by the reset coil which has an a.c. flux in the back iron of the stator. The rotor memory is erased by the suspension system through the one piece rotor.

The quality of any accelerometer is determined by its performance stability. The bias, a_b, of the accelerometer (output with no input) and its stability has another relationship. The torque generator is compensated to be resistive. Upon switching, the current in one winding decays exponentially while it rises exponentially in the other winding. The torque is proportional to the difference of the square of the current.

$$M_{tg} = S_{tg}\,(i_1^2 - i_2^2)$$

If M_{tg} is integrated over one limit cycle period and averaged the bias due to the torque generator is obtained.

$$M_{avg} = \frac{1}{2n\,\Delta T} \int_0^{2n\,\Delta T} S_{tg}\,(i_1^2 - i_2^2)\, dt = ml\, a_b$$

Thus bias acceleration, a_b, is proportional to difference to the current rise time.

$$a_b = \frac{\Delta V}{\Delta T} \frac{\tau_2 - \tau_1}{2n\,\Delta T} \qquad \text{(Eq. 4-17)}$$

It is important to have these two times identical or the bias would be a function of the period $2n\,\Delta T$. The accelerometer itself is the best instrument to use to adjust these two rise times to be identical. By introducing a phase delay (decreasing the damping for example) the moding may be altered. Then the change in bias is proportional to the current time constant differences.

The other parameter of primary significance in an accelerometer is the alignment and stability of the input axis. The mounting flange can be seen on the view of the pendulum. On that flange is a slot. The surface of the flange and the slot then form the reference alignment directions. The stable member contains the mounting surface and pin with the proper tolerances. The input axis is aligned about the output axis by rotating the PIP with respect to the slot. The mounting flange contains two rings which have mating spherical surfaces. Alignment of the input axis about the pendulous reference axis is obtained by sliding between these surfaces. The two rotations are uncoupled for small rotations. The pendulum is thus prealigned prior to its assembly into the IMU. Like the gyro it also contains a module of the necessary suspension capacitors and other normalizing components. For alignment reasons this module fastens into the stable member and not the pendulum.

CHAPTER 4–3

THE COUPLING DATA UNIT (CDU)

The Coupling Data Unit provides the central angle junction box between the IMU, Optics, Computer and certain portions of the spacecraft analog electrical interfaces. There are three basic portions of the CDU. They are the angle read system or analog to digital conversion process, the digital to analog conversion process, and a portion of the moding controls for the guidance system The analog to digital system will be covered in some detail and other portions only mentioned.

Analog to Digital Conversion – Angle information is stored in a two speed resolver system of a control member, for example a gimbal axis or an optical axis see Fig. 4–25. The output of the resolver is proportional to sin θ, cos θ, sin $\eta\theta$, cos $\eta\theta$, where η is a binary number. It is a common technique to have both the single speed and multiple speed resolver use the same iron and utilize a single excitation winding. The second excitation winding space, phased 90° with respect to the primary excitation, is used for electrical zero adjustment. The elements of the angle read system are an analog multiplication of the resolver output, an analog summation, a sampler and quantizer, a storage counter to control the analog multiplication and a.c. switches controlled by the counter to gate inputs to the analog multipliers.

The equation mechanized is:

$$\sin\theta\cos\psi - \cos\theta\sin\psi = \sin(\theta-\psi) \qquad \text{(Eq. 4–18)}$$

$$\cos\theta\cos\psi + \sin\theta\sin\psi = \cos(\theta-\psi) \qquad \text{(Eq. 4–19)}$$

Where ψ is a quantized angle in increments of $11\frac{1}{4}$ electrical degrees, and

θ is the angle of the control member

As shown in Fig. 4–26 this output is summed with a quantized linear interpolation of difference between sin $(\theta-\psi)$ and θ. The selection of the quantized angle ψ and the quantized linear interpolation angle ϕ, is based upon the contents of an angle counter register. The angle counter inputs are gated by the phase of the summed voltages. Thus when the contents of the counter are equal to the control member angle:

$$\sin(\theta-\psi) + K\cos(\theta-\psi) = 0 \qquad \text{(Eq. 4–20)}$$

The inputs to the counter are angle increments of the control member and these are parallel fed to the computer where the same control member angle information is stored.

Analog multiplication of the resolver sin θ and cos θ voltage is accomplished by the use of an a.c. operational amplifier with the ratio of the feedback resistor to the input resistor equal to the cosine of the angle ψ_1. S is an a.c. transistorized switch gated closed or open by contents of the angle counter resistor. The switch is in series with the feedback resistor to take

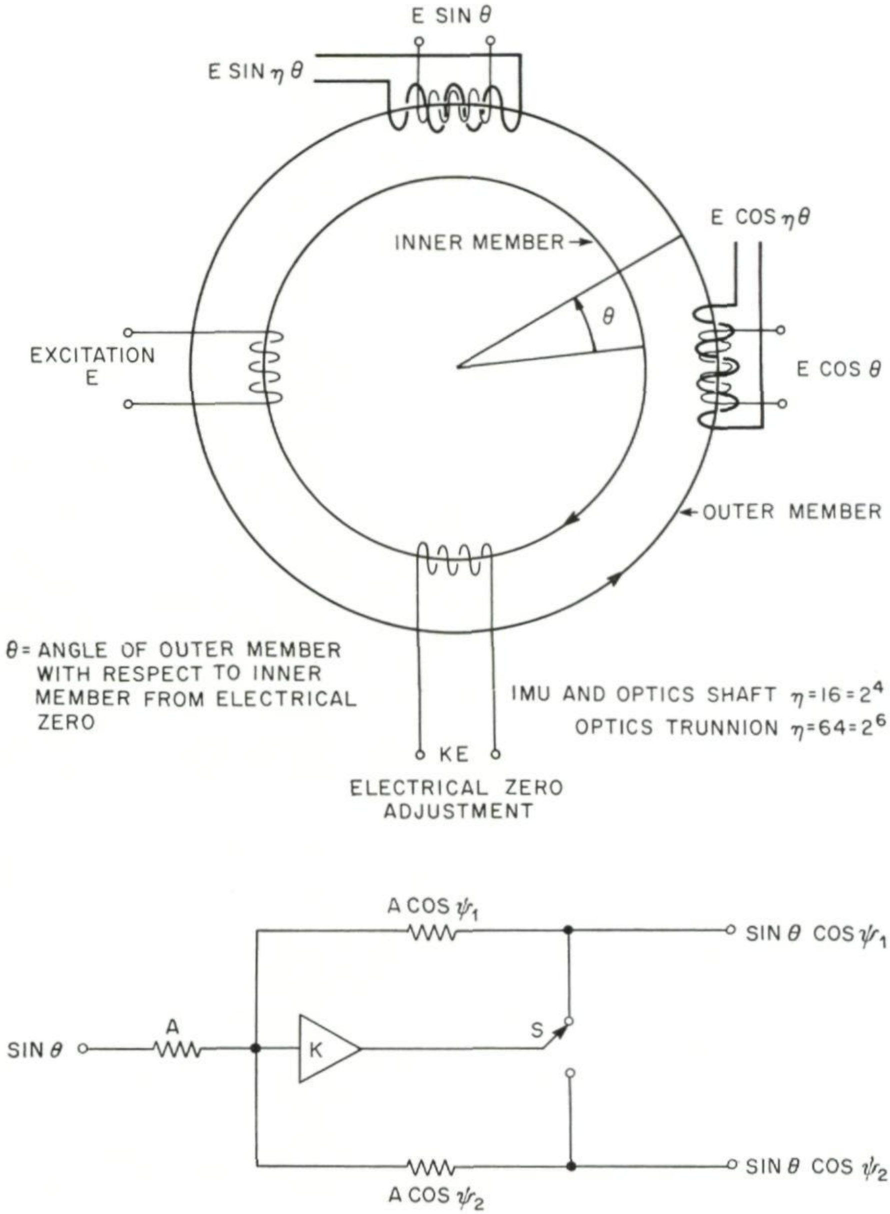

FIG. 4–25 Resolver schematic

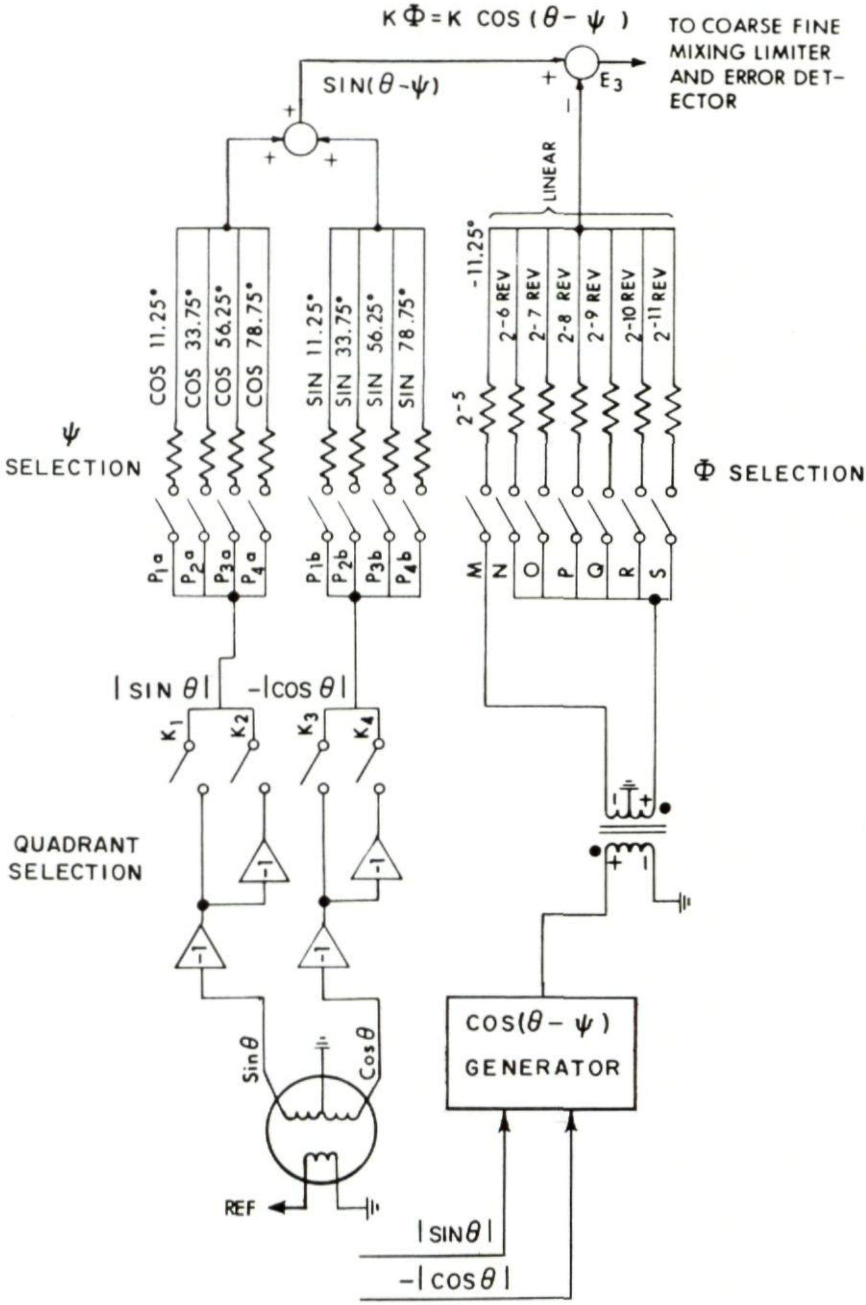

NOTE (2^{-11} REV = $\widehat{10.5}$ min FOR 16 SPEED RESOLVER = $\widehat{39.6}$ sec OF GIMBAL ANGLE)

FIG. 4–26 Selection logic–16 speed resolver digitizing loop

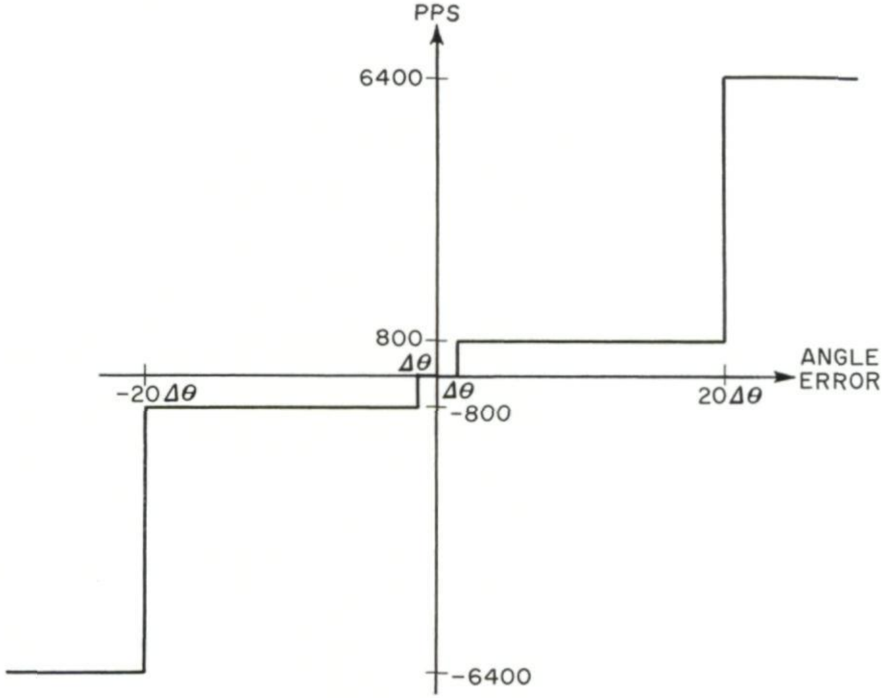

FIG. 4–27a Angle error/PPS: error detector

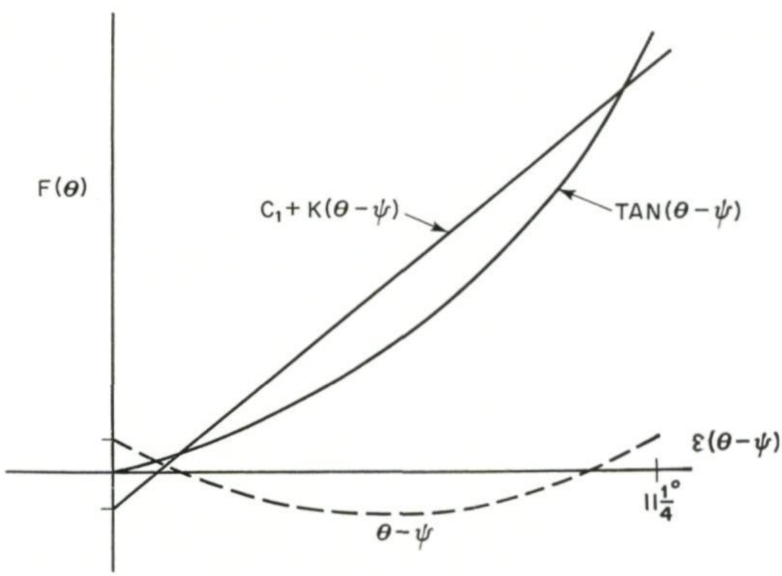

FIG. 4–27b θ–ψ/F(θ): speed resolver error

advantage of the high impedance open condition and low impedance closed condition which makes the impedance equivalent to a portion of the amplifier gain, K. Since the switch is effectively a single pole double throw switch the output of the open side differs from zero only by the input signal divided by the amplifier gain. Using the technique of transistorized a.c. switches and operational amplifiers the read system is mechanized. The read counter contains 16 bits. The lowest order bit is used to eliminate transmitting any limit cycle operation to the computer and thus creating unnecessary activity. The four highest order bits are used for quadrant selection and multiplication of the single speed resolver (ψ_1). In addition, the bits $2^9 - 2^{12}$ are used as an approximate linear interpolation of the single speed resolver to within 2.81° of the actual angle. The multiple speed resolver (sixteen speed) is the precision angle transmitting device. The zero-to-peak errors of this resolver are less than 20 seconds of arc. There is crossover between the sixteen speed and the single speed resolvers to assure synchronization of the reading of the sixteen speed resolver within the proper cycle. The lowest order bits are a linear interpolation of error using the voltage of the cos $(\theta-\psi)$ as a source. This voltage has the same phase relation as the sin $(\theta-\psi)$ of the sixteen speed resolver and is scaled correctly by the resolver attenuation.

Referring to Fig. 4–27 the input to the error detector is the sum of the single speed multiplication, the sixteen speed multiplication and the linear interpolation. There is a coarse-fine mixing network to assure synchronization and angle measurement using the precision resolver. The error detector contains an active feedback quadrature rejector network which for large error signals will not introduce dynamic errors for reading the angle, but for small errors will yield the proper precision. The output of the error detector is fed to both the rate selection logic and up-down counter logic. The contents of the counter are used to control the a.c. switches for the multiplication of the resolver voltages and the linear interpolator.

The error detector has three-state or ternary logic. The lowest order pulse rate command to the counter is 800 pulses per second. Using this as the lowest order assures switching of equal multiples of the resolver carrier frequency of 800 cps. This prevents rectification of the switched signal and altering of the dynamic operation of the read system.

The high speed rate following command reduces dynamic error for high angular velocity inputs and the low speed command rate reduces the limit cycle error.

The linear interpolation constant K is adjusted to minimize the peak error:

$$E = \sin(\theta-\psi) - K\cos(\theta-\psi) \qquad \text{(Eq. 4–21)}$$

By suitably choosing K the error for the speed resolver system can be reduced to less than 10 sec arc. For a 64 speed system as used on the optics trunnion this error is reduced to less than 3 sec arc.

In addition, a bias is added to further reduce the errors over the entire range of linear interpolation. This results in a system whose errors are within the predicted errors.

All digital functions including the memory are mechanized with the three input NOR gate, a silicon semiconductor micro-integrated circuit. This is the same element used in the computer. Direct coupled transistorized logic is

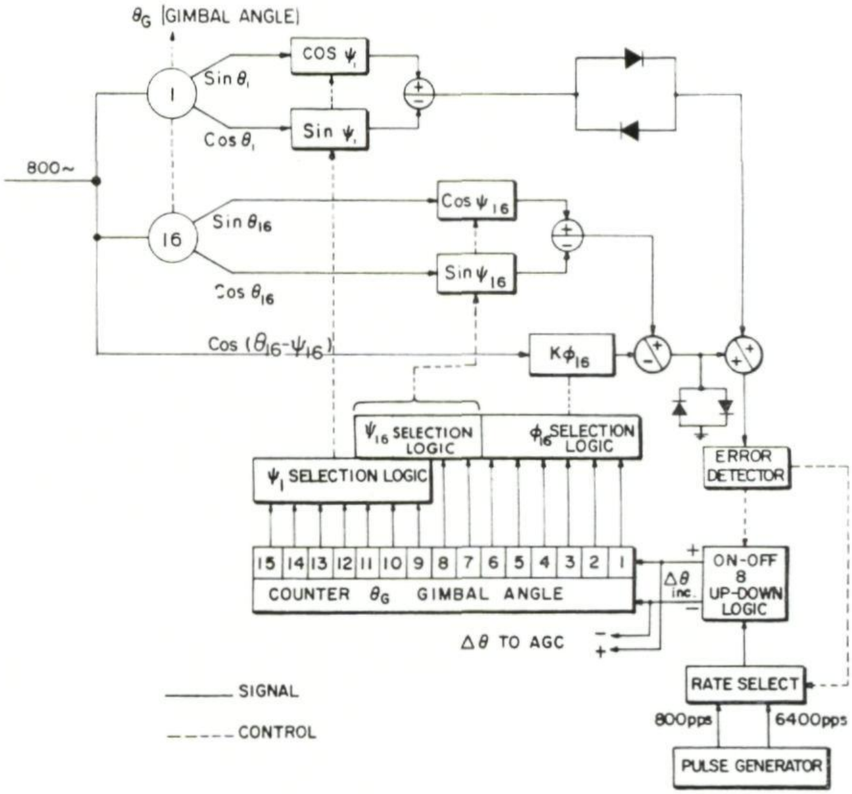

FIG. 4–28 Coarse-fine mixing (1 and 16 speed resolver)

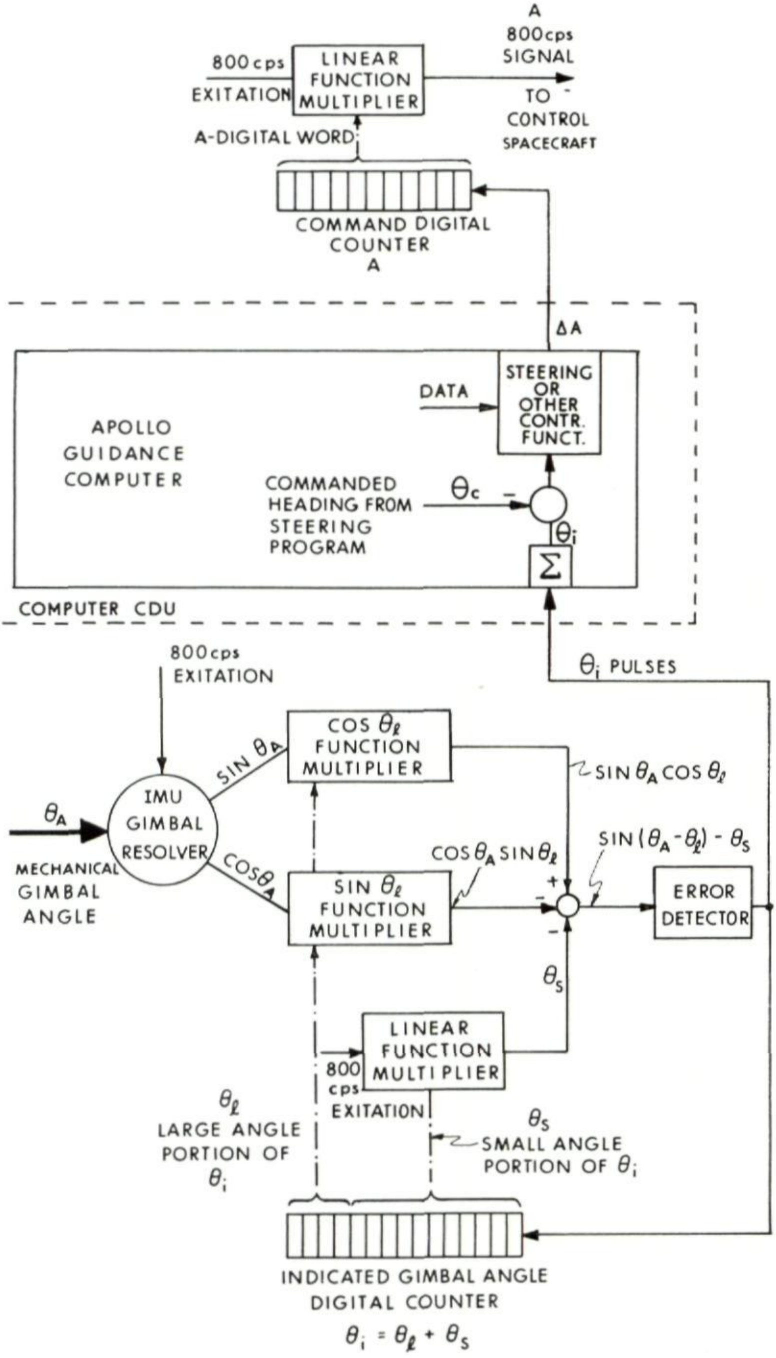

FIG. 4–29 Electronic coupling data unit, schematic

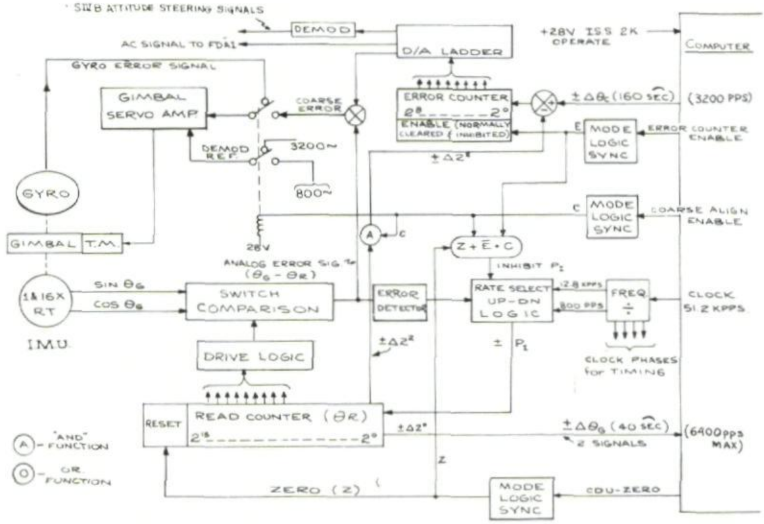

FIG. 4–30 IMU-CDU moding

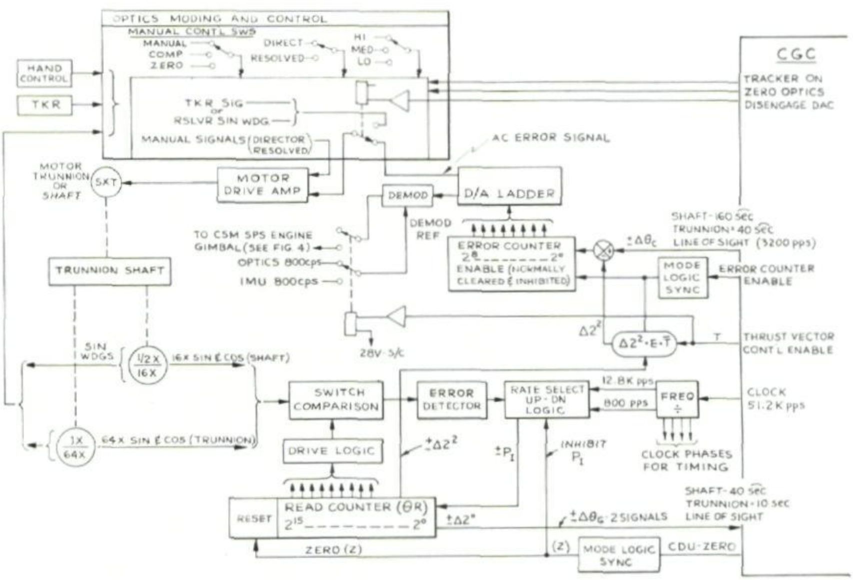

FIG. 4–31 Optics – CDU moding (CSM only)

used throughout. A multiple phase clock system, generated within the CDU and synchronized to the guidance computer, is used to control all functions.

Moding and Digital to Analog Conversion – The guidance computer serves as the important link between the spacecraft and the sensing device. All angle transformations are made by the guidance computer based upon IMU gimbal angles or optics angles. For any steering function utilizing the IMU the computer, through the use of knowledge of the gimbal angles, provides steering and attitude commands to the spacecraft via the digital to analog converter. The angle information is always stored in the resolvers and no mechanical rezeroing of the IMU is necessary to establish, within the counter, the IMU gimbal angle within the uncertainty of the resolver, the error of the read system and the bit size of the analog to digital converter.

The digital to analog converter system is required to accept digital commands from the guidance computer and generate analog voltages (a.c. and d.c.) proportional to these commands. The error angle counter is an eight bit up-down counter. Computer commands are stored in this counter. The counter is logically controlled to prevent it from being reset to zero in the event it is commanded to more than 2^8 increments. The analog error signals are developed by an 800 cps source gated by the counter contents through a resistance ladder to the input of an operational amplifier. Polarity reversal by switching is used to command the 0 phase or π phase 800 cps input to the ladder. All analog voltages used as steering commands to the LEM, spacecraft or other portions of the Apollo launch vehicle are d.c. isolated from the guidance system either by transformers or an isolated demodulator.

The moding of the system is almost entirely controlled by the computer. Provision is made for two modes to be controlled by the astronaut. One mode is the cage function. In the event of a spacecraft tumble and loss of attitude, provision is made for the astronaut to cage the IMU gimbals with respect to the spacecraft after he has first stabilized the craft. This then gives him a means of obtaining a new reference in a very short time. The other manual mode is similar in that with the computer not operating he can use the same switch to cage the IMU with respect to the spacecraft, release it, and again use the IMU as an attitude reference.

All other moding is controlled by the computer as can be seen from Fig. 4–30 for the IMU. Optics moding has more manual control and is shown in Fig. 4–31. This moding will be described elsewhere. There are a number of interesting modes possible because of the flexibility of the CDU. The Coarse Align Mode, that of commanding the IMU gimbal angles by the resolvers, is rate controlled to limit angular velocity input to the gyroscopes. The input to the error detector is summed with the analog command from the computer to provide stable operation. The gimbal angle pulse increments from the read system are used as feedback pulse to the error angle counter.

REFERENCES

1. Draper, C. S., Wrigley, W., and Grohe, L. R., "The Floating Integrating Gyro and Its Application to Geometrical Stabilization Problems on Moving Bases", Institute of the Aeronautical Sciences Preprint 503, presented January 25, 1955.
2. Gilinson, Jr. P. J., Denhard, W. G., and Frasier, R. H., "A Magnetic Support for Floated Inertial Instruments". Report No. R-277 Instrumentation Laboratory, M.I.T., Cambridge, Massachusetts, April 1960.
3. Wiener, T. F., "Theoretical Analysis of Gimballess Inertial Reference Equipment Using Delta-Modulated Instruments", M.I.T., Cambridge, Massachusetts, Sc.D. Thesis.

ACKNOWLEDGEMENTS

Hickey, E. S., M.I.T. Instrumentation Laboratory.
Sitomer, J. L., M.I.T. Instrumentation Laboratory.
Crisp, R., M.I.T. Instrumentation Laboratory.
Cushman, G., M.I.T. Instrumentation Laboratory.

PART 5

OPTICAL MEASUREMENTS AND NAVIGATION PHENOMENA

D. Alexander Koso

D. ALEXANDER KOSO

D. Alexander Koso, Assistant Director of Instrumentation Laboratory, Massachusetts Institute of Technology, heads the Laboratory group responsible for development of the optical subsystem – space sextant, scanning telescope and the associated electronics – used in the guidance system the Laboratory is developing for the Project Apollo spacecraft.

Mr. Koso was born in Bratislava, Czechoslovakia, March 13, 1935, and came to the United States in 1949. He was graduated from University High School, Minneapolis, Minn., in 1952. He received both the B.S. and M.S. degrees from M.I.T. in Electrical Engineering in 1957 and the degree of Electrical Engineer from M.I.T. in 1959.

While an undergraduate at M.I.T., Mr. Koso studied under the Institute's cooperative plan and was employed by the Philco Corporation. As a graduate student studying for the E.E. degree, he was a research assistant at the M.I.T. Electronic Systems Laboratory. Mr. Koso joined the Instrumentation Laboratory in 1959 and worked a few years on navigation studies for manned boost-glide space vehicles. He was appointed an Assistant Director in 1963.

PART 5

OPTICAL MEASUREMENTS AND NAVIGATION PHENOMENA

INTRODUCTION

During the orbital and midcourse phases of a space mission, inertial components (due to a lack of force) can no longer provide information about the position of the vehicle. The gyroscope can be used to provide an artificial set of fixed stars usable as a basic reference for measurements. However, external sensors have to be used to update the position information within the vehicle.

During the orbital phases of a mission, it is possible to treat the navigational problem with relative ease, because one can write a set of linear constant coefficient equations which describe the propagation of errors with time. Each measurement then provides a linear equation between certain of these errors. In this chapter on-board measurements are considered which can be used to determine the orbit of a satellite.

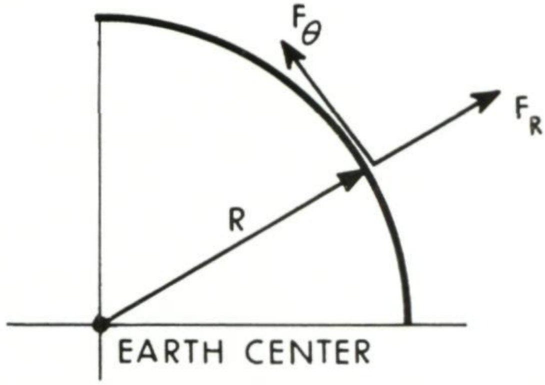

FIG. 5–1 Equations of motion

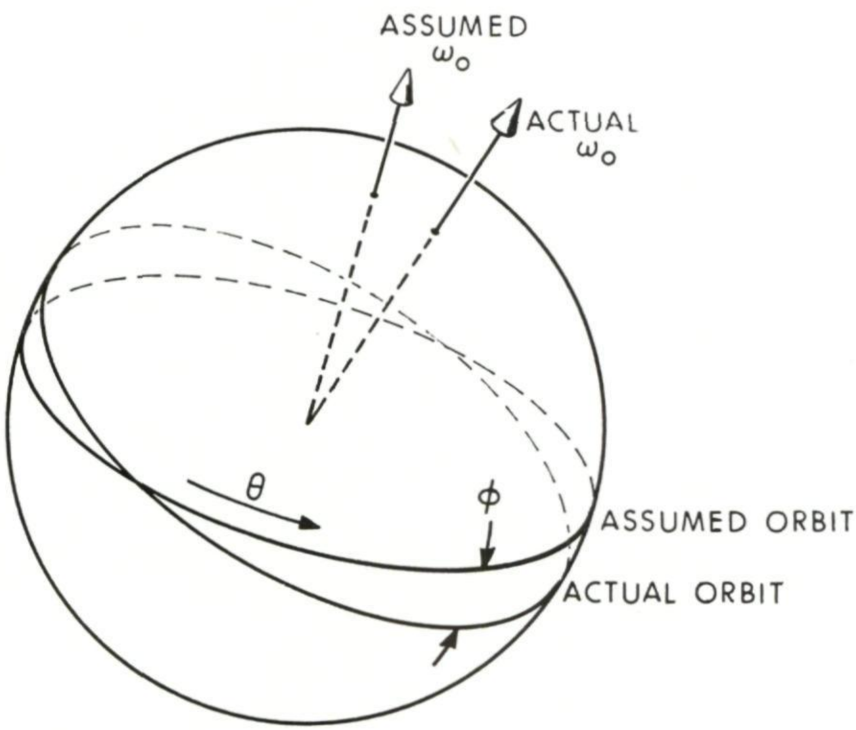

FIG. 5–2 Orbital geometry

CHAPTER 5–1

NAVIGATION IN ORBIT

ERROR PROPAGATION IN ORBIT

The equations of motion in this analysis are written in polar coordinates to make linear approximation of these equations easier. Thus, the equations presented are closer to the equations of a local-vertical system; however, the analysis applies irrespective of the coordinate system used in the actual computation.

The equations of motion in polar coordinates are:

$$\ddot{R} = F_R + R\Omega^2 - E/R^2 \qquad \text{(Eq. 5–1a)}$$

$$R\frac{d^2\theta}{dt^2} = R\Omega = F\theta - 2\dot{R}\Omega \qquad \text{(Eq. 5–1b)}$$

where F_R and F_θ are the forces (per unit mass of the vehicle) in the radial and range direction respectively as illustrated in Fig. 5–1.

For the purpose of analysis, set:

$$R = r_o + r \qquad \text{(Eq. 5–2a)}$$

$$\Omega = \omega_o + \omega \qquad \text{(Eq. 5–2b)}$$

where r_o and ω_o are constants.

Thus:

$$\dot{R} = \dot{r};\ \ddot{R} = \ddot{r};\ \dot{\Omega} = \dot{\omega};\ \theta - \omega_o t = \int_o^t \omega(x)dx$$

One can also assume without loss of generality that:

$$\omega_o^2 = E/r_o^3 \qquad \text{(Eq. 5–3)}$$

If r_o is assumed to be about 300 kilometers above mean earth radius, then for orbits ranging from 150 to 450 kilometers altitude:

$$r/r_o < .02 \qquad \text{(Eq. 5–4)}$$

Similarly:

$$\omega/\omega_o < .05 \qquad \text{(Eq. 5–5)}$$

Thus, the equations of motion can be linearized for satellites confined to nearly circular orbits.

Under the assumption that:

$$E/R^2 = E/r_o^2 - [2E/r_o^3]r \qquad \text{(Eq. 5–6)}$$

Eq. 5–1a and 5–1b can be written as:

$$\ddot{r} = F_R + (r_o + r)(\omega_o^2 + 2\omega_o\omega + \omega^2) - E/r_o^2 + 2E/r_o^3 r \qquad \text{(Eq. 5–7a)}$$

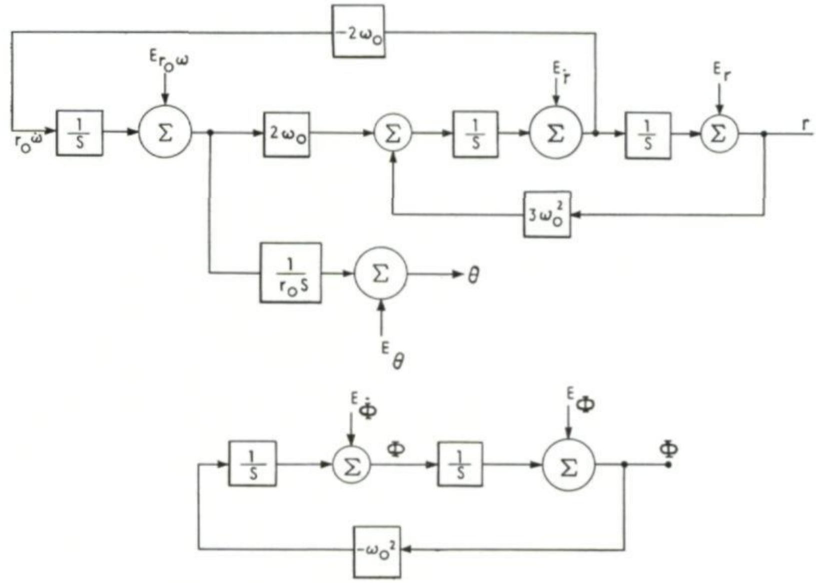

FIG. 5-3 Block diagram of error propagation

Error Source	Range	Range Rate	Altitude	Altitude Rate	Track	Track Rate
E_r	$\frac{6}{r_o}(\sin\omega_o t - \omega_o t)$	$6\omega_o(\cos\omega_o t - 1)$	$3(1 - \cos\omega_o t) + 1$	$3\omega_o \sin\omega_o t$	0	0
$E_{\dot r}$	$\frac{2}{r_o\omega_o}(\cos\omega_o t - 1)$	$-2\sin\omega_o t$	$\frac{1}{\omega_o}\sin\omega_o t$	$\cos\omega_o t$	0	0
E_θ	1	0	0	0	0	0
$E_{r_\theta\omega}$	$\frac{4}{r_o\omega_o}(\sin\omega_o t - \omega_o t) + \frac{1}{r_o}t$	$4(\cos\omega_o t - 1) + 1$	$\frac{2}{\omega_o}(1 - \cos\omega_o t)$	$2\sin\omega_o t$	0	0
E_ϕ	0	0	0	0	$\cos\omega_o t$	$\frac{1}{\omega_o}\sin\omega_o t$
$E_{\dot\phi}$	0	0	0	0	$\omega_o \sin\omega_o t$	$\cos\omega_o t$

TABLE 5-1 Summary of errors due to initial conditions at some time T, after insertion into orbit

$$(r_o+r)\dot{\omega} = F_\theta - 2\dot{r}(\omega_o+\omega) \qquad \text{(Eq. 5–7b)}$$

Substitution of Eq. 5–3 into Eq. 5–7a and Eq. 5–7b gives:

$$\ddot{r} = F_R + 3\omega_o^2 r + 2\omega_o\omega(r_o+r)+(r_o+r)\omega^2 \qquad \text{(Eq. 5–8a)}$$

$$(r_o+r)\dot{\omega} = F_\theta - 2(\omega_o+\omega)r \qquad \text{(Eq. 5–8b)}$$

Using the approximations of Eq. 5–4 and Eq. 5–5:

$$r << r_o;\ \omega << \omega_o$$

Eq. 5–8a and Eq. 5–8b become:

$$\ddot{r} = F_R + 3\omega_o^2 r + 2\omega_o r_o \omega \qquad \text{(Eq. 5–9a)}$$

$$r_o\dot{\omega} = F_\theta - 2\omega_o\dot{r} \qquad \text{(Eq. 5–9b)}$$

Eq. 5–9a and Eq. –59b represent very closely the errors in the position computation of an orbiting vehicle. For relatively short flights, the two force inputs F_R and F_θ are also negligible, so that the major contribution of error is due to the uncertainty in initial conditions at the end of injection into orbit. There is another error which can exist in an orbit determination. This one is due to a lack of knowledge of the exact direction of the ω_o vector (see Fig. 5–2).

If the angular displacement is small, the error in the out of plane position is given by:

$$\Phi = E_\Phi \cos(\omega_o+\omega)t + \frac{E_{\dot{\phi}}}{\omega_o} \sin(\omega_o+\omega)t \qquad \text{(Eq. 5–10)}$$

For relatively small range errors, the ω term can be neglected. From a control viewpoint, the error in the position computation can be represented very closely by the two linear constant-coefficient systems show in Fig. 5–3. One set of equations is fourth order, the other second order. E_Φ is a step input representing the particular initial condition error.

Two conclusions can be drawn from Table 5–1:

Only range error grows with time

There is no error coupling between range and track errors

Generally, depending on the particular problem on hand, the navigation system has to be able to determine the position and velocity errors at some time, T, after injection into orbit. However, since this time T, depends on a specific mission phase only the problem of initial condition determination will be treated here. The actual errors at the specified time, T, can then easily be obtained from the initial condition errors and the expressions of Table 5–1.

POSSIBLE MEASUREMENTS

As can be seen from the block diagram, Fig. 5–3, there are six possible sources of error which have to be considered. The measurements which are taken have to provide some information about the Φ and θ errors. Thus, while a good altimeter can be used to determine $E_{r_o w}$, $E_{\dot{r}}$ and E_r, it cannot provide information about E_θ, E_Φ, and $E_{\dot{\phi}}$. Similarly, a velocity meter, even if it could provide information about E_Φ and $R_{\dot{\phi}}$ in addition to the variables provided for by the altimeter, would provide no information about E_θ.

While most of these considerations are of academic interest on the earth

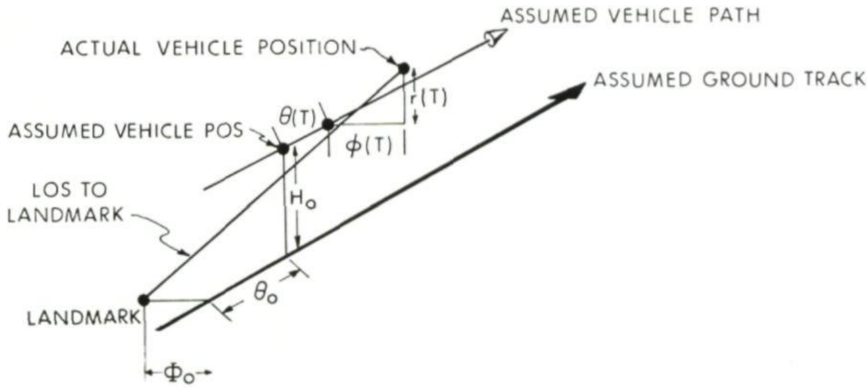

FIG. 5-4 Known landmark measurement geometry

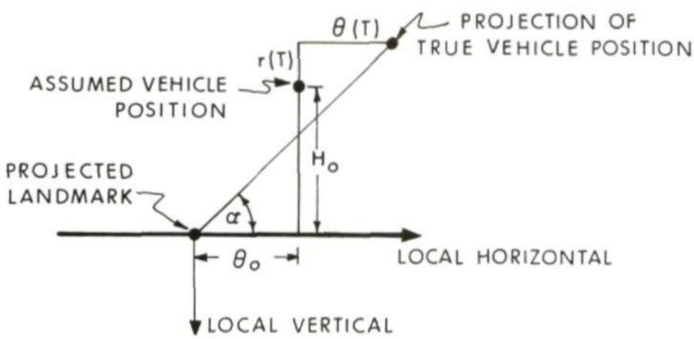

FIG. 5-5 In plane measurement geometry

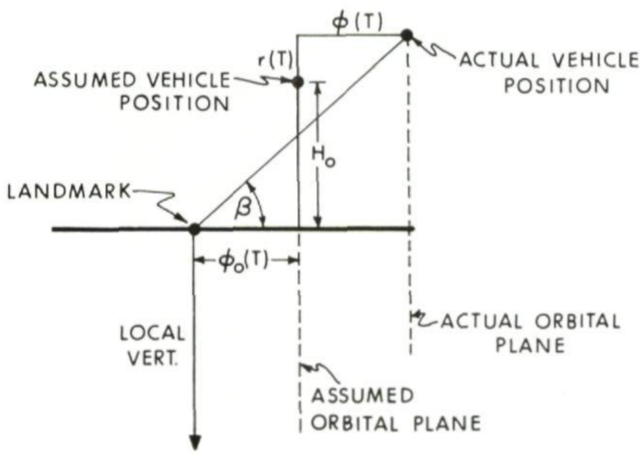

FIG. 5-6 Out of plane measurement geometry

where radar tracking coverage is provided, they do become important during lunar operations, where – especially on the far side of the moon – ground based information is not available. Thus, the following measurements have been considered:

(a) Bearing measurements to known landmarks
(b) Bearing measurements to unknown landmarks
(c) Star occultation measurements
(d) Star horizon measurements
(e) Star known landmark measurements

Measurements of two or three horizons simultaneously were rejected because the lines of sight have to be able to see almost a full hemisphere. This requires a sensor too close to the skin of the vehicle to make this type of a measurement feasible.

In midcourse, where the subtended angle of the planet is smaller, and this measurement becomes feasible from an equipment standpoint, the error sensitivities are so low that the accuracy requirement was deemed not feasible.

While this is not an exhaustive list of possible measurements, it does cover a large variety of applications and it can be instrumented with a relatively simple optical system.

KNOWN LANDMARK BEARING MEASUREMENT

Consider a known point on the earth's surface and an assumed vehicle position as shown in Fig. 5–4. The assumed position of the vehicle at time, T, is at a range $\theta_o(T)$ and $\phi_o(T)$ and an altitude $H_o(T)$ from the known landmark. Now consider a projection of the landmark into the assumed orbital plane as shown in Fig. 5–5. The angle α is the angle between the local horizontal at the landmark, and the projection of the vehicle into the assumed orbital plane.

Figure 5–5 provides the first equation of orbit determination from a bearing measurement to a known landmark:

$$\frac{\theta_o(T) + \theta(T)}{H_o(T) + r(T)} = \cot \alpha \qquad \text{(Eq. 5–11)}$$

Now consider a projection of Fig. 5–4 into a plane which is orthogonal to the assumed orbital plane and which also contains the landmark local vertical as shown in Fig. 5–6.

This measurement provides the second equation of orbit determination:

$$\frac{\Phi_o(T) + \Phi(T)}{H_o(T) + r(T)} = \cot \beta \qquad \text{(Eq. 5–12)}$$

The cotangent has been chosen because $H_o(T) + r(T) > 0$ at all times and the equations are well behaved. Let us assume that a landmark can be tracked when the angle between the local vertical at the landmark and the line of sight is less than 45°. For a 150 kilometer orbit, this means that the landmark can be tracked for a period of less than 40 seconds. The exact amount depends on the distance between the landmark and the ground track of the vehicle.

Consider the time, T_1, when the landmark is first acquired. It is immediately possible to write two equations, Eq. 5–11 and Eq. 5–12, in the three

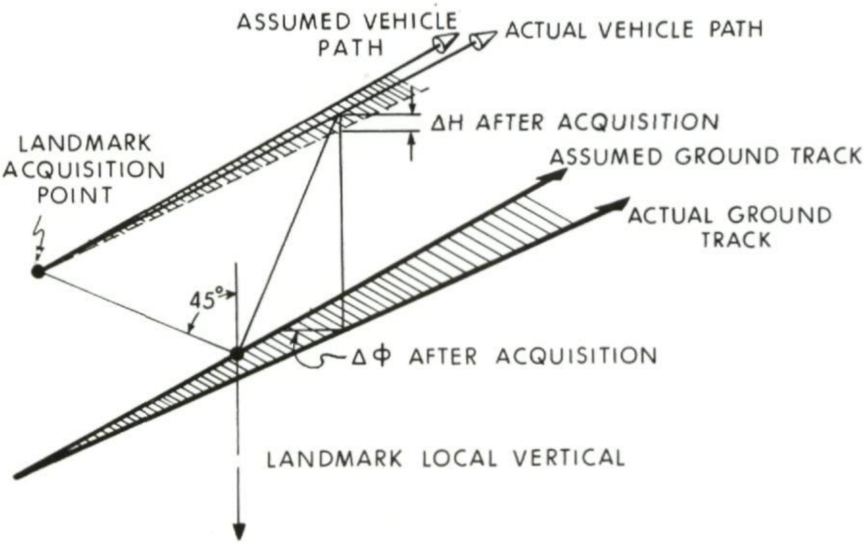

FIG. 5–7 Measured geometry for an unknown landmark

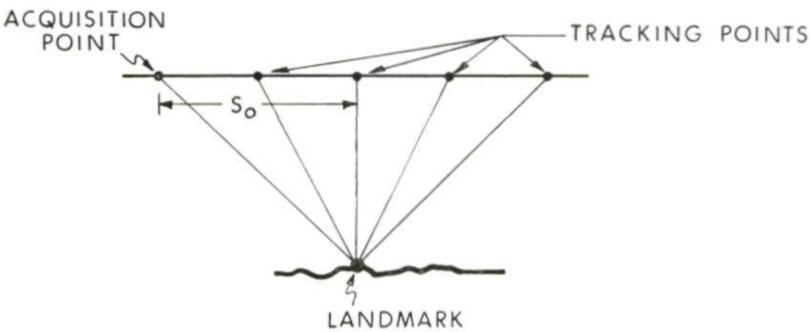

FIG. 5–8 Nominal tracking sequence

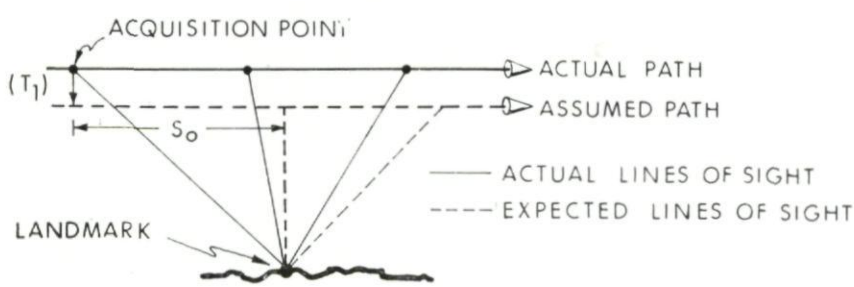

FIG. 5–9 Tracking with an erroneous vehicle or landmark altitude

unknowns $r(T_1)$, $\theta(T_1)$, and $\phi(T_1)$. Consider now the determination of other variables at time, T_1, by further bearing measurements to the same landmark. At the time, $t > T_1$, the position errors of the vehicle will have changed. The new variables are:

$$\theta(t) = \theta(T_1) + \omega(T_1)(t - T_1) \qquad \text{(Eq. 5-13a)}$$

$$r(t) = r(T_1) + \dot{r}(T_1)(t - T_1) + r_o\omega_o\theta(T_1) \qquad \text{(Eq. 5-13b)}$$

$$\phi(t) = \phi(T_1) + \phi(T_1)(t - T_1) \qquad \text{(Eq. 5-13c)}$$

Substituting Eq. 5-13 into Eq. 5-11 and Eq. 5-12 provides a complete solution to the orbital navigational problem:

$$\theta(T_1) + (t - T_1)\omega(T_1) - \cot a(t)r(T_1) - \cot a(t)(t - T_1)[\dot{r}(T_1) + r_o\omega_o\theta(T_1)] = H_o(t) \cot a\ (t) - \theta_o(t) \qquad \text{(Eq. 5-14a)}$$

$$\phi(T_1) + (t - T_1)\dot{\phi}(T_1) - \cot a(t)r(T_1) - \cot a(t)(t - T_1)[\dot{r}(T_1) + r_o\omega_o\theta(T_1)] = H_o(t) \cot \beta\ (t) - \Phi_o(t) \qquad \text{(Eq. 5-14b)}$$

However, four bearing measurements to a single landmark are required before Eq. 5-14a and 5-14b can be solved. Three measurements do provide six equations in the six unknowns; but they are not independent.

UNKNOWN LANDMARK BEARING MEASUREMENT

When the point on the earth's surface has unknown coordinates, the navigational system has to rely on the changes in the tracking angle as the vehicle passes over the landmark. Let us assume that the astronaut can lock-on to an identifiable but otherwise unknown point on the earth's surface when the angle between the computed (or assumed) velocity vector and the line of sight to the point is approximately 45°. The exact number will depend on the skill of the astronaut and on the range error which the navigational system has accumulated by the time of the measurement.

Consider the measurement geometry of Fig. 5-7 and the projections of this geometry into the orbital plane as shown in Fig. 5-8.

The problem is the determination of the errors: $r(T_1)$, $\dot{r}(T_1)$, $\theta(T_1)$, $r_o\omega(T_1)$, $\phi(T_1)$, $\dot{\phi}(T_1)$ at the time of unknown landmark acquisition. As will be seen, it is not possible to determine all of the errors after the tracking of a single landmark; at least four landmarks have to be tracked before all of the orbital parameters of a vehicle can be determined.

Let us assume that the distance between the intersection of the landmark local vertical and assumed velocity vector and the point where tracking begins is S_o (Fig. 5-8). For a general time, τ, after T_1(T_1 is the time when tracking begins), the computed bearing measurement is given by:

$$\cot a_c = \frac{S_o - r_o\omega_o\tau}{H_o} \qquad \text{(Eq. 5-15)}$$

This variation in the bearing angle has to be compared to the angle which actually gets measured.

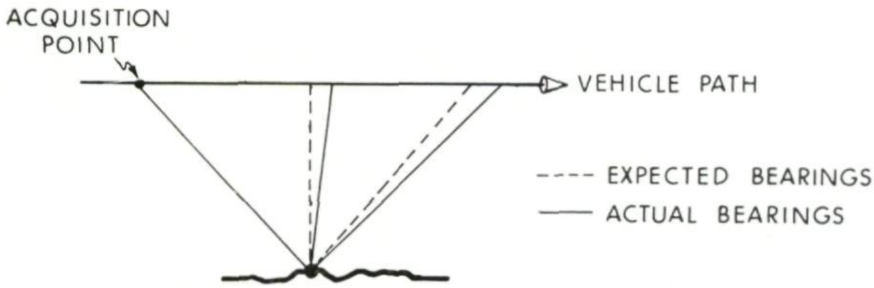

Fig. 5–10 Tracking with an erroneous velocity along range

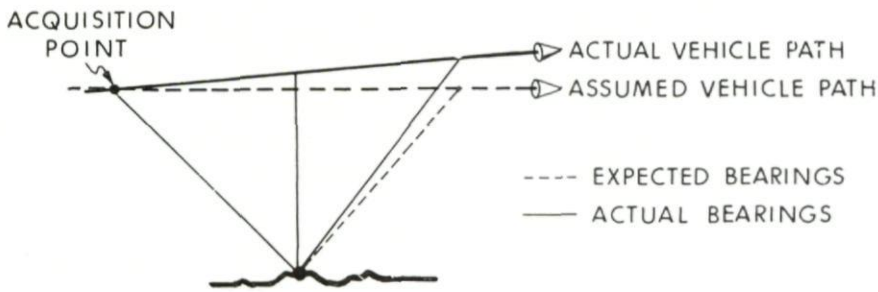

Fig. 5–11 Tracking with an erroneous vertical velocity

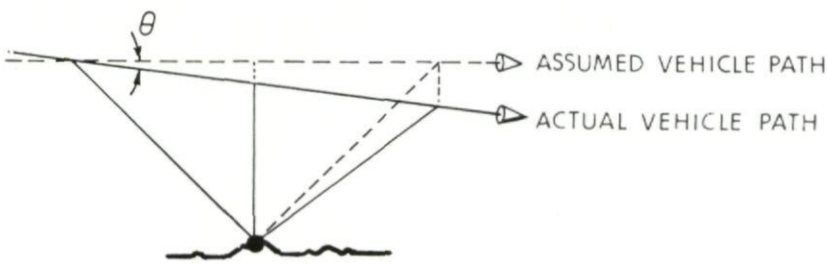

Fig. 5–12 Tracking with an erroneous range error

Consider first an erroneous altitude of the vehicle $r(T_1)$.

As can be seen from Fig. 5–9, it is impossible to determine the difference between an altitude error in the vehicle path and a lack of knowledge in the altitude of the landmark. For a general time, τ, after T_1, the actual bearing measurement given

$$\cot \alpha_a = \frac{S_o - r_o\omega_o\tau}{H_o + r(T_1) - \Delta H} + \frac{\cot \alpha(0)(r(T_1) - \Delta H)}{H_o + r(T_1) - \Delta H} \qquad \text{(Eq. 5–16)}$$

where ΔH is the altitude uncertainty of the landmark.

If the vehicle has an error $\omega(T_1)$ when tracking begins, then the measurement geometry is as shown in Fig. 5–10. The actual bearing measurements in this case are:

$$\cot \alpha_a = \frac{S_o - (\omega_o + \omega(T_1))r_o\tau}{H_o} \qquad \text{(Eq. 5–17)}$$

Again τ is the time after landmark acquisition.

Tracking with an initial vertical velocity error provides the geometry of Fig. 5–11. In this case the bearing measurements are:

$$\cot \alpha_a = \frac{S_o - r_o\omega_o\tau}{H_o + \dot{r}(T_1)\tau} \qquad \text{(Eq. 5–18)}$$

An initial range $(\theta(T_1))$ error appears identical to a vertical velocity error, because at the time, T_1, the computed and actual velocity vectors differ by the angle $\theta(T_1)$ as shown in Fig. 5–12. Thus it is impossible to distinguish between a range error at time, T_1, and a vertical velocity error at time, T_1.

The bearing measurement made along the actual trajectory is:

$$\cot \alpha_a = \frac{S_o - r_o\omega_o\tau}{H_o - \theta(T_1)r_o\omega_o\tau} \qquad \text{(Eq. 5–19)}$$

Since the error terms in Eq. 5–16 to Eq. 5–19 are generally small, further linear approximations of these equations can be made. Using the approximation:

$$\frac{1}{1 + \delta} = 1 - \delta$$

Eq. 5–16 can be approximated by:

$$\cot \alpha_a = \frac{S_o - r_o\omega_o\tau}{H_o} + \frac{r_o\omega_o\, t(r(T_1) - \Delta H)}{H_o^2} \qquad \text{(Eq. 5–20)}$$

(since $S_o = H_o \cot \alpha\ (0)$)

Eq. 5–17 can be approximated by:

$$\cot \alpha_a = \frac{S_o - r_o\omega_o\tau}{H_o} - \frac{\omega(T_1)r_o}{H_o}\,\tau \qquad \text{(Eq. 5–21)}$$

Eq. 5–18 can be approximated by:

$$\cot \alpha_a = \frac{S_o - r_o\omega_o\tau}{H_o} - \frac{S_o\dot{r}(T_1)}{H_o^2}\,\tau + \frac{r_o\omega_o\dot{r}(T_1)}{H_o^2}\,\tau^2 \qquad \text{(Eq. 5–22}$$

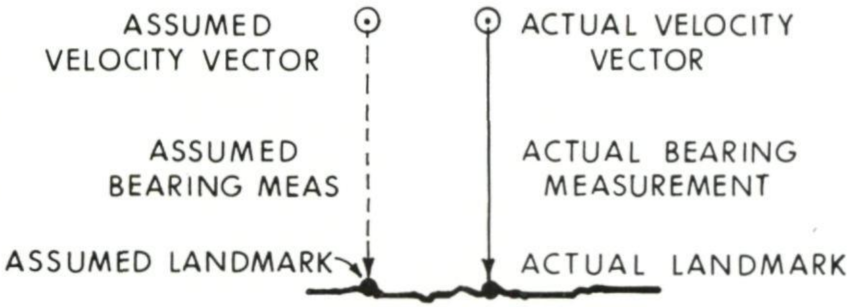

FIG. 5–13 Tracking with erroneous track position

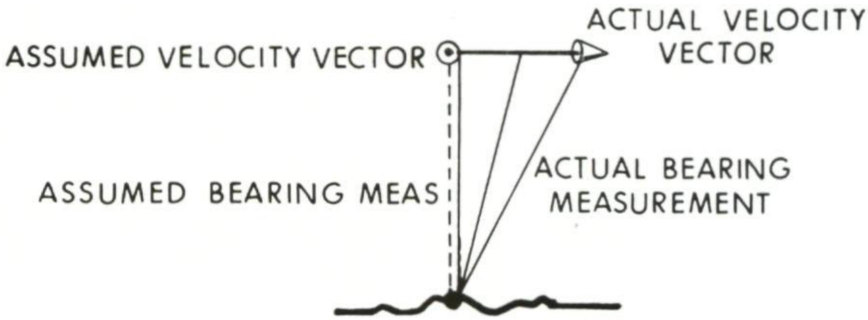

FIG. 5–14 Tracking with erroneous track velocity

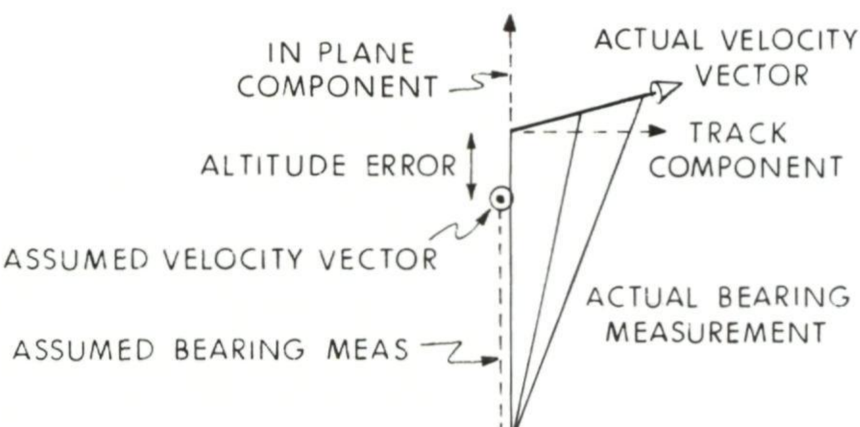

FIG. 5–15 Tracking with erroneous track velocity, altitude error and vertical velocity error

Eq. 5–19 can be approximated by

$$\cot a_a = \frac{S_o - r_o\omega_o\tau}{H_o} + \frac{S_o r_o\omega_o\theta(T_1)}{H_o^2}\tau - \frac{r_o^2\omega_o^2\theta(T_1)}{H_o^2}\tau^2 \qquad \text{(Eq. 5–23)}$$

The first term on the right hand side of Eq. 5–20 through Eq. 5–23 is cot a_c. Thus, one can write in general:

$$\cot a_a - \cot a_c = \frac{1}{H_o^2}\Bigg[r_o\omega_o[r(T_1) - \Delta H]$$
$$\frac{r_o}{H_o}\,\omega(T_1) - S_o\,[r(T_1) - r_o\omega_o\theta(T_1)]\Bigg]\tau \qquad \text{(Eq. 5–24)}$$
$$+ \frac{r_o\omega_o}{H_o^2}\,[\dot{r}(T_1) - r_o\omega_o\theta(T_1)]\tau^2$$

When one considers the magnitude of the terms in Eq. 5–24, it becomes apparent that the $r_o\omega(T_1)(H_o)$ term can also be neglected. This leaves the relatively simple expression:

$$\cot a_a - \cot a_c = \frac{1}{H_o^2}\Bigg[r_o\omega_o\,[r(T_1) - \Delta H]$$
$$+ S_o\,[r_o\omega_o\theta(T_1) - r(T_1)]\Bigg]\tau \qquad \text{(Eq. 5–25)}$$
$$+ \frac{r_o\omega_o}{H_o^2}\Bigg[\dot{r}(T_1) - r_o\omega_o\theta(T_1)\Bigg]\tau^2$$

To determine the track errors in the vehicle trajectory, consider the projection of Fig. 5–7 into a plane normal to the assumed velocity vector. The unknown landmark should also be contained in this plane. This measurement provides no information about the position error ϕ as shown in Fig. 5–13.

However, the measurement does provide information about the track velocity error ϕ as shown in Fig. 5–14.

To determine ϕ, two variables from the in plane component of this measurement have to be known:

The distance between the landmark and the vehicle velocity vector (just the sum – not the individual components)

The sum of the vertical velocity and range error (again only the sum).

These variables, though, are available from the in plane computation (Eq. 5–25). The measurement geometry is as shown in Fig. 5–15.

Consider the angle, β, between the assumed bearing measurement and the actual bearing measurement.

$$\sin\beta = \frac{\phi r_o\tau}{H_o + r(T_1) - \Delta H + (r(T_1) - r_o\omega_o\theta(T_1))\tau} \qquad \text{(Eq. 5–26)}$$

Depending on the particular orbit, the denominator terms with exception of H_o or possibly $H_o + r(T_1) - \Delta H$ will be negligible. For small values of β $\sin\beta \approx \beta$ and in general:

$$\phi = \frac{\beta(\tau)\ [H_o + r(T_1) - \Delta H]}{r_o t} \qquad \text{(Eq. 5–27)}$$

Eq. 5–25 and Eq. 5–27 form the two basic equations which have to be solved

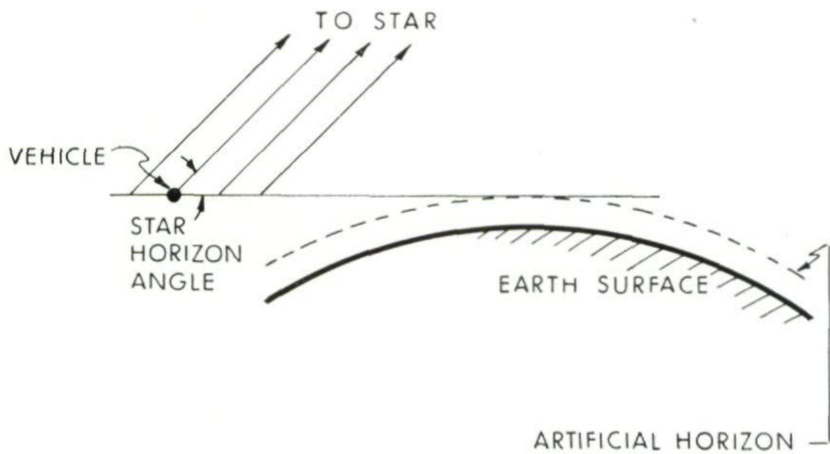

FIG. 5–16 Star horizon measurement

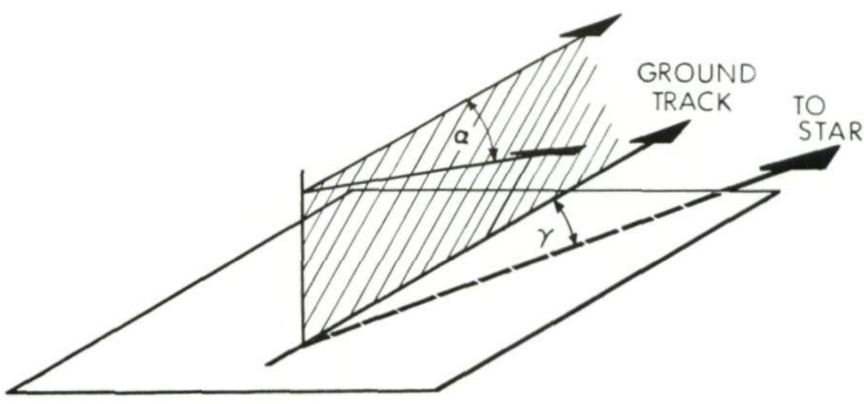

FIG. 5–17 Star horizon measurement geometry

to determine the orbital parameters when unknown landmarks are used.

Thus, as contrasted with the known landmark measurement, the unknown landmark measurement provides information about the velocity vector of the vehicle. Since each measurement to an unknown landmark provides only one equation for the determination of the four in plane orbital parameter unknowns, it is necessary to track four unknown landmarks to determine the initial condition errors. The first two of these measurements completely determine the track errors. The remaining two track computations – if carried out – serve only for redundancy. The requirement for four landmarks instead of three appears here again, similar to the requirements for four bearing measurements to a known landmark.

NAVIGATION USING STAR HORIZON MEASUREMENTS

Let us assume for the moment that it is possible to define an earth horizon by some means. A possible method is discussed in a later section of this paper where a horizon is defined at approximately 30 kilometers above the earth's surface. The astronaut then maneuvers the vehicle so that the plane formed by the two lines of sight (star line of sight and horizon line of sight) also contains the center of the earth and measures the angle between the star and horizon. This places the vehicle on a surface which touches the earth at the earth's artificial horizon as shown in Fig. 5–16.

Since the artificial horizon is at an altitude of approximately 30 kilometers, the angle between the local horizontal and the line to the horizon is about 0.2 radians.

Again it is possible to make a flat earth approximation for this measurement. Figure 5–17 illustrates the star horizon measurement when there is no error in the vehicle position. The angle, γ, is the angle between the assumed orbital plane, and a plane containing the vehicle, earth center, and a vector from the vehicle to the star. Thus, when γ is zero, the measurement is insensitive to ϕ errors, when γ is $90°$, the measurement is insensitive to θ errors. The angle, $90° - \alpha$ is the angle between the velocity vector at time, T_1, and the normal to the plane established by this measurement.

If the measurement is taken at a time, t, when the star horizon angle is equal to the expected star horizon angle at time, T_1, the vehicle is located on a plane (taking the position of the vehicle at time, T_1, as the origin) given by Eq. 5–28. One equation relating the errors:

$$r(t)\cos\alpha + \gamma(t)\sin\alpha\cos\gamma + \phi(t)\sin\alpha\sin\gamma = 0 \qquad \text{(Eq. 5–28)}$$

at time, T_1, can be obtained by substitution of Eq. 5–13a, Eq. 5–13b, and Eq. 5–13c into Eq. 5–28. Thus, only one equation between the orbital parameter errors can be obtained from this type of measurement, since the measurement involves only one angle and time. The angle, α, depends only on the orbital altitude. The angle, γ, depends on star direction. It can be chosen to favor either the range error (by making γ small) or the track error (by choosing γ close to $90°$). The star horizon angle only determines the time, T_1, when the vehicle should pass through the plane given by Eq. 5–28.

Since each measurement provides only one equation in the six unknown orbital errors, it is necessary to take at least six star horizon measurements to determine the orbital parameters.

STAR OCCULTATION MEASUREMENT

As a vehicle moves in an orbit around the earth or moon, stars will rise and set. Whenever a star sets, the disk of the moon or earth occults this star and the vehicle is at that moment crossing a cylinder with its axis in the direction of the star. The diameter of this cylinder is equal to the diameter of the earth or moon.

The measurement is very useful when the vehicle is in a lunar orbit. However, in earth orbit – due to the atmosphere – it is very difficult to determine when a star is occulted, since attenuation of the starlight in the atmosphere will take place due to differential refraction and due to attenuation. This measurement can be considered as a special case of the star horizon measurement with a zero star horizon angle.

The position of the vehicle is given by the plane defined by Eq. 5–28 and the error at time, T_1, by substitution of Eq. 5–13a, Eq. 5–13b, and Eq. 5–13c into Eq. 5–28. Again, six star occultation measurements have to be performed to completely determine the orbital parameters of the vehicle.

The measurements described in this chapter require different configurations of equipment. They also have certain constraints imposed on their usage as described below:

Known Landmark Bearing Measurement:

Advantages:

Good error sensitivity
Moderate equipment accuracy requirement with man made beacons usable on both the light and dark side of the earth

Disadvantages:

Landmarks have to be chosen for ease of recognition and unambiguity. Cloud cover can make landmarks not usable. Large map requirements. Surveying of some landmarks required. Barely usable on the moon due to poor maps. Requires a reference (e.g. inertial system)

Unknown Landmark Bearing Measurement:

Advantages:

Reasonable error sensitivity. Usable anywhere on sunlit side and whereever there are lights on dark side of earth. No maps required. Usable even on the far side of the moon

Disadvantages:

Relatively high equipment accuracy required
Requires a reference (e.g. inertial system)

Star Horizon Measurement:

Advantages:

Reasonable error sensitivity
No reference required

Disadvantages:

High equipment accuracy required usable only against sunlit earth or moon, requires automatic star tracker and photometer

Star Occultation Measurement:

Advantages:

Good error sensitivity
No equipment required

Disadvantages:

Usable on moon only

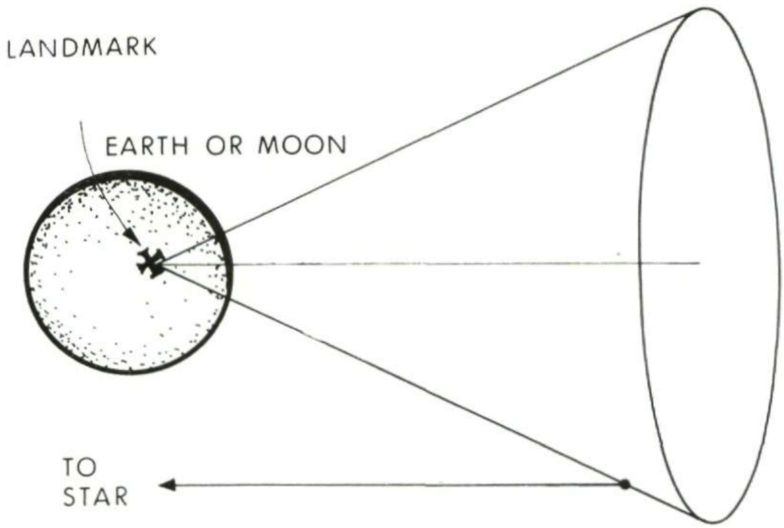

FIG. 5–18 Star landmark measurement geometry

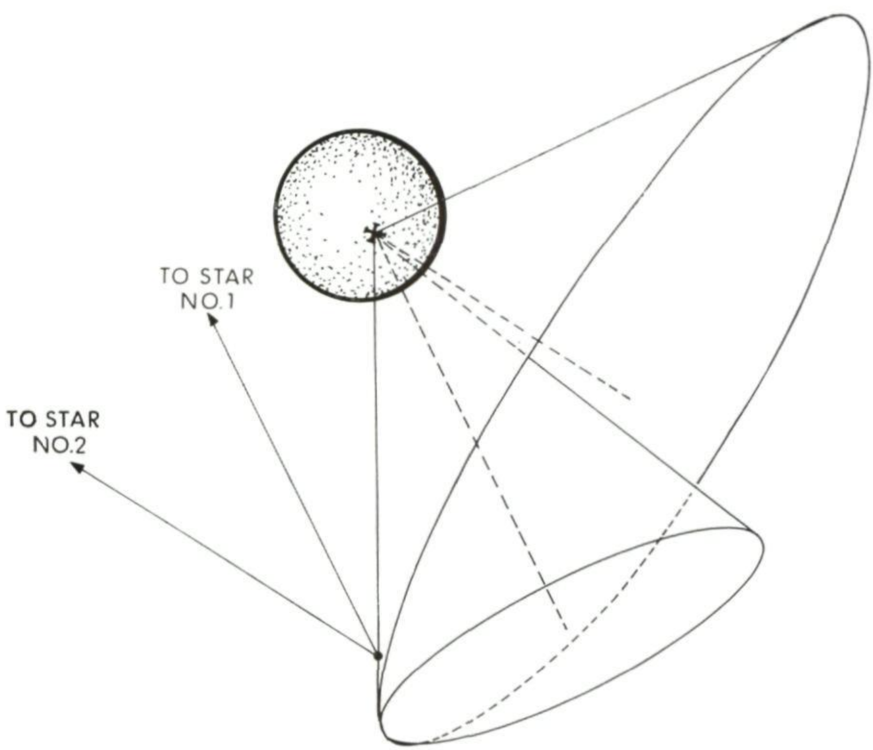

FIG. 5–19 Measurement geometry, conical surfaces

CHAPTER 5-2

MIDCOURSE NAVIGATION

After injection into translunar or transearth orbit, it is no longer possible to use the simplifying assumptions of Eq. 5-4 and Eq. 5-5. Thus, one generally has to resort to computer solutions to solve the navigational problem. Navigation from ground based stations is again possible and has been used quite successfully. However, in this part only on-board measurements will be considered.

POSSIBLE MEASUREMENTS

Again in midcourse, as in the orbital case, use is made of optical measurements. However, the accuracy requirements in midcourse are so much greater than the accuracy requirements in orbit that bearing measurements with the inertial system used as a reference are no longer possible. As can be seen from Fig. 5-4 and Fig. 5-5 a measurement uncertainty of one milliradian produces position uncertainties of 0.15 to 0.2 km in earth orbit. A measurement with similar accuracy, however, is not too useful at a distance of 100000 km.

At distances from the earth, which are comparable to the lunar distance, it is possible to use features on the earth or on the moon, or to use planets within our celestial system. Among these choices, the earth and moon provide the best accuracy because of their proximity to the trajectory.

Another factor is of great importance in midcourse. The bearing angles to landmarks or to the horizon change very slowly. In orbit these rates are (see again Fig. 5-4 or Fig. 5-7) in the order of degrees per second. In midcourse the rates reach low values of arc-seconds per second. Thus, considerably more time can be taken by the operator to complete each measurement.

Measurements which have been considered are:

Star Landmark Angle Measurements
Star Horizon Angle Measurements
Star Occultation Measurements

The first two of these measurements are sextant measurements. Only one angle has to be read with great accuracy to complete the navigational measurement. The third measurement does not require any instrumentation when a star is occulted by the lunar disk. However, occultation measurements against the earth's disk require relatively precise knowledge of starlight attenuation through the atmosphere to determine a point of occultation. A photometer to make this measurement has not been included in the optical unit used in Project Apollo.

STAR LANDMARK MEASUREMENT

One precision angular measurement between a star and a landmark places a vehicle on a cone as shown in Fig. 5-18. The apex of the cone is located at

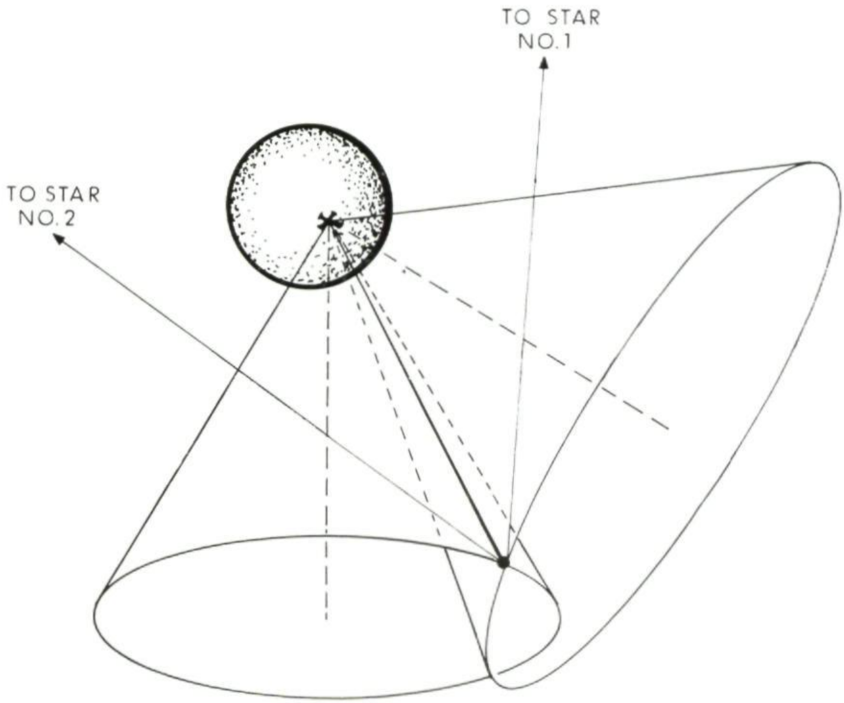

FIG. 5–20 Measurement geometry, conical intersection

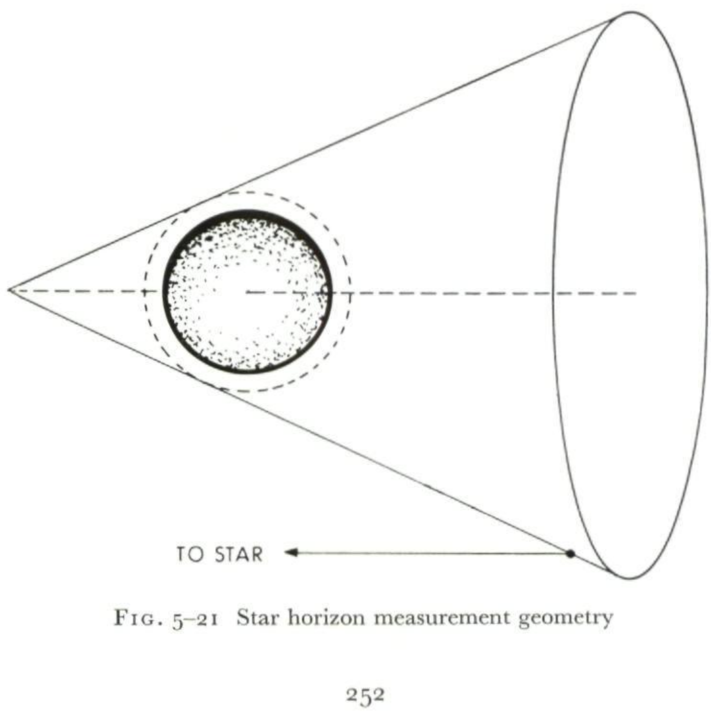

FIG. 5–21 Star horizon measurement geometry

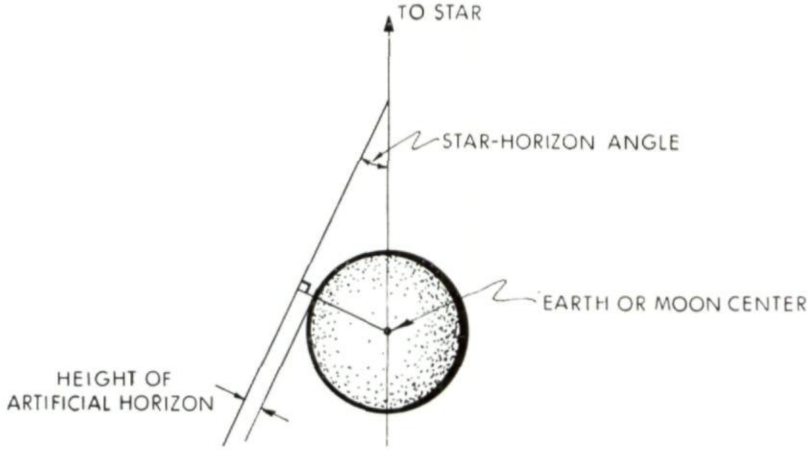

FIG. 5–22 Star horizon cone apex location

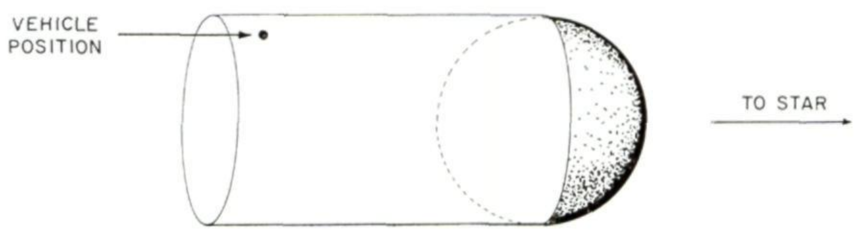

FIG. 5–23 Star occulation measurement geometry

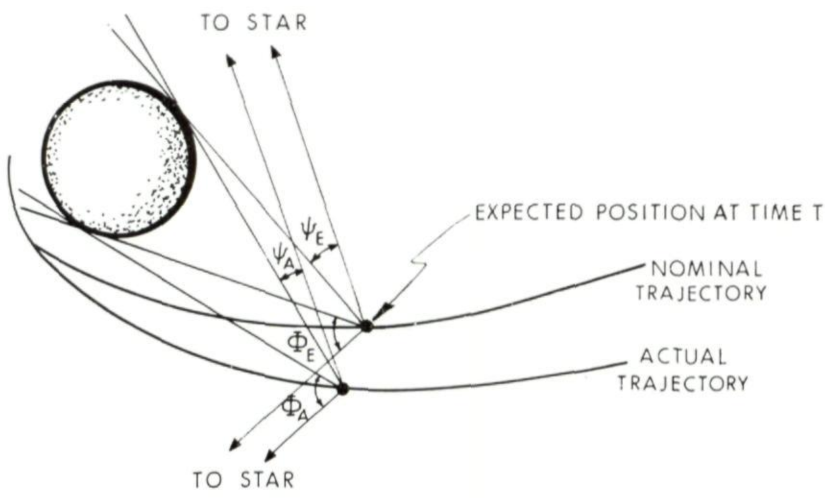

FIG. 5–24 Measurements to both horizons

ASSOCIATED WITH ΔR_o

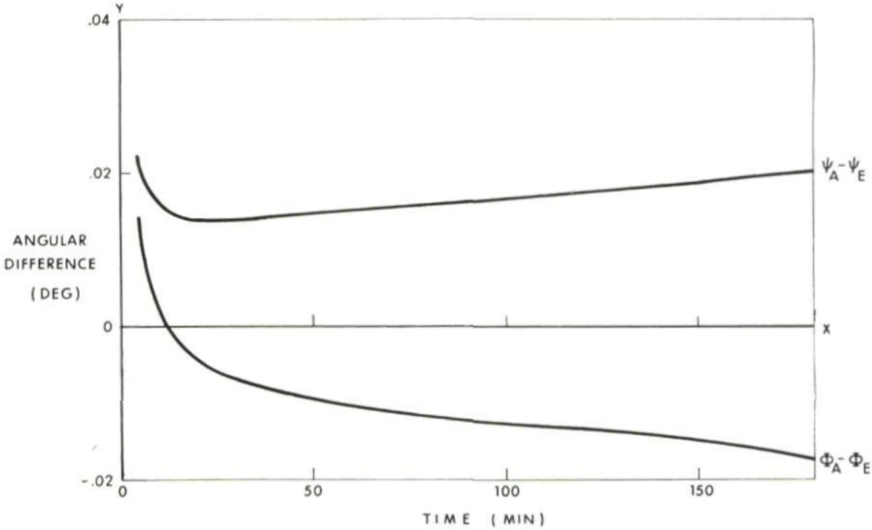

FIG. 5–25 Change in angle measurement due to initial altitude error

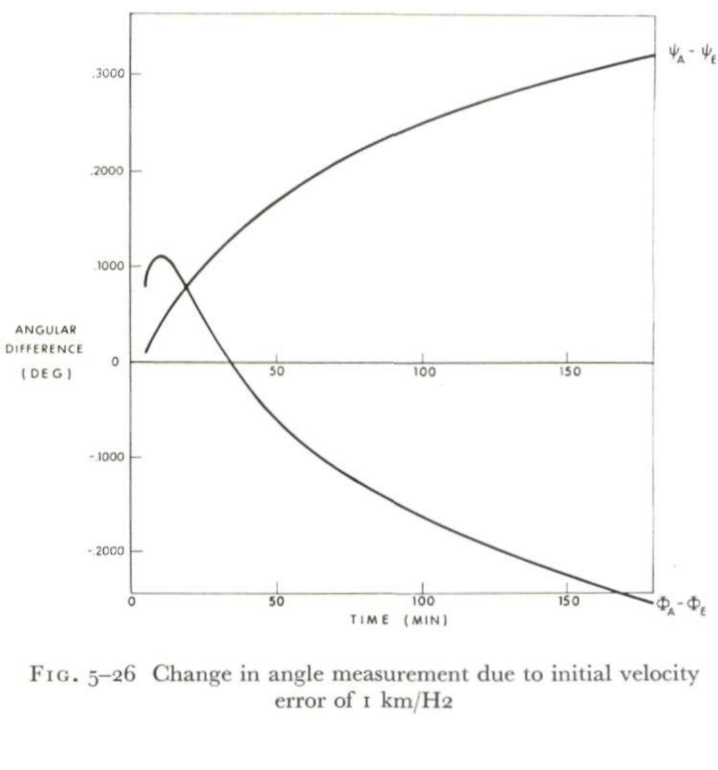

FIG. 5–26 Change in angle measurement due to initial velocity error of 1 km/H2

the landmark. The direction of the center line of the cone is parallel to the direction to the star. The cone half angle is equal to the measured star landmark angle. Consider the plane formed by the vector from the vehicle to the landmark and the vehicle to the star. If another navigational measurement is made using the same landmark, and another star within this plane, then another cone of position is established as shown in Fig. 5–19. The two conical surfaces touch at the line containing the vehicle and landmark. Locally, in the vicinity of the vehicle (assuming a distance to the landmark greater than 20000 km and a star landmark angle greater than five degrees) this conical surface can be approximated by a plane; the only difference is that for a larger star landmark angle the flat plane approximation is better. No other information is provided by this measurement.

To obtain information for a second degree of freedom it is necessary to choose another star so that the plane containing the vectors from the vehicle to the second star and vehicle to the first star is approximately orthogonal to the plane shown in Fig. 5–18. The resultant locus of position of the vehicle is a line as shown in Fig. 5–20. Any other measurement using the chosen landmark only provides redundant information. The uncertainty of the vehicle along this line can only be reduced if another landmark is used.

Let us assume that a landmark can be used as long as the angle between the line-of-sight and the local vertical at the landmark is less than 45°, then at a 20000 km distance from the earth the error along the line established in Fig. 5–20 is about 0.4 km per arc-second of error in the measurement. At 100000 km from the earth star landmark measurements to two earth landmarks provide essentially no additional information when compared to measurements made with only one landmark. Conversely, it can be said that the choice of earth (or moon) landmarks does not matter for star landmark measurement in midcourse. Any landmark, as long as its position is known and clouds are not present, can be used as well as any other landmark.

STAR HORIZON MEASUREMENT

Let us assume again that a suitable earth horizon as seen from space can be defined. The lunar horizon can be defined by the lunar disk. The astronaut maneuvers the vehicle so that the horizon scan takes place in a plane normal to the horizon. When the measurement between star and horizon is made, the vehicle is located on a cone as shown in Fig. 5–21. The center line of the cone is parallel to the starlight. The half angle of the cone is equal to the star horizon measurement angle. The location of the apex of the cone can be obtained from Fig. 5–22, where R is the radius of the earth or moon respectively. Thus, as can be seen, the geometry of a star horizon measurement and a star landmark measurement is almost identical. The only difference between the two measurements is the location of the apex of the cone which defines the vehicle position.

STAR OCCULTATION MEASUREMENT

When a star is occulted by the earth's or moon's disc, the vehicle is located on a cylinder as shown in Fig. 5–23. The center of the cylinder passes through the center of the earth. The diameter of the cylinder is equal to the earth's or moon's disc. Since star occultations depend on the trajectory of

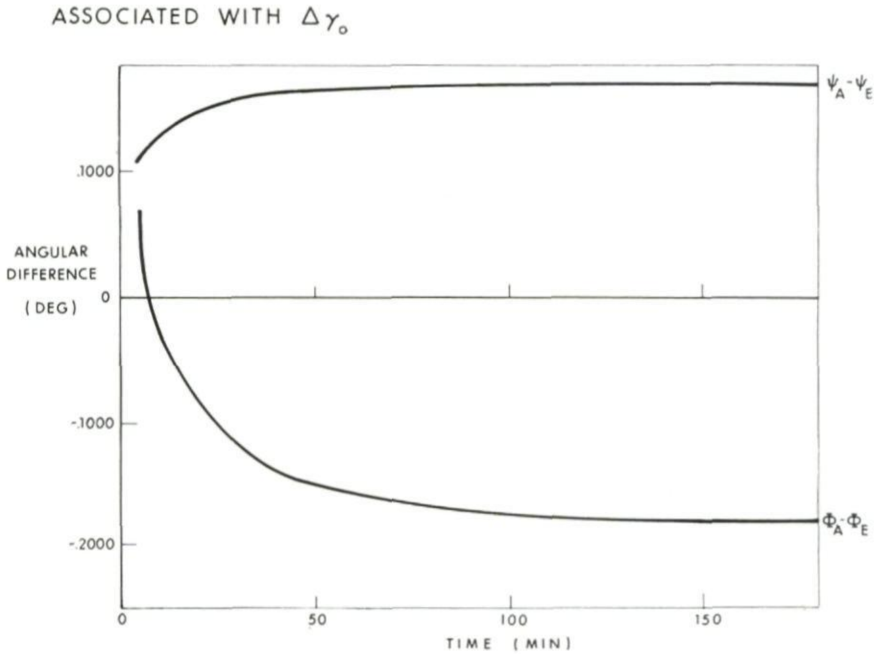

FIG. 5–27 Change in angle measurement due to initial velocity direction error of 1 milliradian

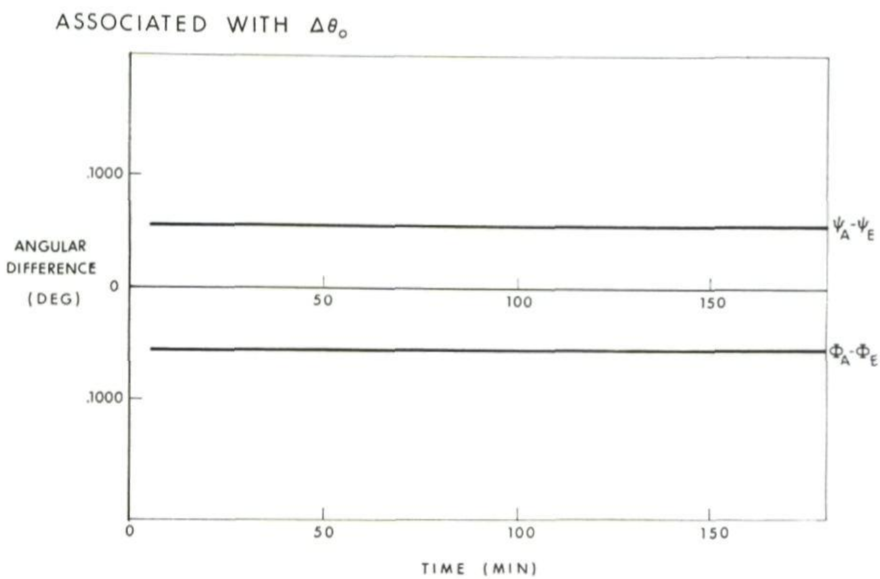

FIG. 5–28 Change in angle measurement due to initial range error of 1 milliradian

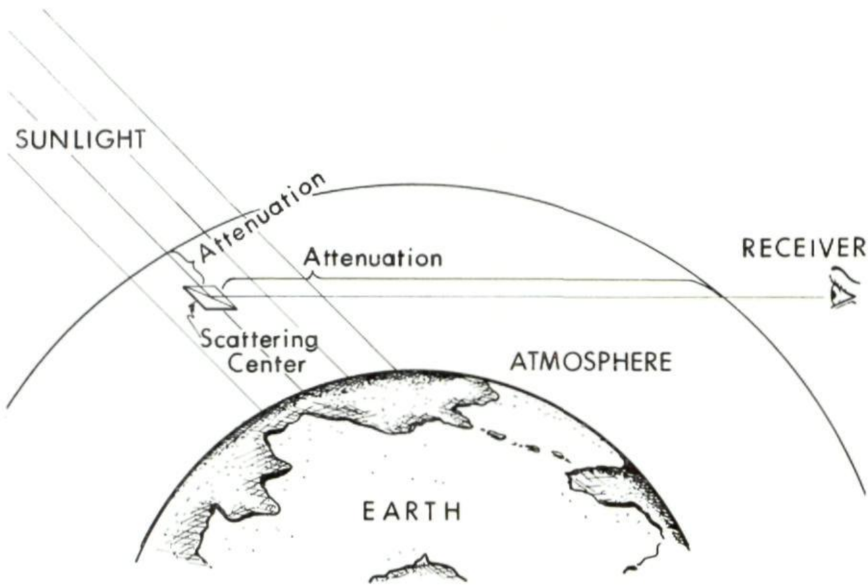

FIG. 5–29 Location of horizon phenomena

the vehicle, it is not possible to choose the measurement geometry to any extent. However, the measurement does have the advantage that no equipment is required to perform it. The only requirement is timing of the star occultation.

ERROR SENSITIVITIES NEAR THE EARTH AND MOON

When the distance between the earth or moon and the vehicle is less than about 20 000 km, the angle between the two horizons is sufficiently large so that an advantage can be gained from star horizon measurements using first one horizon and then the other horizon. Since errors at injection are costliest (from a correction fuel requirement standpoint) when they are made in the trajectory, it is important to determine their magnitudes early during the midcourse phase.

Let us assume that at the end of injection the vehicle has an error in the magnitude of the velocity vector. The direction of the velocity vector and position of the vehicle are assumed to be correct. Figure 5–24 shows in exaggerated fashion how the path of the vehicle deviates from the nominal (or expected) path. The differences between the actual angles and expected angles are shown in Fig. 5–25 to Fig. 5–29. Let us assume that the vehicle is injected with an altitude error of 1 km. The difference between the expected and actual star horizon angle as defined in Fig. 5–24 is shown in Fig. 5–25. The error sensitivity for readings taken against either horizon is almost identical when the vehicle reaches a distance of about 30 000 km from earth center (100 minutes after injection). Similar conclusions can be reached from Fig. 5–26 (error sensitivity due to wrong injection velocity) and Fig. 5–27 (error sensitivity due to an error in the direction of the velocity vector at burnout). A range error (θ in Chapter 1) simply rotates the transfer ellipse by the angular range error θ. Thus, the error sensitivity is constant during the first part of the mission.

If navigational sightings cannot be taken during the first one or one-half hours, either due to crew tasks or constraints imposed by radiation belts, the astronaut or computer has to choose only between an earth feature or a lunar feature. Choosing between specific landmarks or horizon on either the earth or the moon does not provide any major improvement in the knowledge of the vehicle position.

AN ARTIFICIAL EARTH HORIZON

Clouds and atmosphere on the earth make it generally impossible to see the earth's surface near the horizon; thus it is necessary to define a horizon which is sufficiently high above the clouds to be visible during most of the mission time. To date, most of the horizon sensing has been accomplished in the infrared region of the spectrum. However, sunlight scattered within the earth's atmosphere also provides a possible horizon. Since the upper atmosphere scatters most of the blue and near ultraviolet light, a horizon model based on scattered sunlight is being used. Figure 5–29 illustrates the measurement geometry used. A comparison is made between the maximum intensity and half of the maximum. The half maximum establishes a horizon located about 30 km above the earth's surface.

CHAPTER 5–3

THE APOLLO OPTICAL UNIT

The varied navigational measurements which are made during the Apollo mission are used as a basis for the design of the optical unit shown in Fig. 5–30. The unit consists of a sextant, an automatic star tracker and photometer and a scanning telescope. During midcourse when it is necessary to make accurate star landmark and star horizon measurements, the sextant is used. The scanning telescope is used only as an instrument for target acquisition.

Both instruments are used during the orbital portion of the mission. The scanning telescope is used for known landmark bearing measurements. Its large field of view is essential for landmark identification and acquisition. The movable line-of-sight of the sextant is used for unknown landmark tracking. The automatic features are used for star-horizon measurements. Star occultation measurements need no particular bearing readout, since only the time of occultation is required. Either instrument or a window can be used for this particular measurement.

SPACE SEXTANT

The sextant consists of a 28 power, 1.8 degree field of view telescope located within the optical base (see Fig. 5–30). Before light enters the telescope, it passes through the sextant head, where the two lines-of-sight of the instrument are combined. The landmark line-of-sight passes through the beamsplitter and from there directly into the telescope. To move this line-of-sight, it is necessary to move the vehicle. The beamsplitter passes about 20% of the light to the telescope. Also contained within the beamsplitter is a filter which attenuates most of the blue and green light entering the landmark line-of-sight. This reduces the blue haze which is generally visible on the earth from high altitudes without appreciably degrading the characteristics of lunar landmarks.

The star line-of-sight is directed to the telescope by a movable mirror, two fixed mirrors and the beamsplitter. About 80% of the starlight passes through the beamsplitter into the telescope. The movable mirror is positioned by a conventional a.c. servo system. The readout of the mirror position (this is the most accurate angle readout within the guidance system) depends on a 64 speed (128 pole) resolver. The angles of this resolver are read by a coupling data unit as described in Part 4.

Angles ranging from zero to 50 degrees between the two lines-of-sight can be read with this instrument. The mirror can be moved further to 90 degrees, where the image of the reticle is reflected back upon itself. The astronaut can use this point as a check of the alignment stability of the instrument. Viewing of a bright star or planet with the line-of-sight angle set to zero degrees provides another point where the sextant angular readout can be easily checked.

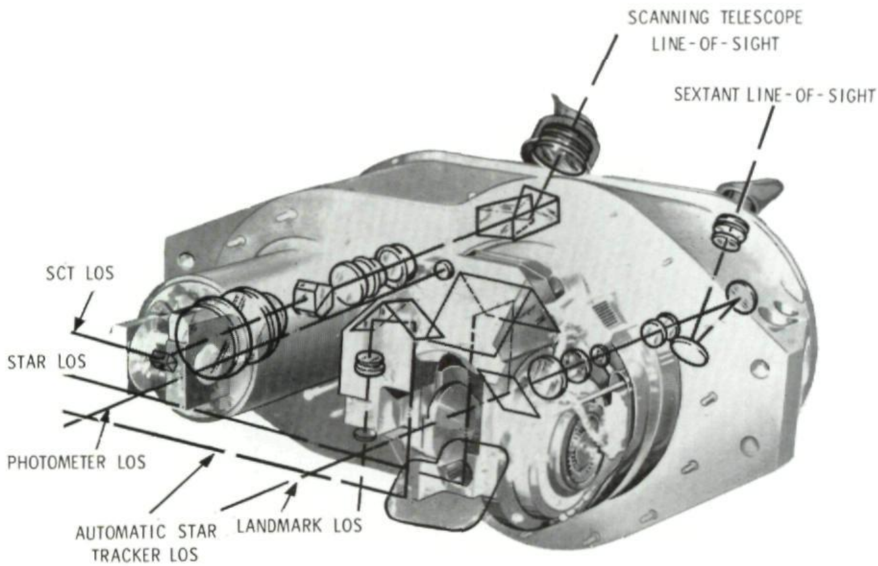

FIG. 5–30 Apollo optical unit

These self-checking features have been incorporated to make sure that a check of the instrument accuracy can be made before and after each midcourse navigational sighting.

The head assembly and telescope rotate within the optical base. This motion provides the second degree of freedom of motion for the star line-of-sight. Motion in this direction is limited to $\pm$ 270 degrees from a predetermined zero. The power to the components located on the sextant head is carried through a flex cable. Limitation of the freedom of motion of the sextant thus makes use of slip rings not required.

STAR TRACKER-PHOTOMETER

The star tracker is included within the optical unit to enable the astronaut to make measurements between the earth's horizon and a star. Both instruments including their detectors and preamplifiers are completely located on the sextant head. The photometer measures the intensity of the near ultraviolet sunlight scattered by the earth's atmosphere. Light collected by the photometer aperture is filtered and modulated by a vibrating reed before it reaches the photodetector. The signal is further amplified and the level of the signal is detected with circuitry within the power and servo assembly of the guidance system.

The star tracker is a narrow, field-of-view ($\frac{1}{2}$ deg. $\times$ $\frac{1}{2}$ deg.) instrument. Star light is directed into the aperture of the telescope by the star line-of-sight movable mirror and two redirection mirrors. Crossed tuning forks are used to provide information about the star position within the tracker's field of view. The electronics required to process the star tracker signal are also located in the power and servo assembly.

The two degrees of freedom required to position the star tracker are identical to the degrees of freedom provided for the star line-of-sight. Thus, when a star is tracked the astronaut can compare the star position in the sextant field to the center of the reticle. This provides a visual check on the operation of the star tracker.

SCANNING TELESCOPE

The scanning telescope is a single line-of-sight, unit power, 60 degree field of view instrument used for making known landmark bearing measurements in earth and lunar orbit and also for general use, such as acquisition of landmarks and stars for sextant sightings. The complete telescope assembly rotates within the optical base, similar to the sextant. The two shafts are continuously tied together with a conventional a.c. servo system.

The light enters the telescope through a double dove prism. This prism can be positioned so that the telescope line-of-sight is parallel to the landmark line-of-sight (for midcourse landmark acquisition) or parallel to the star line-of-sight for star acquisition. A third position, offset from the landmark line-of-sight by 25 degrees, is also provided. In this position the scanning telescope covers the complete sextant field of view. This position is used when the astronaut tries to hold one image in one of the sextant lines-of-sight while searching for the second image.

To provide backup in case of an electrical failure, the scanning telescope also contains two mechanical counters connected to the movable parts of the

telescope. These counters can be read and the angles manually entered into the computer in case of a malfunction within the angle encoding loop. Two knobs which can be used for manual positioning of the telescope line-of-sight are also provided. These provide a backup for the a.c. servo components which are normally used to position the sextant and scanning telescope.

REFERENCES

1. CHANDRASEKHAR, S., "Radiactive Transfer". Dover Publications, 1960.
2. PETERSON, R., "Final Report on Special Techniques for Space Navigation". Control Data Corporation, July 1964.
3. SEWARD, H. H., "The Blue-White Boundary Horizon Sensor". M.I.T. Instrumentation Laboratory Report E-1206, September 1962.
4. WOLFF, M., "The Profile of an Exponential Atmosphere Viewed from Outer Space and Consequences for Space Navigation". M.I.T. Instrumentation Laboratory Report E-1634, September 1964.
5. ZUCHERBRAUN, J., "High-Reliability Scanners for Stellar Navigation". Electronics, May 11, 1962.

PART 6

GUIDANCE COMPUTER DESIGN

Dr. Albert Hopkins

DR. ALBERT L. HOPKINS, JR.

Dr. Albert L. Hopkins, Jr., Assistant Director of Instrumentation Laboratory, Massachusetts Institute of Technology, is a specialist in the development of computers for inertial guidance and navigation systems. In his present assignment in the Laboratory's Digital Development Group, Dr. Hopkins is responsible for the design of memory circuits and logic employed in the guidance system computer for the Project Apollo spacecraft.

Dr. Hopkins was born in Chicago, Ill., May 6, 1931, and was graduated from Exeter Academy, Exeter, N.H., in 1949. He attended Harvard University, where he received the A.B. degree in Engineering Sciences in 1953, the A.M. degree in Applied Mathematics in 1954 and the Ph.D. degree in Applied Mathematics in 1957. He was Instructor in Control Systems Engineering in the Harvard Division of Engineering and Applied Physics from 1957 to 1960 under Professor Howard Aiken. Dr. Hopkins joined Instrumentation's Digital Development Group in 1960.

PART 6

GUIDANCE COMPUTER DESIGN

INTRODUCTION

Some twenty-two years have elapsed since the first digital computer was completed. For the past several years, digital guidance computers have flown in airplanes, missiles and rockets. Some of these vehicles are scarcely bigger than an early computer, whose performance is surpassed by the guidance computers they carry.

The first general-purpose computer and the first high speed electronic number processor were each put into use in about 1943. Numbers were stored in relay controlled counter wheels and in vacuum tube ring counters. The next few years brought the high speed general-purpose computer, the acoustic delay line and the electrostatic storage tube. In the early 1950s higher densities were achieved in logic by the use of semiconductor diodes and in memory by the introduction of magnetic cores, drums and tapes. The transistor was developed in 1948, and was employed in some experimental small computers intended as prototype airborne computers in the early 1950s. Transistors began to be employed in large-scale computers in the late 1950s, beginning with computers for military applications. Only now are semiconductor components beginning to match the enormous density which was achieved in magnetic memories ten years ago. In today's guidance computers, we are realizing an overall density thousands of times greater than in computers of fifteen years ago. Part of this difference is due to advances in mechanical design which have been made purely because of the extreme importance of weight and volume in airborne applications. In cases where size is not an important factor, densities are lower by an order of magnitude.

Performance has been increased over the years by advances in logical design as well as in component size and speed. Early contributions of the number bus, binary arithmetic and common storage have been followed by such improvements as methods of fast arithmetic, indexing and other address modification schemes, multiprogramming and program interrupt. Progress in mathematical areas has been a significant factor in our ability to employ digital computers in airborne guidance at this stage of their development. Computer programming developments have given us automatic programming and internal "software" routines such as executive control and interpretive programs. Recent efforts have produced numerical methods of celestial mechanics which do not overtax the limited resources of today's guidance computers. Sampled-data theory has given rise to methods of stable control of unstable vehicles using digital techniques. Vast amounts of programming and analysis are needed before today's missions become tractable for existing computer performance. It is the purpose of the remainder of this essay to discuss the present state of the art of logical design, hardware and software, particularly as it is applied in the Apollo Guidance Computer.

The reasons for having an airborne computer are so numerous that the computer engineer is apt to take the parochial viewpoint that the guidance computer is the principal part of the guidance system and that the other parts such as inertial, optical, radar and radio elements are ancillary units for sensing and communication. This picture of a guidance system is somewhat distorted but not entirely so. In 1962, J. F. Shea, then Deputy Director of Manned Space Flight at NASA and presently Apollo Project Manager, said, "Although engineers in each discipline tend to regard their particular developments as the most critical, once the propulsion capability has been provided, the key to reliable execution of a wide range of complex long-duration missions is the computational capacity provided aboard the spacecraft." (1).

The Apollo Guidance Computer will be incorporated into the Guidance and Navigation Systems in the Command and Lunar Excursion Modules. Its functions are to aid in operating the inertial and optical subsystems, to provide steering signals where human reaction is too slow, to perform spacecraft attitude control with minimum fuel expenditure, to maintain timing references, to communicate with the Astronauts via display lights and keyboard, to communicate with ground tracking stations via digital data links and to perform the calculations necessary to deduce position and velocity relative to the earth and the moon from the input data available during all flight phases from boost through lunar landing and rendezvous to final entry and landing.

CHAPTER 6–1

CHARACTERISTICS OF GUIDANCE COMPUTERS

GENERAL

Guidance computers are designed to meet a number of severe constraints. The extent to which the constraints are met depends upon the ingenuity of the designers; but to judge from comparisons among existing computers, it depends far more strongly on the limitations of available hardware. The more significant differences in performance among computers can be traced to the degree to which their designers are willing to commit themselves to advanced technology and processes previously untried. Today, the complex micro-circuit and the multi-layer etched board are areas in which some computer makers are attempting to attain significant advantages, while others wait and watch to see the inevitable problems arise and become solved before venturing.

Requirements for guidance computers are extreme reliability, low weight and power consumption, high performance in terms of mathematical answers per second and inputs and outputs serviced and flexibility to grow with the scope of the mission. Although immense achievements have been made within the last few years, the present generation of guidance computers rapidly becomes obsolete; missions already in the planning stages call for much greater achievements in design, programming, production, test and repair than have so far been realized.

Some feeling for the range of guidance computer characteristics may be obtained from the tabulation in Table 6–1 of published data (1, 2, 3) on computers designed within the past few years. Comparisons are often misleading, especially if one is trying to prove superiority of one computer over another. It is reasonable and often necessary to choose among computers for a specific application, but it is not easy, for subtle differences can be of great importance. It is less difficult and more valid to draw conclusions about the similarities of various computers from a chart of comparative characteristics. Size and weight data have been omitted here because they tend to be particularly misleading in the absence of knowledge of the particular input and output configuration of the computers. This, in turn, is hard to present because of its detailed nature in some cases and its scanty description in others. Sizes range from 0.2 to 2 cubic feet (0.005 to 0.05 cubic meters), and densities are close to that of water.

LOGICAL DESIGN (4, 5)

Word Length – *It is desirable to minimize word length in a guidance computer.* Memory sense amplifiers being high-gain class A amplifiers, are considerably harder to operate with wide margins of temperature, voltages and input signal than, for example, circuits made of NOR gates. Memory digit drivers are also critical circuits whose number is equal to the number of bits

	Serial or Parallel	Negative Numbers	Word Length Bits	Number of Operations
Univac type 1824	Parallel	2's complement	24	41
AC Spark Plug "Magic"	Serial	2's complement	24	16 (?)
Burroughs D-210	Parallel	2's complement	24	32
Arma Micro Computer	Serial	2's complement	22	19
IBM Saturn V Computer	Serial	2's complement	28	18
Autonetics D26C	Parallel	2's complement	30	100
MIT/IL Apollo Computer	Parallel	2's complement	16	34

	Addition Time	Multiplication Time	Power Consumption	Bits of Memory
Univac type 1824	8 μsec	64 μsec	110 watts	2×10^5
AC Spark Plug "Magic"	70	258	90	1×10^5
Burroughs D-210	30	570	1-100	7×10^4
Arma Micro Computer	27	135	50	5×10^4
IBM Saturn V Computer	82	328	131	5×10^5
Autonetics D26C	6	18	192	3×10^5
MIT/IL Apollo Computer	24	48	90	6×10^5

TABLE 6–1 Selected characteristics of several guidance computers

in a word. Similarly, the time required for carry propagation in a parallel adder or for circulation in a serial machine is proportional to word length, and moreover the very size of a computer is dependent on word length.

Factors which discourage the minimization of word length are the numbers of bits required for data words, input and output variables and instruction words. These numbers are functions of mission requirements and details of logical design. Most guidance computers have word lengths of around 24 bits. The Apollo Guidance Computer is unique among those listed in having 16 bits of which one is a parity check bit. As explained later, the difference is due largely to a decision to use multiple-precision arithmetic for variables concerned with guidance and navigation. Even the longest word in the list (30 bits) is short by comparison to the large scale computer installations, where size is not of as great concern as are speed and programming ease.

Instruction Repertoire – The implicit requirements for any Von Newmann-type computer demand that facilities exist for:

(a) Fetching from memory
(b) Storing in memory
(c) Negating (complementing)
(d) Combining two operands (e.g. addition)
(e) Address modification
(f) Normal sequencing (specifying the location of the next instruction)
(g) Conditional sequence changing.

A single instruction can provide several of these facilities, so that a very limited repertoire is possible (6), although a large burden is thereby placed on program storage and speed is limited. For a relatively small additional cost in complexity, a more comfortable repertoire is obtained. An operation set of eight instructions can provide flexibility without sacrificing simplicity. All of the computers listed go beyond this, however, and in general it is done to obtain speed at a cost in hardware. In some instances, the taking of square roots and the conversion of numbers between binary and decimal appear as single instructions. More commonly, the instruction sets contain convenient data handling, branching, and arithmetic operations with from about 2^4 to 2^5 codes.

Speed – It is well known that the overall speed of a computer can be enhanced by its logical design, usually at an equipment cost. This may take the form of having separate adders in a parallel machine for indexing and arithmetic, or it may consist of providing circuits to speed up multiplication by processing several multiplier bits at a time. Alternatively, speed can be obtained by providing single instructions which perform complex jobs such as the two mentioned in the preceding paragraph. Speed is important in guidance computers and logical complexities are employed in order to gain speed in virtually every guidance computer design, but size and reliability restrictions are of sufficient importance to limit the number and extent of such complexities. In data processing computers, where size is less important and where speed is a competitive issue, logic circuits are employed somewhat into the area of diminishing returns. Guidance computers as a result are generally slower than their ground based relatives.

Input and Output – Guidance computers and control computers in general,

differ from data processors most significantly in the area of input and output. Modern data processors generally communicate with peripheral equipment which is complex and sophisticated enough to send and receive data over parallel channels without the computer having to spend much time overseeing the process. In some cases the computer sends data to a remote buffer register upon receipt of an indication that the remote unit is ready. In other cases the remote unit interrogates the computer memory as often as necessary thus eliminating the buffer. In guidance computers, however, the input and output are not generally exchanged with such sophisticated machines. Owing partly to the non-digital nature of such electromechanical machines as inertial measurement units and rocket steering servos and partly to the strong desire to keep interface circuits and cables as small as possible, the guidance computer spends a substantial part of its time (or equipment) budget on maintaining communication with these units.

Another interesting contrast exists between data processors and guidance computers. The former are designed to spread a work load out over a period of time to achieve a good balance between internal computing and input-output activity. One figure of merit of a data processing installation is the degree to which it can keep its various facilities busy by time-sharing them among various independent users. If a large demand occurs for time on a printer, for example, the results to be printed will be buffered on a magnetic tape to be printed later when the facility is available. In a guidance computer, the central processor is time-shared among numerous jobs, but the allowable delays in reacting to a large demand for input-output service are measured in milliseconds rather than minutes, and the logical design of computers and systems must reflect this fact.

Fault Diagnosis – Another area of interesting contrast between data processors and guidance computers is in the area of self-checking or fault diagnosis. Since time on a large computer is valued at hundreds of dollars per hour, it is economically necessary to locate and correct faults very rapidly. For this reason modern computers are equipped with circuits whose function is to make fault location nearly automatic.

Guidance computers cannot afford to carry extra hardware for this purpose. It is important, however, to be able to detect that an error has occured in flight so that the proper course of action may be taken. This action might be to switch to a back-up computer or other means of control, or possibly it may mean that a missile must be destroyed in order that it may not stray far off course. The most common means of fault detection is by a programmed self-check which is run at all times when the computer is not otherwise occupied. More refined checking may be done by a limited amount of circuitry. For example, some guidance computers employ a parity test on the contents of memory. Still other types of alarms are included in the Apollo Guidance Computer, including tests for prolonged or insufficient interrupt activity and various sorts of program freezes. The sum total of these checks and alarms reduces to a small value the probability that a malfunction shall go undetected.

HARDWARE

Memory Devices – The ferrite coincident current core memory is the

cornerstone of computer technology, providing fast random access at a few cents per bit in the megabit range. Thin film memories have had a large research investment and have surpassed core memories in speed and bit density by little or none at all. Their cost is relatively high and their capacity is more limited than core. Plated wire promises to be a substantial improvement, but is not yet advanced enough to be producible or reliable in data processing or guidance applications.

Core memory is clearly ahead of thin film in data processing applications. The matter is controversial with respect to guidance computers, where the higher cost and the capacity limitations of film are less important. Film offers somewhat higher speed, where core offers the economy of coincident selection plus a large output signal. Density and reliability are unresolved issues between the two.

High capacity electromechanical memories such as drums and disks are disappearing from guidance computer use. This is so for three reasons: a substantial increase in packaging density of core and film memories, the serial access nature of disks and drums, and the limited time that disks and drums can operate without maintenance. The high bit densities and large capacities attainable with electromechanical memories make them virtually indispensable to large scale data processing installations, however.

Fixed memory is not used in data processing to any large degree except as a means of implementing internal machine logic such as in a program sequence generator. Its broader use in guidance computers stems from its potential for indestructibility and high density. Indestructibility is a two-edged sword. It requires that program and data be determined well in advance of use, moreover it places a limitation on changes in mission plan such as may be required periodically in ballistic missile applications. Wherever these limitations are not overly constraining, a fixed memory offers assurance that the computer program is identical through all phases of testing and in flight. It moreover permits recovery from temporary malfunctions which would alter the contents of an erasable memory.

Some types of memories compromise between reliability and unchangeability by having the ability to be electrically alterable. Modifications of film and core memories have this property, although coincident selection is less apt to be possible in the core versions, most of which are relatives of transfluxors. The bit densities of such memories have been well below those which are available in permanent memories.

Logic Devices – In the past few years integrated circuits or microcircuits have been adopted nearly universally by guidance computer designers for at least the logic portion of their computer designs. Prior to the advent of microcircuits, magnetic cores were strong contenders as logic elements against all-transistor circuitry. Core circuits were no larger, and in addition were capable of operating on substantially lower power than all-transistor circuits. Although special applications may yet exist which favor the magnetic core, the very small size of microcircuits and their high speed and proven reliability make them preferred in nearly all instances over cores. With each passing year, moreover, the power consumption of new microcircuit logic devices has been substantially reduced. One can now expect to consume less power with microcircuits than with cores at full speed. The latter elements still

retain the advantage of reduced power consumption at low speed operation.

Data processing machines are only now beginning to use microcircuit techniques, because of numerous problems which have attended the large scale production of microcircuits. If these problems are solved, we may expect to see the same increase in the ratio of performance to size in the logic area of data processors which was seen in guidance computers a few years ago.

The primary area in which advances need to be made is in interconnection of logic units (7). A poor job of mechanical design results in unreliable connections or low component density or both, yet it has so far proven quite difficult to arrive at a structure which is satisfactory in all respects. Some of the essential and important requirements are reliability, ease of manufacture, thermal conductance, mechanical soundness, convenient shape, means of inspection and repair and high density. Some of the methods which achieve high density are seriously lacking in some of the other attributes listed. The multi-layer etched board appears to be a means whereby the technology of interconnection can be advanced but there exists some disagreement as to its qualifications in its present state of development. A highly satisfactory, though somewhat less dense method, is the welded wire matrix which is also a multi-layer device, but not made in an integral unit and not so small as the etched board.

CHAPTER 6–2

CHARACTERISTICS OF THE APOLLO GUIDANCE COMPUTER

LOGICAL DESIGN

General – The AGC has three principal sections. The first is a memory, the fixed (read only) portion of which has 36 864 words, and the erasable portion of which has 2 048 words. The next section may be called the central section; it includes an adder, an instruction decoder (SQ), a memory address decoder (S), and a number of addressable registers with either special features or special use. The third section is the sequence generator which includes a portion for generating various microprograms and a portion for processing various interrupting requests. The backbone of the AGC is the set of 16 write buses; these are the means for transferring information between the various registers shown in Fig. 6–1. The arrowheads to and from the various registers show the possible directions of information flow. In Fig. 6–1, the data paths are shown as solid lines, the control paths are shown as broken lines.

The Fixed Memory is made of wired-in "ropes" which are compact and reliable devices. The number of bits so wired is in excess of 5×10^5. The cycle time is 12 μsec. The erasable memory is a coincident current ferrite core system with the same cycle time as the fixed memory. Instructions can address registers in either memory and can be stored in either memory. The only logical difference between the two memories is the inability to change the contents of the fixed part by program steps. Each word in memory is 16 bits long (15 data bits and an odd parity bit). Data words are stored as signed 14 bit words using a one's complement convention. Instruction words consist of 3 order code bits and 12 address code bits.

The contents of the address register S do not always determine uniquely the address of the memory word. For example, the 2 048 erasable registers are accessed via a 1 024 word address field. This is done with a 3-bit auxiliary address contained in the "Erasable Bank" register which is under program control. Part of the address field is one-to-one: addresses between 0 and 1 377 (octal or base eight) always refer to the same registers. Addresses 1 400–1 777 (octal) are ambiguous and refer to one of 5 sets of 256 words according to the number stored in the Erasable Bank register.

The 3 072 word fixed-memory address field encompasses 36 864 words by means of a 5-bit "Fixed Bank" register and a 1-bit "Fixed Extension" channel. Addresses between 2 000 and 3 777 (octal) are ambiguous and refer to one of 34 banks of 1 024 words each according to the number in the Fixed Bank register. If this number exceeds 30 (octal) then the bank selection further depends on the Fixed Extension bit. The Bank registers and the Extension channel are addressable and are all in the non-ambiguous portions of the erasable memory and channel fields.

Word Length	15 Bits + 1 Parity
Number System	One's Complement
Memory Cycle Time	11.7 μsec
Fixed Memory Registers	36,864 Words
Erasable Memory Register	2,048 Words
Number of Normal Instructions (Interrupt, Increment, etc.)	10
Interrupt Options	10
Addition Time	23.4 μsec
Multiplication Time	46.8 μsec
Double Precision Addition Time	35.1 μsec
Double Precision Multiplication Time Subroutine	575 μsec
Increment Time	11.7 μsec
Number of Counters	29
Power Consumption	100 Watts (AGC + DSKY's)
Weight	58 Pounds (Computer Only)
Size	1.0 Cubic Foot (Computer Only)

TABLE 6–2 AGC characteristics

Transfers in and out of memory are made by way of a memory local register G. For certain specific addresses, the word being transferred into G is not sent directly but is modified by a special gating network. The transformations on the word sent to G are right shift, right cycle, left cycle and 7-position right shift for editing interpretive instruction words.

The middle part of Fig. 6–1 shows the central section in block form. It contains the address register S and the memory bank registers which were mentioned above. There is also a block of addressable registers called "central and special registers", which will be discussed later, an arithmetic unit and an instruction decoder register, SQ. The arithmetic unit is an adder with shifting gates and control logic. The SQ register bears the same relation to instructions as the S register bears to memory locations; neither S nor SQ are explicitly addressable. The central and special registers are A, L, Q, Z and a set of input and output channels. Their properties are shown in Table 6–3.

The sequence generator provides the basic memory timing and the sequences of control pulses (microprograms) which constitute instructions. It also contains the priority interrupt circuitry and a scaling network which provides various pulse frequencies used by the computer and the rest of the navigation system.

Instructions are arranged so as to last an integral number of memory cycles. The list of instructions is treated in detail later. In addition to these there are a number of "involuntary" sequences, not under normal program control, which may break into the normal sequence of instructions. These are triggered either by external events, or by certain overflows within the AGC, and may be divided into two categories: counter incrementing and program interruption.

Counter incrementing may take place between any two instructions. External requests for incrementing a counter are stored in a counter priority circuit. At the end of every instruction a test is made to see if any incrementing requests exist. If not, the next instruction is executed directly. If a request is present an incrementing memory cycle is executed. Each "counter" is a specific location in erasable memory. The incrementing cycle consists of reading out the word stored in the counter register, incrementing it (positively or negatively) or shifting it and storing the results back in the register of origin. All outstanding counter incrementing requests are processed before proceeding to the next instruction. This type of interrupt provides for asynchronous incremental or serial entry of information into the working erasable memory. The program steps may refer directly to a counter register to obtain the desired information and do not have to refer to input buffers. Overflows from one counter may be used as inputs to another. A further property of this system is that the time available for normal program steps is reduced linearly by the amount of counter activity present at any given time.

Program interruption also occurs between program steps. An interruption consists of storing the contents of the program counter and transferring control to a fixed location. Each interrupt option has a different location associated with it. Interrupting programs may not be interrupted, but interrupt requests are not lost and are processed as soon as the earlier interrupted program is resumed.

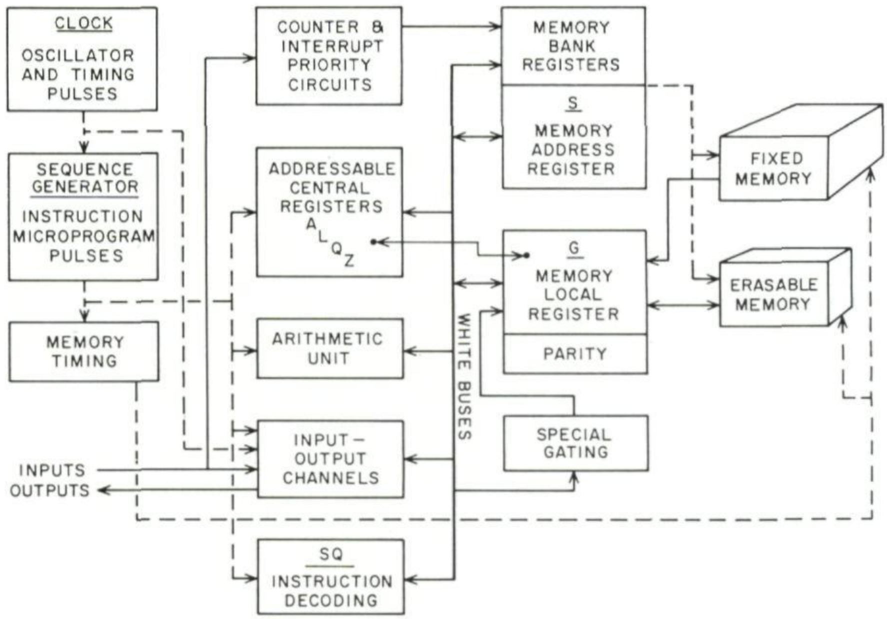

FIG. 6–1 AGC block diagram

REGISTER	OCTAL ADDRESS	PURPOSE
A	0000	Central Accumulator. Most instructions refer to A.
L	0001	Lower accumulator. Used in multiply, divide and all double-precision operations.
Q	0002	Return address register. If a transfer control (TC) operation occurred at line L, (Q) = L + 1.
EB	0003	Erasable bank register, bits 9, 10, 11.
FB	0004	Fixed bank register, bits 11, 12, 13, 14, 15.
Z	0005	Program counter. Contains L + 1, where L is the address of the instruction presently being executed.
BB	0006	Both bank registers: Erasable, bits 1, 2, 3. Fixed, bits 11, 12, 13, 14, 15.
--	0007	Contains Zero.

TABLE 6–3 Addressable special and central registers

Word Length – The AGC is a "common storage" machine which means that instructions may be executed from erasable memory as well as from fixed memory, and that data (obviously constants in the case of fixed memory) may be stored in either memory. The word sizes of both types of memory must be compatible in some sense, the easiest solution is to have equal word lengths. The AGC is somewhat unique in its very short word length and the reasons for it are of some interest. The principal factors in the choice of word length are:

(a) Precision desired in the representation of navigational variables;
(b) Range of the input variables which are entered serially or incrementally;
(c) Instruction word format. Division of instruction words into two fields, one for operation code and one for address.

As a start, the word length (15 bits) for two previous machines in this series (4) was kept in mind as a satisfactory word length from the point of view of mechanization, i.e. the number of sense amplifiers and inhibit drivers and the carry propagation time etc. were all considered satisfactory. The influence of these principal factors will be taken up in turn.

The data words used in the AGC may be divided roughly into two classes: data words used in elaborate navigational computations and data words used in the control of various appliances in the system. Initial estimates of the precision required by the first class ranged from 27 to 32 bits $o(10^{8\pm1})$. The second class of variables could almost always be represented with 15 bits. The fact that navigational variables require about twice the desired 15-bit word length means that there is not much advantage to word sizes between 15 and 28 bits, as far as precision of representation of variables is concerned, because double-precision numbers must be used in any event. Because of the doubly signed number representation for double-precision words, the equivalent word length is 29 bits (including sign) rather than 30, for a basic word length of 15 bits.

The initial estimates for the proportion of 15-bit vs. 29-bit quantities to be stored in both fixed and erasable memories indicated the overwhelming preponderance of the former. It was also estimated that a significant portion of the computing had to do with control, telemetry and display activities, all of which can be handled more economically with short words. A short word allows faster and more efficient use of erasable storage because it reduces fractional word operations, such as packing and editing; it also means a more efficient encoding of small integers.

As a control computer, the AGC must make analog-to-digital conversions, many of which are of angles. Two principal forms of conversion exist; one renders a whole number, the other produces a train of pulses which must be counted to yield the desired number. The latter type of conversion is employed by the AGC, using the counter incrementing feature. When the number of bits of precision required is greater than the computer's word length the effective length of the counter must be extended into a second register, either by programmed scanning of the counter register, or by using a second counter register to receive the overflows of the first. Whether programmed scanning is feasible depends largely on how frequently this scanning must be done. The cost of using an extra counter register is directly

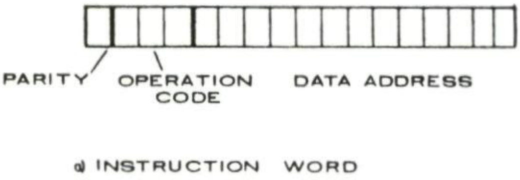

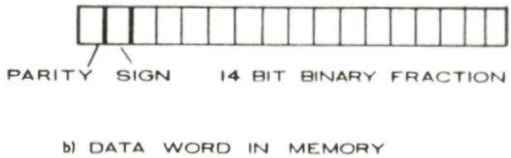

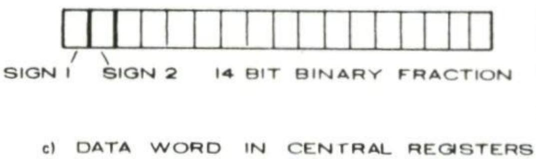

SIGN 2	SIGN 1*	NET SIGN
0	0	POSITIVE
1	1	NEGATIVE
0	1	+OVERFLOW
1	0	-OVERFLOW

* SIGN 1 ACCOMPANIES WORD ON NORMAL TRANSFER TO MEMORY

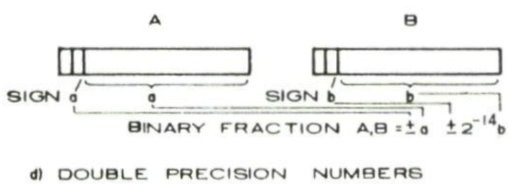

FIG. 6–2 Word formats

measured in terms of the priority circuit associated with it. In the AGC, the equipment saved by reducing the word length below 15 bits would probably not match the additional expense incurred in double-precision extension of many input variables. The question is academic, however, since a lower bound on the word length is effectively placed by the format of the instruction word.

An initial decision was made that instructions would consist of an operation code and a single address. The straightforward choices of packing one two such instructions per word were the only ones seriously considered, although other schemes, such as packing one and a half instructions per word, are possible (1). The two previous computers had a 3-bit field for operation codes and a 12-bit field for addresses, to accommodate their 8 instruction order codes and 4096 words of memory. In the initial core-transistor version of the AGC, the 8 instruction order codes were in reality augmented by the various special registers provided, such as shift right, cycle left, edit, so that a transfer in and out of one of these registers would accomplish actions normally specified by the order code. These registers were considered to be more economical than the corresponding instruction decoding and control pulse sequence generation. Hence the 3 bits assigned to the order code were considered adequate albeit not generous. Furthermore, as will be seen, it is possible to expand the number of order codes.

The address field of 12 bits presented a different problem. At the time of the design of the previous computers it was estimated that 4000 words would satisfy the storage requirements. By the time of redesign it was clear that the requirement was for 10^4 words or more, and the question then became whether the proposed extension of the address field by a bank register was more economical than the addition of bits to the word length. For reasons of modularity of equipment, adding more bits to the word length would result in adding more bits to all the central and special registers which amounts to increasing the size of the non-memory portion of the AGC.

In summary, the 15-bit word length seemed practical enough so that the additional cost of extra bits in terms of size, weight and reliability did not seem warranted. A 14-bit word length was thought impractical because of the problems with certain input variables and it would further restrict the already cramped instruction word format. Word lengths of 17 or 18 bits would result in certain conceptual simplicities in the decoding of instructions and addresses but would not help in the representation of navigational variables. These require 28 bits, so they must be represented in double precision in any event.

Number Representation – In the absence of the need to represent numbers of both signs, the discussion of number representation would not extend beyond the fact that numbers in the AGC are expressed to base two. But the accommodation of both positive and negative numbers requires that the logical designer choose among at least three possible forms of binary arithmetic. These three principal alternatives are: one's complement, two's complement and sign and magnitude.

In one's complement arithmetic, the sign of a number is reversed by complementing every digit, and "end around carry" is required in addition of two numbers. In two's complement arithmetic, sign reversal is effected by

EXAMPLE	STANDARD					MODIFIED					
	S_1	4	3	2	1	S_2	S_1	4	3	2	1
1: Both operands positive; Sum positive, no overflow. Identical results in both systems.	0	0	0	0	1	0	0	0	0	0	1
	0	0	0	1	1	0	0	0	0	1	1
	0	0	1	0	0	0	0	0	1	0	0
2: Both operands positive; positive overflow. Standard result is negative; Modified result is positive using S_2 as sign of the answer. Positive overflow indicated by $S_1 \cdot \overline{S}_2$.	0	1	0	0	1	0	0	1	0	0	1
	0	1	0	1	1	0	0	1	0	1	1
	1	0	1	0	0	0	1	0	1	0	0
3: Both operands negative; Sum negative no overflow. End around carry occurs. Identical results in both systems using either S_1 or S_2 as the sign of the answer.	1	1	1	1	0	1	1	1	1	1	0
	1	1	1	0	0	1	1	1	1	0	0
	1	1	0	1	0	1	1	1	0	1	0
					1 °						1 °
	1	1	0	1	1	1	1	1	0	1	1
4: Both operands negative; negative overflow. Standard result is positive; modified result is negative using S_2 as the sign of the answer. Negative overflow indicated by $\overline{S}_1 \cdot S_2$.	1	0	1	1	0	1	1	0	1	1	0
	1	0	1	0	0	1	1	0	1	0	0
	0	1	0	1	0	1	0	1	0	1	0
					1 °						1 °
	0	1	0	1	1	1	0	1	0	1	1
5: Operands have opposite sign: Sum positive. Identical results in both systems.	1	1	1	1	0	1	1	1	1	1	0
	0	0	0	1	1	0	0	0	0	0	1
	0	0	0	0	1	0	0	0	0	0	1
					1 °						1 °
	0	0	0	1	0	0	0	0	0	1	0
6: Operands have opposite sign; sum negative. Identical results in both systems.	1	1	1	0	0	1	1	1	1	0	0
	0	0	0	0	1	0	0	0	0	0	1
	1	1	1	0	1	1	1	1	1	0	1

° carry

FIG. 6–3 Illustrative example of properties of modified one's complement system

complementing each bit and adding a low order *one,* or some equivalent operation. Sign and magnitude representation is typically used where direct human interrogation of memory is desired, as in "postmortem" memory dumps for example. The addition of numbers of opposite sign requires either one's or two's complementation or comparison of magnitude, and sometimes may use both. The one's complement notation has the advantage of having easy sign reversal which is equivalent to Boolean complementation, hence a single machine instruction performs both functions. Zero is ambiguously represented by all *zero's* and by all *one's,* so that the number of numerical states in a n-bit word is $2^n - 1$. Two's complement arithmetic is advantageous where end around carry is difficult to mechanize, as is particularly true in serial computers. An n-bit word has 2^n states, which is desirable for input conversions from such devices as pattern generators, geared encoders or binary scalers. Sign reversal is awkward, however, since a full addition is required in the process.

In a standard one's complement adder overflow is detected by examining carries into and out of the sign position. These overflow indications must be "caught on the fly" and stored separately if they are to be acted upon later. The number system adopted in the AGC has the advantage of being a one's complement system with the additional feature of having a static indication of overflow. The implementation of the method depends on the AGC's not using a parity bit in most central registers. Because of certain modular advantages 16, rather than 15, columns are available in all of the central registers including the adder. Where the parity bit is not required the extra bit position is used as an extra column. The virtue of the 16-bit adder is that the overflow of a 15-bit sum is readily detectable upon examination of the two high order bits of the sum (see Fig. 6–3). If both of these bits are the same, there is no overflow. If they are different, overflow has occurred with the sign of the highest order bit.

The interface between the 16-bit adder and the 15-bit memory is arranged so that the sign bit of a word coming from memory enters both of the two high order adder columns. These are denoted S_2 and S_1 since they both have the significance of sign bits. When a word is transferred to memory, only one of these two signs can be stored. In the AGC the S_2 bit is stored which is the standard one's complement sign except in the event of overflow, in which case it is the sign of the two operands. This preservation of sign on overflow is an important asset in dealing with carries between component words of multiple-precision numbers.

Multiple-Precision Arithmetic – A short word computer can be effective only if the multiple-precision routines are efficient corresponding to their share of the computer's work load. In the AGC's application there is enough use for multiple-precision arithmetic to warrant consideration in the choice of number system and in the organization of the instruction set. A variety of formats for multiple-precision representation are possible, probably the most common of these is the identical sign representation in which the sign bits of all component words agree. The method used in the AGC allows the signs of the components to be different.

Independent signs arise naturally in multiple-precision addition and subtraction and the identical sign representation is costly because sign recon-

A.	**Sequence Changing**		
1.	Transfer control, set return address	1 MCT	All Memory
2.	Transfer control only	1 MCT	Fixed Only
3.	Four way skip and diminish by one	2 MCT	Erasable
*4.	Branch on zero	1 or 2	Fixed only
*5.	Branch on zero or minus	1 or 2	Fixed only
B.	**Fetching and Storing**		
1.	Clear and add to Accumulator, A	2 MCT	All
2.	Clear and subtract from Accumulator, A	2 MCT	All
*3.	Double clear and add to A and Lower Accumulator, L	3 MCT	All
*4.	Double clear and subtract from A and L	3 MCT	All
5.	Transfer to storage	2 MCT	Erasable
6.	Exchange A with storage	2 MCT	Erasable
7.	Double exchange A and L with storage	3 MCT	Erasable
8.	Exchange L with storage	2 MCT	Erasable
*9.	Exchange Q with storage	2 MCT	Erasable
C.	**Instruction Modification**		
1.	Index (add to next instruction)	2 MCT	Erasable
*2.	Index and extend	2 MCT	All
D.	**Arithmetic and Logic**		
1.	Add to A	2 MCT	All
*2.	Subtract from A	2 MCT	Erasable
3.	Add to Storage and A	2 MCT	Erasable
*4.	Modular subtract from A (mixed number system)	2 MCT	Erasable
5.	Add 1 to storage (Increment)	2 MCT	Erasable
*6.	Increase absolute value of storage by 1 (Augment)	2 MCT	Erasable
*7.	Decrease absolute value of storage by 1 (Diminish)	2 MCT	Erasable
8.	Double add A and L to storage	3 MCT	Erasable
9.	Logical product to A	2 MCT	All
*10.	Multiply; product to A and L	3 MCT	All
*11.	Divide A and L by storage; quotient to A	6 MCT	Erasable
E.	**Input Output**		
*1.	Transfer channel to A	2 MCT	Channels
*2.	Transfer A to channel	2 MCT	Channels
*3.	Logical product (of A and channel) to A	2 MCT	Channels
*4.	Logical product to channel and A	2 MCT	Channels
*5.	Logical sum to A	2 MCT	Channels
*6.	Logical sum to channel and A	2 MCT	Channels
*7.	Exclusive or to A	2 MCT	Channels

*Requires Extend instruction
MCT = Memory Cycle Time

TABLE 6–4 Normal instructions

ciliation is required after every operation. For example, $(+6, +4) + (-4, -6) = (+2, -2)$, a mixed sign representation of $(+1, +8)$. Since addition and subtraction are the most frequent operations it is economical to store the result as it occurs and reconcile signs only when necessary. When overflow occurs in the addition of two components a *one* with the sign of the overflow is carried to the addition of the next higher components. The sum that overflowed retains the sign of its operands. This overflow is termed an interflow to distinguish it from an overflow that arises when the maximum multiple-precision number is exceeded.

For triple and higher orders of precision, multiplication and division become excessively complex, unlike addition and subtraction where the complexity is only linear with the order of precision. Apollo programs do not require greater than double-precision multiplication and division, however. The algorithm for double-precision multiplication is directly applicable to numbers in the independent sign notation. The treatment of interflow is simplified by a double-precision add instruction. Double-precision division is exceptional in that the independent sign notation may not be used; both operands must be made positive in identical sign form and the divisor normalized so that the left-most non-sign bit is *one*. A few triple-precision quantities are used in the AGC. These are added and subtracted using independent sign notation with interflow and overflow features the same as those used for double-precision arithmetic.

Instruction Set – The major goals in the AGC were efficient use of memory, reasonable speed of computing, potential for elegant programming, efficient multiple-precision arithmetic, efficient processing of input and output and reasonable simplicity of the sequence generator. The constraints affecting the order code as a whole were the word length, one's complement notation, parallel data transfer and the characteristics of the editing registers. The following rules governing the design of instructions arose from these goals and constraints: three bits of an instruction word are devoted to operation code, address modification must be convenient and efficient, there should be a multiply instruction yielding a double length product, facility for multiple precision must be available and a Boolean combinatorial operation should be available. These rules are by no means complete, but give a good indication of what kind of instruction set was desired.

The three bits reserved for instruction codes are capable of rendering a selection among eight operations with no further refinement. Two techniques are employed in the AGC to expand the number of operations fourfold. These are called "extension" and "partial codes" respectively. Extension is like using a teletype shift code; when an Extend instruction occurs, it signifies that the next instruction code in sequence is to be interpreted otherwise than normally. By this means, the instruction set could be expanded almost indefinitely at a penalty in speed, for a memory cycle time is required for each extension. In the AGC the size of the instruction set is doubled by an Extend operation, which calls forth the less-often used instructions. For example, code 000 selects the Transfer Control instruction unless it is preceded by an Extend, in which case it selects an Input-Output instruction.

Partial codes are instruction codes which encroach upon the address field. This technique capitalizes upon the essential difference between fixed and

A.	Involuntary		
1.	Transfer to interrupt program, store c (Z) and c(B)	3 MCT	Limited
2.	Increment by 1	1 MCT	Counters
3.	Increment by - 1	1 MCT	Counters
4.	Diminish absolute value by 1	1 MCT	Counters
5.	Shift left	1 MCT	Counters
6.	Shift left and add 1	1 MCT	Counters
B.	Address Dependent		
1.	Resume interrupted program = Index 0017 (octal)	2 MCT	
2.	Extend = Transfer control 0006	1 MCT	
3.	Inhibit interrupt = Transfer control 0004	1 MCT	
4.	Permit interrupt = Transfer control 0003	1 MCT	
5.	Cycle right each access	Address 20 (octal)	
6.	Shift right each access	Address 21 (octal)	
7.	Cycle left each access	Address 22 (octal)	
8.	Shift right seven places each access	Address 23 (octal)	

MCT = Memory Cycle Time

TABLE 6–5 Special instructions

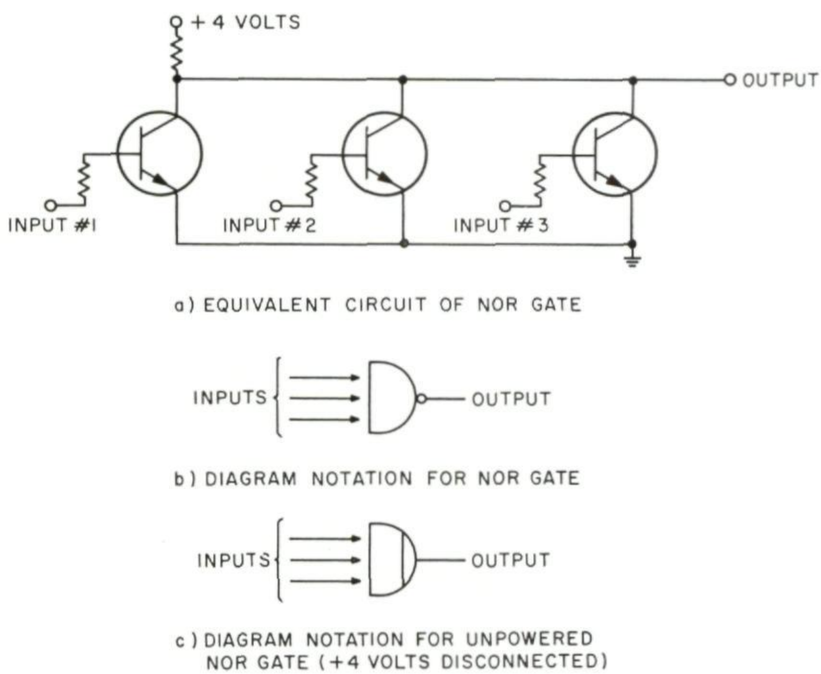

FIG. 6–4 The NOR gate

erasable memory. More specifically, a wider variety of instructions are applicable to erasable than to fixed memory; for example, all instructions which modify the operand register are not fully applicable for fixed memory. Since the fixed memory address field in the AGC is three times as big as the erasable memory field, it is possible to pack three extra erasable memory instructions into that portion of the entire address field. Thus operation code 101 for addresses 0 through 1777 (octal) selects the Index instruction for the erasable memory, whose address field is also 0 through 1777 (octal). The same operation code for addresses 2000–3777 (octal) selects a Double Exchange instruction for erasable memory, whose addresses are obtained by reducing the address modulo 2000 (octal). In a similar way, the Transfer to Storage instruction is selected by the same code for addresses 4000–5777 (octal), and the Exchange A instruction for addresses 6000–7777 (octal), both for erasable memory. Alternatively, the entire fixed memory field may select a different instruction for fixed memory, or else the same instruction may be selected over the entire address field.

Table 6–4 lists the normal AGC instructions. These include facility for double-precision data handling and addition. Many of these instructions are similar to one another and share microprogram steps. Input and output are handled to a large extent by special registers called channels, which are not accessible through the regular address field. In the version of the AGC prior to the present one, this was not true; the input and output registers were addressable for any instruction. Here, the channels are accessible by the input-output instructions alone. A slight extra degree of freedom is provided by making the Lower accumulator (L) and Return address (Q) registers accessible through channels 1 and 2 as well as through regular addresses 1 and 2. This is primarily to allow the programmer to take advantage of the *or* and *exclusive or* input-output instructions.

The remainder of the AGC instructions are involuntary or address dependent, and are listed in Table 6–5. The last four are not really instructions, but are rather editing operations on all words written into the specified four addresses. They are tabulated as instructions only because such operations have instruction status in most computers.

HARDWARE

Logic – The design of the Apollo Guidance Computer began at a time when microcircuits were first being produced. Microcircuits held great promise but were not well enough proven for the design of this computer to be based on them; magnetic core and transistor logic had been used in its immediate ancestry and was scheduled to be used here. Nevertheless, during the first year of design microcircuits were evaluated for possible use in the AGC. When it became clear that microcircuits could be reliably produced with rigid specifications, the decision was made to substitute them for the core-transistor logic. In the course of this change, the power consumption increased by a factor of three but size and weight were reduced by half and performance and speed were doubled. Moreover, though it could not be known at the time, the reliability of the logic hardware was greatly increased.

One of the important decisions made at that time was to confine the use of logic microcircuits to a single type to avoid having to develop successively

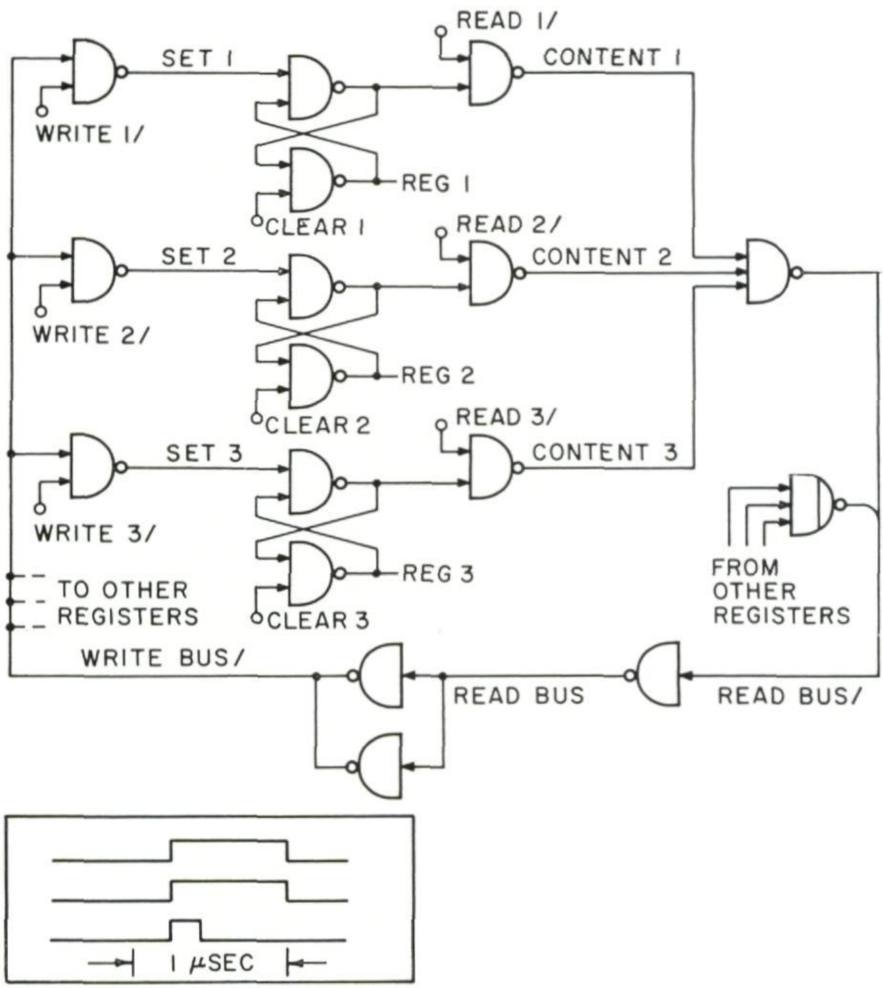

FIG. 6–5 NOR gate circuit resembling one column of AGC central registers

a number of different devices. A logic circuit was required whose operational function was capable of synthesizing all switching functions and which was simple enough to be controllable, testable and producible. The circuit chosen was a NOR gate which employs a configuration known as modified direct-coupled transistor logic (DCTL). Three transistors in parallel, along with four resistors, form a three-input gate with a fan-out capability of approximately 5 and an average propagation delay of about 20 nanoseconds, while dissipating about 12 milliwatts of power. A recent modification of design has resulted in a new unit with approximately the same specifications except for a power dissipation of 5 milliwatts instead of 12. These gates are designed to operate over the temperature range from 0 to 70°C.

The importance of using a single circuit should not be underestimated. Thousands of logic gates are employed in each computer and barring the use of redundancy techniques, every one may be considered critical. Indeed, most redundancy techniques depend on randomness of failures; in general new components and assembly methods introduce failure modes which make erroneous the basic assumptions on which the redundancy is based. High reliability is essential for every gate. It can best be attained by standardization, and can only be demonstrated by the evaluation of large samples (8). Had a second type of logic microcircuit been employed in the AGC, the number of logic elements could have been reduced by about 20%, but it is clear that to have done so would have been false economy, for neither of the two circuits would have accumulated the high mean time to failure and high confidence level that the one NOR-circuit has.

Logic equations expressed in the familiar AND, OR, NOT notation may readily be realized with NOR operators. A two-level and-or expression is realizable in a two-level NOR-circuit. The NOR function of three variables is as follows: $N(x, y, z) = \bar{x}\,\bar{y}\,\bar{z} = \overline{x + y + z}$. An AND function is $A(x, y, z) = x\,y\,z$, and an OR function is $o(x, y, z) = x + y + z$. By comparison, $N(x, y, z) = A(\bar{x}, \bar{y}, \bar{z}) = \overline{o(x, y, z)}$. The NOT operation, or complementation, is the NOR function of one variable i.e. $\bar{x} = N(x)$. Complex Boolean expressions ordinarily arise only in connection with non-sequential or combinational aspects of the computer logic. Sequential operations require storage; and the basic logic storage element is the flip-flop. Two NOR gates form a flip-flop if the output of each is an input to the other and if all other inputs are normally zero. If one of these other inputs is momentarily made equal to *one*, the flip-flop is forced into one state, whereas if a free input on the opposite gate is made equal to *one*, the other state is obtained. Most frequently, the condition for setting a flip-flop to a particular state is that two or more other signals simultaneously take on prescribed values. Detection of such coincidence requires a NOR operation separate from the flip-flop plus any NOR operation required to invert (complement) the inputs.

It is frequently necessary to implement NOR functions of more than three variables and also to be able to drive more than five inputs with a single output. For these reasons, NOR gates may be combined so as to increase either the input (fan-in) capacity, or the output (fan-out) capacity, or both. Fan-in is increased by connecting the outputs of unpowered gates to the output of a powered gate. This provides a fan-in of three times the total number of gates. Fan-out is increased by connecting the outputs of powered

gates together. Both fan-in and fan-out are increased, but the fan-in is not available because it is necessary to have each input signal connected to as many inputs in common as there are powered gates connected together. This is done in order to be able to saturate the transistors whose current gain is limited. By simultaneous application of these techniques however, it is possible to increase both fan-in and fan-out at the same time.

An illustrative example of the employment of NOR logic in the AGC is provided by the central register flip-flops. Digits are transferred from one register to another via common set of wires called write buses. The sending and receiving flip-flops are selected by read and write pulses, respectively, applied to gates which either set or interrogate the flip-flops of the corresponding register. Figure 6–5 shows a hypothetical set of three flip-flops similar to those in one column of the AGC central register section. Dashed lines imply the existence of other registers than the three shown. Diagonal lines, or slashes, after signal names denote inverse polarity. Thus WRITE BUS/ is normally in the *one* state, and changes to *zero* while transferring a *one*. Suppose REG 1 contains a *one*, i.e. the top gate of its flip-flop has an output of *zero*. At the time that the READ 1/ signal goes to *zero* from its normally *one* state, the output of the read gate, CONTENT 1, becomes a *one*. This propagates through a read bus fan-in and an inverter and fan-out amplifier to make WRITE BUS/ become *zero*. Suppose that WRITE 2/ is made *zero* concurrently with READ 1/. Then the coincidence of *zero*'s at the write gate of REG 2 generates a *one* at the input to the upper gate of its flip-flop, thus setting the bit to *one*.

If REG 1 had contained a *zero*, the write bus would have remained at *one*, and no setting input would have appeared at the upper gate of REG 2. The CLEAR 2 pulse, which always occurs during the first half of WRITE 2, would have forced the flip-flop to the *zero* state, where it would remain; whereas when a *one* is transferred, the SET 2 signal persists after the CLEAR 2, and thus forces the register back to the *one* state. Thus the simultaneous occurrence of READ 1/, WRITE 2/, and the short CLEAR 2 pulses transfer the content of REG 1 to REG 2. Only the content of REG 2 may be altered in the process. REG 1 and REG 3 retain their original contents. An instance of gates being used to increase fan-in is shown where several CONTENT signals are mixed together to form the signal READ BUS/. An increase in fan-out is achieved by the two gates connected in parallel to form the signal WRITE BUS/.

The main problem of mechanical design in guidance computer logic is the creation of signal interconnections, indeed approximately three-quarters of the volume of the AGC is used for this purpose. Interconnections are primarily of two types: between modules by wrapped wire, and within a module by welded matrix.

The carrier into which all modules are inserted is called a "tray". The AGC comprises two trays; one for logic, power supply and interface modules, and the other for memory and ancillary circuit modules. The 15000 jacks on the tray into which signal pins are inserted pass through the tray and extend out the other side in the form of posts with square cross-sections. Interconnections between pins are made by wires whose ends are tightly wrapped around the posts without the use of any further contact mechanism

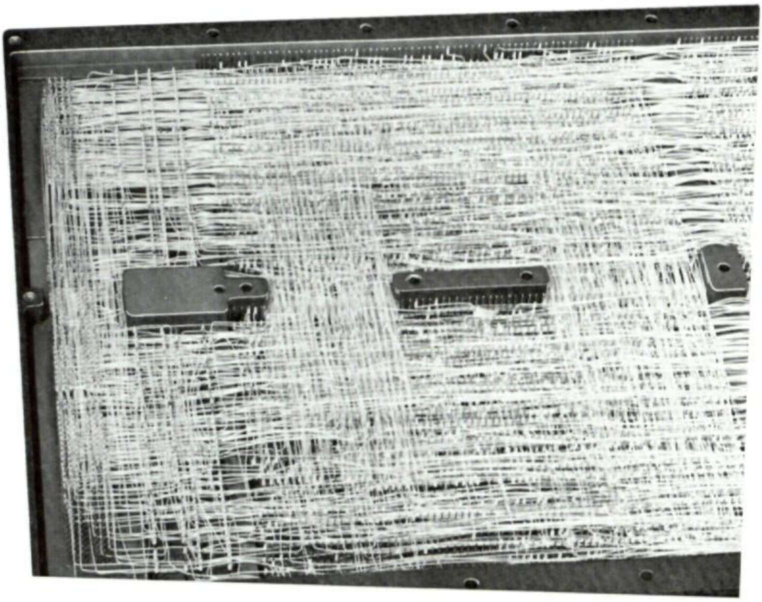

Fig. 6–6 Wire-wrapped tray connections

Fig. 6–7 Logic module containing 120 microcircuit units

such as solder or welds. This method has several advantages; it is executed by a machine, which requires only a few seconds per wire, it is controlled by a punched card input, it can easily be altered if a change is desired, wires can be run point to point if desired and the reliability of the connection is extremely high since there is no single point where bending stress is applied. Moreover, it is compatible with hand wiring, which is required wherever wires are twisted together to protect low level signals or where heavy gauge wire is needed in order to accommodate high currents.

In the AGC, one of the basic goals has been to make the electronic circuits in small pieces which are easily installed and removed, for the sake of producibility, testing, easy diagnosis and economical maintenance. This can only be realized in so far as it does not excessively degrade the overall packaging density of the computer for volume is, of course, critically limited in the spacecraft. It was found expedient to make twenty-four modules each containing 120 microcircuit units, separated into two independent groups of sixty. The 12-milliwatt gates are packaged one to a unit; sixty gates are connected together into a circuit with seventy-two pins to bring signals in and out. The more recent 5-milliwatt gates are packaged two to a unit, because of their less severe heat transfer requirement. These are organized into subgroups of thirty, such that sixty gates are again connected together; and seventy-two pins are again available to each sixty gates. The modules are the same size, so that the low-power units are packaged with double the density of the high power units. Accordingly, the density of pins and interconnections has been doubled along with that of the gates.

The main method of connection internal to the module is by matrix. Gates are disposed in a single row within each sixty-gate sub-group. An array of vertical wires, at right angles to the row of gates provides access to every connection to the gates. Horizontal conductors (parallel to the row of gates) carry signals from gate to gate and from gate to pin. Connections between horizontal and vertical matrix members as well as between matrix members and gate connection pins are made by a spot welding process. The process was developed in an earlier guidance computer project in order to eliminate the problems of cold solder joints.

Power distribution is a special problem in this computer. The current drawn by the gates is about 6 amperes for low power gates and about 13 amperes for high power. For the sake of efficiency, these large currents must be distributed from the power supply to the logic modules with very little d.c. voltage drop. Moreover, the current return, or zero-volt distribution must not sustain any a.c. voltages of such a frequency or amplitude as to turn on or turn off a gate inadvertently. This is all accomplished by building an interlaced gridwork of heavy conductors upon the terminal posts of the tray. Each group of sixty gates shares a ground plane in a module which is brought out at three equally spaced places to connect to this gridwork, which provides multiple paths for return current much the same as a ground plane. The other power line, the positive voltage, is distributed by a gridwork circuit to two points on the power bus shared in a module by each sixty-gate group.

The main tray structure of the AGC is an aluminum alloy frame into which the modules are affixed by jacking screws, providing a good thermal

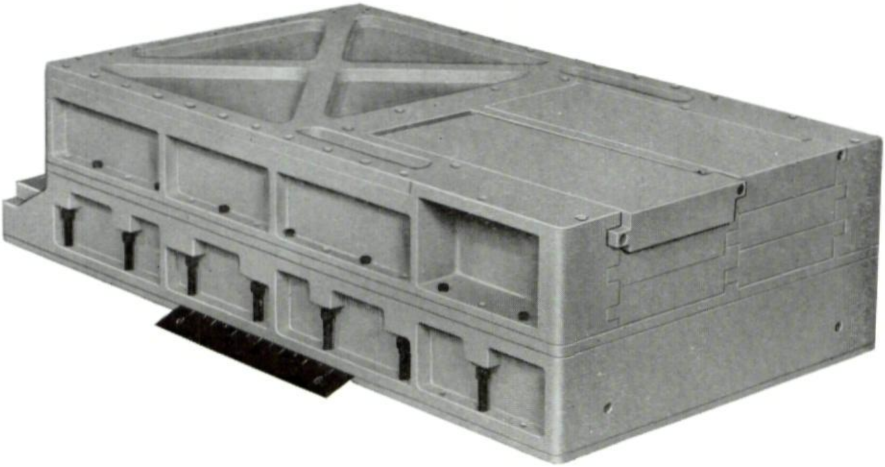

Fig. 6–8 AGC mockup – front view

Fig. 6–9 AGC mockup – rear view

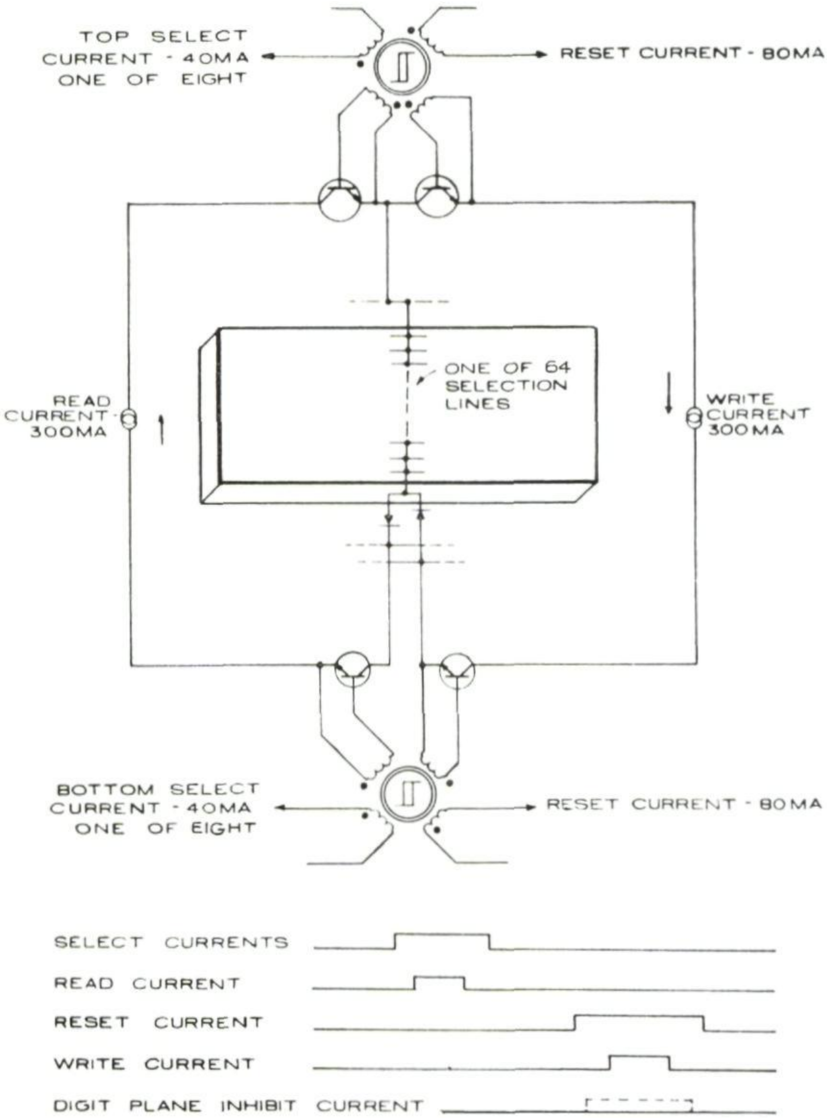

FIG. 6–10 Erasable memory current switching

path between modules and tray. The tray in turn is screwed to a cold plate where heat is removed. A model of the AGC is shown in Fig. 6–8 and Fig. 6–9. The front is shown in the first figure, with the outlines of the six fixed memory modules just visible. One of the six is partially extracted. The second figure shows the rear and the connector deck with system and test connector covers. The ruler is calibrated in inches (1 inch = 2.54 cm).

Memory – The erasable memory of the AGC was inherited from its core-transistor logic ancestor (9). It is a conventional coincident-current ferrite core array whose ferrite compound yields a combination of high squareness and a comparatively low sensitivity to temperature. Moreover, the silicon transistor circuits which drive this memory vary their outputs with temperature in such a way as to match the requirements of the cores over a wide range, from 0°C to 70°C. Coincident current selection affords an economy in selection circuitry at the expense of speed in comparison with linear (word) selection. This is advantageous to the AGC, where the memory cycle time is already long, largely due to the fixed memory. The 2048 word array is wired in 32×64 planes with no splices in the wires for highest reliability. The planes are folded to fit into a 9 cubic inch module along with two diodes for each select line. Bi-directional currents are generated in each selection wire by a double-ended transistor switching network. The selection of one wire in 32 is made by twelve switch circuits in an 8×4 array; the selection of one wire in 64 is made in an 8×8 array. The operation of the switching network is illustrated in Fig. 6–10. The transistors are driven by magnetic cores, which offer two advantages over all-transistor circuits; small size and storage of address for data regeneration. Again, this circuit economy is realized at the expense of speed. The timing of the currents which operate the switch cores is based on the duration of the write current in the memory array, which is 2 microseconds. Two current drivers with controlled rise times, one for reading and one for writing, are used on each of the two drive select networks. Sixteen more such drivers are used to drive the digit lines which control the writing phase of the memory cycle. Current amplitude is governed by the forward voltage drop across a silicon junction, so that temperature compensation is achieved without any circuit complications for changes in coercive force.

The output signal from the memory cores has an amplitude of about 50 millivolts. Transformer coupling to the sense amplifiers provides common mode noise rejection and a voltage gain of two. The sense amplifiers have a differential first stage operated in the linear or class A mode. A second stage provides threshold discrimination, rectification and gating, or strobing. Three reference voltages are generated for the sense amplifiers by a circuit whose temperature characteristics compensate for amplitude and noise changes in the memory.

The sense amplifiers are implemented as integrated circuits in order to realize a number of advantages inherent in single-chip semiconductor circuits. Differential amplifiers pose a special problem in component matching both internal to a single amplifier in achieving balance and among a group of amplifiers in achieving uniform behaviour for common reference voltages. In discrete-component amplifiers a great deal of time and effort go to specifying and selecting matching sets of circuit components. In an integrated

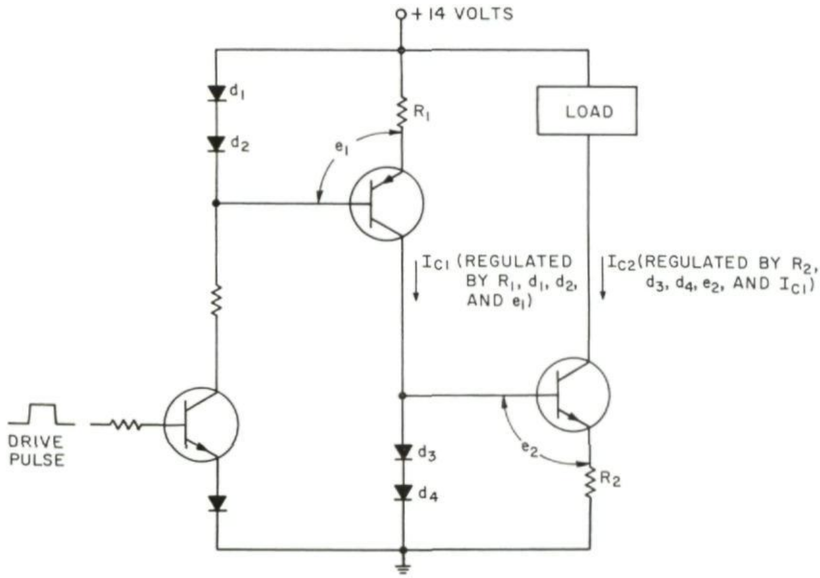

Fig. 6–11 Regulated pulsed current driver circuit

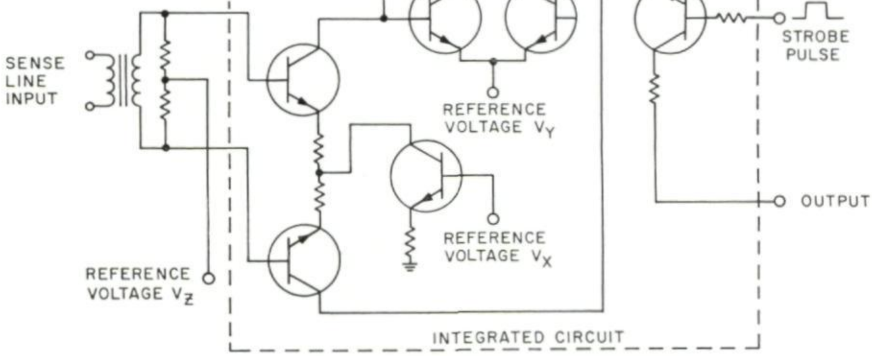

Fig. 6–12 Sense amplifier circuit

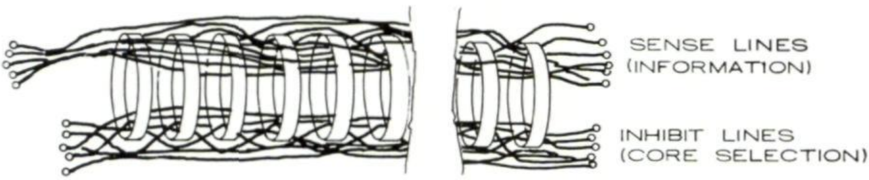

FIG. 6–13 Inhibit and sense lines through a rope, conceptual drawing

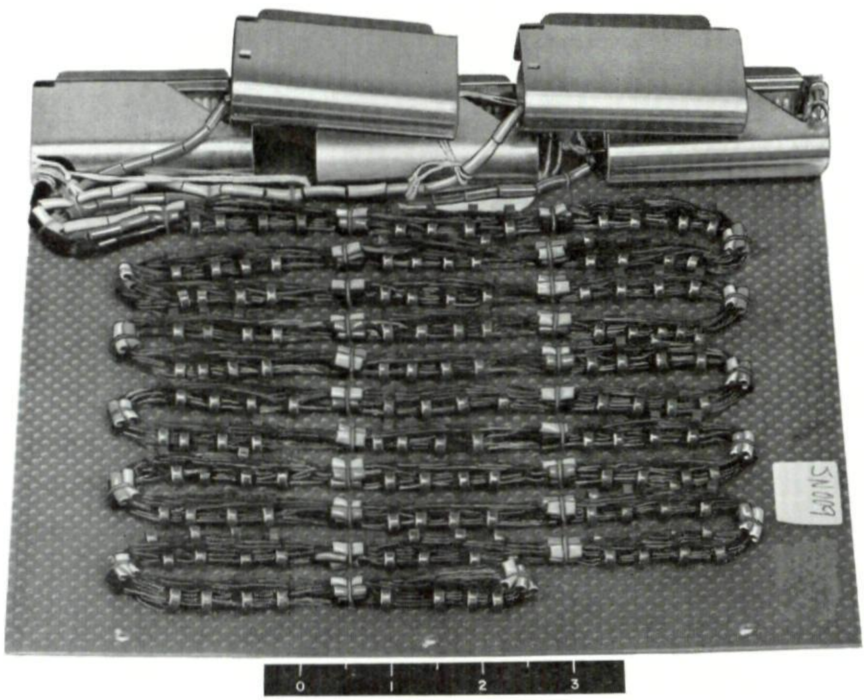

FIG. 6–14 Early model of core rope

FIG. 6–15 Prototype core rope, 1963

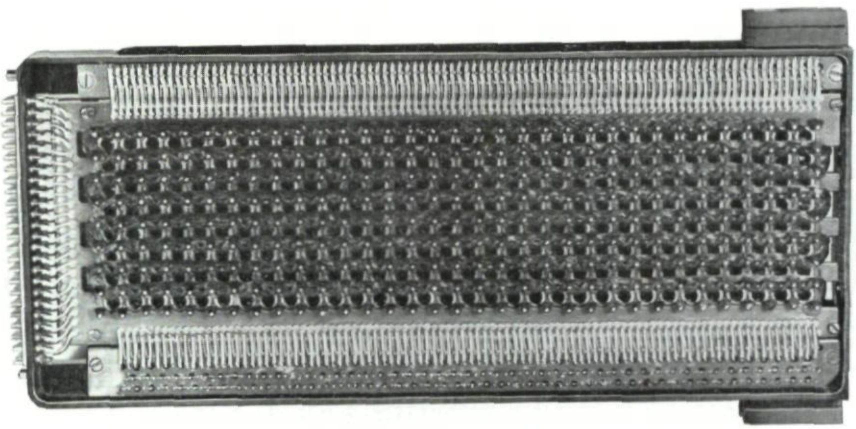

FIG. 6–16 AGC core rope module

circuit, however, balance is readily achieved owing to the extremely close match between transistors on the same silicon chip exposed to the same chemical processes. A similar situation holds for uniformity from one amplifier to another. Within the same batch, amplifiers tend to be very much alike, their differences being easily compensated by external trimming resistors. The efforts expended in specifying the integrated sense amplifier and in a program of reliability testing are little if any more costly than for discrete component amplifiers. Indeed, for a given degree of matching, the cost may be expected to be lower for the integrated circuit.

Considerably more complex than the integrated NOR gate used in the AGC, the sense amplifier is used in far less number (32 per computer), so that it is feasible to test and screen each amplifier more comprehensively than a NOR gate, of which there are over 5 000 in each AGC. Performance of the sense amplifiers has been superior, with no spontaneous failures recorded in about a million operational device-hours as of this writing. Their small size is advantageous in obtaining temperature tracking, since it is not difficult to keep them at a temperature close to that of the memory cores. Where sense amplifiers have historically been the "weak link" of computer memory systems, the integrated sense amplifier has already been proven to be at least on a par with the rest of the memory electronics.

The AGC fixed memory is of the transformer type and was developed at M.I.T., (5, 10). It is designated a "core rope" memory owing to the physical resemblance of early models to lengths of rope. Incorporated into its wiring structure is an address decoding property, because of which its cycle time is not as short as that of some other transformer memories whose address decoding is external. The resulting bit density is extremely high; approximately 1 500 bits per cubic inch (or about 100 bits per cubic centimeter) including all driving and sensing electronics, interconnections and packaging hardware. This high density of storage is achieved by "storing" a large number of bits in each magnetic core. A stored bit is a *one* whenever a sense wire threads a core and is a *zero* whenever it fails to thread a core. The total number of bits is the number of cores multiplied by the number of sense lines having a chance to thread the cores. The AGC's memory is composed of six modules. Each module contains 512 cores and 192 sense lines and hence contains $192 \times 98\,304$ bits of information. This information is permanently wired; once the module has been manufactured not a single bit can be changed, either intentionally or unintentionally, except by physical destruction or by failure of one or more of a number of semiconductor diodes whose functions are described in the following paragraph.

In the operation of the rope memory a core is switched in a module, thus inducing a voltage drop in every sense line which threads the core. Only one word is read at a time so that of the 192 sense lines, only 16 are connected to the sense amplifiers to detect which have voltage drops and hence store *one*'s. Thus it is that each core stores 12 words; and within each module a switching network is included in order to transmit no more than one of the 12 to the module's output terminals. The principle of the switching network is illustrated in Fig. 6–17. It consists of diodes and resistors connected so as to block the sense line's output when sense line diodes are reverse-biased as in the case of d5 and d6, and to transmit it when the sense line diodes are for-

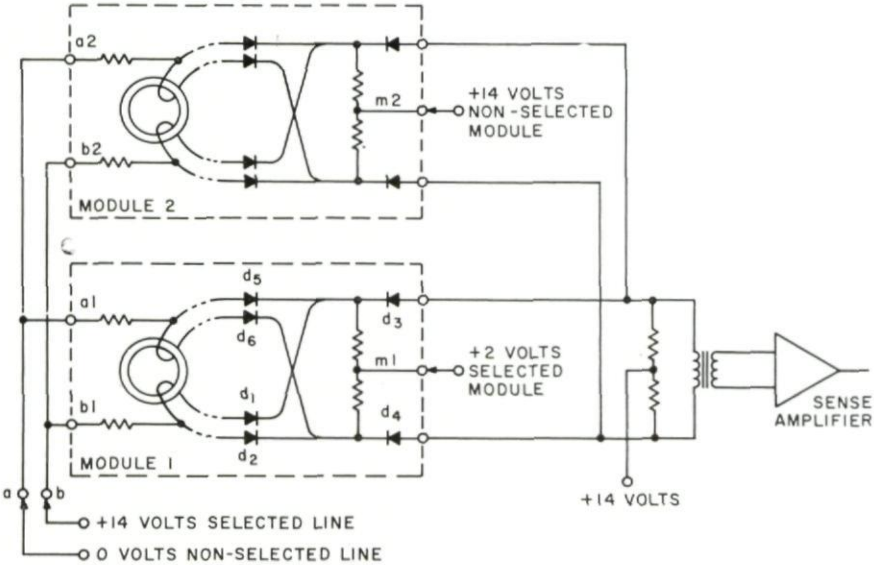

FIG. 6–17 Simplified rope sense line switching diagram

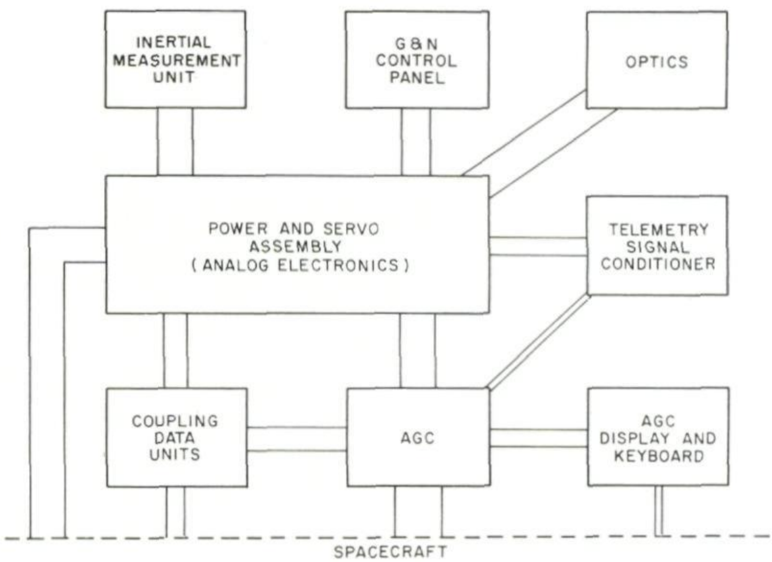

FIG. 6–18 Simplified G and N interconnection diagram

ward biased, as in the case of d1 and d2. A second-stage switch composed of d3 and d4 is used to select one of six modules' outputs to be transmitted to the sense amplifiers. Only the selected line in the selected module is transmitted; all others are blocked by one or two sets of reverse-biased diodes. All of these selection diodes are physically located in the rope modules to minimize the number of terminals necessary for each module. The application of selection voltages to the line and module select terminals is a part of the address decoding which is external to the rope; the balance is internal.

The means by which a single core in a module is caused to switch is as follows: First, a switching current is applied, which attempts to set 128 cores. Four such current lines serve a 512 core module. Second, an inhibit current is simultaneously applied to either the first half or the second half of each group of 128 cores. Two inhibit lines exist for this purpose. Third, another inhibit current is simultaneously applied to either the first or the second half of each half-group. Two more inhibit lines exist for this purpose. Fourth, six more pairs of inhibit lines exist for the purpose of reducing the uninhibited core groups successively by halves until only one core is left uninhibited. One member of each inhibit pair carries current at a time; there are 8 pairs in all to select among 2^7 cores, of which 7 pairs correspond to the 7 low order address bits. The eighth pair is logically redundant, being selected by the parity of the address. The redundancy is used to reduce the amount of current required in each inhibit line. After the selected core has switched, a reset current is passed through all cores. Only the core which was just set will change state, and the sense amplifiers may be gated on during the set or the reset part of the cycle to read information out of the memory. The noise level during reset is lower than during set for a number of reasons, but the access time, which is the time it takes to read the memory after the address is available, is longer that way. Both ways have been used in the AGC; the newer design uses the longer access time and produces the address earlier to make up for it.

INTERFACE METHODS

General – Information transfer between the AGC and its environment occupies a substantial fraction of the computer's hardware and its time budget. An attempt has been made to minimize the number of different types of circuit involved. This minimizes engineering effort and makes the computer more easily produced and tested. The impact of this design philosophy on the system has been substantial and it came about only by active co-operation between subsystem design and system integration groups. The nature of information handled through the interfaces is varied. In some cases computer words are transferred bodily into and out of the computer. Pre-launch and in-flight radio links are maintained between the computer and ground control.

Owing to the great difference in data rates between up and down directions, the mechanizations differ considerably. The down link operates at a relatively high rate (50 AGC words or 800 bits per second) and is made so as to occupy a minimum of the computer's time budget. The circuit is relatively expensive. It serializes a word stored in parallel in a flip-flop register and, upon command, sends the bits in a burst to the central timing system of

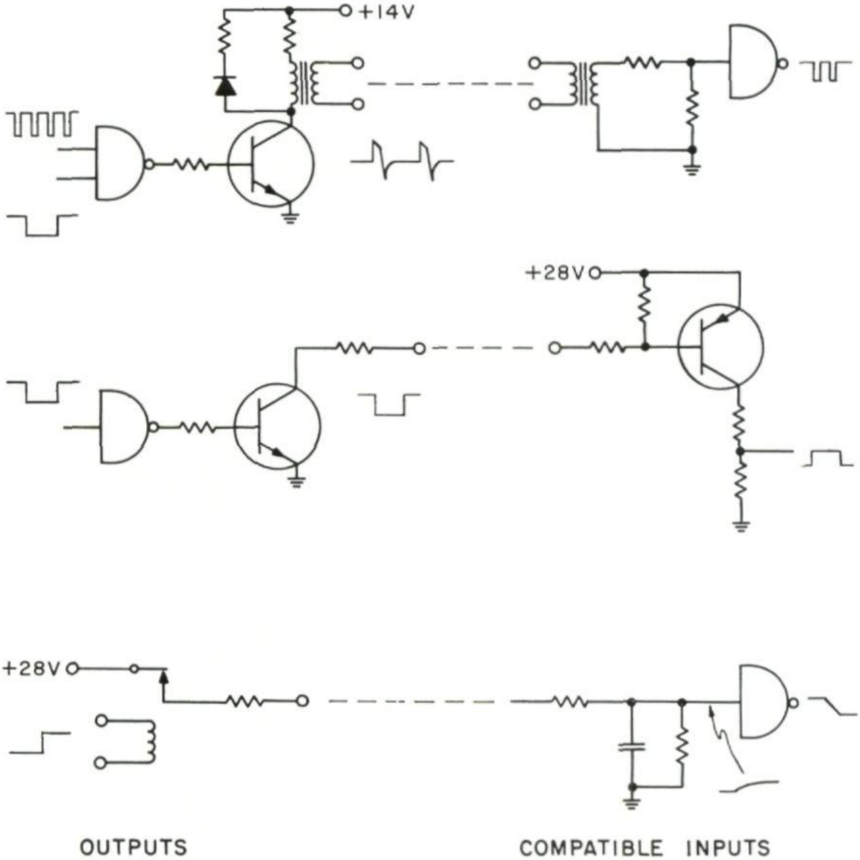

FIG. 6–19 Examples of AGC interface circuits

Number of Discrete Inputs	73
Number of Input Pulses (Serial and Incremental)	33
Number of DC Output Discretes	68
Number of Variable Pulsed Outputs (Serial, Incremental, and Discrete)	43
Number of Fixed Pulsed Outputs	10
Number of Connector Wires	365

TABLE 6–6 AGC interface summary

the spacecraft. The up link uses memory cycles to effect a serial to parallel conversion of data. Each bit received requires a memory cycle, a maximum of 160 bits per second are allowed. The cost in equipment is small. The same procedure used in the up link for serial to parallel conversion is used for whole word transfers out of the computer to digital spacecraft display units. It is also used to accept data from the radar measurement subsystem and can be used if desired to communicate between the two AGC's in the command module and the LEM.

Incremental information transfer is similar to serial information transfer in that a sequence of pulses is transmitted over a single channel. It differs in that each pulse represents the same value, or weight, as opposed to serial transfer, where two adjacent pulses differ in weight by a factor of two and where the concept of positional notation is employed. An incremental receiver counts pulses to form a word, where a serial receiver shifts pulses to form a word. Incremental information transfer was adopted as a means of analog data transmission in order to maintain high precision and standardization. In the conversion of gimbal angles and optics angles, an intermediate transformation to incremental form is made in the Coupling Data Units (CDU's), the inputs to which are electrical resolvers. The alternative to having this extra conversion is to measure the time difference between zero crossings of resolver outputs, to do which may involve equally "expensive" hardware. The Apollo accelerometers are incremental by nature, producing a pulse output to the computer for each unit change in velocity. Incremental transfer is also used for angle commands from the computer to the gyros and the CDU's and for thrust control and certain display functions in the spacecraft. Pulses are sent in groups or "bursts" at a fixed rate. Pulse rate multipliers would be required in order to send smooth, continuous pulse trains, and these are more costly in equipment.

Discrete signals are individual or small groups of binary digits which give commands or feedback for discrete actions, such as switch closures, mission phase changes, jet firings, display initiations and many other similar controlled events. The display portion of the computer communicates with the computer proper by discrete signals in groups which carry encoded information. Serial transmission might be suitable for this communication, but would be costlier owing to the small number of bits involved. The computer is the primary source of timing signals for all spacecraft systems; and within the guidance and navigation system it furnishes in the neighborhood of twenty time pulse signals to various subsystems.

The development of the Apollo Guidance system has followed a number of principles which reflect experience gained in previous missile-borne control systems: electrical isolation and asynchronism. Electrical isolation is an important point which has both electrical and logical implications. The computer is connected to the power supply return at a single place thus avoiding "ground loops". Isolation of interface signals is accomplished by transformer coupling, by switch closure (relays), or by a high resistance d.c. current signal. Input and output circuits are designed so that no damage can be caused by improper connections at the interface, such as short circuits to ground. The ability to accept asynchronous inputs, i.e. those not related to computer timing signals, is desirable because it affords a design with

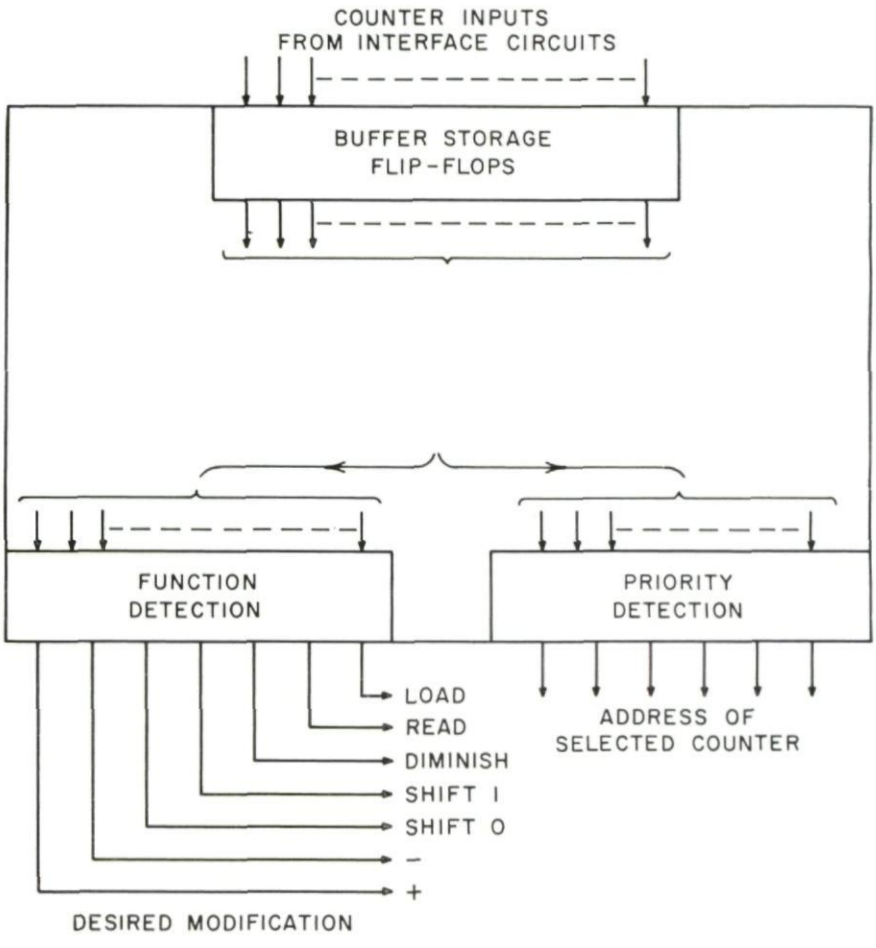

FIG. 6–20 Structure of counter priority circuit

a minimum of reference to signals outside the computer and reduces the number of signals across the interface. This principle is particularly important for signals whose functions are to interrupt normal program sequences.

Inputs – Incremental and serial inputs are received in special erasable memory cells called "counter registers". They are made special by the fact that pulses received by the computer cause short interruptions of the program sequence during which one of these registers is interrogated and modified. Just which counter register is involved and what the modification to its contents is are determined by the particular input being responded to. Since there are twenty-nine of these registers, some provision must be made to accommodate simultaneous requests for servicing several counter registers. The circuit which accomplishes this and in addition satisfies the principle of asynchronism is known as the "Counter Priority" circuit. This circuit stores incoming pulses until they can be processed. If more than one request is pending, preference is given to the one for the counter register whose address is lowest.

When the "Counter Increment" cycle begins, the priority circuit delivers to the S register the address of the counter register having the outstanding request of highest priority. At about the same time, the choice is made as to how the counter's contents will be modified when they are obtained. This choice is based upon the source of the request. The counter word is shifted if it is one of the serial data receiving counters. If the "one" input received the request, a low order *one* is added after shifting; if the "zero" input received the request nothing is added. When the register is full, a program interrupt is requested. For a counter which is an incremental receiver, a low order plus *one* or minus *one* is added, depending upon whether the positive or negative requesting input was received. Since counter words are in the erasable memory, they are always readily accessible by any program. Each increment or shift requires a memory cycle for its execution, so the aggregate counting rate has to be limited in order to avoid an excessive use of the computer's time budget. In some instances, this requires having a logic circuit between the interface and the priority circuit which prevents the input pulse rate from exceeding a chosen level.

Two types of discrete inputs to the computer are distinguished, interrupting and non-interrupting, the latter class being much larger than the former. Non-interrupting discrete inputs are signals which can be interrogated by input-output channel instructions. They are mechanized either as d.c. inputs through a filter to a logic gate, or as a.c. signals, transformer coupled to a flip-flop which is reset after interrogation. Interrupting inputs, in addition to appearing where they can be interrogated, announce their presence to the computer's sequence generator by initiating a program interrupt. A priority circuit similar to the Counter Priority circuit buffers the asynchronism of the inputs and resolves ambiguities caused by simultaneous interrupt requests. At the earliest permissible time, the Interrupt Priority circuit forces a transfer of control to a particular address, where the computer program interrogates the appropriate inputs and initiates any necessary action. The original program is then resumed at the point where it was interrupted. Interrupt programs never exceed a few milliseconds in running time.

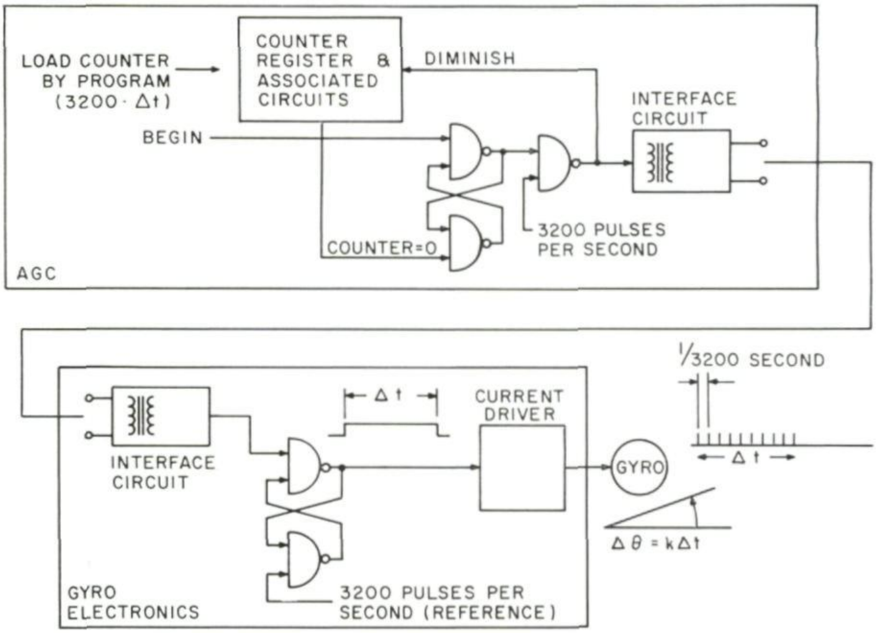

FIG. 6–21 Digital-to-Analog conversion by time duration of precision current

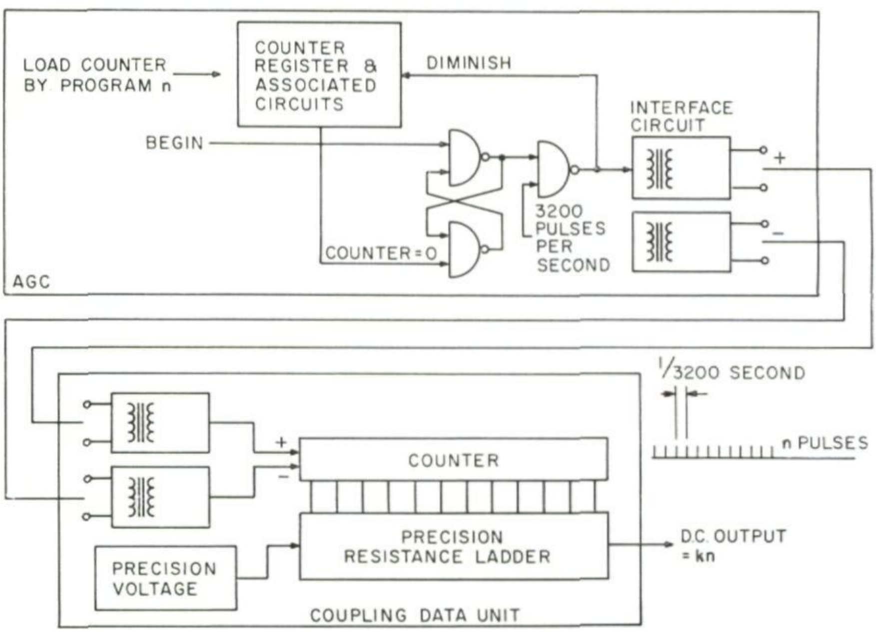

FIG. 6–22 Digital-to-Analog conversion by resistance ladder

Purpose	Serial or Incremental	Nature of Signal	Maximum Rate	Implementation
Digital down data link	S	50 bursts of 40 pulses each	51.2KC	Special circuit
Digital up data link	S	10 or fewer bursts of 16 pulses each	1.0KC	Counter increment
Digital cross links	S	10 or fewer bursts of 16 pulses each	3.2KC	Counter increment
Altitude display	S	2 or fewer bursts of 16 pulses each	3.2KC	Counter increment
Radar data link	S	10 or fewer bursts of 16 pulses each	3.2KC	Counter increment
Gimbal and optics angles	I	All rates to maximum	6.4KC	Counter increment
PIPA velocity increments	I	All rates 0 to maximum	3.2KC	Counter increment
Gyro torquing	I	Occasional bursts of 0 to 2^{14} pulses	3.2KC	Counter increment
Engine thrust control	I	Occasional bursts of 0 to 2^{11} pulses	3.2KC	Counter increment
Engine steering	I	Occasional bursts of 0 to 2^{11} pulses	3.2KC	Counter increment

TABLE 6–7 Partial list of serial and incremental interface characteristics

Fig. 6–23 AGC Display and keyboard

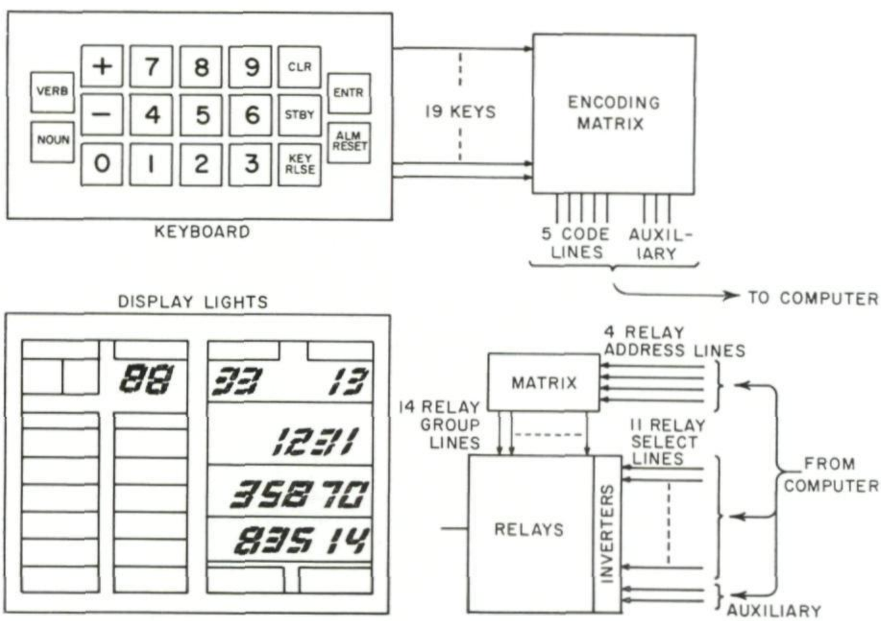

Fig. 6–24 Block diagram of AGC display and keyboard unit

Outputs – With one major exception, the AGC uses its counter register processing facility to make all conversions from parallel words to serial and incremental pulse trains. The exception is the down data link circuit mentioned previously, where a rather costly circuit is used so that the high bit rate will not detract from the time budget. Serial outputs originate from counter registers which contain the word to be transmitted. Fifteen successive shifting requests are applied to the Counter Priority circuit; each time an overflow occurs during the shifting process, a *one* pulse is sent to a transformer output circuit. If no overflow occurs, a pulse representing a *zero* is sent to another output. This is a self-timing form of serial transmission, and is fully compatible with the serial input counter circuits.

Incremental transmission is made by placing a number in an output counter register and activating the Counter Priority circuit at a fixed rate of 3 200 times per second. Each time the counter is processed, the number in the counter register is diminished by a low order *one* of such a sign that the register's contents approach zero. An output pulse is generated concurrently each time on one of two lines, depending on the sign of the number in the counter register. When the number has reached zero, the periodic activation of the Counter Priority circuit ceases and the pulse burst terminates. Bursts of anywhere from one to 1 6384 pulses can be generated this way.

Two forms of digital-to-incremental-to-analog conversion are used in the Apollo Guidance Equipment. The simpler of the two is used for gyro torquing. During an output pulse burst, a precision current source is gated on so that an amount of charge proportional to the desired angle change is forced through the torquing element. A single precision element is used for this form of conversion, but external storage is required for the result. In this case the storage is in the mechanical gyro angle. The second form uses a counting flip-flop register and a resistance ladder. The number in the register controls the switching of a set of precision resistors in an operational amplifier network such that the amplifier output is proportional to that number. These ladder networks are located physically in the Coupling Data Units. An incremental form of information transfer from the computer to the Coupling Data Units is used in order to minimize the interface. Several precision elements are needed for this kind of conversion but no external storage is needed. Thus these analog signals are available as voltages for driving such equipment as attitude displays and steering gimbals for a rocket engine.

Discrete outputs are controlled either directly or indirectly by program. Typically, a discrete output is turned on by placing a *one* in the proper bit position of an output channel, which sets a flip-flop. If the output is transformer coupled, the flip-flop signal drives a transistor output circuit. For higher power levels, the transistor output circuit drives a relay located in the Display and Keyboard unit and the relay's contacts are connected to the interface. Fixed outputs are steady pulse trains which are used to synchronize other equipment. Nearly all of these are transformer coupled and are generated simply by driving the transformer circuit with the appropriate pulse signal.

Display and Keyboard – The Display and Keyboard unit (abbreviated DSKY) is in some respects like an integral computer part, yet it is operated with the same interface circuits used for connection to other subsystems and

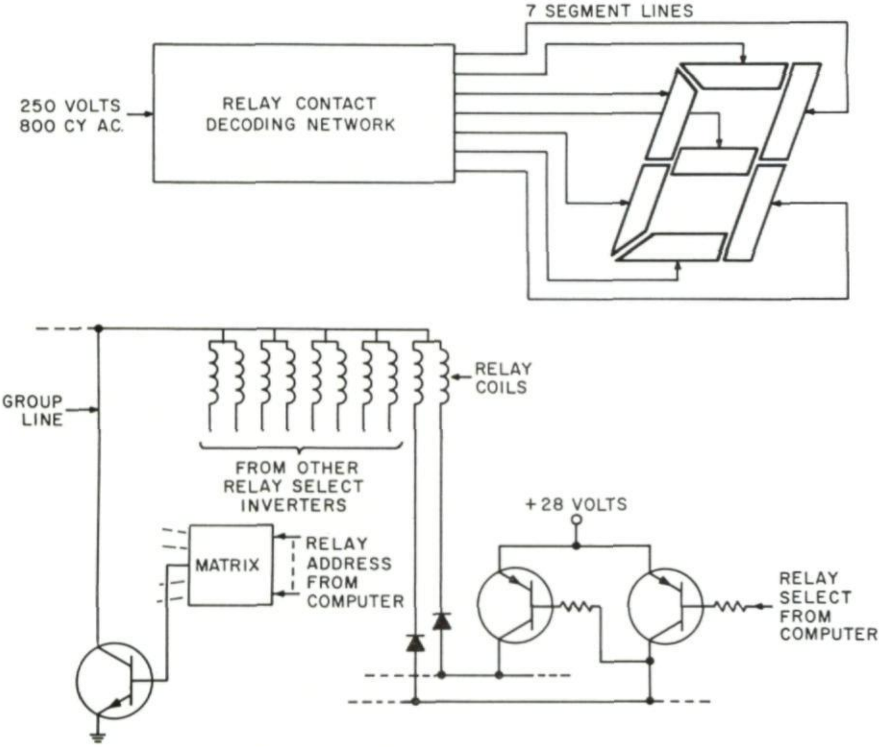

Fig. 6–25 Display circuit scheme

DP = double precision

Operator	Average Execution Time, Milliseconds
DP Add	0.66
DP Subtract	0.66
DP Multiply	1.1
DP Divide	2.5
DP Sine	5.6
DP Cosine	5.8
DP Arc Sine	9.3
DP Arc Cosine	9.1
DP Square Root	1.9
DP Square	0.76
DP Vector Add	0.92
DP Vector Subtract	0.92
DP Vector x Matrix	9.0
DP Matrix x Vector	9.0
DP Vector x Scaler	3.3
DP Vector Cross Product	5.0
DP Vector Dot Product	3.1

Table 6–8 Partial list of interpretive operators

systems. Since it serves as the channel for human communication with the computer it needs a rather high peak data rate without either being very large in itself or having overly many wires between itself and the computer located a few meters distant along a cable. The principal part of the display is the set of three light registers, each containing five decimal digits composed of electroluminescent segmented numerical lights. Five digits are used so that an AGC word of 15 bits can be displayed in one light register by five octal digits. No fewer than three registers are used because of the frequent need to display the three components of a vector. No more than three are used because the extra space and weight penalty cannot be justified. In addition to the numerical lights, a sign position is included in each light register. The convention is used that when a sign appears, the number is to be interpreted as decimal. Otherwise it is taken to be octal.

Electroluminescent lights are small and easy to read, and require relatively little power. They are driven by an 800 cycle alternating voltage supply, switched by miniature latching relays. These have a substantial power advantage over the equivalent electronic circuitry. The contacts, well suited to the high a.c. voltage, are used for decoding, while the latching action provides a storage function. Both latching and non-latching relays are used for interfaces with other subsystems and systems and are located in the DSKY's where they share driving circuits with the light register relays. A double-ended selection matrix is used for actuating the relays. This is organized so that one of fourteen groups of eleven relays is set at a time. Eleven signals are required from the computer to govern the configuration of the eleven relays in a group and four more bits are used to select one group out of fourteen, making fifteen bits. The fact that this is the size of an AGC word is not entirely coincidental. This arrangement allows one word in the DSKY output channel to control enough relays to light two numbers in a light register and one stroke of a sign.

Digits are entered into the computer from a keyboard of nineteen push buttons including the ten decimal digits, plus and minus and a number of auxiliary items. No more than one key is depressed at a time, so the nineteen key functions can be encoded into five signals. This is done by a diode matrix in the keyboard section of the DSKY. In order that each key depression can be quickly gathered and interpreted, the key code inputs to the computer are of the interrupting type. The key input channel is interrogated by the keyboard interrupt program, which also makes a request to the computer's executive program to process the character at the earliest opportunity. A "trap" circuit logically differentiates the leading edge of the key code signal so that no more than one interrupt is made for each depression of a key. This trap circuit is reset by a signal through all of the normally closed contacts of the keys; the reset signal is present only when all keys are released. Problems from key contact bounce are avoided by having flip-flops at the input channel to receive the key code signals.

In addition to the three light registers, the display has other digit displays labeled verb, noun, and program. The keyboard has keys labeled verb, noun, enter, and clear as well as three others. These are used to enable concise yet flexible communication between man and computer. Commands and requests are made in the form of sentences each with an object and an action,

such as "display velocity" or "load desired angle". The first is typical of a command from man to machine; the second is typical of a request from machine to man. The DSKY is designed to transmit such simple commands and requests made up of a limited vocabulary of 63 actions, or "verbs" and 63 objects, or "nouns". These verbs and nouns are, of course, displayed by number rather than by written word; so it is necessary to learn them or else to have a reference document at hand. To command the computer, the operator depresses the verb key followed by two octal digit keys. This enters the desired verb into the computer, where it is stored and also sent back to the DSKY to be displayed in the verb lights. The operator next enters the desired noun in similar fashion using the noun key, and it is displayed in the noun lights. When the verb and noun are specified, the enter key is depressed, whereupon the computer begins to take action on the command.

When the computer requests action from the operator, a verb and a noun are displayed in the lights and a relay is closed which causes the verb and noun lights to flash on and off so as to attract the operator's attention and inform him that the verb and noun are of computer origin. To illustrate the usefulness of the requesting mode, consider the procedure for loading a set of three desired angles for the IMU gimbals. The operator keys in the verb and noun numbers for "load 3 components, IMU gimbal angles". When the enter key is depressed, the computer requests that the first angle be keyed in by flashing and changing the verb and noun lights to read "load first component, IMU gimbal angles". Now the operator keys in the angle digits, and as he does so the digits appear in light register number one. When all five digits have been keyed, the enter key is depressed. The verb and noun lights continue to flash but call for the second component; when it has been keyed and entered, they call for the third component. When the third component has been entered, the flashing stops, indicating that all requests have been responded. If a mistake in keying is observed, the clear key allows the operator to change any of the three angles previously keyed until the third angle has been entered.

Program lights give the operator an indication showing what major programs the computer is running. Additional features of the DSKY are discrete alarm and condition lamps, a condition light reset key and a key with which the operator relinquishes his use of the display lights to the computer. The last named function is useful because it is not always known *a priori* whether the operator's command has a higher priority than the computer's request. This is resolved by having the operator make the decision. If a keyboard entry sequence is in progress at a time when the computer program has a request or a result to display, a condition lamp is turned on to notify the operator of the fact. When he is ready to have the computer use the display, he need only depress this release key.

UTILITY PROGRAMS (11, 12, 13)

Interpreter – Most of the AGC programs relevant to guidance and navigation are written in a parenthesis-free pseudocode notation for economy of storage. In a short word computer, such a notation is especially valuable, for it permits up to 32 768 addresses to be accessible in a single word without sacrificing efficiency in program storage. This notation is encoded and stored

in the AGC as a list of data words. An AGC program called the "interpreter" translates this list into a sequence of subroutine linkages which result in the execution of the pseudocode program. A pseudocode program consists of lists called "equations". Each equation consists of a string of operators followed by a string of addresses to be used by the operators. Two operators are stored in an AGC word, each one being 7 bits long. A partial list of operators appears in Table 6–8.

Use of the interpreter accomplishes a saving in instruction storage over programs generated in an automatic compiler and it affords the programmer a rapid and concise form of program expression which liberates him from the time consuming job of programming in basic machine language. In so doing it expands the instruction set into a comprehensive mathematical language accommodating matrix and vector operations upon numbers of 28 bits and sign. This is made possible at the modest cost of a few hundred words of program storage and the cost of about an order of magnitude in execution time over comparable long word computers.

Executive – All AGC programs operate under control of the Executive routine except those which are executed in the interrupt mode. Executive controlled programs are called "jobs" as distinct from so-called "tasks", which are controlled by the Waitlist routine and completed during interrupt time. The functions of the Executive are to control priority of jobs, to permit time sharing of erasable storage and to maintain a display discrete signal denoting "Computer Activity". Jobs are usually initiated during interrupt by a task program or a keyboard program. The job is specified by its starting address and another number which gives it a priority ranking. As the job runs, it periodically checks to see if another job of higher priority is waiting to be executed. If so, control is transferred away until the first job again becomes the one with highest priority. No more than 20 milliseconds may elapse between these periodic priority checks.

When a job is geared to the occurrence of certain external events and must wait a period of time until an event occurs it may be suspended or "put to sleep". The job's temporary storage is left intact through the period of inactivity. When the anticipated event occurs the job is "awakened" by transfer of control to an address which may be different from its starting address. If a job of higher priority is in progress, the "awakening" will be postponed until it ends. When a job is finished it transfers control to a terminating sequence which releases its temporary storage to be used by another job. Approximately ten jobs may be scheduled for execution or in partial stages of completion at a time.

Waitlist – The function of the Waitlist routine is to provide timing control for other program sections. Waitlist tasks are run in the interrupt mode, and must be of short duration, 4 milliseconds or less. If an interrupt program were to run longer it could cause an excessive delay in other interrupts waiting to be serviced since one interrupt program inhibits all others until it calls for resumption of the normal program. The Waitlist program derives its timing from one of the counter registers in the AGC. The Counter Priority stage which controls this counter is driven by a periodic pulse train from the computer's clock and scaler such that it is incremented every 10 milliseconds. When the counter overflows, the interrupt occurs which calls the Waitlist

program. Before the interrupting program resumes normal program it presets the counter so as to overflow after a desired number of 10 millisecond periods up to a limit of 12 000 for a maximum delay of 2 minutes. If the Waitlist is to initiate a lengthy computation, then the task will initiate an Executive routine call so that the computation is performed as a job during non-interrupted time.

Display and Keyboard – The programs associated with operation of the two Display and Keyboard units are basic to the employment of the AGC in the Apollo Guidance and Navigation system. These programs are long but their duty cycle is low so that their use of the time budget is reasonably small. Key depressions interrupt to a program which samples the key code, makes a job request to the Executive, and then resumes. When this job is initiated, it examines the code and makes numerous branches based on past and present codes to select the appropriate action. Nearly always, a modification of the light registers in the display is called for. A periodic interrupt program similar to Waitlist, but occurring at fixed time intervals, performs the required display interface manipulations after it has been initiated by the job. More complex situations occur as a result of lengthy processing of data and periodic re-activation of a display function. For example, it is possible to call for a periodic decimal display of a binary quantity, for which the Waitlist is required to awaken a sampling and display job every second. This job samples the desired register or registers and makes the conversion to decimal according to the appropriate scaling for the quantity, i.e. whether it is an angle, a fraction, an integer etc. and where the decimal point is located. The Display and Keyboard programs are highly sophisticated routines to which a certain amount of computer hardware is expressly devoted for the sake of efficiency. They also make full use of the Executive and Waitlist functions to furnish a highly responsive and flexible medium of communication.

CHAPTER 6–3

MECHANIZED AIDS TO DESIGN AND PRODUCTION

MANUFACTURING

A number of automated processes are employed in the production of the Apollo Guidance Computer hardware. This has been done largely for the sake of minimizing human error and thus minimizing the consequent problems of reworking parts which were improperly built. The case of the computer consists of metal pieces processed on a numerically controlled milling machine. Signal matrices which interconnect microcircuit logic packages within a 60-package module are made semiautomatically, using punched paper tape to control a punching die which forms a matrix layer from a thin sheet of metal. Layers are insulated and stacked by hand before being hand-welded to the logic packs.

Another tape-controlled semiautomatic process is used for threading sense wires in Core Rope memory modules. Information on paper tape is used to position a rope fixture for an operator to pass a wire bobbin through core holes in which *one*'s are to be stored, bypassing those where zeros belong. The bobbin is passed as many times as there are *one*'s on the particular sense wire; following each pass the tape is advanced so as to cause the fixture to be properly positioned for the next pass. When all 192 wires have been fully threaded and terminated, the module is tested on a rope memory tester which operates the module as it will be operated in the computer. A punched tape input to the tester is compared against the information content of the module.

Interconnections between modules are made by wire which is terminated by tightly wrapping it about a rectangular post. The wrapping process may be done manually or automatically. In the AGC most of the wiring is done automatically by a machine whose information input is in the form of punched cards. The machine positions the wire over the pins with as many as two right angle (90°) bends in it, cuts it, strips the insulation at the ends and wraps both ends.

INTERCONNECTING WIRING

The raw data for interconnection of modules is necessarily originated by hand. There have been several instances of computer makers using automated logical design procedures in which the manual input was in the form of Boolean expressions to be mechanized. Such procedures, attractive as they sound, are difficult to prepare and check out and owing to their necessary inflexibility are not as efficient in hardware utilization as manual design methods. In the AGC, logic circuits are assigned to modules when they are drawn, and terminal assignments are made at the same time. A name is given each terminal signal using the rule that all terminals bearing the same signal

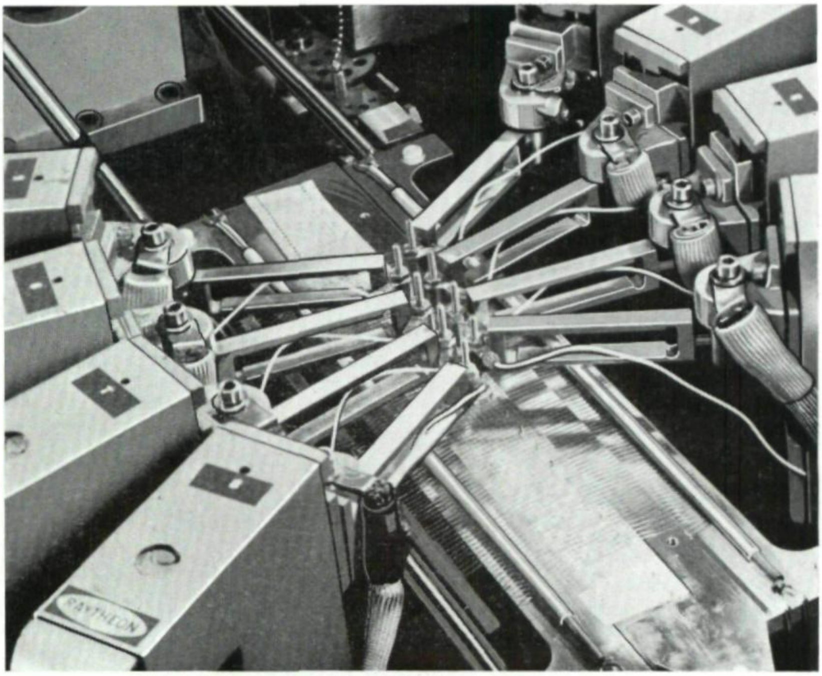

FIG. 6–26 Automatic fabrication of welded matrix

FIG. 6–27 Semiautomatic core rope fabrication

name shall ultimately be connected together and no connections shall be made between terminals bearing different names.

A punched card is prepared for every used terminal of every module, whether it be a logic module or any other kind. These cards are accepted by a so-called "Wirelist" program which sorts the inputs by signal name to show the terminal groups. On each card pertaining to a logic module a number is added stating the loading or generating nature of the circuits connected to the terminal within the module. The Wirelist program processes these numbers showing for each signal name (group) whether the load exceeds the drive or vice versa, and by how much. This is a useful feature, for whereas it is not difficult to analyze loading of a signal entirely contained in a module and hence drawn on a single sheet of paper, it is perplexing to analyze loading on a signal which goes several places and appears on several different drawings. The Wirelist program prepares a printed document showing the terminal groups listed alphabetically and also showing the signal names for each module terminal listed in numerical order. The information file, obtained from the cards and stored on tape, constitutes the input to the program which prepares the card deck for the wire-wrap process.

The preparation of the card deck for wire wrapping would be a tedious task without the aid of automatic data processing. Starting from a magnetic tape file listing all of the interconnections in the AGC, a computer program assigns a path to each wire, punches the card deck and prints a listing of what it has done. The program examines in order each group of terminals which are to be wired together. Since there is no pre-specified order in which the terminals in a group are to be joined to one another, the program tries to minimize the wire length by a sequential trial and error process. Not all possible configurations can be tried owing to the excessive time required, so an algorithm is used which can find an optimal or nearly optimal solution in a short time. The program thus arrives at a definition of the connections within a group, i.e. a list of terminal pairs.

It is next necessary to decide how a wire will proceed from one terminal to the other, a straight line is only possible if the terminals happen to lie in the same row or column. A rectangular layout pattern is used so as to avoid choking the gaps between terminals. The program first tries to assign either a straight wire or one with a single bend. If wires previously assigned have blocked the gaps through which this would have to pass, then another assignment is tried. If all possible assignments have been tried without success, no control card is punched for this wire. Rather an entry is made on the printed listing calling for a manual insertion of the wire after the automatic wrapping is complete.

PROGRAM PREPARATION

Assembler – The standard programming language for the AGC is an assembly language, in which each machine word of program is represented by a symbolic expression on an 80-column punched card. In fact, it can be said that there are two programming languages, basic and interpretive, and that any sizable program contains large amounts of both. As these languages are mutually exclusive, that is, no expression in one can be mistaken for any expression in the other, the assembler readily handles any mixture of the two. The punched-card format consists of three main fields.

Fig. 6–28 Wire wrapping machine – Gardner Denver Co.

(a) Location field, which may be used to assign a symbolic name to the location of the machine word defined on the card.
(b) Operation Code field, containing a symbolic code specifying the operation to be done, which determines whether the expression on the card is in basic or interpretive language.
(c) Address field, which in basic language usually contains a wholly or partially symbolic expression that specifies the address of the location to be operated upon.

There are many exceptions in detail to those definitions, only the most common use of each is given. Ample space is provided also for explanatory remarks, which are an integral part of the assembly-language file of a program. The printed listings made during assemblies, which for complete mission programs run to several hundred pages, thus constitute a medium of communication among the fifty or so engineers who do most of the programming.

The assembly program itself runs on the Instrumentation Laboratory's Honeywell 1800 data processing installation and performs in parallel its two major tasks, assembly and updating. The assembly process translates programs in assembly language into absolute binary form for simulation and manufacturing, prints a listing in which the symbolic and absolute forms of each word of the program are displayed side by side and prints diagnostic information about syntactical errors. The assembly process also allocates memory space to the program and to its variables and constants. The updating process maintains magnetic tape files of current programs in both assembly-language and absolute form, greatly reducing the need to handle large numbers of punched cards. For example, a program may be revised by presenting to the assembler just enough cards to specify the changes. Assembly and updating take from less than 30 seconds to several minutes, depending on the size of the program being assembled and the amount of information on the file tape. The absolute binary files generated by assembly and maintained by updating are the input to the AGC simulator program and to program manufacturing activities that are described in later sections.

It may be instructive to trace briefly the history of part of a mission program, re-entry guidance for example, from the conceptual stage to actual readiness for flight.

(a) The mathematical ideas are blocked out roughly, tolerances guessed, variables and effects judged to be significant or negligible, and some such decisions are left to be settled by trial and error.
(b) A procedure employing the concepts is worked out, using one mathematical model for the spacecraft with its guidance and navigation system and another for the environment. This procedure is then employed in a data processor program for testing.
(c) The program is compiled, tested, revised and retested, until the mathematical properties of the procedure are satisfactory. Because these programs retain 2 to 4 more digits of precision than double-precision AGC programs, the variables at this stage may be considered free of truncation or round-off error. It is desirable to do as much pinning down of the procedure as possible in steps B and C, since these programs run a good deal faster than real time.

(d) An AGC program is written by translating the relevant parts of the program into AGC assembly language, the more mathematical parts such as position and velocity updating, into interpretive language, and the more logical such as turning reaction control jets on and off, into basic.
(e) In combination with the utility programs described previously, the AGC program is assembled. After two or three revisions, when the grammatical errors that can be detected by the assembler are eliminated, the program checkout is begun by use of the AGC simulator, another data processor program, which is described later. In advanced stages of checkout, this simulation incorporates the part of the program of steps (b) and (c) that models the environment. AGC simulation discovers the numerical properties of the procedure, since all effects of scaling, truncation, and roundoff are present. Steps (d) and (e) are repeated until the program fulfills the goals determined in step (a). Severe problems may send the engineers back to step (b), or even to step (a).
(f) Up to this point, everything has been done on the initiative of the 3- or 4-man "working group" whose speciality is the particular phase of the mission. Now, however, this AGC program must be integrated with the rest of the mission program. Using the updating facilities of the assembler, the working group transfers its own coding to the mission program and, in cooperation with the group in charge of program integration, checks out not only its operation but its ability to "get along with" the other parts of the mission program, e.g. staying with its part of the time budget. Here again, the AGC simulator is the primary tool.
(g) At this point, or sometimes before step (f), it is necessary to run an AGC attached to guidance and navigation and ground support equipment. This is the last procedure devoted entirely to the checkout of an AGC program.
(h) When all of steps (a) through (g) for a whole mission program have been completed, the assembly listing of the program is given the status of an engineering drawing. Only now are rope memory modules wired and further testing is for the benefit of other subsystems as much as of the program.

It should be explained that by "mission" is meant not only a flying mission but lesser responsibilities as well. Early mission programs, shipped with computers to other contractors to aid them in testing their systems, consisted mostly of utility programs.

Simulator – The assembler is designed to detect programmer errors of the nature of inconsistencies but it is not capable of checking program validity in general. The hazards are numerous: faulty analysis of a problem, incorrect scaling, wrong use of instructions, interference with other programs, wrong timing, endless loops and many other pitfalls familiar to programmers. Strictly speaking, the AGC program can never be fully tested before it is operated in a system in flight. Short of this, however, it is possible to prove out a program to a high degree of confidence by simulations of the program operating in an environment. Several possible approaches have been taken

to the simulation study. In one, a computer and other parts of the guidance and navigation system are operated in conjunction with a real-time hybrid analog and digital simulation of the environment. The other approach to simulation is an all digital simulation program which is run on the large scale data processing installation at the Instrumentation Laboratory. This is an important tool in the development of system oriented programs. Since it does not run in real time, it is possible to halt for the purpose of recording information relevant to program progress, such as periodic values of control constants or guidance and navigation variables, traces of interpretive instructions, environmental data and so forth. Initial conditions are easily set, and there is no limit, in principle, to the extent to which one can reproduce anticipated operational environments. The penalty is having running times from two to forty times as long as real time (ten times is typical).

The Simulator comprises three major sections. The first simulates the AGC, and even operates an AGC Display and Keyboard (DSKY) connected on-line to the data processor. The second simulates the environment and is constantly being added to and improved as operating experience is gained. These two sections run largely independent of one another as their functions are basically incompatible. One is a function of elapsed time and the other is a function of AGC program execution status. The third section exists for the purpose of communication between the other two. It is capable of representing the environment to the computer over short periods of time while the two operate in isolation. From time to time the simulation halts while the AGC and environment sections reconcile with one another. The communicator section is re-initialized; and the simulation proceeds with the communicator extrapolating the recent past history of the environment. Information which is recorded out is subsequently edited in such a way that system analysts can easily process it with their own programs in order to make error analyses, study correlation of events or perform any other mathematical or editing operation.

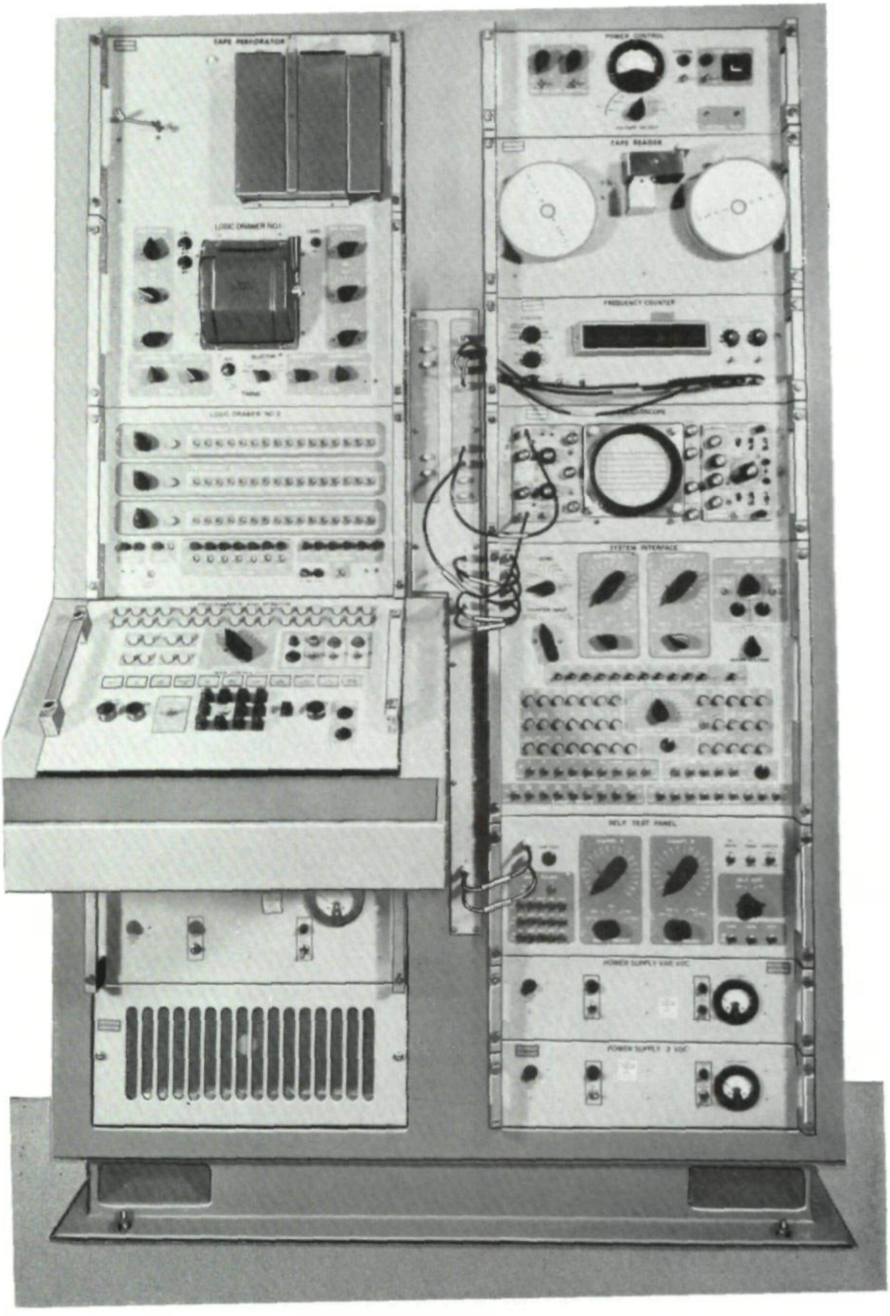

FIG. 6–29 Computer test set

CHAPTER 6-4

GROUND SUPPORT EQUIPMENT

TEST SET

Because of volume and weight restrictions guidance computers are built without the extensive maintenance features found in data processing computers. During all stages of design, assembly and field testing it is important to have the facility for manual intervention into the computer's operation as well as a means for certifying that all circuits are properly operating. This facility is provided by a separate unit which connects to the computer through what is usually a separate interface.

The unit which does this job with the AGC is called the AGC Test Set. It contains a number of flip-flop registers which can be made to serve various roles by selecting among numerous modes of operation. Over 100 signals are exchanged between the AGC and Test Set through an interface called the test connector. The Test Set has access to the AGC's write buses. It can sense them and also force signals upon them. This feature, together with the AGC's timing pulses and central register control pulses, permits the Test Set to follow the progress of AGC programs.

In its monitor mode the Test Set uses flip-flop registers to duplicate or mimic the contents of AGC central registers. Any of these registers may be displayed in lights on the control panel. Since in particular the S, or address, register and the G, or memory local, register are displayed, it is possible to see what is stored in memory. The successive contents of any erasable register can be displayed by commanding the Test Set to sample the G register and display its contents each time the address is the same as the address specified by hand set switches on the panel.

Facility is also available for causing the computer to halt when it interrogates a specified address, or when the content of a specified register reaches a specified value, or at the end of each instruction, memory cycle, or alarm. The computer may be made to proceed from where it is, or it may be started at any desired instruction. Any register may be read to the lights whether or not it is accessed by program, and any erasable location may be loaded from the Test Set with any desired value.

The Test Set contains circuits for exercising and testing all of the AGC's interface circuits. A separate cable connects the Test Set with the AGC's system connector and a switch panel causes an oscilloscope to be connected to an AGC output, or else a signal generator of appropriate characteristics to an AGC input. This feature is used to make a detailed test of output signals, including their rise time, amplitude, duration and any other important characteristics. A faster and less complete check of the interfaces can be made by a special connector which exercises pulse inputs by connecting them to pulse outputs and exercises DC inputs by connecting them to DC outputs and supplying a dummy load. The check can then be made by an AGC program read into the erasable memory.

AGC MONITOR

Before an AGC program is wired into fixed memory modules it must be exercised on an AGC. For this purpose, there exists a form of ground support equipment incorporating some features of the Test Set together with an erasable type of memory whose contents are sent to the AGC when it interrogates a fixed memory address. This machine is the AGC Monitor, so called because it encompasses the monitor feature of the Test Set. The memory control circuits of the Monitor are arranged so that only a part of the AGC fixed memory is read from the Monitor, while the remainder is read from the AGC. This is done, moreover, without having to remove fixed memory modules from the AGC. Rope simulations are done in 1 024 word segments. When the AGC Fixed Bank register and S register are observed to be set to access a simulated bank, the sensing of the AGC fixed memory is inhibited by a signal from the monitor while the simulated word is transferred into the G, or memory local, register of the AGC.

The memory used in the Monitor is a set of nine erasable memory units each containing a 4096 word coincident-current ferrite core stack with driving electronics similar to those in the AGC. The logic in the Monitor and in the Test Set is made from microcircuit NOR gates. One reason this is done is to put to use those gates which are not found qualified for flight hardware but are still satisfactory for less stringent environments.

CHAPTER 6–5

CONCLUSION

Guidance computer engineering is a simultaneous effort in mechanical, electrical and logical design disciplines. In order to obtain high efficiency in terms of performance, volume and power consumption, guidance computers are designed to work in a single specific system unlike most commercial computers. They commonly have fewer and less flexible instructions, shorter word length and less complex arithmetic units. Compactness and short term reliability predominate over considerations of programming ease, maintainability and manufacturing cost. Whereas the commercial computer designer strives to maximize answers per month, the guidance computer designer seeks the capability of handling high peak loads and is concerned with answers per second.

The guidance computer receives data from various sources and delivers answers to various destinations over tens or hundreds of signal paths, each requiring appropriate conditioning circuitry at origin and at destination. One of the challenging design problems is to minimize the number of these interface signals, and moreover to minimize the number of different circuits used.

The AGC is quite representative of the state of the art in guidance computers as contrasted with the rest of computer technology. Most conspicuous of the attributes common in guidance computers are the extensive use of microcircuits and high density interconnections, a dense fixed memory of about half a million bits, a small erasable memory, and a short word length. The computer was designed to employ certain utility programs. The Interpreter program allows efficient expression of double precision matrix programs for navigation, attitude control and steering. The Executive program allots computer time among various jobs according to a priority schedule. The Waitlist program provides interrupted entry to other programs at specified intervals of real time.

Guidance computers are often supported by commercial computers for automatic programming and in various areas of mechanical and electrical design. A large scale computer is used in connection with the Apollo Guidance Computer in several respects. It assembles and makes simulation runs on programs, it generates the input card decks for automatic wire wrapping machinery used in computer manufacture, and it also prepares punched tape for use in fixed memory fabrication and information input to ground support equipment.

The constraints on the guidance computer designer are severe. In addition to the requirements of size, performance and reliability is the urgency for early delivery which stems from trying to get the best equipment possible without introducing unnecessary delay in flight schedules. For this reason, we may expect that guidance computer engineering will continue to be a highly productive competitive discipline for years to come.

REFERENCES

1. "Proceedings of the Conference on Spaceborne Computer Engineering". I.R.E., P.G.E.C., Anaheim, California, October 30–31, 1962.
2. DICKINSON, M. M., JACKSON, J. B., and RANDA, G. C., "Saturn V Launch Vehicle Digital Computer and Data Adapter". Proceedings 1964 Fall Joint Computer Conference, Spartan Books, Inc., Baltimore, Maryland, 1964.
3. WYLE, H., RUBENSTEIN, S. Z., MILLER, L., and GITHENS, S. E., "The Logical Design of the D26C: A Microminiature Real Time Processing System". National Electronics Conference, May 1964.
4. ALONSO, R. L., BLAIR-SMITH, H., and HOPKINS, A. L., "Some Aspects of the Logical Design of a Control Computer: A Cast Study". IEEE Transactions on Electronic Computers, Vol. EC–12, No. 5, December 1963.
5. ALONSO, R. L., and LANING, J. H., Jr., "Design Principles for a General Control Computer". Institute of Aeronautical Sciences, New York, S. M. Fairchild Publication Fund Paper FF-29, April 1960.
6. ALONSO, R. L., GREEN, A. I., MAURER, H. E., and OLEKSIAK, R. E., "A Digital Control Computer; Developmental Model 1B". Report No. R-358, Instrumentation Laboratory, M.I.T., Cambridge, Massachusetts, April 1962.
7. TAYLOR, T. C., "A Proposed Circuit Structure for Computer Logic Based on Semi-conductor Flat Packs Interconnected by Multilayer Circuit Boards". Report No. E-1699, Instrumentation Laboratory, M.I.T., Cambridge, Massachusetts, December 1964.
8. PARTRIDGE, J., HANLEY, L. D., and HALL, E. C., "Progress Report on Attainable Reliability of Integrated Circuits for Systems Application". Report No. E-1679, Instrumentation Laboratory, M.I.T., Cambridge, Massachusetts, November 1964.
9. SHANSKY, D., "Erasable Store Mod 3C". Report No. E-1158, Instrumentation Laboratory, M.I.T., Cambridge, Massachusetts, July 1962.
10. ALONSO, R. L., and HOPKINS, A. L., "The Apollo Guidance Computer". Report No. R-416, Instrumentation Laboratory, M.I.T., Cambridge, Massachusetts, August 1963.
11. MUNTZ, C. A., "User's Guide to the Block II AGC/LGC Interpreter". Report No. R-489, Instrumentation Laboratory, M.I.T., Cambridge, Massachusetts, April 1965.
12. GREEN, A. I., and ROCCHIO, J. J., "Keyboard and Display System Program for AGC". Report No. E-1574, Instrumentation Laboratory, M.I.T., Cambridge, Massachusetts, August 1964.
13. LAWTON, T. J., and MUNTZ, C. A., "Organization of Computation and Control in the Apollo Guidance Computer". Instrumentation Laboratory, M.I.T., Cambridge, Massachusetts, April 1965.

ACKNOWLEDGEMENTS

The Apollo Guidance Computer has been used here to exemplify the state of the art in broad scope, from hardware to software. The AGC owes its existence to the pioneering work of Ramon L. Alonso, Eldon C. Hall, and J. Halcombe Laning, Jr. Its development has encompassed the efforts of many workers, some of whose contributions are referenced. Others, whose contributions are substantial but unwritten include D. J. Bowler, E. J. Duggan, J. S. Miller, R. F. Morse, and H. A. Thaler. To them and to the Raytheon Company, manufacturers of the Apollo Guidance Computer, the author is grateful for advice and assistance in preparing this description of their achievements.

PART 7

SPACE VEHICLE CONTROL SYSTEMS

Dr. Wallace E. Vander Velde

DR. WALLACE E. VANDER VELDE

Dr. Wallace E. Vander Velde is an Associate Professor of Aeronautics and Astronautics and Consultant to the Instrumentation Laboratory at Massachusetts Institute of Technology. In his academic position he is an authority on automatic control systems for fixed wing aircraft, helicopters, missiles, satellites and space vehicles. At the Instrumentation Laboratory he is working with the Apollo Spacecraft Guidance and Navigation Group.

Dr. Vander Velde was born June 4, 1929, at Jamestown, Michigan. He received the B.S. degree in Aeronautical Engineering from Purdue University in 1951. Following military service, in 1953, he entered M.I.T. as a graduate student and received the degree of D.S. in Instrumentation in 1956.

From 1956 to 1957, Dr. Vander Velde was director of applications engineering for the GPS Instrument Co., Inc., Newton, Massachusetts. He returned to M.I.T. in 1957 as Assistant Professor of Aeronautical Engineering and was appointed Associate Professor of Aeronautics and Astronautics in 1961 and Professor of Aeronautics and Astronautics in June 1965.

PART 7

SPACE VEHICLE FLIGHT CONTROL

INTRODUCTION

The development of the theory and practice of automatic control has to a large extent gone hand in hand with the development of aerospace flight control systems. Although the earliest application of feedback control as a deliberately conceived and consciously applied technique preceded the invention of the airplane by about fifty years, it was the exacting requirements of aircraft flight control which for years made the greatest demands on the developing theory of feedback control and which stimulated much of its growth. In recent years the advance of "modern" control theory has been led in large part by workers responding to the need for more sophisticated control theories and techniques for application to aerospace flight control problems. The requirements for control efficiency, accomodation of changing controlled-member characteristics and reliable control in complicated and demanding situations have resulted in a far broader application of optimal controls, adaptive controls and digital-computer control systems to the problems of aerospace vehicle flight control than to any other area of application.

Aerospace flight control problems are not only demanding but quite diverse. Among the many different phases of a space vehicle mission beginning with lift-off from a launching pad and ending perhaps with a return to a designated landing point on earth, one can identify three major classes of flight control problems:

(a) **Powered flight control** – control of the attitude and flight path of the vehicle while thrusting.

(b) **Coasting flight control** – control of the attitude of the vehicle while coasting in free space.

(c) **Atmospheric flight control** – control of the attitude and flight path of the vehicle while gliding in an atmosphere.

The nature of the control problems in these different situations is very different. The environment in which the vehicle operates, the requirements of the control systems, the sources of reference information and of control torques are all quite different. But a single space vehicle operates under all of these conditions during the course of a mission and it is to be hoped that the different control problems will not have to be solved one at a time in isolation. The design of an overall control system which performs well in each phase of the mission, using common equipment whenever possible and which is in addition integrated efficiently with the guidance and navigation system constitutes a most challenging engineering problem. In the following chapters the major characteristics of the control problems in each of these classes is discussed in turn.

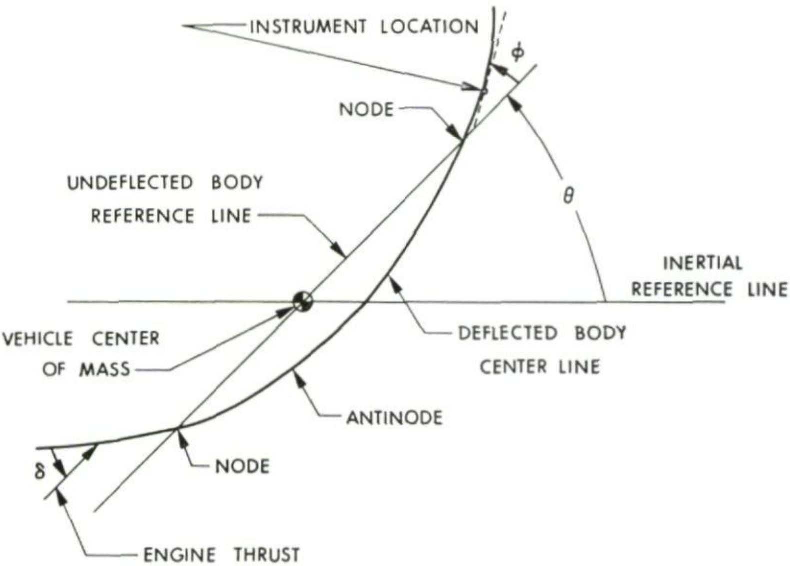

FIG. 7–1 Idealized body bending mode shape

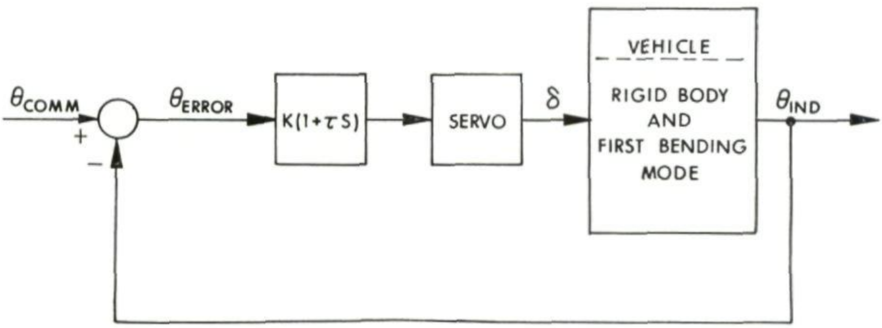

FIG. 7–2 Simplified attitude control system configuration

CHAPTER 7–1

POWERED FLIGHT CONTROL

The function of the powered flight control system is to orient the vehicle thrust acceleration vector in response to commands generated by the guidance system. This function is required during each of the powered flight phases of a mission. These phases might include:

(a) Boost from the launching pad into a parking orbit
(b) Acceleration into the destination transfer trajectory
(c) Midcourse velocity corrections
(d) Deceleration into an orbit around the destination planet or moon
(e) Powered descent to the planet or moon
(f) Comparable phases in the return flight

The thrust acceleration vector is, on the average, oriented in the vicinity of the vehicle longitudinal axis. Thus powered flight control is primarily a problem in attitude control. This problem will be discussed first as it relates to two means of generating the required control moments. Then in the following section, some additional considerations involved in acceleration vector control will be discussed.

ATTITUDE CONTROL WITH A GIMBALED ENGINE

With a rocket engine providing a large force which acts on the vehicle, the most evident source of large control moments is the deflection of the direction of this force so it has some moment arm with respect to the vehicle center of mass. This can be conveniently accomplished in the case of a liquid-fueled rocket by mounting the engine on gimbals and rotating it. A solid-fuel rocket requires rotation of the thrust direction with respect to the engine itself. This has been accomplished by different means; among them are jet vanes, jetavators, rotating canted nozzles and secondary fluid injection. The present discussion supposes a liquid-fueled rocket with a gimbal-mounted engine.

The very first flight control problem encountered in a space mission is probably the most difficult – the control of the unstable, elastic vehicle in its ascent through the gusty atmosphere. In this phase the configuration of the vehicle is largest, the frequencies of body bending and fuel sloshing oscillations are lowest and the need for control system gain and bandwidth is most critical due to the requirements of stabilizing the aerodynamically unstable vehicle and reducing structural loads due to wind disturbances. In most of the powered flight phases following this, there is no atmosphere to contend with and the vehicle configuration is smaller due to the separation from one or more stages. This would not be true if in-orbit assembly of separately boosted payloads were employed.

The most important requirements of the attitude control system during atmospheric exit may be summarized as:

(a) Maintain vehicle stability

(b) Provide adequate performance for execution of commands
(c) Provide adequate alleviation of gust loads
(d) Make reasonably efficient use of control action
(e) Maintain simplicity and reliability

The first requirement dominates the design of this system. For early analysis one might very well model the vehicle and its control system as quasi-stationary and linear. If so, one has only the classical problem of the stability of a linear, invariant feedback system – and the problem would be simple were it not for the very complicated nature of the vehicle being controlled. The basic rigid vehicle is unstable in the atmosphere because of the required distribution of area and mass. It could be stabilized aerodynamically by the addition of fins at the rear of the vehicle but the additional weight and drag would incur too dear a performance penalty. So the alternative of active stabilization through control system feedback is almost universally preferred. This places a lower bound on control system gain for static stability; the restoring control moment due to a rotation of the vehicle must be greater than the diverging aerodynamic moment due to that rotation.

But this requirement of high gain for static stability is in conflict with the requirement of low gain for dynamic stability. The dynamic stability problem is complicated by the fact that the large vehicle is by no means rigid. The launch configuration consists of a number of vehicle stages coupled with light-weight interstage structure. Significant bending occurs at these coupling points. Further, each stage is designed as light-weight as possible with the major requirement being to carry axial compressive loads. The resulting structure has appreciable bending elasticity. Still further non-rigid-body behavior is due to fuel and oxydizer sloshing in their tanks and localized bending of the structure between the points of engine gimbal mounting and gimbal actuator attachment.

The primary body bending deflections are decomposed for analytic purposes into a series of normal modes of oscillation. Each mode has a characteristic frequency and mode shape. These resonant modes are very lightly damped. An idealized picture of a fundamental or first order bending mode is shown in Fig. 7–1. The body centerline, deflected according to the first order mode shape, is shown with an undeflected body reference line. The two points which do not translate in this mode of oscillation are called nodes; the point of greatest translation, which is also the point of zero rotation, is called the antinode. The engine gimbal deflection, δ, is measured and controlled with respect to the deflected body. Also, the body attitude is indicated by an instrument located at a particular body station such as that shown on the figure. It will indicate the local body angle with respect to the inertial reference line; in Fig. 7–1, this angle is $\theta + \phi$. Additional higher ordered bending modes may be excited simultaneously. The body translational or rotational deflection at any station is the sum of the deflections in the different modes.

It is clear that if the control system bandwidth extends to the frequency of a particular bending mode, the effect of the control feedback can either tend to stabilize or destabilize the mode. Consider as an example just the effect of attitude rate feedback on the mode shown in Fig. 7–1. We see that for gross vehicle stability the sense of the rate feedback to gimbal angle must be

positive. That is, a positive $\dot{\theta}$ should cause a positive engine deflection, δ, which will result in a control moment tending to reduce the angular velocity. But now a positive bending rate $\dot{\phi}$ which is also sensed by the indicator also causes a positive increment in engine deflection, δ, and this produces a normal force component on the body which tends to further bend the body in the same sense.

For the configuration shown then, with the engine behind the rear node and the rate indicator forward of the antinode, in-phase rate feedback at the first bending frequency tends to destabilize the mode. If either the engine were forward of the rear node, or the rate indicator were behind the antinode, but not both, such feedback would tend to stabilize the mode. Alternatively, for the configuration shown, rate feedback would stabilize the bending mode if a filter between the rate indicator and engine deflection provided 180 degrees of phase shift at the bending frequency so the engine deflection would be opposite in sign to the indicated bending rate. Notice that for the present purpose it is immaterial whether the 180 degrees of phase shift at the bending frequency is phase lead or lag.

This qualitative view of the effect of the control system on body bending modes may be given quantitative significance using any of the standard methods of studying linear system stability. Consider the system configuration of Fig. 7–2 in which the vehicle is characterized by its rigid body dynamics and first bending mode. The indicated angle is compared with the commanded angle, and the compensated error signal commands the gimbaled engine servo. The lead compensation which is necessary to stabilize even the rigid body dynamics may be thought of as realized either by rate gyro feedback or by an idealized lead network. For a bending mode shape such as that pictured in Fig. 7–1, a simplified root locus plot for this system has the general appearance of that shown in Fig. 7–3. A number of high frequency effects have been omitted from this figure to emphasize the basic problem of stabilizing the aerodynamically unstable vehicle which also suffers elastic deformations. The unstable character of the vehicle is indicated by the rigid body pole in the right half plane. A single pole corresponding to a first order lag approximation to the servo dynamics is shown, as is the zero due to the lead compensation. Were it not for the bending mode, this lead would clearly be adequate to stabilize the rigid body.

The lightly damped bending oscillation is indicated by the pole near the imaginary axis at the bending frequency. The parallel transfer of the rigid body angle plus the bending deformation angle to the attitude indicator gives rise to a zero near this pole. The indicated relation of the zero to the pole corresponds to the situation shown in Fig. 7–1. If it were possible to move the instrument location back along the vehicle, the zero would move toward the pole – *lying on top of the pole and cancelling the effect of the mode in the* control system when the attitude indicator is located at the antinode. In that location the attitude indicator does not sense any angle due to the bending oscillation. If the attitude indicator were moved behind the antinode, the zero would appear below the pole in the upper half of the root locus plot and the small locus of closed loop root locations would lie to the left of the pole and zero. The first bending mode would be a stable oscillation for all control system loop gains in that case. However, higher frequency effects

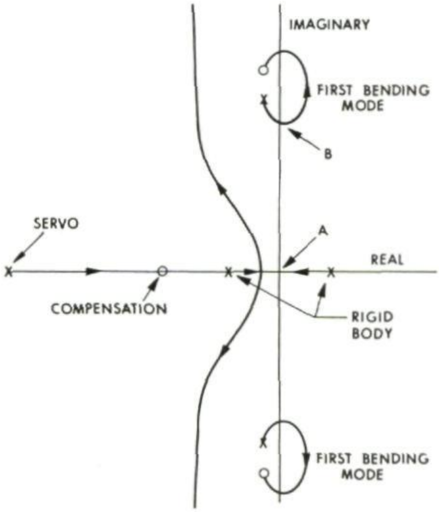

FIG. 7–3 Simplified root locus plot for system with rigid body compensation only

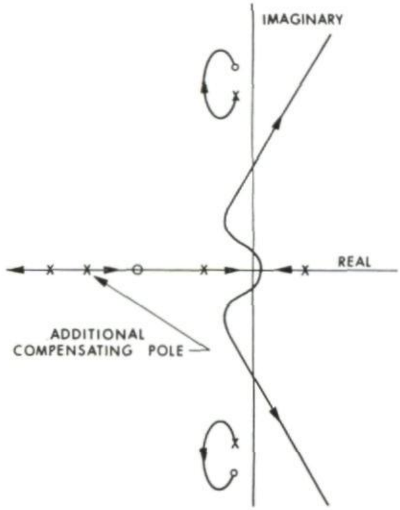

FIG. 7–4 Simplified root locus plot for system with lag compensation for bending mode

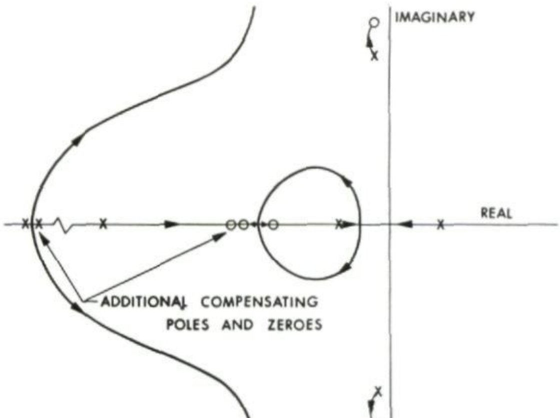

FIG. 7–5 Simplified root locus plot for system with lead compensation for bending mode

not shown in Fig. 7–3 would still be troublesome, so careful placement of the sensors is not generally adequate to solve the problem.

For the configuration shown in Fig. 7–3, which is commonly the case, the design problem results from the fact that for a loop gain high enough to stabilize the rigid body dynamics, which is indicated by the unstable closed loop pole crossing into the left half plane at A, the bending mode pole has already crossed into the right half plane at B. Static stability demands a certain minimum loop gain as noted before, so it is essential to stabilize the bending mode at the required higher gain. This can be thought of as a requirement to turn the bending mode locus from the right to the left of the pole and zero. This can be accomplished by rotating the breakaway angle for the locus from the pole either clockwise or counterclockwise, which corresponds to either lag or lead compensation.

With lag compensation for the bending mode, the root locus has the appearance of that shown in Fig. 7–4. The additional lag has turned the bending mode locus to the left as desired but it has adversely affected the dominant rigid body mode. There is, however, a range of loop gains for which the system is stable. It has a bandwidth well below the frequency of the bending mode. The neglect of any higher frequency effects may well be justified in this case.

With lead compensation for the bending mode, the root locus has the appearance of that shown in Fig. 7–5. The strong lead compensation required to turn the bending mode locus far enough has significantly influenced the locus of the rigid body mode. Considering only the dynamic effects shown in the figure wide bandwidth operation would be possible. However, the additional lead maintains the open loop gain at higher frequencies and makes more high frequency effects important in the system. Higher ordered bending modes must then be included in the analysis. The lead at higher frequencies will not be as great, and there may well be instability indicated in a higher frequency mode.

In addition to all this, there is another source of dynamic modes to complicate the picture still further. For the liquid-fueled rockets under consideration here, the propellants are free to slosh back and forth in their tanks. This oscillatory change of momentum of the fluid particles reacts through the tank walls to affect the dynamic behavior of the vehicle – giving rise to additional lightly-damped modes. The analysis of these effects is facilitated by reference to a mechanical analogy to the sloshing fluid. The analogy can be taken in the form of a spring and mass with a degree of freedom normal to the body longitudinal axis, or a pendulum as shown in Fig. 7–6. The parameters of the mechanical analogies have been derived by a number of authors; among them is Lorell (1). One such pendulum is required to simulate each mode of sloshing to be considered in each tank. For a multi-stage vehicle having two tanks in each stage the complexity compounds rapidly. Fortunately it is often true that only the first sloshing modes in the largest tanks have frequencies in the pass band of the control system.

The coupling of the pendulum oscillation into indicated vehicle attitude is dynamic in this case as opposed to geometric in the case of body bending, so the effect is more difficult to visualize. However, the coupled equations of motion for the vehicle and pendulum produce light damped pole-zero pairs

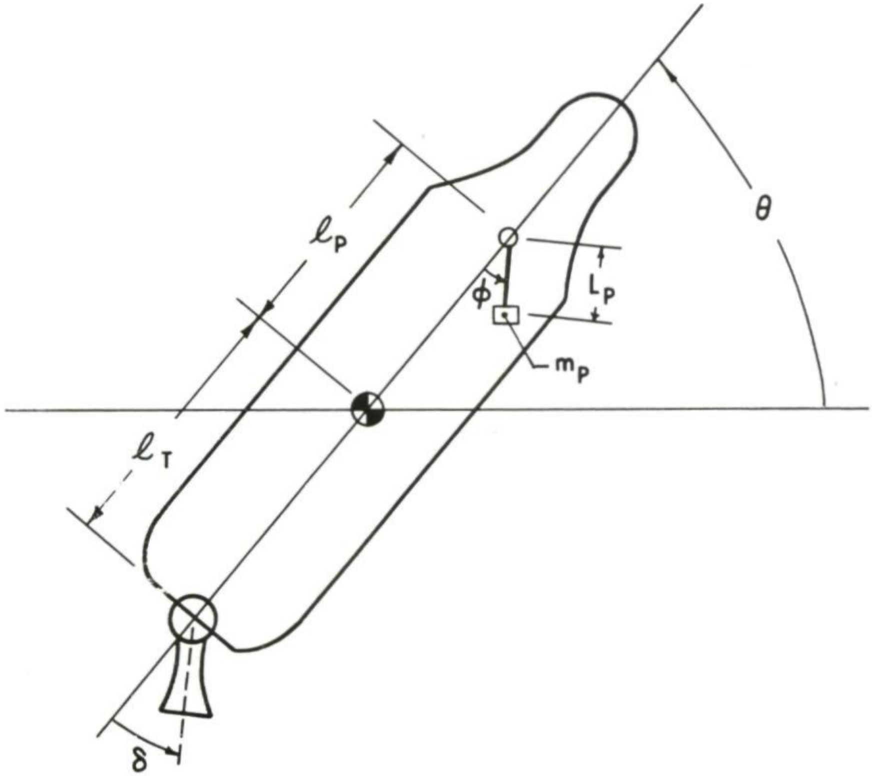

FIG. 7–6 Pendulum analogy to sloshing propellant

in the system open-loop transfer function just like those due to bending. A single tank located well forward of the vehicle center of mass or to the rear of the center of mass has its upper half plane zero located below the pole – the configuration which tends to give stable closed loop roots. There is an intermediate range of tank locations which puts the upper half plane zero above the pole and which would tend to give unstable closed loop roots unless compensated. These locations are characterized by the hinge point of the analogous pendulum lying in front of the rigid vehicle center of mass and the pendulum mass lying to the rear of the instantaneous center of vehicle rotation in response to control moments. This rotation center is forward of the rigid vehicle center of mass by the amount k^2/l_T, where k is the rigid vehicle radius of gyration and l_T is shown in Fig. 7–6. There are two cases in which the zero lies on the pole and the slosh mode has no participation in vehicle dynamics: (a) if the pendulum hinge is at the vehicle center of mass, in which case the pendulum reaction causes no moment about the vehicle center of mass: or (b) if the pendulum mass is at the vehicle rotation center, in which case control moments do not excite pendulum motion. Having coupling between slosh modes and vehicle dynamics, the problem of compensation design is the same as for bending modes.

The controlled member is thus characterized by the unstable rigid body dynamics and an assortment of lightly damped oscillatory modes due to body bending and propellant sloshing. The design of compensation which at any one flight condition will either stabilize these modes or leave them essentially uncoupled is somewhat like juggling a large number of balls. Allowing any *one mode to be badly behaved is like dropping just one ball – the act is a* flop. And to make matters worse, the characteristics of these modes change continuously as the dynamic pressure varies and propellants are consumed. Compensation which works well at one flight condition may result in unstable operation at the flight condition which exists a half minute later. The least sensitive design is usually one which employs lag compensation and simply cuts off the control system bandwidth below the frequencies of the oscillatory modes. This leaves the bending and slosh modes essentially uncoupled from the control system. They are free to display their characteristic oscillations in response to whatever excitation they receive. For the lowest frequency bending and slosh modes particularly this may allow the existence of continuing oscillations which cause substantial structural loads. If so, the total system design is improved by using the control system to actively damp the lowest frequency modes. This requires a wider bandwidth control system. In fact, from just the point of view of structural loads there may well exist, for any vehicle, an optimum control system bandwidth. For lower bandwidths the loads due to poorly damped oscillations tend to dominate and for higher bandwidths the loads due to control action tend to dominate. In the case of the propellant sloshing oscillation, a source of damping other than the active effect of the attitude control system is available and often used. At the cost of some weight, structural baffles may be built into the propellant tanks to break up the large-scale oscillations of the fluid near the free surface.

Fortunately the requirements on the attitude control system, other than stability, are not very demanding in most instances. Very little bandwidth is

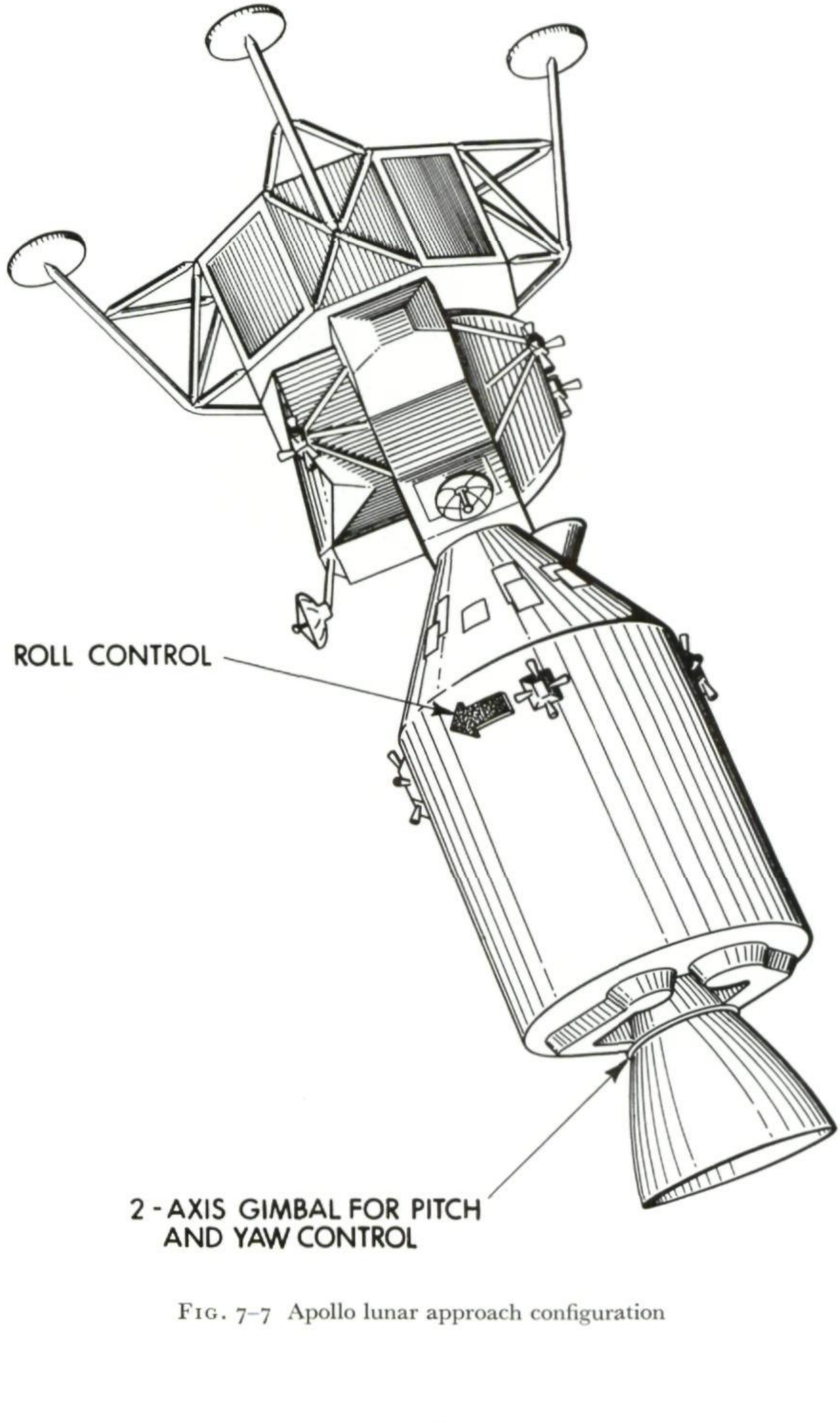

FIG. 7–7 Apollo lunar approach configuration

required to follow the command inputs since the required attitude for efficient powered flights is usually very slowly changing. The requirement for speed of response to alleviate gust loads may be more demanding. In the selection of a system bandwidth to minimize structural loads, as previously discussed, the effects of gust and wind shear inputs should be included. The requirement for efficient use of control action is not usually of crucial importance though there is some weight penalty associated with excessive demand for control moments. System simplicity and reliability is always an object of first importance. In the present context this requires the design of simple compensation using parameter values which can readily be realized and finding simple ways to vary this compensation as needed during the flight.

Another basic choice which bears on the question of reliability is the choice of analog vs. digital data processing to close the control loop. Wide band systems are usually more efficiently implemented with analog equipment but the range of achievable bandwidths in this problem is not very large. On the other hand there is the need for variable compensation and loop gains and the desirability of complex zeros and poles in compensation functions each of which can more readily be implemented by digital computation. Moreover, there is the fact, usually obscure at the outset, that after a system has been designed to serve its primary function it tends to grow to accommodate the additional requirements of the operational situation. One major cause of this growth is the need for a variety of modes of operation: check-out mode, primary mode, back-up mode, pilot control mode etc. Mode switching requires changing connections in an analog system and this increases the component count and decreases the reliability estimate. In a digital system, mode switching is accomplished by branching to another program stored in memory. Since fixed memory is highly reliable, this entails little penalty in the reliability estimate.

The design of a digital attitude control system is quite like the design of a continuous system with the additional requirement to choose the sampling period and quantization of computer input and output variables. The sampling period is chosen primarily on the basis of the desired system bandwidth. If, for example, it is decided that the first bending mode is to be stabilized and higher frequency modes isolated as much as possible, the sampling frequency would be chosen perhaps five times greater than the first bending frequency. If the form of the attitude indicator and analog/digital convertor permits it, insertion of a low-pass filter before the sampler would be wise, in most cases, to attenuate the higher frequency noise which might be modulated down into the control system pass band by the sampling process. The signal quantization levels are chosen to cause no more than some tolerable degree of graininess in the operation of the system.

An example of a digital attitude control system for a large vehicle may be cited from the Apollo program. The configuration of the vehicle as it decelerates from the translunar trajectory into the lunar circular orbit is shown in Fig. 7–7. The Lunar Excursion Module is shown attached to the Command Module in the position that allows the astronauts to move from one vehicle to the other. This configuration is rather flexible, most of the bending occurring in the coupling structure between the vehicles. The frequency of the first bending mode is about 2 cps. Fuel sloshing has little effect on the

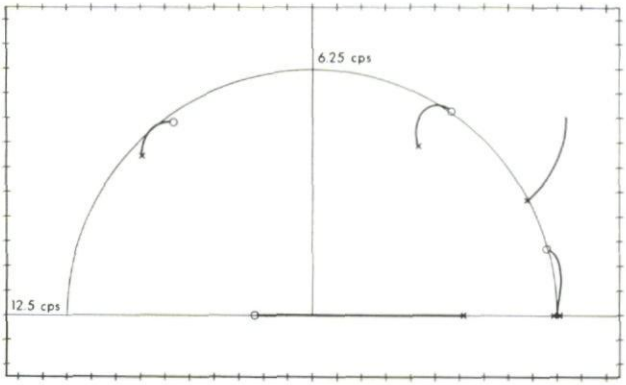

FIG. 7–8 Z plane locus of roots: without compensation

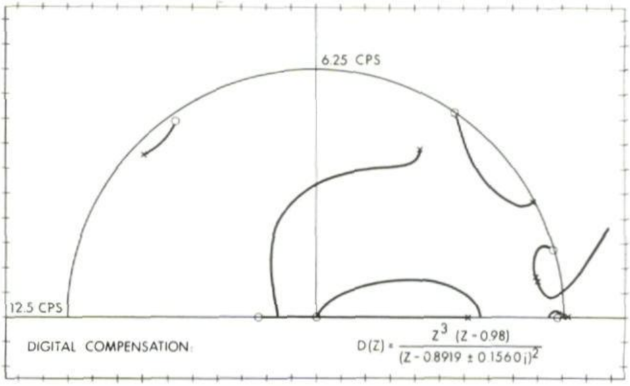

FIG. 7–9 Z plane locus of roots: with lag compensation

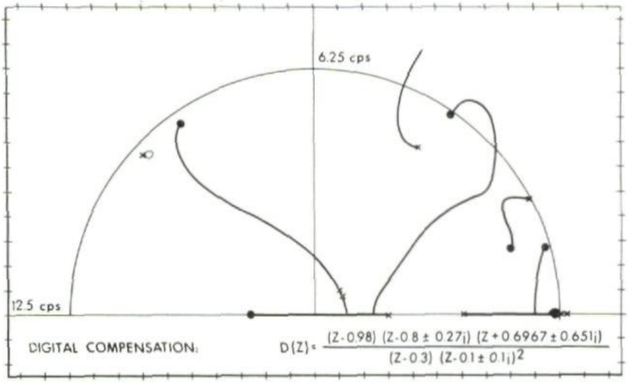

FIG. 7–10 Z plane locus of roots: with lead compensation

dynamics of this vehicle, the mass of fuel which participates in the sloshing oscillation being only a very small fraction of the mass of the vehicle. The analytic manifestation of this small mass ratio is the very close proximity of the zero to the pole in the sloshing pole-zero pair. Thus the zero nearly cancels the pole and both can be ignored in the analysis of this system. The attitude control system uses a sampling frequency of 25 cps and employs angle information only; no rate gyros are required. The attitude information which is the input to the digital Apollo Guidance Computer (AGC) is quantized at 40 arc-sec. The output of the AGC is the command to the engine gimbal servo which is held between the sampling points; this command is quantized at 160 arc-sec.

A Z plane locus of roots for the sampled system without compensation is shown in Fig. 7–8. The rigid body dynamics in the absence of atmosphere are just due to the vehicle inertia, this gives rise to the two poles at $+1$. Pole-zero pairs due to the first two bending modes are included. Without compensation, the first bending mode goes unstable immediately for very low system gain. The locus with lag compensation is shown in Fig. 7–9. In this case a single compensating zero has been used which corresponds to the rigid body compensation mentioned earlier, plus four poles to attenuate higher frequencies sharply. The closed-loop root locus originating at the first bending pole is seen to be pulled well into the stable region. The corresponding locus with lead compensation is shown in Fig. 7–10. In order to provide active damping of the first bending mode considerable lead was required. As can be seen in the figure, compensation involving five zeros and five poles is employed for this purpose. The result shows the first bending mode to be not only stabilized but rather well damped. With each of these forms of compensation the dominant system closed-loop poles have a natural frequency of about 1 rad/sec, roughly one-tenth fundamental bending frequency. With lead compensation, however, there are closed-loop zeros in the vicinity of these poles resulting in a significantly shorter response time to transient inputs. The bandwidth of each system as measured by the frequency at which the magnitude of the open-loop transfer function is unity is nearly the same – about 1 rad/sec – but the lag compensated system has more phase lag at this frequency and cuts off much more sharply for higher frequencies.

The step response of this system with lead compensation is shown in Fig. 7–11. This response was recorded by a simulator which used an analog computer to simulate the vehicle dynamics but used an actual AGC as the controller. The basic system response is seen to follow quite well the transient response characteristics corresponding to the dominant poles in the Z plane. Moreover, the bending oscillation is seen to be reasonably well damped. An interesting problem is pointed up by the occasional bursts of activity after the major response transient is over. These are occasioned by the attitude error drifting far enough to cause an indicated 1 quantum of error. This is a small error and the actual error rate is very small, so very little control is required to return the error to the zero quantum zone. However, the computer has seen an indicated zero error for many sampling periods so when one quantum of error is indicated the lead compensator interprets this change as a significnt rate of change of error with a similar interpretation of higher derivatives. This touches off an unnecessarily long period of control activity during which the bending modes are again excited.

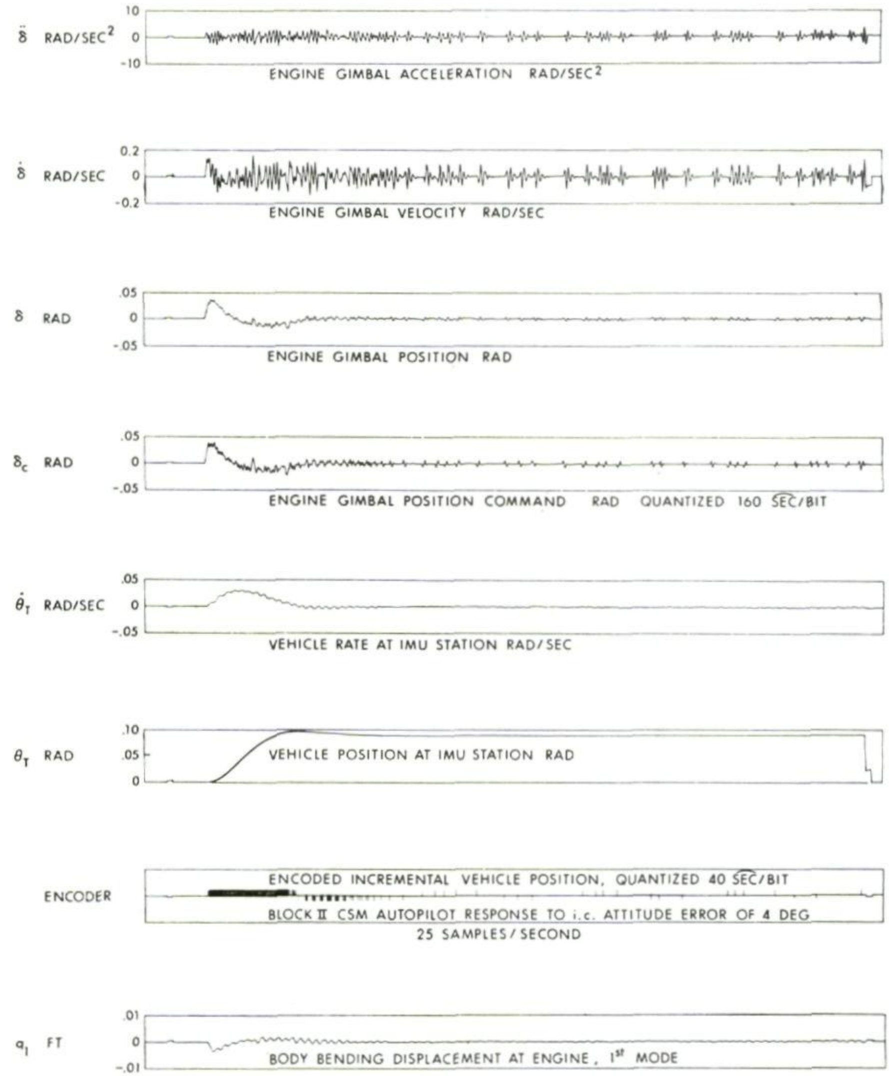

FIG. 7–11 Step response of attitude control system

So the problem of the attitude control of large flexible space vehicles is indeed challenging – and it will become even more so in the future. As the vehicles get larger the bending and slosh frequencies become lower but the performance required of the system does not necessarily decrease. Thus the requirement will be to push the system performance in terms of bandwidth closer to and beyond the bending and slosh frequencies. This can be done, but it makes the stability of the system critically dependent upon the detailed characteristics of these modes – and these characteristics are not altogether predictable in advance of the flight. Thus the interest in self-adaptive control systems for this application. It may also be that modern estimation theory will find some application to this problem. In the meantime, classical linear system analysis techniques remain very useful tools for the system designer, but the complicated character of the controlled member makes hand application of these techniques impractical. A powerful attack on the problem can be launched by preparing a series of digital computer programs to do the tasks that one would otherwise do by hand; tasks such as plotting the frequency response function for an open or closed loop system given the cascade of elements which comprise the open loop system, calculation of the sampled transfer function given the continuous transfer function, plotting the locus of closed loop roots for a sampled or continuous system given the open loop transfer function etc. Programs such as these have been used to carry out the design of the Apollo systems at the M.I.T. Instrumentation Laboratory. It is difficult to see how the job could have been done on a reasonable schedule without automation of these analytic operations.

ATTITUDE CONTROL WITH A FIXED ENGINE

The possible elimination of the massive engine gimbal structure and associated high-power actuators and servo systems is a very appealing step in the direction of system simplicity. The alternative is a control system based on on-off switching of attitude control reaction jets. The control thrusters must in this case be capable of delivering substantial control torque to balance the possible range of thrust axis offsets for the main engine. This offset is due to a number of causes. There is some tolerance in the mounting and aligning of the engine. The thrust axis does not lie along the engine centerline due to unsymmetrical flow and unsymmetrical nozzle ablation. But the major cause is the uncertain location of the vehicle center of mass. During any one mission phase the center of mass may move appreciably as propellants are consumed from off-axis tanks. An interesting compromise design is one which has the main engine gimbaled but provided only with a low-power actuator and very simple servo, such as a constant rate drive, which is switched in sign so the thrust axis tracks the vehicle center of mass. This will permit the use of smaller thrusters for attitude control.

For the present, consider the design of an attitude control system for a vehicle with a fixed engine. This configuration would not be attractive for the control of a very large high-thrust booster in atmosphere. For a smaller vehicle out of atmosphere the vehicle dynamics are essentially just the inertia effects, body bending and propellant sloshing being very high frequency modes. The parameters which dictate the design in the absence of thrust axis offset are the vehicle acceleration due to control moment, the minimum on-

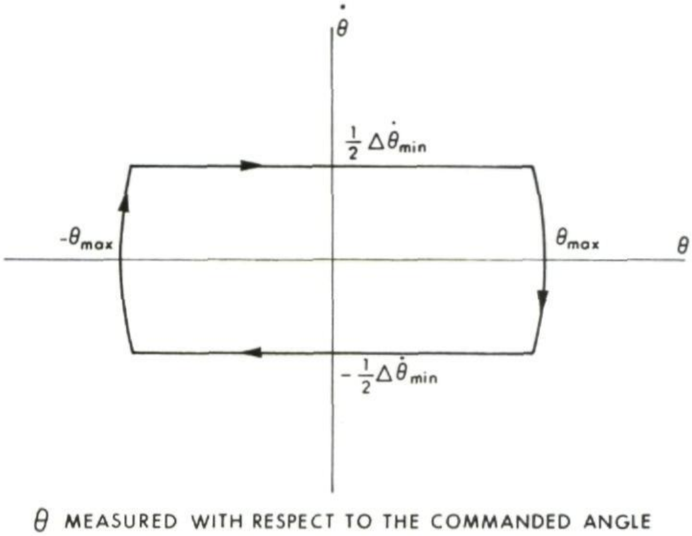

FIG. 7–12 Minimum symmetric limit cycle with no thrust offset

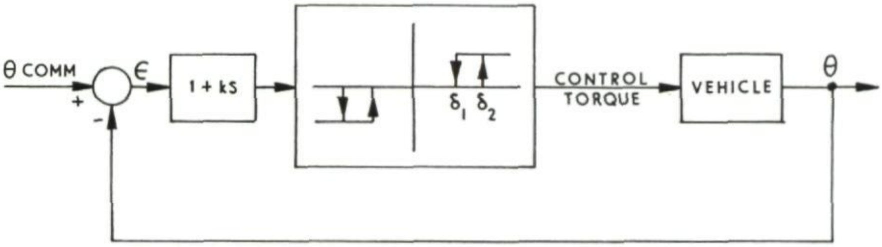

FIG. 7–13 Standard on-off control system

time for the control thrusters and the maximum allowable attitude error. In this situation, with the control moment designed to accommodate the maximum possible thrust axis offset, the acceleration due to control moment is likely to be very large. Also, for any thrusting system, there is a minimum on-time which can reliably be commanded. The product of this control acceleration and minimum on-time then gives the minimum change of vehicle angular velocity which can be commanded, call it $\Delta\dot{\theta}_{\min}$. The most favorable symmetric limit cycle which can be achieved in the absence of thrust offset consists of a coast at the rate of $1/2\ \Delta\dot{\theta}_{\min}$ to the specified error boundary, $\theta_{\max}$, a minimum control impulse at that point which changes the vehicle rate to $-1/2\ \Delta\dot{\theta}_{\min}$, and a coast to the negative $\theta_{\max}$ boundary. This limit cycle is shown in the phase plane in Fig. 7–12. The angle at which the control moment is switched on and off is:

$$\text{Switching angle} = \pm\,(\theta_{\max} - 1/8\ a_c t_{\min}^2) \qquad \text{(Eq. 7–1)}$$

where a_c is the angular acceleration due to the control moment. The thruster duty cycle is:

$$\text{Duty cycle} = \frac{2}{\dfrac{8\ \theta_{\max}}{a_c t_{\min}^2} - 1} \qquad \text{(Eq. 7–2)}$$

If, for example, the maximum allowable error is 1 deg, the angular acceleration due to control is 10 deg/sec^2 and the minimum control on-time is 10 milliseconds, the switching angle is 0.9999 deg and the duty cycle is $2.5\,10^{-4}$. With this large a control acceleration the limit cycle looks rectangular on the phase plane. The thruster duty cycle is quite favorable – the thrusters being on only 0.025% of the time. The vehicle coasts for 40 sec, thrusts for 10 millisec and coasts for 40 sec again. This is of course an idealization which assumes constant input, perfect information and no disturbances. The same performance would result with a constant rate input.

This limit cycle can be achieved in the absence of thrust offset using standard switching logic. Figure 7–13 shows a common system configuration in which a linear combination of error and error rate controls the thrusters through a trigger circuit or switching logic which includes a dead band and hysteresis. The indicated derivative can be thought of either as an idealization of a lead network or the effect of rate gyro feedback. Given the magnitude of the control torque, this system is designed by choosing values for the free parameters k, δ_1, and δ_2. The switching logic is assumed symmetrical. Realization of the limit cycle shown in Fig. 7–12 places two constraints on these free parameters; the two switching lines on each side of the origin must pass through the corners of the desired phase trajectory.

There remains a degree of freedom yet to be specified. This freedom can be used to achieve fast recovery from step changes in command of probable magnitude. If k is very small and δ_1 and δ_2 are chosen to yield the desired steady-state limit cycle, the response to a change in command is poorly damped. Such a phase trajectory is shown in Fig. 7–14. If k is very large and again δ_1 and δ_2 are chosen to yield the desired steady state limit cycle, the response to a change in command is slow and sluggish as indicated in Fig. 7–15. For any given initial error there is a choice of k (and δ_1, δ_2) which will

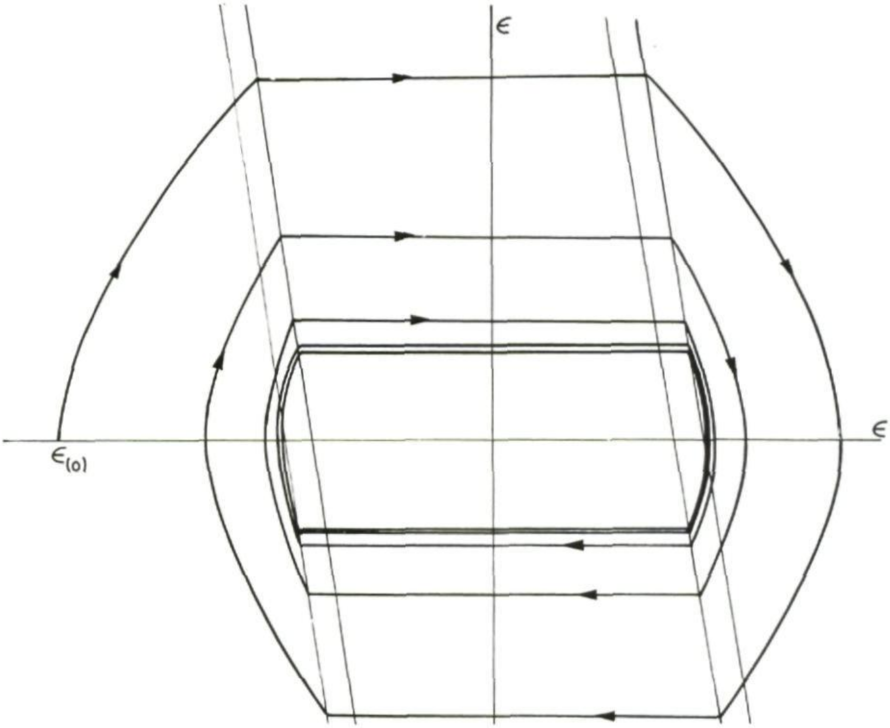

FIG. 7–14 Step response with small rate gain

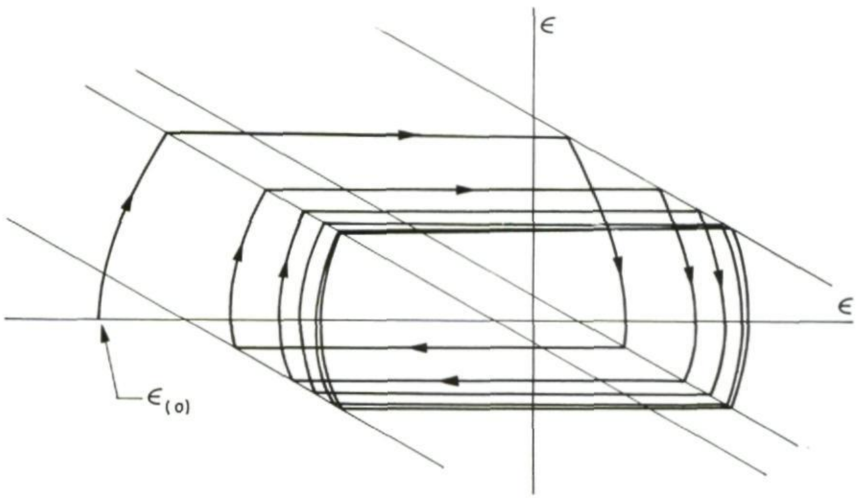

FIG. 7–15 Step response with large rate gain

carry the response into the limit cycle immediately as indicated in Fig. 7–16. The magnitudes of command changes are not predictable, of course, but some are more likely than others – and k (and δ_1, δ_2) can be chosen to yield good response in the most probable cases.

Having such a system designed to yield good step response for inputs of likely magnitude and an efficient limit cycle, it remains to be seen how the performance changes with thrust offset. The performance can be quite adversely affected as suggested by Fig. 7–17. This figure shows one form of limit cycle which may result from a positive offset moment which tends to drive the error rate negative. The trajectory is shown starting from the switching line in the first quadrant. A minimum positive control impulse is commanded at that point, which acting with the offset torque, drives the vehicle to a large negative rate. The negative acceleration then continues due to the offset torque alone until the trajectory hits the lower switching line. From that point the phase trajectory "chatters" between the switching lines moving to the left and approaching a limiting closed cycle. This steady-state operation is undesirable both because of the negative error bias and because of the rapid on-off cycling of the thrusters which is wasteful of fuel.

If the amount of the thrust offset were known, it would be easy to command a much more desirable limit cycle. The thrusters would never be used to add to the offset torque unless the offset were below some threshold. Rather, one portion of the cycle as seen in the phase plane would be the parabola due to the offset moment alone which just stays within the specified error bound. The other portion would be the parabola due to the control moment acting against the offset moment and which also stays just within the specified error bound. Such a trajectory is shown in Fig. 7–18. With the vehicle dynamics modeled as just an inertia, the required conditions for switching the control moment on and off are easily and simply expressed. The remaining requirement is an indication of the offset moment in addition to the error and error rate. It is clear that information about the offset moment is contained in the time history of attitude which results from the known history of control moment. If, for example, one took an estimate of the offset moment and applied it together with the known control moment to a model of the vehicle dynamics and later found that the attitude indicated by the model tended to grow more positive than the attitude of the actual vehicle, this would be evidence that the estimated offset moment was in error in the positive sense. This information could then be fed back to adjust the estimated offset moment.

This is the physical concept which underlies optimal linear estimation theory as formalized primarily by Kalman (2). The form of the Kalman estimating filter is shown in Fig. 7–19 where only one quantity is shown as being measured and several parameters may be estimated. It is also possible to process more than one measurement at a time. A model of the system is used to generate a prediction of the quantity being measured based on the current estimates of all parameters being estimated. The difference between the predicted measurement and the actual measurement feeds back through gains to alter the parameter estimates. A gain computer varies the estimate adjustment gains in an optimal manner depending on the nature of the measurement, the statistics of the measurement errors and of the uncertainties in the

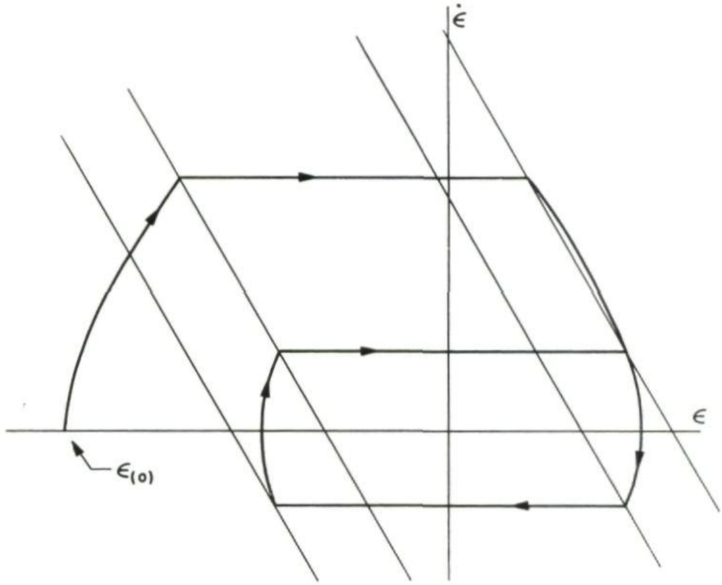

FIG. 7–16 Step response with proper rate gain

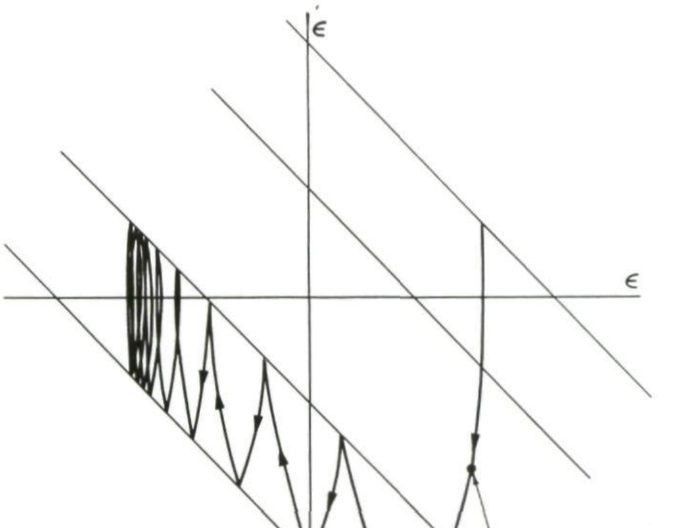

FIG. 7–17 Limit cycle with thrust offset

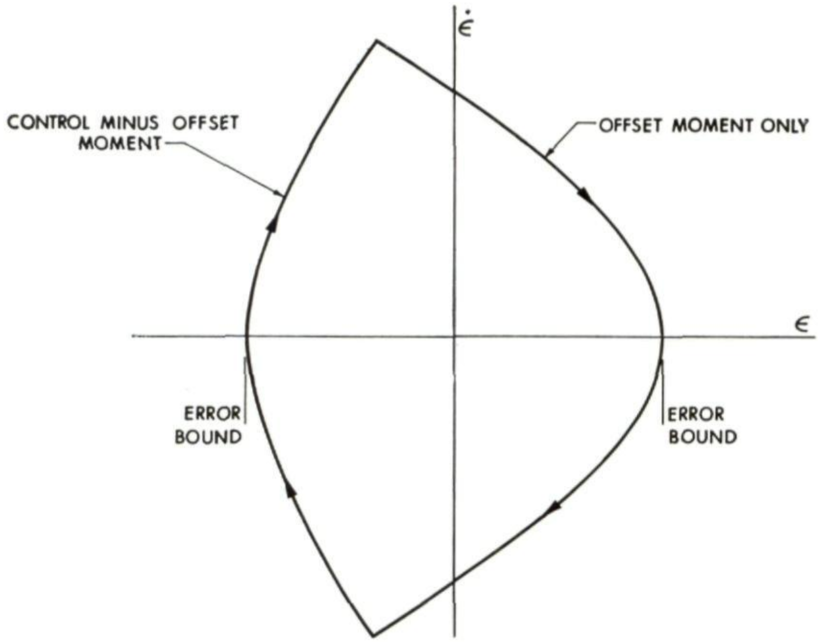

FIG. 7–18 Desirable limit cycle with thrust offset

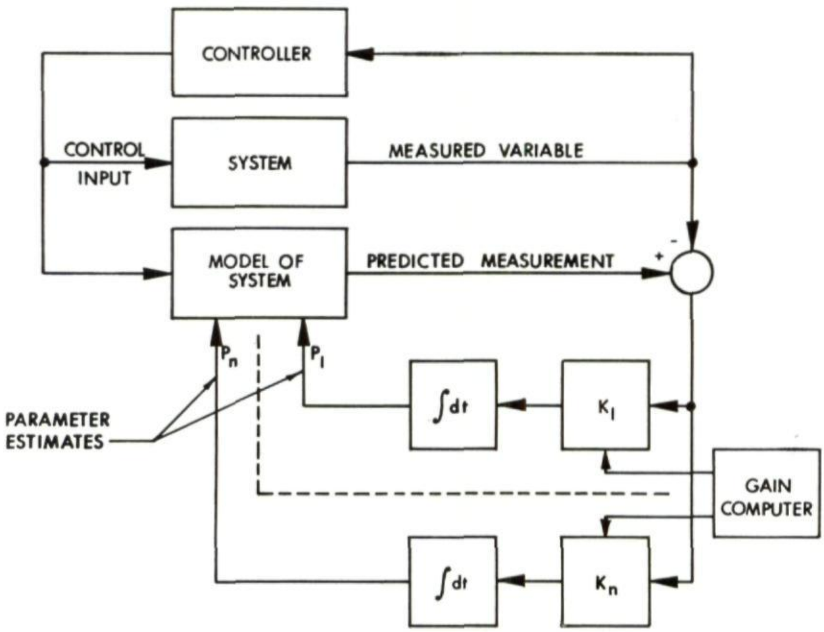

FIG. 7–19 Form of the Kalman estimator

prior knowledge of the estimated quantities. In the present application, the measured quantity is vehicle attitude and the estimated parameters would include vehicle attitude, attitude rate, offset moment and possibly vehicle inertia. Vehicle attitude is included as an estimated parameter, even though it is the measured variable, since the measurement is subject to noise or uncertainties. With an appropriate model of the system being of such simple form in this case, the major computational load is the gain computation. But the optimally varying gains converge quickly to steady-state values and in many mission situations little would be lost by using constant gains. If that is the case, then estimates of all the quantities needed to permit efficient control with arbitrary thrust offsets can be generated with very little required computation.

The resulting system can of course be instrumented with either analog or digital computation. Because of the rapid response of the vehicle to control and offset moments, rather high sampling frequencies would be required if a digital computer were used in the standard way in which control action can be taken only when the computer samples the attitude and processes the control equations. For example, in a limit cycle of the form of that shown in Fig. 7–18 corresponding to a control acceleration of 50 deg/sec^2, an offset acceleration of 10 deg/sec^2 and an error tolerance of 0.5 deg, the control torque is on for a period of 0.2 sec each cycle. If this time is to be resolved with no more than 10% error by the basic computer samples, a sampling frequency of 50 samples/sec would be required. This could impose an appreciable load on the computer. However, if the computer is organized (as is the Apollo Guidance Computer) to count input pulses while processing other calculations and also can be interrupted briefly when a certain count has been reached to issue a discrete output, then control action can be taken at times other than the basic computer sampling times. With this capability, a slower sampling frequency can be used. Each time the attitude is sampled and the estimates of parameters updated, the computation can predict whether control action (either on or off) should be taken before the next sampling point. If so, the time till that event or the change in attitude till that event can be read into a counter and counted down. Each time a thruster is turned on, the time it should be on is calculated and read into a counter so it can be turned off again between samping times.

A fixed-position rocket engine is used in the ascent stage of the LEM. For the purpose of standardization the same hypergolic thrusting system used on the Command and Service Module is also used on the Lunar Excursion Module. Toward the end of the ascent boost the response of the LEM to this control moment is quite lively – about 50 deg/sec^2. The moment due to thrust axis offset from the vehicle center of mass may be as much as half the control moment. Vehicle attitude is derived from the IMU gimbal angles and is indicated by the Coupling and Display Unit with a quantization of 40 arc-sec. No rate gyros are required by the primary attitude control system. Simulation of this system using digital control of standard switching logic has indicated that a sampling frequency of about 40 samples/sec would be required. Even at that sampling rate the effects of timing errors are clearly evident. A system using a Kalman filter to estimate attitude, attitude rate, and thrust axis offset has also been simulated. The model of vehicle dynamics

used in the filter is just an inertia for each axis. This is an incomplete model of three-axis vehicle dynamics but it is quite adequate. Different modes of control are programmed depending on the magnitude of the estimated error and the estimated offset. For steady-state operation with the offset above a threshold value limit cycles of the desired form shown in Fig. 7–18 are commanded. In each case, when a control moment is commanded, the time interval during which it should be on is calculated and read into a counter to be counted down by clock pulses. With this form of control, a sampling rate of 10 per sec yields excellent performance.

ACCELERATION VECTOR CONTROL

The purpose of the control system during powered flight is not just to control the vehicle attitude but rather to control the thrust acceleration vector, $\underline{a_T}$, in response to commands from the guidance system. In fact, it is possible to effect the $\underline{a_T}$ control directly without even feeding back attitude information, but a system which uses velocity information only requires complicated compensation which must be varied rather carefully with the changing flight condition and vehicle characteristics. It seems clearly preferable in most cases to use attitude feedback to stabilize the vehicle. Having a well-behaved attitude control system to work through, the design of the $\underline{a_T}$ controller is not difficult.

One approach is open-loop in nature. Having the desired direction of $\underline{a_T}$ as an input from the guidance system, one can interpret this simply as an attitude command and orient the longitudinal axis of the vehicle in the desired direction for $\underline{a_T}$. The discrepancy in so doing is that the thrust acceleration vector is not necessarily aligned with the longitudinal vehicle axis. In addition, if the vehicle center of mass moves off the longitudinal axis, the attitude control system develops a forced error large enough to point the average $\underline{a_T}$ direction through the offset center of mass location. For a vehicle with a gimbaled engine, the resulting angular error about one axis is:

Angle between actual $\underline{a_T}$ direction and desired $\underline{a_T}$ direction

$$\text{is equal to } \left(1 + \frac{1}{K}\right)\delta_{ss} \qquad \text{(Eq. 7–3)}$$

where K is the attitude control system forward gain – the gimbal angle per unit attitude error – and δ_{ss} is the steady-state engine deflection required to point $\underline{a_T}$ through the vehicle center of mass. The use of integral control in the attitude control system makes K in effect infinite, but the angular deviation between the direction of $\underline{a_T}$ and the vehicle longitudinal axis cannot be accounted for directly by an $\underline{a_T}$ control system which commands attitude in an open-loop manner. The resulting offset $\underline{a_T}$ direction feeds back through the guidance system to influence subsequent $\underline{a_T}$ commands but there does result from this a forced guidance error at cutoff proportional to the $\underline{a_T}$ directional error indicated above. In some mission situations this forced error may be tolerable. If the powered flight phase under consideration is followed by another guided phase, such as a translunar or transplanetary midcourse phase, the cost of the forced error will very likely be measured in terms of the fuel required to accommodate the error in the subsequent phase. In other

situations the inaccuracy resulting from the forced guidance error is of more direct consequence.

Such a forced error can be eliminated, if desired, by commanding the attitude control system through a closed-loop scheme in which the actual $\underline{a_T}$ direction as indicated by the IMU accelerometers is compared with the desired $\underline{a_T}$ direction and the vehicle commanded to rotate at a rate proportional to the angular deviation. This can be instrumented conveniently by noting that the cross product of the indicated unit $(\underline{a_T})$ with the desired unit $(\underline{a_T})$ is a vector which gives in magnitude and direction the rotation required to carry the indicated $\underline{a_T}$ into the direction of the desired $\underline{a_T}$. If the command is taken to be an angular rate proportional to this angular error, the resulting control law is:

$$\underline{W_c} = S(la_{\text{ind}} \pm la_{\text{com}}) \qquad \text{(Eq. 7–4)}$$

where $\underline{W_c}$ is the commanded angular rate, S a sensitivity or gain to be designed, la_{ind} a unit vector in the direction of the indicated $\underline{a_T}$, and la_{com} a unit vector in the commanded or desired direction for $\underline{a_T}$. If a rate-responding autopilot is used, this rate command can be transformed into body coordinates and applied as the command input. Only pitch and yaw components of the commanded rate in body axes would be computed and used. If an attitude autopilot or attitude control system is used, this commanded angular rate is transformed into the corresponding rate of change of direction for the vehicle longitudinal axis using:

$$\underline{i_l} = \underline{W_c} \pm \underline{I_l} \qquad \text{(Eq. 7–5)}$$

which is then integrated to the desired direction for the longitudinal axis. $\underline{I_l}$ is a unit vector along the longitudinal axis of the vehicle. It is compared with actual vehicle attitude to provide pitch and yaw attitude errors for the attitude control systems to null. In many mission situations the computing axis system can be chosen favorably with respect to the general direction of desired $\underline{a_T}$ so some of the indicated computation can be abbreviated. Toward the end of the powered flight phase when the cutoff condition is approached, the computed direction for the desired $\underline{a_T}$ tends to change rapidly. However, $\underline{W_c}$ can be limited in magnitude or even clamped to zero for a brief period of time prior to cutoff with little loss in guidance accuracy.

This closed-loop $\underline{a_T}$ control renders the system insensitive to any static thrust axis offset or offset center of mass location. The vehicle is simply commanded to rotate until the desired condition is achieved, regardless of what vehicle attitude is required to achieve it. The forced guidance error is in this case proportional to the rate of change of the offset angle rather than the angle itself. It is then primarily the rate of change of vehicle center of mass which designs the system sensitivity, S. This sensitivity can often be quite low; for example, in the Apollo lunar approach configuration, a gain of 0.06 rad/sec/rad is adequate.

CHAPTER 7–2

COASTING FLIGHT CONTROL

During periods of coasting flight when there are no significant forces acting on the spacecraft, control over the vehicle implies attitude control only. In mid-course flight through free space the most common requirements for attitude control result from the requirements for:

(a) **Sun pointing** – Very often a space vehicle is designed to operate most of the time with one face pointed to the sun. This allows efficient operation of solar cell panels and heat radiators and provides a predictable heat load on the vehicle which eases the thermal control problem. In addition, the sun line constitutes the most easily acquired and identified reference direction in solar space.

(b) **Antenna pointing** – A communication or telemetry antenna oriented toward earth is an almost universal requirement. This requirement can be accommodated by vehicle roll control around the sun line plus one degree of freedom of the antenna with respect to the vehicle.

(c) **Orienting for navigation sights** – Depending upon the design of the on-board optical equipment, vehicle reorientation may be required in taking navigation sightings. Measurement of the angle between a star line and the line of sight to a landmark on a near body, for example, requires orienting the sextant precision drive axis normal to the plane of the measurement. This is a two-degree of-freedom specification. If for reasons of mechanical simplicity and instrument accuracy only one degree of freedom of the precision drive axis with respect to the vehicle is provided, the additional degree of freedom must be provided by vehicle reorientation about one axis.

(d) **Orienting for thrusts** – Prior to starting the spacecraft propulsive engine for a thrusting period, the vehicle is oriented with its longitudinal axis in the direction along which velocity is to be gained. This requires a two-axis vehicle reorientation.

The attitude references usually used during midcourse coasting flight are sun and star lines during quiescent periods and an inertial reference during reorientations. A two-axis sun sensor serves as the reference for control of one axis of the vehicle along the sun line. The degree of freedom in roll about the sun line is controlled against a reference provided by a star tracker. The star Canopus is a popular choice for the reference star because of its location well out of the ecliptic plane. The Canopus line thus makes a large angle with respect to the Sun line as seen from a vehicle travelling near the ecliptic and it is not confused by neighboring stars of comparable magnitude. Orienting for a navigation sight or a thrust requires giving up one or both of these optical references. An inertial reference must then be provided. The accuracy required of such a reorientation is not so demanding as to require the use of the navigation system IMU. A set of body-mounted single-degree-of-freedom

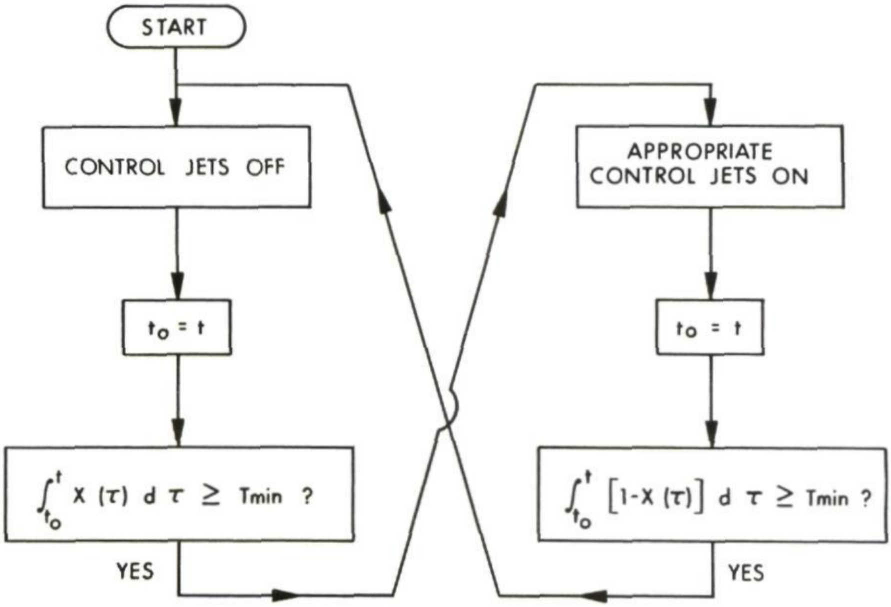

FIG. 7–20 Control logic for Shaefer or pulse ratio modulator

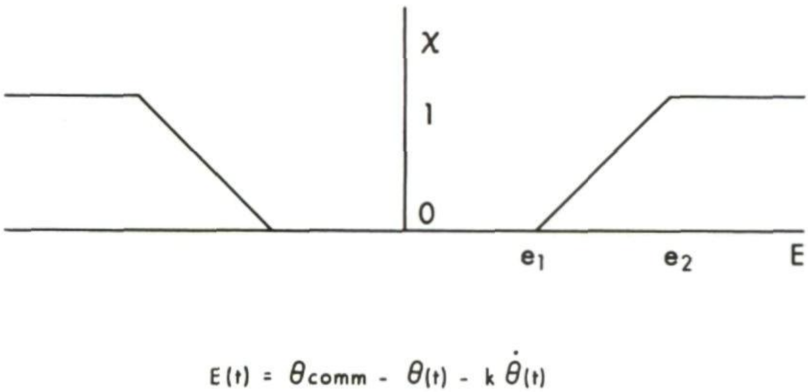

FIG. 7–21 Typical definition of x(t)

integrating gyros is a convenient and simple alternative. If these gyros are used as pulse-rebalanced instruments, communication with the central digital computer is particularly easy. A two-axis reorientation is accomplished by rotating from the reference orientation through a prescribed angle about one axis followed by a prescribed rotation about a second axis. The vehicle control system holds the third gyro at null during this process. The reference orientation can then be recovered by executing negative rotations in the reverse order.

The sources of control moments during midcourse space flight are reaction jets or momentum exchange systems. Reaction jets can employ either cold or hot gas, hypergolic thrusters being preferable for the larger vehicles. Cold gas systems, most commonly employing pressurized nitrogen, have been used in many missions but they have a restricted specific impulse capability – about 60 to 80 sec – and require even more weight in tankage than the weight of control gas stored. On-off control systems for vehicles using reaction jets are of the same type as those discussed in the preceding chapter under "Attitude Control with a Fixed Engine". As described there, the thruster duty cycle in steady-state limit cycling with no external moments acting on the vehicle depends on the minimum impulse which can reliably be commanded and the maximum attitude error which can be tolerated. The presence of an external moment, such as a moment due to unbalanced solar pressure forces, can actually be used to advantage to further reduce the rate of control fuel consumption. But this saving can only be achieved if the control system is capable of recognizing the presence of the moment and only thrusting against it, waiting for the external moment to return the attitude error to the limit.

Momentum exchange systems derive moments either by accelerating wheels about their spin axes or by precessing wheels which are maintained continuously spinning as gyros. In either case it is possible to design a linear control system around such a torque generator. Steady-state operation of such a system does not necessarily include a limit cycle and very accurate attitude control – essentially as accurate as the basic attitude reference – can be maintained if needed. On the other hand, there is an upper limit to the amount of angular momentum such a system can exchange. The saturated condition is represented by an inertia wheel spinning at its maximum speed in the case of the accelerating wheel system, and by the gyros having turned through 90 degrees in the case of the precessing gyro system. Control saturation must be prevented either by adjusting the attitude or configuration of the vehicle to prevent an external moment from acting in the same sense over a long period of time, or by applying a moment to the vehicle with a reaction jet system in such a sense as to move the momentum exchange controllers away from the saturated condition.

A number of forms of control logic have been devised for use with reaction jet controllers in an effort to achieve some approximation to linear or proportional, control. The simplest of these are pulse rate modulation and pulse width modulation. In the former case, control torque pulses of constant width are commanded to recur at a rate proportional to a control signal which may be attitude error or vehicle-rate-damped attitude error. The major disadvantage of this logic is the high pulse repetition rate at large errors when it would be less wearing on valves and more efficient in fuel use to simply leave

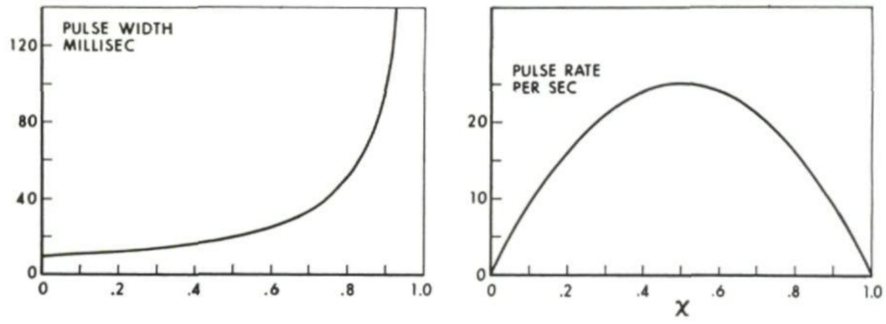

FIG. 7–22 Performance of the pulse ratio modulator

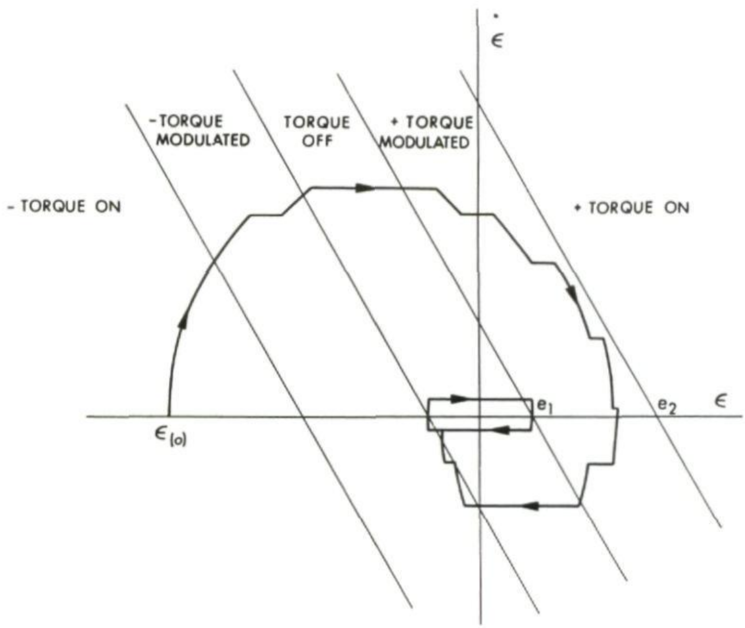

FIG. 7–23 Typical step response of pulse ratio modulated system

the control jets on. In the latter case, control torque pulses are commanded to recur at a fixed rate – the width of these pulses being proportional to the control signal. The disadvantage of this scheme is the repeated operation of the thrusters even at small errors when it would be preferable to leave them off.

More sophisticated schemes attempt to relieve these disadvantages through additional data processing. One such scheme due to R. A. Schaefer (3) is known as the Schaefer modulator or pulse ratio modulator. The control logic is pictured in Fig. 7–20. The variable $x(t)$ shown in that figure is a function of the rate-damped attitude error signal; it must range between 0 and +1 and is often taken in the form shown in Fig. 7–21. In operation, the control logic moves repeatedly around the flow graph of Fig. 7–20, turning the appropriate jets on long enough for the integral of $1 - x(t)$ to accumulate to T_{min}, then turning the jets off long enough for the integral of $x(t)$ to accumulate to T_{min}. Clearly, if the control signal remains within the dead zone of Fig. 7–21, the jets would remain continuously off and if the control signal remains in the saturated regions of that figure, the jets would remain continuously on. For intermediate values of the control signal, the control jets are pulsed on and off, the pulse width, pulse rate and pulse duty ratio all varying with the control signal. If $x(t)$ is treated as quasi-stationary, the operating characteristics are:

$$\text{Pulse width} = t_{on} = \frac{T_{min}}{1 - x} \qquad \text{(Eq. 7–6)}$$

$$\text{Pulse rate} = \frac{1}{t_{on} + t_{off}} = \frac{1}{T_{min}} x(1 - x) \qquad \text{(Eq. 7–7)}$$

$$\text{Duty ratio} = \frac{t_{on}}{t_{on} + t_{off}} = x \qquad \text{(Eq. 7–8)}$$

The variable x thus measures directly the duty ratio of the control history. The pulse width and pulse rate are plotted in Fig. 7–22 for $T_{min} = 10$ millisec. It may be seen from these curves that for small values of x (control signals near the dead zone) the pulse ratio modulator acts essentially as a pulse rate modulator using minimum width pulses. For larger errors, the pulse width increases as desired to prevent very large pulse rates. The maximum pulse rate for quasi-static x is $\frac{1}{4\,T_{min}}$.

Even the performance of such a control logic leaves something to be desired. A typical response to a command input using the pulse ratio modulator is shown in Fig. 7–23. The control jets are turned on and off unnecessarily often before reaching the final limit cycle. If the performance of the system (its acceleration level and time lags) is known well enough, only two control pulses are needed to enter the limit cycle. A set of switching curves which

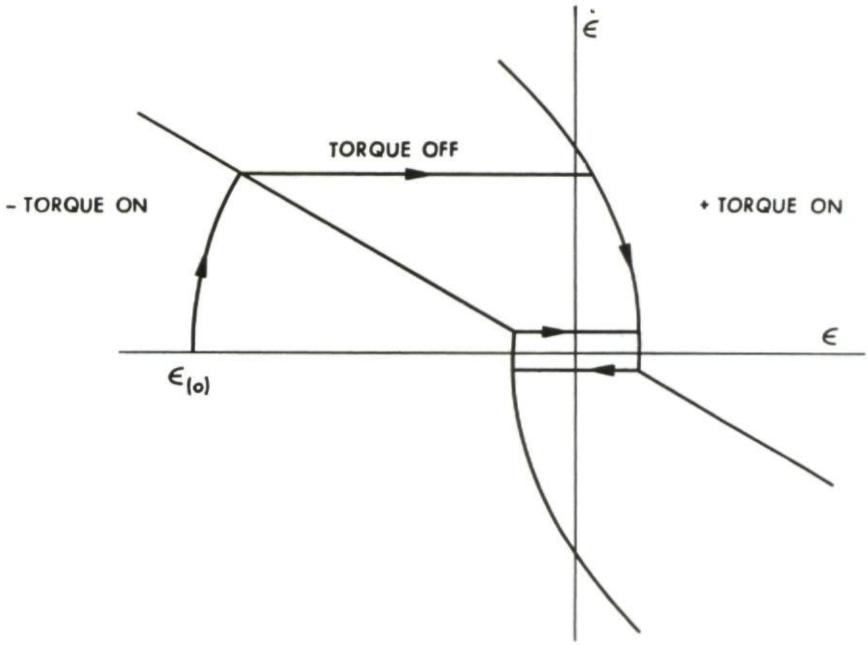

FIG. 7–24 Step response with straight-line and parabolic switching curves

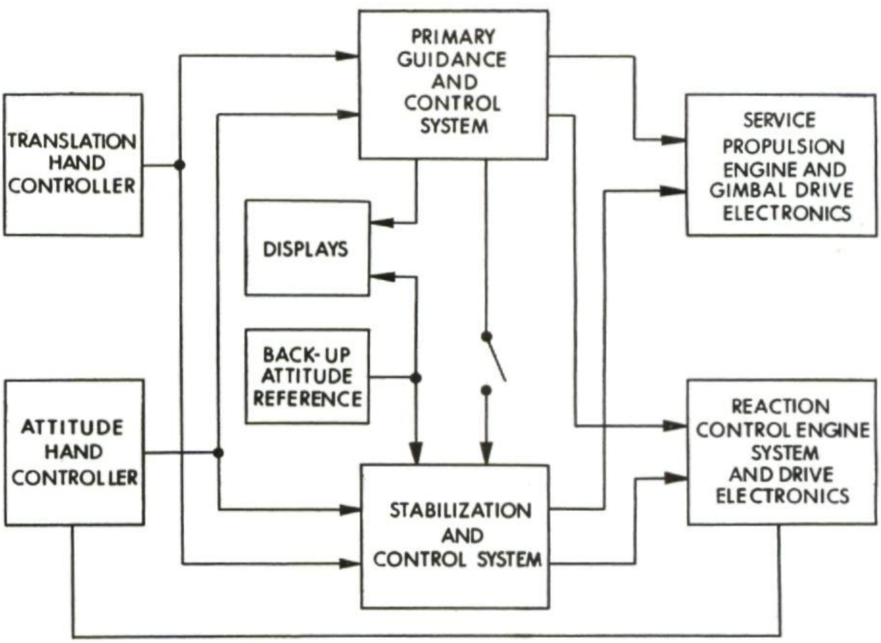

FIG. 7–25 CSM guidance and control system block diagram, Block II configuration

achieve this is shown in Fig. 7–24. The slope of the straight-line torque-off switching lines may be varied as desired to compromise between fuel used and response time. If a digital controller is employed, switching logic such as this is easy to implement.

Choice of a momentum exchange or reaction jet system or both should be based on an analysis of system weight, performance and reliability. If high accuracy attitude control is required, such as in the case of a vehicle carrying a large telescope fixed to the body, a momentum exchange system would seem to be a clear choice. Most space missions do not require exceptional attitude accuracy, however, and a reaction jet system may be selected on the grounds of reliability. The reliability advantage would be especially significant if one interpreted successful operation of a momentum exchange system to require the operation of a reaction jet system used for desaturation as well. If it is understood at the outset of a system design that accurate attitude control is costly, the vehicle and its subsystems can often be designed with a view to avoiding the need for accurate control. For example, it is easy to imagine designs for an optical measurement unit which would require precise vehicle control to track some reference line. But it may also be possible to design that unit, as in the Apollo system, to tolerate a slow drift in vehicle attitude. Rather than controlling the vehicle precisely to a reference condition the vehicle is allowed to drift through the reference condition – and the event of passage through the reference is noted.

An additional factor bearing on the choice of a momentum exchange or reaction jet system, especially for space missions of extended lifetime, is difficult to assess quantitatively. This is the possibility of consuming all available fuel for a reaction jet system. A momentum exchange system has the advantage of consuming a quantity which can be replenished in space – electrical energy. There is no obvious threat of running out. But a reaction jet system consumes mass which cannot yet be replenished in space. So although the analysis may show a very low probability of exhausting all control fuel, the threat of this possibility hangs over the mission during its entire lifetime.

During its midcourse flight the Apollo spacecraft (4) effects attitude control with a system of hypergolic rocket engines which are also used for vernier translational control when needed. They employ hydrazine and nitrogen tetroxide or variations of them as fuel and oxidizer. They are capable of reliable operation in pulses as short as 10 milliseconds. Sixteen of these engines are mounted on the sides of the service module in quadruple sets at four locations. They are normally fired in pairs to produce control couples. A variety of operational modes can be selected by the crew. These are suggested by the simplified block diagram shown in Fig. 7–25. In the primary mode, the Apollo Guidance Computer operates the jet solenoid valve drivers directly based on attitude reference information only. The analog Stabilization and Control System is used as a back-up mode. It employs both attitude reference and rate gyro information. Crew-operated modes include attitude-hold and rate-command modes in addition to direct actuation of the reaction jets by the pilot through a three-axis hand controller.

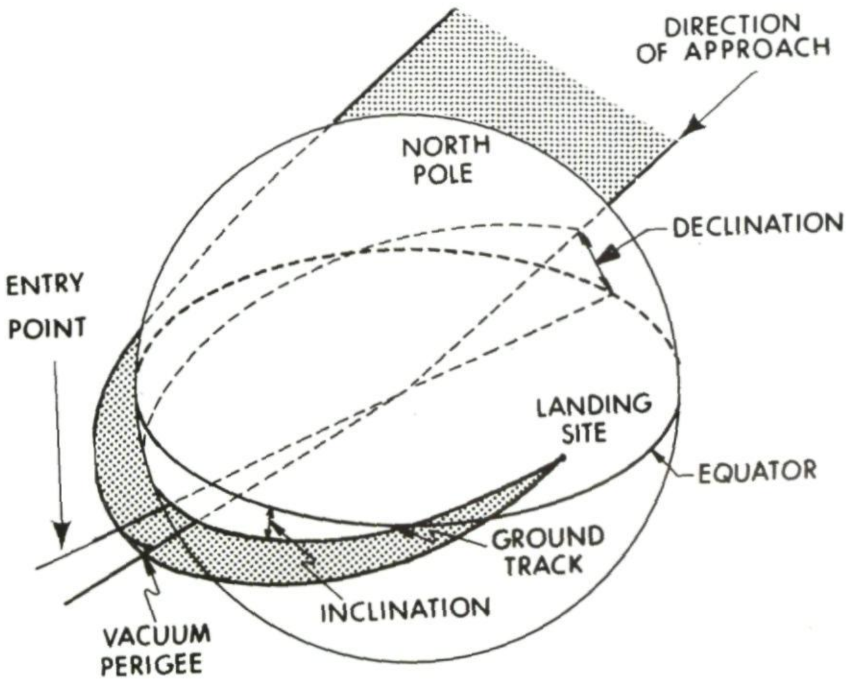

FIG. 7–26 Geometry of entry trajectories

CHAPTER 7–3

ATMOSPHERIC FLIGHT CONTROL

INTRODUCTION

A significantly different control problem is encountered in the high-speed atmospheric flight phase or phases of a space mission. Attention is here centered on flight following entry into a planetary atmosphere in which the path of the vehicle is controlled entirely or primarily by control of the aerodynamic force acting on the vehicle. This would include the final phase of an earth-return mission; re-entry into earth's atmosphere and control of the vehicle to a desired landing point. It would include a pass through the atmosphere of a planet for the purpose of reducing the energy of the vehicle's orbit relative to that planet prior to a propulsive transfer into a planetary orbit. We do not consider in this chapter the brief period of atmospheric flight which occurs at the beginning of a mission, the boost from the pad out of earth's atmosphere. The control problem during boost is dominated primarily by the propulsive force rather than the atmospheric force and was considered earlier in Chapter 7–1.

Control over the flight path of the vehicle as well as attitude control of the vehicle itself is discussed here. Flight path control is also called guidance, and as such could well have been treated in Part 3. However, the distinction between guidance and control is arbitrary, and it was thought better to consolidate in one section the discussion of the unique problems of guidance and control in the high-speed atmospheric flight situation.

FLIGHT PATH CONTROL

The discussion of this section will center on the re-entry and landing control problem. An atmospheric braking pass which involves entry into and subsequent exit from a planetary atmosphere is in fact a truncated version of a landing trajectory, which often requires a controlled skip out of the atmosphere to achieve the required range. The geometry of entry trajectories leading to a landing point is indicated in Fig. 7–26. The direction of approach relative to earth is constrained by the nature and timing of the mission. However, when the spacecraft is a substantial distance from earth its velocity vector is oriented nearly along the direction to the earth's center, so it is possible with little expenditure of fuel to rotate the plane of the approach trajectory arbitrarily about the local vertical line. Thus it is possible to orient the trajectory plane so the vehicle will fly to any selected landing point with no lateral control under nominal conditions. The trajectory plane required to achieve this is not immediately obvious because the landing point is moving due to the rotation of the earth and the vehicle without lateral control does not fly in an inertial plane.

Prior to entering significant atmosphere, the vehicle's trajectory does lie essentially in a single inertial plane. But except for winds, the atmosphere

rotates with the earth and the vehicle is gradually captured by the rotating air mass, and eventually flies essentially in a plane which rotates with the earth. None the less, it is possible to determine by iteration a plane for the approach trajectory such that no lateral control would nominally be required to fly to the landing point. The required range after entry is then given by the distance from the entry point to the landing site. The entry point is defined as that point at which the approach trajectory passes through an arbitrary altitude – often taken to be 400000 ft. The entry point thus occurs slightly before the perigee point for the approach trajectory computed as if there were no atmosphere.

This problem is further constrained by the desire to hold the azimuth of the approach to the landing site within certain bounds. This requirement is due to the desire to fly over well-instrumented areas and the desire to avoid hostile areas. This hostility may be either natural or political. Especially in a manned mission one would want to avoid over-flying certain countries and would want to avoid the colder regions of the earth. If it were possible to select and reach a landing site nearly along the line of the approach direction, then by rotation of the approach trajectory plane about the local vertical line while the vehicle is some distance from earth it would be possible to approach that landing point with any desired azimuth. But in many cases this would represent a severe re-entry range requirement.

The other extreme is a landing point near the plane normal to the approach direction. In that case the plane of the approach trajectory must be taken to give a reasonable lateral range requirement after entry, and very little freedom remains to adjust the approach azimuth. These requirements may very well conflict to such an extent that it is impossible to select one or even several landing sites which can be reached by the vehicle with the desired azimuth or orbital inclination under all conditions of timing of the mission. In that case an alternative is to use a water landing and move the landing point continuously with the changing mission situation. In the Apollo mission, for example, the direction of return to earth depends on the declination of the moon which changes from day to day. A band of possible landing sites is chosen at low latitudes in the Pacific Ocean so the actual landing point toward which the re-entry system guides is moved from day to day if a take-off is delayed.

Another concept associated with atmospheric entry trajectories is that of the entry corridor. This is simply recognition of the fact that a given vehicle cannot fly an acceptable atmospheric flight for arbitrary initial conditions at the entry point. If the flight path angle at that point is too steep, the vehicle will later suffer excessive aerodynamic loading even if its maximum lift is directed upward. Or if the flight path angle at entry is too shallow, the vehicle will exit the atmosphere again with a supercircular velocity even if its maximum lift is directed downward. These boundaries of entry flight path angle are often taken to define the corridor of acceptable entry conditions. The corridor can also be specified in terms of the range of acceptable virtual perigees – the perigee altitude computed as if there were no atmosphere. The corridor depends on the specific definitions of its boundaries, such as 10 g's for the undershoot boundary and on the entry velocity and vehicle L/D (Lift/Drag) capability. For a lunar return with an entry velocity of about

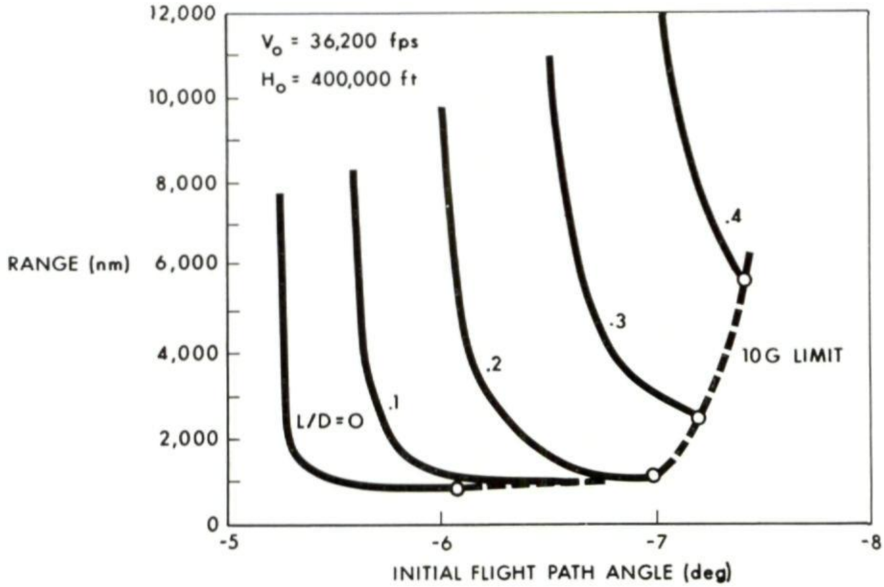

FIG. 7–27 Re-entry range capability for lunar return conditions, constant L/D

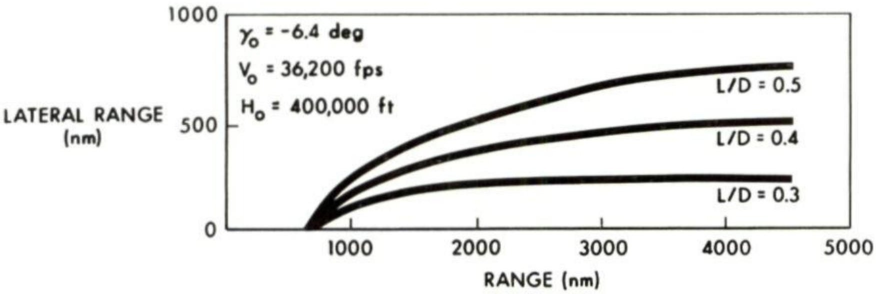

FIG. 7–28 Lateral range capability for lunar return conditions, constant L/D

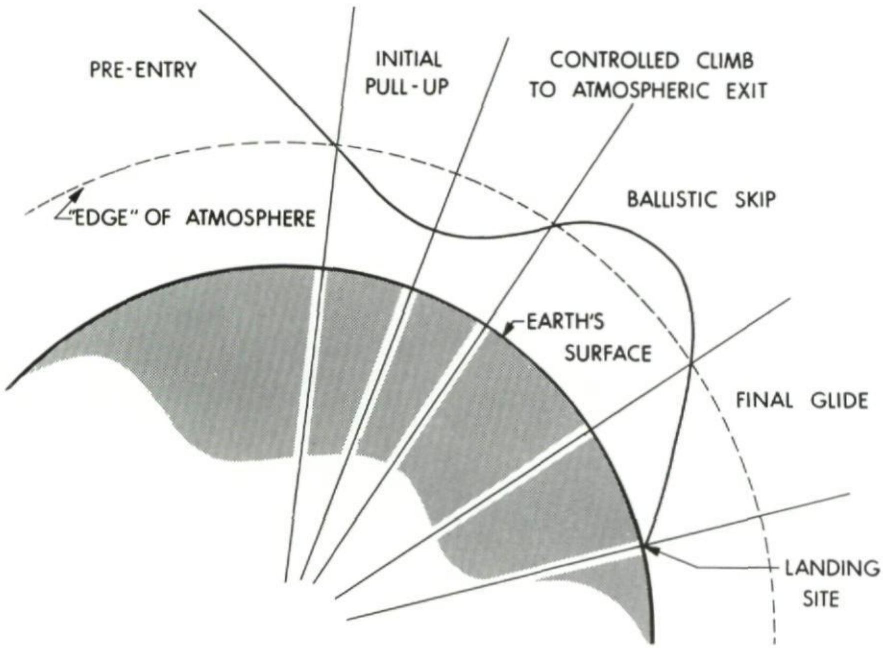

FIG. 7–29 Typical re-entry trajectory

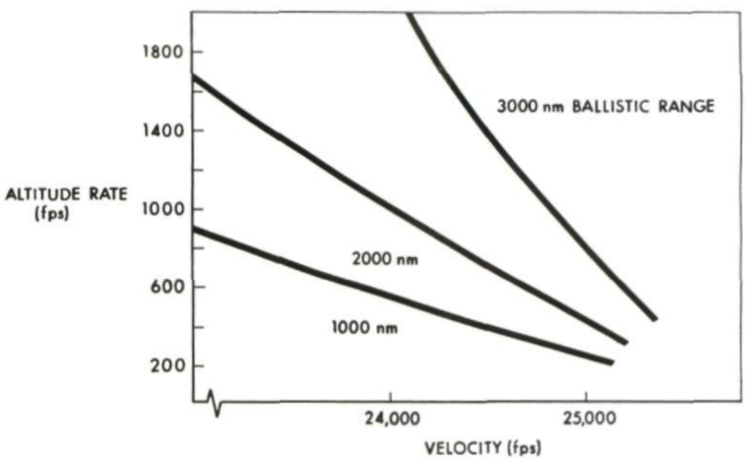

FIG. 7–30 Ballistic range for different exit conditions

considered logical in nature – the decision to direct lift up or down depending on the indicated entry conditions and continuing trajectory. If not all the lift of which the vehicle is capable is required to avoid excessive g's or skip-out and if substantial lateral range is required to reach the landing point, at least some component of lift may be used in the lateral direction. To achieve near-maximum lateral range it is essential to begin turning the trajectory as early as possible. The end objective of this phase might be taken to be a horizontal flight path angle at a suitably low g level and a low enough velocity so the vehicle can maintain capture in the atmosphere. This means the velocity and altitude at the end of pull-up must be such that the maximum lift of which the vehicle is capable is nearly enough to balance the excess of centripetal over gravitational acceleration.

Controlled Climb to Atmospheric Exit – In most instances, if the vehicle is to make the required range it must climb and do an out-of-atmosphere skip to a new entry point close enough to the landing point so the remaining range can be covered in a steady glide. This is the most sensitive maneuver of the re-entry flight. The range achieved in the ballistic portion of the flight is shown in Fig. 7–30 as a function of velocity and altitude rate at exit which is taken as 400 000 ft altitude. It is clear that there is a one parameter infinity of exit conditions which will realize the desired ballistic range. For a given required range, a lower exit velocity can be compensated for by a steeper flight path angle resulting in a larger altitude rate. These different trajectories resulting in the same ballistic range have very different sensitivities to errors in knowledge of or control over exit conditions. This is indicated in Fig. 7–31 which shows the sensitivity of ballistic range to exit velocity and in Fig. 7–32 which shows the sensitivity of ballistic range to exit altitude rate. In each case the sensitivity decreases sharply with velocity, so a slow, steep exit is preferable to a fast, shallow exit from the point of view of error sensitivity. For example, if 2 000 nm range is required in the ballistic portion of the flight, it can be achieved with an exit velocity of 24 600 fps and an altitude rate of about 680 fps or an exit velocity of 25 400 fps and an altitude rate of about 230 fps – among other combinations. The range derivatives with respect to both velocity and altitude rate are roughly three times larger in the second case than is the first. Since the navigation information used by the guidance system may have appreciable errors, due chiefly to the imperfect initial conditions supplied to the navigator at the end of midcourse flight, control over sensitivity to errors must play a dominant role in the design of the flight control system for this phase of the flight.

Two fundamentally different approaches to this flight control problem are often considered: predicted final value control and nominal-following control. The final value control scheme involves prediction of the effect of an assumed control history on the conditions at the end of flight. This trajectory prediction can be done analytically if possible, or otherwise by high speed computer runs starting from the indicated present state. If the terminal conditions are not as desired, in this case if the terminal range is not the desired range, the assumed form of the control is altered and a new predicted trajectory is computed. This iterative process converges on a suitable control history. This form of control can accommodate large off-nominal perturbations in initial conditions, it does not attempt to fly back to a pre-selected

36 000 ft/sec and L/D = $\frac{1}{2}$, the 10 g entry corridor is about 2.5 degrees wide in terms of entry flight path angle. For a planetary return with an entry velocity of perhaps 50 000 ft/sec the same corridor shrinks to about 0.7 degree.

For lunar return conditions, the range control which is available to vehicles of different hypersonic L/D capability is shown in Fig. 7–27. (Data from Ref. 5.) For each L/D, the short range limit is determined by the 10 g constraint. The maximum range increases essentially without limit with decreasing entry flight path angle. This is indicative of trajectories which turn upward after entry and exit the atmosphere for a long ballistic skip. Such long range performance is not necessarily usable in practice due to the extreme sensitivity of range to errors in exit conditions. The data of Fig. 7–27 is for constant L/D flight. The minimum range for a given initial flight path angle and L/D capability can be improved somewhat by controlling the lift during the flight. The gain is realized by reducing the lift as the vehicle approaches a 10 g acceleration so as to reduce the total aerodynamic load and prevent a violation of the 10 g limit. The lateral control capability of vehicles of various hypersonic L/D as a function of the downrange distance travelled is shown in Fig. 7–28 (5).

Some of the basic requirements which must be placed on an atmospheric flight control system are the following:

(a) Avoid excessive aerodynamic loads.
(b) Avoid uncontrolled skip-out in the presence of navigation, vehicle and atmospheric uncertainties.
(c) Achieve the necessary range and cross-range.
(d) Maintain a suitably low heating load, perhaps heating rate.
(e) Achieve adequate accuracy at landing point.

These requirements will be considered within the context of a standard flight plan as indicated in Fig. 7–29.

Pre-Entry – A large part of the responsibility for meeting the first two requirements above rests with the midcourse guidance system. Throughout the mission each guided phase has been followed by another, so the cost of guidance inaccuracies is measured primarily in terms of the fuel required to accommodate the errors in the next mission phase. A more serious cost, however, is associated with the last midcourse correction prior to entry into an atmosphere. That correction must yield entry conditions within the acceptable corridor or it will be beyond the capability of the atmospheric flight control system to fly a proper trajectory. For reasons of simplicity and reliability, the midcourse corrections prior to the last one may be made under the control of an abbreviated inertial system – such as one based on three body-mounted pulse-rebalanced gyros for attitude control and a single body-mounted longitudinal accelerometer for engine cutoff. But due to the premium on accuracy for the last correction, it will be delayed as long as possible so as to benefit from the best possible navigation information, and be executed under the control of the primary instruments of the guidance and navigation system. The IMU will have been aligned for this purpose and prior to atmospheric entry the inertial navigator is provided with initial conditions.

Initial Pull-Up – During the initial portion of the entry trajectory, attention may well be centered not on reaching the landing point but on avoiding excessive g's or uncontrolled skip-out. Control during this phase may be

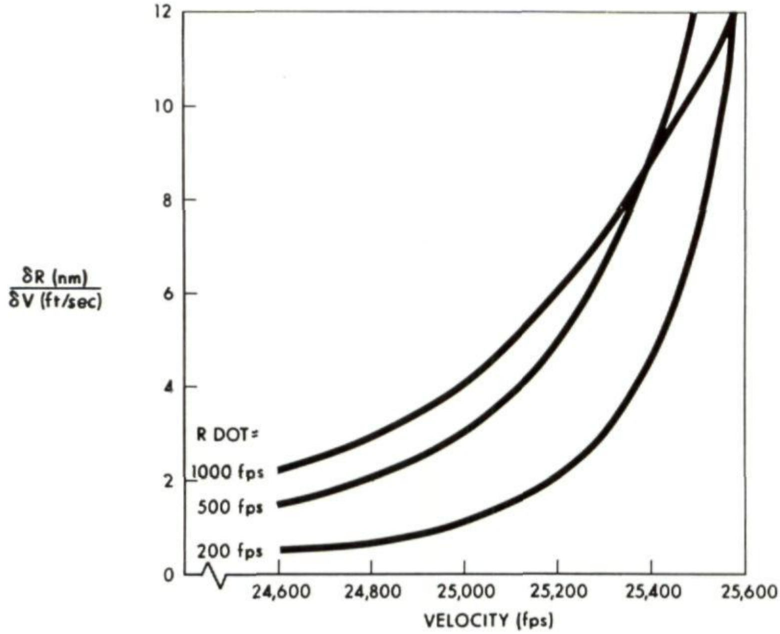

FIG. 7–31 Sensitivity of ballistic range to exit velocity

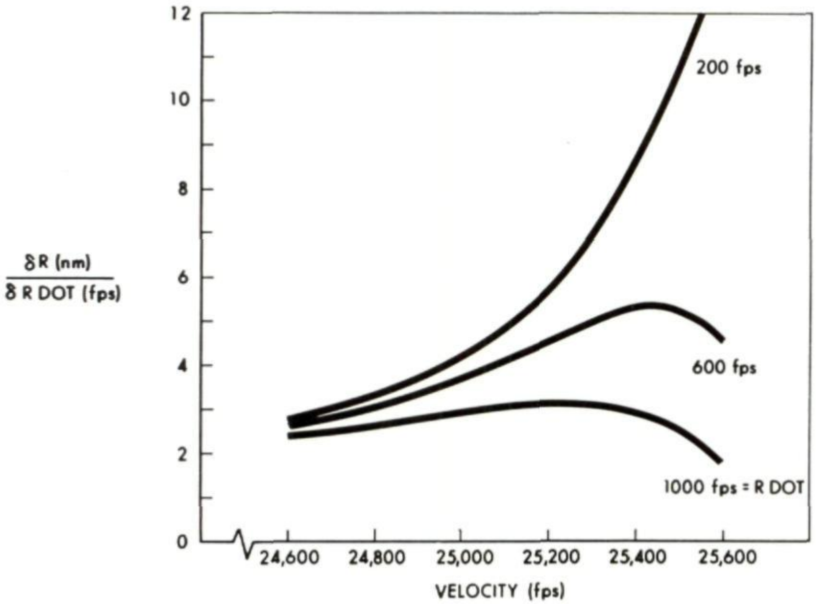

FIG. 7–32 Sensitivity of ballistic range to exit altitude rate

nominal trajectory which may be a costly maneuver and with proper choice for the form of control history it can direct the vehicle along trajectories which are desirable for other reasons than terminal accuracy – such as low heat load. A nominal-following control scheme would be undesirable if it referred to a nominal trajectory selected prior to the start of the mission. This would be a severe constraint for a flight control system which must be able to bring the vehicle home under the wide variety of circumstances resulting, for example, from aborts at all possible times during the mission. However, for this climb-to-exit phase of re-entry flight it has been demonstrated (5) that some simplifying approximations to trajectory equations permit on-board calculation of a reference trajectory which is based on the existing conditions at the end of the initial pull-up and which reflects the conditions desired at exit so as to achieve the required ballistic range. With such an analytical reference trajectory available, the nominal-following scheme has complete flexibility. Moreover, with the feedback gains in the nominal-following system time programmed to minimize the mean squared range perturbation at the end of ballistic flight due to the ensemble of expected errors in navigation information, a surprising degree of insensitivity to these errors is achieved (6). In spite of a range sensitivity to altitude rate which is typically about 3 nm/fps, this system yields trivial control errors with errors in knowledge of altitude rate as large as 200 fps. This insensitivity to error is probably the most important criterion by which to judge the merit of a flight control system for this critical phase of the flight.

Ballistic Skip – No effective aerodynamic control can be exercised during this phase of the flight. For a vehicle with no propulsive capability remaining, this skip is then uncontrolled. This just serves to emphasize the importance of achieving accurate exit conditions – or what is closer to the case, achieving a combination of errors at exit such that a desired ballistic trajectory results.

Final Glide – Again during the final glide to the landing point either predicted final value control or nominal-following control can be employed. If the vehicle has a reasonable lifting capability, say L/D of 0.5 or greater, a particularly simple range predictor is available for use in a final value control scheme. If the control history is taken to be just a constant L/D, the range to which the vehicle will glide is given to good accuracy by the simple equilibrium glide relation:

$$\text{Range angle} = \frac{1}{2}\frac{L}{D}\ \ln\left(\frac{1-\overline{V}_f^2}{1-\overline{V}_i^2}\right) \qquad \text{(Eq. 7–9)}$$

where $\overline{V}_i$ and $\overline{V}_f$ are the initial and final velocities divided by the circular satellite velocity at some mean altitude. In fact, the form of this range expression is so simple as to allow direct calculation of the required L/D given the range to go. This expression for L/D, modified by correction terms to account for the fact that the initial altitude and flight path angle may not be consistent with equilibrium glide at the required L/D (7), results in a direct closed-loop flight control system for the final glide.

The Apollo vehicle has an L/D of only 0.3. With such little lift, the assumptions underlying the equilibrium glide relations are not well satisfied, and the nominal-following philosophy seems preferable. This scheme is especially amenable to this last phase of the flight since the ballistic skip was

intended to bring the vehicle into the final glide at a nominal range from the landing point. Thus trajectory data calculated before the start of the mission and stored in the on-board computer is perfectly usable in this phase. The nominal distance flown by the Apollo vehicle in this final glide phase is about 640 nm and the control capability for accommodating range errors at the end of the ballistic skip is about ± 200 nm. It is expected that the errors will be no more than about 20 nm.

VEHICLE CONTROL

The result of the flight control schemes discussed above is a desired or commanded L/D. It still remains for a vehicle control system to execute these commands. For many reasons it would be desirable to have full aerodynamic control available, that is, to be able to roll to any desired bank angle and to trim the vehicle to any desired lift or L/D. But aerodynamic trimming poses a most difficult problem. This requires something like control surfaces or trim tabs which will not burn up when deflected into the hot gas flow, will not jam if heat-protecting material from the vehicle forebody flows back and condenses, which are reasonably small and light-weight, have modest power requirements for actuation and so on. It seems fair to say that this problem has no satisfactory solution at present.

A perfectly reasonable alternative is the use of a fixed vehicle trim at some L/D and the use of roll only to control the flight. In this case the L/D referred to throughout the discussion of in-plane flight is interpreted as the vertical component of L/D. The vehicle is then rolled to whatever bank angle is required to achieve the commanded vertical component of L/D. The resulting lateral component of lift can be directed either to the right or left. An evident logic for lateral control is to reverse the direction of roll when the predicted lateral error exceeds some limit. This limit can be set large initially and decreased during flight – perhaps in proportion to the vehicle's lateral control capability. Roll control in the Apollo mission is exercised by on-off operation of hypergolic thrusters using attitude information derived from the IMU gimbal angles. The vehicle is aerodynamically stable in pitch and yaw, additional control engines are used for rate damping about these axes.

The re-entry flight control problem for lunar return missions seems well in hand. The problem becomes much more challenging as one looks ahead to planetary return missions. It may be that new techniques will be required to satisfactorily solve that problem. The entry corridor will be considerably narrowed; perhaps large area controllable drag devices may be useful to broaden the corridor or propulsion may be useful to rotate the flight path somewhat at a strategic point during entry. The vehicle energy which must be dissipated in the atmosphere will be much greater, thus complicating considerably the problem of heat protection. Perhaps different flight plans can be used to assist in this problem – very long flights around the earth at high altitude to dissipate the energy under radiative equilibrium may be useful. Trajectory sensitivity to error will be greater, control responsiveness will have to be faster and more accurate. But one thing is certain: there will be space missions ending with atmospheric flight to a landing point. So workable solutions to the re-entry flight control problem will have to be found for all such missions.

REFERENCES

1. LORELL, J., "Forces Produced by Fuel Oscillations". Report 20–149, Jet Propulsion Laboratory, Pasadena, Calif., October 1951.
2. KALMAN, R. E., "A New Approach to Linear Filtering and Prediction Problems". Transactions of the ASME, Journal of Basic Engineering, March 1960.
3. SCHAEFER, R. A., "A New Pulse Modulator for Accurate D.C. Amplification with Linear or Nonlinear Devices". IRE Transactions on Instrumentation, Vol. I–11, No. 2, September 1962.
4. CHILTON, R. G., "Apollo Spacecraft Control Systems". Presented at I.F.A.C. Symposium on Automatic Control in the Peaceful Uses of Space, Stavanger, Norway, June 1965.
5. LICKLY, D. J., MORTH, H. R., and CRAWFORD, B. S., "Apollo Reentry Guidance". Report R-415, M.I.T. Instrumentation Laboratory, Cambridge, Mass., July 1963.
6. CRAWFORD, B. S., "Optimization of Reentry 'Up-Phase' Guidance". Space Guidance Analysis Memo #35–64, M.I.T. Instrumentation Laboratory, Cambridge, Mass., September 1964.
7. ROSENBAUM, R., "Longitudinal Range Control for a Lifting Vehicle Entering a Planetary Atmosphere". A.R.S. Paper 1911–61; August 1961.

ACKNOWLEDGEMENTS

CHERRY, G. W., M.I.T. Instrumentation Laboratory.
FRASER, D. C., M.I.T. Instrumentation Laboratory.

INDEX

FUTURE PUBLICATIONS

AGARDograph 95

"SPREAD F AND ITS EFFECTS UPON RADIOWAVE PROPAGATION AND COMMUNICATION"

This book, edited by P. Newman of the U.S.A.F. Cambridge Research Laboratories describes the irregularities in the F region observed by a number of workers in various parts of the world. Differing methods of observation were used including backscatter radar, topside sounding, oblique frequency sweeping, etc. The recent observations of radio star and satellite signals and scintillations are included.

AGARDograph 106

"SOME EFFECTS OF RAISED INTRAPULMONARY PRESSURE IN MAN"

This monograph by Sqdn. Ldr. S. Ernsting, Ph.D., B.Sc., M.B., B.S., R.A.F., is concerned with the effects on the body of raised intrapulmonary pressure and the reduction of these effects by applying compensating pressures to specific regions of the body. The information is of special value to those concerned with the protection of personnel engaged in high altitude or space flight and of considerable general interest to those engaged in the physiology of the respiration and circulation systems.

AGARD Conference Proceedings Series No. 3

"PROPAGATION FACTORS IN SPACE COMMUNICATIONS"

This volume, edited by W. T. Blackband of the R.A.E. Farnborough, presents the text of papers read (and the ensuing discussions) at the 1965 annual symposium dealing with the propagation of electromagnetic waves in space. The information covers a broad field and includes radar measurements, radio communications, propagation in a plasma sheath and some information on the ionosphere of Mars. The frequency spectrum covered extends from V.L.F. to laser beams.

Space Navigation Guidance and Control

J. E. MILLER

TECHNIVISION